

Enclosure 2 to SBK-L-16153

Simpson Gumpertz & Heger, Inc., "Evaluation and Design Confirmation of As-Deformed CEB, 150252-CA-02," Revision 0, July 2016 (Seabrook FP#100985)

CALCULATION REPORT COVER SHEET

☒ Safety Related
☐ Important to Safety
☐ Other

SIMPSON GUMPERTZ & HEGER



Engineering of Structures
and Building Enclosures

Client: NextEra Energy Seabrook

Project No.: 150252

Project: Investigate Apparent Movement of Containment Enclosure Building at NextEra Energy Seabrook Facility, Seabrook, NH

Calculation No.: 150252-CA-02

Title: Evaluation and Design Confirmation of As-Deformed CEB

Rev. No.: 0

OBJECTIVE OVERVIEW

Perform a structural evaluation and design confirmation of the as-deformed Unit 1 Containment Enclosure Building (CEB) at NextEra Energy Seabrook Station in Seabrook, New Hampshire. The as-deformed condition of the CEB is based on field measurements recorded by Simpson Gumpertz & Heger in 2015 and 2016.

OVERVIEW OF METHOD AND ASSUMPTIONS

Simulate the as-deformed condition of the CEB by applying sustained loads and self-straining forces such as alkali-silica reaction (ASR) expansion, shrinkage, swelling, and creep where applicable. Apply loads included in the original design criteria (self-weight, earth pressure, seismic load, wind load, etc.) to the CEB structure in its as-deformed state. Seismic loads are applied using a static-equivalent method utilizing the design-basis maximum acceleration profiles, which were computed during original design from response spectra analysis. Amplify ASR loads by a threshold factor to account for potential future ASR expansion. Evaluate capacity based on ACI 318-71 criteria with combined demands from all design loads, including the self-straining loads associated with the as-deformed condition.

There are eleven justified assumptions in this calculation (see Section 5.1). There is one unverified assumption in this calculation. The unverified assumption is that the CEB is statically and seismically isolated from other buildings at all locations where isolation joints are specified in design drawings. This calculation shows that the gap between the CEB and CB at missile shield block locations must be at least 1 in. to maintain seismic isolation. This unverified assumption must be tracked until resolved.

KEY REFERENCES

ACI Committee 318, *Building Code Requirements for Reinforced Concrete and Commentary*, ACI 318-71.

Seabrook, *System Description For Structural Design Criteria For Public Service Company of New Hampshire Seabrook Station Unit Nos. 1 & 2*, Document No. 9763-SD-66, Revision 2, 2 March 1984.

Simpson Gumpertz & Heger Inc., *Additional ASR-Related Inspections and CI Measurements at Forty-Two Locations to Support the Root Cause Evaluation of Apparent Movement of CEB, NextEra Energy Seabrook Facility, Seabrook NH, 150252-SVR-05-R0*, July 2016.

OVERVIEW OF RESULTS AND CONCLUSIONS

The deformed shape of the CEB model, when subjected to sustained loads and self-straining loads, simulates field measurements of deformations. The CEB meets evaluation criteria of ACI 318-71 for all factored load combinations and analysis cases analyzed when ASR loads are amplified by a threshold factor of 1.2 to account for future ASR expansion. Evaluation of deformations indicates that existing seismic gaps are sufficient at all assessed locations (excluding missile shields) and that a seismic gap of at least 1 in. must be provided at missile shields. Chapter 8 identifies recommended methods to quantitatively monitor the structure to identify if the selected threshold limit is exceeded.

Software/Version	QA Verified
ANSYS v15	<input checked="" type="checkbox"/> Yes <input type="checkbox"/> No
spColumn v4.81	<input checked="" type="checkbox"/> Yes <input type="checkbox"/> No

Software/Version	QA Verified
	<input type="checkbox"/> Yes <input type="checkbox"/> No
	<input type="checkbox"/> Yes <input type="checkbox"/> No

No.	Reason for Revision	Total No. of Sheets	Last Sheet No.	No. CD-ROM	Prepared By / Date	Independently Verified By / Date	Approved By / Date
0	Initial document	526	Z11	1	Ryan Mon	A. Sarawit	S. Bolourchi
					R. Mones	A. Sarawit	S. Bolourchi
					7/31/2016	7/31/2016	7/31/2016

Form EP3.1 EX3.1 R2
Date: 1 September 2012

150252-CA-02

- i -

Revision 0

INDIVIDUAL CALCULATION SIGNOFF SHEET

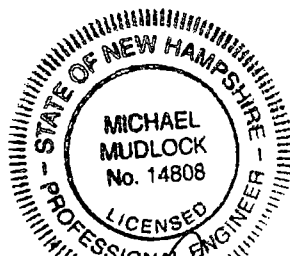
SIMPSON GUMPERTZ & HEGER

Engineering of Structures
and Building Enclosures

Section	Pages	Rev.	Prepared By		Verified By	
		No.	Name	Initial and Date	Name	Initial and Date
Cover Sheets	i-ii	0	R.M. Mones	RMM 7/31/2016	A.T. Sarawit	ATS 7/31/2016
Calculation Body	3-159	0	R.M. Mones	RMM 7/31/2016	A.T. Sarawit	ATS 7/31/2016
Appendix A	A1-A7	0	A.T. Sarawit	ATS 7/31/2016	-	7/31/2016
Appendix B	B1-B13	0	R.M. Mones	RMM 7/31/2016	A.T. Sarawit	ATS 7/31/2016
Appendix C	C1-C3	0	R.M. Mones	RMM 7/31/2016	A.T. Sarawit	ATS 7/31/2016
Appendix D	D1-D20	0	R.M. Mones	RMM 7/31/2016	A.T. Sarawit	ATS 7/31/2016
Appendix E	E1-E9	0	R.M. Mones	RMM 7/31/2016	A.T. Sarawit	ATS 7/31/2016
Appendix F	F1-F22	0	R.M. Mones	RMM 7/31/2016	A.T. Sarawit	ATS 7/31/2016
Appendix G	G1-G12	0	R.M. Mones	RMM 7/31/2016	A.T. Sarawit	ATS 7/31/2016
Appendix H	H1-H95	0	R.M. Mones	RMM 7/31/2016	A.T. Sarawit	ATS 7/31/2016
Appendix I	I1-I9	0	R.W. Keene	RWK 7/31/2016	A.T. Sarawit	ATS 7/31/2016
Appendix J	J1-J20	0	R.M. Mones	RMM 7/31/2016	A.T. Sarawit	ATS 7/31/2016
Appendix K	K1-K11	0	R.M. Mones	RMM 7/31/2016	A.T. Sarawit	ATS 7/31/2016
Appendix L	L1-L13	0	R.M. Mones	RMM 7/31/2016	A.T. Sarawit	ATS 7/31/2016
Appendix M	M1-M11	0	R.M. Mones	RMM 7/31/2016	A.T. Sarawit	ATS 7/31/2016
Appendix N	N1-N30	0	J.B. Deaton	JD 7/31/2016	A.T. Sarawit	ATS 7/31/2016
Appendix O	O1-O70	0	N.E. Castaneda	NCA 7/31/2016	A.T. Sarawit	ATS 7/31/2016
Appendix Y	Y1-Y11	0	R.M. Mones	RMM 7/31/2016	A.T. Sarawit	ATS 7/31/2016
Appendix Z	Z1-Z11	0	R.M. Mones	RMM 7/31/2016	A.T. Sarawit	ATS 7/31/2016

Note: Appendices P through X are not used.

Form EP 3.1 EX 3.3 R2
Date: 1 September 2012



Michael Mudlock
07-31-2016



TABLE OF CONTENTS

LIST OF APPENDICES.....	5
LIST OF ATTACHMENTS.....	5
LIST OF TABLES.....	6
LIST OF FIGURES.....	7
SYMBOLS AND NOTATIONS.....	11
SIGN AND LABELING CONVENTIONS USED IN THIS REPORT.....	12
1. REVISION HISTORY.....	13
1.1 REVISION 0.....	13
2. OBJECTIVE OF CALCULATION.....	14
3. CONCLUSIONS AND RECOMMENDATIONS.....	15
4. DESIGN DATA / CRITERIA.....	18
4.1 MATERIAL PROPERTIES.....	18
4.2 COMBINATIONS OF LOADS.....	19
4.3 EVALUATION ACCEPTANCE CRITERIA.....	19
4.4 FIELD MEASUREMENTS AND OBSERVATIONS.....	19
5. ASSUMPTIONS.....	22
5.1 JUSTIFIED ASSUMPTIONS.....	22
5.2 UNVERIFIED ASSUMPTIONS.....	25
6. STRUCTURAL ANALYSIS.....	26
6.1 DESCRIPTION OF STRUCTURE.....	26
6.1.1 Structure Geometry.....	26
6.1.2 Structure Reinforcement.....	26
6.1.3 Backfill Concrete and Surrounding Structures.....	29
6.2 ANALYSIS METHODOLOGY.....	29
6.2.1 Analysis Models.....	30
6.2.2 Analysis Cases.....	33
6.2.3 Standard-Plus Analysis Case to Simulate Inward Radial Deformations at Azimuth 230°.....	34
6.2.4 Methodology for Study of Impact of As-Deformed Condition on Maximum Acceleration Profiles.....	35
6.3 DESCRIPTION OF APPLIED LOADS.....	35
6.3.1 Self-Straining Loads.....	35
6.3.2 Original SD-66 Loads.....	42
6.4 ANALYSIS RESULTS.....	46
6.4.1 Comparison of ASR Strains and Crack Index Measurements.....	46
6.4.2 Comparison of Simulated Deformations and Field Measurements.....	47
6.4.3 Results of Study on Impact of As-Deformed Condition on Maximum Acceleration Profiles.....	48



6.4.4	Summary of Computed Demands.....	49
7.	STRUCTURAL EVALUATION	52
7.1	ELEMENT-BY-ELEMENT EVALUATION METHODOLOGY	52
7.1.1	Axial Compression	52
7.1.2	Axial-Flexure Interaction.....	53
7.1.3	Axial Tension.....	55
7.1.4	In-Plane Shear.....	55
7.1.5	Out-of-Plane Shear	56
7.2	SECTION CUT METHODOLOGY.....	58
7.2.1	In-Plane Shear.....	59
7.2.2	Shear Friction	61
7.2.3	Axial-Flexure Interaction.....	61
7.2.4	Torsion.....	61
7.3	DEFINITION AND SELECTION OF ASR THRESHOLD FACTOR.....	62
7.4	RESULTS OF EVALUATION WITHOUT SELF-STRAINING LOADS	62
7.5	EVALUATION RESULTS	62
7.5.1	Axial Compression in the Hoop Direction.....	64
7.5.2	Axial Compression in the Meridional Direction.....	64
7.5.3	In-Plane Shear.....	65
7.5.4	Out-of-Plane Shear Acting on the Hoop-Radial Plane.....	66
7.5.5	Out-of-Plane Shear Acting on the Meridional-Radial Plane.....	67
7.5.6	Axial-Flexure Interaction in the Hoop Direction.....	67
7.5.7	Axial-Flexure Interaction in the Meridional Direction.....	69
7.6	RESULTS OF ALTERNATIVE EVALUATIONS	71
7.6.1	Evaluation of Base of Wall Adjacent to Penetrations.....	71
7.6.2	Moment Redistribution Analysis and Evaluation.....	74
7.7	EVALUATION OF CEB DISPLACEMENTS	76
7.8	EVALUATION OF GLOBAL STABILITY	78
8.	ESTABLISH THRESHOLD MEASUREMENTS FOR CONDITION MONITORING	79
8.1	CRACK INDEX THRESHOLD MEASUREMENTS AND THRESHOLD LIMITS.....	80
8.2	DEFORMATION THRESHOLD MEASUREMENTS AND THRESHOLD LIMITS	81
9.	TABLES.....	83
10.	FIGURES.....	105
11.	REFERENCES	157

BODY OF CALCULATION:

157 PAGES TOTAL

PROJECT NO: 150252DATE: 31 July 2016CLIENT: NextEra Energy SeabrookBY: R.M. MonesSUBJECT: Evaluation and Design Confirmation of As-Deformed CEBVERIFIER: A.T. Sarawit**LIST OF APPENDICES**

Appendix A	Independent Verifier and Checker Comments
Appendix B	Computer Run Identification Log
Appendix C	Description of 150252-CA-02-CD-01 Contents
Appendix D	Computation of Creep Coefficient and Shrinkage Strain
Appendix E	Computation of PM Interaction using spColumn
Appendix F	Input Seismic Accelerations for 3D Analysis
Appendix G	Evaluation Results for Load Combinations for Original Design Analysis Case without As-Deformed Condition Demands
Appendix H	Documentation of Moment Redistribution
Appendix I	Global Stability of CEB Structure
Appendix J	Parametric Studies
Appendix K	Evaluation Computation Examples
Appendix L	Moment Redistribution Validation Examples
Appendix M	Analysis and Evaluation of Meridional Demands At El. +45.5 ft
Appendix N	Section Cut Definitions
Appendix O	Evaluation of Reinforced Concrete Section Ductility Demand
Appendix Y	Source Code of Project-Specific Computer Routines
Appendix Z	FEA Model Definition

Note: Appendices P through X do not exist.

LIST OF ATTACHMENTS

150252-CA-02-CD-01 CD containing all computer run files

Form EP 3.1 EX 3.2 R2
Date: 1 September 2012



LIST OF TABLES

CONCLUSION TABLE 1. SUMMARY OF THRESHOLD LIMITS	17
TABLE 1. LIST OF LOAD SYMBOLS AND NOTATION*	83
TABLE 2. LIST OF LOADS NOT CONSIDERED IN EVALUATION	83
TABLE 3. DEFINITION OF TORNADO WIND LOAD, W_T	84
TABLE 4. COMBINATIONS FOR COMPUTATION OF DEFORMATIONS	84
TABLE 5. LIST OF LOAD COMBINATIONS	85
TABLE 6. SEISMIC EXCITATION COMBINATIONS USING 100-40-40 RULE	86
TABLE 7. DESCRIPTION AND PURPOSE OF ANALYSIS CASES	87
TABLE 8. SUMMARY OF ANALYSIS CASES	88
TABLE 9. SUMMARY OF ANALYSIS RESULTS NAMING CONVENTION	89
TABLE 10. WIND VELOCITY PRESSURES (SECTION 4.4.1.1 OF SD-66 [8])	90
TABLE 11. SSE AND OBE SPECTRA [8]	91
TABLE 12. CRACK INDEX MEASUREMENT DATA	92
TABLE 13. ASR REGION SUMMARY	93
TABLE 14. SUMMARY OF EVALUATION RESULTS FOR STANDARD ANALYSIS CASE AT THRESHOLD FACTOR OF 1.2	94
TABLE 15. SUMMARY OF CONTROLLING EVALUATION RESULTS FOR STANDARD-PLUS ANALYSIS CASE AT THRESHOLD FACTOR OF 1.2	95
TABLE 16. SUMMARY OF DISPLACEMENT EVALUATION FOR STANDARD ANALYSIS CASE ^{1,4}	96
TABLE 17. SUMMARY OF DISPLACEMENT EVALUATION FOR STANDARD-PLUS ANALYSIS CASE ^{1,4}	97
TABLE 18. LIST OF REFERENCE DRAWINGS	98
TABLE 19. THRESHOLD MEASUREMENT SET A	102
TABLE 20. THRESHOLD MEASUREMENT SET B	103
TABLE 21. THRESHOLD MEASUREMENT SET C	104



LIST OF FIGURES

FIGURE 1. IMAGE OF CONTAINMENT ENCLOSURE BUILDING WITH OPENINGS LABELED	105
FIGURE 2. MEASUREMENTS OF TANGENTIAL MOVEMENT AT BASE OF CEB WALL [2]	106
FIGURE 3. CONCRETE FILL AND SOIL ON EXTERIOR OF CEB WALL (NOT TO SCALE)	107
FIGURE 4. ASR REGIONS AND CRACK INDEX MEASUREMENT LOCATIONS	108
FIGURE 5. WIND PRESSURE COEFFICIENTS FOR CYLINDER AND SPHERE	109
FIGURE 6. EXTERNAL WIND PRESSURES ACTING ON CEB AT VARIOUS ELEVATIONS	110
FIGURE 7. MAXIMUM ACCELERATION PROFILES FOR OBE	111
FIGURE 8. MAXIMUM ACCELERATION PROFILES FOR SSE	112
FIGURE 9. HORIZONTAL SSE SPECTRA [8]	113
FIGURE 10. VERTICAL SSE SPECTRA [8]	114
FIGURE 11. COMPARISON OF BELOW-GRADE HORIZONTAL ASR STRAINS WITH CRACK INDEX MEASUREMENTS	115
FIGURE 12. COMPARISON OF BELOW-GRADE MERIDIONAL ASR STRAINS WITH CRACK INDEX MEASUREMENTS	116
FIGURE 13. COMPARISON OF ABOVE-GRADE HOOP ASR STRAINS WITH CRACK INDEX MEASUREMENTS	117
FIGURE 14. COMPARISON OF ABOVE-GRADE MERIDIONAL ASR STRAINS WITH CRACK INDEX MEASUREMENTS	118
FIGURE 15. COMPARISON BETWEEN AS-DEFORMED CONDITION SIMULATIONS AND FIELD MEASUREMENTS AT EL. 6 FT	119
FIGURE 16. COMPARISON BETWEEN AS-DEFORMED CONDITION SIMULATIONS AND FIELD MEASUREMENTS AT EL. 22 FT	120
FIGURE 17. COMPARISON BETWEEN AS-DEFORMED CONDITION SIMULATIONS AND FIELD MEASUREMENTS AT EL. 50 FT	121
FIGURE 18. COMPARISON BETWEEN AS-DEFORMED CONDITION SIMULATIONS AND FIELD MEASUREMENTS AT EL. 119 FT	122
FIGURE 19. AXIAL FORCE ACTING IN HOOP DIRECTION FOR COMBINATION NO_1 FOR THE STANDARD ANALYSIS CASE	123
FIGURE 20. AXIAL FORCE ACTING IN HOOP DIRECTION FOR COMBINATION OBE_1 FOR THE STANDARD ANALYSIS CASE	123
FIGURE 21. AXIAL FORCE ACTING IN HOOP DIRECTION FOR COMBINATION NO_1 FOR THE STANDARD-PLUS ANALYSIS CASE	124
FIGURE 22. AXIAL FORCE ACTING IN MERIDIONAL DIRECTION FOR COMBINATION NO_1 FOR THE STANDARD ANALYSIS CASE	124
FIGURE 23. AXIAL FORCE ACTING IN MERIDIONAL DIRECTION FOR COMBINATION OBE_1 FOR THE STANDARD ANALYSIS CASE	125
FIGURE 24. AXIAL FORCE ACTING IN MERIDIONAL DIRECTION FOR COMBINATION NO_1 FOR THE STANDARD-PLUS ANALYSIS CASE	125
FIGURE 25. IN-PLANE SHEAR FORCE FOR COMBINATION NO_1 FOR THE STANDARD ANALYSIS CASE	126
FIGURE 26. IN-PLANE SHEAR FORCE FOR COMBINATION OBE_1 FOR THE STANDARD ANALYSIS CASE	126
FIGURE 27. IN-PLANE SHEAR FORCE FOR COMBINATION NO_1 FOR THE STANDARD-PLUS ANALYSIS CASE	127



FIGURE 28. OUT-OF-PLANE SHEAR FORCE (ALONG MERIDIONAL-RADIAL PLANE) FOR COMBINATION NO_1 FOR THE STANDARD ANALYSIS CASE	127
FIGURE 29. OUT-OF-PLANE SHEAR FORCE (ALONG MERIDIONAL-RADIAL PLANE) FOR COMBINATION OBE_1 FOR THE STANDARD ANALYSIS CASE	128
FIGURE 30. OUT-OF-PLANE SHEAR FORCE (ALONG MERIDIONAL-RADIAL PLANE) FOR COMBINATION NO_1 FOR THE STANDARD-PLUS ANALYSIS CASE	128
FIGURE 31. OUT-OF-PLANE SHEAR FORCE (ALONG HOOP-RADIAL PLANE) FOR COMBINATION NO_1 FOR THE STANDARD ANALYSIS CASE	129
FIGURE 32. OUT-OF-PLANE SHEAR FORCE (ALONG HOOP-RADIAL PLANE) FOR COMBINATION OBE_1 FOR THE STANDARD ANALYSIS CASE	129
FIGURE 33. OUT-OF-PLANE SHEAR FORCE (ALONG HOOP-RADIAL PLANE) FOR COMBINATION NO_1 FOR THE STANDARD-PLUS ANALYSIS CASE	130
FIGURE 34. OUT-OF-PLANE BENDING MOMENT (ABOUT MERIDIONAL AXIS) FOR COMBINATION NO_1 FOR THE STANDARD ANALYSIS CASE	130
FIGURE 35. OUT-OF-PLANE BENDING MOMENT (ABOUT MERIDIONAL AXIS) FOR COMBINATION OBE_1 FOR THE STANDARD ANALYSIS CASE	131
FIGURE 36. OUT-OF-PLANE BENDING MOMENT (ABOUT MERIDIONAL AXIS) FOR COMBINATION NO_1 FOR THE STANDARD-PLUS ANALYSIS CASE	131
FIGURE 37. OUT-OF-PLANE BENDING MOMENT (ABOUT HOOP AXIS) FOR COMBINATION NO_1 FOR THE STANDARD ANALYSIS CASE	132
FIGURE 38. OUT-OF-PLANE BENDING MOMENT (ABOUT HOOP AXIS) FOR COMBINATION OBE_1 FOR THE STANDARD ANALYSIS CASE	132
FIGURE 39. OUT-OF-PLANE BENDING MOMENT (ABOUT HOOP AXIS) FOR COMBINATION NO_1 FOR THE STANDARD-PLUS ANALYSIS CASE	133
FIGURE 40. DCRs FOR AXIAL COMPRESSION IN HOOP DIRECTION FOR COMBINATION NO_1 FOR THE STANDARD ANALYSIS CASE	133
FIGURE 41. DCRs FOR AXIAL COMPRESSION IN HOOP DIRECTION FOR COMBINATION OBE_1 FOR THE STANDARD ANALYSIS CASE	134
FIGURE 42. DCRs FOR AXIAL COMPRESSION IN HOOP DIRECTION FOR COMBINATION NO_1 FOR THE STANDARD-PLUS ANALYSIS CASE	134
FIGURE 43. DCRs FOR AXIAL COMPRESSION IN MERIDIONAL DIRECTION FOR COMBINATION NO_1 FOR THE STANDARD ANALYSIS CASE	135
FIGURE 44. DCRs FOR AXIAL COMPRESSION IN MERIDIONAL DIRECTION FOR COMBINATION OBE_1 FOR THE STANDARD ANALYSIS CASE	135
FIGURE 45. DCRs FOR AXIAL COMPRESSION IN MERIDIONAL DIRECTION FOR COMBINATION NO_1 FOR THE STANDARD-PLUS ANALYSIS CASE	136
FIGURE 46. DCRs FOR IN-PLANE SHEAR FOR COMBINATION NO_1 FOR THE STANDARD ANALYSIS CASE	136
FIGURE 47. DCRs FOR IN-PLANE SHEAR FOR COMBINATION OBE_1 FOR THE STANDARD ANALYSIS CASE	137
FIGURE 48. DCRs FOR IN-PLANE SHEAR FOR COMBINATION NO_1 FOR THE STANDARD-PLUS ANALYSIS CASE	137
FIGURE 49. DCRs FOR OUT-OF-PLANE SHEAR (ACTING ON HOOP-RADIAL PLANE) FOR COMBINATION NO_1 FOR THE STANDARD ANALYSIS CASE	138
FIGURE 50. DCRs FOR OUT-OF-PLANE SHEAR (ACTING ON HOOP-RADIAL PLANE) FOR COMBINATION OBE_1 FOR THE STANDARD ANALYSIS CASE	138
FIGURE 51. DCRs FOR OUT-OF-PLANE SHEAR (ACTING ON HOOP-RADIAL PLANE) FOR COMBINATION NO_1 FOR THE STANDARD-PLUS ANALYSIS CASE	139



FIGURE 52. DCRs FOR OUT-OF-PLANE SHEAR (ACTING ON MERIDIONAL-RADIAL PLANE) FOR COMBINATION NO_1 FOR THE STANDARD ANALYSIS CASE	139
FIGURE 53. DCRs FOR OUT-OF-PLANE SHEAR (ACTING ON MERIDIONAL-RADIAL PLANE) FOR COMBINATION OBE_1 FOR THE STANDARD ANALYSIS CASE	140
FIGURE 54. DCRs FOR OUT-OF-PLANE SHEAR (ACTING ON MERIDIONAL-RADIAL PLANE) FOR COMBINATION NO_1 FOR THE STANDARD-PLUS ANALYSIS CASE	140
FIGURE 55. DCRs FOR AXIAL-FLEXURE INTERACTION IN THE HOOP DIRECTION FOR COMBINATION NO_1 FOR THE STANDARD ANALYSIS CASE	141
FIGURE 56. DCRs FOR AXIAL-FLEXURE INTERACTION IN THE HOOP DIRECTION FOR COMBINATION OBE_1 FOR THE STANDARD ANALYSIS CASE	141
FIGURE 57. DCRs FOR AXIAL-FLEXURE INTERACTION IN THE HOOP DIRECTION FOR COMBINATION NO_1 FOR THE STANDARD-PLUS ANALYSIS CASE	142
FIGURE 58. DCRs FOR AXIAL-FLEXURE INTERACTION IN THE MERIDIONAL DIRECTION FOR COMBINATION NO_1 FOR THE STANDARD ANALYSIS CASE	142
FIGURE 59. DCRs FOR AXIAL-FLEXURE INTERACTION IN THE MERIDIONAL DIRECTION FOR COMBINATION OBE_1 FOR THE STANDARD ANALYSIS CASE	143
FIGURE 60. DCRs FOR AXIAL-FLEXURE INTERACTION IN THE MERIDIONAL DIRECTION FOR COMBINATION NO_1 FOR THE STANDARD-PLUS ANALYSIS CASE	143
FIGURE 61. SECTION CUT RESULTANT FORCES AND MOMENTS AT CUT CENTROID	144
FIGURE 62. PM INTERACTION DIAGRAM AT SECTION CUT 28 SHOWING ELEVATED TENSILE DEMANDS (PRIOR TO ADJUSTMENT OF MERIDIONAL STIFFNESS AT EL. +45.5 FT AND AZ 240)	145
FIGURE 63. PM INTERACTION DIAGRAM AT SECTION CUT 28 AFTER ADJUSTMENT OF MERIDIONAL STIFFNESS AT EL. +45.5 FT AND AZ 240)	145
FIGURE 64. PM INTERACTION CHECK FOR STANDARD ANALYSIS CASE PRIOR TO MOMENT REDISTRIBUTION (SECTION CUT 19)	146
FIGURE 65. PM INTERACTION CHECK FOR STANDARD ANALYSIS CASE PRIOR TO MOMENT REDISTRIBUTION (SECTION CUT 22)	146
FIGURE 66. PM INTERACTION CHECK FOR STANDARD ANALYSIS CASE AFTER MOMENT REDISTRIBUTION (SECTION CUT 19)	147
FIGURE 67. PM INTERACTION CHECK FOR STANDARD ANALYSIS CASE AFTER MOMENT REDISTRIBUTION (SECTION CUT 22)	147
FIGURE 68. PM INTERACTION CHECK FOR STANDARD-PLUS ANALYSIS CASE PRIOR TO MOMENT REDISTRIBUTION (SECTION CUT 19)	148
FIGURE 69. PM INTERACTION CHECK FOR STANDARD-PLUS ANALYSIS CASE PRIOR TO MOMENT REDISTRIBUTION (SECTION CUT 22)	148
FIGURE 70. PM INTERACTION CHECK FOR STANDARD-PLUS ANALYSIS CASE AFTER MOMENT REDISTRIBUTION (SECTION CUT 19)	149
FIGURE 71. PM INTERACTION CHECK FOR STANDARD-PLUS ANALYSIS CASE AFTER MOMENT REDISTRIBUTION (SECTION CUT 22)	149
FIGURE 72. PM INTERACTION CHECK FOR STANDARD-PLUS ANALYSIS CASE (SECTION CUT 14) (NO MOMENT REDISTRIBUTION NEEDED)	150
FIGURE 73. PM INTERACTION CHECK FOR STANDARD-PLUS ANALYSIS CASE (SECTION CUT 15) (NO MOMENT REDISTRIBUTION NEEDED)	150
FIGURE 74. PM INTERACTION CHECKS AT BASE OF WALL BETWEEN AZ 270° AND 360° FOR STANDARD-PLUS ANALYSIS CASE PRIOR TO MOMENT REDISTRIBUTION	151
FIGURE 75. PM INTERACTION CHECKS AT BASE OF WALL BETWEEN AZ 270° AND 360° FOR STANDARD-PLUS ANALYSIS CASE AFTER MOMENT REDISTRIBUTION	151



FIGURE 76. ILLUSTRATION OF AXIAL FORCE COUPLE RESISTING OUT-OF-PLANE PRESSURES AT THE BASE OF WALL	152
FIGURE 77. DCRs FOR IN-PLANE SHEAR FOR COMBINATION OBE_1 (100% E., 40% N., 40% VERT. DOWN) FOR THE STANDARD ANALYSIS CASE	153
FIGURE 78. DCRs FOR IN-PLANE SHEAR FOR COMBINATION OBE_3 (100% E., 40% N., 40% VERT. DOWN) FOR THE STANDARD ANALYSIS CASE	153
FIGURE 79. DCRs FOR IN-PLANE SHEAR FOR COMBINATION OBE_1 (40% E., 100% N., 40% VERT. DOWN) FOR THE STANDARD ANALYSIS CASE	154
FIGURE 80. DCRs FOR OUT-OF-PLANE SHEAR FOR COMBINATION OBE_1 (100% E., 40% N., 40% VERT. DOWN) FOR THE STANDARD ANALYSIS CASE	154
FIGURE 81. DCRs FOR IN-PLANE SHEAR FOR COMBINATION OBE_3 (100% W., 40% N., 40% VERT. UP) FOR THE STANDARD-PLUS ANALYSIS CASE	155
FIGURE 82. DCRs FOR IN-PLANE SHEAR FOR COMBINATION OBE_1 (100% W., 40% N., 40% VERT. UP) FOR THE STANDARD-PLUS ANALYSIS CASE	155
FIGURE 83. DCRs FOR IN-PLANE SHEAR FOR COMBINATION OBE_1 (100% W., 40% N., 40% VERT. UP) FOR THE STANDARD-PLUS ANALYSIS CASE	156
FIGURE 84. DCRs FOR OUT-OF-PLANE SHEAR FOR COMBINATION OBE_3 (100% E., 40% N., 40% VERT. DOWN) FOR THE STANDARD-PLUS ANALYSIS CASE	156



SYMBOLS AND NOTATIONS

ASR	alkali-silica reaction
AZ	azimuth
CB	Containment Building
CCI	Combined Crack Index
CI	Crack Index
C/D	cover-to-bar diameter
CEB	Containment Enclosure Building
CEVA	Containment Enclosure Ventilation Area
DCR	demand to capacity ratio
EI	elevation
E-W	east-west
f'_c	compressive strength of concrete
f_y	yield strength of steel
FEA	finite element analysis
FEM	finite element model
FSB	Fuel Storage Building
FSEL	Ferguson Structural Engineering Laboratory
ILC	independent load case
JA	Justified Assumption
k_{th}	ASR threshold factor (Sections 7.3 and 8)
NEE	NextEra Energy
N-S	north-south
OBE	operating basis earthquake
PM	axial-flexure (interaction)
psf	pounds per square foot
psi	pounds per square inch
psig	pounds per square inch gage (relative to atmospheric pressure)
QANF	Quality Assurance Manual for Nuclear Facility Work
RCE	Root Cause Evaluation
SD-66	System Description 66, Original structural design criteria [8]
SGH	Simpson Gumpertz & Heger Inc.
SRSS	square root of sum of squares
SSE	safe-shutdown earthquake
UA	Unverified Assumption
UE	United Engineers and Constructors
UFSAR	Updated Final Safety Analysis Report

Original SD-66 Loads	All design loads included in the original structural design criteria document (SD-66).
As-Deformed Condition	Deformed state of the CEB as measured and documented by SGH
Mech. Pen.	Mechanical Penetration (Figure 1)
Electrical Pen.	Electrical Penetration (Figure 1)

**SIGN AND LABELING CONVENTIONS USED IN THIS REPORT**

- Tensile forces, stresses, and strains are positive values unless otherwise noted.
- Bending moments are positive if tension occurs on the outside surface of the wall.
- For evaluation of axial and flexure interaction, axial-flexure demands that cause stress in the reinforcement aligned in the circumferential (hoop) direction are referred to as "hoop direction" interaction demands. Similarly, axial-flexure interaction capacity in the "hoop direction" is related to the bars aligned with in the hoop direction. This convention is extended to axial-flexure interaction in the meridional (or vertical) direction.
- For evaluation of out-of-plane shear, out-of-plane shear acting on a vertical plane is referred to as "out-of-plane shear in the hoop direction" because axial stresses acting in the hoop direction cause compression or tension on this plane and because reinforcement aligned in the hoop direction resist shear on this plane through shear friction. This convention is extended to out-of-plane shear in the meridional direction, which acts on a horizontal plane.



PROJECT NO: 150252

DATE: 31 July 2016

CLIENT: NextEra Energy Seabrook

BY: R.M. Mones

SUBJECT: Evaluation and Design Confirmation of As-Deformed CEB

VERIFIER: A.T. Sarawit

1. REVISION HISTORY

1.1 Revision 0

Initial document.



2. OBJECTIVE OF CALCULATION

The objective of this calculation is to perform a structural evaluation and design confirmation for the as-deformed Containment Enclosure Building (CEB) structure at NextEra Energy Seabrook Station in Seabrook, New Hampshire. The evaluation and design confirmation is performed in accordance with the project Criteria Document, 150252-CD-03 Rev. 0 [1]. The as-deformed condition used in the evaluation is based on measurements recorded by Simpson Gumpertz & Heger (SGH) during field inspections in March 2015, September 2015, and April 2016 [2, 3, 5]. Structural demands are computed using load combinations and load factors defined in SGH Report 160268-R-01 [6], which modifies load combinations defined in the Updated Final Safety Analysis Report (UFSAR) [7] and the Seabrook structural design criteria document, SD-66 [8], to include demands caused by ASR expansion. Alkali-silica reaction (ASR) demands are selected based on extensive field measurements of strain on the CEB [9] and are increased by a load factor to account for uncertainty in the demands and a threshold factor to account for limited future ASR expansion. Aside from the deformed condition, all other conditions of the structure, including material properties and reinforcement configurations, are considered to be in accordance with the structural design basis.

The structural evaluation and design confirmation are based on design drawings and project specifications. This calculation does not consider potential deviations from the as-designed conditions due to construction tolerances; approved change orders during construction unless incorporated into the referenced design drawings; aging effects (such as potential carbonation, leaching, or reinforcement corrosion); or local defects, repairs, etc. The evaluation of work platforms, ladders, tie-off points, and equipment braces and the associated anchorage is not in the scope of this calculation. Additionally, evaluation and design confirmation of the reinforced concrete missile shields at El. 22 ft, El. 31 ft-6 in., and El. 49 ft-6 in. against missile loading are not in the scope of this calculation.

The work is performed in accordance with the SGH Quality Assurance Manual for Nuclear Facility Work (QANF) [10] and related Engineering Procedures.



3. CONCLUSIONS AND RECOMMENDATIONS

The CEB is analyzed for the Original Design, Standard, and Standard-Plus Analysis Cases. Each of these analysis cases is briefly defined below, and is described in more detail in Section 6.2.2.

- The Original Design Analysis Case considers all original design loads with the CEB in its undeformed configuration without self-straining loads such as ASR (S_a) and swelling (S_w).
- The Standard Analysis Case considers all original design loads as well as self-straining loads, and simulates deformation measurements while conforming to all construction details specified in the original design drawings.
- The Standard-Plus Analysis Case is identical to the Standard Analysis Case, but provides an improved simulation of deformation measurements near AZ 230° by assuming that the concrete fill is in contact with the CEB at AZ 200° between El. +19 and +54 ft. Note that this assumed condition differs from that shown on the design drawings.

The conclusions of the analysis and evaluation are provided below:

- **Comparison to Field Measurements**

- The strains due to ASR expansion simulated by the finite element model (FEM) reasonably approximate crack index measurements (see Section 6.4.1 for more information).
- The as-deformed condition of the CEB is simulated by combining unfactored sustained loads and unfactored self-straining loads including ASR of the CEB and ASR of the concrete fill. Deformation comparisons are presented in Section 6.4.2 and are summarized below:
 - Deformations for the Standard Analysis Case simulate field measurements of deformation in all locations except near AZ 230°.
 - Deformations for the Standard-Plus Analysis Case simulate field measurements at AZ 230° more favorably than the Standard Analysis Case while continuing to match deformations elsewhere.

- **Design Evaluation**

- A study of the dynamic properties of the as-deformed CEB (from the Standard and Standard-Plus Analysis Cases) concludes that the as-deformed condition does not significantly impact the dynamic properties of the structure, and therefore the maximum seismic acceleration profiles for OBE and SSE excitation used in the original design remain valid.



- The Original Design, Standard, and Standard-Plus Analysis Cases are evaluated for the load combinations listed in Table 5 using the strength criteria of ACI 318-71. All ASR loads are amplified by a threshold factor of 1.2 in addition to the load factors for ASR. The threshold factor accounts for additional ASR loads that may occur in the future.
 - For the Original Design Analysis Case, which does not include self-straining loads such as ASR (S_a) and swelling (S_w), the CEB is shown to meet evaluation criteria. This conclusion is consistent with the original design of the CEB.
 - For the Standard and Standard-Plus Analysis Cases, the CEB is shown to meet evaluation criteria with the use of moment redistribution and with the consideration of localized concrete cracking.
- Clearance evaluations are performed to assess if existing seismic gaps between the CEB and other adjacent structures (with consideration given to UA01 in Section 5.1) are sufficient to reasonably ensure that the CEB will not contact other structures during a seismic event. The clearance evaluations account for existing (reduced) seismic gap widths, additional ASR-related deformations associated with the selected threshold factor, simulated CEB seismic deformations, and predicted seismic deformations of the adjacent structures (computed by others).
 - With the exception of the missile shield locations, existing gap widths at all assessed locations are sufficient to ensure that contact between buildings will not occur.
 - For missile shield locations, a minimum seismic gap of 1 in. is needed to prevent contact with the adjacent structure (CB).
- Global stability of the CEB is evaluated in Section 7.8. Stability evaluation with consideration of ASR demands demonstrates that a factor of safety against sliding, overturning, and flotation meeting the requirements of SD-66 [8] is provided.



Threshold Monitoring

- Systematic monitoring of strains and structure deformations is appropriate to detect when measured ASR strains have reached the selected threshold limits and when the distance between the CEB and adjacent structures is approaching the minimum required seismic separation. Chapter 8 presents an approach and a prospective threshold monitoring plan to meet the monitoring objectives. The monitoring consists of field measurements of CI, CCI, or expansion measurements, and seismic isolation joint widths. The measurements are divided into two sets, and monitoring is performed by comparing the average measurement for strain in regions or seismic gap widths.
- For strain; the average threshold strain limits for below grade areas are 20% above the strain values provided in Table 13 for regions R1, R2, and R3. Alternatively the average strain threshold limits based on CCI measurements for two regions using the existing 15 CCI measurement locations are provided in Conclusion Table 1 as Sets A and B.
- The average seismic gap threshold value is provided in Conclusion Table 1 as Set C.
- As averaged field measurements approach the threshold limits, or if any seismic gap measurement approaches the required minimum gap widths provided in Tables 16 and 17 corrective actions should be taken to ensure validity of the calculation conclusions.

Conclusion Table 1. Summary of Threshold Limits

Prospective Threshold Measurement Set**	Mean of Baseline Measurement Values	Threshold Limit
A (Crack Index)	0.13 mm/m	0.16 mm/m
B (Crack Index)	0.37 mm/m	0.44 mm/m
C (Seismic Gap)*	1.50 in.	1.70 in.

*Note: Data shown in this table are based on projected measurement values.

**See Tables 19, 20, and 21 for identification for measurements within Prospective Threshold Measurement Sets A, B, and C, respectively.



4. DESIGN DATA / CRITERIA

Design data and criteria are provided in the SGH Criteria Document 150252-CD-03 Rev. 0 [1]. Key information from this criteria document is summarized in Sections 4.1 through 4.3 for clarity. Field measurements and observations that are used to calibrate the as-deformed condition of the CEB are presented in Section 4.4.

4.1 Material Properties

The following material properties are used in this calculation:

- CEB Concrete
 - Compressive Strength: $f_c = 4,000$ psi ([12] 9763-F-101448)
 - Elastic Modulus: $E = 57,000 (f_c)^{1/2} = 3,605,000$ psi [8]
 - Poisson's Ratio: $\nu = 0.15$ [8]
 - Shear Modulus: $G = E/(2(1 + \nu)) = 1,567,000$ psi [11]
 - Unit Weight: $w = 150$ pcf [8]
- CEB Foundation Concrete
 - Compressive Strength: $f_c = 3,000$ psi ([12] 9763-F-101448)
 - Elastic Modulus: $E = 57,000 (f_c)^{1/2} = 3,120,000$ psi [8]
 - Poisson's Ratio: $\nu = 0.15$ [8]
 - Shear Modulus: $G = E/(2(1 + \nu)) = 1,357,000$ psi [11]
 - Unit Weight: $w = 150$ pcf [8]
- Backfill Concrete
 - Compressive Strength: $f_c = 2,000$ psi ([12] 9763-F-101842)
 - Elastic Modulus: $E = 57,000 (f_c)^{1/2} = 2,550,000$ psi [8]
 - Poisson's Ratio: $\nu = 0.15$ [8]
 - Shear Modulus: $G = E/(2(1 + \nu)) = 1,109,000$ psi [11]
 - Unit Weight: $w = 150$ pcf [8]
- Steel Reinforcement
 - Yield Strength: ASTM A615 Grade 60 ($f_y = 60,000$ psi) [8]
 - Elastic Modulus: $E_s = 29,000,000$ psi

The elastic modulus of concrete is not reduced due to ASR damage. This is further discussed in justified assumption JA03 (Section 5.1).



4.2 Combinations of Loads

Load combinations evaluated in this calculation are defined in SGH Report No. 150252-R-01 [6]. In Ref. 6, demands caused by ASR expansion are incorporated into the load combinations defined in the Seabrook UFSAR. Load factors for ASR demands are computed using a probabilistic approach that maintains the level of reliability inherent in ACI 318-71 [11, 13].

Load combinations are listed in Table 5. Load symbols are defined in Table 1. Loads not considered in this evaluation are listed in Table 2. Tornado wind loads are defined in Table 3. Additional information on each load type is provided in Section 6.3.

ACI 318-71 Section 9.3.7 [11] specifies that demands from differential settlement, creep, shrinkage, and temperature change shall be included with dead load. In this calculation, concrete swelling demands are also included with dead load due to the similarities between swelling and shrinkage. Demands due to creep and shrinkage generally cause compression in the reinforcement of the CEB and are therefore conservatively neglected when computing demands in this calculation. However, deformations caused by creep and shrinkage are considered when comparing deformations of the finite element model to field measurements.

Each load combination in Table 5 is also evaluated without the effects of self-straining forces (i.e., without ASR and swelling demands) to verify that the original design of the CEB meets design requirements. This evaluation is summarized in Section 7.4 and is presented in detail in Appendix G.

4.3 Evaluation Acceptance Criteria

Acceptance criteria for evaluation and design of reinforced concrete components are defined by ACI 318-71 [11]. No reductions in capacity are made to account for material degradation due to ASR (Justified Assumption JA11, Section 5.1). Physical testing performed by others [16] has indicated that ASR expansion does not reduce structural capacities if the total out-of-plane expansion is less than the limits defined in Ref. 16.

4.4 Field Measurements and Observations

ASR strains simulated by the finite element model are based on crack index (CI) field measurements presented in SGH Site Visit Report 150252-SVR-05-R0 [9]. The CI data come



from a total of forty-two ASR monitoring grids located throughout the CEB structure. The CI data are summarized in Tables 12 and 13, as well as in Figure 4.

Measurements of CEB displacements are presented in the SGH Site Visit Reports listed below. These site visit reports contain relative measurements between the CEB and other adjacent structures including the Containment Building (CB), the Mechanical Penetration (Mech. Pen.), the West Pipe Chase, the Containment Enclosure Ventilation Area structure (CEVA), the East Pipe Chase, and the Electrical Penetration Structure (Electrical Pen.). A brief description of each report is provided below.

- **SGH Site Visit Report 150252-SVR-01-R1 [2]:** This site visit report documents measurements of relative building movement/deformation recorded during CEB walkdowns that were initiated by the CEB Root Cause Evaluation (RCE).
- **SGH Site Visit Report 150252-SVR-02-R0 [3]:** This site visit report contains follow-up measurements of relative building movement / deformation at twenty-five seismic isolation joint locations that were previously measured and documented in Ref. 2. These twenty-five locations generally had seismic isolation joint widths of 2 in. or less.
- **SGH Site Visit Report 150252-SVR-03-R0 [4]:** This site visit report contains measurements of the annulus width between the CB and CEB at the springline elevation. Also, this report documents surveyor markings on the exterior surface of the CB at the springline elevation, which can be used to obtain the as-built radius of the CB at each azimuth. Additionally, this site visit report contains qualitative observations of ASR on the exterior surface of the CEB.
- **SGH Site Visit Report 160144-SVR-03-R0 [5]:** This site visit report contains follow-up measurements of relative building movement / deformation at twenty-five seismic isolation joint locations that were previously measured and documented in Ref. 2 and 3.

This calculation generally interprets all relative measurements between buildings using the following two assumptions (JA08 in Section 5.1):

- The CEB and all adjacent structures were originally constructed in accordance with design drawings
- No structures other than the CEB are deforming or displacing (except during seismic events)

Using these two assumptions, relative measurements between the CEB and other adjacent structures can be compared to corresponding design dimensions on drawings; any difference



between the design dimension and the measurement is generally attributed to CEB deformation. These assumptions have exceptions, as listed below:

- Preliminary field observations indicate that the isolation gap between the CEB and the CB at the missile shield above the CEVA structure has zero or near-zero width. This indicates that there is a larger inward radial deformation at this location than measured elsewhere on the CEB, and the deformation may be higher than indicated by the Standard Analysis Case, which assumes that the concrete fill was placed as indicated on the design drawings. To reach this level of inward deformation, an alternative analysis case (referred to as the Standard-Plus Analysis Case) is performed with the assumption that the concrete fill placed between the CEVA structure, FSB, and CEB (between El. +19 and +54 ft) was constructed without the 3 in. seismic isolation joint specified on the design drawings. CEB demands from the Standard and the Standard-Plus Analysis Case are both evaluated against the ACI 318-71 acceptance criteria in this calculation (see Section 6.2.2 for more information).
- Site visit report 150252-SVR-03-R0 [4] documents surveyor markings that were painted on the exterior surface of the CB at the springline elevation. These markings are used to compute the as-built radius of the CB at the springline elevation. Measurements of radial deformation of the CEB at the springline elevation are adjusted for the as-built radius of the CB.



5. ASSUMPTIONS

5.1 Justified Assumptions

Justified assumptions (JAs) are listed below.

- **JA01:** The as-deformed condition of the CEB can be represented by a finite element model subjected to sustained loads and self-straining forces including ASR expansion, creep, shrinkage, and swelling.

Justification: It is demonstrated in Section 6.4.2 that sustained loads and self-straining forces (including ASR expansion, creep, shrinkage, and swelling) can be applied to the finite element model to generally simulate the deformed shape of the CEB measured by SGH [2, 3, 4, 5].

- **JA02:** ASR causes expansion of concrete, which creates a tension in the reinforcement and corresponding compression in the concrete (in the direction of expansion).

Justification: Many researchers [14] show that ASR in reinforced concrete forms cracks that become filled with an expansive gel. A tensile force in the reinforcement bars develops as the concrete attempts to expand. The tensile force in the reinforcement is balanced by a corresponding compression force in the concrete. The magnitude of ASR expansion (and the associated tensile and compressive forces) used in this evaluation and design confirmation is based on field measurements.

- **JA03:** Unreduced design material stiffness properties can adequately represent ASR-impacted reinforced concrete sections of the CEB structure.

Justification: A physical test program by MPR Associates and the Ferguson Structural Engineering Laboratory (FSEL) concludes that structural evaluations of ASR-affected structures at Seabrook Station with through-thickness expansion within certain limits should use the material properties specified in the original design specifications [17]. These limits bound the current conditions. Additionally, a parametric study (described in Appendix J) demonstrates that larger demands are computed from the as-deformed condition if an unreduced elastic modulus is used. Therefore, an unreduced elastic modulus based on the design concrete compression strength (f_c) is used in the Standard and Standard-Plus Analysis Cases in this calculation.

- **JA04:** Concrete fill undergoes ASR expansion.

Justification: Testing has not been performed to assess whether the concrete fill is undergoing ASR expansion. However, the same aggregate source was used for the concrete fill as for the CEB concrete. In the absence of such test data, this calculation assumes that ASR is present in the fill concrete and concrete fill expansion will produce a radial pressure on the CEB proportional to the overburden pressure at the



depth of concrete fill. The actual pressure due to concrete fill expansion plus all other sustained loads should result in deformations that simulate the field measurements of deformation.

- **JA05:** Live loading of work platforms and ladder landings is neglected.

Justification: Live loading of work platforms and ladder landings is considered to be negligible relative to the self-weight of the CEB concrete structure. These live loads are excluded from original design calculations [24] and are neglected in this calculation.

- **JA06:** The mass, stiffness, and wind loading of the Plant Vent Stack attached to the outside surface of the CEB at AZ 230° do not affect the behavior of the CEB model.

Justification: The Plant Vent Stack is constructed of stainless steel sheet metal and steel channel sections. An approximate self-weight take-off indicates that the Plant Vent Stack and adjacent ladders and platforms weigh approximately 900 lbf per linear foot and are about 170 ft long. The mass of the Plant Vent Stack is equivalent to about 20% of its supporting concrete (assuming that the mass of the vent stack is resisted by a strip of CEB concrete that is twice the width of the vent stack). Additionally, the total mass of the vent stack is about 10% of the design snow load (74 psf) and about 6% of the unusual snow load (126 psf). Based on this information, the mass of the Plant Vent Stack is considered to be negligible. Additionally, the sheet metal and light weight steel channels are judged to have negligible stiffness relative to the reinforced concrete CEB.

Due to the small size of the Plant Vent Stack relative to the CEB structure, wind loads acting on the Plant Vent Stack are judged to be insignificant relative to the loading on the concrete cylinder and dome.

- **JA07:** Observed cracking at the springline elevation (El. +119 ft) is at least partially related to non-ASR structural demands.

Justification: Ref. 9 notes that the orientation and pattern of cracks at the springline elevation are not necessarily indicative of ASR expansion. ASR cracking typically has a map pattern, which is generally less apparent at the springline elevation than other ASR monitoring locations. Additionally, the cracking on the interior of the CEB at the springline does not show signs of moisture intrusion, efflorescence, or ASR gel. Furthermore, a parametric study documented in Appendix J evaluates the impact of modeling ASR demands at the springline.

- **JA08:** In the Standard Analysis Case, the calculations assume that the CEB structure was constructed as specified in design drawings. In the Standard-Plus Analysis Case, the calculations assume additional inward pressure, corresponding to the location of the concrete fill wedge between the CEVA, CEB, and FSB at El. +19 to +54 ft, to improve the CEB deformation in a localized area at about AZ 230°. For the Standard-Plus Analysis Case, the assumed additional pressure could be due to ASR expansion of the concrete fill wedge if it has come in contact with the CEB (even though a gap is



indicated in design drawings). In all analysis cases, it is assumed that no structures other than the CEB are deforming or displacing, except for seismic joint measurement that accounts for seismic displacements of adjacent structures.

Justification: Analysis cases are described fully in Section 6.2.2. In the Standard Analysis Case, it is assumed that the CEB conforms to original design drawings. For this case all analyses are based on original design assumptions except accounting for additional deformations and stresses in the CEB due to self-straining loads. Therefore this assumption for the Standard Analysis Case is justified since it is fully consistent with the original design.

The additional pressure assumed for the Standard-Plus Analysis Case was done to improve the CEB radial deformation at AZ 230° compared to observed deformation. This additional pressure is assumed to be due to ASR expansion of the wedge of concrete fill between the CEVA, FSB, and CEB. Assuming the additional pressure is due to concrete fill expansion is justified since ASR has the largest load factor for the controlling static load combination. However this assumption inherently implies that the designed seismic gap between the concrete fill wedge and CEB is closed. The Standard-Plus Analysis Case does not account for the effects from or potential interaction with the wedge of concrete fill. It is expected that the wedge of concrete fill is self-supporting and sufficiently stiff to prevent imparting lateral demands to the CEB. Motion of the CEB toward the fill may result in contact along the height of the wedge, which is expected to reduce seismic demands lower in the structure.

The assumption that no structures are deforming or displacing other than the CEB causes all observed seismic gap movements to be conservatively attributed to CEB deformation. While there is potential for other buildings to be deforming or displacing, this assumption is justified because it results in the most conservative deformation profile for the CEB. When evaluating clearance between the CEB and adjacent structures, the seismic deformations of other structures [31] are considered.

- **JA09:** Maximum acceleration profiles for seismic analysis are not impacted by the as-deformed condition and are unchanged from the original design. Additionally, the maximum acceleration profiles are not impacted by concrete cracking.

Justification: A study has been performed to demonstrate that the dynamic properties of the CEB structure are not impacted by the as-deformed condition. The methodology and results of this study are summarized in Sections 6.2.4 and 6.4.3. Additional documentation for this study is provided in Appendix F.

The OBE and SSE maximum acceleration profiles used in the original design of the CEB are used in this analysis. These acceleration profiles were computed by UE and are presented on Sheets 22 through 26 of UE Calculation SBSAG 4CE [24] (replicated in this calculation as Figure 7).

- **JA10:** The CEB material properties are not reduced due to irradiation.



Justification: Section 3.8.3.4 (b).4 of the Seabrook UFSAR [7] states that the primary shield wall is the only concrete subjected to relatively high irradiation.

- **JA11:** ASR expansion impacts the total demand on reinforced concrete elements, but does not reduce the resistance (capacity) of reinforced concrete elements so long as the strain does not exceed the limits defined in Ref. 16.

Justification: A physical testing program performed by MPR Associates and the University of Texas at Austin Ferguson Structural Engineering Laboratory (FSEL) [16] has shown that ASR does not reduce the design properties and capacities for the levels of ASR currently identified in the CEB.

5.2 Unverified Assumptions

Unverified Assumptions (UAs) are listed below.

- **UA01:** The CEB is statically and seismically isolated from other buildings at all locations where isolation joints are specified in design drawings.

Description: Preliminary field observations indicate that the isolation gap between the CEB and the CB at the missile shield above the CEVA structure has zero or near-zero width. In order for this calculation to be valid, a seismic gap of at least 1 in. must be provided at the missile shield above the CEVA structure.

Required Action: This unverified assumption must be tracked until confirmation or resolution.



6. STRUCTURAL ANALYSIS

Structural analysis is performed using finite element analysis. The CEB structure is described in Section 6.1. The analysis methodology, including the analysis models, is described in Section 6.2. Applied loads are described in Section 6.3. Analysis results (i.e., deformations, strains, and structural forces and moments computed using the finite element model) are summarized in Section 6.4. Methodology and results of the evaluation (i.e., comparison of structural demands and structural capacities) are presented in Chapter 7 of this calculation.

6.1 Description of Structure

6.1.1 Structure Geometry

Based on the UE design drawings [12], the CEB is a cylindrical reinforced concrete structure, 228 ft tall, with an inside radius of 79 ft-0 in. that is enclosed at the top by a 1 ft-3 in. thick hemispherical reinforced concrete dome. The wall thickness varies from 3 ft-0 in. at the base to 2 ft-3 in. from El. 11 ft to El. 40 ft, and 1 ft-3 in. above El. 40 ft.

Several large openings penetrate the CEB wall. The Mech. Pen. and adjoining West Pipe Chase are located on the west side of the CEB and are approximately 60 ft wide and 50 ft tall. The Electrical Pen. is located on the north side of the CEB and is approximately 40 ft wide and 57 ft tall. Both the Mech. Pen. and the Electrical Pen. extend to the base of the structure. Other openings of significant size include the East Pipe Chase, the Equipment Hatch, the Personnel Hatch, and openings adjacent to the CEVA and the FSB. Openings in the CEB wall are illustrated in Figure 1.

The CEB wall is supported on a 10 ft thick concrete ring base footing. The top of the footing is at El. (-)30 ft, approximately 50 ft below finished grade. The foundation is interrupted at the Mechanical and Electrical Penetrations on the west and north sides of the CEB.

6.1.2 Structure Reinforcement

The reinforcement in the hoop direction is described below:

- **Between El. (-)30 ft and El. (-)11 ft:** #11@12 in. on each face, with the following exceptions:



- The region between the Mechanical Penetration and the Electrical Penetration, which has #11@6 in. on each face
- The pilasters adjacent to the Mechanical Penetration and the Electrical Penetration are reinforced with additional #6@6 in. on each face.
- A 30 ft long region on the east side of the Electrical Penetration has #11@6 in. on each face and #8@6 in. on the outside face.
- **Between El. (-)11 ft and El. 22 ft:** #10@12 in. on each face, with the following exceptions:
 - The region around the Equipment Hatch, which has #10@6 in.
 - A 30 ft long region to the east of the Electrical Penetration, which has #10@12 in. on each face and additional #8@12 in. on the inside face up to El. 0 ft.
 - The region between the Electrical Penetration and the Mechanical Penetration has #10@6 in. on each face between El. (-)11 ft and El. 3 ft-3 in.
- **Between El. 22 ft and 45 ft-6 in.:** #10@12 in. on each face, with the following exceptions:
 - #10@6 in. on the inside face and two layers #10@6 in. on the outside face directly above the Electrical Penetration.
 - #10@6 in. on each face in the region around the Equipment Hatch.
 - #10@6 in. on the outside face and #10@12 in. on the inside face directly above the Mechanical Penetration.
- **Between El. 45 ft-6 in. and 75 ft-6 in.:** #9@6 in. on each face above the electrical penetration, #10@6 in. on each face above the Equipment Hatch up to El. 61 ft, and #9@12 in. on each face elsewhere.
- **Between El. 75 ft-6 in. and the Springline at El. 119 ft:** #8@6 in. on each face above the electrical penetration and #8@12 in. on each face elsewhere.
- **Between El. 119 ft and El. 170 ft (40 deg above the Springline on the dome):** #8@12 in. on each face.
- **Between El. 170 ft-2 in. and El. 197 ft (80 deg above the Springline on the dome):** #6@12 in. on each face.
- **Within the top 10 deg of the dome:** No hoop bars provided, however meridional bars form a grid in this region.

The reinforcement in the meridional direction is described below:

- **Between El. (-)30 ft and El. (-)11 ft:** One layer of #11@6 in. on inside face and two layers of #11@6 in. on outside face, with the following exceptions:



- To the east of the Electrical Penetration, one layer of #11@12 in. and #14@12 in. (alternating, such that there is one bar per 6 in.) on the inside face and two layers of #14@6 in. on the outside face.
- To the north of the Mechanical Penetration, one layer of #11@6 in. on the inside face and two layers of #14@6 in. on the outside face.
- Additional #11@6 in. bars provided on the edge of the wall within the pilasters on either side of the Mechanical Penetration and Electrical Penetration.
- **Between El. (-)11 ft and El. 11 ft:** One layer of #11@6 in. on inside face and two layers of #11@6 in. on outside face. Additional #11@6 in. bars provided on the edge of the wall within the pilasters on either side of the Mechanical Penetration and Electrical Penetration.
- **Between El. 11 ft and El. 22 ft:** #11@6 in. on each face. Additional #11@6 in. bars provided on the edge of the wall within the pilasters on either side of the Mechanical Penetration and Electrical Penetration.
- **Between El. 22ft and El. 45 ft-6 in.:** #11@6 in. on each face.
- **Between El. 45 ft-6 in. and 75 ft-6 in.:** #9@6 in. on each face above the Electrical Penetration, #11@6 in. on each face adjacent to and above the Equipment Hatch up to El. 69 ft, #9@12 in. on each face elsewhere.
- **Between El. 75 ft-6 in. and the Springline at El. 119 ft:** #8@6 in. on each face above the Electrical Penetration, #8@12 in. on each face elsewhere.
- **Between El. 119 ft and El. 170 ft (40 deg above the Springline on the dome):** #8@12 in. on each face.
- **Between El. 170 ft-2 in. and El. 197 ft (80 deg above the Springline on the dome):** #6@12 in. on each face.
- **Within the top 10 deg of the dome:** #6@6 in. on each face forming a grid pattern.

Transverse reinforcement (stirrups) are described below:

- **Between El. (-)30 ft and El. (-)11 ft:** #8 stirrups spaced at 12 in. in both hoop and meridional direction.
- **Between El. (-)11 ft and El. 22 ft:** #4 stirrups spaced at 12 in. in both hoop and meridional direction.
- **Surrounding the Equipment Hatch:** #4 stirrups spaced at 12 in. in both hoop and meridional direction.

In addition to the reinforcement described above, additional "C-shaped" reinforcement is provided around several of the penetrations, and diagonal reinforcement bars are provided at



reentrant corners of penetrations. This calculation does not explicitly consider additional capacity from this reinforcement.

6.1.3 Backfill Concrete and Surrounding Structures

As illustrated in Figure 3, concrete backfill occupies the space between the outside surface of the wall and the bedrock up to El. 0 ft. A waterproofing membrane separates the outside surface of the wall from the concrete backfill. Soil structural backfill is used between El. 0 ft and finished grade at El. 20 ft.

The triangular space between the CEVA structure, FSB, and CEB is filled with concrete fill material up to El. +54 ft. According to design drawings, the CEB and FSB are isolated from this wedge of concrete fill along its full height by a 3 in. wide seismic joint. In the Standard-Plus Analysis Case, the calculations assume (JA08, Section 5.1) that this wedge of concrete fill may be in contact with the CEB structure.

The CEB is structurally separated from all adjacent structures by nominally 3 in. wide seismic gaps except for the inside edge of the CEB footing, which is directly adjacent to the CB footing. Field measurements of the seismic gaps [2, 3, 5] have indicated that the actual width of seismic gaps deviates from the 3 in. nominal design width at several locations. If the measured width of the gap is less than 3 in., then the reduced seismic gap width is considered when evaluating building clearances in this calculation.

6.2 Analysis Methodology

Structural analyses are performed to obtain structural demands due to self-straining loads and all loads included in the original design criteria (referred to as "original SD-66 loads"). The as-deformed condition of the CEB is simulated by applying unfactored sustained loads and self-straining loads. All loads except for self-straining loads are applied to the structure when it is in its as-deformed condition. The analysis procedure to compute demands is broken into two analysis steps:

- **Analysis Step One**



- Simulate the as-deformed condition by applying unfactored sustained loads and unfactored self-straining loads to the Undeformed 3D Model defined in Section 6.2.1.1.
 - Extract nodal deformations caused by these unfactored loads, which are used to generate the As-Deformed 3D Model.
 - Extract structural demands (forces and moments) caused by self-straining loads (ASR and swelling) for combination with original SD-66 loads.
- **Analysis Step Two**
- Apply non-seismic loads to the As-Deformed 3D Model generated in Analysis Step One. Extract non-seismic demands (forces and moments).
 - Perform a static equivalent seismic analysis by applying the maximum seismic acceleration profiles to the As-Deformed 3D Model. Extract seismic demands (forces and moments).

This analysis methodology follows the procedure defined in Section 9.1 of the criteria document [1].

The methods that are used to apply loads are listed in Section 6.3. Following completion of Analysis Steps One and Two, structural demands are combined using the combinations and load factors presented in Table 5. ASR-related demands are multiplied by the load factors in Table 5 as well as by a threshold factor to account for possible future ASR expansion. The threshold factor is defined in Section 7.3. Chapter 8 identifies recommendations for monitoring the CEB structure to detect when ASR loads have met the selected threshold factor. When measurements of field conditions show that the threshold limits are met or exceeded, then the validity of the evaluations made in this calculation must be assessed.

6.2.1 Analysis Models

Analyses are performed using the models described in this section. All models are created with ANSYS Mechanical APDL Version 15.0 finite element modeling software [18]. ANSYS Version 15 was procured as a nuclear QA software package and has been validated and verified in accordance with the SGH QANF Program [19, 20].

6.2.1.1 Undeformed 3D Model

The undeformed 3D model is generated based on design drawings [12] and is used in Analysis Step One to simulate the as-deformed shape of the CEB.



Undeformed 3D Model Geometry

The undeformed 3D model consists of the entire CEB cylinder walls, dome, and foundation. The CEB walls and dome concrete consist of four-node shell elements (SHELL181 [18]) modeled using centerline geometry. The CEB foundation consists of eight-node solid elements (SOLID185). The CEB wall connects to the foundation using rigid beam elements (MPC184). The concrete fill that is not separated from the CEB wall with a seismic isolation gap is modeled using spring elements (COMBIN14) that are assigned stiffness in the radial direction only. Membrane elements (SHELL181 with membrane stiffness only) model the steel reinforcement in the CEB wall. These membrane elements are included in the model only to facilitate computation of ASR expansion and concrete swelling related stresses, and are not included in the model during application of other loads. The model contains a total of 13,613 shell elements, 3,660 solid elements, 27,226 membrane elements, 3,334 spring / connector elements, and 21,967 nodes. The model is in units of pounds-force (lbf) and inches (in.). In the model's rectangular global coordinate system, the positive x-direction is east, the positive y-direction is north, and the positive z-direction is vertically upward. In the model's cylindrical global coordinate system, the x-direction is radial, the y-direction is tangential, and the positive z-direction is vertically upward.

Shell elements representing the CEB wall are approximately 3 ft by 3 ft in size. Penetrations in the CEB wall exceeding this typical element size are included in the model. The penetrations included in the model are listed below.

- Electrical Pen., centered at AZ 0°
- East Main Steam and Feed Water Pipe Chase opening, centered at AZ 90°
- FSB Penetration, centered at AZ 185°
- Equipment Hatch opening, centered at AZ 150°
- CEVA opening, centered at AZ 230°
- Mech. Pen. and West Main Steam and Feed Water Pipe Chase opening, centered at AZ 270°
- Personnel Hatch opening, centered at AZ 315°



Walls / slabs extending perpendicularly from the CEB wall, including the walls / slabs extending towards the Main Steam and Feed Water Pipe Chases and missile shields, are modeled using shell elements (SHELL181).

Undeformed 3D Model Boundary Conditions

The boundary conditions for the ASR expansion of the CEB wall and concrete swelling load cases are described below:

- The base of the CEB foundation is restrained vertically.
- The base of the CEB foundation is permitted to slide in the tangential direction. Spring elements with low stiffness are provided to provide numerical stability to the CEB model. Sliding is permitted in these cases because the capacity for the CEB foundation to resist sliding through friction is limited. Field measurements of movement at the base of the CEB wall indicate between 0.5 and 1.0 in. of tangential displacement (Figure 2), which is matched in the as-deformed condition simulations.
- The CEB wall below El. 0 ft and the outside surface of the foundation are supported radially with spring elements that are given stiffness equivalent to 10 ft of fill concrete. The springs have no stiffness in the tangential and vertical directions.

The boundary conditions for the shrinkage, hydrostatic pressure, and ASR expansion of backfill cases are described below. Note that the shrinkage load case is used to compute deformations of the as-deformed condition, but is not used to compute structural demands.

- The base of the CEB foundation is restrained vertically.
- The base of the CEB foundation is restrained in the tangential direction.
- The outside surface of the foundation is supported radially with spring elements that are given stiffness equivalent to 10 ft of fill concrete. The springs have no stiffness in the tangential and vertical directions.

The boundary conditions for other loads are described below:

- The base of the CEB foundation is restrained vertically.
- The base of the CEB foundation is restrained in the tangential direction.
- The CEB wall below El. 0 ft and the outside surface of the foundation are supported radially with spring elements that are given stiffness equivalent to 10 ft of fill concrete. The springs have no stiffness in the tangential and vertical directions.



6.2.1.2 As-Deformed 3D Models

The original SD-66 seismic and non-seismic loads are applied to the As-Deformed 3D Models. Demands obtained from the As-Deformed 3D Models are combined with demands from self-straining loads (ASR and swelling) as shown in Table 5.

As-Deformed 3D Model Geometry

The "As-deformed 3D Model" is generated using the deformed shape of the "Undeformed 3D Model" with unfactored sustained loads and unfactored self-straining loads. The as-deformed model approximates the measured deformations presented in Section 4.4.

As-Deformed 3D Model Boundary Conditions

The boundary conditions for all original SD-66 loads are described below:

- The base of the CEB foundation is restrained vertically.
- The base of the CEB foundation is restrained in the tangential direction.
- The CEB wall below El. 0 ft and the outside surface of the foundation are supported radially with unidirectional spring elements that are given stiffness equivalent to 10 ft of fill concrete. The springs have stiffness in the radial direction only.

6.2.2 Analysis Cases

The CEB is analyzed and evaluated under four analysis cases (excluding analyses documented in parametric studies). These cases are defined below, and the computer run identifier for each analysis case is written in parenthesis beside each analysis case name.

- **Original Design Analysis Case (10D_r0):** This case uses the CEB model without any self-straining loads (e.g., without ASR expansion of the wall, ASR expansion of the fill, creep, shrinkage, and swelling). In this analysis case, loads are limited to those considered during the original design of the CEB.
- **Standard Analysis Case (10A_r0):** This case uses the CEB model and simulates self-straining loads in addition to all other design loads included in the original design criteria. Applied expansion representing ASR expansion of the wall is tuned to generally match field measurements (listed in Section 4.4), and applied pressures representing ASR expansion of the fill is tuned such that deformations (due to unfactored sustained loads and self-straining loads) match field measurements of deformation at all locations except for AZ 230°.



- Standard-Plus Analysis Case (10B7_r0):** This case is identical to the Standard Analysis Case, except additional radial-inward pressures are applied to the wall near AZ 200° to better simulate field measurements of deformation in that particular region. The additional pressures are applied in an area where concrete fill is adjacent to the CEB, but is designed to be separated from the CEB with a 3 in. gap (based on design drawings [12]). The additional pressures are applied in this area because (a) it is possible that the concrete fill is currently in contact with the CEB at this location and (b) the demands caused by this deformation are conservatively large if it is assumed they are caused by an externally applied ASR load due (since ASR has a large load factor). Additional information on the Standard-Plus Analysis Case is provided in Section 6.2.3.

The purpose and use of each analysis case is shown in Table 7. A summary of the features of each analysis case is shown in Table 8. The design confirmation evaluation is performed on the Standard Analysis Case (09A_r0) and the Standard-Plus Analysis Case (10B7_r0). Moment redistribution is performed for elements that have axial-flexure interaction demands exceeding capacity in the Standard and Standard-Plus Analysis Cases; the moment redistribution analyses are labeled "Standard Analysis Case with Moment Redistribution (10AR_r0)" and "Standard-Plus Analysis Case with Moment Redistribution (10BR7_r0)."

6.2.3 Standard-Plus Analysis Case to Simulate Inward Radial Deformations at Azimuth 230°

The "Standard" analysis case described in Section 6.2.2 is performed using the assumption that the CEB and all adjacent structures are constructed as shown on design drawings (JA08, Section 5.1). In the "Standard" analysis case, the CEB deformations generally simulate field measurements of relative building movement with the exception of inward radial movement near AZ 230°. Preliminary field observations indicate that the isolation gap between the CEB and the CB at the missile shield above the CEVA structure has zero or near-zero width, indicating possible radial deformations of up to 3 in. at this location.

A "Standard-Plus" analysis case is performed in addition to the "Standard" analysis case. The "Standard-Plus" analysis differs from the "Standard" analysis in the following way:

- Inward pressures representing concrete fill are extended to include the portion of CEB wall that is adjacent to the triangular "wedge" of concrete between the CEVA, FSB, and CEB (from AZ 180° to 212°, El. +19 to +54 ft). See Assumption JA08 in Section 5.1.

Concrete fill pressure simulating ASR within the region adjacent to the concrete fill "wedge" is taken as 50% of the overburden pressure acting on the fill at the top of the "wedge" and 100% of the overburden pressure at the bottom of the "wedge."



The pressure profile described above was selected based on the parametric study provided in Appendix J, such that the deformed shape at this location better simulates the observed deformation.

Unfactored sustained loads and self-straining loads in the “Standard-Plus” analysis case result in increased deformation at AZ 230°, as discussed in Section 6.4.2. Demands from the “Standard Plus” analysis case are evaluated using the same acceptance criteria as the “Standard” analysis case.

6.2.4 Methodology for Study of Impact of As-Deformed Condition on Maximum Acceleration Profiles

To analyze the impact of the as-deformed condition of the CEB on the OBE and safe-shutdown earthquake (SSE) maximum acceleration profiles, a study is performed by comparing the dynamic properties of the CEB with and without the deformations computed in Analysis Step One. The parameters evaluated in this study include center of mass, shear center, and stick model moment of inertia. Cracked section properties are not considered by this study since they do not affect the global seismic response of the CEB. Results of this study are summarized in Section 6.4.3. Detailed documentation of this study is provided in Appendix F.

6.3 Description of Applied Loads

Loads applied to the CEB in both Analysis Step One and Analysis Step Two are described in this section. A full description of these loads can be found in the SGH Criteria Document 150252-CD-03 [1].

6.3.1 Self-Straining Loads

Self-straining loads are applied to the model during Analysis Step One, as described in Section 6.2.

Deflections caused by unfactored self-straining loads listed in this section are combined with unfactored sustained loads to simulate the field measurements of the CEB as-deformed condition recorded by SGH in March 2015, September 2015, and April 2016 [2, 3, 5].



Creep

Creep causes deformations of hardened concrete subjected to sustained loads to increase over time. The rate of creep deformations varies with time, among other factors, and is dependent on the magnitude of stress caused by the sustained loads. Creep generally causes a portion of a sustained load initially carried by concrete to transfer to the steel reinforcement over time. Creep generally causes sustained load stresses (which are primarily compressive in the CEB) to shift from the concrete to the reinforcement. Therefore, it is reasoned that excluding the demands from creep will conservatively result in higher tensile stress in steel and higher compressive stress in concrete. Although the demands associated with creep are neglected from this analysis, the deflections caused by creep are included when simulating the as-deformed condition of the CEB.

Lower-bound and upper-bound creep coefficients are computed in Appendix D using ACI 209R-92 [21]. The lower-bound creep coefficient of 1.3 is used to model creep deformations for the following two reasons:

- Using a smaller creep coefficient causes more of the as-deformed condition to be attributed to other self-straining loads (such as ASR and swelling), which contribute to the overall demands acting on the structure. Therefore, using the lower-bound creep coefficient leads to more conservative demands.
- The ACI 209R-92 [21] computations do not explicitly account for the effects of reinforcement on the creep coefficient. Reinforcement generally reduces creep deformations; therefore, it is judged that the lower-bound creep coefficient is more reasonable.

Creep deflections are computed by multiplying the sustained load deflections by the computed creep coefficients. For example, if the sustained load deflection is 0.20 in., and the creep coefficient is 1.3, then the creep deflection is 0.26 in. and the total deflection is 0.46 in.

Shrinkage

Shrinkage is the volume change that occurs during the hardening of concrete that is caused by the loss of water as the concrete cures. Shrinkage strains are independent of the sustained loads acting on a concrete section. The magnitude of shrinkage strains are computed in Appendix D as (-)0.025% for 15 in. walls, (-)0.020% for 27 in. thick walls, and (-)0.010% for 36 in. thick walls.



Shrinkage can cause a small compression stress in reinforcement. If included in the finite element analysis, it would negate a portion of the ASR demands. For this reason, shrinkage demands are excluded from this analysis. However, similar to creep, the deformations associated with shrinkage are included when simulating the as-deformed condition of the CEB.

Shrinkage is applied to the model using thermal contraction (i.e., subjecting the elements to a decrease in temperature). Varying levels of thermal loads are applied to the model based on element thickness to achieve the desired shrinkage effects.

ASR Expansion of the CEB Wall

ASR is a chemical reaction between the alkali contained in cement and reactive silica minerals contained in some concrete aggregates. The reaction produces an alkali-silica gel that swells if moisture is present and causes the concrete to expand and crack.

Varying magnitudes of ASR expansion are applied to the CEB finite element model based on field measurements of CI. Physical tests have shown that CI measurements provide a reasonable and conservative approximation of the true engineering strain at a point in time for a reinforced concrete member undergoing ASR expansion [16, 22]. CI measurements have been recorded at forty-two locations on the CEB wall [9]. Of these forty-two CI measurements, thirty-two are located at interior locations, ten are located at exterior locations, twenty-one are located below-grade, and twenty-one are located above-grade. All CI measurements are shown in Table 12.

Using the CI data, the CEB is divided into regions. Regions are selected to contain CI values that are generally within the limits of an ASR Severity Zone. ASR Severity Zones are defined in SGH Report 160268-R-01 [6] as shown below:

- Zone I: CI from 0 to 0.5 mm/m
- Zone II: CI from 0.5 to 1.0 mm/m
- Zone III: CI from 1.0 to 2.0 mm/m
- Zone IV: CI from 2.0 to 3.5 mm/m



Consideration is given to significant aspects of the CEB structure when selecting the extents of each region; for example, the upper elevation of Regions R1, R2, and R3 is the approximate elevation of grade (El. +20 ft). The extents of the five regions (Region R1, R2, R3, R4, and R5) are shown in Figure 4.

The amount of nominal ASR expansion applied to the CEB wall in each direction (i.e., hoop and meridional) for each region is approximately equivalent to the mean of all CI measurements within the region for the corresponding direction. Nominal ASR expansion magnitudes for each region are shown in Table 13.

The mean CI for each region indicates that all regions belong to Severity Zone I, except for meridional expansion in Region R3, which falls into Severity Zone II. A small number of individual CI grids assigned to Severity Zone I regions exceed the upper limit of Severity Zone I (0.5 mm/m). However, these are judged to be acceptable because the probability distribution that is used to characterize Severity Zone I in Ref. 6 accounts for a small probability of exceeding the upper limit of the selected zone. Furthermore, reliability computations in Ref. 6 show that Severity Zone I results in the highest load factors for ASR. The load factors for ASR recommended by Ref. 6 are used in this calculation, and no reduction to the ASR load factors is taken for ASR loads exceeding the upper limit of Severity Zone I.

Since ASR expansion of the wall is largest below-grade, applying a small amount of ASR expansion in the above-grade portion of the wall lessens the transition in expansion that occurs around El. +22 ft and reduces the tension demands acting on the wall in that area. Therefore, for the above-grade portion of the wall, using a lower ASR leads to a more severe transition in expansion and is conservative for evaluation. For this reason, an ASR expansion magnitude of 0.01% (which is slightly smaller than the mean CI expansion of 0.016%) is used in the above-grade region (Region R4).

Although CI measurements recorded at the springline indicate strains of about 0.1% in the hoop direction and about 0.05% in the vertical direction, the Site Visit Report [9] notes that the orientation and pattern of cracks at the springline elevation are not necessarily indicative of ASR expansion. ASR cracking typically has a map pattern, which is generally less apparent at the springline elevation than other ASR monitoring locations. Additionally, the cracking at the



interior of the CEB at the springline does not show signs of moisture intrusion, efflorescence, or ASR gel. ASR expansion is not applied to the CEB wall from El. +114 ft and above in the Standard and Standard-Plus Analysis Cases. However, a study documented in Appendix J shows that applying ASR expansion at the springline elevation causes elevated (but still acceptable) demands local to the springline, but does not impact the demands elsewhere in the CEB.

Abrupt transitions in ASR expansion can cause concentrated stresses near the locations of the transition. These concentrated stresses are considered to be fictitious because their effects are not observed in the field. For this reason, a taper is used between each region to gradually transition between differing ASR magnitudes. The tapers are generally about 60 ft long, except for the below-grade to above-grade ASR taper, which is given a shorter length due to the short distance between groundwater and grade. The below-grade ASR magnitudes are applied up to EL. +2 ft (the upper estimate of normal groundwater depth [29]), and then are linearly tapered to the above-grade magnitudes which begin at El. +20 ft. The above-grade expansion magnitude tapers downward to zero from El. +50 ft to El. +114 ft (just below the springline elevation). Horizontal transitions between different ASR magnitudes are applied gradually over a distance of 40 deg (equivalent to about 55 ft).

The applied ASR expansion magnitudes and distribution are verified through comparison with field measurement data in two different ways, as described below.

- Strain in the finite element model caused by unfactored ASR expansion of the CEB wall is compared with field measurements of CI in Section 6.4.1. The comparisons show that the finite element simulation of ASR expansion generally matches the CI values measured in the field.
- Deformations of the finite element model caused by unfactored sustained loads plus unfactored self-straining loads are compared to field measurements of seismic gap widths in Section 6.4.2. This comparison shows that the finite element model simulation of the as-deformed condition generally provides a good match to field measurements.

A method of applying ASR expansion to the model is developed to capture the behavior observed by researchers in which the ASR in unrestrained or partially restrained reinforced concrete causes the reinforcement to be stressed in tension and concrete to be subjected to compression. This method of applying ASR expansion is summarized below.



- ASR expansion is simulated by applying a thermal expansion to the elements representing the CEB concrete. Steel reinforcement membrane elements are included in the model and are given thickness based on the total area of reinforcement provided. The expansion of the concrete creates tension in the steel membrane elements, which also causes a corresponding compression force in the concrete elements.
- In the absence of external restraint, the steel tensile force due to ASR and the concrete compressive force due to ASR will sum to zero. However, external boundary conditions, applied loading, and restraint from other portions of the structure can restrict the concrete from expansion and cause a net force or moment to be developed.
- The steel membrane elements are only included in the model when applying ASR expansion of the CEB wall and concrete swelling.

An alternative analysis (referred to as the Standard-Plus Analysis Case) is performed with additional external pressure close to AZ 230 that could be due to ASR expansion of the concrete fill wedge to better simulate deformation measurements on the CEB missile shield at AZ 230° El. +31.5 ft. Input parameters for the alternative analysis are documented in Section 6.2.3.

ASR Expansion of Concrete Fill

ASR expansion of the concrete fill causes a radial inward pressure on the CEB wall. Design drawings [12] indicate that the concrete fill is directly in contact with the exterior surface of the CEB wall at El. 0 ft and below. Field data showing ASR expansion of the concrete fill is not available; therefore, this calculation conservatively assumes that the concrete fill is expanding due to ASR (JA04 in Section 5.1).

The magnitude of the concrete fill expansion is unknown. Therefore, ASR expansion of the fill is modeled as an inward pressure acting on the wall with magnitude tuned such that the deformed shape of the CEB due to unfactored sustained and unfactored self-straining loads (including ASR expansion of the fill) generally matches field measurements [2, 3, 5]. Through comparison with field measurements, it is found that modeling ASR expansion of the fill with an inward pressure equivalent to 50% of the overburden pressure acting on the fill leads to a deformed shape that reasonably approximates field measurements.

Since ASR expansion tends to occur in the direction of least resistance [30], it can be reasoned that the concrete fill will initially expand in the radial inward direction (because expansion in the



vertical direction is resisted by the overburden pressure of the concrete fill). ASR expansion in the tangential direction will also occur, and is dependent on the stiffness and configuration of the structures surrounding the CEB (such as the Electrical Pen., Mech. Pen., FSB, etc.). Expansion occurring in the tangential direction does not directly impact the CEB and is therefore considered to be negligible. Once the compression in the concrete fill in the radial direction is equivalent to the overburden pressure acting on the fill, further expansion will generally occur in the vertical direction.

Demands caused by the pressure representing ASR expansion of concrete fill are factored by the load factor for ASR (which is as high as 2.0 in the static NO_1 combination defined in Table 5) and an additional threshold factor (as defined in Section 7.3). Therefore, the maximum concrete fill pressure considered in this evaluation is larger than the total overburden pressure at each depth.

Since the contractor was given the option to use either structural fill or backfill concrete to backfill between El. 0 and El. +20 ft, the overburden pressure is conservatively computed using the density of concrete (150 pcf). Therefore, the nominal pressure is equal to 1,500 psf at El. 0 ft and it increases linearly to 3,750 psf at El. -30 ft.

An alternative analysis, referred to as the "Standard-Plus Analysis Case," is performed with modified pressures representing ASR of concrete fill to better match deformation measurements recorded on the CEB missile shield at AZ 230° El. +31.5 ft. Input parameters for the alternative analysis are documented in Section 6.2.3.

Concrete Swelling

While concrete that cures in typical environments is caused to shrink due to loss of moisture, concrete that is subjected to long-term water exposure exhibits a net increase in volume and mass over time due to swelling. Based on an assessment of the groundwater exposure conditions, the Seabrook CEB can be reasonably expected to have undergone swelling [23]. Research referenced by this assessment indicates that unreinforced concrete (if in conditions similar to the CEB) can be expected to swell approximately 0.02% and reinforced concrete can be expected to swell by approximately 0.01%.



An assessment of groundwater conditions [29] indicates that normal groundwater is between El. -10 ft and +2 ft. Therefore, swelling of 0.01% is applied to the wall below El. -10 ft where the concrete is permanently exposed to groundwater. The swelling strains are tapered from 0.01% to 0% along the width of two elements (approximately 6 ft) from El. -7 ft to -13 ft to reduce large fictitious strains caused by an abrupt transition in applied expansion. Much like ASR expansion, concrete swelling generally causes tension in the reinforcement and compression in the concrete. As with ASR expansion, membrane elements representing reinforcement are coincident with the concrete elements during application of concrete swelling, and the swelling is simulated by applying a thermal load to the concrete elements.

6.3.2 Original SD-66 Loads

Original SD-66 loads are applied to the structure during Analysis Step Two, as defined in Section 6.2. These loads are listed in the UFSAR [7] and are defined with additional detail in SD-66 [8]. These loads are described in this section as follows:

Dead Load

Dead load includes the weight of all CEB and foundation concrete as well as the permanently installed formwork in the CEB dome. The total weight of the permanently installed formwork is 260 kips [24]. Hydrostatic pressure is considered as a dead load and is computed using a unit weight of 64.4 pcf [24]. The water table is taken at El. 20 ft. As explained in Justified Assumptions JA05 and JA06, the self-weight of ladders, walkways, and the Plant Vent Stack are excluded from this analysis.

Self-weight is modeled by applying a uniform acceleration equal to 1g to the model in the vertical downward direction. The density of the concrete dome elements is increased to include the permanently installed formwork. Hydrostatic pressure loads are modeled by applying surface pressures to the shell elements representing the CEB wall. The surface pressures are computed as $\gamma_w \times h$, where γ_w is the unit weight of water and h is the depth of the shell element centroid below the water table.

**Live Load**

Live load includes a normal snow load of 74 psf on the dome of the CEB [8]. No reduction is used for the sloping roof of the CEB [8].

Snow loads are modeled by adjusting the density of CEB dome elements based on their projected area on a horizontal plane.

Wind Load

Wind pressures acting on the CEB are computed using the ANSI A58.1-71 approach [8]. A basic wind velocity of 110 mph at 30 ft above ground is used to calculate the wind velocity pressures listed in Table 10. For the calculation of internal wind pressures, the structure is considered enclosed without any openings. External pressure coefficients for a cylinder and sphere are plotted in Figure 5. External wind pressures applied to the CEB (for the case where wind hits the CEB at AZ 90°) are illustrated at various elevations in Figure 6.

Wind loads are modeled by applying surface pressures to the shell elements representing the above-grade portions of the CEB wall and dome.

Tornado Wind Load

Tornado wind pressure acting on the CEB is computed using the ANSI A58.1-71 approach (Section 4.4.2.2.1 [8]). The average velocity pressure due to tornado winds is computed as 235 psf (based on a maximum velocity pressure of 332 psf and a size factor of 0.70). For the calculation of internal tornado wind pressures, the structure is considered enclosed without any openings. A pressure drop of 432 psf caused by the design tornado is considered (Section 4.4.2.3 [8]). Tornado missile loads acting on the CEB are not considered (Table 3.3-1 [8]).

Tornado wind loads are modeled by applying surface pressures to the shell elements representing the above-grade portions of the CEB wall and dome.

Static Soil Pressure

To be consistent with the original design-basis, buoyant soil unit weight, γ_1 , is taken as 62.5 psf and a coefficient of static (at rest) soil pressure, K_o , of 0.5 is used when computing lateral soil



pressure [8]. The CEB wall is considered a rigid wall [8]. In addition to the above load, a 300 psf compaction load and a 500 psf surcharge load are applied as design loads [8]. The surcharge load and compaction loads are not applied to the structure during Analysis Step One when computing the deformations of the as-deformed condition. During Analysis Step Two, the full static soil pressure (including surcharge and compaction loads) is used.

Static soil pressures are modeled by applying surface pressures to the shell elements representing the CEB wall at locations of soil backfill.

Unusual Snow Load

A credible but highly improbable unusual snow load of 126 psf is used (Section 4.2.2.1 [8]). No reductions in snow load are used for the sloping roof of the CEB.

Snow loads are modeled by adjusting the density of CEB dome elements based on their projected area on a horizontal plane.

Accidental Pressure

Accidental differential pressure load of (+)3 psig due to a postulated pipe break is considered (Section 4.8 [8]).

Accidental pressure is modeled by applying surface pressures to the shell elements representing the CEB wall and dome.

Seismic Loads

The original design-basis maximum acceleration profiles for SSE and OBE computed by UE are used in this calculation [24]. The maximum acceleration profiles are presented in Figures 7 and 8 for OBE and SSE, respectively. These maximum acceleration profiles were originally computed by UE using the spectra shown in Figures 9 and 10 and tabulated in Table 11. As specified in SD-66 [8], 7% and 4% of critical damping was used for SSE and OBE analyses, respectively. Response spectra analysis was performed using a simplified "stick" model. For lateral analyses, the model was fully fixed below El. 0 ft. For vertical analyses, the model was fixed at the base at El. (-)30 ft.



The as-deformed condition of the CEB is analyzed to verify that the observed deformations do not significantly impact the seismic response of the structure. See Sections 6.2.4 and 6.4.3 for more information.

The final acceleration profile in each direction (east-west, north-south, and vertical) is computed by combining the in-line acceleration profile with cross-term accelerations using the square root of the sum of squares (SRSS) approach. For example, the north-south (N-S) maximum acceleration profile is computed by combining the N-S accelerations due to N-S excitation with the N-S accelerations due to east-west (E-W) excitation using SRSS. N-S and E-W accelerations due to vertical motion are not provided by UE and therefore are not included in this calculation.

Seismic loads are applied independently for each direction (E-W, N-S, and vertical) using a static equivalent approach. A force is applied to all nodes of the CEB equivalent to the acceleration at the given elevation multiplied by the node's tributary mass. The seismic mass of the CEB dome is increased by an amount equivalent to 25% of the design snow load (74 psf) acting on the total area of the dome projected onto a horizontal plane. Linear interpolation is used to obtain the maximum acceleration at elevations not provided in the UE acceleration profiles. Demands from the east-west, north-south, and vertical cases are combined using the 100-40-40 rule as shown in Table 6.

Dynamic Soil Loads

Dynamic soil loads are computed in accordance with Section 8.2.2.2 of SD-66 [8]. The CEB wall is considered a rigid wall. To be consistent with the original design calculations, the water table is considered to be at El. 20 ft. The saturated soil unit weight, γ_s , is taken as 125 pcf. The coefficient of dynamic earth pressure, K_D , is taken as 0.28 for SSE and 0.15 for operating basis earthquake (OBE) [8].

Dynamic soil loads are modeled by applying surface pressures to the shell elements representing the CEB wall at locations of soil backfill.



6.4 Analysis Results

Strains and deformations computed for the as-deformed condition are compared with field measurements in Sections 6.4.1 and 6.4.2. Results of the study on the impact of the as-deformed condition on seismic acceleration profiles are presented in Section 6.4.3. Computed demands (i.e., forces and moments) are summarized in Section 6.4.4, and are presented more thoroughly in the attached 150252-CA-02-CD-01 (which is summarized in Appendix C).

6.4.1 Comparison of ASR Strains and Crack Index Measurements

In this section, strains computed from the ASR load case (for the standard analysis without a load factor) are compared with CI measurements recorded in April 2016 [9]. Computed strains due to concrete swelling and shrinkage are not included in this comparison for the following reasons:

- **Concrete Swelling:** Swelling causes concrete to expand directly, whereas ASR causes an expansive gel to crack the concrete. Therefore, swelling strains would not be captured by a crack index measurement and are not used while comparing the simulation of the as-deformed condition to measured CI values.
- **Shrinkage:** Shrinkage and ASR both cause concrete cracking, but through different mechanisms. Shrinkage cracks are early age cracks that are caused by the outer layer of concrete shrinking more quickly than the inner-core concrete. Since ASR strain and shrinkage strain have opposite signs, including both strains would seemingly reduce the total strain; however, cracks from shrinkage and ASR would both increase a measured CI value. To address this, this calculation generally assumes that cracks measured by CI are not shrinkage related. This is a conservative assumption because it ultimately increases the ASR expansion magnitude.

Results of comparisons between ASR Strains and Crack Index Measurements are provided below:

- **Below Grade:** Comparisons of CI recorded at below-grade ASR monitoring locations to ASR strains computed by FEA are shown in Figures 11 and 12 for horizontal (hoop) and meridional directions, respectively. These figures show that the FEA strains provide a reasonable representation of CI data, and the FEA simulations provide a good match of the mean of CI data.
- **Between Grade and Springline:** CI measurements indicate that above-grade ASR strains are smaller than those below grade. The transition from high to low ASR expansion causes an axial tension in the hoop direction at the location of transition. The axial tension is made worse if the transition between below-grade and above-grade ASR magnitudes is made larger. Therefore, it is reasoned that targeting an



above-grade ASR expansion magnitude slightly smaller than measured CI values is conservative in the areas of highest concern. Comparisons of CI strains to ASR strains computed by FEA are shown in Figures 13 and 14 for hoop and meridional directions between El. +25 ft and +50 ft. The FEA strains are, on average, slightly smaller than recorded CI values at these elevations.

- **Springline:** Ref. 9 notes that the orientation and pattern of cracks at the springline elevation are not necessarily indicative of ASR expansion. ASR cracking typically has a map pattern, which is generally less apparent at the springline elevation than other ASR monitoring locations. Additionally, the cracking on the interior of the CEB at the springline does not show signs of moisture intrusion, efflorescence, or ASR gel. ASR expansion is not applied to the CEB wall from El. +114 ft and above in the FEA analyses; therefore, no comparison is made at these elevations in this section. A study documented in Appendix J evaluates the impact of modeling ASR demands at the springline.
- **Above Springline:** CI measurements are not available above the springline elevation, since the original formwork is left in place and the concrete surface is not exposed from the inside.

6.4.2 Comparison of Simulated Deformations and Field Measurements

Field deformation measurements, recorded and interpreted as described in Section 4.4, are compared to deformations simulated by the finite element model in this section. Finite element deformations are computed as listed in the first row of Table 4. The ASR threshold factor k_{th} (defined in Section 7.3) is not used when comparing the finite element simulation to recent field measurements.

Section cuts comparing the simulated deformations with field measurements are provided at several different elevations, as listed below. Deformations in these section cuts are magnified to improve visibility. The deformations associated with different analysis cases (e.g., Standard and Standard-Plus) are shown in different colors in the following figures.

- Figure 15: Elevation approx. +6 ft
- Figure 16: Elevation approx. +22 ft
- Figure 17: Elevation approx. +50 ft
- Figure 18: Elevation approx. +119 ft

These figures show that the deformed shape for all analysis cases generally simulates the deformed shape indicated by field measurements. Field measurements tend to have a large



variability due to irregularities in concrete surfaces, such as formwork imperfections and construction tolerances; additionally, seismic isolation joints are covered in seal material, limiting measurement accuracy. For these reasons, measurements are estimated to have an accuracy of $\pm 1/2$ in. [2] and the extent that finite element analysis can simulate field measurements is limited. These figures show that the Standard analysis case generally approximates the magnitude of radial deformations throughout the CEB with the exception of the area around AZ 230°. The Standard-Plus analysis case simulates additional deformation around AZ 230° by applying additional radial pressures in that area, which could be due to ASR of the concrete fill adjacent to the CEVA structure (see Section 6.2.3 for a description of the Standard-Plus analysis case). This additional pressure also impacts the deformations between AZ 270° and 360°.

Sustained loads and self-straining loads are unfactored when comparing FEA simulations to field measurements of deflections. It should be noted that the CEB structure is evaluated under the factored conditions presented in Table 5, and the deformations associated with these factored load combinations greatly exceed those presented in this section.

6.4.3 Results of Study on Impact of As-Deformed Condition on Maximum Acceleration Profiles

A study is performed by analyzing the change of the CEB center of mass, shear center, and stick model equivalent moment of inertia at a selection of elevations due to the as-deformed condition of each analysis case. The study shows that the center of gravity and shear center of the CEB moved less than 1 in. due to the as-deformed condition at all elevations analyzed, which is considered very small for a structure with an inside radius of 79 ft. The moment of inertia of the CEB changed by less than 0.5% at all elevations analyzed.

The information above demonstrates that the effects of the as-deformed condition on the CEB structural dynamic properties are negligible. Therefore, the OBE and SSE maximum acceleration profiles are not impacted by the as-deformed condition obtained in Analysis Step One (defined in Section 6.2).

Additional documentation for this study is provided in Appendix F.



6.4.4 Summary of Computed Demands

Forces and moments computed for the static and representative seismic OBE cases are presented in this section. The primary purpose of this section is to describe the mechanisms leading to demands in the CEB structure. In this section, demands are shown for static load combination NO_1 (as defined in Table 5) and seismic combination OBE_1 with 100% acceleration in the east direction, 40% acceleration in the north direction, and 40% acceleration in the vertical-up direction. Similar figures for other load combinations are provided in the attached 150252-CA-02-CD-01 (see Appendix C for description of CD contents).

All element demands presented in this calculation are computed by combining demands of the concrete element, with the coincident hoop and meridional reinforcement membrane elements. The coincident reinforcement membrane elements are active in the model only when analyzing the ASR of wall and swelling load cases. The ASR portion of the demands in each combination is multiplied by the threshold factor of 1.2 in addition to the corresponding load factor for ASR, as described in Section 7.3.

Demands are shown in this section using contour plots, which highlight regions of the structure with different colors based on the magnitude of demands. Colors used for each contour do not have any inherent meaning (i.e., red and orange colors for these plots do not necessarily indicate regions of overstress). Axial and shear demands are presented with units of lbf per inch of element width. The sign convention for axial demands is that tension is positive and compression is negative. Bending moments are presented with units of lbf-in. per inch of element width. The sign convention for bending moments is that positive moment causes tension on the outside face of the wall.

Axial forces acting in the hoop direction are plotted for the NO_1 and the representative OBE_1 load combinations for the Standard analysis case in Figures 19 and 20. The region of axial compression between El. -30 ft and 0 ft are caused primarily by the applied ASR and swelling expansion being constrained by internal stiffnesses of the CEB structure. The regions of hoop tension between El. 0 ft and +30 ft are caused by the transition from below-grade to above-grade magnitudes of applied ASR expansion. The regions of axial tension at the base of the wall are caused by the mechanism resisting out-of-plane loads acting on the base of the wall, which is described with more detail in Section 7.6.1. Axial forces acting in the hoop direction for



the NO_1 load combination for the Standard-Plus Analysis Case are plotted in Figure 21. The additional concrete fill pressures modeled in the Standard-Plus Analysis Case primarily cause additional hoop tension demands at the base of the wall between AZ 180° and 270° and additional hoop compression demands about 10 to 20 ft above the base of the wall within the same range of azimuths.

Axial forces acting in the meridional direction are plotted for the NO_1 and the representative OBE_1 load combinations for the Standard analysis case in Figures 22 and 23. The pilasters on either side of the Electrical and Mechanical Penetrations attract meridional demands because of their high stiffness relative to the CEB wall. The pilaster on the east side of the Electrical Penetration has more tensile demand than that on the west side due to the dissimilar vertical ASR expansion magnitudes acting on the wall on either side of the penetration (0.06% on the west side, 0.015% on the east side). Seismic overturning also contributes to the axial demands acting on the wall and pilasters; in the OBE_1 combination plotted in Figure 23, the resultant of lateral accelerations is in the northeast direction, causing additional tension in the pilaster on the south side of the Mech. Pen. Dead loads cause meridional compression in the wall; however, these compressive demands are small relative to those from ASR and seismic overturning. Axial forces acting in the meridional direction for the NO_1 load combination for the Standard-Plus Analysis Case are plotted in Figure 24. The additional concrete fill pressures modeled in the Standard-Plus Analysis Case cause additional meridional tension at the base of the wall near AZ 225° and additional meridional compression at the base of the wall near AZ 180° and AZ 240°.

In-plane shear forces are plotted for the NO_1 and the representative OBE_1 load combinations for the Standard analysis case in Figures 25 and 26. Regions of elevated in-plane shear demand are located adjacent to each of the penetrations at the base of the CEB. In-plane shear demands in these regions are caused by ASR expansion of the concrete fill. Elevated in-plane shear demands are also computed near the reentrant corners of openings where additional diagonal reinforcement is provided. The seismic accelerations lead to additional in-plane shear demands at the base of the CEB. In-plane shear forces for the NO_1 load combination for the Standard-Plus Analysis Case are plotted in Figure 27. The additional concrete fill pressures modeled in the Standard-Plus Analysis Case further increase the elevated in-plane shear demands near the opening on the south side of the Mech. Pen.



Out-of-plane shear forces are plotted for the NO_1 and the representative OBE_1 load combinations for the Standard analysis case in Figures 28, 29, 31, and 32. Out-of-plane shear forces can act along the hoop-radial or the meridional-radial planes, and corresponding demands are plotted separately. The most significant of the out-of-plane shear demands are those acting on the hoop-radial plane near the base of the CEB. Other out-of-plane shear demands are generally localized near openings and changes in geometry. Out-of-plane shear forces for the NO_1 load combination for the Standard-Plus Analysis Case are plotted in Figures 30 and 33. The additional concrete fill pressures modeled in the Standard-Plus Analysis Case further increase the elevated out-of-plane shear demands at the base of the wall between AZ 180° and 270°.

Bending moments about the meridional axis are plotted for the NO_1 and the representative OBE_1 load combinations for the Standard analysis case in Figures 34 and 35. Positive bending moments occur above the Electrical and Mechanical Penetrations, where sustained loads and self-straining forces cause outward deformation. Negative bending moments occur on either side of the West Pipe Chase (e.g., near the Personnel Hatch and the CEVA opening), where inward deformation occurs. Bending moments about the meridional axis for the NO_1 load combination for the Standard-Plus Analysis Case are plotted in Figure 36. The additional concrete fill pressures modeled in the Standard-Plus Analysis Case increase the elevated bending moments further, particularly positive bending moments above the West Pipe Chase.

Bending moments about the hoop axis are plotted for the NO_1 and the representative OBE_1 load combinations for the Standard analysis case in Figures 37 and 38. Elevated bending moments are computed at the base of the CEB where the wall connects to the foundation; these demands are caused primarily by the pressures representing ASR expansion of the concrete fill. The pilasters adjacent to the Electrical Penetration and Mechanical Penetration generally attract more bending moments than the wall due to their higher stiffness. The pilasters have positive bending moment demand at the base, and negative bending moment demand at approximately El. 0 ft where the concrete fill pressures subside. Bending moments about the hoop axis for the NO_1 load combination for the Standard-Plus Analysis Case are plotted in Figure 39. The additional concrete fill pressures modeled in the Standard-Plus Analysis Case lead to additional bending moments at the base of the CEB wall between AZ 180° and AZ 270°.



7. STRUCTURAL EVALUATION

Structural capacities are evaluated for all analysis cases listed in Section 6.2.2 and for load combinations in Table 5 using the element-by-element approach described in Section 7.1 as well as the section cut approach described in Section 7.2. Evaluation criteria for strength of reinforced concrete components are taken from ACI 318-71 [11]. The threshold factor, which amplifies ASR demands to account for future ASR expansion, is described and quantified in Section 7.3. Results of the evaluation are given in Section 7.5. Special cases are evaluated using “Alternative Evaluation” procedures, which are documented in Section 7.6. Maximum displacements of the CEB are evaluated against clearances with adjacent structures in Section 7.7. Global stability of the CEB is evaluated in Section 7.8.

7.1 Element-by-Element Evaluation Methodology

The computation of capacities for the element-by-element evaluation is outlined in this section. Evaluating a structure on an element-by-element basis is considered a conservative approach because it does not allow for concentrations of high demands to be distributed locally within the structure. Factored demand exceeding capacity in the element-by-element evaluation does not necessarily indicate a structural deficiency. Since a relatively small finite element size is used in the analyses, stress concentrations can cause localized capacity exceedances in the element-by-element evaluation which may not have any real structural impact. If an element's capacity is exceeded in the element-by-element evaluation, the area is evaluated again using a section cut approach. If the element-by-element capacity exceedance is identified as insignificant (i.e., a stress concentration that will not impact structural performance), then further analysis/evaluation is not performed.

7.1.1 Axial Compression

Axial compression is evaluated using the criteria in Chapter 10 of ACI 318-71 [11]. The equation used to compute axial compressive strength is shown in Equation 1. While computing axial compression capacity, the strain in the reinforcement at the point of concrete crushing is computed by taking into account the strains caused by self-straining loads. This computation is consistent with ACI 318-71 Section 10.2.4 [11].



ACI 318-71 Section 10.3.6 specifies that the reinforced concrete member must be designed for a minimum eccentricity of 0.1h. Modern versions of ACI 318 have replaced this requirement with a constant reduction factor of 0.8 applied to computed axial compression capacities. The ACI code commentary explains that the 0.8 factor is intended to be approximately equal to the ACI 318-71 approach. For simplicity of implementation, the constant reduction factor approach is used in this calculation. The use of this factor has been verified for four section configurations of varying thicknesses and reinforcement, which show that the constant 0.8 factor is either equivalent to or more conservative than the 0.1h minimum eccentricity.

$$\phi P_n = \phi \times 0.8 [0.85f'_c(A_c - A_s) + \min(-\varepsilon_{sc}E_s, f_y)A_s] \quad \text{Equation 1}$$

$$\varepsilon_{sc} = \varepsilon_{SQ} + \varepsilon_{cc} - \varepsilon_{CQ}$$

Where:

ϕ	=	Strength reduction factor for compression, 0.70
P_n	=	Nominal axial compressive strength
f'_c	=	Design concrete compressive strength
A_c	=	Area of concrete
ε_{sc}	=	Compressive strain in the steel when concrete reaches compressive strain of ε_{cc} . Following typical unit convention for this analysis, ε_{sc} is negative to represent compression.
E_s	=	Elastic modulus of steel
f_y	=	Yield strength of steel
A_s	=	Total area of steel oriented in direction of evaluation
ε_{SQ}	=	Strain in steel due to as-deformed condition. Typically this strain is positive (tensile) because ASR and swelling cause the steel to lengthen.
ε_{cc}	=	Strain at which concrete crushes, -0.003
ε_{CQ}	=	Strain in concrete due to as-deformed condition. Typically this strain is negative (compressive) because ASR and swelling cause the compression in restrained concrete.

7.1.2 Axial-Flexure Interaction

Axial-flexure interaction is evaluated using the criteria in Chapter 10 of ACI 318-71 [11]. Axial-flexure interaction capacities are calculated using the computer program spColumn [25]. spColumn has been verified and validated in accordance with the SQH QANF program [10, 26].



Additional information on the computation of axial-flexure interaction capacities can be found in Appendix E.

Flexural demands for the axial-flexure interaction evaluation are computed using Equation 2.

$$M_{hoop,1} = M11 + |M12| \quad \text{Equation 2}$$

$$M_{hoop,2} = M11 - |M12|$$

$$M_{meridional,1} = M22 + |M12|$$

$$M_{meridional,2} = M22 - |M12|$$

Where:

$M_{hoop,1}$ and $M_{hoop,2}$	are bending moments that are combined with hoop-direction axial demands during axial-flexure interaction checks
$M_{meridional,1}$ and $M_{meridional,2}$	are bending moments that are combined with meridional-direction axial demands during axial-flexure interaction checks
$M11$ and $M22$	are the element bending moments acting about the meridional and hoop axes, respectively
$M12$	is the element torsional bending moment

Axial-flexure interaction checks do not include a reduction of the compressive strength due to accidental eccentricity because compressive strength is evaluated independently (Section 7.1.1).

Note that in the present calculation, the torsional moments are explicitly considered in evaluation of flexural reinforcement following the methodology outlined by Wood and Armer [27]. This approach differs from that used in the UE calculations, where UE determined that the level of torsion was small enough to not warrant explicit consideration as allowed by ACI 318-71. The $M12$ contribution to total flexural demands is often most pronounced at discontinuities such as reentrant corners, which could lead to larger flexural demands at corners and openings in this calculation compared to those computed by UE.



7.1.3 Axial Tension

Axial tension is evaluated as part of the axial-flexure interaction checks. The axial tensile strength is proportional to the amount of reinforcement developed in the section. Although ASR expansion causes the reinforcement to develop tensile stress, no reduction to axial tensile strength due to ASR is considered because the corresponding ASR-induced compressive stress in the concrete must be unloaded by an applied tension before the entire cross section loses its tensile stiffness [15].

7.1.4 In-Plane Shear

In-plane shear is evaluated using the criteria in Sections 11.4 and 11.16 of ACI 318-71 [11]. The formulation used to compute in-plane shear capacity for the element-by-element evaluation is presented as Equation 3.

$$v_{c,a} = 2 \left(1 + 0.0005 \frac{N_u}{A_g} \right) \sqrt{f'_c} \quad \text{Equation 3}$$

$$v_{c,b} = 3.5 \sqrt{f'_c} \sqrt{1 + 0.002 \frac{N_u}{A_g}}$$

$$v_{c,c} = \max \left[2 \left(1 + 0.002 \frac{N_u}{A_g} \right) \sqrt{f'_c}, 0.0 \right]$$

$$v_c = v_{c,c} \text{ if } N_u \text{ is tensile, otherwise } v_c = \min(v_{c,a}, v_{c,b})$$

$$v_s = \frac{A_v f_y}{b_w s}$$

$$\phi v_n = \phi \times \min(v_c + v_s, 10 \sqrt{f'_c})$$

Where:

$v_{c,a}$	=	Nominal concrete shear strength for section in compression
$v_{c,b}$	=	Nominal concrete shear strength upper limit for section in compression
$v_{c,c}$	=	Nominal concrete shear strength for section in tension
v_s	=	Nominal shear strength of steel reinforcement
ϕ	=	Strength reduction factor for shear, 0.85
v_n	=	Nominal shear strength of reinforced concrete section



N_u	=	Axial force (lbf) normal to the cross section occurring simultaneously with the design shear force, taken as positive for compression and negative for tension*
A_g	=	Gross area of the section
A_v	=	Area of shear reinforcement
b_w	=	Width of wall strip under consideration
s	=	Spacing of shear reinforcement

**Note: This sign convention differs from the convention used throughout this analysis. Reinforcement oriented in the hoop direction is used when evaluating the in-plane shear reinforcement, as stipulated by ACI 318-71 Section 11.16.4.1. Since axial compression increases in-plane shear capacity, axial loads caused by self-straining loads (such as ASR and swelling) are excluded if they are compressive.*

In the element-by-element evaluation, in-plane shear demand is computed as shown below.

$$Vu_A = |Vu_{cd}| \quad \text{Equation 4}$$

$$Vu_B = |Vu_{cd} + Vu_{c,swell}|$$

$$Vu_C = |Vu_{cd} + Vu_{c,ASR}|$$

$$Vu_D = |Vu_{cd} + Vu_{c,swell} + Vu_{c,ASR}|$$

$$Vu = \max(Vu_A, Vu_B, Vu_C, Vu_D)$$

Where:

Vu_{cd} = Factored in-plane shear demand due to design loads (excluding self-straining loads)

$Vu_{c,swell}$ = Factored in-plane shear demand due to concrete swelling

$Vu_{c,ASR}$ = Factored in-plane shear demand due to ASR loads (includes threshold factor)

Vu = Factored shear demand

7.1.5 Out-of-Plane Shear

Out-of-plane shear is evaluated using two separate approaches. In the first approach, the criteria of ACI 318-71 Section 11.4 are used, in which the design shear capacity ϕv_n is calculated as shown in Equation 3 and v_s is computed using the amount of transverse reinforcement provided (v_s is taken as zero in areas without stirrups). Alternatively, the shear



capacity is also calculated using a shear friction approach, which is based on ACI 318-71 Section 11.15. The exceedance of criteria of the first approach does not imply a non-conformance as the section may still have sufficient shear friction capacity. In the shear friction approach, the amount of reinforcement available to resist out-of-plane shear is computed by subtracting the reinforcement area utilized by tensile demands and in-plane shear demands (Equation 5 and Equation 6) from the total amount of reinforcement provided. The amount of reinforcement required to resist out-of-plane demands (Equation 7) is compared to the remaining reinforcement available to obtain a demand-to-capacity ratio for the shear-friction approach. A friction coefficient of 1.0 is used (as opposed to 1.4 for monolithic concrete) in shear-friction calculations to account for the construction joints within the CEB wall.

The smaller demand-to-capacity ratio of the ACI 318 71 Section 11.4 and 11.15 approaches is taken as the DCR for out-of-plane shear.

$$RA_{st} = \frac{P_u}{\phi_t f_y} \quad \text{Equation 5}$$

$$RA_{svip} = \frac{(V_{uip} - V_c) \times (1/2)}{f_y} \quad \text{Equation 6}$$

$$RA_{svoop} = \frac{V_{uoop}}{\phi_v \mu f_y} \quad \text{Equation 7}$$

$$DCR_{voop} = \frac{RA_{svoop}}{A_s - RA_{st} - RA_{svip}} \quad \text{Equation 8}$$

Where:

RA_{st}	=	Area of steel reinforcement required to resist tensile demand
P_u	=	Axial tensile demand
ϕ_t	=	Strength reduction factor for tension, 0.9
f_y	=	Yield strength of reinforcement
RA_{svip}	=	Area of steel reinforcement required to resist in-plane shear demand
V_{uip}	=	In-plane shear demand
V_c	=	In-plane shear capacity of concrete
RA_{svoop}	=	Area of steel reinforcement required to resist out-of-plane shear demand
V_{uoop}	=	Out-of-plane shear demand
ϕ_v	=	Strength reduction factor for shear, 0.85



μ	=	Friction coefficient for concrete placed against hardened concrete, 1.0
f_y	=	Yield strength of reinforcement
A_s	=	Area of steel provided

7.2 Section Cut Methodology

Structural evaluation on an element-by-element basis is a conservative approach because the behavior of reinforced concrete is generally represented by the section response due to its capability for local inelastic redistribution of demands. Generally most physical tests supporting the strength criteria of ACI are based on section behavior, not localized behavior represented by element-by-element evaluation. Therefore, in regions where a conservative element-by-element evaluation shows exceedance, section cuts are used to evaluate compliance with the requirements of ACI 318-71 [11]. A section cut approach is applied to investigate whether, after load redistributions within the CEB wall, the capacity is sufficient for a given failure mode. Particular section cuts are only evaluated for limit states deemed significant based on exceedances identified in the element-by-element evaluation.

Section cuts are defined in the model along a series of nodes comprising a cross-section of the CEB wall in a region of interest. A post-processing script identifies all wall elements acting along one side of this set of nodes, forms a local coordinate system with orientation specific to that cut, and calculates the sum of forces and moments acting at the centroid of the cut cross section. For ASR-affected regions where reinforcing bars are modeled with equivalent shell elements, reinforcement elements are also considered in the calculation of total section forces acting on the cut. For a given cut, this approach calculates a resultant axial force, in-plane shear force, out-of-plane shear force, in-plane (overturning) moment, out-of-plane moment, and torsion. The resultant moments are comprised of both the sum of element nodal moments acting at each node along the section cut and the moment effects arising from element nodal forces acting at each node along the section cut with associated internal moment arms back to the cut centroid. An illustration of a section cut, selected elements which contribute demand to the cut, formation of the cut coordinate system, and orientation of section cut resultant forces and moments is shown in Figure 61.

The average section geometry over the length of the cut is used for the evaluation. The thickness is taken as the average thickness of all concrete wall elements along the cut. The



length of the cut is taken as the chord length for limit states involving overturning and in-plane shear. It is slightly conservative to use the chord length for in-plane shear evaluations, rather than the arc length. The average hoop and meridional steel reinforcement area is calculated along the section cut using the same reinforcing bar definitions used in the element-by-element evaluation. In-plane shear effects are evaluated using the total reinforcement parallel to the cut that is effective for the section. Axial-flexure interaction checks are performed based on the average reinforcement per foot length of the section. Evaluation of horizontal shear is performed on cuts up to a length of a quarter of the building perimeter. For other limit states the length is limited to eight times the wall thickness. This limit is based on engineering judgment and is analogous to approaches used for calculating effective influence areas for shear in other design contexts. Since the element size is approximately 36 in. square, for 36 in. thick regions the section cut may be eight elements wide, for 27 in. thick regions six elements wide, and for 15 in. thick regions three to four elements wide.

Section cut capacities are calculated as discussed in the following subsections.

7.2.1 In-Plane Shear

In-plane shear is evaluated using the criteria in Section 11.16 of ACI 318-71 [11]. The formulation used to compute in-plane shear capacity for the section cut evaluation includes ACI 318-71 Equations 11-31 through 11-33 and is presented in this calculation as Equation 9. Reinforcement oriented in the hoop direction is used when evaluating the in-plane shear reinforcement, as stipulated by ACI 318-71 Section 11.16.4.1.



Equation 9

$$v_{c,a} = 3.3\sqrt{f'_c} + \frac{N_u}{4l_w h}$$

$$v_{c,b} = 0.6\sqrt{f'_c} + \frac{l_w \left(1.25\sqrt{f'_c} + 0.2 \frac{N_u}{l_w h} \right)}{\frac{M_u}{V_u} - \frac{l_w}{2}}$$

$$v_{c,c} = 2\sqrt{f'_c}$$

$$v_c = \min(v_{c,a}, v_{c,b})$$

In compression, v_c may be taken as $2\sqrt{f'_c}$

$$v_s = \frac{A_v f_y}{b_w s}$$

$$\phi v_n = \phi \times \min(v_c + v_s, 10\sqrt{f'_c})$$

Where:

$v_{c,a}$	=	Concrete shear strength upper limit 1
$v_{c,b}$	=	Concrete shear strength upper limit 2
$v_{c,c}$	=	Concrete shear strength for section in compression
v_c	=	Nominal concrete shear strength
v_s	=	Nominal shear strength of steel reinforcement
ϕ	=	Strength reduction factor for shear, 0.85
v_n	=	Nominal shear strength of reinforced concrete section
N_u	=	Design axial force (lbf) normal to the cross section occurring simultaneously with the design shear force, taken as positive for compression and negative for tension
V_u	=	Design shear force (lbf) parallel to the cross section axis
M_u	=	Design in-plane (overturning) moment (lbf-in) occurring simultaneously with the design shear force
l_w	=	Length of wall
h	=	Thickness of wall
A_v	=	Area of shear reinforcement
b_w	=	Width of wall strip under consideration
s	=	Spacing of shear reinforcement



7.2.2 Shear Friction

Section cuts at the base of the structure are evaluated for shear demands following shear-friction provisions in Section 11.15 of ACI 318-71 [11]. The shear capacity ϕv_n is calculated using the equations in ACI 318-71 Section 11.15.3 and 11.15.3 and is presented in this calculation as Equation 7, which is also used for the element-by-element evaluation.

This evaluation at the base of the wall considers a reduction in the available length for shear friction to account for in-plane overturning moment. At each end of the wall, 15% of the wall length is allocated for tension and compression zones to resist overturning. Therefore, only 70% of the wall length is assumed available to resist shear by shear-friction; this assumption is confirmed by hand calculation for the most critical case for shear-friction. The vertical area of steel reinforcement required to resist net tension on the section is calculated, and the vertical reinforcing steel in the remaining length of the section is reduced by this amount to calculate the total area of vertical steel available to resist shear. For all cases, the coefficient of friction is taken as 1.0, which corresponds to the case of concrete placed against hardened concrete. The section is evaluated for the SRSS of the in-plane and out-of-plane resultant shear forces.

7.2.3 Axial-Flexure Interaction

Axial-flexure (PM) interaction for section cuts is evaluated using the criteria in ACI 318-71 [11]. Axial-flexure interaction capacities are calculated using the computer program spColumn [25], which has been validated and verified in accordance with the SGH QANF program [10, 26]. PM capacities for section cuts are computed using concrete cover over reinforcement bars that is between 1 to 2 inches larger than actual design values. This is done to conservatively account for possible variations in reinforcement configuration within the section. The total axial force and out-of-plane moment are calculated and used to compute the average axial force and moment demand acting on a per-foot basis along the wall section using the average vertical reinforcement available over the length of the section cut.

7.2.4 Torsion

The effect of torsion is discussed in ACI 318-71 Section 11.7 (Combined Torsion and Shear for Nonprestressed Members) [11]. These provisions suggest that resultant torsional effects acting on a cross-section may be decomposed as acting on a series of component rectangles, each



subjected to a shear stress with magnitude calculated from the total torsion. This section of the code focuses on rectangular and / or flanged cross sections and is not appropriate for cross sections that are restrained due to participation in a monolithic shell structure such as the CEB. Therefore, no further evaluation is provided using section cuts for torsion on the basis of engineering judgment. Torsional demands are considered when evaluating flexural demands in the element-by-element evaluation as discussed in Section 7.1.2.

7.3 Definition and Selection of ASR Threshold Factor

In the analysis and evaluation of the CEB, ASR loads are amplified by a threshold factor (referred to as k_{th}) in addition to a load factor. While the load factor accounts for uncertainty in the ASR load, the threshold factor accounts for additional ASR load that may occur in the future. The threshold factor is selected to be the largest factor in which the structure meets evaluation criteria using the approaches described in this calculation. Selection of the threshold factor for the CEB is primarily governed by axial-flexure interaction and tensile demands acting on the CEB wall. A threshold factor of 1.2 is selected for evaluation of the CEB, which indicates that ASR-related demands are amplified by 20% beyond the factored values.

7.4 Results of Evaluation without Self-Straining Loads

Each load combination in Table 5 is evaluated without the effects of self-straining forces (i.e., without ASR and swelling demands) to verify, with the modeling and analysis procedures used in this calculation, that the original design of the CEB meets design requirements. This evaluation is defined as the Original Design Analysis Case in Section 6.2.2 and Table 7. The evaluation indicates that the CEB meets ACI 318-71 evaluation criteria for the Original Design Analysis Case. Additional information on this analysis case is provided in Appendix G.

7.5 Evaluation Results

In this section, evaluation results are presented for each resistance mechanism (i.e., axial compression, in-plane shear, out-of-plane shear, etc.). Evaluations are first performed using the element-by-element approach described in Section 7.1. The element-by-element evaluations are conservative and are used to identify regions of the structure that require further evaluation. Based on the element-by-element evaluation results, section cut evaluations are performed. The section cut evaluations are more representative of structural behavior than the element-by-



element evaluations because they can account for local redistribution of loads that is known to occur within reinforced concrete structures. Evaluations are performed for all Section Cuts defined in Appendix N for all load combinations and analysis cases. Additional section cut checks (beyond those shown in Appendix N) are used in this section to supplement the element-by-element evaluation as needed. Additional evaluations are performed if a section cut evaluation is unable to qualify a localized region of the structure.

The evaluation of the CEB in the as-deformed condition is governed by static and OBE load combinations. Static load combinations often govern the evaluation due to the relatively large load factor for ASR demands (S_a) in the static combinations. The large ASR load factors are related to the high reliability against structural deficiency that is targeted by the static combinations [6]. OBE load combinations govern a portion of the evaluation because these combinations include the largest non-self-straining lateral forces affecting the CEB. This finding is consistent with the original design calculation for the CEB, which states that OBE combinations control design [24]. Wind, tornado, and SSE load combinations generally have lower lateral loads and/or use lower ASR load factors than the static and OBE load combinations, and therefore generally do not govern the evaluation.

For each evaluation check, contour plots of element-by-element evaluation results are shown for static load combination NO_1 (as defined in Table 5) and a representative seismic combination OBE_1 with 100% acceleration in the east direction, 40% acceleration in the north direction, and 40% acceleration in the vertical-up direction. Demands for these two load combinations were provided in Section 6.4.4. Although the static load combination NO_1 often controls the design, evaluation results for these two particular load combinations are shown in this section to provide an understanding of behavior as well as the regions of high demands. Similar figures with DCRs for other load combinations are provided in the attached 150252-CA-02-CD-01. The naming convention of load combination results is described in Table 9, and additional description of CD contents are provided in Appendix C. The evaluation is performed for all load combinations, and the most critical combinations are discussed in the following sections.



Element-by-element evaluation DCRs are illustrated using contour plots with fixed contour limits. Note that DCRs exceeding the upper limit of the contour intervals (1.5) are colored light gray.

7.5.1 Axial Compression in the Hoop Direction

Contour plots of DCRs for axial compression in the hoop direction from the element-by-element evaluation for load combination NO_1 and the representative OBE_1 load combination for the Standard Analysis Case are plotted in Figures 40 and 41. In the standard analysis case, the portion of the wall between El. -20 ft and El. 0 ft is in compression, but the DCRs in this area are generally below 0.7. Contour plots of DCRs for axial compression in the hoop direction for load combination NO_1 for the Standard-Plus Analysis Cases are plotted in Figure 42. This analysis case shows an increase to the size of the region of compression demand below the CEVA opening (near AZ 230°); however, the DCRs remain below 0.7.

This evaluation shows that axial compression in the hoop direction meets evaluation criteria for all analysis cases and all load combinations.

7.5.2 Axial Compression in the Meridional Direction

Contour plots of DCRs for axial compression in the meridional direction from the element-by-element evaluation for load combinations NO_1 and the representative OBE_1 load combination for the Standard analysis case are plotted in Figures 43 and 44. Compression in the meridional direction is generally low and DCRs for the Standard Analysis are generally below 0.5. The pilasters have higher meridional compression demands than the wall, and have single-element localized capacity exceedances at the base in the controlling OBE load combinations. These single-element exceedances are less severe than those identified in the Standard-Plus Analysis Case; therefore, further evaluation of this exceedance is deferred to that case (see below).

A contour plot of DCRs for axial compression in the meridional direction for load combination NO_1 for the Standard-Plus Analysis Case is plotted in Figure 45. The additional concrete fill pressure modeled in the Standard-Plus analysis case causes increased compression demands, particularly in the pilaster on the south side of the Mechanical Penetration. The controlling load combination for compression in this pilaster is static combination NO_1, due to its large load



factor for ASR loads. As a bounding case, meridional compression in this pilaster (and the adjacent wall) is evaluated for load combination NO_1 using Equation 1 below. The evaluation is performed using a section cut length equal to four wall thicknesses, which is computed using the width of the CEB wall (36 in.) rather than the width of the pilaster (48 in.). The average axial compression demand along this cut is -72,100 lbf/in or 72.1 kip/in.

$$\varepsilon_{sc} = \varepsilon_{SQ} + \varepsilon_{cc} - \varepsilon_{CQ}$$

$$\varepsilon_{sc} = (1.12 \times 10^{-3}) + (-3.00 \times 10^{-3}) - (-1.08 \times 10^{-5}) = -0.00187$$

$$\phi P_n = \phi \times 0.8 [0.85 f'_c (A_c - A_s) + \min(-\varepsilon_{sc} E_s, f_y) A_s]$$

$$A_s = 3\#11@6" = \frac{3 * 1.56 \text{ in}^2}{6 \text{ in}} = 0.780 \text{ in}^2/\text{in}$$

$$A_c = \frac{48 \text{ in} \times 5 \text{ ft} + 36 \text{ in} \times 13 \text{ ft}}{18 \text{ ft}} = 39 \text{ in}^2/\text{in}$$

$$\min(-\varepsilon_{sc} E_s, f_y) = \min[(0.00187) \times (29 \times 10^6 \text{ psi}), (60,000 \text{ psi})] = 54,230 \text{ psi}$$

$$\phi P_n = (0.7) \times (0.8) [(0.85)(4,000 \text{ psi})(39 \text{ in} - 0.78 \text{ in}) + (54,230 \text{ psi})(0.78 \text{ in})]$$

$$\phi P_n = 96,400 \frac{\text{lbf}}{\text{in}} = 96.4 \frac{\text{kip}}{\text{in}}$$

$$\phi P_n = 96.4 \frac{\text{kip}}{\text{in}} > P_u = 72.1 \frac{\text{kip}}{\text{in}} \quad (\text{OK- Compressive strength is adequate, DCR}=0.75)$$

This evaluation shows that axial compression in the meridional direction meets evaluation criteria for all analysis cases and all load combinations.

7.5.3 In-Plane Shear

Contour plots of DCRs for in-plane shear from the element-by-element evaluation for load combination NO_1 and the representative OBE_1 load combination for the Standard analysis case are plotted in Figures 46 and 47. A contour plot of DCRs for in-plane shear for load combination NO_1 for the Standard-Plus Analysis Case is plotted in Figure 48. Several regions of the CEB are critical for in-plane shear; each region is assessed below.

- Based on the element-by-element evaluation, in-plane shear demand exceeds capacity beside each of the large openings at the base of the wall. The mechanism resisting



out-of-plane loads at the base of the wall causes in-plane shear stress to occur, as described in Section 7.6.1. However, in-plane shear demands engage a large portion of a wall structure as a membrane, and are therefore more reasonably evaluated using section cuts. The in-plane shear forces acting at the base of the wall are assessed in Section 7.6.1 along with other strength checks associated with the aforementioned resistance mechanism.

- The element-by-element evaluation shows in-plane shear exceedances at the reentrant corners above the Mechanical and Electrical Penetrations. This exceedance is most severe at the west side of the Electrical Penetration (approximately AZ 330°, El. +27 ft) in the Standard-Plus Analysis Case. Shear on this side of the Electrical Penetration is particularly critical due to the short distance between the Electrical and Mechanical Penetration. In-plane shear in this area is evaluated using a section cut (Section Cut 7 in Appendix N). The maximum DCR for in-plane shear for Section Cut 7 is 0.37, which occurs in load combination OBE_1. The Section Cut in-plane shear check is performed using horizontal reinforcement bars; however, additional diagonal steel is provided at the corners of the Electrical Penetration, which are not considered in this evaluation. Based on these assessments, in-plane shear strength at the reentrant corners is judged to be adequate.

This evaluation shows that in-plane shear meets evaluation criteria for all analysis cases and all load combinations.

7.5.4 Out-of-Plane Shear Acting on the Hoop-Radial Plane

Contour plots of DCRs for out-of-plane shear acting on the hoop-radial plane from the element-by-element evaluation for load combination NO_1 and the representative OBE_1 load combination for the Standard analysis case are plotted in Figures 49 and 50. The base of the wall has high out-of-plane shear demands due to the pressures caused by ASR of the concrete fill and hydrostatic loads. The element-by-element evaluation shows that these out-of-plane shear demands are less than capacity for the Standard analysis case. A contour plot of DCRs for out-of-plane shear acting on the hoop-radial plane for load combination NO_1 for the Standard-Plus Analysis Case is plotted in Figure 51. The element-by-element evaluation of the Standard-Plus Analysis Case shows a minor single-element capacity exceedance near the reentrant corner above the electrical penetration; this exceedance is judged to be insignificant when consideration is given to local averaging of stresses. Section cut evaluations of out-of-plane shear at the base of the structure (utilizing shear-friction) show maximum DCRs of 0.58 for the Standard and Standard-Plus Analysis Cases, occurring between AZ 0 and AZ 90.



This evaluation shows that out-of-plane shear meets evaluation criteria for all analysis cases and all load combinations.

7.5.5 Out-of-Plane Shear Acting on the Meridional-Radial Plane

Contour plots of DCRs for out-of-plane shear acting on the meridional-radial plane from the element-by-element evaluation for load combination NO_1 and the representative OBE_1 load combination for the Standard Analysis Case are plotted in Figures 52 and 53. A contour plot of DCRs for out-of-plane shear acting on the meridional-radial plane for load combination NO_1 for the Standard-Plus Analysis Case is plotted in Figure 54. Only minor and localized capacity exceedances are identified for out-of-plane shear acting on the meridional-radial plane, occurring at the corners of openings. These exceedances are judged to be insignificant by giving consideration to local averaging of demands.

7.5.6 Axial-Flexure Interaction in the Hoop Direction

Contour plots of DCRs for axial-flexure (PM) interaction in the hoop direction from the element-by-element evaluation for load combination NO_1 and the representative OBE_1 load combination for the Standard analysis case are plotted in Figures 55 and 56. The deformed shape of the CEB, consisting of outward radial movement at AZ 270 and inward radial movement at AZ 225 and AZ 300 between El. 0 and El. +50 ft, indicates that high flexural demands will occur within these regions. The element-by-element evaluation reflects this by showing capacity exceedances near the Personnel Hatch (AZ 315) and the CEVA opening (AZ 230°). The flexural demands are primarily caused by ASR loads, and therefore are most severe in the static case where the ASR load factor is highest. The transition from high ASR load in the below-grade region of the CEB to lower ASR load above grade causes a tension in the hoop direction in the region where this flexure is occurring, which reduces the section's capacity for PM interaction. Axial-flexure evaluation results for the Standard Analysis Case are discussed below.

- Axial-flexure demands in the hoop direction at the base of the CEB wall meet evaluation criteria for the Standard Analysis Case.
- Based on the element-by-element evaluation of the Standard Analysis Case, PM demands in the hoop direction exceed capacity in the areas adjacent to the Personnel Hatch and the CEVA opening between El. 0 ft and El. 50 ft. These capacity



exceedances are addressed by redistributing the bending moment in excess of the PM interaction capacity. The redistribution causes changes in bending moments and, to a lesser extent, membrane forces in adjacent areas of the structure. For the Standard Analysis Case, the moment redistribution study is performed for the controlling static load combination (NO_1). Documentation of the moment redistribution is provided in Appendix H. A summary of the moment redistribution is provided in Section 7.6.2.

A contour plot of DCRs for PM interaction in the hoop direction for load combination NO_1 for the Standard-Plus Analysis Case is plotted in Figure 57. Evaluation of PM interaction for the Standard-Plus Case shows similar regions of capacity exceedance as the Standard Case, and some additional regions of exceedance caused by the added pressures between AZ 180 and 270. Evaluation results for PM interaction in the hoop direction for the Standard-Plus Analysis Case are discussed below.

- Based on element-by-element evaluation, the base of the wall between AZ 180 and 270 shows capacity exceedance for PM interaction in the hoop direction. Due to the nearby foundation and out-of-plane restraint of the concrete fill, the capability of the wall to bend about the vertical axis at the base is limited; therefore, the bending demand at this section is small (less than 100 kip-ft/ft). This exceedance is primarily driven by tensile demands caused by the out-of-plane force resistance mechanism acting at the base of the wall (this mechanism is described in Section 7.6.1). These tensile demands are evaluated below using a section of length equal to three wall thicknesses, which is equivalent to the entire width of the tensile region. The average tensile demand in this cut is 5,500 lbf/in (5.5 kip/in).

$$A_s = 2\#11@12" = \frac{2(1.56 \text{ in}^2)}{12 \text{ in}} = 0.26 \text{ in}^2/\text{in}$$

$$\phi P_n = \phi A_s f_y = (0.9) \left(0.26 \frac{\text{in}^2}{\text{in}} \right) (60,000 \text{ psi}) = 14,000 \frac{\text{lbf}}{\text{in}} = 14 \frac{\text{kip}}{\text{in}}$$

$$\phi P_n = 14 \frac{\text{kip}}{\text{in}} > P_u = 5.5 \frac{\text{kip}}{\text{in}} \quad (\text{OK- Tensile strength is adequate, DCR}=0.39)$$

- Based on the element-by-element evaluation of the Standard-Plus Analysis Case, PM demands in the hoop direction exceed capacity in the areas adjacent to the Personnel Hatch and the CEVA opening between El. 0 ft and El. 50 ft as well as a localized region at El. +60 to +90 ft at AZ 200 (above the location where additional concrete fill pressures are applied). These capacity exceedances are addressed by redistributing the bending moment in excess of the PM interaction capacity. The redistribution causes changes in bending moments and, to a lesser extent, membrane forces in adjacent areas of the structure. For the Standard-Plus Analysis Case, the moment redistribution study is performed for the controlling static load combination (NO_1) as well as an OBE load combination (OBE_4). Documentation of the moment



redistribution is provided in Appendix H. A summary of the moment redistribution is provided in Section 7.6.2.

- Based on the element-by-element evaluation of the Standard-Plus Analysis Case, PM demands in the hoop direction exceed capacity in an area to the east of the Electrical Penetration. This exceedance is evaluated using two section cuts (Section Cuts 14 and 15, as defined in Appendix N). The section cut evaluations show that the wall meets acceptance criteria for PM interaction in this region for all load combinations (Figures 72 and 73).

The information presented above shows axial-flexure interaction meets evaluation criteria for all analysis cases and all load combinations.

7.5.7 Axial-Flexure Interaction in the Meridional Direction

Contour plots of DCRs for PM interaction in the meridional direction from the element-by-element evaluation for load combination NO_1 and the representative OBE_1 load combination for the Standard Analysis Case are plotted in Figures 58 and 59. Meridional flexure demands (i.e., bending about the hoop axis) are most critical at the base of the CEB wall and at the pilasters on either side of the Electrical and Mechanical Penetrations. Axial-flexure evaluation results for the Standard Analysis Case are discussed below.

- The element-by-element evaluation of the Standard Analysis Case indicates meridional axial-flexure interaction capacity exceedances at the base of the wall between AZ 270 and 360. This portion of the wall is between the two large penetrations (Electrical and Mechanical Penetrations). Out-of-plane ASR of fill loads contributes most to the out-of-plane flexure demands at the base of the wall. The evaluation of these demands is controlled by the static NO_1 load combination because of the large ASR load factors. This wall segment is subdivided into three section cuts, each between 15 and 27 ft wide (approximately eight wall thicknesses wide), for evaluation of axial-flexure interaction. The section cuts on either end of this wall segment have increased PM capacity due to the pilasters adjacent to the penetrations. The section cut evaluations also indicate exceedance of axial-flexure interaction capacity. Therefore a moment redistribution analysis is performed at the base of the wall to redistribute bending moment in excess of the PM interaction capacity. The redistribution causes changes in bending moments and, to a lesser extent, membrane forces in adjacent areas of the structure. For the Standard Analysis Case, the moment redistribution study is performed for the controlling static load combination (NO_1). Documentation of the moment redistribution is provided in Appendix H. A summary of the moment redistribution is provided in Section 7.6.2.
- The element-by-element evaluation of the Standard Analysis Case indicates meridional axial-flexure interaction capacity exceedances at the pilasters on either side of the Electrical and Mechanical Penetrations. Section cut evaluations of these locations (Section Cuts 8, 9, 10, and 11, as defined in Appendix N) indicate that the pilasters on



either side of the Electrical Penetration (Section Cuts 8 and 11) exceed capacity, while the pilasters on either side of the Mechanical Penetration (Section Cuts 9 and 10) meet evaluation criteria. Moment redistribution analysis is performed at these pilasters to redistribute bending moment in excess of the PM interaction capacity. The redistribution causes changes in bending moments and, to a lesser-extent, membrane forces in adjacent areas of the structure. For the Standard Analysis Case, the moment redistribution study is performed for the controlling static load combination (NO_1). Documentation of the moment redistribution is provided in Appendix H. A summary of the moment redistribution is provided in Section 7.6.2.

- The element-by-element evaluation of the Standard Analysis Case indicates small regions of minor and localized capacity exceedances at El. +45.5 ft near AZ 30 and 240. These capacity exceedances are primarily caused by tensile demands acting on the wall due to different ASR expansion magnitudes acting at different portions of the wall. As shown in Table 13, between AZ 0 and 180 the applied ASR strain is 0.015% in the vertical direction and between AZ 180 & 270 and 270 & 360 the applied ASR strain is 0.04% and 0.06% in the vertical direction, respectively. These changes in vertical expansion cause tensile demands in the wall. These tensile demands are studied for the most severe case, which occurs in the Standard-Plus Analysis Case (see additional info below).

Contour plots of DCRs for PM interaction in the meridional direction for load combination NO_1 for the Standard-Plus Analysis Case are plotted in Figure 60. Axial-flexure evaluation results for the Standard-Plus Analysis Case are discussed below.

- Similar to the Standard Analysis Case, element-by-element evaluation of the Standard-Plus Analysis Case shows regions of capacity exceedance at the base of the wall between AZ 270 and 360 as well as at the pilasters on either side of the Electrical and Mechanical Penetrations. The Standard-Plus Analysis Case also shows a region of meridional PM interaction exceedance along the base of the wall between AZ 180 and 270; this exceedance is caused by the added pressures considered in this analysis case. These exceedances are confirmed by section-cut analyses, and moment redistribution analysis is performed for these exceedances for the controlling static (NO_1) combination as well as an OBE combination. Documentation of the moment redistribution is provided in Appendix H. A summary of the moment redistribution is provided in Section 7.6.2.
- The element-by-element evaluation of the Standard-Plus Analysis Case indicates a localized region of capacity exceedance at El. +45.5 ft near AZ 240. This demands in this region are similar to those previously identified at El +45.5 ft in the Standard Analysis Case. This exceedance is most critical in the static combination (NO_1) of the Standard-Plus Analysis Case at AZ 240 because meridional tension demands caused by additional pressure possibly due to ASR of the concrete fill wedge are additive to those caused by the differential ASR expansion of the CEB wall. The transition in wall thickness from 27 in. to 15 in between El +40 and +45.5 ft causes the



wall's centerline to shift by 6 in., which causes the tensile demands to impart a bending moment on the wall about the hoop axis.

The tension demands at El +45.5 ft AZ 240 for this localized area are larger than the modulus of concrete rupture (as defined in ACI 318-71 Section 9.5.2.2 [11]). In the linear elastic model of the CEB, demands are computed conservatively by not considering stiffness reductions associated with concrete cracking. Concrete cracking occurring in this area would reduce the meridional stiffness of the area, and promote further tensile demands to take alternate load paths with higher stiffness. Furthermore, the differential ASR expansion loads causing these tensile demands are displacement controlled, which indicates that demands would be partially reduced by the reduction in stiffness due to concrete cracking.

An analysis is performed by reducing the stiffness of a strip of elements at El. +45.5 AZ 240 to be equivalent to the stiffness of the steel reinforcement in that area to simulate concrete cracking. This reduction in stiffness is only used in ASR load cases (ASR of CEB wall and ASR of concrete fill). This analysis shows that concrete cracking reduces the tensile and flexural demands acting on the section, and a section cut evaluation shows that evaluation criteria are met. The PM interaction diagram before and after the adjustment to stiffness is shown in Figures 62 and 63. Additional information on this analysis is provided in Appendix M.

The information presented above shows axial-flexure interaction meets evaluation criteria for all analysis cases and all load combinations.

7.6 Results of Additional Evaluations

Additional evaluations are performed if the element-by-element and section cut evaluations are unable to qualify a region of the structure. In the additional evaluations, areas with elevated demands are identified, and the mechanisms resisting the demands are identified. A detailed analysis of the resistance mechanisms is performed, and all critical aspects of the mechanism are checked against evaluation criteria.

7.6.1 Evaluation of Base of Wall Adjacent to Penetrations

The base of the CEB wall resists out-of-plane demands using a resistance mechanism that consists of out-of-plane shear, flexure about the hoop axis, and the formation of a compression-tension couple as illustrated in Figure 76. The ASR expansion of the concrete fill contributes the most to the out-of-plane loads, and the factored demands caused by these loads must be resisted along with those from all other factored design loads. To maintain this resistance mechanism, the following items are evaluated:



- Out-of-plane shear strength at the base of the wall
- Meridional axial tension at the base of the wall
- Meridional axial compression at the base of the wall near openings
- Axial tension at the base of the wall in the hoop direction
- In-plane shear strength at the base of the wall
- Out-of-plane bending about the hoop axis at the base of the wall

Many of these items have already been qualified in Section 7.5 using element-by-element and section cut evaluations. However, the evaluation of each of these items is discussed below within the context of the base of the CEB wall.

Out-of-Plane Shear Strength at the Base of the Wall

Out-of-plane shear at the base of the wall is evaluated using section cuts taken at the base of the wall. For each section cut, shear demand is computed as the SRSS of the in-plane shear and out-of-plane shear demands. Shear demand is compared to the shear friction capacity, which is computed using a friction coefficient of 1.0 to account for a construction joint between the foundation and CEB wall concretes. As stated in Section 7.5.4, the maximum DCR for out-of-plane shear at the base of the wall is 0.58.

Therefore, it is concluded that out-of-plane shear at the base of the wall meets evaluation criteria.

Meridional Axial Tension at the Base of the Wall

The tension-compression couple illustrated in Figure 76 occurs due to the curved shape of the CEB wall. This couple creates a region of meridional tension demand at locations away from large penetrations (i.e. Electrical and Mechanical Penetrations). The tension demand is most severe in the Standard-Plus Analysis Case at approximately AZ 225° due to the additional concrete fill pressure in this case, and the controlling load combination is the static NO_1 combination (as defined in Table 5). The maximum net axial demand on the wall at this location is 9,800 lbf/in or 9.8 kip/in, which is significantly lower than the axial tension capacity of 42 kip/in., as computed below.



$$\phi P_n = \phi A_s f_y = (0.9) \times \left(\frac{1.56 \text{ in}^2 \times 3}{6 \text{ in}} \right) \times 60 \text{ ksi} = 42 \text{ kip/in}$$

Therefore, it is concluded that axial tension at the base of the wall meets evaluation criteria.

Meridional Axial Compression at the Base of the Wall on the Edge(s)

The tension-compression couple illustrated in Figure 76 occurs due to the curved shape of the wall. The couple creates meridional compression in the pilasters adjacent to the Electrical and Mechanical Penetrations. Section 7.5.2 shows that compression demands meet evaluation criteria at these locations.

Axial Tension at the Base of the Wall in the Hoop Direction

The tension-compression couple illustrated in Figure 76 also causes a narrow region of hoop tension demand at the base of the wall. The element-by-element evaluation indicates that this tensile demand exceeds capacity in the Standard-Plus Analysis Case. However, the section cut evaluation performed in Section 7.5.6 demonstrates that the wall meets evaluation criteria.

In-Plane Shear Strength at the Base of the Wall

In-plane shear is evaluated at the base of the CEB wall using section cuts. Since in-plane shear demands engage a large portion of the wall as a membrane, in-plane shear is typically evaluated using longer section cuts than out-of-plane demands. For evaluation of in-plane shear for the CEB, section cuts up to 90° in length are used. In some cases, such as between the Electrical and Mechanical Penetrations, ASR loads can cause in-plane shear demands to act in two different directions within a single section cut. In these cases, in-plane shear is evaluated for the net demand in the entire section cut and the potential for the wall to split apart is evaluated by checking membrane demands in the hoop and meridional directions. Section cut evaluations of in-plane shear at the base of the wall indicate a maximum DCR of 0.56, which occurs in Section Cut 3 (between AZ 180° and 270°) in the OBE_3 combination in the Standard-Plus Analysis Case.

Out-of-Plane Bending about the Hoop Axis at the Base of the Wall



Out-of-plane bending about the hoop axis occurs at the base of the wall and is caused by out-of-plane pressures applied to the wall (primarily caused by ASR of concrete fill). The base of the wall is subdivided into sections with length approximately equal to eight wall thicknesses, and each section is evaluated for PM interaction. It is found that sections between AZ 270 and 360 exceed PM capacity in the Standard Analysis Case. For the Standard-Plus Analysis Case, it is found that PM interaction capacity is exceeded for sections between AZ 180 and 270 as well as section between AZ 270 and 360. Both of these exceedances are controlled by the static load combination (NO_1), as defined in Table 5. Moment redistribution analyses are performed for these areas of exceedance. The analysis is summarized in Section 7.6.2 and documented with additional detail in Appendix H.

7.6.2 Moment Redistribution Analysis and Evaluation

In areas where axial-flexure interaction capacity is exceeded by factored demands, a moment redistribution analysis is performed to simulate possible localized cracking and formation of localized plastic hinges to account for the impact of this redistribution on other parts of the CEB structure. In moment redistribution analyses, all moment that is in excess of the computed capacity is redistributed in the structure; this is to account for localized cracking and plastic hinge behavior. This procedure causes changes in bending moments and, to a lesser extent, membrane forces in adjacent areas of the structure. The moment redistribution analyses simulate local plasticity within the structure, and simulate the redistribution of loads associated with the plasticity.

Since a linear elastic model is used in this calculation, the moment redistribution is performed with an approach that utilizes several conservative approximations. These conservative approximations are listed below:

- In the moment redistribution analyses, the plastic moment capacity of each evaluated wall section is taken as the code flexural capacity. Since the code flexural capacity is computed using strength reduction (ϕ) factors, the wall may have remaining flexural stiffness when the code flexural capacity (ϕM_n) is exceeded. This means that the amount of moment that must be redistributed is over-predicted in these analyses. This over-prediction is conservative because it requires adjacent wall sections to carry the excess moment demand.



- Cracked section properties are not considered in the analyses leading to moment redistribution. Flexural cracking reduces the stiffness of the section, and therefore reduces the demand in the element due to certain types of load.
- All moment redistributions are assumed to occur concurrently. This is a conservative assumption because loads in all areas of the structure may not necessarily reach their fully factored value at the same time.

The moment redistribution approach is documented and validated in Appendix L.

Three moment redistribution analyses are performed in this calculation. For the Standard Analysis Case, moment redistribution is performed for the static load combination (NO_1) only, which is the controlling case. For the Standard-Plus Analysis Case, moment redistribution is performed for the static load combination (NO_1) as well as an OBE combination (OBE_4) that is found to control over other OBE combinations at several section cuts.

In all moment redistribution analyses, the moment in excess of capacity is redistributed such that, after redistribution is complete, the PM interaction demand point is generally within the capacity of the section. Impact on membrane forces due to moment redistribution is generally small, as identified in Appendix H.

Section cuts (as shown in Appendix N) are defined in critical areas of the structure for PM interaction. After moment redistribution is performed, demands at all relevant defined section cuts are analyzed to determine if redistributed demands sufficiently increase in PM interaction to cause capacity exceedance. If needed, additional iterations of moment redistribution are performed to resolve such exceedances.

Diagrams illustrating PM interaction prior to moment redistribution for the Standard Analysis Case are shown for Section Cuts 19 and 22 in Figures 64 and 65. It can be seen in these figures that the static load combination NO_1 controls evaluation in these cuts. The PM interaction diagrams after moment redistribution are shown in Figures 66 and 67. It can be seen that the demand for static combination NO_1 at these cut locations has sufficiently been redistributed. Similar diagrams are shown for the Standard-Plus Analysis Case for Section Cuts 19 and 22 in Figures 68 through 71. PM interaction diagrams for Section Cuts 14 and 15, which do not require moment redistribution in the Standard-Plus Analysis Case, are shown in Figures 72 and 73. Diagrams illustrating PM interaction before and after moment redistribution for



section cuts at the base of the structure between AZ 270 and 360 for the NO_1 combination in the Standard-Plus Analysis Case are shown in Figures 74 and 75.

Additional documentation on the moment redistribution analyses, including assessment of membrane forces, is provided in Appendix H of this calculation. This appendix shows that, in some cases, moment redistribution can result in small increases in DCR for effects other than PM interaction. However, these increases are small and they impact evaluations (in-plane shear, out-of-plane shear, compression) that have sufficient remaining.

The ductility of the sections where moment redistribution is performed is evaluated in Appendix O. Ductility is defined as the total strain in the tension reinforcement divided by the strain at which the reinforcement yields. Appendix O shows that the maximum ductility computed in this evaluation is 3.5, occurring in Section Cut 22 (as defined in Appendix N). All other section cuts have a maximum ductility of 2.5 or less.

7.7 Evaluation of CEB Displacements

Potential interaction between the CEB and other adjacent structures is evaluated in this section. When available, measurements made of the widths of the seismic gaps between the CEB and the adjacent structures (West Pipe Chase, Electrical Pen., FSB, and CB) are used when performing these computations. The finite element analysis results are used to obtain (a) seismic and transient load displacements of the CEB and (b) the reduction in seismic gap widths due to possible progression of ASR associated with the threshold factor of 1.2. Although the results of this computation are not greatly affected by the use of the Standard-Plus Analysis Case rather than the Standard Analysis Case, the CEB displacements are checked for both the Standard and the Standard-Plus Analysis Cases.

The remaining clearance between the CEB and an adjacent structure is computed using Equation 10. The relative seismic movements of the CEB and adjacent structures are combined as $2\sqrt{L_s^2 + L_a^2}$, which is based on Section 7.3 of ASCE 43-05 [28]. This equation provides a factor of safety against building contact due to seismic and transient motions.



$$C = L_{des} - k_{th}^* \times L_{obs} - L_R \quad \text{Equation 10}$$

$$L_R = 2 \times \sqrt{(L_s + L_{ns})^2 + L_a^2}$$

Where:

- C = Minimum remaining joint clearance between CEB and adjacent structure.
- L_{des} = Design seismic gap width, 3 in. [12].
- k_{th}^* = Factor representing the increase in radial CEB deformation when ASR loads are amplified by the threshold factor k_{th} (See Section 7.3). This factor is computed as the FEA-simulated radial deformation amplified by the ASR threshold factor divided by the FEA-simulated radial deformation without the ASR threshold factor.
- L_{obs} = Measured radial displacement of CEB, taken as positive if in direction toward adjacent structure. If seismic gap measurement is not available, L_{obs} is taken as the displacement from FEA simulations of the as-deformed condition.
- L_{ns} = Computed factored non-seismic displacement of the CEB, not including sustained loads (such as self-weight, hydrostatic pressure, and static soil pressure) which are already included in L_{obs} . L_{ns} is taken as positive if in direction toward the adjacent structure. L_{ns} is taken as zero if it is in the direction away from the adjacent structure.
- L_s = Computed factored seismic displacement of CEB, taken as absolute value.
- L_a = Maximum lateral displacement of adjacent structure. L_a values are taken from [31] whenever possible; otherwise it is assumed that L_a is equal in value to L_s .

Clearance evaluations are shown in Tables 16 and 17 for the Standard and Standard-Plus Analysis Cases. For Locations 7 and 8 in this table, existing seismic gaps are unknown; therefore, it is assumed that the minimum remaining seismic gap during a seismic event is 0.0 in., and a minimum as-deformed condition seismic gap (i.e., due to sustained loads and self-straining loads only) is computed. This computation takes into account a decrease in isolation gap width due to possible progression of ASR related to the threshold factor of 1.2.

Results of the clearance evaluations are summarized below:

- With the exception of the locations at missile shields, the existing gap widths are sufficient at all assessed locations to ensure that contact between buildings will not occur.
- For missile shield locations, the minimum current seismic gap to prevent contact with the adjacent structure (CB) is 1 in. at the missile shield above the Personnel Hatch and 5/8 in. at the missile shield above the CEVA.



7.8 Evaluation of Global Stability

The concrete fill that surrounds the CEB from El. 0 ft and below provides a substantial resistance to global sliding and overturning. However, since ASR expansion of the CEB and the surrounding fill introduces a new load the CEB, a conservative evaluation against sliding and overturning is performed. The original design calculations checking for global flotation were confirmed in Ref. 29 and are not affected by the addition of ASR loads; therefore flotation is not reevaluated in this calculation.

The conservative stability evaluation with consideration of ASR demands is performed in Appendix I and demonstrates that a factor of safety against sliding and overturning meeting the requirements of SD-66 [8] is provided. This evaluation is considered to be conservative because it accounts for demands caused by ASR expansion of the fill, but it does not consider the resistance to sliding and overturning provided by the concrete fill.



8. ESTABLISH THRESHOLD MEASUREMENTS FOR CONDITION MONITORING

In the analysis and evaluation of the CEB, ASR loads are amplified by a threshold factor in addition to a load factor. While the load factor accounts for uncertainty in the ASR load, the threshold factor accounts for additional ASR load that may occur in the future. As noted in Section 7.3, a threshold factor of 1.2 is selected for the CEB, which means that ASR-related demands are amplified by 20% beyond their factored values. Simulated ASR expansion of the CEB is based on Crack Index (CI) strain measurements performed in the regions of the structure defined in Table 13. The analysis shows that ASR expansions occurring in the below-grade portions of the structure (regions R1, R2, and R3) have a larger impact on demands and deformations than those occurring above-grade.

Systematic monitoring of the CEB is required to verify that ASR loads have not exceeded the selected threshold and to inform when threshold values are being approached to allow for appropriate corrective action measures. Monitoring of strains and structure deformations is appropriate to inform of potential internal ASR expansion to evaluate against the strain limits established by the large-scale testing at FSEL, to understand the impact of potential ASR expansion of concrete backfill, and to capture potential movement or deformation of adjacent structures. Strains can be monitored by different means such as through CI, CCI, and expansion measurements.

Because the analysis uses a mean strain value for each region, monitoring must be able to track strains sufficiently to justify the use of a mean value in each of the below-grade regions defined in Table 13 for below grade regions not to exceed 20% above strain values provided in Table 13 for regions R1, R2, and R3. This may be achieved by using existing monitoring locations within each region if sufficient data can be collected or by establishing new locations to supplement or replace existing locations.

For purposes of explaining the methodology, this chapter discusses the use of CCI measurements to monitor strains. While the use of the selected monitoring locations is expected to produce the desired results, the intent is not to restrict development of threshold monitoring program to the specific methods and monitoring locations identified in the text. Similarly, this chapter discusses the use of the existing seismic gap measurement locations to monitor structure deformations; alternative means and locations may be appropriate.



A proposed approach is to monitor regions R1, R2, and R3 to confirm the average strains in these regions don't exceed 20% above the strain values provided in Table 13. Another alternative prospective approach for monitoring of ASR strain using CCI is described below where threshold measurements are divided into sets based on regions of the CEB structure. A threshold limit is established for each set of threshold measurements. The average change in the set of threshold measurements is compared to the threshold limit to determine if the predefined threshold of ASR load is met. Averaging of threshold measurements is done because the threshold amplification is applied to all ASR loads on the entire structure and a localized increase in a monitored quantity is not indicative of threshold conditions being met.

Prospective threshold measurement sets and their corresponding limits are summarized in Section 3. Further information on these measurements and limits is provided in the preceding sections of this report. As field measurements approach the threshold limits, corrective actions should be taken to ensure validity of the calculation conclusions. If needed, further evaluation may be required to qualify the structure under a larger set of ASR loads.

8.1 Alternate Prospective Crack Index Threshold Measurements and Threshold Limits

The fifteen ASR monitoring grids established in 2011 [32] and re-measured in 2016 [9] comprise a representative sample of the most severe regions of the CEB for ASR expansion. These monitoring grids are located below-grade where ASR expansion tends to be the most severe. Additionally, these monitoring grids are approximately evenly distributed at different azimuths on the CEB.

These fifteen ASR monitoring grids are divided into two sets: one set consists of monitoring grids on the east side of the CEB (between AZ 0° and 180°) where ASR strains are generally lower, and the other set consists of grids on the west side of the CEB (AZ 180° to 360°) where ASR strains tend to be higher. Monitoring is performed using combined crack index (CCI), which takes into account both vertical and horizontal strains [33]. Threshold limits are established by multiplying the average of the most recent CCI values by the threshold factor of 1.20. The two measurement sets are referred to as Threshold Measurement Set A and B, and their corresponding threshold limits are referred to as Threshold Limit A and B. These measurements and limits are shown in Tables 19 and 20.



8.2 Prospective Deformation Threshold Measurements and Threshold Limits

A set of deformation threshold measurements throughout the CEB structure is defined in this section. This set of threshold measurements is referred to as Threshold Measurement Set C. The measurements within this group consist of seismic gap measurements and annulus width measurements. The threshold limit for this set, referred to as Threshold Limit C, is defined and evaluated using the equations below.

$$\overline{TM}_C \leq TL_C$$

$$\overline{TM}_C = \sum_{i=0}^n |d_{n,field} - d_{n,design}| \times \left(\frac{1}{n}\right)$$

$$TL_C = \sum_{i=0}^n [|d_{n,baseline} - d_{n,design}| \times k_{n,thf}] \times \left(\frac{1}{n}\right)$$

$$k_{n,thf} = \frac{d_{n,FEA,1.2}}{d_{n,FEA,baseline}}$$

Where:

\overline{TM}_C = Average deformation for locations in Threshold Measurement Set C

TL_C = Threshold Limit C

n = Number of measurement locations in Threshold Measurement Set C

$d_{n,field}$ = Field measurement of threshold measurement n at time of monitoring

$d_{n,design}$ = Design dimension of threshold measurement n

$d_{n,baseline}$ = Field measurement of threshold measurement n at time when TL_C is established and CEB evaluation is performed

$d_{FEA,1.2}$ = Radial deformation of the CEB at location of threshold measurement n due to unfactored sustained loads plus unfactored self-straining loads with a 1.2 threshold factor

$d_{n,FEA,baseline}$ = Radial deformation of the CEB at location of threshold measurement n due to unfactored sustained loads plus unfactored self-straining loads without threshold factor amplification

The locations in Threshold Measurement Set C are listed in Table 21. For each threshold measurement, a method must be established to perform the measurement in a repeatable way. It is particularly important to perform the measurement in a well-defined location, otherwise seemingly small deviations in the concrete surfaces can have a significant impact on the repeatability of the threshold measurements. For some of the locations in Threshold Measurement Set C, a repeatable measurement method has already been established and a



baseline measurement has been obtained [3, 5]. Other locations in this set have previously been measured, but they have not been measured in a suitably repeatable way for continued monitoring. Once a baseline measurement is established for all locations in Threshold Measurement Set C, then Threshold Limit C can be computed. A projected value of Threshold Limit C is provided in Table 21 based on currently available measurement data.



9. TABLES

Table 1. List of Load Symbols and Notation*

Load Symbol	Description
D	Dead load (includes hydrostatic pressure)
L	Live load
H	Lateral static soil pressure
W	Wind load
E _o	Operating basis earthquake (OBE)
E _{ss}	Safe shutdown earthquake (SSE)
H _e	Dynamic earth pressure due to OBE
H _s	Dynamic earth pressure due to SSE
W _t	Tornado wind load
P _a	Accidental Pressure load
L _s	Unusual snow load
F	Design basis flood load
S _a	ASR expansion of wall and backfill concrete (self-straining force)
S _c	Creep (self-straining force)
S _h	Shrinkage (self-straining force)
S _w	Concrete swelling (self-straining force)

*Note: This table includes loads that are considered in this evaluation

Table 2. List of Loads Not Considered in Evaluation

Load Symbol	See Note	Description
W _m	1	Tornado missile loading
R _o	2	Pipe reaction loads during normal conditions
R _a	2	Accident piping load
R _{ij}	2	Jet impingement load
R _{rr}	2	Jet force reaction
R _{rm}	2	Pipe whip load
T _a	2	Accidental temperature load
T _o	2	Operational temperature load
P _o	2	Operational pressure load

1: Evaluation of Tornado Missile Loads is not required according to SD-66 [8]

2: Evaluation of piping loads, temperature loads, and operational pressure loads are not part of the original design performed by UE [24].



Table 3. Definition of Tornado Wind Load, W_t

Combination ¹
$W_t = W_{w1} + W_{w2}$
$W_t = W_p$
$W_t = W_{w1} + 0.5W_p$

¹ W_{w1} : Tornado wind external pressure load

W_{w2} : Tornado wind internal pressure load

W_p : Tornado differential pressure load

Table 4. Combinations for Computation of Deformations

Combination
For Comparison with Field Measurements: $1.0D + 1.0H + 1.0S_a + 1.0S_w + 1.0S_c + 1.0S_h$
To Establish Threshold Measurement Limits¹: $1.0D + 1.0H + 1.0k_{th}S_a + 1.0S_w + 1.0S_c + 1.0S_h$
For Computation of Demands Associated with the As-Deformed Condition: $1.0D + 1.0H + 1.0k_{th}S_a + 1.0S_w$

Notes:

¹ The threshold factor k_{th} is selected to be 1.2, see Section 7.3.



Table 5. List of Load Combinations

Label ^{1,2}	Combination
NO_1	$(2.0 \times k_{th})S_a + 1.4S_w + 1.4D + 1.7L + 1.7H$
NO_2	$(1.5 \times k_{th})S_a + 1.4S_w + 1.05D + 1.28L + 1.28H$
NO_3	$(1.0 \times k_{th})S_a + 1.4S_w + 1.0D + 1.0L + 1.0H + 1.5P_a$
OBE_1	$(1.3 \times k_{th})S_a + 1.4S_w + 1.4D + 1.7L + 1.9E_o + 1.7H + 1.9H_e$
OBE_2	$(1.0 \times k_{th})S_a + 1.4S_w + 1.05D + 1.28L + 1.43E_o + 1.28H + 1.43H_e$
OBE_3	$(1.3 \times k_{th})S_a + 1.4S_w + 1.2D + 1.9E_o + 1.7H + 1.9H_e$
OBE_4	$(1.0 \times k_{th})S_a + 1.4S_w + 1.0D + 1.0L + 1.25E_o + 1.0H + 1.25H_e + 1.25P_a$
SSE_1	$(1.0 \times k_{th})S_a + 1.4S_w + 1.0D + 1.0L + 1.0E_{ss} + 1.0H + 1.0H_s$
SSE_2	$(1.0 \times k_{th})S_a + 1.4S_w + 1.0D + 1.0L + 1.0E_{ss} + 1.0H + 1.0H_s + 1.0P_a$
W_1	$(1.7 \times k_{th})S_a + 1.4S_w + 1.4D + 1.7L + 1.7W + 1.7H$
W_2	$(1.28 \times k_{th})S_a + 1.4S_w + 1.05D + 1.28L + 1.3W + 1.28H$
W_3	$(1.7 \times k_{th})S_a + 1.4S_w + 1.2D + 1.7W + 1.7H$
W_4	$(1.0 \times k_{th})S_a + 1.4S_w + 1.0D + 1.0L + 1.0W_t + 1.0H$
W_5	$(1.0 \times k_{th})S_a + 1.4S_w + 1.0D + 1.0L + 1.0W + 1.0L_s$
W_6	$(1.0 \times k_{th})S_a + 1.4S_w + 1.0D + 1.0L + 1.0W + 1.0L_s + 1.0F$

¹ NO: Normal load combinations (non-seismic and non-wind)

OBE = Load combinations including operating basis earthquake E_o

SSE = Load combinations including safe shutdown earthquake E_{ss}

W = Load combinations including wind, W, and tornado wind, W_t

² OBE and SSE combinations are performed for each of the directional combinations shown in Table 6



Table 6. Seismic Excitation Combinations using 100-40-40 Rule

	Seismic Excitation Directions
1	100% East 40% North 40% Vertical Up
2	100% East 40% South 40% Vertical Up
3	100% East 40% North 40% Vertical Down
4	100% East 40% South 40% Vertical Down
5	100% West 40% North 40% Vertical Up
6	100% West 40% South 40% Vertical Up
7	100% West 40% North 40% Vertical Down
8	100% West 40% South 40% Vertical Down
9	40% East 100% North 40% Vertical Up
10	40% West 100% North 40% Vertical Up
11	40% East 100% North 40% Vertical Down
12	40% West 100% North 40% Vertical Down
13	40% East 100% South 40% Vertical Up
14	40% West 100% South 40% Vertical Up
15	40% East 100% South 40% Vertical Down
16	40% West 100% South 40% Vertical Down
17	40% East 40% North 100% Vertical Up
18	40% West 40% North 100% Vertical Up
19	40% East 40% South 100% Vertical Up
20	40% West 40% South 100% Vertical Up
21	40% East 40% North 100% Vertical Down
22	40% West 40% North 100% Vertical Down
23	40% East 40% South 100% Vertical Down
24	40% West 40% South 100% Vertical Down



Table 7. Description and Purpose of Analysis Cases

Analysis Case Name	Computer Run	Conditions	Purpose/Use
Original Design Analysis Case	10D_r0	CEB model without self-straining loads.	Evaluate CEB structure to assess if original design was sufficient and to verify performance of FEA model.
Standard Analysis Case	10A_r0	<ul style="list-style-type: none"> ASR loads matching field measurements of CI. CEB deformations generally matching field measurements of building movement at all locations except for AZ 230°. Concrete fill constructed in accordance with design drawings. See Section 6.2.2 for full description of analysis case.	Evaluate CEB structure.
Standard Analysis Case with Moment Redistribution	10AR_r0	Same as the Standard Analysis Case, except moment redistribution is used at localized areas where axial-flexure interaction demands are in exceedance of capacity in the Standard Analysis Case. See Appendix H for documentation of moment redistribution.	<ul style="list-style-type: none"> Evaluate axial-flexure interaction at localized areas with exceedance in the Standard Analysis Case. Identify areas where moment redistribution may impact membrane demands.
Standard-Plus Analysis Case	10B7_r0	<ul style="list-style-type: none"> ASR loads matching field measurements of CI. CEB deformations are more representative of those measured in the field at AZ 230°, and continue to reasonably match field measurements elsewhere. Inward pressures representing concrete fill are extended to include the portion of CEB wall that is adjacent to the triangular "wedge" of concrete between the CEVA, FSB, and CEB (from AZ 180° to 212°, El. +19 to +54 ft). This assumes that the concrete fill is in contact with the CEB and exerting lateral pressure from ASR expansion. See Section 6.2.3 for full description of analysis case.	Evaluate CEB structure.
Standard-Plus Analysis Case with Moment Redistribution	10BR7_r0	Same as the Standard-Plus Analysis Case, except moment redistribution is used at localized areas where axial-flexure interaction demands are in exceedance of capacity in the Standard-Plus Analysis Case. See Appendix H for documentation of moment redistribution.	<ul style="list-style-type: none"> Evaluate axial-flexure interaction at localized areas with exceedance in the Standard-Plus Analysis Case. Identify areas where moment redistribution may impact membrane demands.



Table 8. Summary of Analysis Cases

Analysis Case Name	Loads Considered	Consistent with Design Drawings?	Generally Simulates CI Measurements?	Generally Simulates Deformation Measurements?	Moment Redistribution
Original Design Analysis Case	All Table 5 combinations ¹	Yes	No	No	No
Standard Analysis Case	All Table 5 combinations	Yes	Yes	Yes ³	No
Standard Analysis Case with Moment Redistribution	Load combination NO_1 in Table 5 (controlling load combination)	Yes	Yes	Yes ³	Yes
Standard-Plus Analysis Case	All Table 5 combinations	Design-Plus ²	Yes	Yes	No
Standard Plus Analysis Case with Moment Redistribution	Load combination NO_1 and OBE_4 in Table 5 (controlling load combination and an OBE load combination)	Design-Plus ²	Yes	Yes	Yes

¹ In the Original Design Analysis Case, all self-straining loads (including S_a and S_w) are excluded

² "Design-Plus" indicates that additional ASR loads are applied due to the assumption that the concrete fill is not isolated from the CEB at certain Azimuths (see JA08 in Section 5.1)

³ The Standard Analysis Case generally simulates deformation measurements at all locations except AZ 230° (see Section 6.2.2)



Table 9. Summary of Analysis Results Naming Convention

Example load combination output name: (See notes on naming convention below)		SR_evA_LCB_D12_t12_r0
Note		Options
①	Analysis and evaluation descriptor	Specified as "SR" for all CEB analyses/evaluations
②	Analysis Case Descriptor	evA: Standard Analysis Case evAR: Standard Analysis Case evB7: Standard-Plus Analysis Case evD: Original Design Analysis Case evBR7: Standard-Plus Analysis Case with Moment Redistribution See Section 6.2.2 for more information on analysis cases
③	Specifies if output is for an independent load case or load combination	ILC: Independent load case (i.e. one single type of unfactored load applied to the structure, such as hydrostatic pressure) LCB: Load combination (i.e., several factored loads applied to the structure) See Table 5 for a list of load combinations considered in this evaluation.
④	Letter to specify load combination group	A: Combinations for computation of building deformations (See Table 4 for additional information) B: Combinations consisting of ASR loads or other self-straining loads only (Not used for evaluation) C: Load combinations NO_1, NO_2, and NO_3 (as defined in Table 4) D, E, F, G: Load combinations OBE_1, OBE_2, OBE_3, and OBE_4 (as defined in Table 4) H, I: Load combinations SSE_1, and SSE_2 (as defined in Table 4) J: Load combinations W_1, W_2, and W_3 (as defined in Table 4) K: Load combinations W_4, and W_5 (as defined in Table 4) (No letter is used for independent load cases)
⑤	Independent load case or load combination number	Can range from 1 to 41, See Appendix B for more information
⑥	Descriptor for threshold factor k_{th}	t00: Threshold factor of zero (i.e., no self-straining loads) t10: Threshold factor of one (i.e., ASR loads equivalent to currently observed conditions) t12: Threshold factor of 1.2 See Section 7.3 for a description of threshold factors.
⑦	Version number	Generally specified as "r0" for items discussed in this document



Table 10. Wind Velocity Pressures (Section 4.4.1.1 of SD-66 [8])

Height	q_t , psf	q_p , psf	q_m , psf
30 ft or less	40	46	31
Over 30 ft and up to 50 ft	46	51	36
Over 50 ft and up to 100 ft	53	59	44
Over 100 ft and up to 150 ft	58	65	49
Over 150 ft and up to 200 ft	62	69	53
Over 200 ft and up to 250 ft	65	72	57


Table 11. SSE and OBE Spectra [8]

SSE Horizontal Spectra at 7% Damping					
Control Pt		A	B	C	D
f, Hz	60	33	9.0	2.5	0.25
T, s	0.017	0.030	0.11	0.40	4.0
a, g	0.25	0.25	0.57	0.68	0.11
SSE Vertical Spectra at 7% Damping					
Control Pt		A	B	C	D
f, Hz	60	33	9.0	3.5	0.25
T, s	0.017	0.030	0.11	0.29	4.0
a, g	0.25	0.25	0.57	0.65	0.072
OBE Horizontal Spectra at 4% Damping					
Control Pt		A	B	C	D
f, Hz	60	33	9.0	2.5	0.25
T, s	0.017	0.030	0.11	0.40	4.0
a, g	0.13	0.13	0.38	0.46	0.066
OBE Vertical Spectra at 4% Damping					
Control Pt		A	B	C	D
f, Hz	60	33	9.0	3.5	0.25
T, s	0.017	0.030	0.11	0.29	4.0
a, g	0.13	0.13	0.38	0.43	0.044

Notes:

f = Frequency, T = Period, a = Acceleration

See Reference 4 for Control Point definitions

Table 12. Crack Index Measurement Data

ASR Monitoring Location ¹	Azimuth	Elevation	CI, Hoop Direction, mm/m	CI, Meridional Direction, mm/m	Region ²
CI-1	32	-27.5 ft	0.22	0.11	R1
CI-2	40	-20.5 ft	0.07	0.06	R1
CI-3	53	-23.5 ft	0.00	0.11	R1
CI-4	73	-24.5 ft	0.12	0.17	R1
CI-5	95	-24 ft	0.14	0.14	R1
CE101-05	104	+9.5 ft	0.08	0.06	R1
CE101-03	104	-23.5 ft	0.26	0.08	R1
CE101-04	106	-8.5 ft	0.04	0.41	R1
CI-6	113	-27.5 ft	0.12	0.13	R1
CI-7	124	-27.5 ft	0.11	0.14	R1
CI-8	144	-24 ft	0.12	0.14	R1
CI-9	163	-27.5 ft	0.20	0.23	R1
CI-10	175	-20 ft	0.09	0.28	R1
CI-11	197	-19 ft	0.24	0.33	R2
CI-13	214	+6 ft	0.96	0.22	R2
CI-12	230	-19 ft	0.12	0.46	R2
CE101-10	302	+9.5 ft	0.58	0.41	R3
CI-14	309	-24 ft	0.14	0.15	R3
CI-15	318	-24 ft	0.22	0.87	R3
CE101-11	322	-22.5 ft	0.12	0.89	R3
CE101-12	332	-22.0 ft	0.35	0.52	R3
CEBE-05	0	+51.5 ft	0.15	0.22	R4
CEBE-07	35	+29.5 ft	0.13	0.06	R4
CEBE-02	45	+25.5 ft	0.14	0.03	R4
CEBE-09	65	+25.5 ft	0.19	0.03	R4
CE101-06	106	+26 ft	0.14	0.09	R4
CE101-07	108	+46.5 ft	0.25	0.16	R4
CE101-08	108	+81.5 ft	0.16	0.23	R4
CEBE-03	125	+23 ft	0.10	0.11	R4
CEBE-08	125	+29 ft	0.09	0.08	R4
CEBE-01S	150	+55 ft	0.67	0.82	R4
CEBE-10	200	+58.5 ft	0.05	0.03	R4
CEBE-06	275	+68.5 ft	0.02	0.11	R4
EM401-01	305	+25 ft	0.05	0.18	R4
CEBE-04	315	+55 ft	0.08	0.03	R4
CE101-18	47	+116.5 ft	0.84	0.31	R5
CE101-09	103	+116.5 ft	0.39	0.49	R5
CE101-13	163	+116.5 ft	1.27	0.74	R5
CE101-14	205	+116.5 ft	1.76	0.76	R5
CE101-15	245	+116.5 ft	0.53	0.28	R5
CE101-16	284	+116.5 ft	1.64	0.58	R5
CE101-17	347	+116.5 ft	0.45	0.58	R5

Notes:

¹All measurements recorded in April and May of 2016 except for location CEBE-01S which was most recently inspected in April 2014.

²ASR monitoring locations are divided into regions based on ASR severity. See Table 13, Section 6.3.1, and Figure 4 for more information.



Table 13. ASR Region Summary

Region	R1	R2	R3	R4	R5
Description	Below grade, AZ 0 to 180	Below grade, AZ 180 to 270	Below grade, AZ 270 to 360	From grade to springline, AZ 0 to 360	Above Springline, AZ 0 to 360
Number of CI Measurements Contained Within	13	3	5	14	7
Average Hoop CI, mm/m (%)	0.12 mm/m (0.012%)	0.44 mm/m (0.044%)	0.28 mm/m (0.028%)	0.16 mm/m (0.016%)	0.98 mm/m (0.098%)
Average Meridional CI, mm/m (%)	0.16 mm/m (0.016%)	0.34 mm/m (0.034%)	0.57 mm/m (0.057%)	0.16 mm/m (0.016%)	0.57 mm/m (0.057%)
Hoop expansion applied to model, mm/m (%)	0.15 mm/m (0.015%)	0.40 mm/m (0.040%)	0.30 mm/m (0.030%)	0.10 mm/m (0.010%)	0.00 mm/m (0.00%)
Meridional expansion applied to model, mm/m (%)	0.15 mm/m (0.015%)	0.40 mm/m (0.040%)	0.60 mm/m (0.060%)	0.10 mm/m (0.010%)	0.00 mm/m (0.00%)

Notes:

See Table 12 for individual CI measurements. See Section 6.3.1 and Figure 4 for additional information on regions.

Table 14. Summary of Evaluation Results for Standard Analysis Case at Threshold Factor of 1.2

Evaluation	Load Combination (See Table 5 for Notation)	Location	Demand- to- Capacity Ratio	Notes	Figure, Table, or Section Reference
In-Plane Shear at Base	OBE_1 (100% E., 40% N., 40% Vert. Down)	Base of CEB between AZ 270 and 360 (Section Cut 4)	0.47	2	Figure 77
In-Plane Shear at Base	OBE_3 (100% E., 40% N., 40% Vert. Down)	Base of CEB between AZ 270 and 360 (Section Cut 4)	0.47	2	Figure 78
In-Plane Shear above Base	OBE_1 (40% E, 100% N, 40% Vert. Down)	Wall between Mech. Pen. and Electrical Pen.	0.36		Figure 79
Out-of-Plane Shear at Base	NO_1 (Static)	Base of CEB between AZ 0 and 90 (Section Cut 1)	0.58	2	Figure 49
Out-of-Plane Shear at Base	OBE_1 (100% E., 40% N., 40% Vert. Down)	Base of CEB between AZ 270 and 360 (Section Cut 4)	0.54	2	Figure 80
Axial Compression in Hoop Direction	NO_1 (Static)	Between El. -20 and 0 ft	<0.7	1	Figure 40
Axial Compression in Meridional Direction	NO_1 (Static)	Pilaster on south side of Mech. Pen.	0.75	2	Figure 43
PM Interaction in the Hoop Direction	NO_1 (Static)	Areas adjacent to CEVA opening (AZ 230) and Personnel Hatch Opening (AZ 300)	<1	3	Appendix H
PM Interaction in the Meridional Direction	NO_1 (Static)	Base of wall between AZ 270 and 360, pilasters on either side of Electrical Pen.	<1	3	Appendix H

¹ Based on element-by-element evaluation, DCR value would further reduce if section cut evaluation performed for this load combination and location.

² Based on section cut evaluation.

³ Based on moment redistribution analysis (Appendix H).


Table 15. Summary of Controlling Evaluation Results for Standard-Plus Analysis Case at Threshold Factor of 1.2

Evaluation	Load Combination	Location(s)	Demand-to-Capacity Ratio	Notes	Figure, Table, or Section Reference
In-Plane Shear	OBE_3 (100% W., 40% N., 40% Vert. Up)	Base of CEB between AZ 180 and 270 (Section Cut 3)	0.56	2	Figure 81
In-Plane Shear	OBE_1 (100% W., 40% N., 40% Vert. Up)	Base of CEB between AZ 180 and 270 (Section Cut 3)	0.55	2	Figure 82
In-Plane Shear above Base	OBE_1 (40% E., 100% N., 40% Vert. Down)	Wall between Mech. Pen. and Electrical Pen.	0.37	2	Figure 83
Out-of-Plane Shear	NO_1 (Static)	Base of CEB between AZ 0 and 90 (Section Cut 1)	0.58	2	Figure 51
Out-of-Plane Shear	OBE_1 (100% E., 40% N., 40% Vert. Down)	Base of CEB between AZ 270 and 360 (Section Cut 4)	0.55	2	Figure 84
Axial Compression in Hoop Direction	NO_1 (Static)	Between El. -20 and 0 ft, most critical at AZ 230	<0.7	1	Figure 42
Axial Compression in Meridional Direction	NO_1 (Static)	Pilaster on south side of Mechanical Pen. (AZ 240)	0.75	2	Figure 45
PM Interaction in the Hoop Direction	NO_1 (Static)	Areas adjacent to CEVA opening (AZ 230) and Personnel Hatch Opening (AZ 300)	<1	3	Appendix H
PM Interaction in the Meridional Direction	NO_1 (Static)	Base of wall between AZ 180 and 360, pilasters on either side of Electrical Pen. and Mech. Pen.	<1	3	Appendix H

¹ Based on element-by-element evaluation, DCR value would further reduce if section cut evaluation performed for this load combination and location.

² Based on section cut evaluation.

³ Based on moment redistribution analysis (Appendix H).



Table 16. Summary of Displacement Evaluation for Standard Analysis Case^{1, 4}

Label		Point 1	Point 2	Point 3	Point 4	Point 5	Point 6	Point 7	Point 8
	Elevation, ft	6.0	21.0	0.0	5.5	1.0	-22.0	50.0	31.5
	Azimuth, degrees	260	305	335	182	20	175	315	225
	Node Number	2200142	2201562	2101350	2205657	2101473	2100493	2202850	2203006
	Direction of CEB Displacement to Cause Contact	Radial+	Radial+	Radial+	Radial-	Radial+	Radial-	Radial-	Radial-
L_{des}	Design Seismic Gap Width	3.000	3.000	3.000	3.000	3.000	3.000	3.000	3.000
	Adjacent Structure ³	WPC	WPC	EP	CB	EFW	CB	CB	CB
	Seismic Gap Measurement ID (if available)	2a.01	2d.02	2f.02	3a.01	6a.02	3b.01	Note 2	Note 2
$L_{des} - L_{obs}$	Minimum Seismic Gap Width ²	2.000	1.938	2.000	1.500	1.625	1.188	0.925	0.614
k_{th}^*	Increase factor in CEB deformation to account for ASR threshold	1.079	1.015	1.073	1.012	1.069	1.039	1.027	1.070
	Minimum Measured Seismic Gap Width (adjusted for ASR threshold)	1.921	1.922	1.927	1.482	1.530	1.116	0.950	0.657
$L_s + L_{ns}$	Max. Factored Radial Seismic and Non-Seismic Disp. of CEB in direction of Adjacent Structure ⁵	0.616	0.361	0.002	0.063	0.008	0.000	0.430	0.259
L_a	Maximum Displacement of Adjacent Structure in Direction of CEB	0.009	0.121	0.145	0.085	0.145	0.085	0.202	0.202
L_R	Required Minimum Gap Width, $2 \times \sqrt{(L_s + L_{ns})^2 + L_a^2}$	1.232	0.762	0.290	0.212	0.290	0.170	0.950	0.657
	Remaining Joint Clearance (Equation 10)	0.688	1.160	1.637	1.271	1.240	0.946	0.000 ²	0.000 ²

For footnotes, see Table 17.

SIMPSON GUMPERTZ & HEGER

Engineering of Structures
and Building Enclosures

PROJECT NO: 150252

DATE: 31 July 2016

CLIENT: NextEra Energy Seabrook

BY: R.M. Mones

SUBJECT: Evaluation and Design Confirmation of As-Deformed CEB

VERIFIER: A.T. Sarawit

Table 17. Summary of Displacement Evaluation for Standard-Plus Analysis Case^{1,4}

Label		Point 1	Point 2	Point 3	Point 4	Point 5	Point 6	Point 7	Point 8
	Elevation, ft	6.0	21.0	0.0	5.5	1.0	-22.0	50.0	31.5
	Azimuth, degrees	260	305	335	182	20	175	315	225
	Node Number	2200142	2201562	2101350	2205657	2101473	2100493	2202850	2203006
	Direction of CEB Displacement to Cause Contact	Radial+	Radial+	Radial+	Radial-	Radial+	Radial-	Radial-	Radial-
L_{des}	Design Seismic Gap Width	3.000	3.000	3.000	3.000	3.000	3.000	3.000	3.000
	Adjacent Structure ³	WPC	WPC	EP	CB	EFW	CB	CB	CB
	Seismic Gap Measurement ID (if available)	2a.01	2d.02	2f.02	3a.01	6a.02	3b.01	Note 2	Note 2
$L_{des} - L_{obs}$	Minimum Seismic Gap Width ²	2.000	1.938	2.000	1.500	1.625	1.188	0.923	0.612
k_{th}^*	Increase factor in CEB deformation to account for ASR threshold	1.081	1.012	1.073	1.043	1.069	1.042	1.026	1.072
	Minimum Measured Seismic Gap Width (adjusted for ASR threshold)	1.919	1.925	1.927	1.435	1.531	1.113	0.948	0.656
$L_s + L_{ns}$	Max. Factored Radial Seismic and Non-Seismic Disp. of CEB in direction of Adjacent Structure ⁵	0.614	0.360	0.002	0.063	0.008	0.000	0.429	0.258
L_a	Maximum Displacement of Adjacent Structure in Direction of CEB	0.009	0.121	0.145	0.085	0.145	0.085	0.202	0.202
L_R	Required Minimum Gap Width, $2 \times \sqrt{(L_s + L_{ns})^2 + L_a^2}$	1.229	0.760	0.290	0.212	0.290	0.170	0.948	0.656
	Remaining Joint Clearance (Equation 10)	0.690	1.165	1.637	1.223	1.240	0.943	0.000²	0.000²

¹ All displacements are in inches

² Points 7 and 8 are located on the missile shields above the CEVA and Personnel Hatch openings; all other points are located on the CEB wall. The remaining joint clearance for Points 7 and 8 is set to zero, and the minimum seismic gap width is computed.

³ WPC = West Pipe Chase, EP = Electrical Penetration, CB = Containment Building.

⁴ If displacements are noted as "towards adjacent structure" or "towards CEB", then positive displacements are in the direction that would cause contact between the two considered structures. Otherwise, positive displacements are in the radial outward direction and negative displacements are in the radial inward direction.

⁵ As discussed in the text with Equation 10, non-seismic displacements are taken as zero if they are in the direction away from the adjacent structure.

⁶ Adjacent structure displacements are obtained from Reference 31 whenever possible. The displacement of the CB is not provided at El. +50, so this displacement is linearly extrapolated from the provided displacements of 0.077" at El. +3 ft and 0.085" at El. +6 ft.

Table 18. List of Reference Drawings

Drawing Label	Reference Information
D-1	United Engineers & Constructors Inc., 9763-F-101013 - <i>Excavation Civil Plan - Sheet 5</i> , Rev. 5, 19 March 1981.
D-2	United Engineers & Constructors Inc., 9763-F-101024 - <i>Site Boring Plan Civil Topo & Rock Contours</i> , Rev. 1, 4 June 1976.
D-3	United Engineers & Constructors Inc., 9763-F-101434 - <i>Containment Concrete Sections and Elevations - CEVA dimensions</i> , Rev. 3, 14 April 2015.
D-4	United Engineers & Constructors Inc., 9763-F-101440 - <i>Containment Concrete Equipment Hatch Reinf - Sheet 1</i> , Rev. 10, 30 November 1990.
D-5	United Engineers & Constructors Inc., 9763-F-101446 - <i>Containment Enclosure Building Concrete Shield Wall for Equipment Hatch</i> , Rev. 3, 21 October 1983.
D-6	United Engineers & Constructors Inc., 9763-F-101448 - <i>Containment Enclosure Building Concrete Section & Typical Dome Details</i> , Rev. 11, 5 August 1983.
D-7	United Engineers & Constructors Inc., 9763-F-101451 - <i>Containment Enclosure Building Concrete Plan at EL. (-)30 ft - 0 in., South</i> , Rev. 8, 22 October 1979.
D-8	United Engineers & Constructors Inc., 9763-F-101452 - <i>Containment Enclosure Building Concrete Plan at EL (-)30 ft - 0 in., North</i> , Rev. 9, 16 December 1983.
D-9	United Engineers & Constructors Inc., 9763-F-101453 - <i>Containment Enclosure Building Concrete Plan at EL. 10 ft -0 in., South</i> , Rev. 11, 27 January 1984.
D-10	United Engineers & Constructors Inc., 9763-F-101454 - <i>Containment Enclosure Building Concrete Plan at EL 10 ft -0 in., North</i> , Rev. 3, 19 March 1982.
D-11	United Engineers & Constructors Inc., 9763-F-101455 - <i>Containment Enclosure Building Concrete Plan at EL 37 ft-0 ½ in., South</i> , Rev. 11, 11 November 1983.
D-12	United Engineers & Constructors Inc., 9763-F-101456 - <i>Containment Enclosure Building Concrete at EL 37 ft- 0 1/2 in. North</i> , Rev. 3, 20 August 1982.
D-13	United Engineers & Constructors Inc., 9763-F-101457 - <i>Containment Enclosure Building Concrete Sections - Sheet 1</i> , Rev. 12, 17 September 1982.
D-14	United Engineers & Constructors Inc., 9763-F-101458 - <i>Containment Enclosure Building Concrete Sections - Sheet 2</i> , Rev. 14, 27 January 1984.
D-15	United Engineers & Constructors Inc., 9763-F-101459 - <i>Containment Enclosure Building Concrete Inside Elev. Stretch-out, East Half</i> , Rev. 9, 22 October 1982.
D-16	United Engineers & Constructors Inc., 9763-F-101460 - <i>Containment Enclosure Building Concrete Inside Elev. Stretch-out, West Half</i> , Rev. 7, 20 August 1982.
D-17	United Engineers & Constructors Inc., 9763-F-101545 - <i>Pri. Aux. Bldg., RHR & CS Eqpt. Vault Concrete Sections - SH. 20</i> , Rev. 9, 22 December 1983.
D-18	United Engineers & Constructors Inc., 9763-F-101560 - <i>Fuel Storage Building Concrete Plan at EL. (-) 16 ft - 4 3/4 & (-) 11 ft 9 1/2</i> , Rev. 3, 8 September 1978.
D-19	United Engineers & Constructors Inc., 9763-F-101565 - <i>Concrete Typical Details</i> , Rev. 17, 18 March 1983.
D-20	United Engineers & Constructors Inc., 9763-F-101610 - <i>Electrical Tunnel Concrete Plans at EL. (-) 26 ft -0 in. & (-) 20 ft -0 in.</i> , Rev. 11, 21 June 1985.
D-21	United Engineers & Constructors Inc., 9763-F-101611 - <i>Electrical Tunnel Concrete Plans at EL. 0 ft-0 in. & 8 ft - 2 in.</i> , Rev. 13, 21 June 1985.


Table 18. List of Reference Drawings

Drawing Label	Reference Information
D-22	United Engineers & Constructors Inc., 9763-F-101612 - <i>Electrical Tunnel Concrete Sections Sheet 1</i> , Rev. 10, 2 December 1983.
D-23	United Engineers & Constructors Inc., 9763-F-101613 - <i>Electrical Tunnel Concrete Sections Sheet 2</i> , Rev. 4, 29 December 1983.
D-24	United Engineers & Constructors Inc., 9763-F-101619 - <i>Containment Enclosure Ventilation Area Concrete Plans at EL 21 ft-6 in. & 53 ft-0 in.</i> , Rev. 11, 6 March 1985.
D-25	United Engineers & Constructors Inc., 9763-F-101620 - <i>Containment Enclosure Ventilation Area Concrete Section - Sheet 1</i> , Rev. 5, 13 January 1984.
D-26	United Engineers & Constructors Inc., 9763-F-101621 - <i>Containment Enclosure Ventilation Area Concrete Section - Sheet 2</i> , Rev. 5, 6 March 1985.
D-27	United Engineers & Constructors Inc., 9763-F-101622 - <i>Containment Enclosure Ventilation Area Steel Framing Plan at EL. 53 ft - 0 in.</i> , Rev. 5, 13 December 1984.
D-28	United Engineers & Constructors Inc., 9763-F-101625 - <i>Mechanical Penetration Area Concrete Plans at EL. (-) 34 ft - 6 in. & (-) 8 ft-6in.</i> , Rev. 10, 6 May 1983.
D-29	United Engineers & Constructors Inc., 9763-F-101626 - <i>Main Steam & Feedwater Pipe Chase (West) Concrete Plans at EL 3 ft-0 in. & (-) 11 ft-2 1/2 in.</i> , Rev. 14, 10 February 1984.
D-30	United Engineers & Constructors Inc., 9763-F-101627 - <i>Main Steam & Feedwater Pipe Chase (West) Concrete Section - Sheet 1</i> , Rev. 13, 18 November 1983.
D-31	United Engineers & Constructors Inc., 9763-F-101628 - <i>Main Steam & Feedwater Pipe Chase (West) Concrete Section - Sheet 2</i> , Rev. 9, 29 December 1983.
D-32	United Engineers & Constructors Inc., 9763-F-101629 - <i>Main Steam & Feedwater Pipe Chase (West) Concrete Section - Sheet 3</i> , Rev. 7, 5 August 1983.
D-33	United Engineers & Constructors Inc., 9763-F-101630 - <i>Main Steam & Feedwater Pipe Chase (West) Concrete Plans at EL 51 ft-6 in. & 64 ft-6 in.</i> , Rev. 9, 2 December 1983.
D-34	United Engineers & Constructors Inc., 9763-F-101631 - <i>Main Steam & Feedwater Pipe Chase (West) Concrete Section - Sheet 4</i> , Rev. 7, 16 June 1982.
D-35	United Engineers & Constructors Inc., 9763-F-101632 - <i>Main Steam & Feedwater Pipe Chase (West) Concrete Section - Sheet 5</i> , Rev. 8, 29 December 1983.
D-36	United Engineers & Constructors Inc., 9763-F-101633 - <i>Main Steam & Feedwater Pipe Chase (West) Concrete Section - Sheet 6</i> , Rev. 5, 29 July 1983.
D-37	United Engineers & Constructors Inc., 9763-F-101641 - <i>Pipe Tunnel Concrete Plans at EL. 4 ft-11 in. & 21 ft-6 in.</i> , Rev. 2, 18 June 1981.
D-38	United Engineers & Constructors Inc., 9763-F-101649 - <i>Main Stm. & Feedwater Pipe Chase (West) Steel Roof Framing Plan at EL. 50 ft-3 in.</i> , Rev. 7, 4 November 1983.


Table 18. List of Reference Drawings

Drawing Label	Reference Information
D-39	United Engineers & Constructors Inc., 9763-F-101650 - Main Steam & Feedwater Pipe Chase (East) Concrete Plans at EL. 3 ft-0 in. & 22 ft-0 in., Rev. 12, 14 November 1985.
D-40	United Engineers & Constructors Inc., 9763-F-101651 - Main Steam & Feedwater Pipe Chase (East) Concrete Plans at EL. 5 ft-6 in. & 64 ft-6 in., Rev. 8, 14 November 1985.
D-41	United Engineers & Constructors Inc., 9763-F-101652 - Main Steam & Feedwater Pipe Chase (East) Concrete Sections - Sheet 1, Rev. 7, 14 November 1985.
D-42	United Engineers & Constructors Inc., 9763-F-101653 - Main Steam & Feedwater Pipe Chase (East) Concrete Sections - Sheet 2, Rev. 8, 27 January 1984.
D-43	United Engineers & Constructors Inc., 9763-F-101659 - Main Steam & Feedwater Pipe Chase (West) Steel Plan and Sections - South Stair, Rev. 1, 8 April 1983.
D-44	United Engineers & Constructors Inc., 9763-F-101660 - Emergency Feedwater Pump Building Concrete Plan at EL. 27 ft-0 in. & 47 ft-0 in., Rev. 9, 2 December 1983.
D-45	United Engineers & Constructors Inc., 9763-F-101661 - Emergency Feedwater Pump Building Concrete Sections - Sheet No. 2, Rev. 4, 16 June 1982.
D-46	United Engineers & Constructors Inc., 9763-F-101662 - Emergency Feedwater Pump Building Concrete Sections - Sheet No. 3, Rev. 5, 1 July 1982.
D-47	United Engineers & Constructors Inc., 9763-F-101842 - Concrete General Notes & Reinforcing Splice Lengths, Rev. 14, 21 October 1983.
D-48	United Engineers & Constructors Inc., 9763-F-101847 - Dewatering Systems for Plant Bldgs & Structures Civil, Rev. 1, 27 June 1978.
D-49	United Engineers & Constructors Inc., 9763-F-101918 - Containment Enclosure Building Steel - Pressure Seal Plate Assembly - Sheet 1, Rev. 1, 10 February 1984.
D-50	United Engineers & Constructors Inc., 9763-F-102153 - Containment Building Enclosure Building Platform, Rev. 5, 10 February 1984.
D-51	United Engineers & Constructors Inc., 9763-F-103232 - Fill & Backfill Concrete Sections, Rev. 2, 30 December 1983.
D-52	United Engineers & Constructors Inc., 9763-F-111574 - Fuel Storage Building Concrete Sections - Sheet 4, Rev. 6, 31 July 1981.
D-53	United Engineers & Constructors Inc., 9763-F-113225 - Fill & Backfill Concrete Profiles - Sheet 1, Rev. 3, 30 December 1983.
D-54	United Engineers & Constructors Inc., 9763-F-113226 - Fill & Backfill Concrete Profiles - Sheet 2, Rev. 3, 30 December 1983.
D-55	United Engineers & Constructors Inc., 9763-F-113229 - Fill & Backfill Concrete Plan & Sections, Rev. 5, 30 December 1983.



Table 18. List of Reference Drawings

Drawing Label	Reference Information
D-56	United Engineers & Constructors Inc., 9763-F-113230 - <i>Backfill Concrete Schedule</i> , Rev. 5, 3 September 1982.
D-57	Bishopric Products Company, FP10980 - <i>Plant Vent Stack Elevation</i> , Rev. 1, 2 February 1984.
D-58	United Engineers & Constructors Inc., 9763-F-101912 – <i>Containment Enclosure Building Concrete Dome Reinforcing</i> , Rev. 3, 5 August 1983.
D-59	United Engineers & Constructors Inc., 9763-F-101494 – <i>Plant Vent Stack Plans, Elevations, Sections & Details – Sheet 1</i> , Rev. 2, 30 May 1986.
D-60	United Engineers & Constructors Inc., 9763-F-101917 – <i>Plant Vent Stack Plans, Elevations, Sections & Details – Sheet 3</i> , Rev. 3, 30 May 1986.
D-61	United Engineers & Constructors Inc., 9763-F-101493 – <i>Plant Vent Stack Breeching Plans, Sections & Details</i> , Rev. 2, 30 May 1986.



Table 19. Prospective Threshold Measurement Set A

Threshold Measurement	Measurement Type	Elevation & Azimuth	Baseline Measurement ¹ , CCI, mm/m	Baseline Measurement ¹ Date
CI-1	CCI	El. -27.5 ft, AZ 32	0.16±0.04	April 2016
CI-2	CCI	El. -20.0 ft, AZ 40	0.06±0.02	April 2016
CI-3	CCI	El. -23.0 ft, AZ 53	0.05±0.01	April 2016
CI-4	CCI	El. -24.0 ft, AZ 73	0.14±0.04	April 2016
CI-5	CCI	El. -24.0 ft, AZ 95	0.14±0.04	April 2016
CI-6	CCI	El. -27.5 ft, AZ 113	0.12±0.04	April 2016
CI-7	CCI	El. -27.5 ft, AZ 124	0.12±0.04	April 2016
CI-8	CCI	El. -24.0 ft, AZ 144	0.13±0.04	April 2016
CI-9	CCI	El. -27.5 ft, AZ 163	0.21±0.06	April 2016
CI-10	CCI	El. -20.0 ft, AZ 175	0.18±0.05	April 2016
Average of Baseline CCI Measurements			0.13 mm/m	
Threshold Limit			0.16 mm/m	

¹ "Baseline measurement" refers to the measurements that are used to establish the Threshold Limit, but do not represent the first time the ASR monitoring grid was measured.



Table 20. Prospective Threshold Measurement Set B

Threshold Measurement	Measurement Type	Elevation & Azimuth	Baseline Measurement ¹ , CCI, mm/m	Baseline Measurement ¹ Date
CI-11	CCI	El. -19.0 ft, AZ 197	0.28±0.05	April 2016
CI-12	CCI	El. -19.0 ft, AZ 230	0.28±0.05	April 2016
CI-13	CCI	El. 7.5 ft, AZ 214	0.61±0.08	April 2016
CI-14	CCI	El. -24.0 ft, AZ 309	0.15±0.04	April 2016
CI-15	CCI	El. -24.0 ft, AZ 318	0.53±0.11	April 2016
Mean of Baseline CCI Measurements			0.37 mm/m	
Threshold Limit			0.44 mm/m	

¹ "Baseline measurement" refers to the measurements that are used to establish the Threshold Limit, but do not represent the first time the ASR monitoring grid was measured.



Table 21. Prospective Threshold Measurement Set C

Measurement ID	3a.01-01	2d.02-01	2d.02-02	2f.02-02	6a.02-01	1h.01-07	1h.01-06	1h.01-05	3a.01-08	3a.01-09
Measurement Type	Seismic Gap	Seismic Gap	Seismic Gap	Seismic Gap	Seismic Gap	Seismic Gap	Seismic Gap	Seismic Gap	Annulus Width	Annulus Width
Measurement Azimuth	180	305	310	335	20	260	270	280	220	240
Measurement Elevation	+5.5 ft	+21 ft	+21 ft	0 ft	+1 ft	+22 ft	+22 ft	+22 ft	+9 ft	+9 ft
Relative-to Structure	CB	Personnel Hatch	Personnel Hatch	W. Pipe Chase	EFW Pump Bldg	CB	CB	CB	CB	CB
Direction of deformation	Inward	Inward	Inward	Inward	Inward	Outward	Outward	Outward	Inward	Inward
Measurement taken from Inside or Outside of Annulus	Inside	Outside	Outside	Outside	Outside	Inside	Inside	Inside	Inside	Inside
Baseline Measurement Date and Report Reference	April 2016 [5]	April 2016 [5]	April 2016 [5]	April 2016 [5]	April 2016 [5]	Mar. 2015 [2]	TBD	TBD	TBD	TBD
$d_{n,baseline}$, in.	1.5	1.97	2.41	1.99	1.63	4.25	4.50 ^A	4.75 ^A	51.00 ^A	52.00 ^A
$d_{n,design}$, in.	3.0	3.0	3.0	3.0	3.0	3.00	3.00	3.00	54.00	54.00
Baseline Measurement, in. $ d_{n,baseline} - d_{n,design} $	1.50	1.03	0.59	1.01	1.37	1.25	1.50	1.75	3.00	2.00
$d_{n,FEA,baseline}$, in. ^B	-0.34	-0.65	-0.94	-0.66	-0.47	0.94	1.13	0.96	-1.01	-0.41
$d_{n,FEA,1.2}$, in. ^B	-0.34	-0.69	-1.01	-0.75	-0.53	1.09	1.32	1.12	-1.18	-0.48
$k_{n,thf}$	1.01	1.05	1.07	1.13	1.14	1.16	1.16	1.17	1.17	1.17
Local Threshold Limit, in. $ d_{n,baseline} - d_{n,design} \times k_{n,thf}$	1.52	1.08	0.63	1.14	1.56	1.45	1.74	2.05	3.51	2.34
Average of Baseline Measurements			1.50 in.							
Threshold Limit (based on projected baseline values)			1.70 in.							

^A Baseline measurement not yet taken, value for $d_{n,baseline}$ shown in this table is a projected baseline value using measurements recorded during walkdowns in March 2015.

^B FEA simulated deformations are taken from Standard Analysis Case (as defined in Section) except for the locations at Azimuths 220 and 240 which use the Standard-Plus Analysis Case, which was performed to increase inward deformation at these azimuths.

10. FIGURES

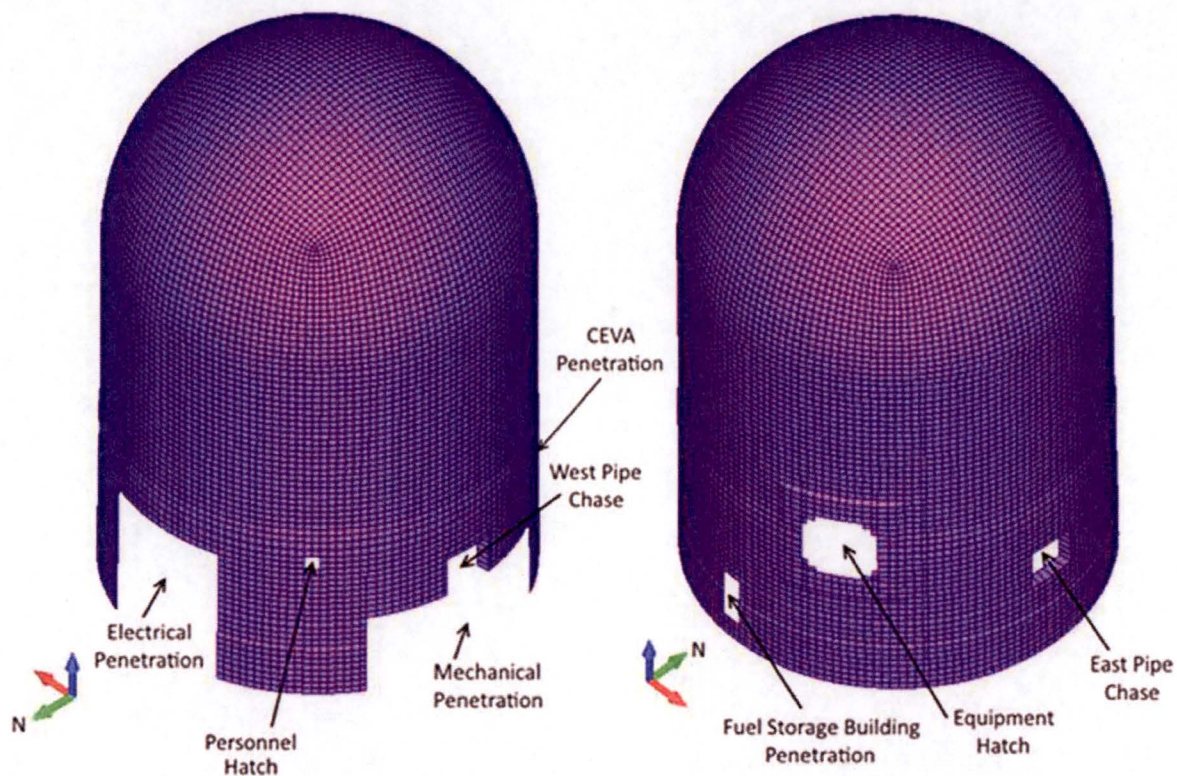


Figure 1. Image of Containment Enclosure Building with Openings Labeled

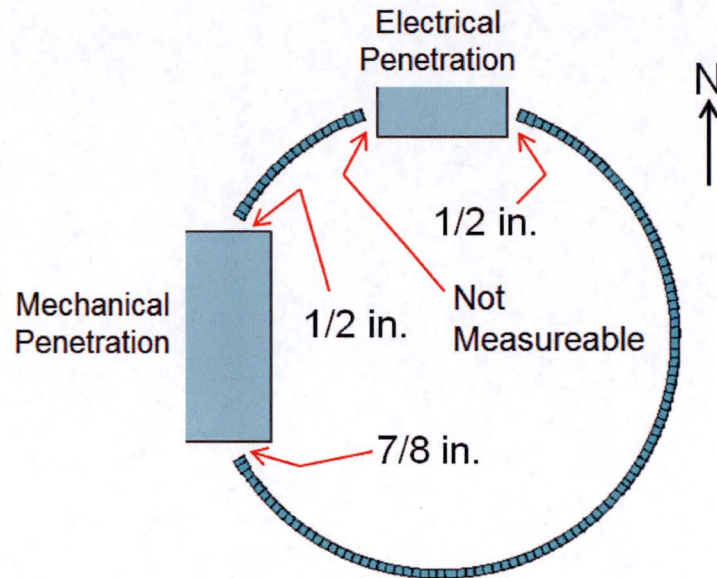


Figure 2. Measurements of Tangential Movement at Base of CEB Wall [2]

Note: Seismic isolation joint between CEB and west wall of the Electrical Penetration could not be accessed for measurement.

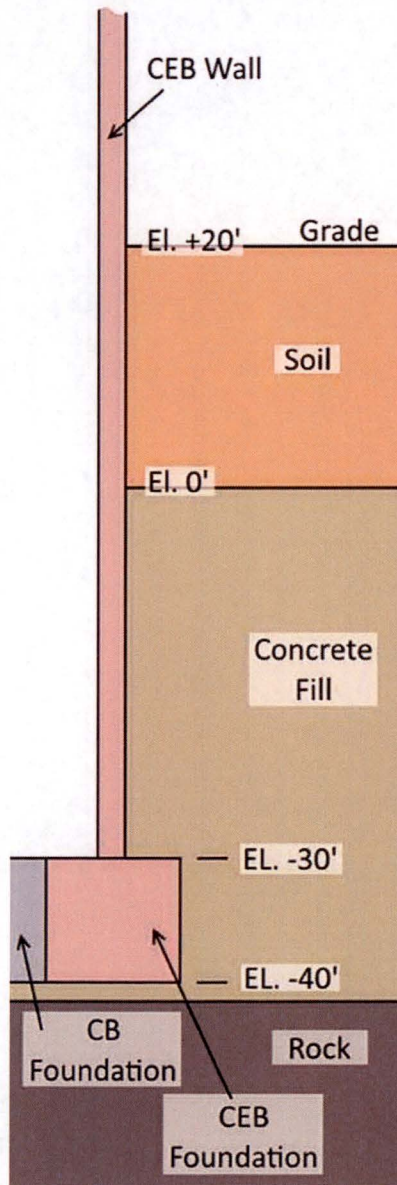


Figure 3. Concrete Fill and Soil on Exterior of CEB Wall (Not to Scale)

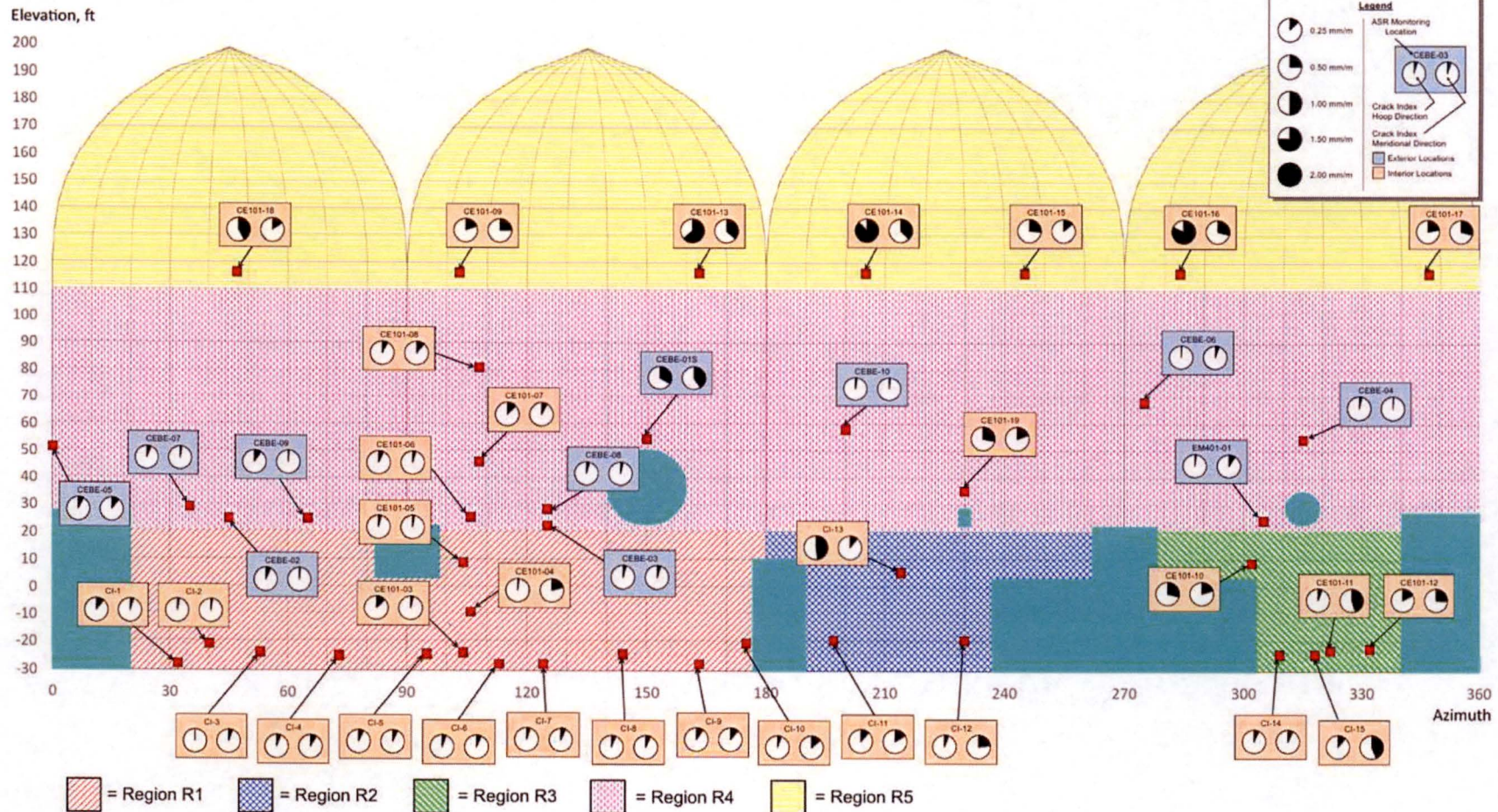


Figure 4. ASR Regions and Crack Index Measurement Locations

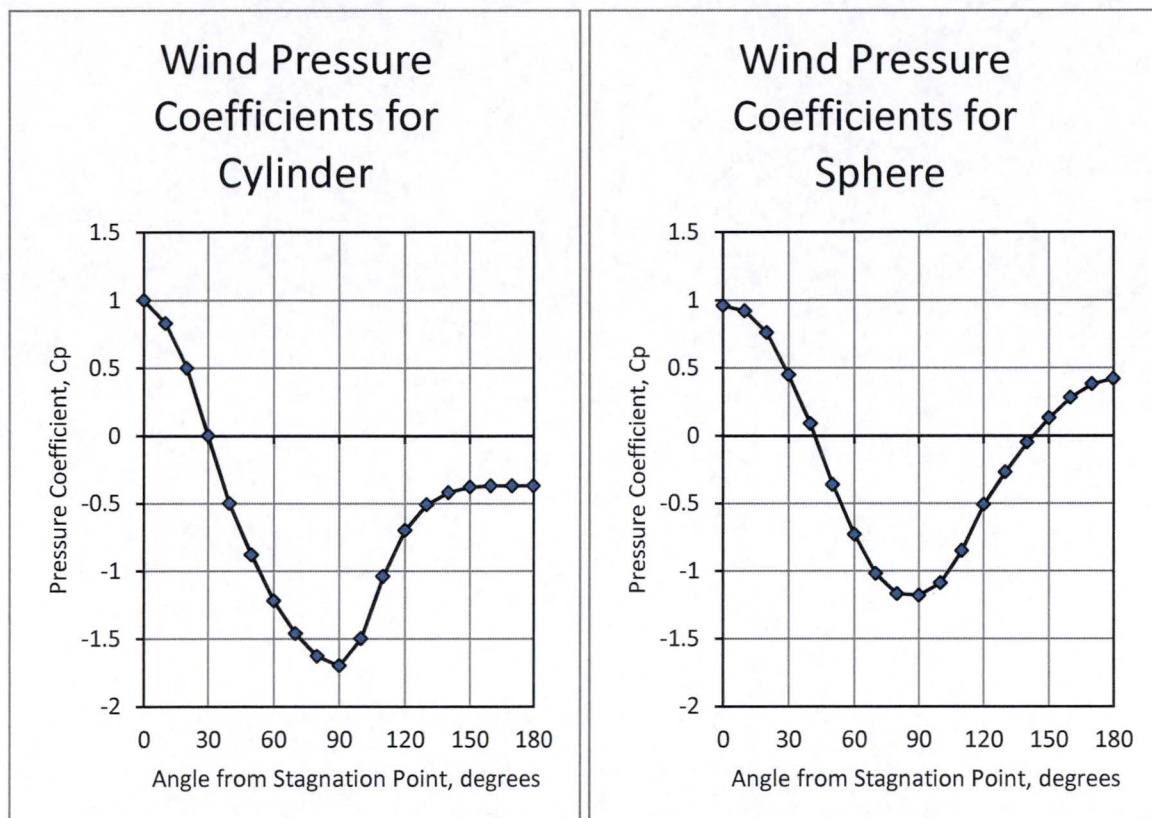


Figure 5. Wind Pressure Coefficients for Cylinder and Sphere

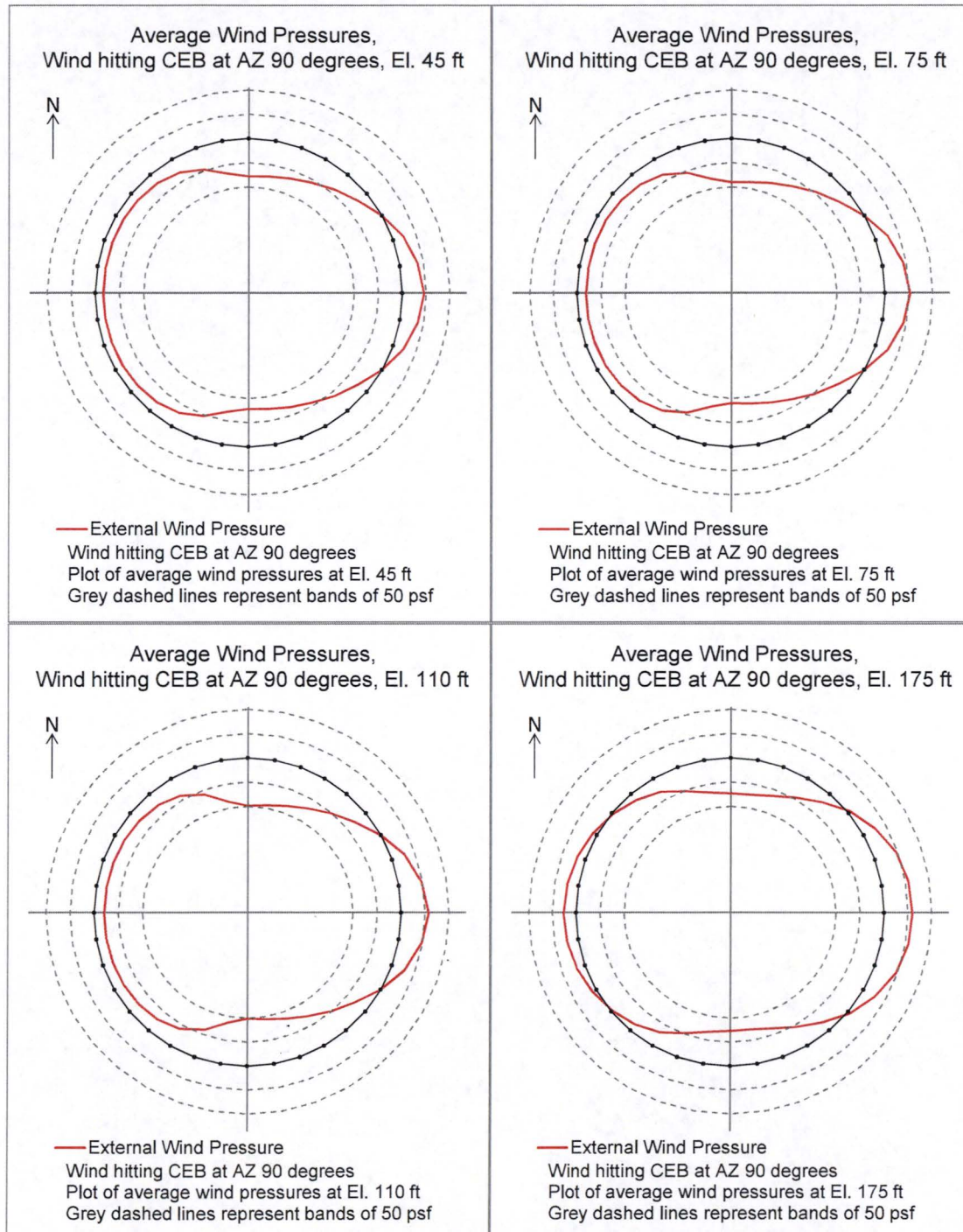


Figure 6. External Wind Pressures Acting on CEB at Various Elevations

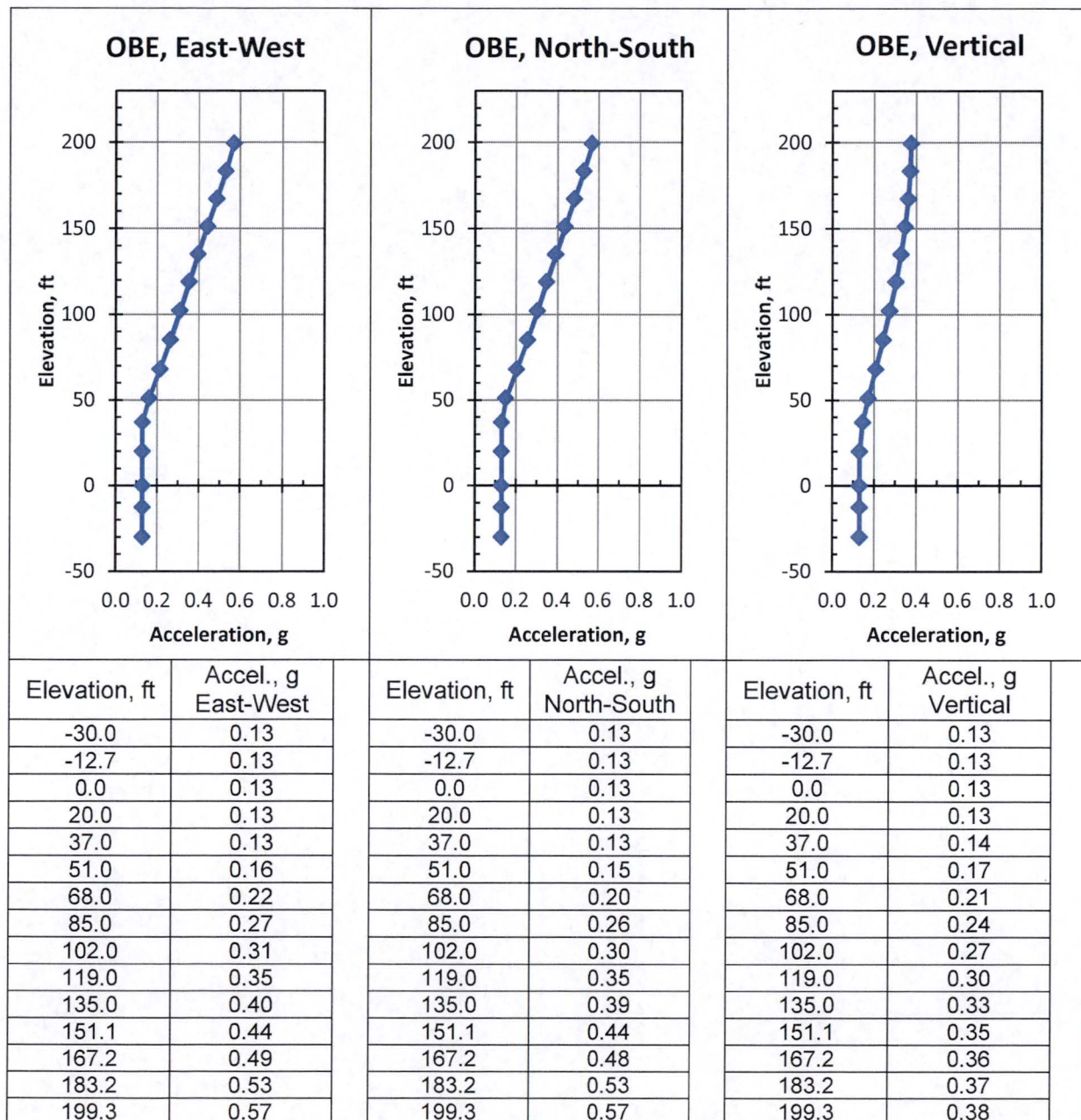


Figure 7. Maximum Acceleration Profiles for OBE

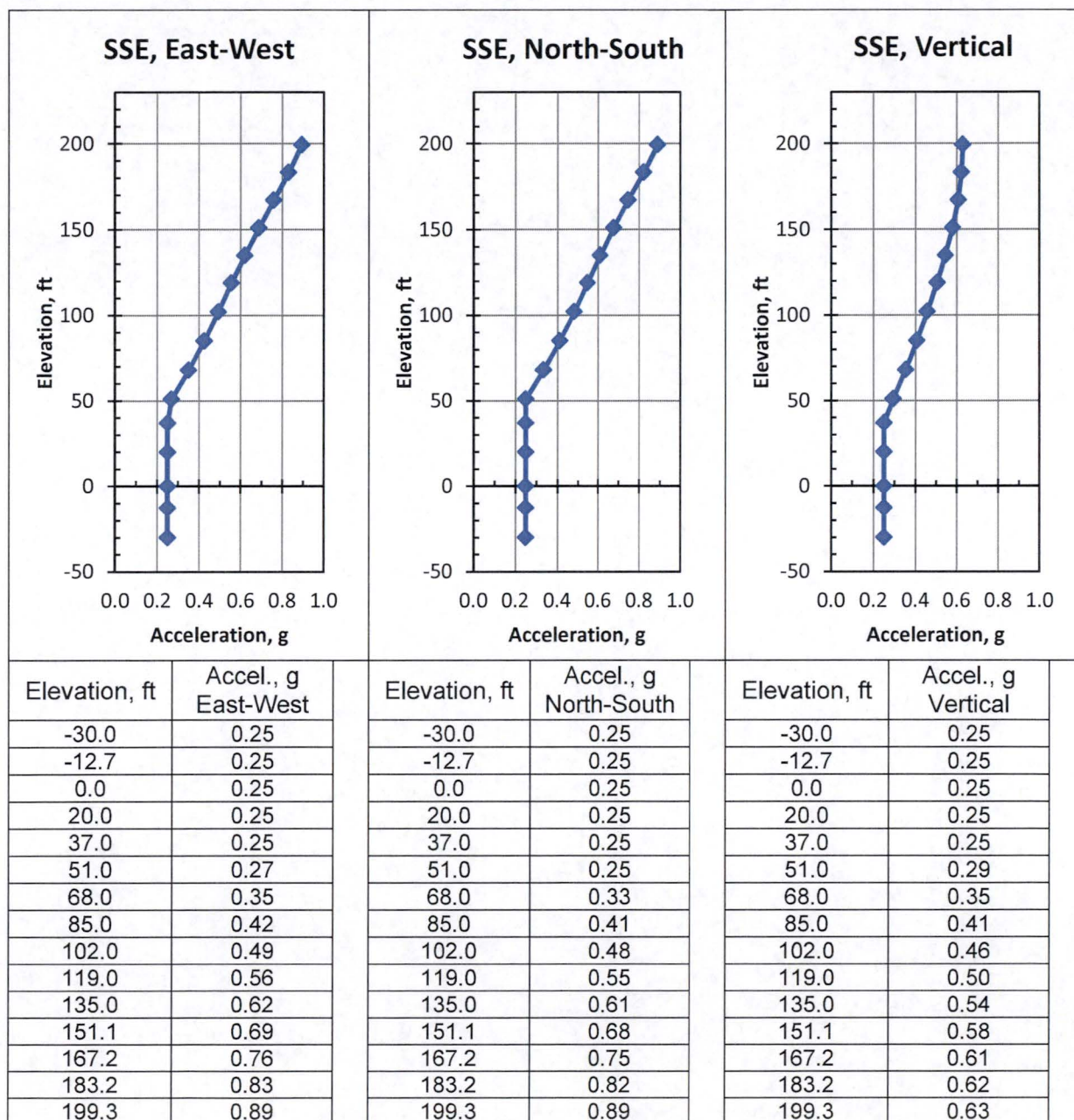


Figure 8. Maximum Acceleration Profiles for SSE

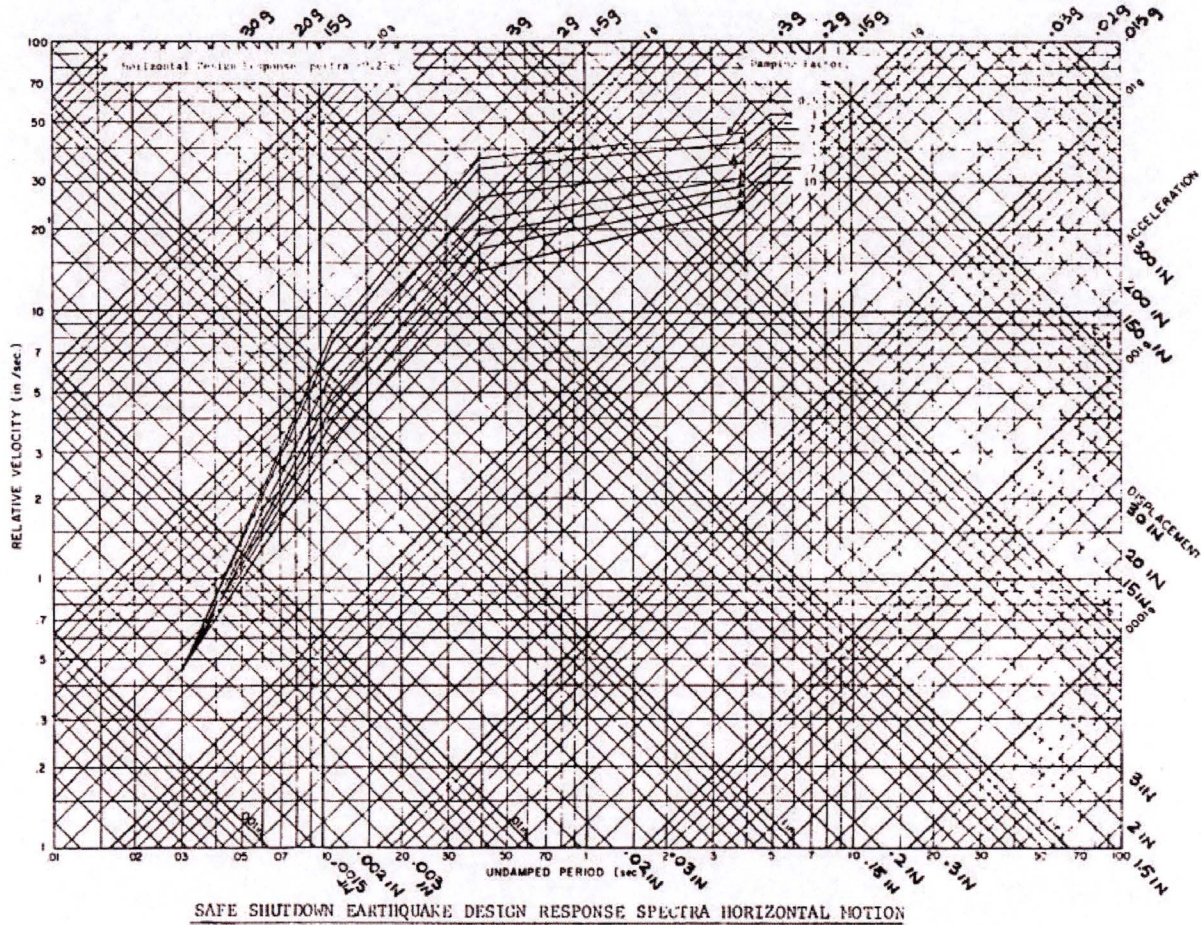


Figure 9. Horizontal SSE Spectra [8]
(Horizontal OBE Spectra are obtained by reducing SSE values by 50%)

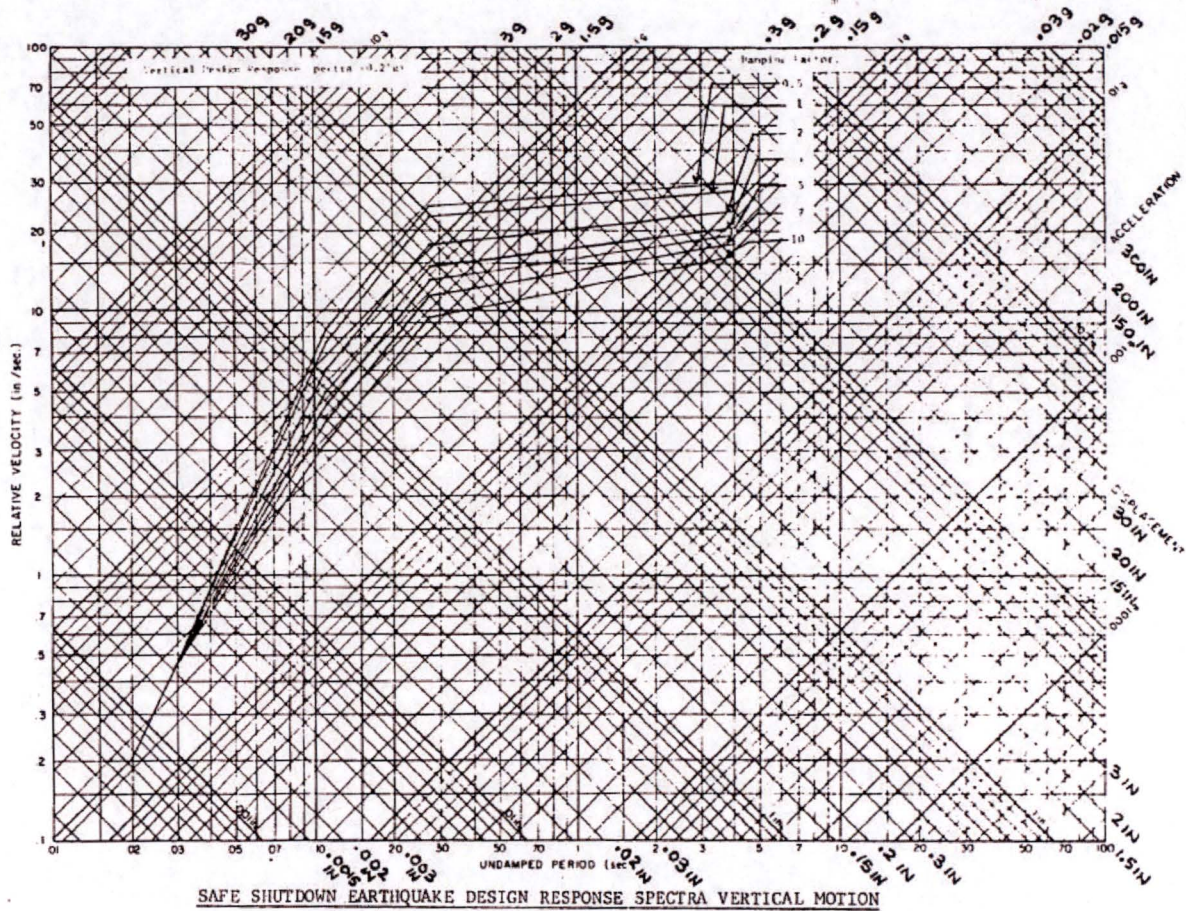


Figure 10. Vertical SSE Spectra [8]

(Vertical OBE Spectra are obtained by reducing SSE values by 50%)

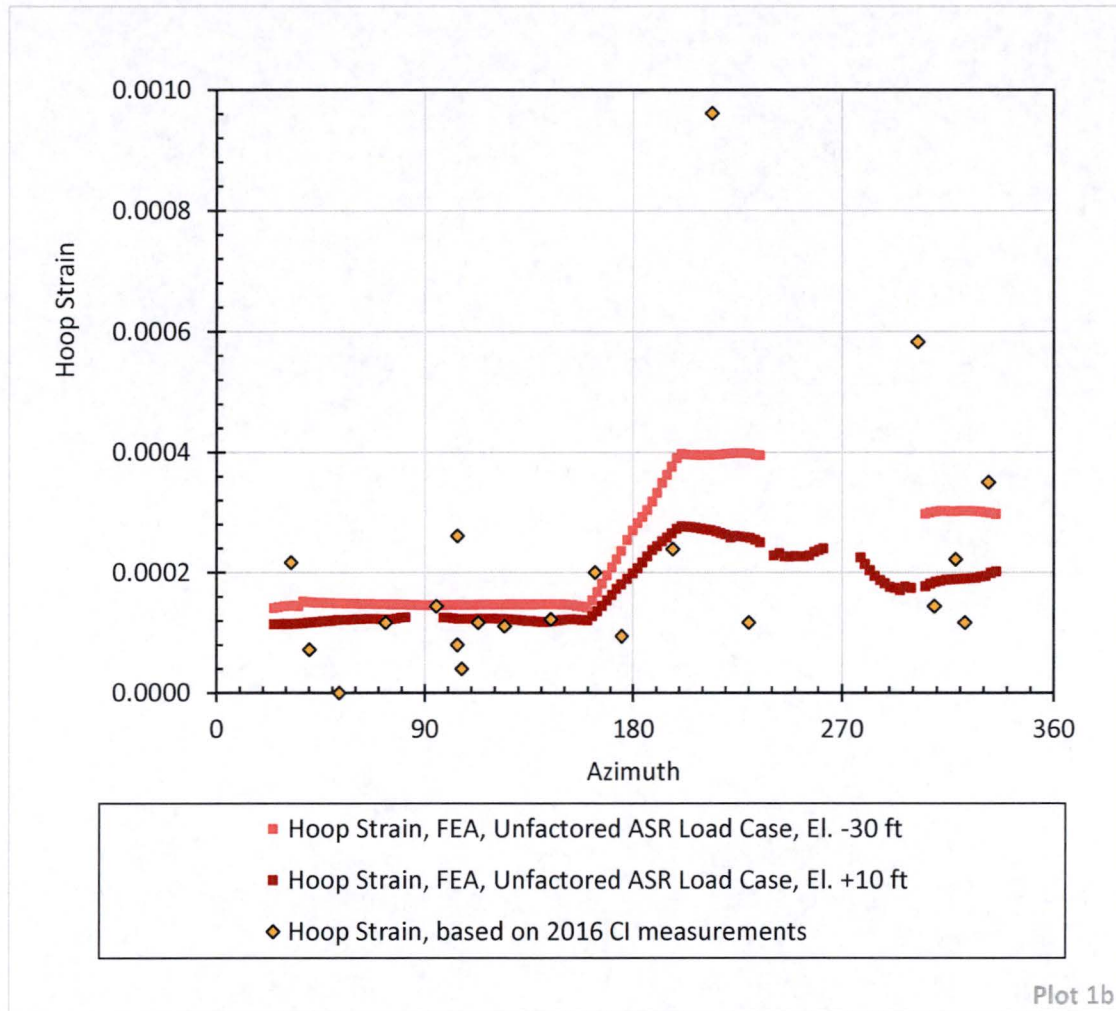


Figure 11. Comparison of Below-Grade Hoop ASR Strains with Crack Index Measurements

Note: FEA Strains for ASR are plotted at El. -30 ft and El. +10 ft, which correspond to the minimum and maximum elevations of below-grade CI grids.

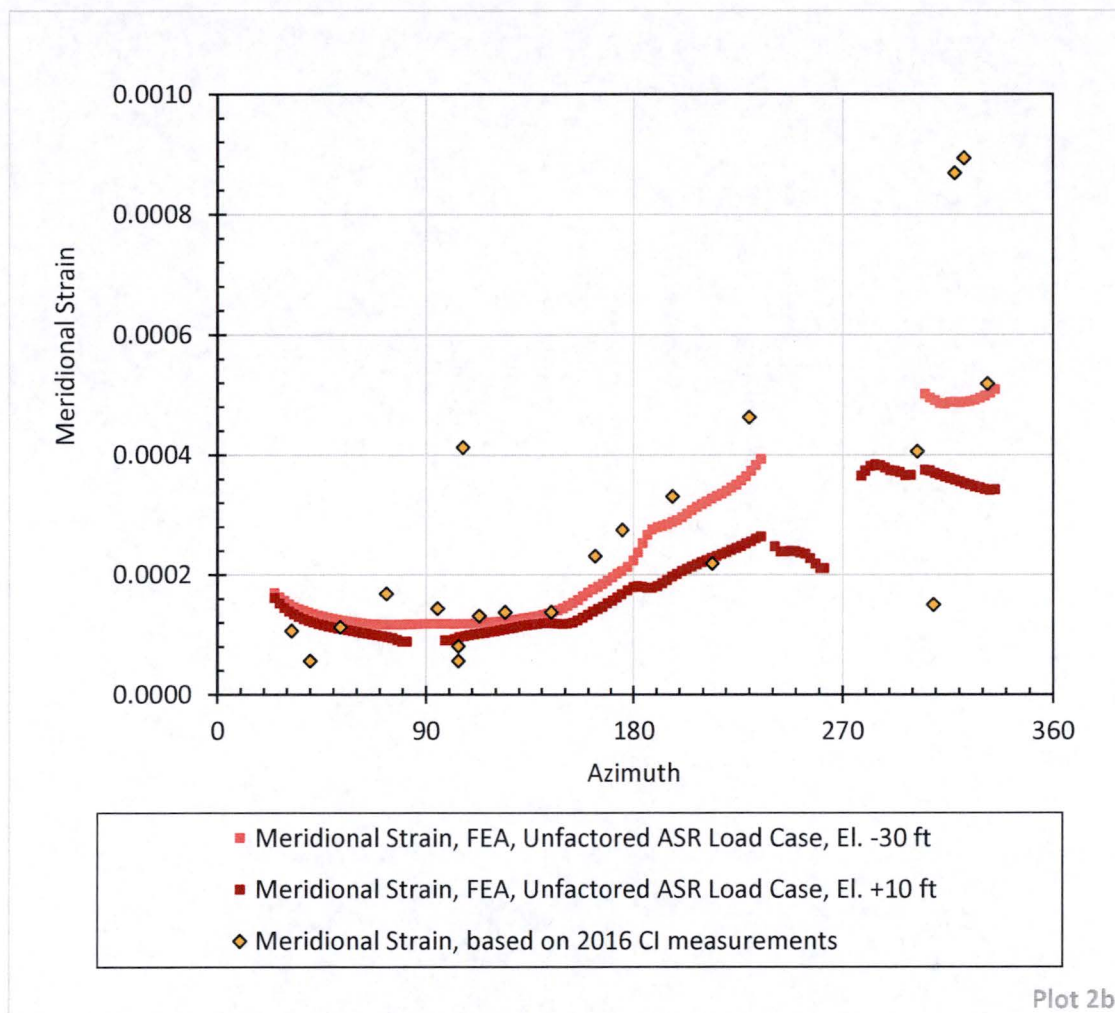


Figure 12. Comparison of Below-Grade Meridional ASR Strains with Crack Index Measurements

Note: FEA Strains for ASR are plotted at El. -30 ft and El. +10 ft, which correspond to the minimum and maximum elevations of below-grade CI grids.

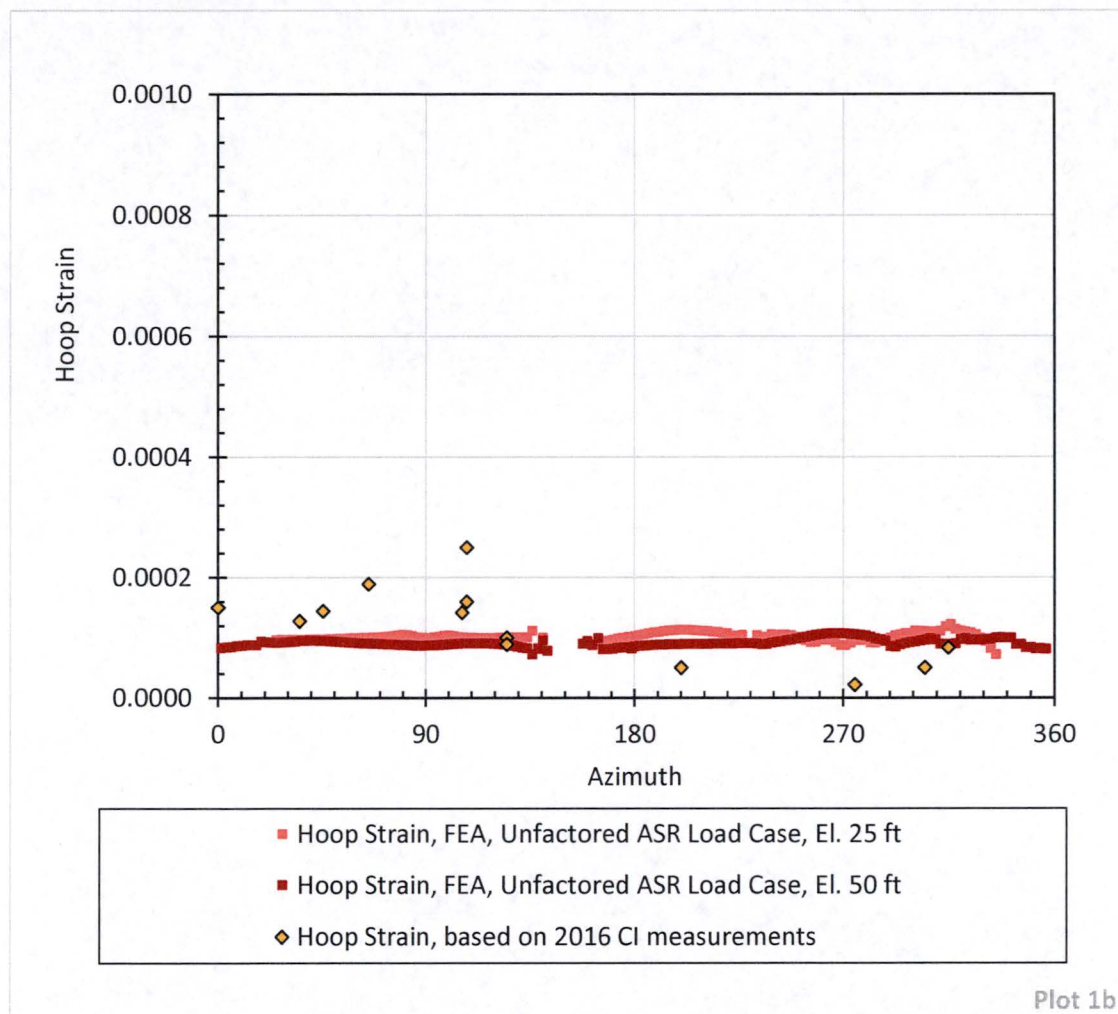


Figure 13. Comparison of Above-Grade Hoop ASR Strains with Crack Index Measurements

Note: Comparison is for strains and CI measurements between grade (El. +20 ft) and the springline (El. +119 ft).

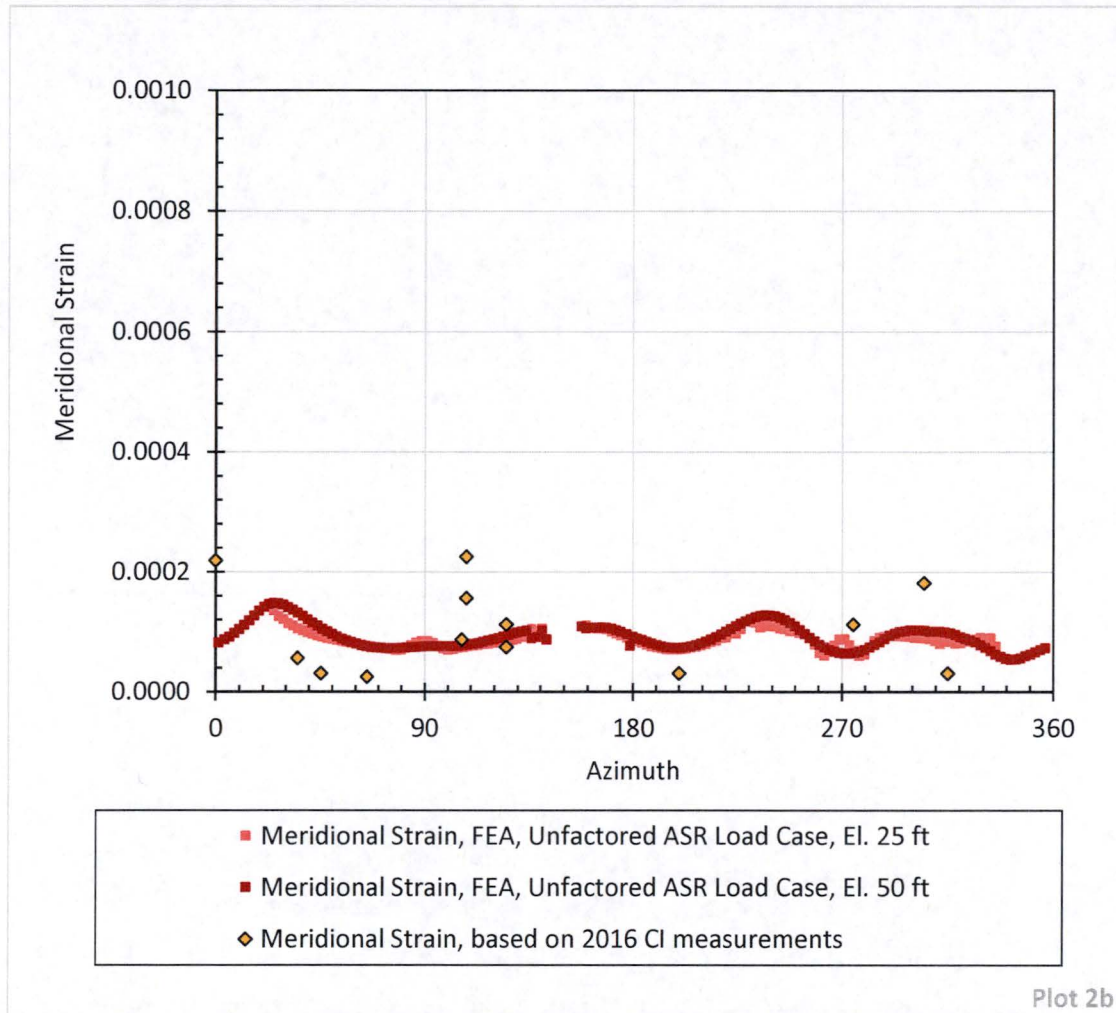


Figure 14. Comparison of Above-Grade Meridional ASR Strains with Crack Index Measurements

Note: Comparison is for strains and CI measurements between grade (El. +20 ft) and the springline (El. +119 ft).

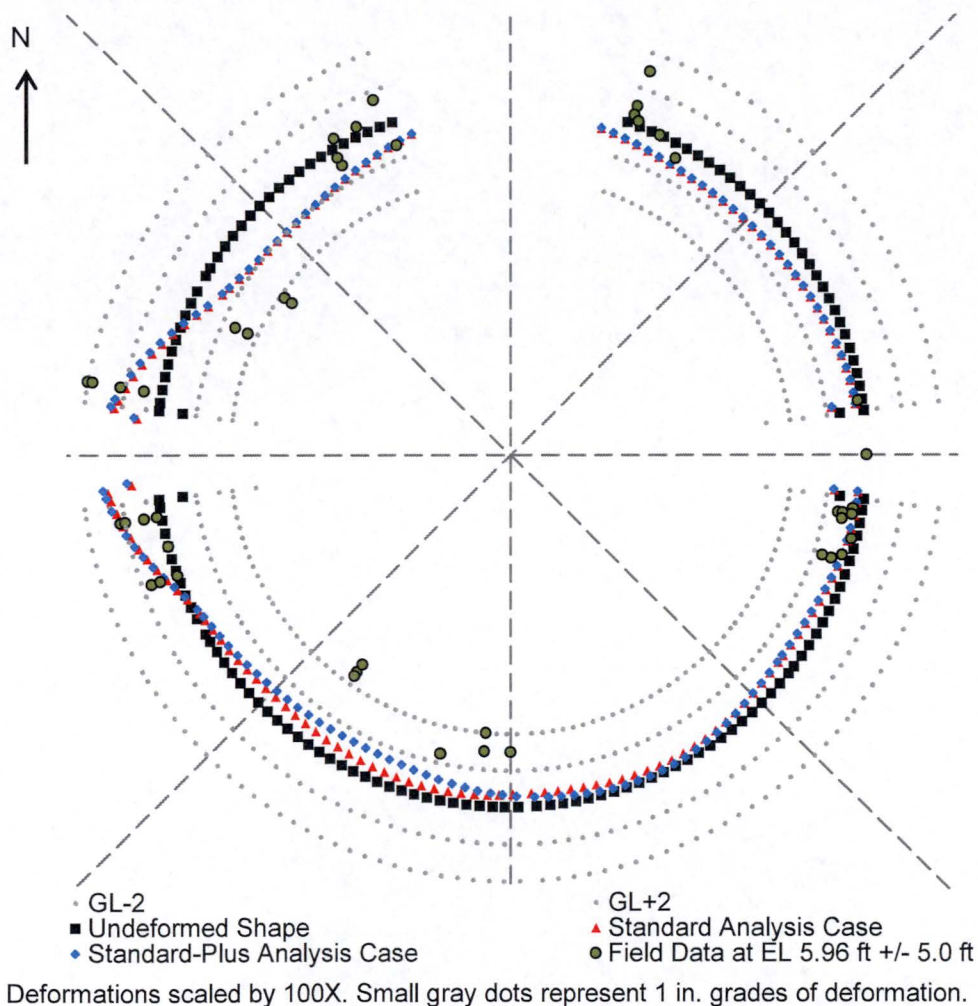
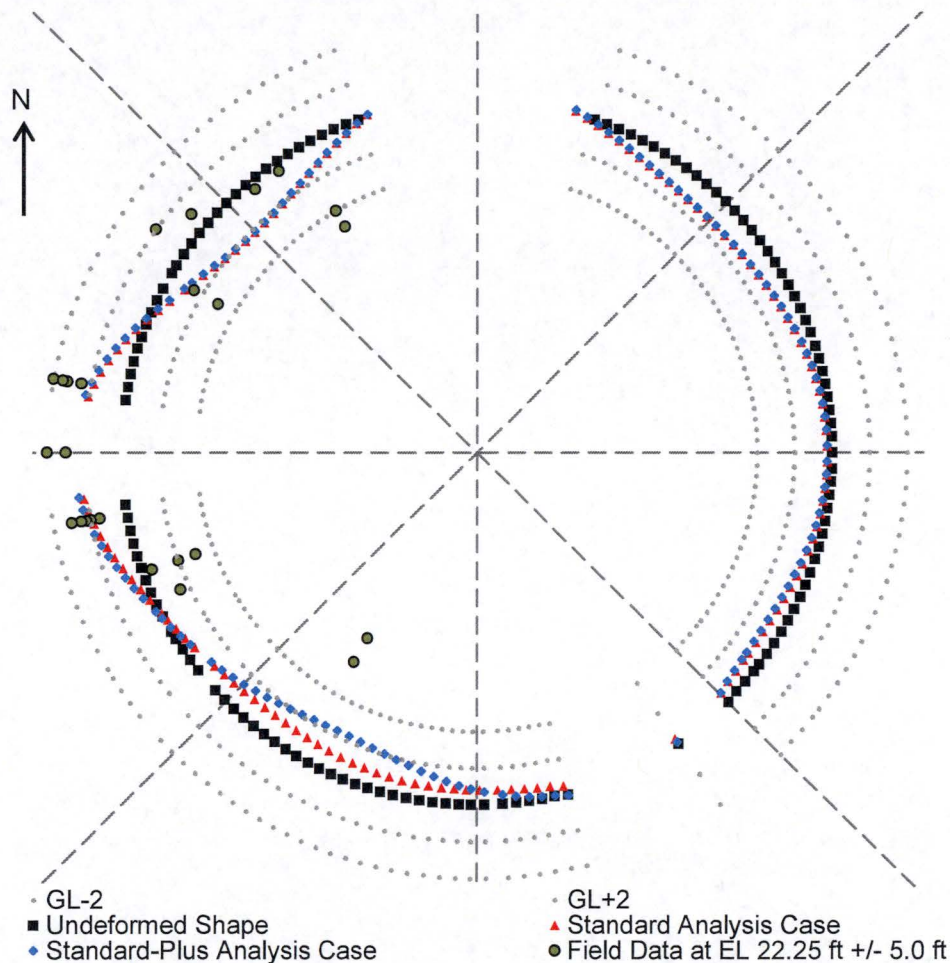
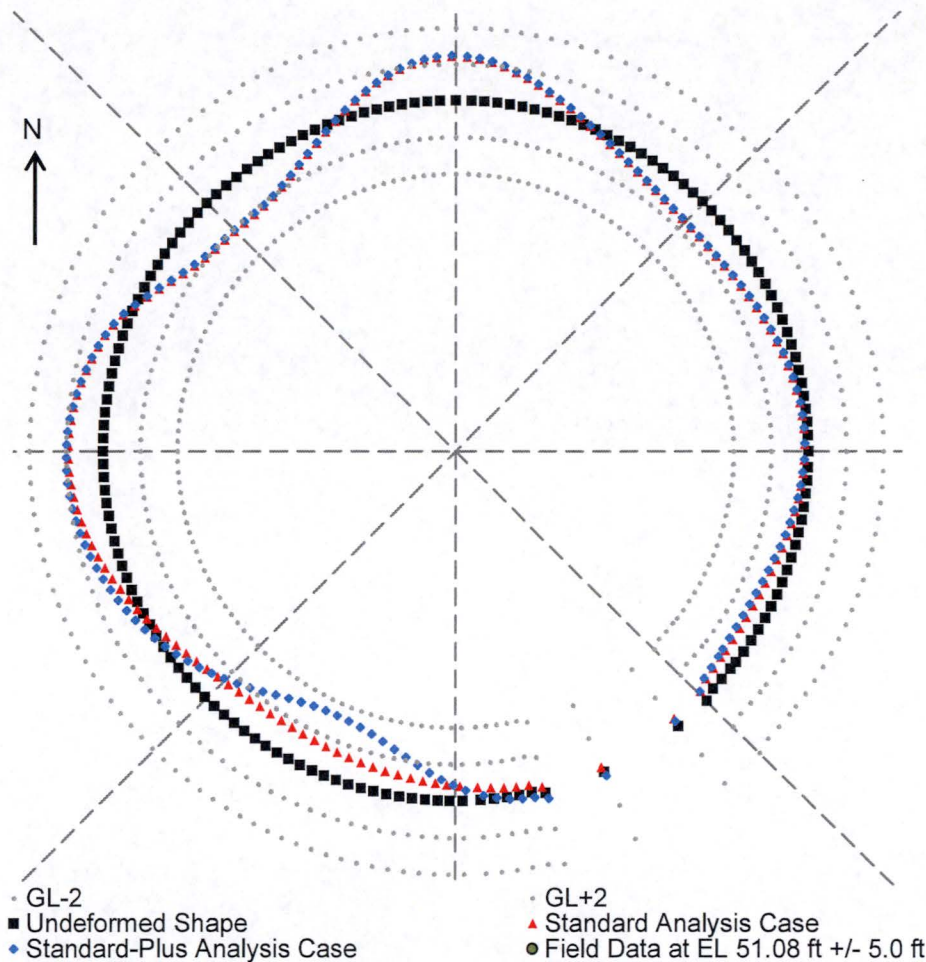


Figure 15. Comparison between As-Deformed Condition Simulations and Field Measurements at El. 6 ft



Deformations scaled by 100X. Small gray dots represent 1 in. grades of deformation.

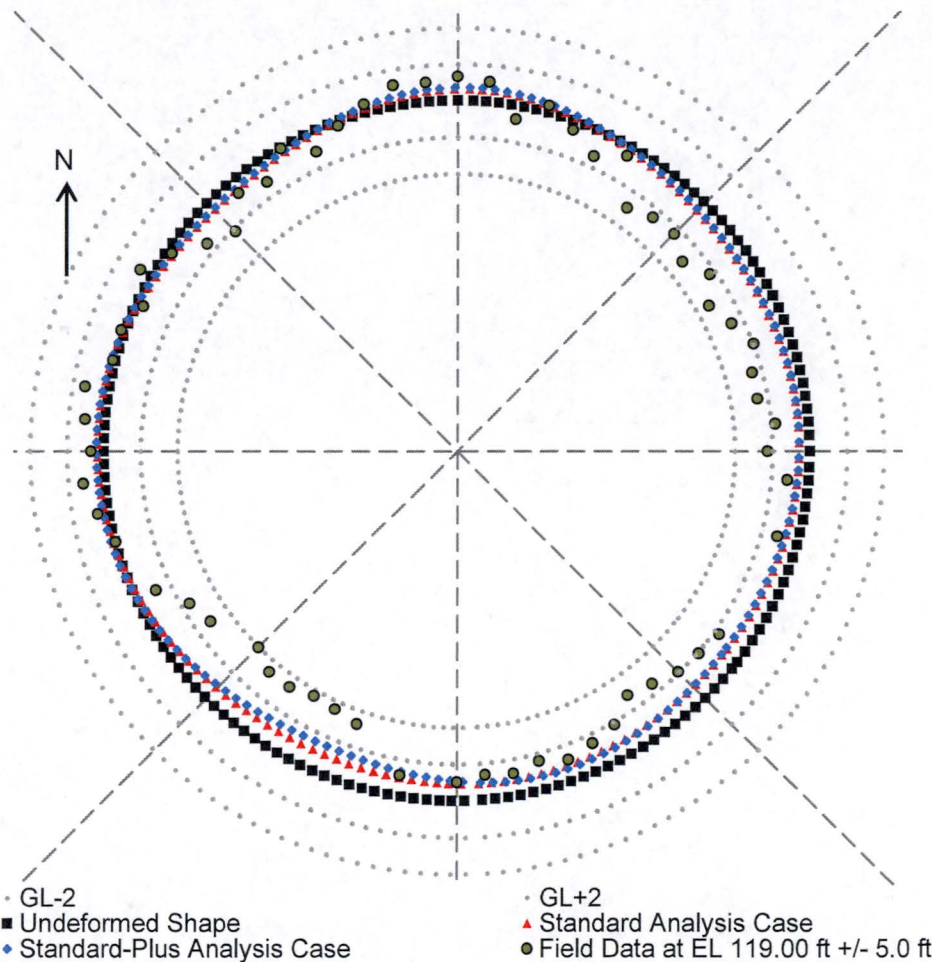
Figure 16. Comparison between As-Deformed Condition Simulations and Field Measurements at El. 22 ft



Deformations scaled by 100X. Small gray dots represent 1 in. grades of deformation.

Figure 17. Comparison between As-Deformed Condition Simulations and Field Measurements at El. 50 ft

Note: Field measurements not recorded at El. 50 ft.



Deformations scaled by 100X. Small gray dots represent 1 in. grades of deformation.

Figure 18. Comparison between As-Deformed Condition Simulations and Field Measurements at El. 119 ft

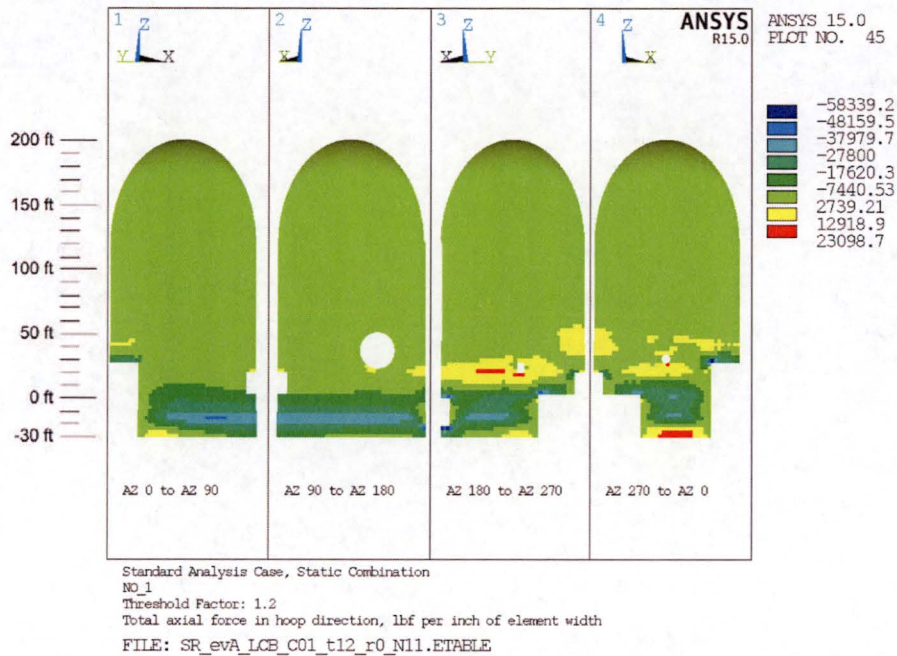


Figure 19. Axial Force Acting in Hoop Direction for Combination NO_1 for the Standard Analysis Case

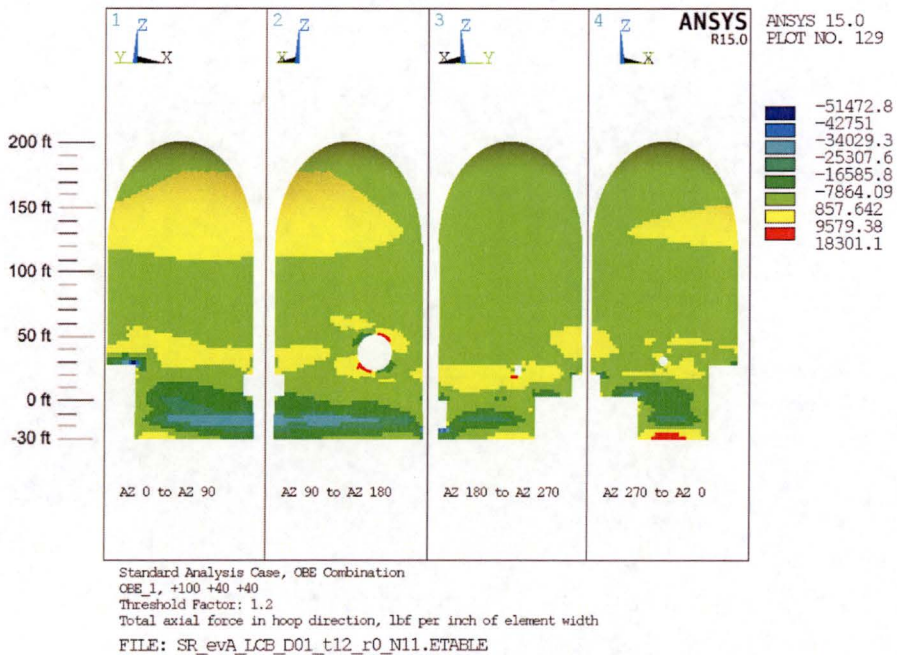


Figure 20. Axial Force Acting in Hoop Direction for Combination OBE_1 for the Standard Analysis Case

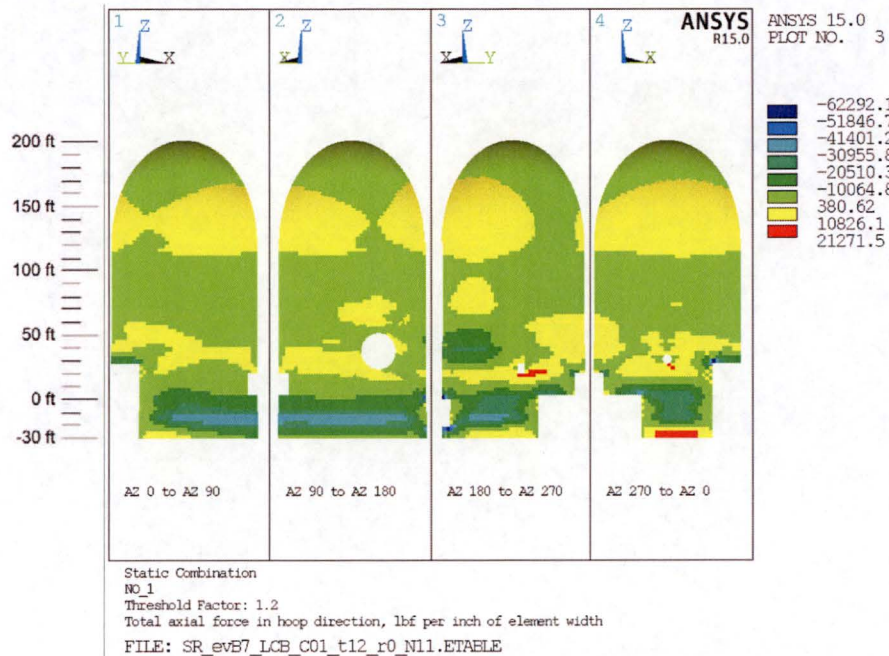


Figure 21. Axial Force Acting in Hoop Direction for Combination NO_1 for the Standard-Plus Analysis Case

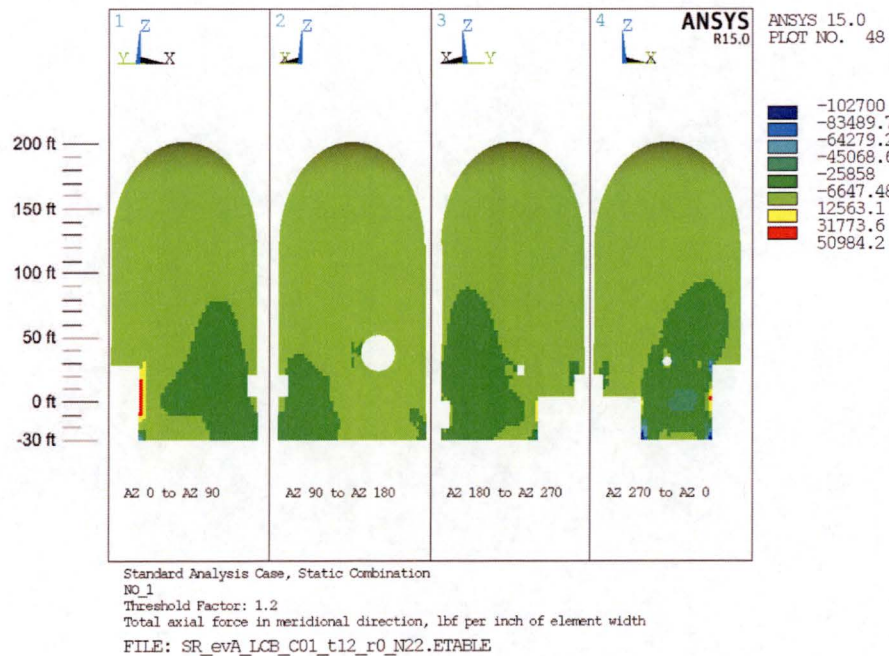


Figure 22. Axial Force Acting in Meridional Direction for Combination NO_1 for the Standard Analysis Case

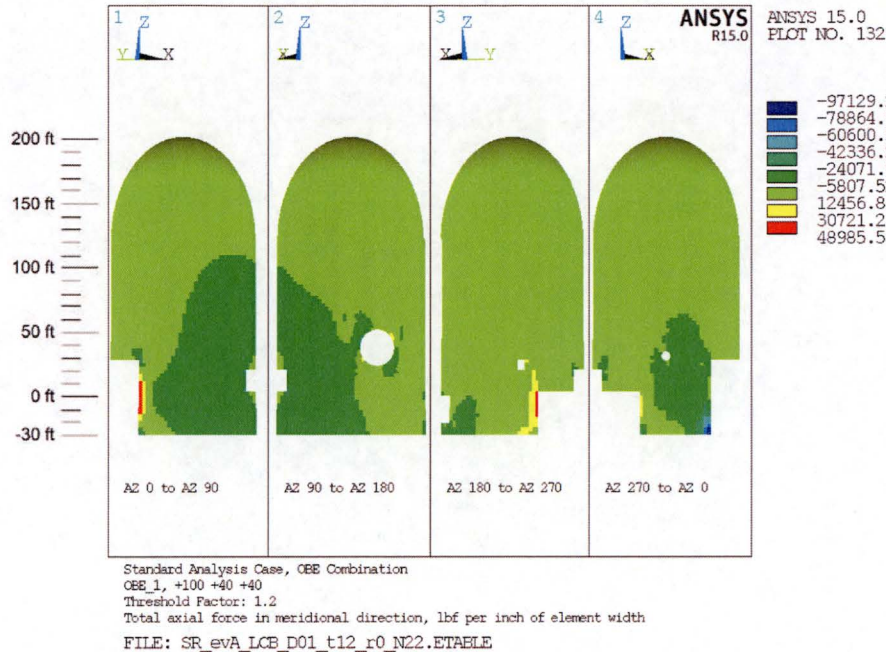


Figure 23. Axial Force Acting in Meridional Direction for Combination OBE_1 for the Standard Analysis Case

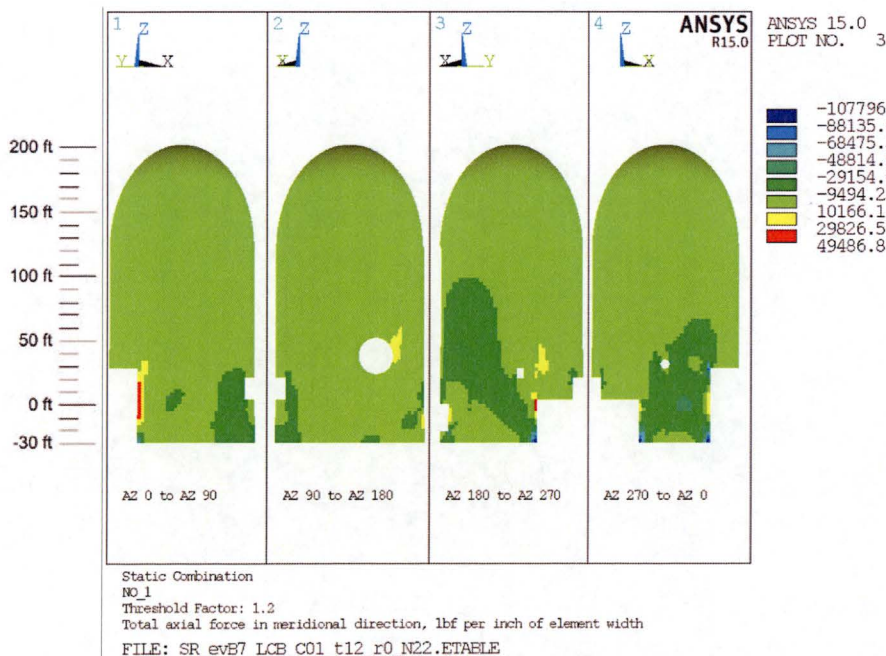


Figure 24. Axial Force Acting in Meridional Direction for Combination NO_1 for the Standard-Plus Analysis Case

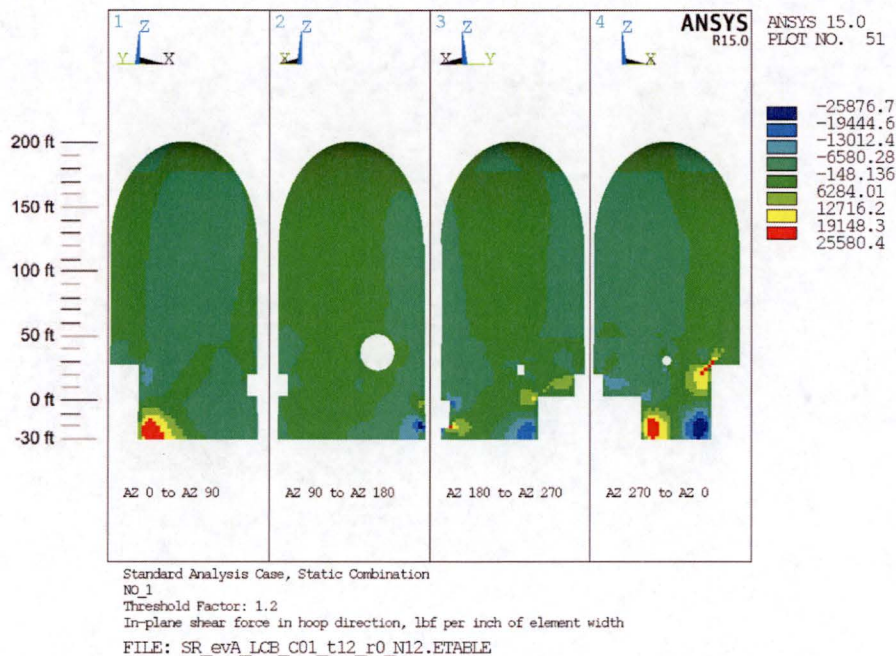


Figure 25. In-Plane Shear Force for Combination NO_1 for the Standard Analysis Case

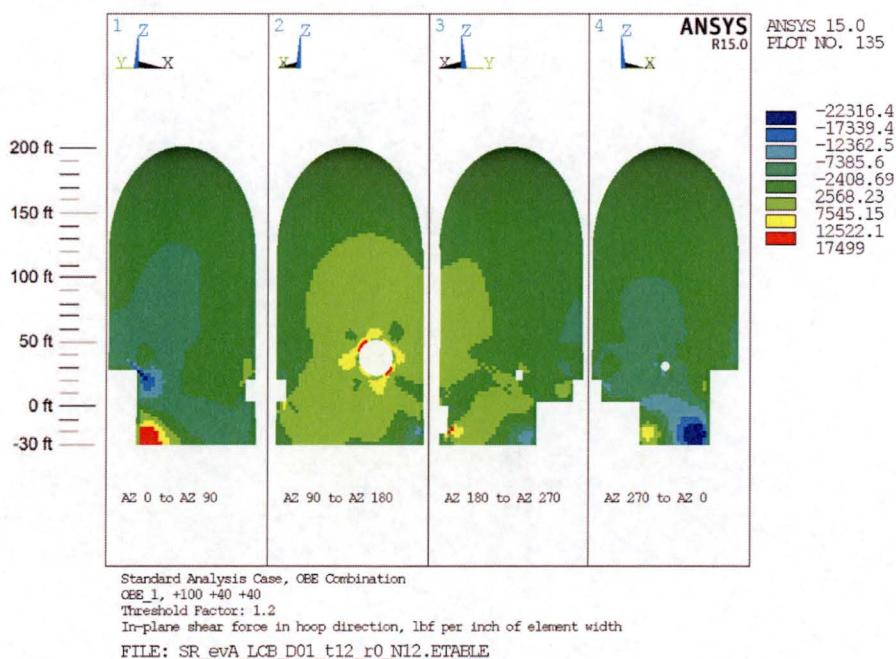


Figure 26. In-Plane Shear Force for Combination OBE_1 for the Standard Analysis Case

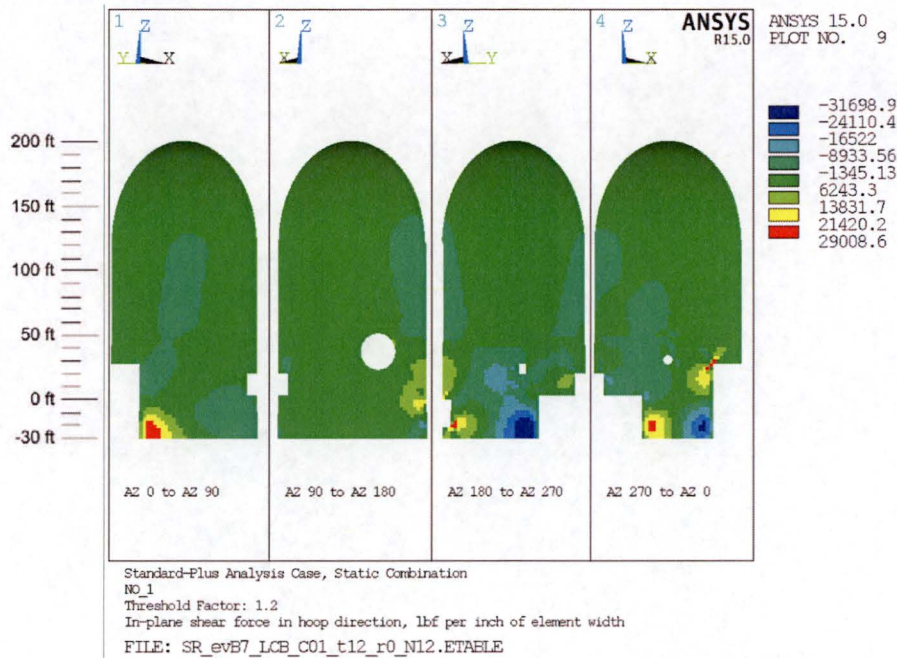


Figure 27. In-Plane Shear Force for Combination NO_1 for the Standard-Plus Analysis Case

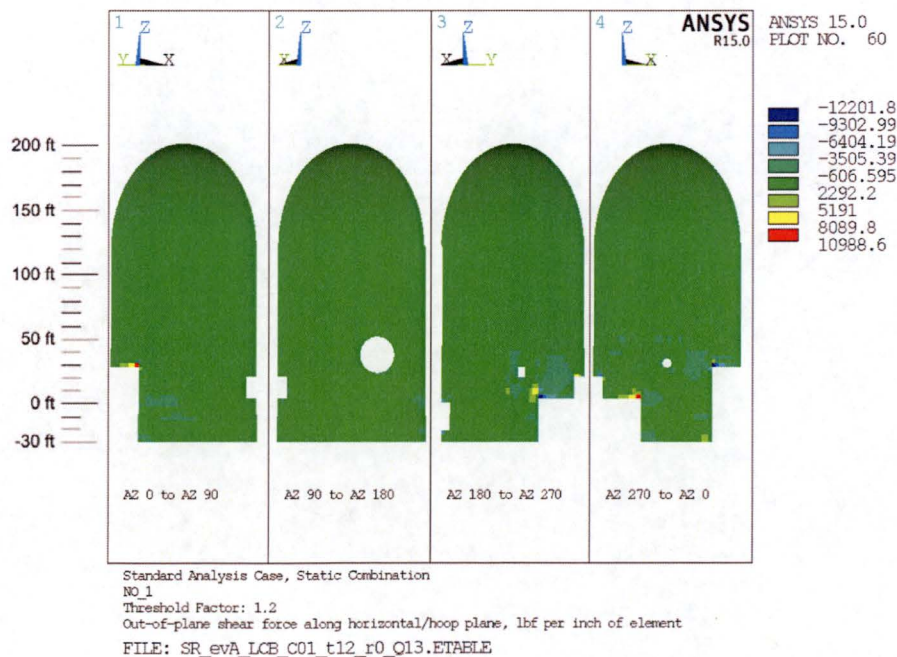


Figure 28. Out-of-Plane Shear Force (Along Meridional-Radial Plane) for Combination NO_1 for the Standard Analysis Case

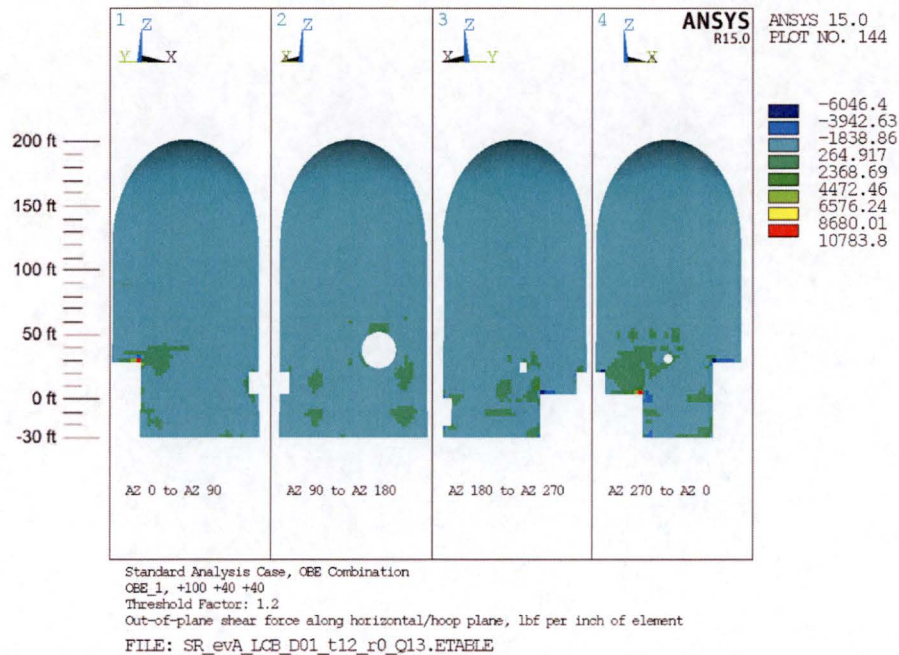


Figure 29. Out-of-Plane Shear Force (Along Meridional-Radial Plane) for Combination OBE_1 for the Standard Analysis Case

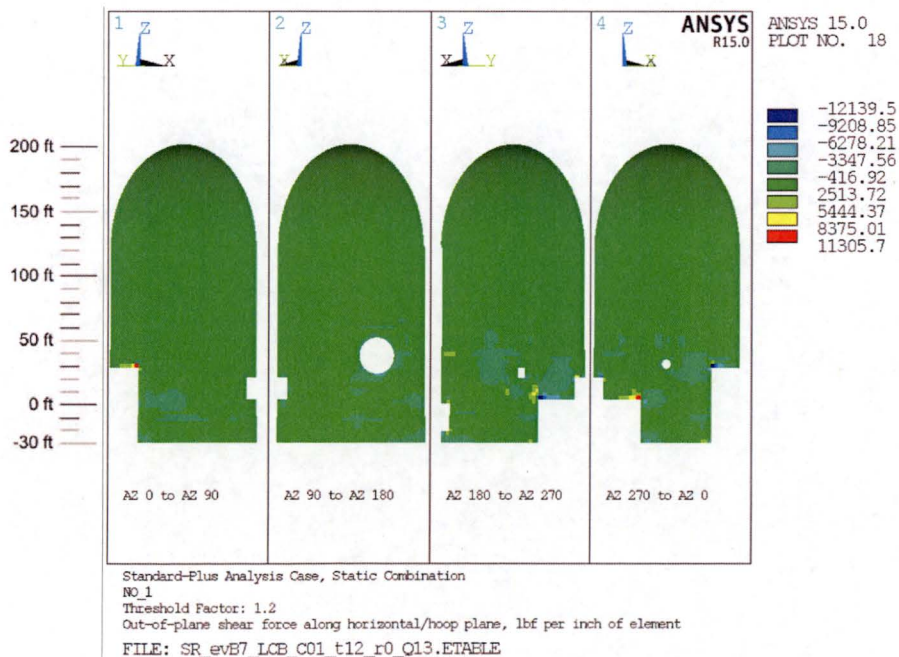


Figure 30. Out-of-Plane Shear Force (Along Meridional-Radial Plane) for Combination NO_1 for the Standard-Plus Analysis Case

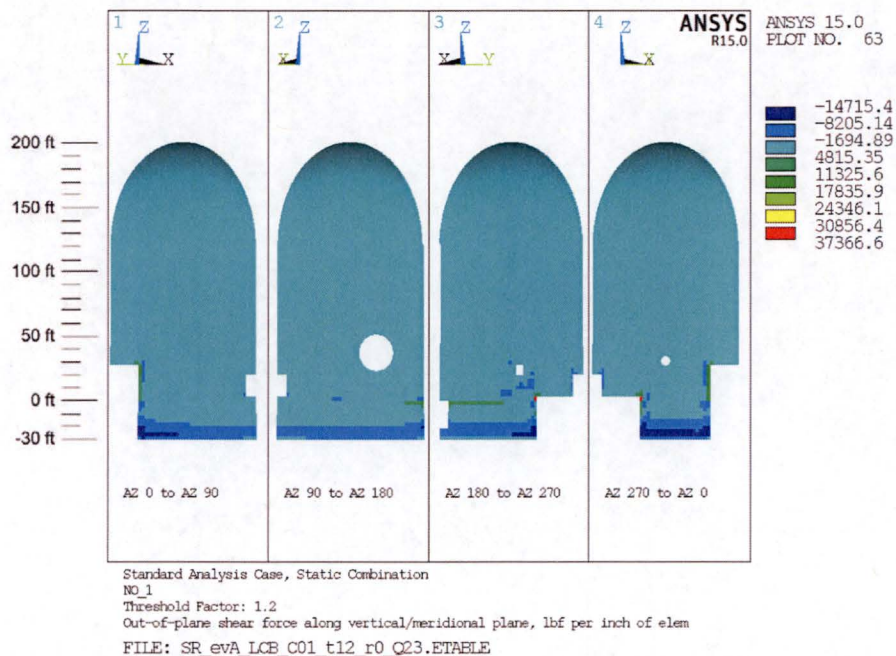


Figure 31. Out-of-Plane Shear Force (Along Hoop-Radial Plane) for Combination NO_1 for the Standard Analysis Case

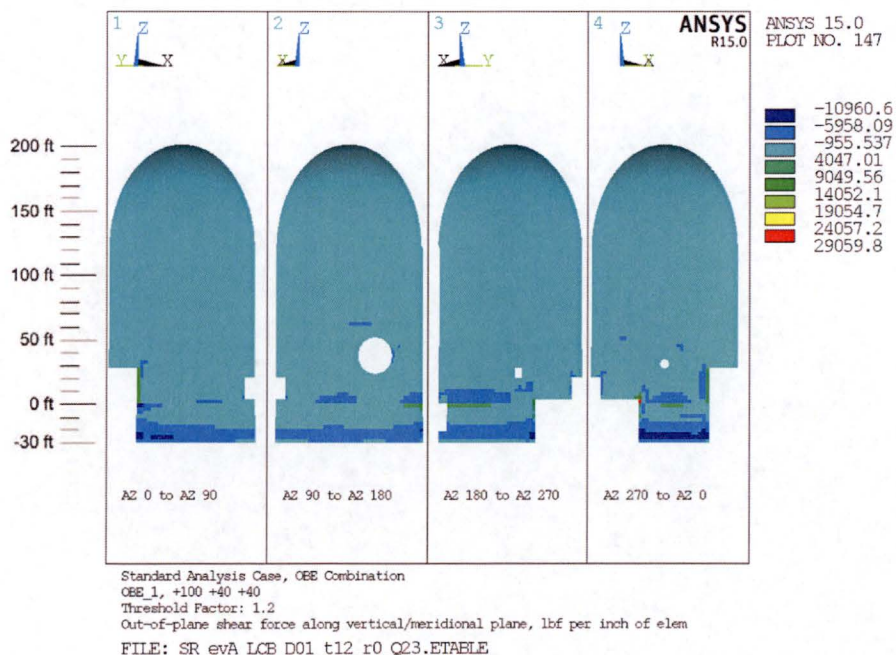


Figure 32. Out-of-Plane Shear Force (Along Hoop-Radial Plane) for Combination OBE_1 for the Standard Analysis Case

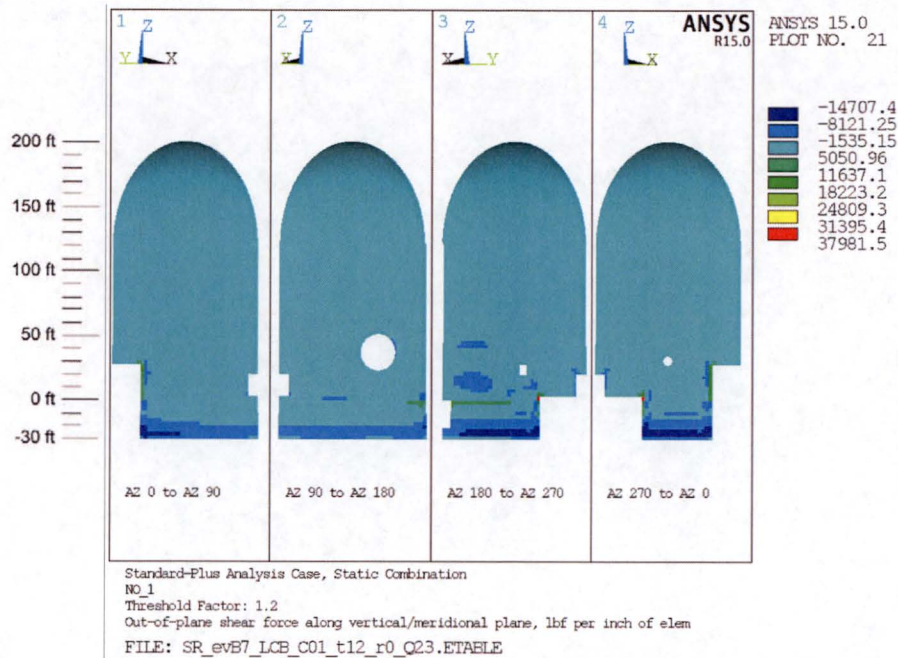


Figure 33. Out-of-Plane Shear Force (Along Hoop-Radial Plane) for Combination NO_1 for the Standard-Plus Analysis Case

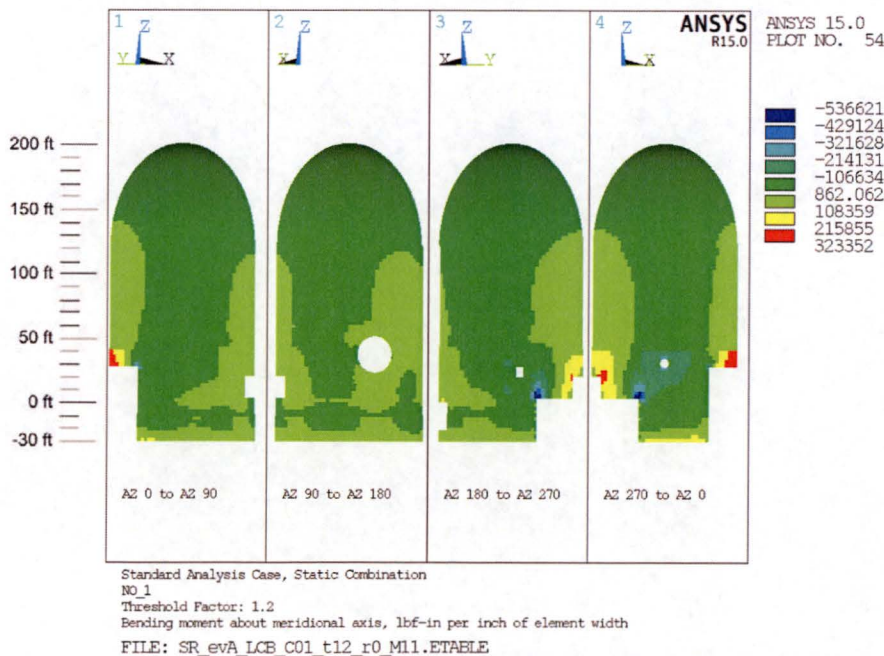


Figure 34. Out-of-Plane Bending Moment (About Meridional Axis) for Combination NO_1 for the Standard Analysis Case

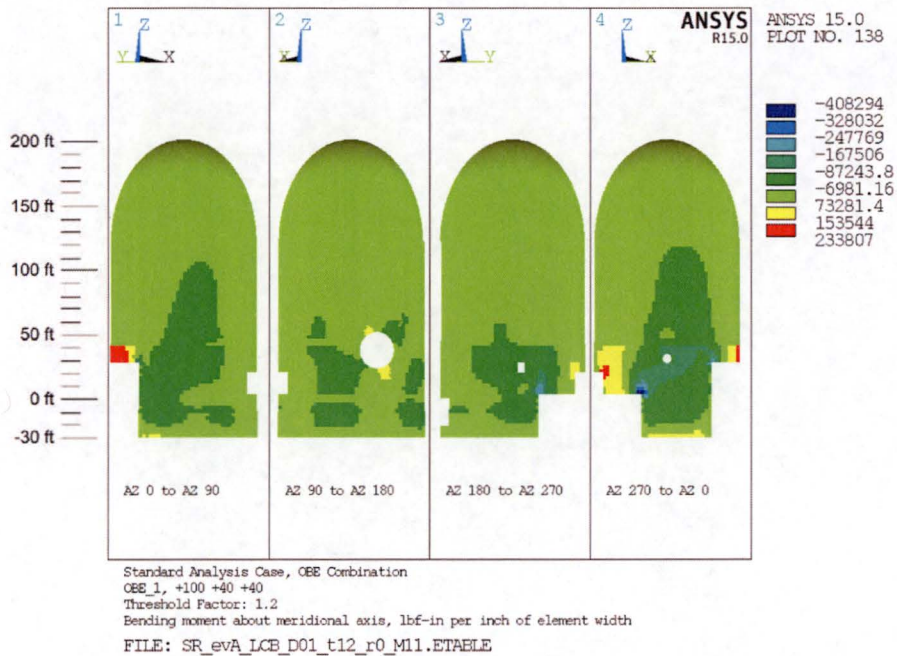


Figure 35. Out-of-Plane Bending Moment (About Meridional Axis) for Combination OBE_1 for the Standard Analysis Case

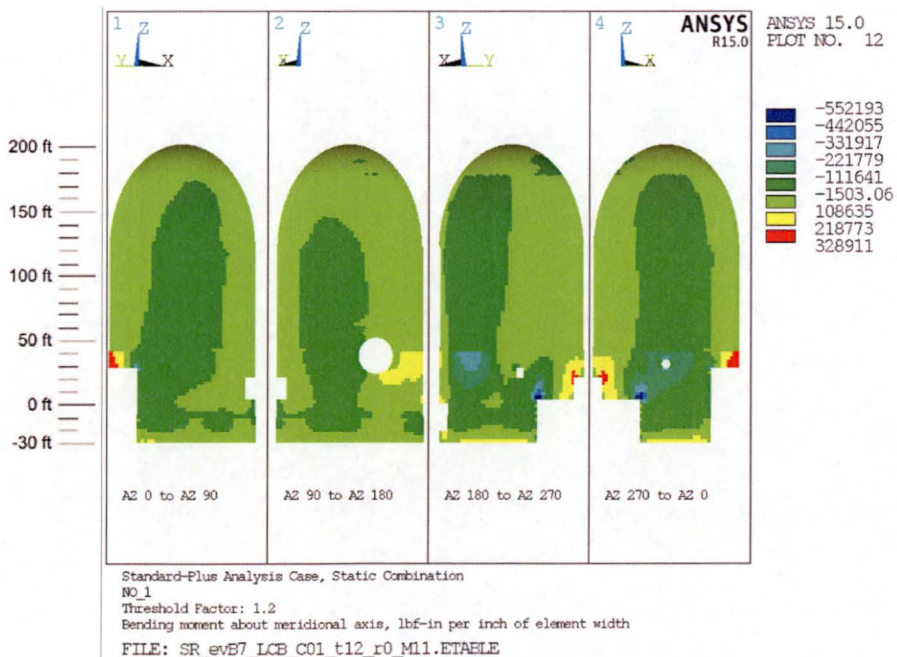


Figure 36. Out-of-Plane Bending Moment (About Meridional Axis) for Combination NO_1 for the Standard-Plus Analysis Case

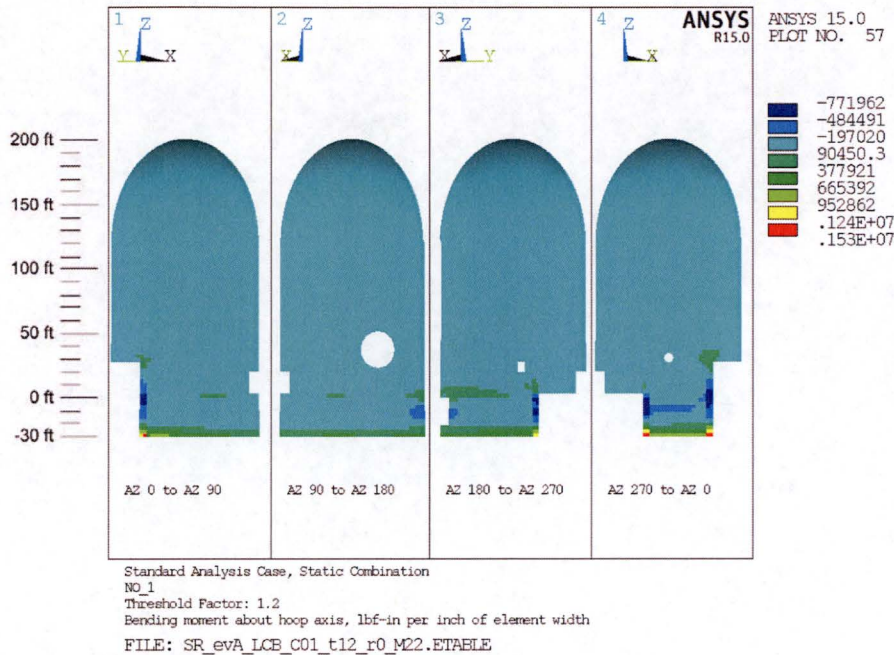


Figure 37. Out-of-Plane Bending Moment (About Hoop Axis) for Combination NO_1 for the Standard Analysis Case

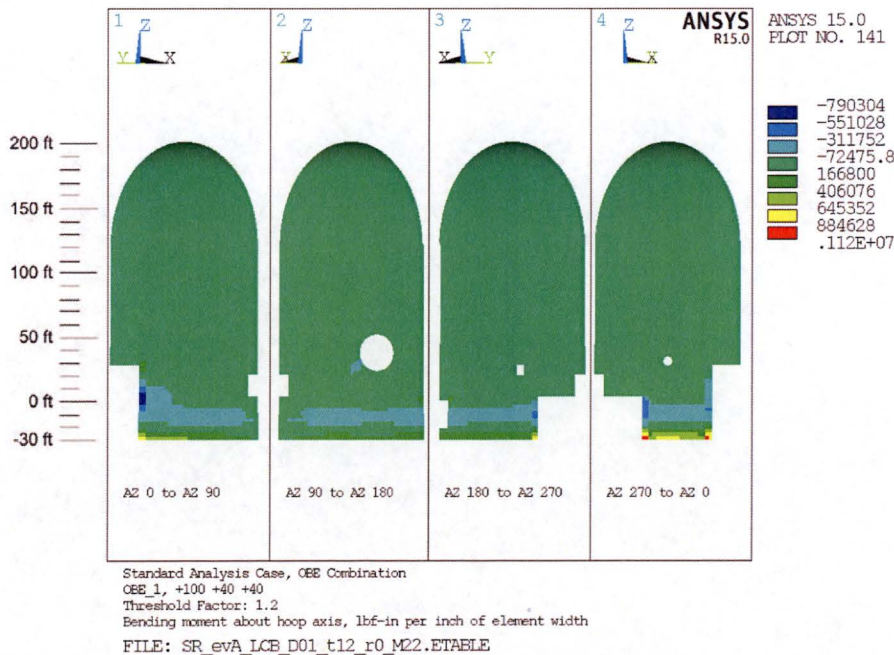


Figure 38. Out-of-Plane Bending Moment (About Hoop Axis) for Combination OBE_1 for the Standard Analysis Case

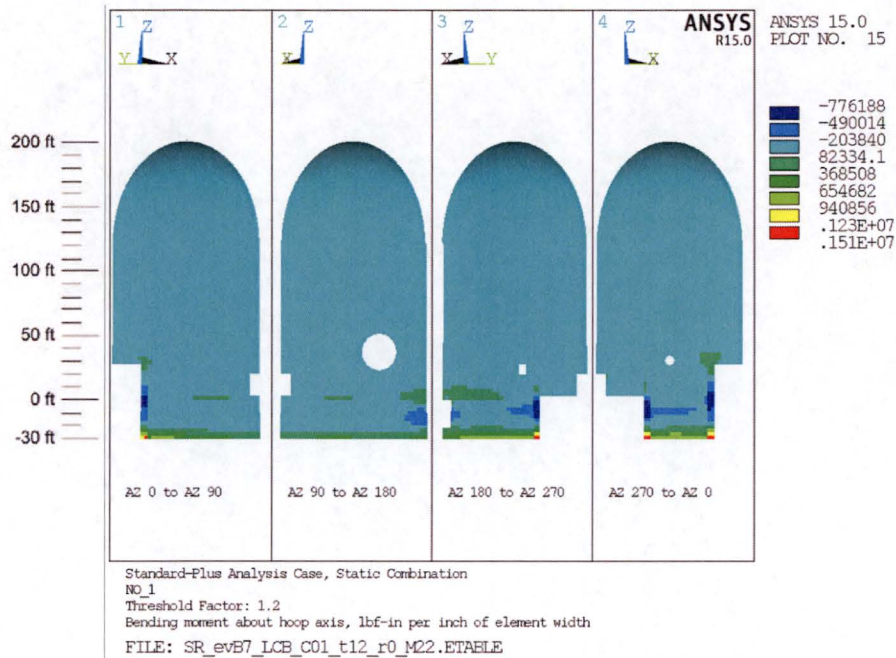


Figure 39. Out-of-Plane Bending Moment (About Hoop Axis) for Combination NO_1 for the Standard-Plus Analysis Case

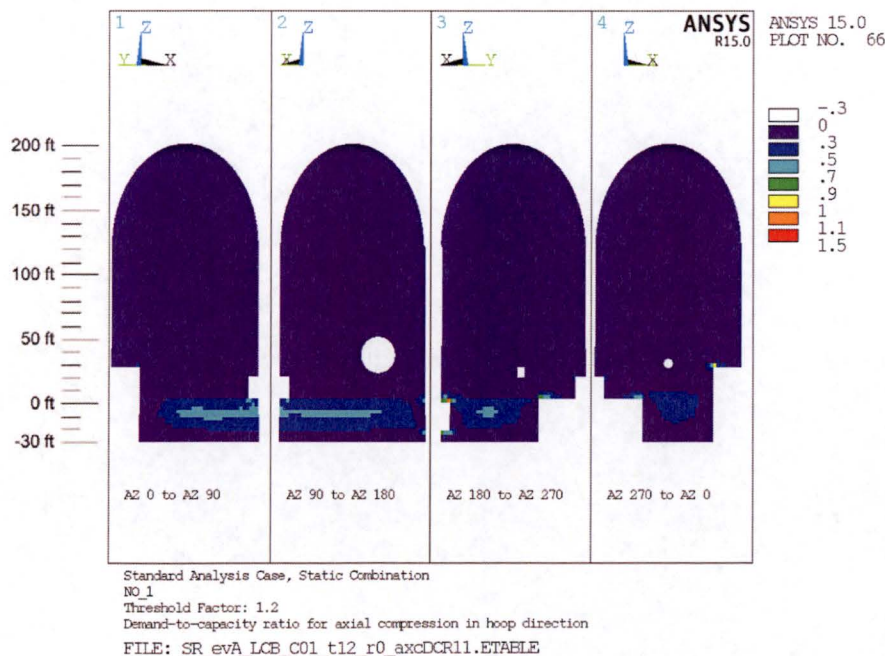


Figure 40. DCRs for Axial Compression in Hoop Direction for Combination NO_1 for the Standard Analysis Case

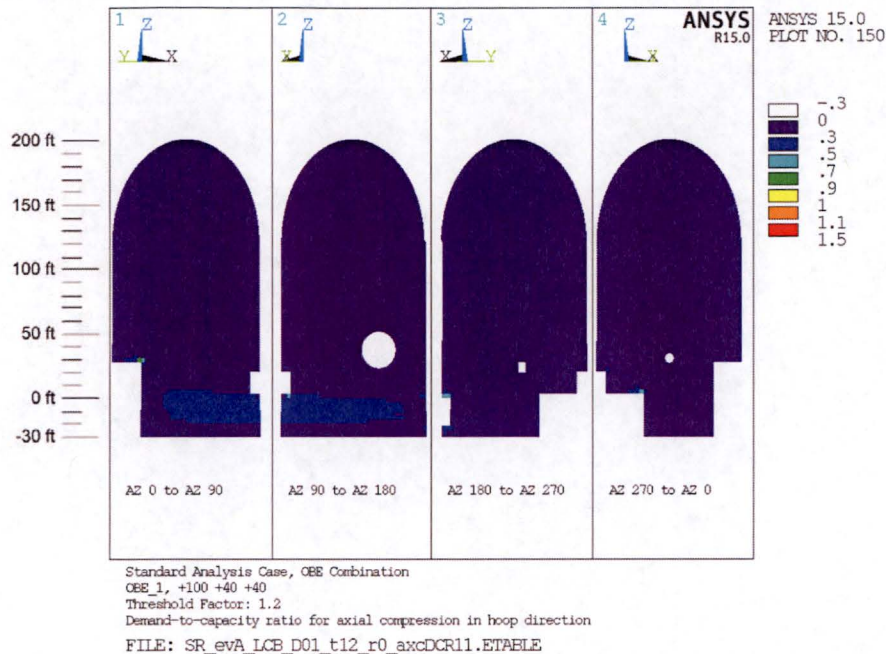


Figure 41. DCRs for Axial Compression in Hoop Direction for Combination OBE_1 for the Standard Analysis Case

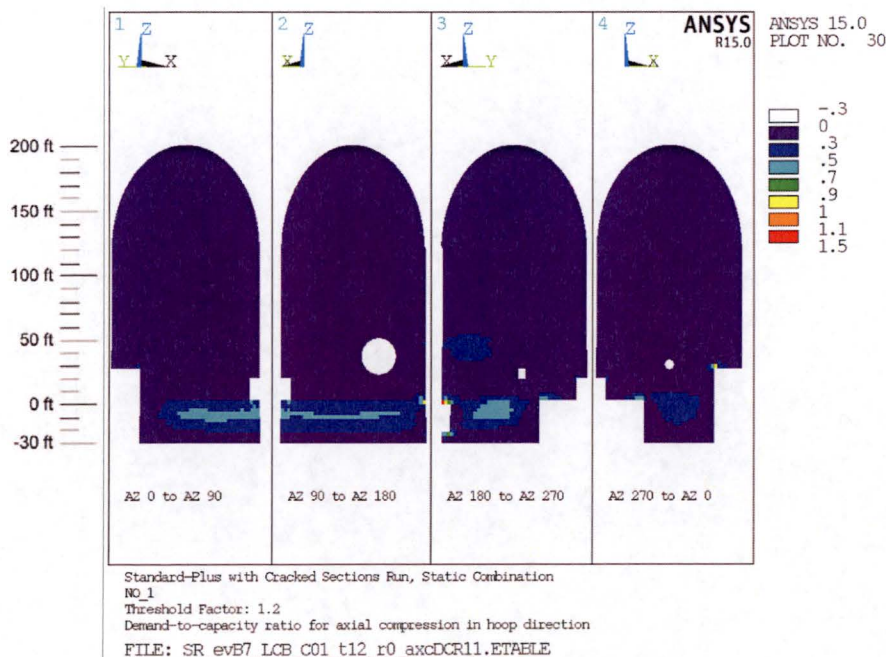


Figure 42. DCRs for Axial Compression in Hoop Direction for Combination NO_1 for the Standard-Plus Analysis Case

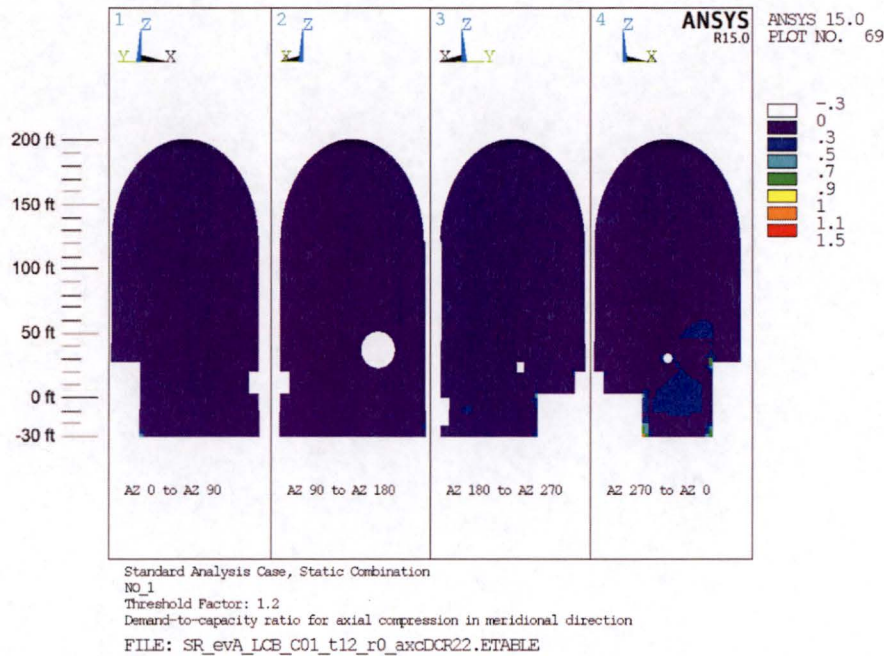


Figure 43. DCRs for Axial Compression in Meridional Direction for Combination NO_1 for the Standard Analysis Case

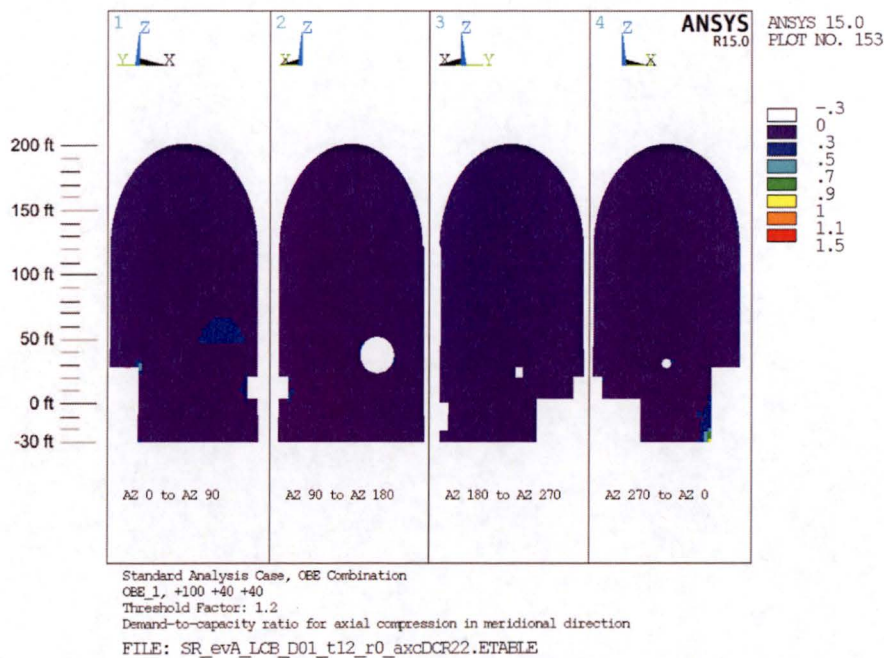


Figure 44. DCRs for Axial Compression in Meridional Direction for Combination OBE_1 for the Standard Analysis Case

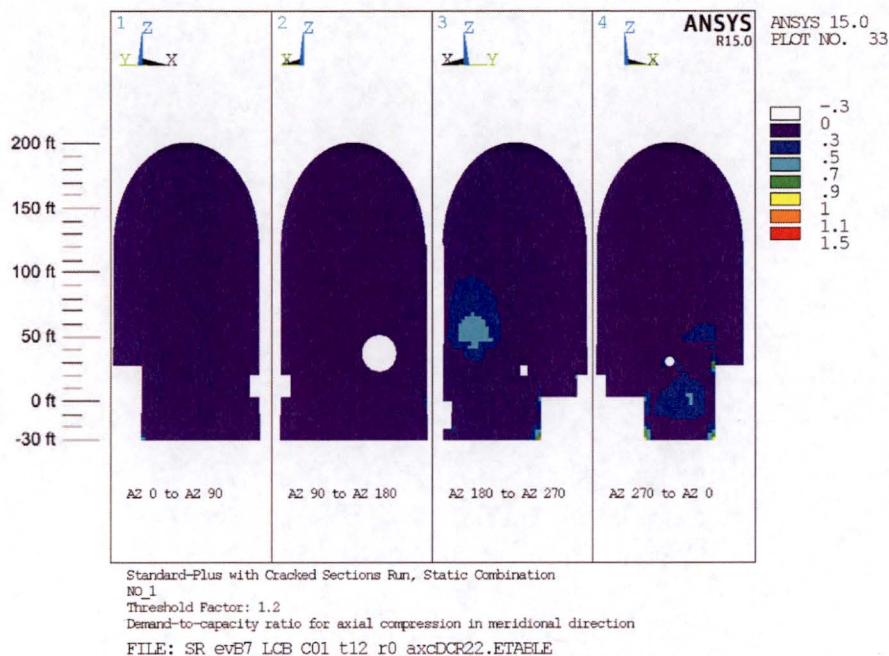


Figure 45. DCRs for Axial Compression in Meridional Direction for Combination NO_1 for the Standard-Plus Analysis Case

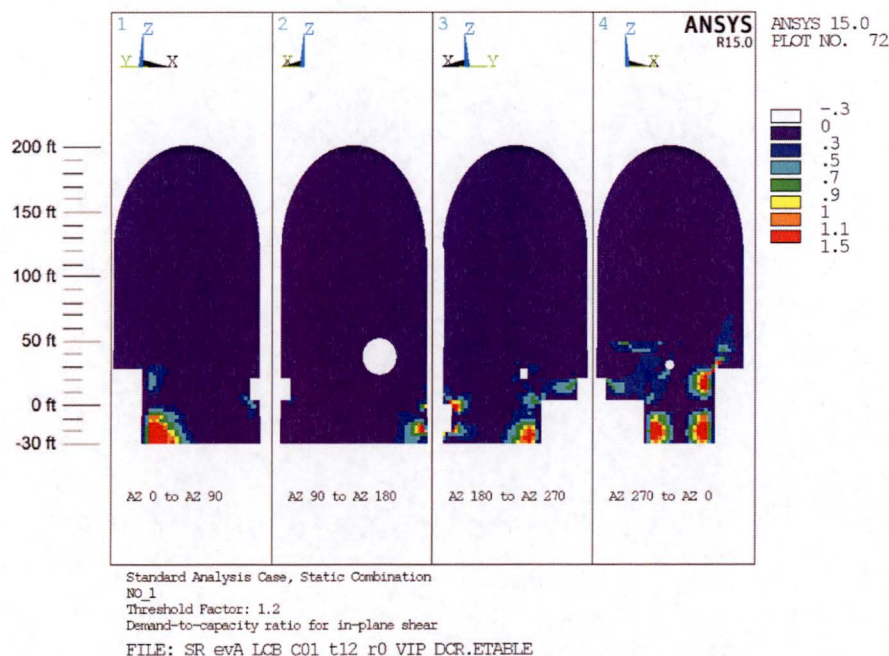


Figure 46. DCRs for In-Plane Shear for Combination NO_1 for the Standard Analysis Case

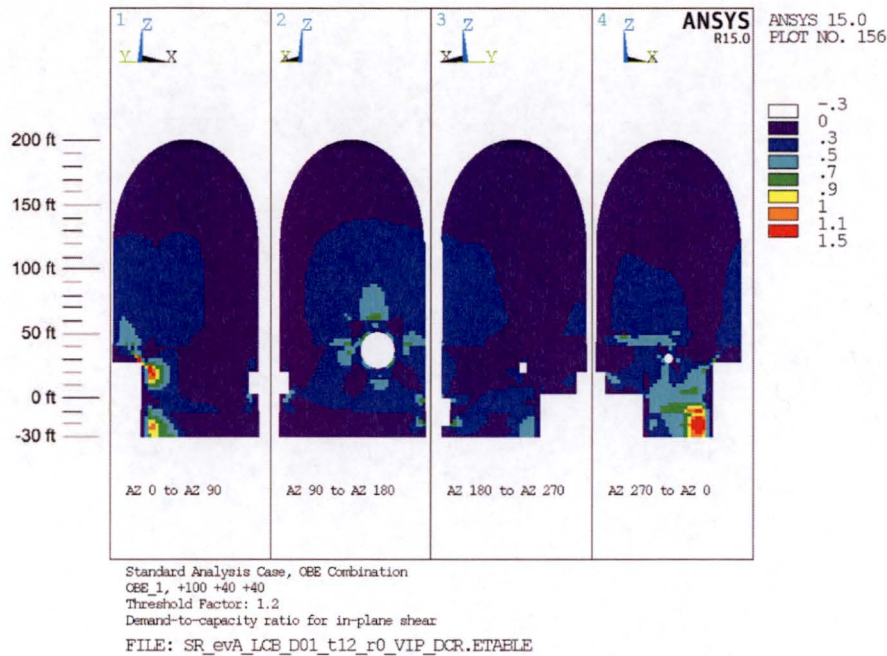


Figure 47. DCRs for In-Plane Shear for Combination OBE_1 for the Standard Analysis Case

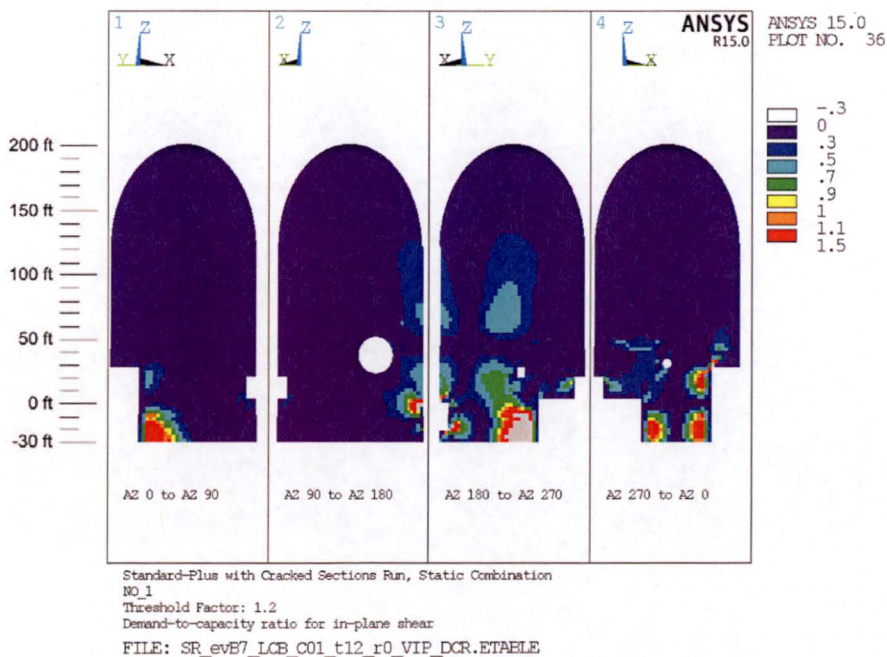


Figure 48. DCRs for In-Plane Shear for Combination NO_1 for the Standard-Plus Analysis Case

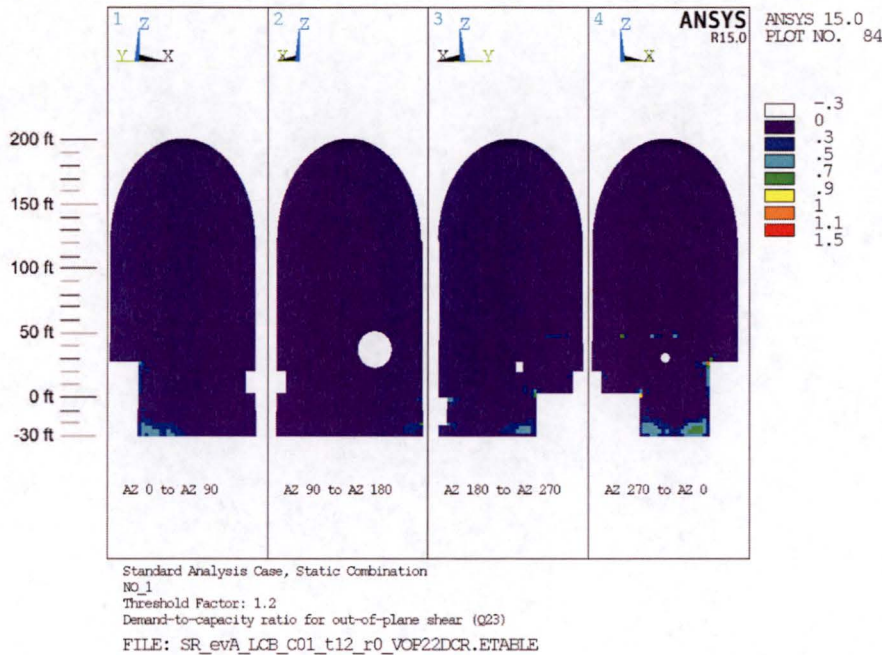


Figure 49. DCRs for Out-of-Plane Shear (acting on hoop-radial plane) for Combination NO_1 for the Standard Analysis Case

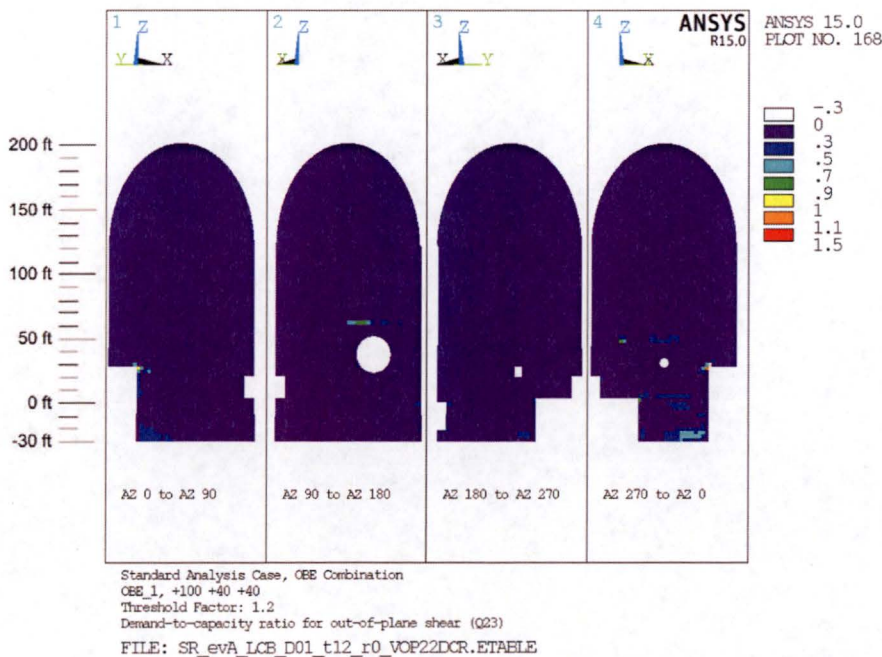


Figure 50. DCRs for Out-of-Plane Shear (acting on hoop-radial plane) for Combination OBE_1 for the Standard Analysis Case

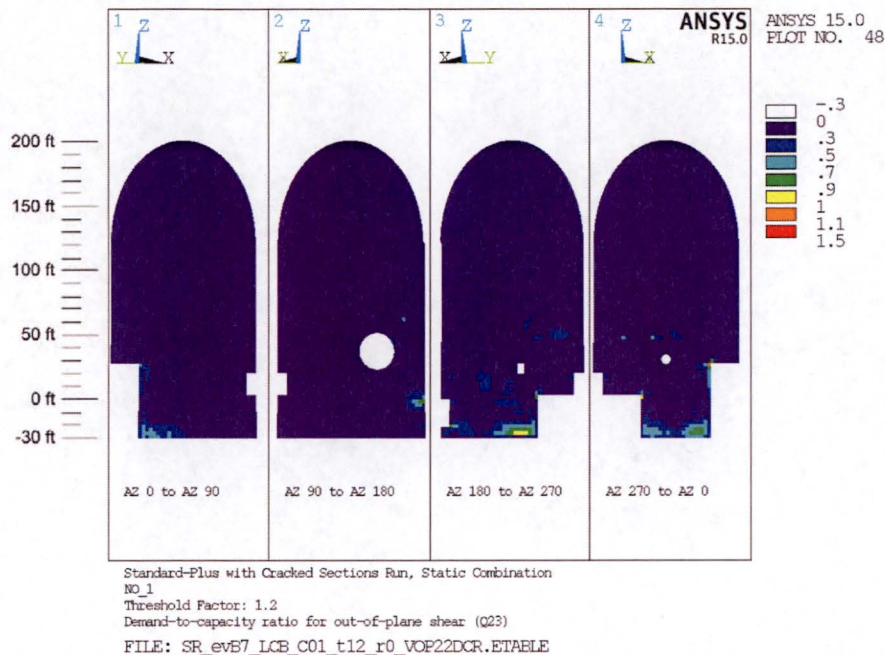


Figure 51. DCRs for Out-of-Plane Shear (acting on hoop-radial plane) for Combination NO_1 for the Standard-Plus Analysis Case

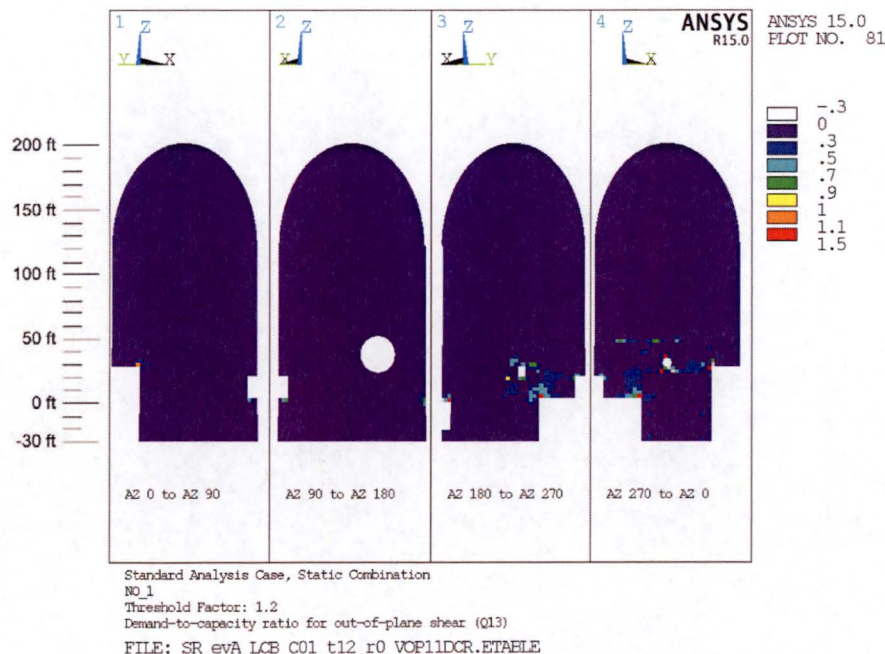


Figure 52. DCRs for Out-of-Plane Shear (acting on meridional-radial plane) for Combination NO_1 for the Standard Analysis Case

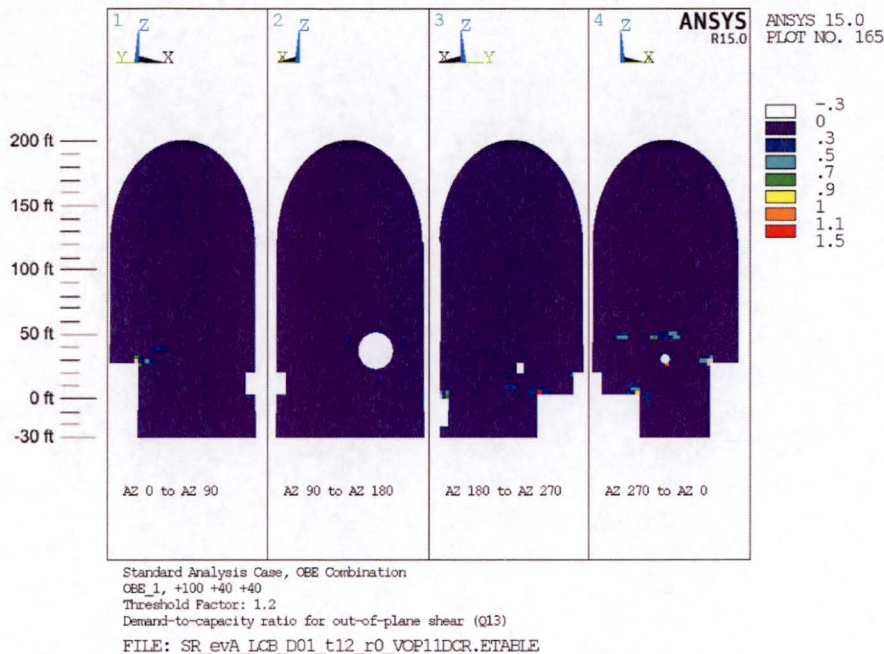


Figure 53. DCRs for Out-of-Plane Shear (acting on meridional-radial plane) for Combination OBE_1 for the Standard Analysis Case

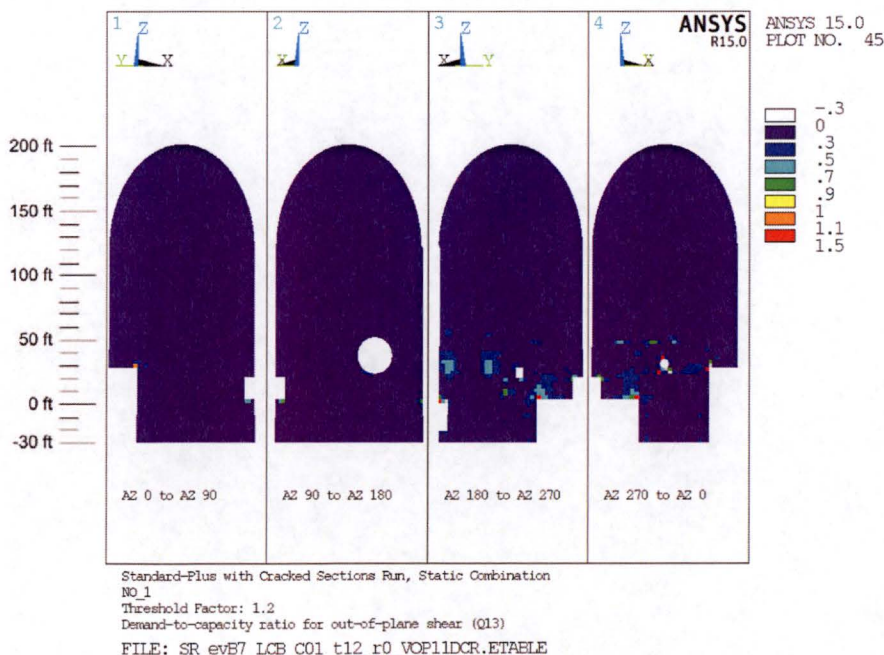


Figure 54. DCRs for Out-of-Plane Shear (acting on meridional-radial plane) for Combination NO_1 for the Standard-Plus Analysis Case

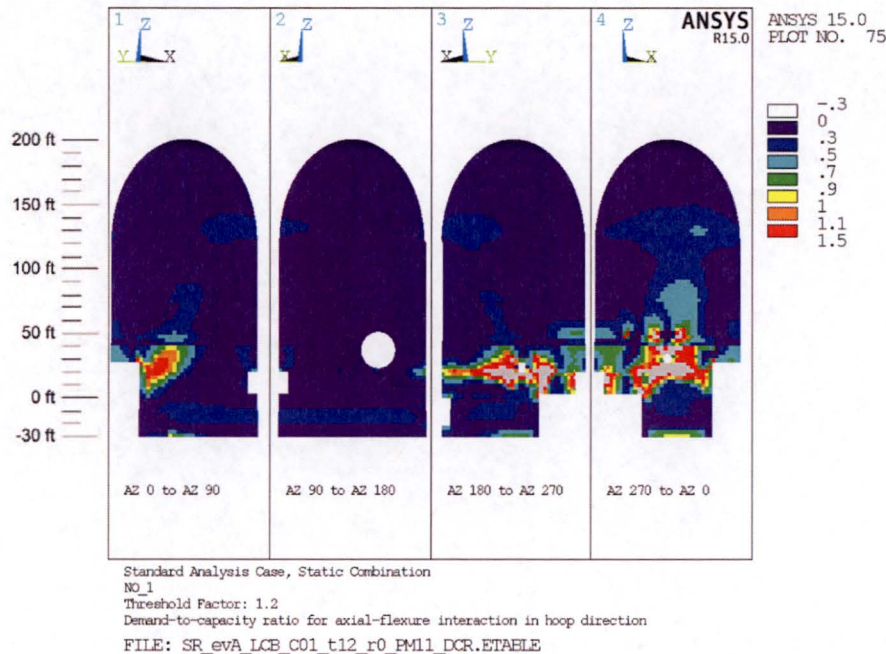


Figure 55. DCRs for Axial-Flexure Interaction in the Hoop Direction for Combination NO_1 for the Standard Analysis Case

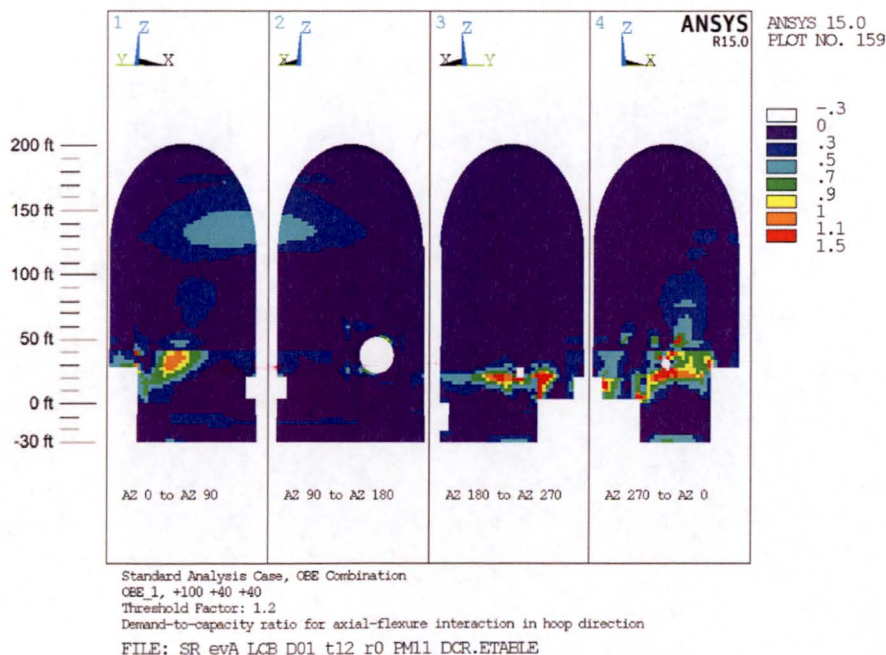


Figure 56. DCRs for Axial-Flexure Interaction in the Hoop Direction for Combination OBE_1 for the Standard Analysis Case

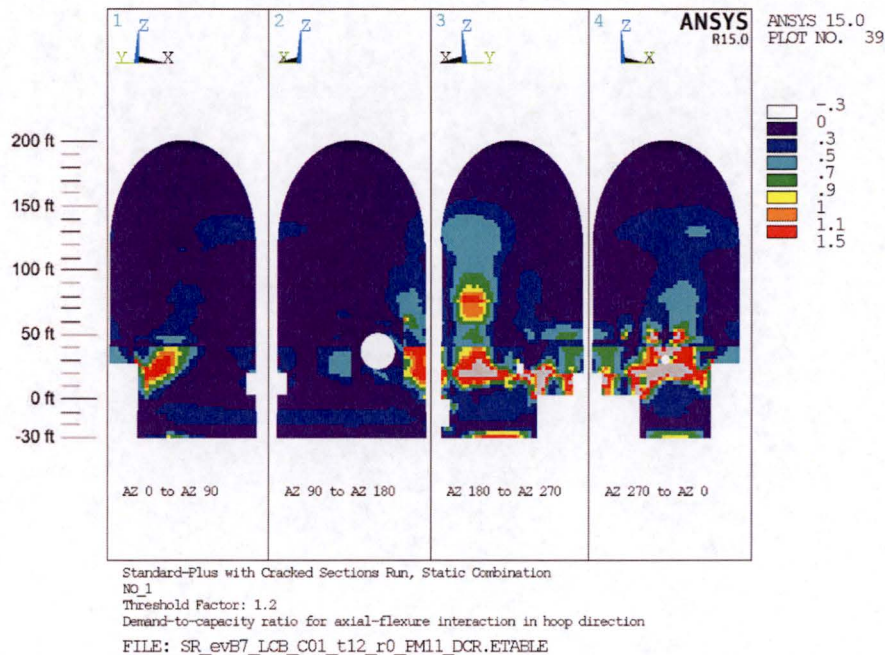


Figure 57. DCRs for Axial-Flexure Interaction in the Hoop Direction for Combination NO_1 for the Standard-Plus Analysis Case

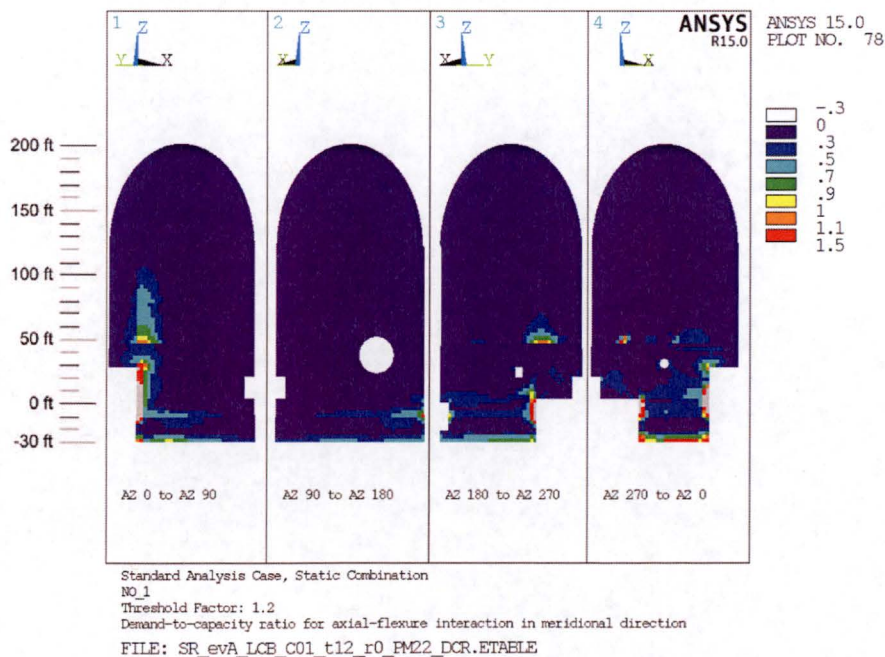


Figure 58. DCRs for Axial-Flexure Interaction in the Meridional Direction for Combination NO_1 for the Standard Analysis Case

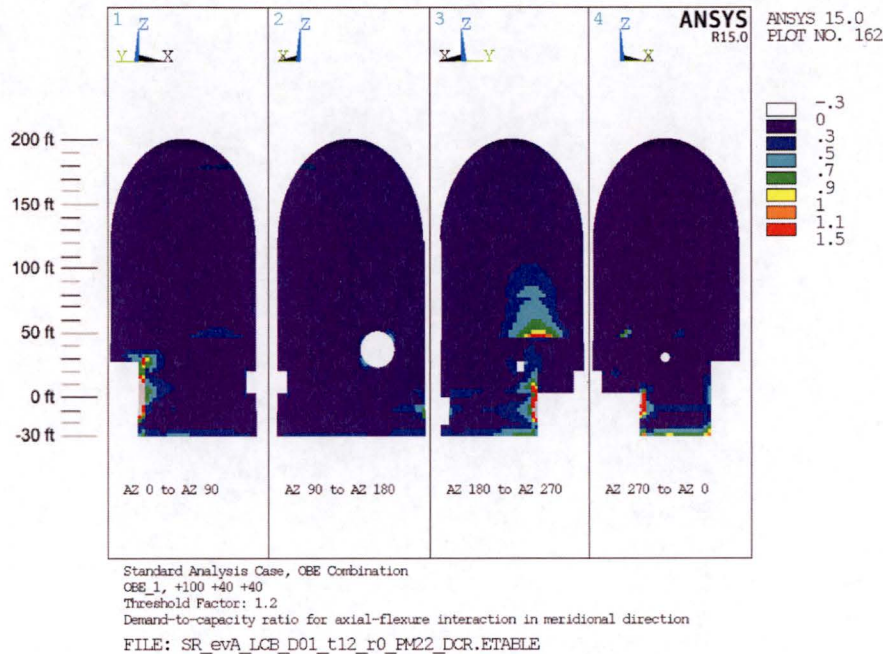


Figure 59. DCRs for Axial-Flexure Interaction in the Meridional Direction for Combination OBE_1 for the Standard Analysis Case

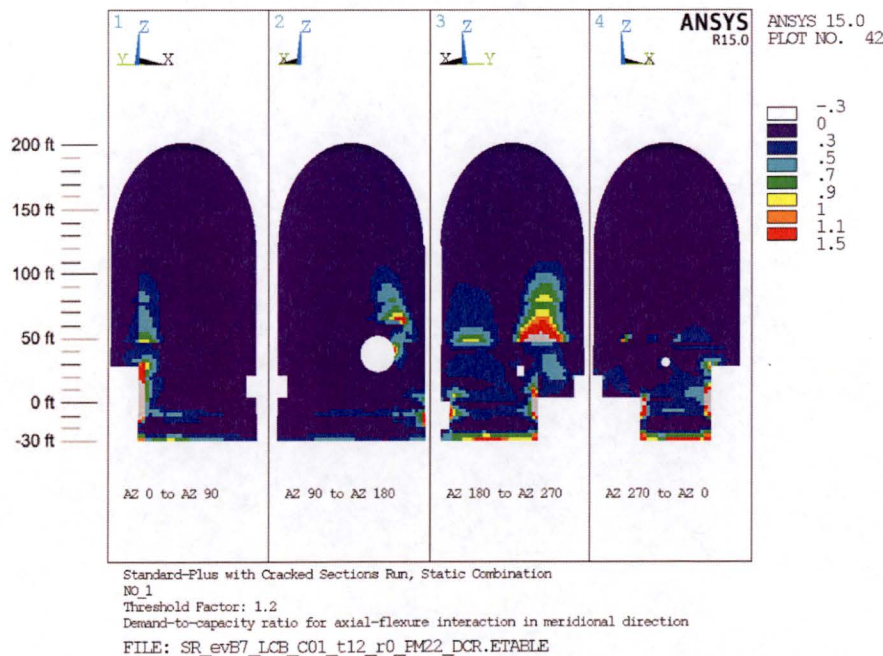


Figure 60. DCRs for Axial-Flexure Interaction in the Meridional Direction for Combination NO_1 for the Standard-Plus Analysis Case

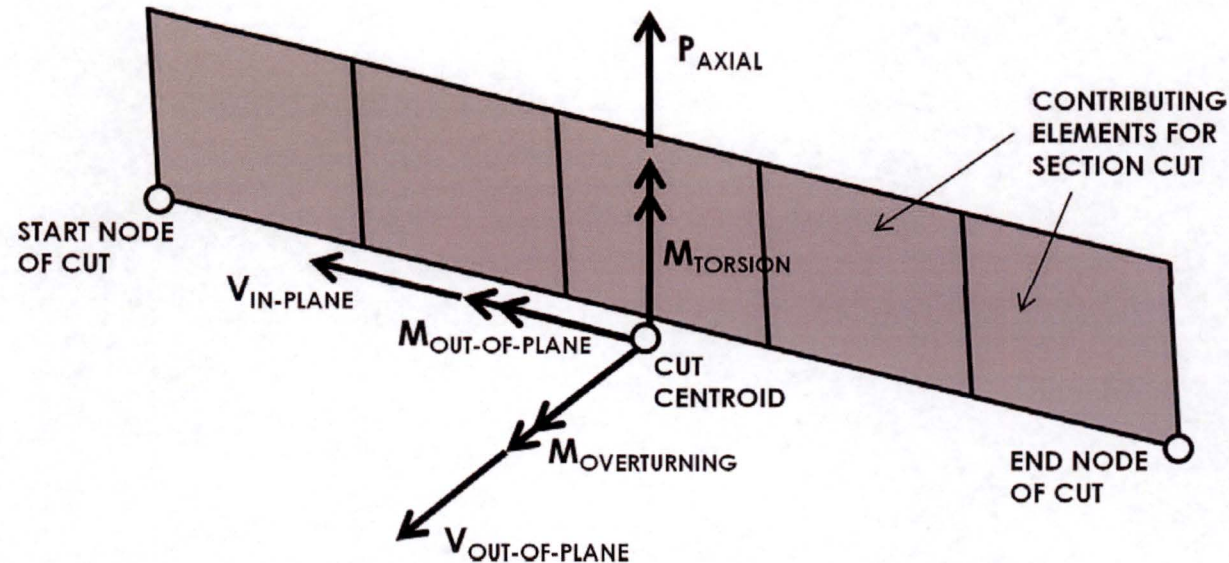


Figure 61. Section Cut Resultant Forces and Moments at Cut Centroid

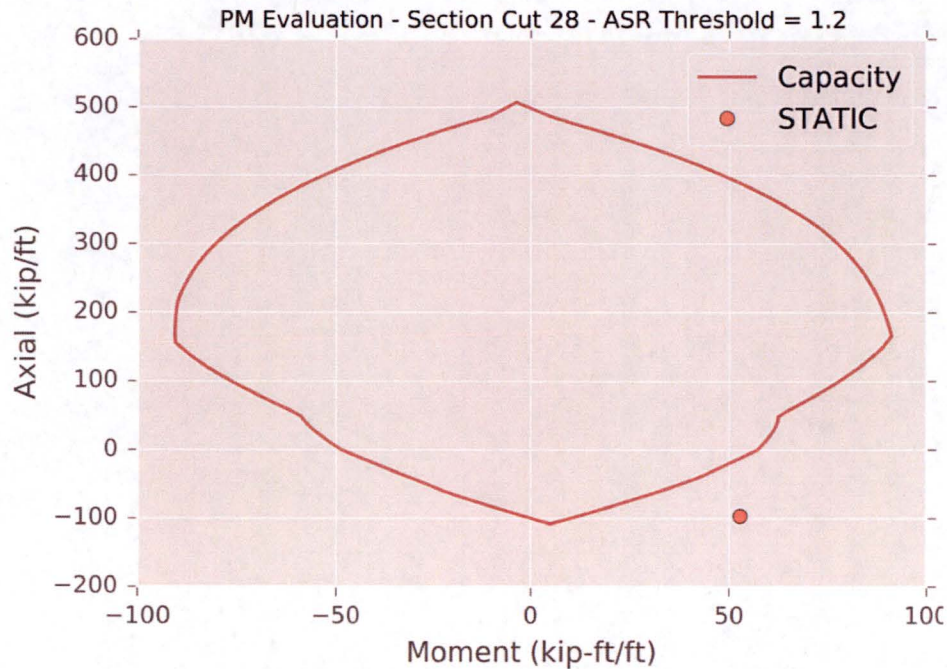


Figure 62. PM Interaction Diagram at Section Cut 28 Showing Elevated Tensile Demands (Prior to Adjustment of Meridional Stiffness at El. +45.5 ft and AZ 240)

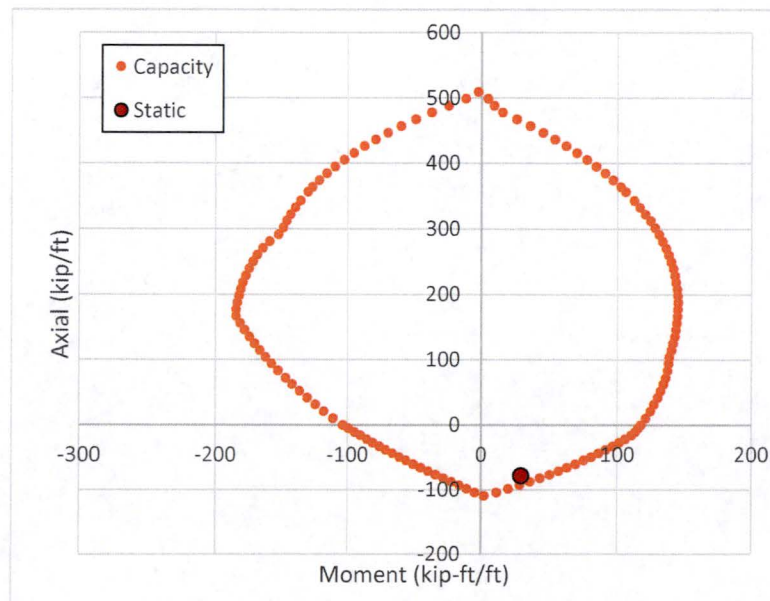


Figure 63. PM Interaction Diagram at Section Cut 28 after Adjustment of Meridional Stiffness at El. +45.5 ft and AZ 240)

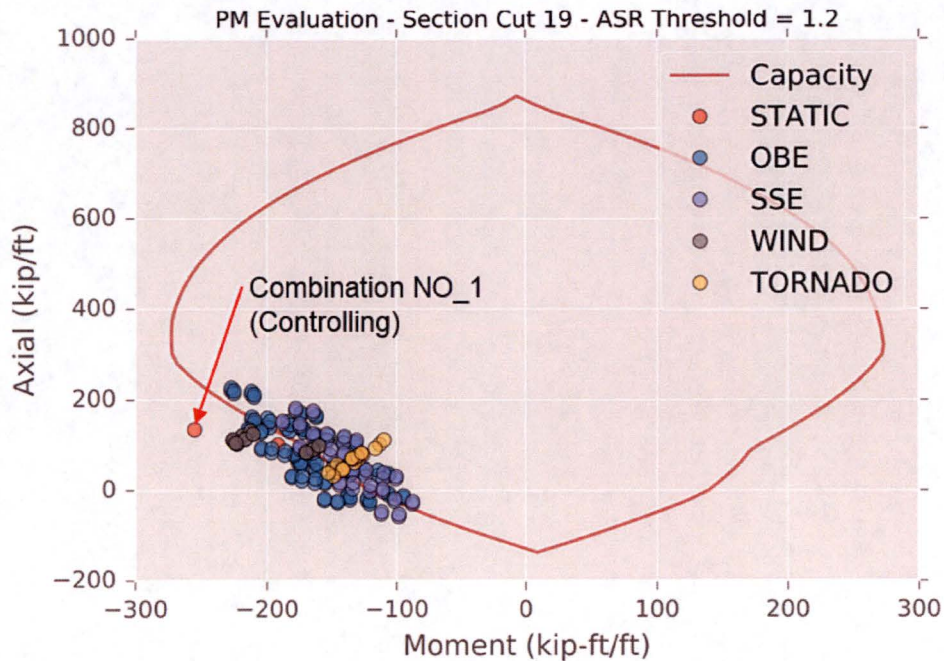


Figure 64. PM Interaction Check for Standard Analysis Case prior to Moment Redistribution (Section Cut 19)

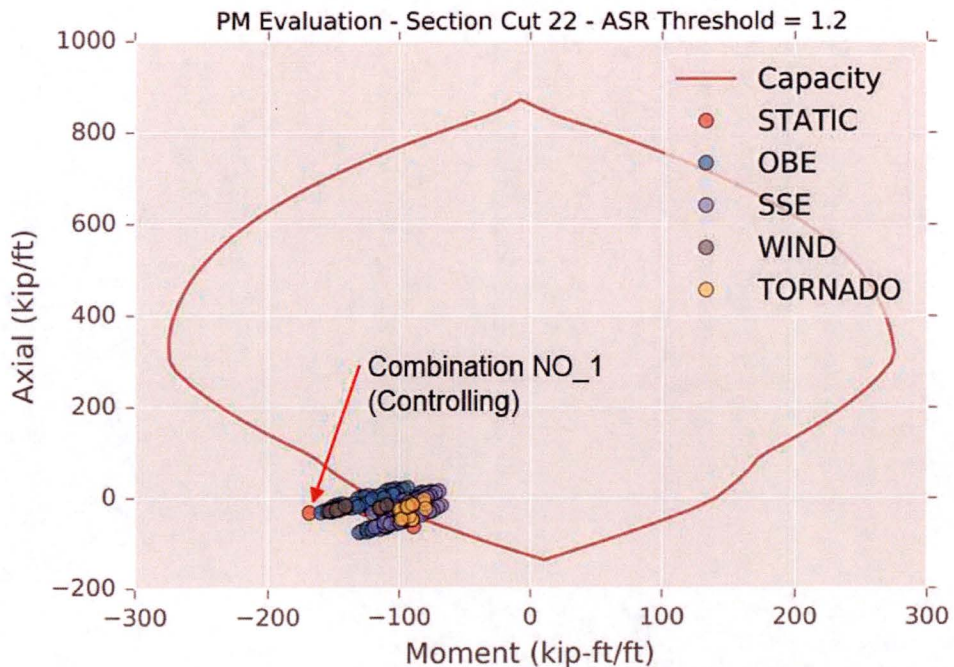


Figure 65. PM Interaction Check for Standard Analysis Case prior to Moment Redistribution (Section Cut 22)

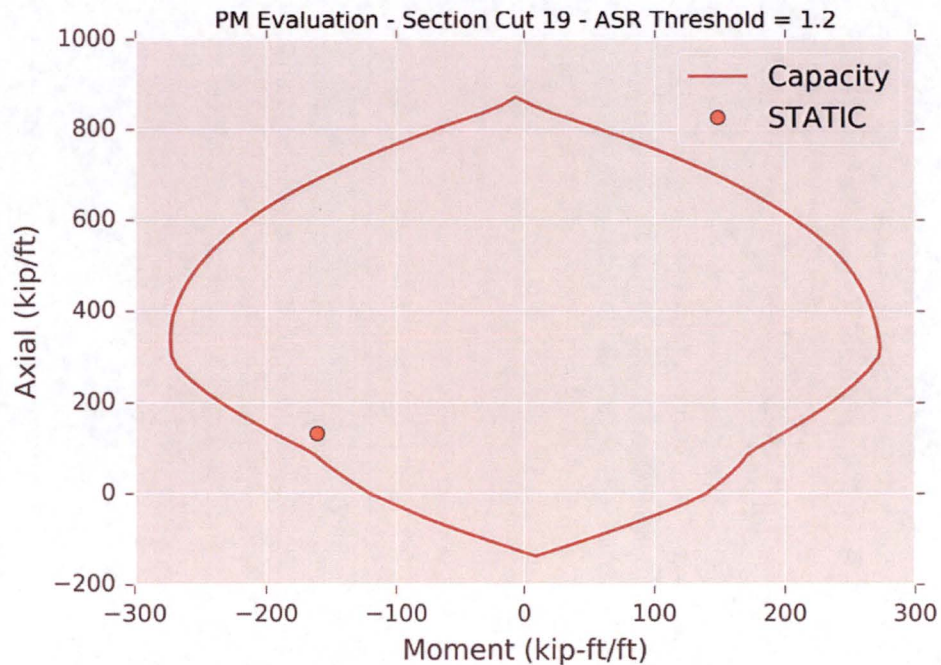


Figure 66. PM Interaction Check for Standard Analysis Case after Moment Redistribution (Section Cut 19)

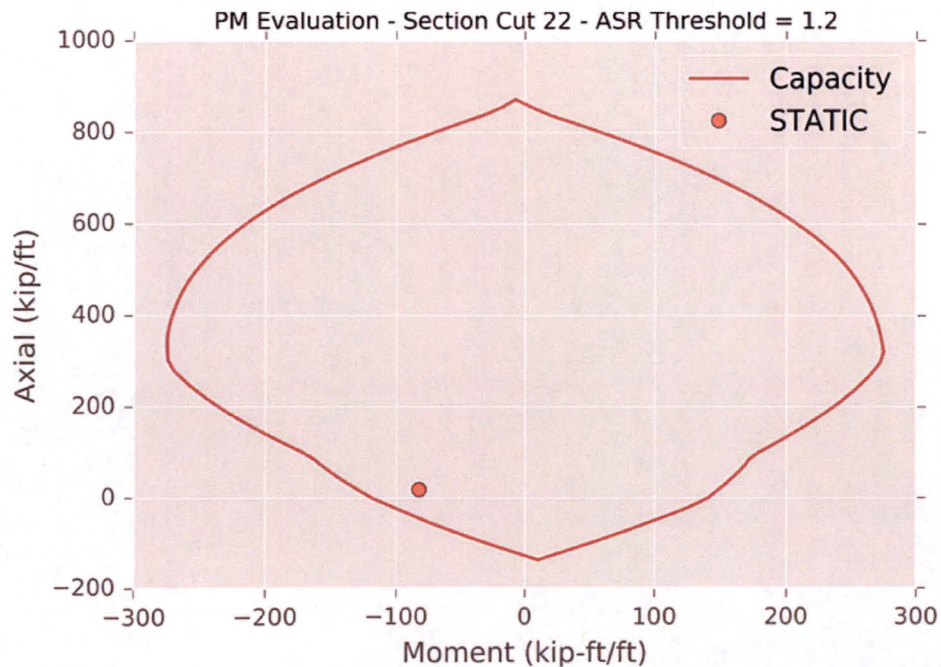


Figure 67. PM Interaction Check for Standard Analysis Case after Moment Redistribution (Section Cut 22)

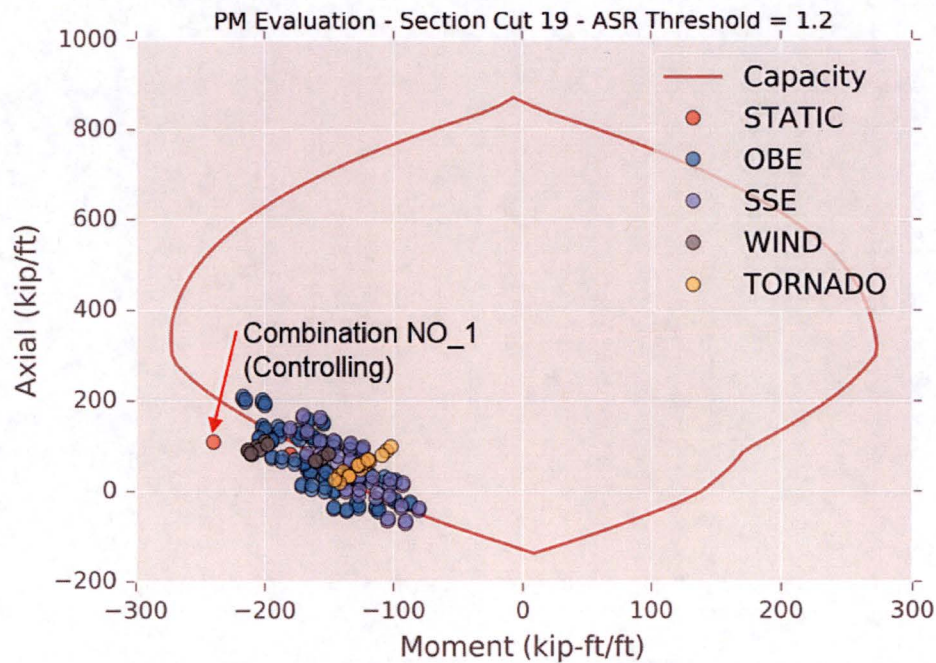


Figure 68. PM Interaction Check for Standard-Plus Analysis Case prior to Moment Redistribution (Section Cut 19)

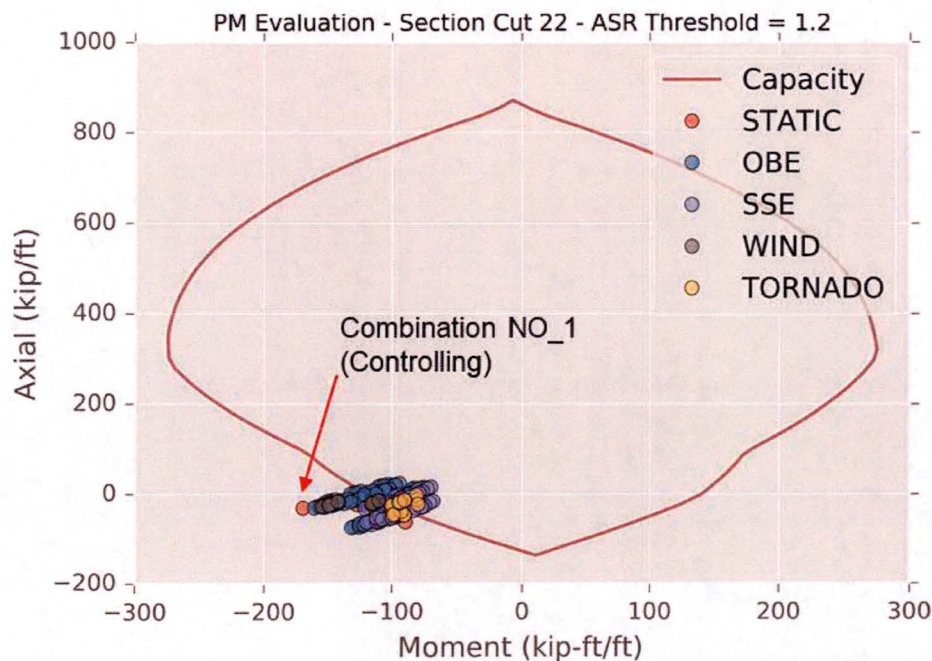


Figure 69. PM Interaction Check for Standard-Plus Analysis Case prior to Moment Redistribution (Section Cut 22)

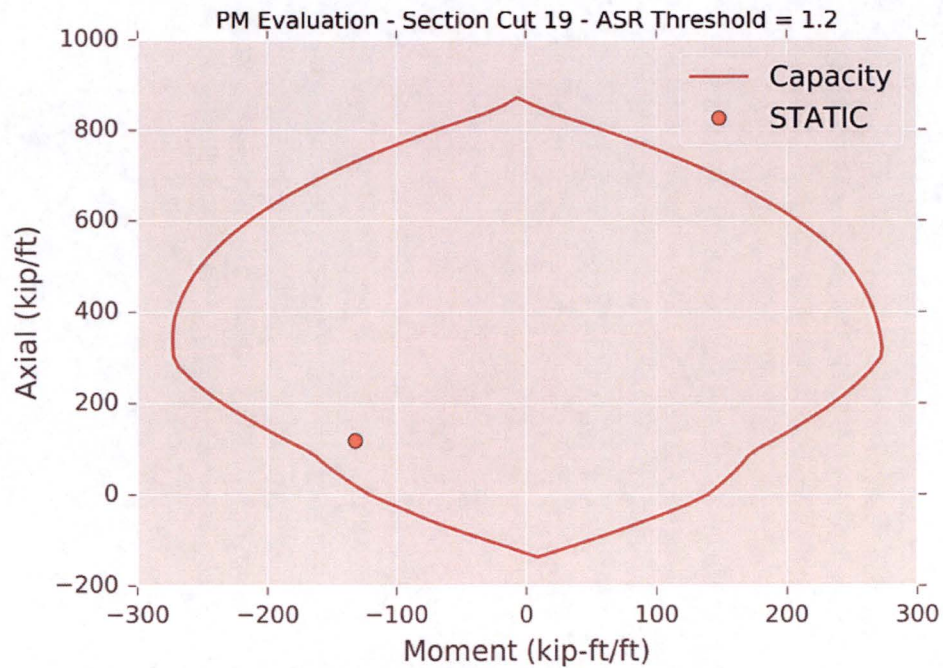


Figure 70. PM Interaction Check for Standard-Plus Analysis Case after Moment Redistribution (Section Cut 19)

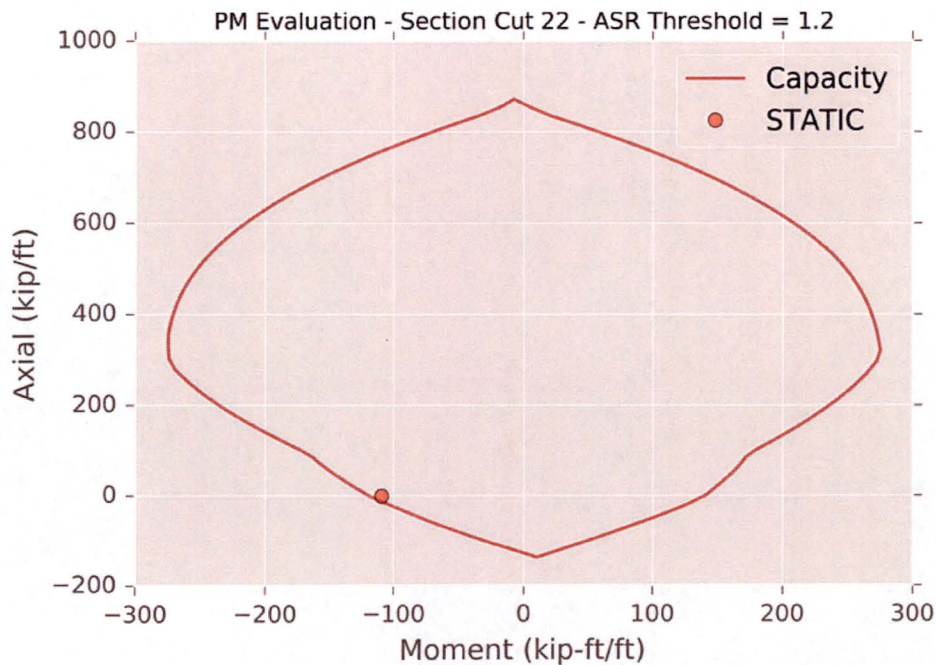
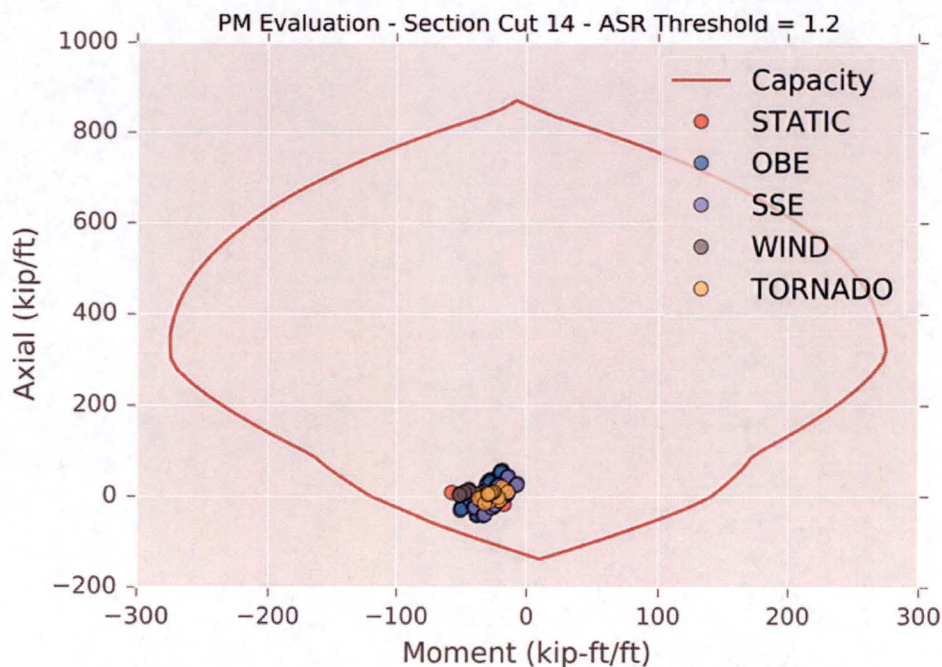
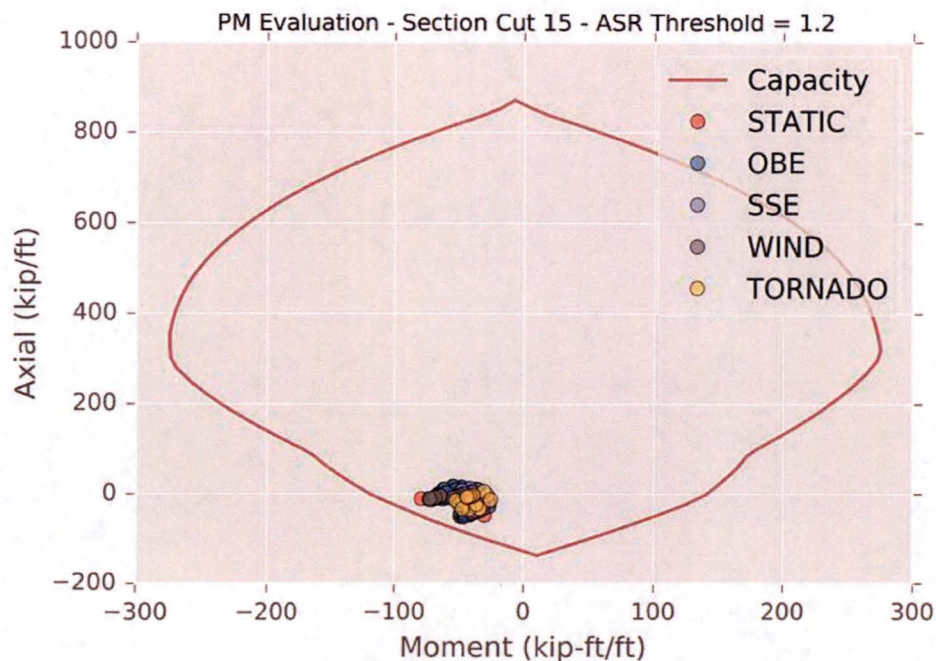


Figure 71. PM Interaction Check for Standard-Plus Analysis Case after Moment Redistribution (Section Cut 22)



**Figure 72. PM Interaction Check for Standard-Plus Analysis Case (Section Cut 14)
(No Moment Redistribution Needed)**



**Figure 73. PM Interaction Check for Standard-Plus Analysis Case (Section Cut 15)
(No Moment Redistribution Needed)**

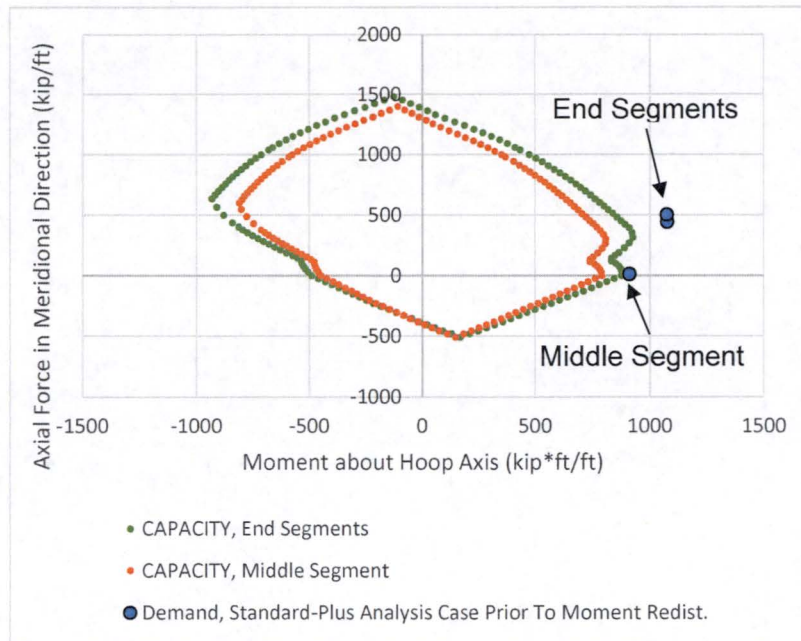


Figure 74. PM Interaction Checks at Base of Wall between AZ 270° and 360° for Standard-Plus Analysis Case prior to Moment Redistribution

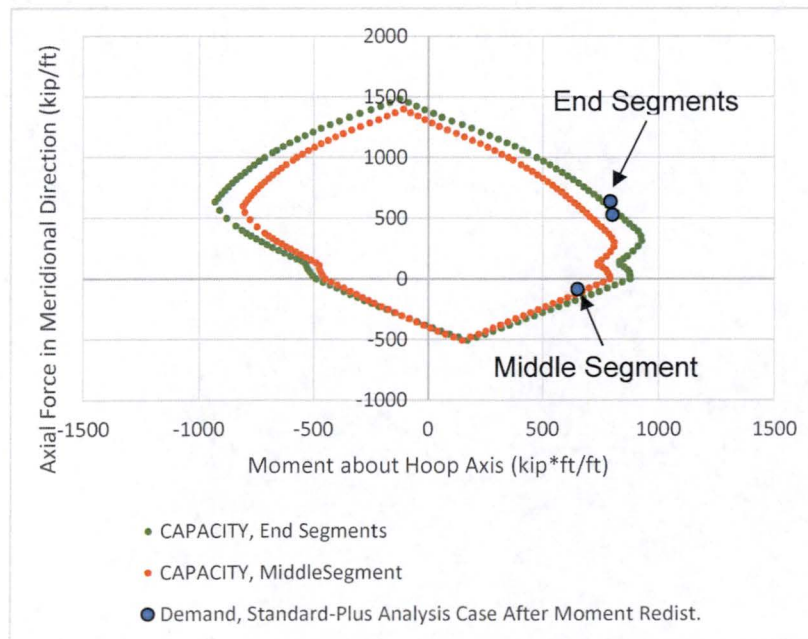


Figure 75. PM Interaction Checks at Base of Wall between AZ 270° and 360° for Standard-Plus Analysis Case after Moment Redistribution

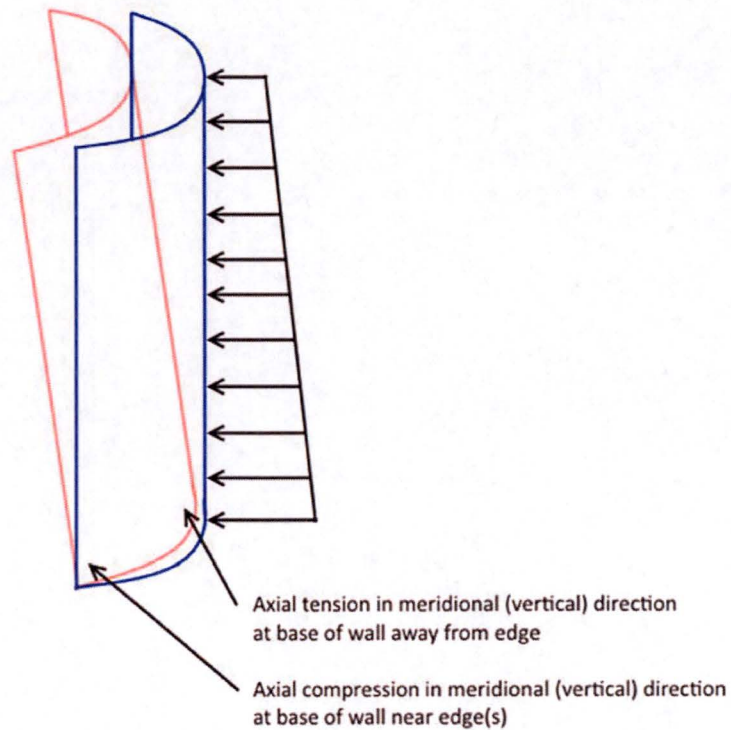


Figure 76. Illustration of Axial Force Couple Resisting Out-of-Plane Pressures at the Base of Wall
(sketch only, not to scale)

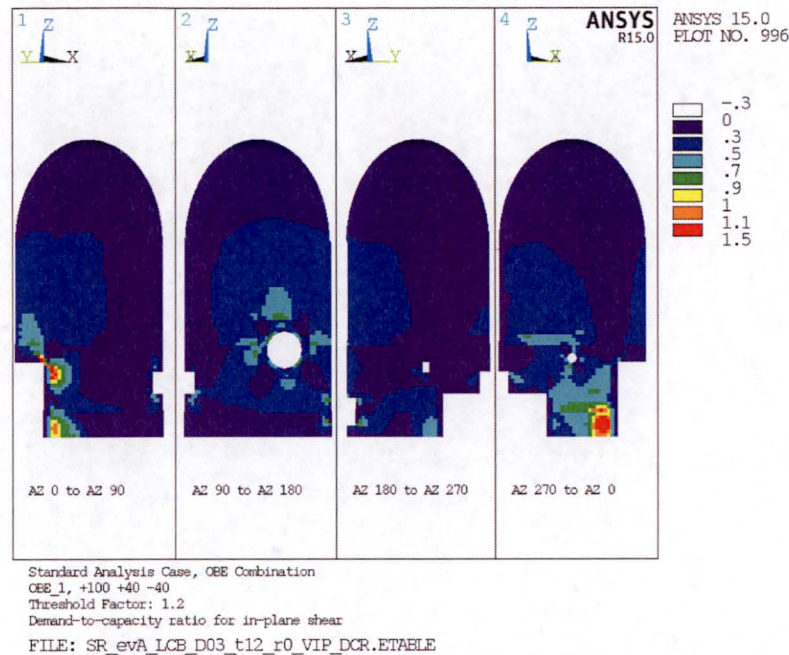


Figure 77. DCRs for In-Plane Shear for Combination OBE_1 (100% E., 40% N., 40% Vert. Down) for the Standard Analysis Case

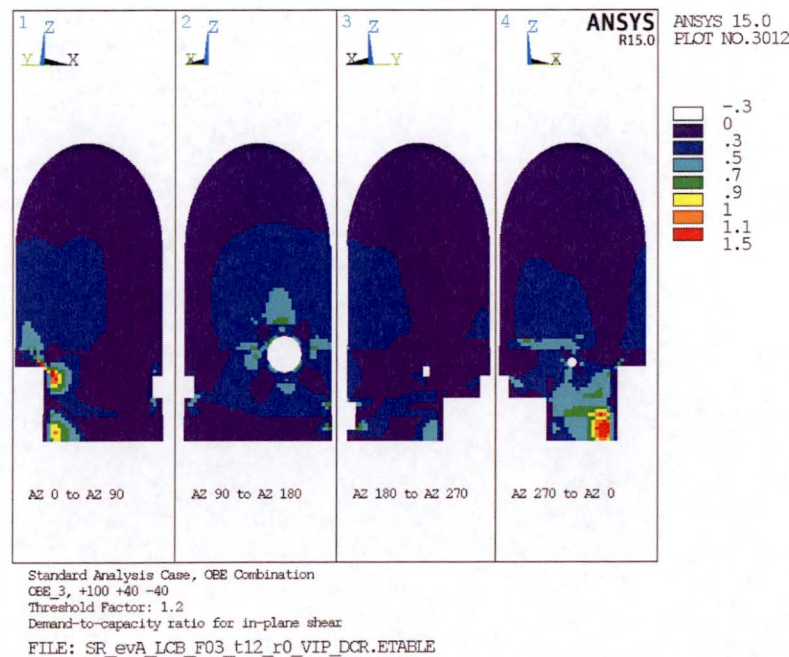


Figure 78. DCRs for In-Plane Shear for Combination OBE_3 (100% E., 40% N., 40% Vert. Down) for the Standard Analysis Case

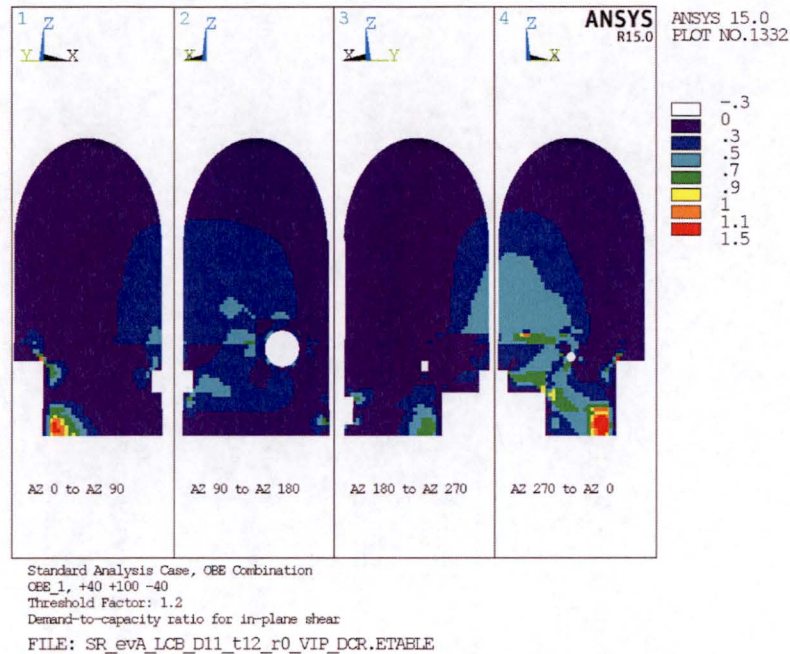


Figure 79. DCRs for In-Plane Shear for Combination OBE_1 (40% E., 100% N., 40% Vert. Down) for the Standard Analysis Case

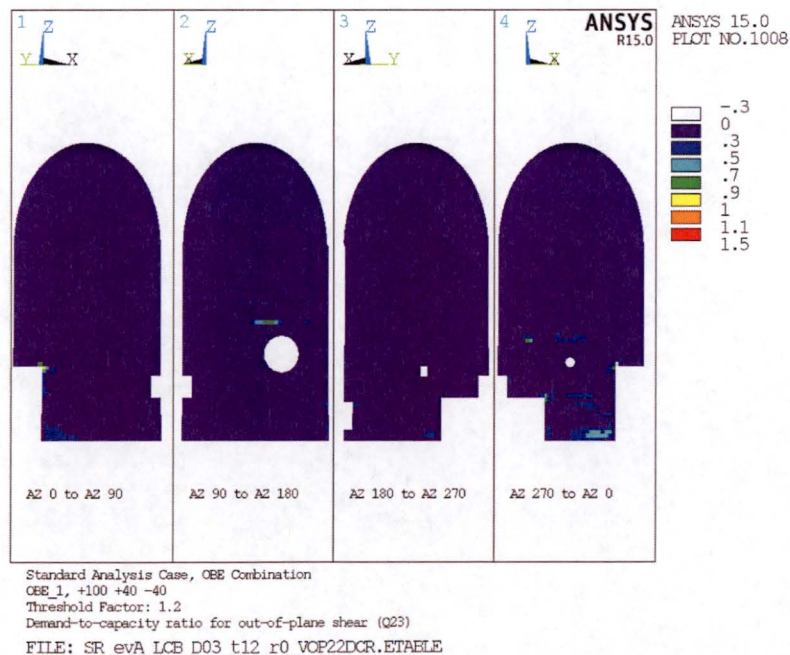


Figure 80. DCRs for Out-of-Plane Shear for Combination OBE_1 (100% E., 40% N., 40% Vert. Down) for the Standard Analysis Case

CLIENT: NextEra Energy Seabrook

SUBJECT: Evaluation and Design Confirmation of As-Deformed CEB

PROJECT NO: 150252

DATE: 31 July 2016

BY: R.M. Mones

VERIFIER: A.T. Sarawit

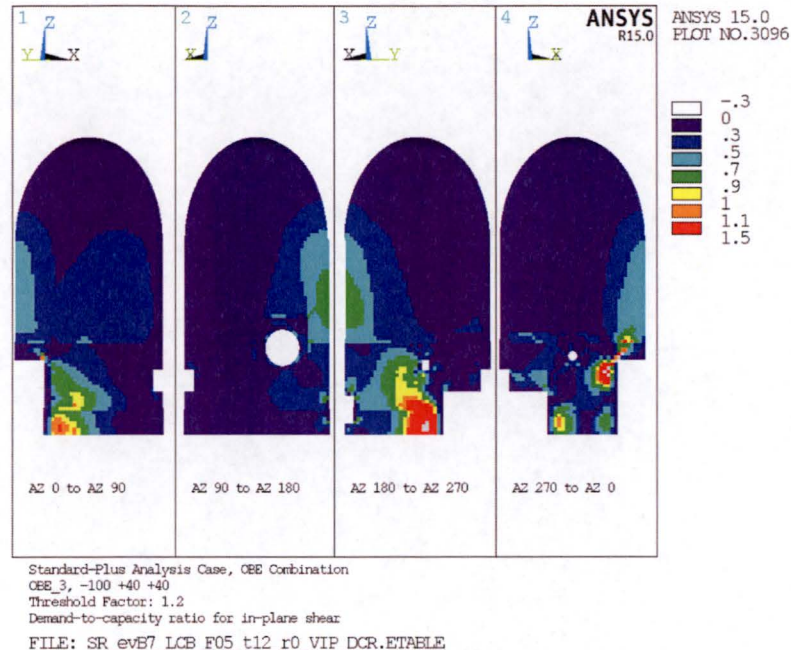


Figure 81. DCRs for In-Plane Shear for Combination OBE_3 (100% W., 40% N., 40% Vert. Up) for the Standard-Plus Analysis Case

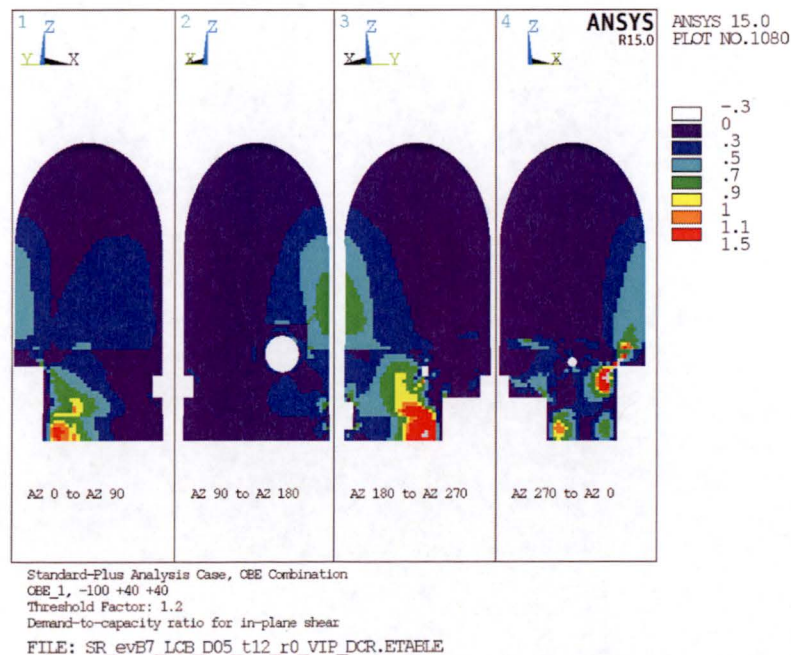


Figure 82. DCRs for In-Plane Shear for Combination OBE_1 (100% W., 40% N., 40% Vert. Up) for the Standard-Plus Analysis Case

CLIENT: NextEra Energy Seabrook

SUBJECT: Evaluation and Design Confirmation of As-Deformed CEB

PROJECT NO: 150252

DATE: 31 July 2016

BY: R.M. Mones

VERIFIER: A.T. Sarawit

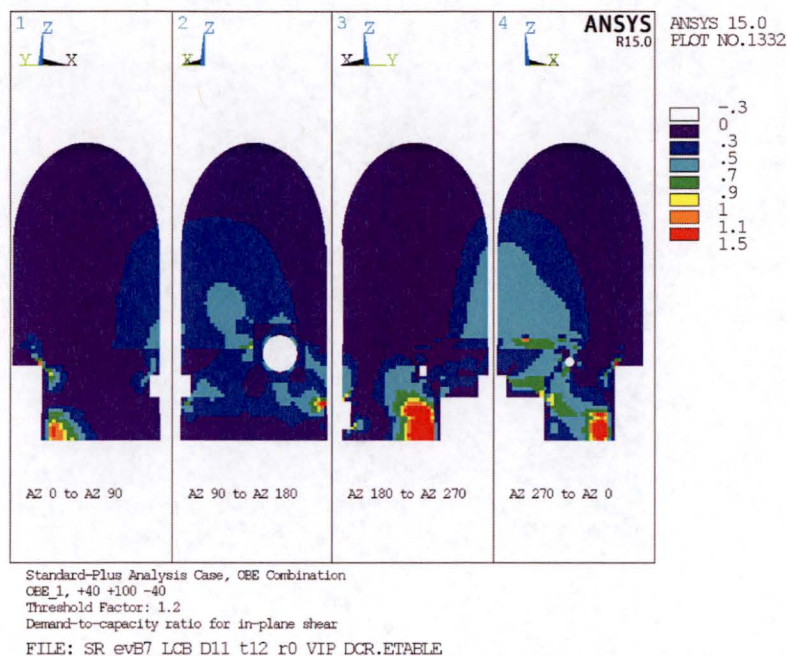


Figure 83. DCRs for In-Plane Shear for Combination OBE_1 (40% E., 100% N., 40% Vert. Down) for the Standard-Plus Analysis Case

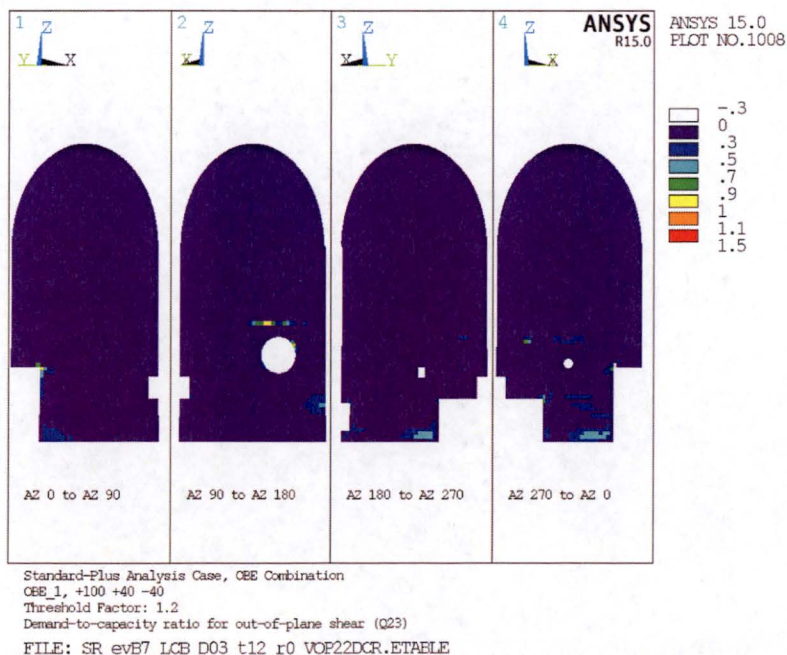


Figure 84. DCRs for Out-of-Plane Shear for Combination OBE_3 (100% E., 40% N., 40% Vert. Down) for the Standard-Plus Analysis Case



11. REFERENCES

- [1] Simpson Gumpertz & Heger, Inc., *Criteria Document for Evaluation and Design Confirmation of As-Deformed Containment Enclosure Building at Seabrook Station in Seabrook, NH*, Document No. 150252-CD-03, Revision 0, Waltham, MA, 27 July 2016.
- [2] Simpson Gumpertz & Heger, Inc., *Phase 1A Investigation of Apparent Movement of the Containment Enclosure Building at the NextEra Energy Seabrook Station, NH*, Report No. 150252-SVR-01-R1, Revision 1, Waltham, MA, 25 June 2015.
- [3] Simpson Gumpertz & Heger, Inc., *Joint Width Measurements at Twenty-Five Seismic Isolation Joint Locations to Support Root Cause Evaluation of Apparent Movement of CEB, NextEra Energy Seabrook Facility, Seabrook, NH*, Report No. 150252-SVR-02-R1, Revision 1, Waltham, MA, 28 September 2015.
- [4] Simpson Gumpertz & Heger, Inc., *Annulus Width Measurements between CEB and CB at Springline, Investigation of Movement between CEB and CEVA Building, and ASR Inspection on the Exterior of the CEB at NextEra Energy Seabrook Station, Seabrook, NH*, Report No. 150252-SVR-03-R0, Revision 0, Waltham, MA, 25 March 2016.
- [5] Simpson Gumpertz & Heger, Inc., *March 2016, Joint Width Measurements at Twenty-Five Seismic Isolation Joint Locations to Support Root Cause Evaluation of Apparent Movement of CEB, NextEra Energy Seabrook Facility, Seabrook, NH*, Report No. 160144-SVR-03-R0, Revision 0, Waltham, MA, 27 May 2016.
- [6] Simpson Gumpertz & Heger, Inc., *Development of ASR Load Factors for Seismic Category I Structures at Seabrook Station, Seabrook, NH*, Report No. 160268-R-01, Revision 0, Waltham, MA, 27 July 2016.
- [7] Seabrook, *Updated Final Safety Analysis Report*.
- [8] Seabrook, *System Description for Structural Design Criteria for Public Service Company of New Hampshire Seabrook Station Unit Nos. 1 & 2*, Document No. SD-66, Revision 2, 2 March 1984.
- [9] Simpson Gumpertz & Heger, Inc., *Additional ASR-Related Inspections and CI Measurements at Forty-Two Locations to Support the Root Cause Evaluation of Apparent Movement of CEB, NextEra Energy Seabrook Facility, Seabrook, NH*, Report No. 150252-SVR-05-RA, Revision A, Waltham, MA, 11 July 2016.
- [10] Simpson Gumpertz & Heger, Inc., *Quality Assurance Manual for Nuclear Facility Work*, Revision 7, Waltham, MA, 18 November 2013.
- [11] American Concrete Institute, *Building Code Requirements for Reinforced Concrete and Commentary*, ACI 318-71, ACI Committee 318, American Concrete Institute, Detroit, MI, 1971.



- [12] United Engineers & Constructors Inc., Seabrook Station Structural Drawings. ¹
- [13] Ellingwood, B. et al., *Development of a Probability Based Load Criterion for American National Standard A58*, NBS Special Publication 577, June 1980.
- [14] The Institution of Structural Engineers, *Structural effects of alkali-silica reaction*, 1992.
- [15] Clark, L.A., "Critical Review of the Structural Implications of the Alkali Silica Reaction in Concrete", Transport and Road Research Laboratory Contractor Report 169, 1989.
- [16] MPR, "Seabrook Station - Implications of Large-Scale Test Program Results on Reinforced Concrete Affected by Alkali-Silica Reaction," MPR-4273 (Seabrook FP# 101050), Revision 0, July 2016.
- [17] MPR, "Seabrook Station: Impact of Alkali-Silica Reaction on the Structural Design Evaluations," MPR-4288 (Seabrook FP# 101020), Revision 0, July 2016.
- [18] ANSYS Inc., ANSYS Mechanical APDL, Release 15, 2013.
- [19] Simpson Gumpertz & Heger Inc., *Verification and Validation of ANSYS 15.0 Structural*, Revision 0, Waltham, MA, 28 May 2015.
- [20] Simpson Gumpertz & Heger Inc., *ANSYS 15.0 Structural Software Requirements Specification (SRS)*, Revision 0, Waltham, MA, 28 May 2015.
- [21] American Concrete Institute, *Prediction of Creep, Shrinkage, and Temperature Effects in Concrete Structures*, ACI 209R-92, 1992.
- [22] Mohammed, T. U. et al., "Alkali-Silica Reaction-Induced Strains over Concrete Surface and Steel Bars in Concrete", ACI Materials Journal, V. 100, No. 2, March-April 2003.
- [23] Simpson Gumpertz & Heger, Inc., *Letter Report*, Report No. 150252-L-04, Revision 0, Waltham, MA, 26 June 2015.
- [24] United Engineers & Constructors Inc., *Containment-Enclosure Building (019), Calculations CE-3 (Rev. 3), CE-4 (Rev. 6), CE-5 (Rev. 3), CE-7 (Rev. 4), SBSAG-3CE (Rev. 1), and SBSAG-4CE (Rev. 0)*, Mar 1977 to Aug. 1983.
- [25] Structure Point, spColumn, Release v4.81, 2013.
- [26] Simpson Gumpertz & Heger Inc, *spColumn v4.81 Commercial Grade Software Dedication Plan/Report*, Revision 0, Waltham, MA, July 2014.
- [27] Wood, R. H., "The reinforcement of slabs in accordance with a pre-determined field of moments", Concrete, Vol. 2 (2), February, pp. 69-76, May 1968.



- [28] American Society of Civil Engineers, *Seismic Design Criteria for Structures, Systems, and Components in Nuclear Facilities*, ASCE/SEI 43-05, 2005.
- [29] Simpson Gumpertz & Heger, Inc., *Geotechnical Assessment of the CEB*, Report No. 150252-R-01, Revision 0, Waltham, MA, 22 June 2015.
- [30] Saouma, V. and Perotti, L., "Constitutive Model for Alkali-Aggregate Reactions", *ACI Materials Journal*, V. 103, No. 3, May-June 2006.
- [31] Seabrook, *Seismic Isolation Gaps Between Structures Less Than Specified Value*, AR02044627, AR Assignment 2, Revision 2, 1 July 2015.
- [32] Simpson Gumpertz & Heger, Inc., *Field Investigation*, Calculation No. 110594-CA-01, Revision 0, Waltham, MA, 20 March 2012.
- [33] Simpson Gumpertz & Heger, Inc., *Cracking Index (CI) Determination*, SGH Z014-13, Revision 2, Waltham, MA, 27 May 2015.



PROJECT NO: 150252

DATE: July 2016

CLIENT: NextEra Energy Seabrook BY: A.T. Sarawit

SUBJECT: Evaluation and Design Confirmation of As-Deformed CEB VERIFIER: N/A

INDEPENDENT VERIFICATION CHECKLIST

Project Number: 150252		Document No. and Revision No.: 150252-CA-02 Rev. 0		Document Type: Calculation
Scope of Review: Calculation Body and Appendices				
Method of Verification: <input checked="" type="checkbox"/> Design Review <input type="checkbox"/> Alternate Calculation <input type="checkbox"/> Qualification Test				
Y	N	N/A		
<input checked="" type="checkbox"/>	<input type="checkbox"/>	<input type="checkbox"/>	Are assumptions, opinions, judgments, and technical approaches correct?	
<input checked="" type="checkbox"/>	<input type="checkbox"/>	<input type="checkbox"/>	1) Are assumptions, used to perform the design or analysis activity identified?	
<input checked="" type="checkbox"/>	<input type="checkbox"/>	<input type="checkbox"/>	2) Are the assumptions adequately described and reasonable?	
<input checked="" type="checkbox"/>	<input type="checkbox"/>	<input type="checkbox"/>	1) Are applicable codes, standards, and regulatory requirements properly identified?	
<input type="checkbox"/>	<input type="checkbox"/>	<input checked="" type="checkbox"/>	2) Are their requirements for design or analysis met?	
<input checked="" type="checkbox"/>	<input type="checkbox"/>	<input type="checkbox"/>	Is an appropriate design or analysis method used?	
<input checked="" type="checkbox"/>	<input type="checkbox"/>	<input type="checkbox"/>	Are the calculations, drawings, graphs, and tables technically complete?	
<input type="checkbox"/>	<input type="checkbox"/>	<input checked="" type="checkbox"/>	Are the design inputs correctly selected and incorporated into design?	
<input checked="" type="checkbox"/>	<input type="checkbox"/>	<input type="checkbox"/>	1) Is the name and version of the computer program(s) or routine(s) used stated?	
<input checked="" type="checkbox"/>	<input type="checkbox"/>	<input type="checkbox"/>	2) Have they been verified and approved for use in accordance with SGH approved procedures?	
<input checked="" type="checkbox"/>	<input type="checkbox"/>	<input type="checkbox"/>	3) Is their use appropriate for the problem?	
<input checked="" type="checkbox"/>	<input type="checkbox"/>	<input type="checkbox"/>	Are results interpreted correctly?	
<input checked="" type="checkbox"/>	<input type="checkbox"/>	<input type="checkbox"/>	Are results, conclusions, and recommendations reasonable?	
<input checked="" type="checkbox"/>	<input type="checkbox"/>	<input type="checkbox"/>	Are the organization and clarity of calculations or other design documents adequate?	
<input type="checkbox"/>	<input type="checkbox"/>	<input checked="" type="checkbox"/>	Are the necessary design inputs for interfacing organization specified in the design documents or in supporting procedures or instructions?	
<input type="checkbox"/>	<input type="checkbox"/>	<input checked="" type="checkbox"/>	Are Checker Assignment and Review Sheets Exhibit 3.7 used (see sheet attached) and properly completed?	
<input type="checkbox"/>	Other items for checklist, if necessary, added by the PIC or PM.			
<input type="checkbox"/>				
<input type="checkbox"/>				
Independent Verifier:				
Andrew T. Sarawit				31 July 2016
Printed Name		Signature		Date
*Any calculations, comments, or notes generated as part of this review should be signed, dated, and attached to this checklist. Such material should be labeled and recorded in such a manner as to be intelligible to a technically qualified third party.				

EP 3.1 EX 3.5 R4
Date: 12 October 2015


INDEPENDENT VERIFICATION COMMENT SHEET
SIMPSON GUMPERTZ & HEGER

 Engineering of Structures
and Building Enclosures

Calculation Number: 150252-CA-02 Rev. C

Independent Verifier: Andrew T. Sarawit

Comments	Resolution
Technical comments: 1) Page i, Objective Overview – What about measurements prior to 2015, are they used at in this calculation? 2) Page 18, 3 rd bullet – Is it true that the assessment of CEB deformations is based on measurements relative to the CB which is assumed to not have deformed or moved? If so, this should be stated as an assumption. 3) Page 19, JA03, last sentence – please describe how the crack section is modeled in terms of flexural and axial stiffnesses. 4) Page 21, 1st paragraph, please clarify what is meant by “performed <u>and qualified</u> ” 5) Page 26, Section 6.2, description of Analysis Steps 1 and 2 – In Step 1, sustained load includes gravity. In step 2, gravity load is applied again so the deflections from step 2 double counts gravity. Unlikely not an issue for strength check, but deflections from step 2 would be off. This should be stated in this section.	Technical comments: 1) For each measurement (including crack indices), the most recent measurement is used in this calculation. Measurements prior to 2011 are available, but those measurements have been superseded by more recent measurements. 2) This has been added to JA08. 3) The model has been revised to not use cracked section properties. 4) This paragraph is describing that both the Standard and the Standard-Plus Analysis Cases are evaluated against ACI 318-71 criteria. The text has been clarified. 5) This has been addressed in the Revision 0 criteria document for this calculation. A reference to Section 9.1 of the Criteria Document has been added to the calculation report after listing analysis steps.



Comments	Resolution
6) Page 44, last sentence of Section 6.4.1 – Why would the ASR strains computed by the FEA be a conservative representation of the CI measurement?	6) It is assumed that all cracking associated with the CI measurement is from ASR of the wall. This is conservative because some of the cracks are realistically from effects such as shrinkage and external loads.
7) Page 46, 3rd paragraph – why are the tensile forces at the base of wall considered to be fictitious?	7) This statement has been removed and the tensile forces at the base of the wall are described and evaluated.
8) Page 50, Section 7.1.2 – Why is it okay to not take into account the effect the ASR-induced prestress when performing axial-flexure interaction evaluations?	8) This sentence was misleading and has been removed. ASR demands are included when performing PM interaction evaluations. The section is evaluated as a reinforced concrete section. Prestressed concrete provisions are not used.
9) Page 66, Section 7.4.6 – Add evaluation results discussion for the springline location.	9) The elevated demands at the springline identified in this section were related to misplaced boundary conditions in a development model and have been resolved.
10) Page 69, Section 7.5.1 – Add discussion on axial tension, in-plane shear, and out-of-plane bending at the base of the wall.	10) See Section 7.6.1.
11) Page 70, Section 7.6 – Add a discussion to mention that preliminary field inspections found gap between CEB and CB at the missile shield is zero or near-zero.	11) This has been added as Unverified Assumption UA01.
12) Appendix H – Figures H27, H59, H88, show high in-plane shear forces. The in-plane shear demand forces goes down as the wall section cut length increases, because the shear demand at some point starts to reverse direction. Please discuss and justify the section cut wall length selected for evaluation.	12) Section cut evaluations for in-plane shear use cut lengths up to 90 degrees or about 125 ft. The use of this wall length is justified because design in-plane shear demands would cause the CEB wall to crack and redistribute load to mobilize the entire wall segment. Since these section cuts are used for evaluation of in-plane shear in the main body of the calculation, this is clarified in Section 7.6.1 (within the in-plane shear subheading)
13) Appendix I, Revise stability calculations to consider buoyancy.	13) Appendix I has been revised.



Comments	Resolution
14) Appendix O, Revise cover quantities for critical section cut (Section Cut 22) to use actual design values rather than conservative values.	14) Revised in Appendix O.
15) Cover page, overview of method of approach - reads like it is unclear to us if CEB and CB are already in contact at some locations. Why can't we just give this as a fact based on our field inspection findings.	15) The site visit report containing specific measurement data has not been issued at this time, therefore specific conditions at the missile shield cannot be stated.
16) Page 18, "... monitoring is performed by comparing the average measurement" - okay for CCI but for gap clearance I think should be minimum instead.	16) Threshold monitoring revised to recommend performing that corrective action when a threshold limit for a given displacement measurement is approached.
17) page 18, "... action should be taken to ensure validity if the calculation conclusions" - recommend to change to say that corrective action should be taken.	17) See response to item 16 above.
18) page 59, we should say some where before "The small demand-to-capacity ratio ..." that exceedance of the first criteria does not imply a non-conformance as the section may still have sufficient shear friction capacity	18) Revised.
19) It isn't clear from reading on how we came up with the 1 inch of needed clearance at the missile shield.	19) The 1 inch of clearance needed at the missile shield is computed by assuming a 0.0 in. remaining joint clearance and then back-calculating the required seismic gap width. Additional clarity has been added to the equations in Section 7.7 and Tables 16 and 17.
20) Figures 68, 69, are not referenced.	20) Figure references have been added to the text.
Editorial comments/suggestions: 1) Page i, Overview of Method and Assumptions - Revise "... <u>by performing</u> response spectrum analysis" to "... <u>from</u> response spectrum analysis"	Editorial comments/suggestions: 1) Revised



Comments	Resolution
2) Page 19, JA02, revise "... as the section attempts to expand." to "... as the <u>concrete</u> attempts to expand."	2) Revised
3) Page 22 and 99 – Figure 1 is not referred to in the text body of the calculation.	3) Revised
4) Page 27, Section 6.2.11 – Revise "Membrane elements (Shell181)" to "Membrane elements (Shell181 <u>with membrane stiffness only</u>)"	4) Revised
5) Page 32, 3rd bullet – adding a figure would help describe the inward pressure distributions.	5) The inward pressure distributions are illustrated in Appendix J. Reference to Appendix J added to this section.
6) Page 39, Section 6.3.2 – add a sentence before subheading loads, "These loads are described in this section as follows".	6) Revised
7) Page 42, Section 6.4 – revise "...profiles <u>in</u> presented in..." to "...profiles <u>is</u> presented in..."	7) Revised
8) Page 49, Section 7.1, last sentence – revise "exceedance is identified and justified" to "structure satisfies the requirements"	8) This sentence has been changed to be clearer.
9) Page 54, Section 7.2, 1st sentence – revised "although" to "because"	9) Revised
10) Page 61, last equation, revise " $> P_u$ " to " $< P_u$ ".	10) Revised
11) Page 67, Section 7.5.1, 3rd bullet, revise "wall on the edge(s)" to "wall near the openings"	11) Revised
12) Page 75, Table 4, in the 2nd equation, revise "... $1.0S_h + 1.0 S_w$ " to "... $1.0S_h$ "	12) Revised
13) Page 79, Table 8 – Revise "Table 4" to "Table 5", at multiple places.\	13) Revised



Comments	Resolution
14) Appendix E – EF, IF, and OF should be defined somewhere in the calculation as “Each Face”, “Inside Face”, and “Outside Face”.	14) Revised
15) Appendix F, Section F7, 1st sentence – revise “Figure 1” to “Figure F.1”	15) Revised
16) Appendix G, Page J-1 – Revise appendix title “...Load Combinations without As-Deformed...” to “...Load Combinations for Original Design Analysis Case without As-Deformed...”	16) Revised
17) Appendix G, Section G3 – Revise “... are <u>neglected</u> in this analysis...” to “... are <u>excluded</u> in this analysis...”	17) Revised
18) Appendix H, Page H-1 – Revise wording of sentence beginning with “The goal of the moment redistribution...” to more clearly explain that moment redistribution simulates plasticity behavior.	18) Revised
19) Appendix J, no comments	19) No revisions required
20) Appendix K, Update PM Interaction diagram example figures to match updated example computation results	20) Revised
21) Appendix K, Clarify why DCR for out-of-plane shear taken as minimum of two computed values.	21) Section 7.1.5 in the main body of the calculation discusses the out-of-plane shear evaluation methodology.
22) Appendix L, Page L-2 – revise “a stress profile that satisfies” to “a stress profile that satisfies <u>static equilibrium</u> ”	22) Revised
23) Appendix L, Page L-2 – revise “initial stress of ± 100 psi” to “initial stress <u>gradient</u> of ± 100 psi”	23) Revised
24) Appendix L, Figures L6, L7, and L8 legend labels, revise “Redistribution, Case M” to “Redistribution, 12.2*Case M”	24) Revised



PROJECT NO: 150252

DATE: July 2016

CLIENT: NextEra Energy Seabrook BY: A.T. Sarawit

SUBJECT: Evaluation and Design Confirmation of As-Deformed CEB VERIFIER: N/A

Comments	Resolution
25) Appendix M, Page M-2 - Revise "The static load combination NO_1 for the <u>Standard</u> Analysis Case is reevaluated", to <u>Standard-Plus</u> .	25) Revised
26) Appendix M, Page M-2, Explain why Figures M1 and M5 use different PM interaction capacities.	26) Sentence added to the appendix to clarify.
27) Appendix N – Revise "Figure M-1" to "Figure N-1", "Figure M-2" to "Figure N-2", and "[M-1]" to "[N-1]".	27) Revised
28) Appendix N, Table N-1 – Revise "T" to "Thickness", and "in^2" to "in. ² ".	28) Revised
29) Figures are not in sequence	29) Some figures/tables have been resorted to be in order, but not all.
30) On page 25, revise "Figure 7 and 8" to "Figures 7 and 8"	30) Revised

Resolution by: Rye Mor 7/31/2016

Accepted by: AS 7/31/2016

Form EP3.1 EX3.6 R2
Date: 28 April 2010



PROJECT NO: 150252

DATE: July 2016

CLIENT: NextEra Energy Seabrook BY: R.M. Mones

SUBJECT: Evaluation and Design Confirmation of As-Deformed CEB VERIFIER: A.T. Sarawit

APPENDIX B

COMPUTER RUN IDENTIFICATION LOG

SIMPSON GUMPERTZ & HEGER



Engineering of Structures
and Building Enclosures

Client: NextEra Energy Seabrook Page 1 of 13

Project: Evaluation and Design Confirmation of As-Deformed CEB

Project No.: 150252 Subcontract No.: N/A Calculation No.: 150252-CA-02

Run No.	Title	Program/Ver. ^A	Hardware	Date	Files	
10A_r0	Standard Analysis Case	ANSYS 15	Cluster3g ^B	7/19/2016	Note C	
10B7_r0	Standard-Plus Analysis Case	ANSYS 15	Cluster3g ^B	7/25/2016	Note C	
10D_r0	Evaluation w/o ASR and SS loads	Note D	Cluster3g ^B	7/19/2016	Note D	
10E_r0	Parametric Study on ASR at Springline	ANSYS 15	Cluster3g ^B	7/19/2016	Note C	
10G_r0	Analysis and Evaluation of Standard-Plus Analysis Case for Combination NO_1 with Simulated Concrete Cracking at El. +45.5 and AZ 240	ANSYS 15	Cluster3g ^B	7/28/2016	Note C	
10AR_r0	Standard Analysis Case with Moment Redistribution (limited to combination NO_1)	ANSYS 15	Cluster3g ^B	7/26/2016	Note C	
10BR7_r0	Standard-Plus Analysis Case with Moment Redistribution (limited to combination NO_1)	ANSYS 15	Cluster3g ^B	7/30/2016	Note C	
10BR7E_r0	Standard-Plus Analysis Case with Moment Redistribution (limited to combination OBE_4)	ANSYS 15	Cluster3g ^B	7/27/2016	Note C	



Run No.	Title	Program/Ver. ^A	Hardware	Date	Files	
10B_r0	Standard-Plus Analysis Case (for comparison with Analysis Case 10E_r0 in Appendix J)	ANSYS 15	Cluster3g ^B	7/18/2016	Note C	
10B4_r0	Parametric Study Comparison Case 1 (Referenced in Appendix J)	ANSYS 15	Cluster3g ^B	7/21/2016	Note C	
10B5_r0	Parametric Study Comparison Case 2 (Referenced in Appendix J)	ANSYS 15	Cluster3g ^B	7/22/2016	Note C	
Parametric_Study_Set_A	Baseline for comparison of with Parametric Study Set H (Referenced in Appendix J)	ANSYS 15	Cluster3g ^B	9/11/2015	Note C	
Parametric_Study_Set_H	Parametric Study with Reduced Concrete Elastic Modulus (Referenced in Appendix J)	ANSYS 15	Cluster3g ^B	9/14/2015	Note C	
H_15_601_705	Compute PM Interaction Capacity of Section H_15_601_705	spColumn 4.81	Cluster3a ^B	6/6/2016	Note D	
H_15_602_703	Compute PM Interaction Capacity of Section H_15_602_703	spColumn 4.81	Cluster3a ^B	6/6/2016	Note E	
H_15_603_705	Compute PM Interaction Capacity of Section H_15_603_705	spColumn 4.81	Cluster3a ^B	6/6/2016	Note E	
H_15_603_706	Compute PM Interaction Capacity of Section H_15_603_706	spColumn 4.81	Cluster3a ^B	6/6/2016	Note E	
H_15_604_702	Compute PM Interaction Capacity of Section H_15_604_702	spColumn 4.81	Cluster3a ^B	6/6/2016	Note E	
H_15_604_704	Compute PM Interaction Capacity of Section H_15_604_704	spColumn 4.81	Cluster3a ^B	6/6/2016	Note E	
H_15_604_705	Compute PM Interaction Capacity of Section H_15_604_705	spColumn 4.81	Cluster3a ^B	6/6/2016	Note E	
H_15_604_706	Compute PM Interaction Capacity of Section H_15_604_706	spColumn 4.81	Cluster3a ^B	6/6/2016	Note E	
H_15_605_702	Compute PM Interaction Capacity of Section H_15_605_702	spColumn 4.81	Cluster3a ^B	6/6/2016	Note E	
H_15_605_705	Compute PM Interaction Capacity of Section H_15_605_705	spColumn 4.81	Cluster3a ^B	6/6/2016	Note E	



Run No.	Title	Program/Ver. ^A	Hardware	Date	Files	
H_15_606_704	Compute PM Interaction Capacity of Section H_15_606_704	spColumn 4.81	Cluster3a ^B	6/6/2016	Note E	
H_15_606_708	Compute PM Interaction Capacity of Section H_15_606_708	spColumn 4.81	Cluster3a ^B	6/6/2016	Note E	
H_15_607_713	Compute PM Interaction Capacity of Section H_15_607_713	spColumn 4.81	Cluster3a ^B	6/6/2016	Note E	
H_15_609_703	Compute PM Interaction Capacity of Section H_15_609_703	spColumn 4.81	Cluster3a ^B	6/6/2016	Note E	
H_15_615_703	Compute PM Interaction Capacity of Section H_15_615_703	spColumn 4.81	Cluster3a ^B	6/6/2016	Note E	
H_24_603_704	Compute PM Interaction Capacity of Section H_24_603_704	spColumn 4.81	Cluster3a ^B	6/6/2016	Note E	
H_24_604_706	Compute PM Interaction Capacity of Section H_24_604_706	spColumn 4.81	Cluster3a ^B	6/6/2016	Note E	
H_27_602_703	Compute PM Interaction Capacity of Section H_27_602_703	spColumn 4.81	Cluster3a ^B	6/6/2016	Note E	
H_27_609_703	Compute PM Interaction Capacity of Section H_27_609_703	spColumn 4.81	Cluster3a ^B	6/6/2016	Note E	
H_27_612_701	Compute PM Interaction Capacity of Section H_27_612_701	spColumn 4.81	Cluster3a ^B	6/6/2016	Note E	
H_27_615_701	Compute PM Interaction Capacity of Section H_27_615_701	spColumn 4.81	Cluster3a ^B	6/6/2016	Note E	
H_27_615_703	Compute PM Interaction Capacity of Section H_27_615_703	spColumn 4.81	Cluster3a ^B	6/6/2016	Note E	
H_27_615_709	Compute PM Interaction Capacity of Section H_27_615_709	spColumn 4.81	Cluster3a ^B	6/6/2016	Note E	
H_27_617_709	Compute PM Interaction Capacity of Section H_27_617_709	spColumn 4.81	Cluster3a ^B	6/6/2016	Note E	
H_36_610_712	Compute PM Interaction Capacity of Section H_36_610_712	spColumn 4.81	Cluster3a ^B	6/6/2016	Note E	

SIMPSON GUMPERTZ & HEGER

Engineering of Structures
and Building Enclosures

PROJECT NO: 150252

DATE: July 2016

CLIENT: NextEra Energy Seabrook

BY: R.M. Mones

SUBJECT: Evaluation and Design Confirmation of As-Deformed CEB

VERIFIER: A.T. Sarawit

Run No.	Title	Program/Ver. ^A	Hardware	Date	Files	
H_36_614_709	Compute PM Interaction Capacity of Section H_36_614_709	spColumn 4.81	Cluster3a ^B	6/6/2016	Note E	
H_36_616_707	Compute PM Interaction Capacity of Section H_36_616_707	spColumn 4.81	Cluster3a ^B	6/6/2016	Note E	
H_36_616_709	Compute PM Interaction Capacity of Section H_36_616_709	spColumn 4.81	Cluster3a ^B	6/6/2016	Note E	
H_36_617_703	Compute PM Interaction Capacity of Section H_36_617_703	spColumn 4.81	Cluster3a ^B	6/6/2016	Note E	
H_39_608_711	Compute PM Interaction Capacity of Section H_39_608_711	spColumn 4.81	Cluster3a ^B	6/6/2016	Note E	
H_39_613_710	Compute PM Interaction Capacity of Section H_39_613_710	spColumn 4.81	Cluster3a ^B	6/6/2016	Note E	
H_39_615_703	Compute PM Interaction Capacity of Section H_39_615_703	spColumn 4.81	Cluster3a ^B	6/6/2016	Note E	
H_39_619_710	Compute PM Interaction Capacity of Section H_39_619_710	spColumn 4.81	Cluster3a ^B	6/6/2016	Note E	
H_39_620_710	Compute PM Interaction Capacity of Section H_39_620_710	spColumn 4.81	Cluster3a ^B	6/6/2016	Note E	
H_39_620_711	Compute PM Interaction Capacity of Section H_39_620_711	spColumn 4.81	Cluster3a ^B	6/6/2016	Note E	
H_39_622_711	Compute PM Interaction Capacity of Section H_39_622_711	spColumn 4.81	Cluster3a ^B	6/6/2016	Note E	
H_48_611_710	Compute PM Interaction Capacity of Section H_48_611_710	spColumn 4.81	Cluster3a ^B	6/6/2016	Note E	
H_48_618_710	Compute PM Interaction Capacity of Section H_48_618_710	spColumn 4.81	Cluster3a ^B	6/6/2016	Note E	
H_48_621_710	Compute PM Interaction Capacity of Section H_48_621_710	spColumn 4.81	Cluster3a ^B	6/6/2016	Note E	
M_15_601_705	Compute PM Interaction Capacity of Section M_15_601_705	spColumn 4.81	Cluster3a ^B	6/6/2016	Note E	



PROJECT NO: 150252

DATE: July 2016

CLIENT: NextEra Energy Seabrook

BY: R.M. Mones

SUBJECT: Evaluation and Design Confirmation of As-Deformed CEB

VERIFIER: A.T. Sarawit

Run No.	Title	Program/Ver. ^A	Hardware	Date	Files
M_15_602_703	Compute PM Interaction Capacity of Section M_15_602_703	spColumn 4.81	Cluster3a ^B	6/6/2016	Note E
M_15_603_705	Compute PM Interaction Capacity of Section M_15_603_705	spColumn 4.81	Cluster3a ^B	6/6/2016	Note E
M_15_603_706	Compute PM Interaction Capacity of Section M_15_603_706	spColumn 4.81	Cluster3a ^B	6/6/2016	Note E
M_15_604_702	Compute PM Interaction Capacity of Section M_15_604_702	spColumn 4.81	Cluster3a ^B	6/6/2016	Note E
M_15_604_704	Compute PM Interaction Capacity of Section M_15_604_704	spColumn 4.81	Cluster3a ^B	6/6/2016	Note E
M_15_604_705	Compute PM Interaction Capacity of Section M_15_604_705	spColumn 4.81	Cluster3a ^B	6/6/2016	Note E
M_15_604_706	Compute PM Interaction Capacity of Section M_15_604_706	spColumn 4.81	Cluster3a ^B	6/6/2016	Note E
M_15_605_702	Compute PM Interaction Capacity of Section M_15_605_702	spColumn 4.81	Cluster3a ^B	6/6/2016	Note E
M_15_605_705	Compute PM Interaction Capacity of Section M_15_605_705	spColumn 4.81	Cluster3a ^B	6/6/2016	Note E
M_15_606_704	Compute PM Interaction Capacity of Section M_15_606_704	spColumn 4.81	Cluster3a ^B	6/6/2016	Note E
M_15_606_708	Compute PM Interaction Capacity of Section M_15_606_708	spColumn 4.81	Cluster3a ^B	6/6/2016	Note E
M_15_607_713	Compute PM Interaction Capacity of Section M_15_607_713	spColumn 4.81	Cluster3a ^B	6/6/2016	Note E
M_15_609_703	Compute PM Interaction Capacity of Section M_15_609_703	spColumn 4.81	Cluster3a ^B	6/6/2016	Note E
M_15_615_703	Compute PM Interaction Capacity of Section M_15_615_703	spColumn 4.81	Cluster3a ^B	6/6/2016	Note E
M_24_603_704	Compute PM Interaction Capacity of Section M_24_603_704	spColumn 4.81	Cluster3a ^B	6/6/2016	Note E



Run No.	Title	Program/Ver. ^A	Hardware	Date	Files	
M_24_604_706	Compute PM Interaction Capacity of Section M_24_604_706	spColumn 4.81	Cluster3a ^B	6/6/2016	Note E	
M_27_602_703	Compute PM Interaction Capacity of Section M_27_602_703	spColumn 4.81	Cluster3a ^B	6/6/2016	Note E	
M_27_609_703	Compute PM Interaction Capacity of Section M_27_609_703	spColumn 4.81	Cluster3a ^B	6/6/2016	Note E	
M_27_612_701	Compute PM Interaction Capacity of Section M_27_612_701	spColumn 4.81	Cluster3a ^B	6/6/2016	Note E	
M_27_615_701	Compute PM Interaction Capacity of Section M_27_615_701	spColumn 4.81	Cluster3a ^B	6/6/2016	Note E	
M_27_615_703	Compute PM Interaction Capacity of Section M_27_615_703	spColumn 4.81	Cluster3a ^B	6/6/2016	Note E	
M_27_615_709	Compute PM Interaction Capacity of Section M_27_615_709	spColumn 4.81	Cluster3a ^B	6/6/2016	Note E	
M_27_617_709	Compute PM Interaction Capacity of Section M_27_617_709	spColumn 4.81	Cluster3a ^B	6/6/2016	Note E	
M_36_610_712	Compute PM Interaction Capacity of Section M_36_610_712	spColumn 4.81	Cluster3a ^B	6/6/2016	Note E	
M_36_614_709	Compute PM Interaction Capacity of Section M_36_614_709	spColumn 4.81	Cluster3a ^B	6/6/2016	Note E	
M_36_616_707	Compute PM Interaction Capacity of Section M_36_616_707	spColumn 4.81	Cluster3a ^B	6/6/2016	Note E	
M_36_616_709	Compute PM Interaction Capacity of Section M_36_616_709	spColumn 4.81	Cluster3a ^B	6/6/2016	Note E	
M_36_617_703	Compute PM Interaction Capacity of Section M_36_617_703	spColumn 4.81	Cluster3a ^B	6/6/2016	Note E	
M_39_608_711	Compute PM Interaction Capacity of Section M_39_608_711	spColumn 4.81	Cluster3a ^B	6/6/2016	Note E	
M_39_613_710	Compute PM Interaction Capacity of Section M_39_613_710	spColumn 4.81	Cluster3a ^B	6/6/2016	Note E	



Run No.	Title	Program/Ver. ^A	Hardware	Date	Files	
M_39_615_703	Compute PM Interaction Capacity of Section M_39_615_703	spColumn 4.81	Cluster3a ^B	6/6/2016	Note E	
M_39_619_710	Compute PM Interaction Capacity of Section M_39_619_710	spColumn 4.81	Cluster3a ^B	6/6/2016	Note E	
M_39_620_710	Compute PM Interaction Capacity of Section M_39_620_710	spColumn 4.81	Cluster3a ^B	6/6/2016	Note E	
M_39_620_711	Compute PM Interaction Capacity of Section M_39_620_711	spColumn 4.81	Cluster3a ^B	6/6/2016	Note E	
M_39_622_711	Compute PM Interaction Capacity of Section M_39_622_711	spColumn 4.81	Cluster3a ^B	6/6/2016	Note E	
M_48_611_710	Compute PM Interaction Capacity of Section M_48_611_710	spColumn 4.81	Cluster3a ^B	6/6/2016	Note E	
M_48_618_710	Compute PM Interaction Capacity of Section M_48_618_710	spColumn 4.81	Cluster3a ^B	6/6/2016	Note E	
M_48_621_710	Compute PM Interaction Capacity of Section M_48_621_710	spColumn 4.81	Cluster3a ^B	6/6/2016	Note E	
Cut01_PM_mer	Compute PM Interaction Capacity of Section Cut 01	spColumn 4.81	Cluster3a ^B	6/28/2016	Note E	
Cut02_PM_mer	Compute PM Interaction Capacity of Section Cut 02	spColumn 4.81	Cluster3a ^B	6/28/2016	Note E	
Cut03_PM_mer	Compute PM Interaction Capacity of Section Cut 03	spColumn 4.81	Cluster3a ^B	6/28/2016	Note E	
Cut04_PM_mer	Compute PM Interaction Capacity of Section Cut 04	spColumn 4.81	Cluster3a ^B	6/28/2016	Note E	
Cut07_PM_mer	Compute PM Interaction Capacity of Section Cut 07	spColumn 4.81	Cluster3a ^B	6/28/2016	Note E	
Cut08_PM_mer	Compute PM Interaction Capacity of Section Cut 08	spColumn 4.81	Cluster3a ^B	6/28/2016	Note E	
Cut09_PM_mer	Compute PM Interaction Capacity of Section Cut 09	spColumn 4.81	Cluster3a ^B	6/28/2016	Note E	



Run No.	Title	Program/Ver. ^A	Hardware	Date	Files	
Cut10_PM_mer	Compute PM Interaction Capacity of Section Cut 10	spColumn 4.81	Cluster3a ^B	6/28/2016	Note E	
Cut11_PM_mer	Compute PM Interaction Capacity of Section Cut 11	spColumn 4.81	Cluster3a ^B	6/28/2016	Note E	
Cut14_PM_hoop	Compute PM Interaction Capacity of Section Cut 14	spColumn 4.81	Cluster3a ^B	6/28/2016	Note E	
Cut15_PM_hoop	Compute PM Interaction Capacity of Section Cut 15	spColumn 4.81	Cluster3a ^B	6/28/2016	Note E	
Cut16_PM_hoop	Compute PM Interaction Capacity of Section Cut 16	spColumn 4.81	Cluster3a ^B	6/28/2016	Note E	
Cut17_PM_hoop	Compute PM Interaction Capacity of Section Cut 17	spColumn 4.81	Cluster3a ^B	6/28/2016	Note E	
Cut18_PM_hoop	Compute PM Interaction Capacity of Section Cut 18	spColumn 4.81	Cluster3a ^B	6/28/2016	Note E	
Cut19_PM_hoop	Compute PM Interaction Capacity of Section Cut 19	spColumn 4.81	Cluster3a ^B	6/28/2016	Note E	
Cut20_PM_hoop	Compute PM Interaction Capacity of Section Cut 20	spColumn 4.81	Cluster3a ^B	6/28/2016	Note E	
Cut21_PM_hoop	Compute PM Interaction Capacity of Section Cut 21	spColumn 4.81	Cluster3a ^B	6/28/2016	Note E	
Cut22_PM_hoop	Compute PM Interaction Capacity of Section Cut 22	spColumn 4.81	Cluster3a ^B	6/28/2016	Note E	
Cut23_PM_hoop	Compute PM Interaction Capacity of Section Cut 23	spColumn 4.81	Cluster3a ^B	6/28/2016	Note E	
Cut24_PM_hoop	Compute PM Interaction Capacity of Section Cut 24	spColumn 4.81	Cluster3a ^B	6/28/2016	Note E	
Cut25_PM_hoop	Compute PM Interaction Capacity of Section Cut 25	spColumn 4.81	Cluster3a ^B	6/28/2016	Note E	
Cut26_PM_hoop	Compute PM Interaction Capacity of Section Cut 26	spColumn 4.81	Cluster3a ^B	6/28/2016	Note E	



PROJECT NO: 150252

DATE: July 2016

CLIENT: NextEra Energy Seabrook

BY: R.M. Mones

SUBJECT: Evaluation and Design Confirmation of As-Deformed CEB

VERIFIER: A.T. Sarawit

Run No.	Title	Program/Ver. ^A	Hardware	Date	Files	
Cut27_PM_hoop	Compute PM Interaction Capacity of Section Cut 27	spColumn 4.81	Cluster3a ^B	6/28/2016	Note E	
Cut28_PM_mer	Compute PM Interaction Capacity of Section Cut 28	spColumn 4.81	Cluster3a ^B	7/26/2016	Note E	
Cut29_PM_hoop	Compute PM Interaction Capacity of Section Cut 29	spColumn 4.81	Cluster3a ^B	7/26/2016	Note E	
Cut30_PM_hoop	Compute PM Interaction Capacity of Section Cut 30	spColumn 4.81	Cluster3a ^B	7/26/2016	Note E	
m_15_el45az240	Compute PM Interaction Capacity of Section at El. +45.5 ft and AZ 240 (Referenced in Appendix M)	spColumn 4.81	Cluster3a ^B	6/28/2016	Note E	

See notes on next page



PROJECT NO: 150252

DATE: July 2016

CLIENT: NextEra Energy Seabrook

BY: R.M. Mones

SUBJECT: Evaluation and Design Confirmation of As-Deformed CEB

VERIFIER: A.T. Sarawit

Notes:

- A ANSYS 15 is QA verified
 spColumn 4.81 is QA verified
- B Cluster3g information is provided below:
 Model: Compute Blade E55A2
 Serial Number: 4600E70 T201000293
 Manufacturer: American Megatrends Inc.
 Operating System: Microsoft Windows NT Server 6.2 (x64)
- Cluster3a information is provided below:
 Model: Compute Blade E55A2
 Serial Number: 4600E70 T148000168
 Manufacturer: American Megatrends Inc.
 Operating System: Microsoft Windows NT Server 6.2 (x64)
- C Input and output files for ANSYS computer runs are listed in Table B1 and B2
- D Item "10D_r0" is treated as a computer run, but consists of a subset of the output
 from 10A_r0.
- E Input and output files for spColumn computer runs are listed in Table B3



Table B1. Input files for ANSYS Computer Runs

SR_ILC_01_I_r0.apdl	SR_ILC_26_I_r0.apdl	SR_MISC_ACCPROF_r0.apdl
SR_ILC_02_I_r0.apdl	SR_ILC_27_I_r0.apdl	SR_MISC_NODEMASS_r0.apdl
SR_ILC_03_I_r0.apdl	SR_ILC_28_I_r0.apdl	SR_MODEL1_BOUNDARY_A_r0.apdl
SR_ILC_04_I_r0.apdl	SR_ILC_29_I_r0.apdl	SR_MODEL1_CONN_BASE_HINGE_r0.apdl
SR_ILC_05_I_r0.apdl	SR_ILC_30_I_r0.apdl	SR_MODEL1_CONN_BASE_r0.apdl
SR_ILC_06_I_r0.apdl	SR_ILC_31_I_r0.apdl	SR_MODEL1_CONN_RADIAL_r0.apdl
SR_ILC_07_I_r0.apdl	SR_ILC_32_I_r0.apdl	SR_MODEL1_CONN_TANGENT_r0.apdl
SR_ILC_08_I_r0.apdl	SR_ILC_33_I_r0.apdl	SR_MODEL1_ELEMENTS_CONCRETE_r0.apdl
SR_ILC_09_I_r0.apdl	SR_ILC_34_I_r0.apdl	SR_MODEL1_ELEMENTS_STEEL_r0.apdl
SR_ILC_10_I_r0.apdl	SR_ILC_35_I_r0.apdl	SR_MODEL1_NODES_DEFORMED_r0.apdl
SR_ILC_11_I_r0.apdl	SR_ILC_36_I_r0.apdl	SR_MODEL1_NODES_r0.apdl
SR_ILC_12_I_r0.apdl	SR_ILC_38_I_r0.apdl	SR_MODEL1_PROPERTIES_A_r0.apdl
SR_ILC_13_I_r0.apdl	SR_ILC_39_I_r0.apdl	SR_MODEL1_PROPERTIES_B_r0.apdl
SR_ILC_14_I_r0.apdl	SR_ILC_40_I_r0.apdl	SR_MODEL1_PROPERTIES_C_r0.apdl
SR_ILC_15_I_r0.apdl	SR_ILC_41_I_r0.apdl	SR_MODEL1_PROPERTIES_D_r0.apdl
SR_ILC_16_I_r0.apdl	SR_ILC_42_I_r0.apdl	SR_RUN_DEFINE_CASENAMES_r0.apdl
SR_ILC_17_I_r0.apdl	SR_ILC_43_I_r0.apdl	SR_RUN_DEFINE_ILC_r0.apdl
SR_ILC_18_I_r0.apdl	SR_ILC_44_I_r0.apdl	SR_RUN_DEFINE_LCB_r0.apdl
SR_ILC_19_I_r0.apdl	SR_ILC_45_I_r0.apdl	SR_RUN_EXECUTE_r0.apdl
SR_ILC_20_I_r0.apdl	SR_ILC_46_I_r0.apdl	SR_RUN_SWITCHCOMBOSET_r0.apdl
SR_ILC_21_I_r0.apdl	SR_ILC_47_I_r0.apdl	SR_MODEL1_MKADJ5_r0.apdl
SR_ILC_22_I_r0.apdl	SR_ILC_48_I_r0.apdl	SR_MODEL1_MKADJ6_r0.apdl
SR_ILC_23_I_r0.apdl	SR_ILC_49_I_r0.apdl	
SR_ILC_24_I_r0.apdl	SR_ILC_50_I_r0.apdl	
SR_ILC_25_I_r0.apdl	SR_ILC_51_I_r0.apdl	

Notes:

- Computer runs that use ANSYS 15 program utilize the input files listed in the above table
- Files SR_ILC_43_I_r0.apdl through SR_ILC_51_I_r0.apdl, SR_MODEL1_PROPERTIES_D_r0.apdl, and SR_MODEL1_CONN_BASE_HINGE_r0.apdl are used in computer runs 10AR_r0, 10BR7_r0, and 10G_r0 only.
- Files SR_MODEL1_MKADJ5_r0.apdl and SR_MODEL1_MKADJ6_r0.apdl are used in computer run 10G_r0 only.
- File SR_MISC_NODEMASS_r0.apdl can be generated by SR_ILC_02_I_r0.apdl



Table B2. Output files for ANSYS Computer Runs

SR_COMBOS_A_r0.db	SR_ILC_13_I_r0.db	SR_ILC_36_I_r0.db
SR_COMBOS_B_r0.db	SR_ILC_14_I_r0.db	SR_ILC_37_I_r0.db
SR_COMBOS_C_r0.db	SR_ILC_15_I_r0.db	SR_ILC_38_I_r0.db
SR_COMBOS_D_r0.db	SR_ILC_16_I_r0.db	SR_ILC_39_I_r0.db
SR_COMBOS_E_r0.db	SR_ILC_17_I_r0.db	SR_ILC_40_I_r0.db
SR_COMBOS_F_r0.db	SR_ILC_18_I_r0.db	SR_ILC_41_I_r0.db
SR_COMBOS_G_r0.db	SR_ILC_19_I_r0.db	SR_COMBOS_A_r0.I**
SR_COMBOS_H_r0.db	SR_ILC_20_I_r0.db	SR_COMBOS_B_r0.I**
SR_COMBOS_I_r0.db	SR_ILC_21_I_r0.db	SR_COMBOS_C_r0.I**
SR_COMBOS_J_r0.db	SR_ILC_22_I_r0.db	SR_COMBOS_D_r0.I**
SR_COMBOS_K_r0.db	SR_ILC_23_I_r0.db	SR_COMBOS_E_r0.I**
SR_ILC_01_I_r0.db	SR_ILC_24_I_r0.db	SR_COMBOS_F_r0.I**
SR_ILC_02_I_r0.db	SR_ILC_25_I_r0.db	SR_COMBOS_G_r0.I**
SR_ILC_03_I_r0.db	SR_ILC_26_I_r0.db	SR_COMBOS_H_r0.I**
SR_ILC_04_I_r0.db	SR_ILC_27_I_r0.db	SR_COMBOS_I_r0.I**
SR_ILC_05_I_r0.db	SR_ILC_28_I_r0.db	SR_COMBOS_J_r0.I**
SR_ILC_06_I_r0.db	SR_ILC_29_I_r0.db	SR_COMBOS_K_r0.I**
SR_ILC_07_I_r0.db	SR_ILC_30_I_r0.db	
SR_ILC_08_I_r0.db	SR_ILC_31_I_r0.db	
SR_ILC_09_I_r0.db	SR_ILC_32_I_r0.db	
SR_ILC_10_I_r0.db	SR_ILC_33_I_r0.db	
SR_ILC_11_I_r0.db	SR_ILC_34_I_r0.db	
SR_ILC_12_I_r0.db	SR_ILC_35_I_r0.db	

Notes:

- File extension ".I**" in above table represent ".I01", ".I02", ".I03", etc. up to ".I75".
- ANSYS computer runs generate one or more of these output files depending on the purpose of the computer run.



Table B3. Input and Output files for spColumn Computer Runs

Input Files	{RunNumber}.cti
Output Files	{RunNumber}.out {RunNumber}.emf {RunNumber}.csv {RunNumber}.iad

Notes:

- The label {RunNumber} represents any spColumn run listed in the Computer Run Identification Log



Appendix C
Description of 150252-CA-02-CD-01 Contents

C1. REVISION HISTORY**Revision 0:**

Initial document.

C2. DESCRIPTION OF CD CONTENTS

The CD attached to this calculation (150252-CA-02-CD-01) contains key analysis input and output files. These files are summarized below.

- The provided analysis cases are listed in Table C1.
- For each analysis case, the files listed and described in Table C2 are provided.
- Input and output files related to computation of axial-flexure (PM) interaction capacity are provided, as described in Table C3.



C3. TABLES

Table C1. List of Analysis Cases Provided on 150252-CA-02-CD-01

Run No.	Title/Description of Analysis Case	Notes
10A_r0	Standard Analysis Case	This analysis case contains all load combinations listed in Table 5 of the calculation main body.
10B7_r0	Standard-Plus Analysis Case	This analysis case contains all load combinations listed in Table 5 of the calculation main body.
10D_r0	Evaluation w/o ASR and SS loads	This analysis case is treated as a computer run, but consists of a subset of the output from 10A_r0. For this reason, database files (*.db) and load case files (*.I01, *.I02, etc.) are not provided
10E_r0	Parametric Study on ASR at Springline	This analysis case is limited to deformation combinations (Combination Set A)
10G_r0	Analysis and Evaluation of Standard-Plus Analysis Case for Combination NO_1 with Simulated Concrete Cracking at El. +45.5 and AZ 240	This analysis case is limited to combination sets A, B, and C.
10AR_r0	Standard Analysis Case with Moment Redistribution (limited to combination NO_1)	This analysis case is limited to combination sets A, B, and C. Combination C01 represents load combination NO_1 without moment redistribution. Combination C02 represents load combination NO_1 with the moment redistributions discussed in Appendix H.
10BR7_r0	Standard-Plus Analysis Case with Moment Redistribution (limited to combination NO_1)	This analysis case is limited to combination sets A, B, and C. Combination C01 represents load combination NO_1 without moment redistribution. Combination C02 represents load combination NO_1 with the moment redistributions discussed in Appendix H.
10BR7E_r0	Standard-Plus Analysis Case with Moment Redistribution (limited to combination OBE_4)	This analysis case is limited to combination sets A, B, and G. Combination G07 contains the load redistribution analysis for the selected OBE load combination (as documented in Appendix H).


Table C2. Description of Files Provided for Analysis Cases

File Type	Description
*.apdl	ANSYS input files. These files are used to define the CEB model, modify the CEB model, define loads applied to the model, or define parameters that are used by the CEB model (such as load factors).
*.db	ANSYS database files. All database files contain the CEB model (nodes, elements, properties, boundary conditions, etc.). Database files for independent load cases (ILCs) contain loads, forces, moments, reactions, and displacements/deformations related to the specific ILC. Database files for combination sets (such as SR_COMBOS_A_r0.db) contain the CEB model, but are otherwise a shell for importing load case files (see next row).
*.l01, *.l02, etc.	Load case files. These files contain forces, moments, reactions, and displacements/deformations related to a specific load combination. Load combinations are defined in the files named SR_RUN_DEFINE_LCB_r0.apdl and SR_RUN_DEFINE_CASENAMES_r0.apdl. These files may be imported by ANSYS using the LCFIL and LCASE commands.
*.png	PM Interaction results. These image files contain PM interaction diagrams with results for the given analysis case.
*.tif	Element contour plots. These image files show contour plots for specific ILCs or load combinations. File names named according to the convention described in Table 9 of the calculation main body.

Table C3. Description of Files Provided for PM Interaction Capacity Computations

File Type	Description
*.cti	spColumn input files
*.emf	spColumn image output files
*.out	spColumn output file
*.csv	spColumn comma-separated output of PM Capacity
*.pmd	Same as *.csv file, but with capacities adjusted to meet ACI 318-71 strength reduction (ϕ) factors.



Appendix D

Calculation of Creep Coefficient and Shrinkage Strain

D1.0 Revision History

- Revision 0: Initial document

D2.0 Objective

In this calculation, the creep coefficient and shrinkage strain of the containment enclosure building (CEB) concrete are calculated. The calculated values are to be used in the evaluation and design confirmation of the as-deformed CEB. All creep and shrinkage calculations are performed using ACI 209R-92 [D1].

D3.0 Results and Conclusions

Creep is calculated using two different approaches from ACI 209R-92; one approach is for standard structures (Section 2.4 of ACI 209R-92) while the other approach is specifically for massive structures that are more than 12 in. thick (Section 2.8 of ACI 209R-92). Using the creep model for standard structures, the creep coefficient is calculated as 1.3. The creep coefficient is 2.3 if the massive structures model is used. According to the ACI 209R-92 creep model, the creep coefficient is not dependent on wall thickness.

Shrinkage strain is calculated using as 1.0×10^{-4} for 36 in. thick walls, 2.0×10^{-4} for 27 in. thick walls, and 2.5×10^{-4} for 15 in. thick walls.

D4.0 Design Data / Criteria

The CEB mix design information below has been provided by Ted Vassallo [D2, D3, D4].

- Design compressive strength = 4000 psi
- Air entraining admixture (Master Builders MB-AE-10). Design air content of 4 to 8%. Actual measured air content from 5.1 to 7.1%.
- Water to cement ratio (w/c) of 0.5. Water reducing admixture (Master Builders Pozzolith 300N).
- Design slump of 2 to 4 inches. Actual measured slump of 2.75 to 3.75 inches.
- Cement content of 560 lbf, fine aggregate content of 1300 lbf, #67 coarse aggregate content of 1780 lbf, water content of 280 lbf.

This mix was used for CEB concrete placement from elevation (-)26'-0" to (-)11'-0" from Azimuth 18 to 33 degrees. However, it has been indicated that this is a typical concrete mixture for the CEB, therefore the properties of this mix are used to approximate the creep coefficient and shrinkage strain throughout the entire CEB.

Typical relative humidity in Seabrook, NH is approximated using weather data [D5] from Portsmouth, NH, which is approximately 15 miles to the north of Seabrook Station. Relative humidity varies throughout the year, a constant relative humidity of 65% is used in this calculation. A plot of relative average relative humidity throughout the year can be seen in Section 7.1 of this calculation.

D5.0 Assumptions

It is assumed that the CEB concrete is allowed to moist cure for 7 days, and that additional (non-self weight) loads are not applied to the CEB concrete during this 7 days.

It is assumed that the relative humidity of the environment surrounding the CEB concrete is constantly 65%. The actual relative humidity in Southern New Hampshire varies between from about 40% to 90%. Relative humidity within the annulus of the operational facility are typically lower (about 25%); however, these relative humidities have a smaller impact because creep and shrinkage primarily occur during the first year after placement.

D6.0 Methodology

Calculation of creep coefficient and shrinkage strain use the models presented ACI 209R-92 [D1]. Shrinkage strain and creep coefficient are calculated using Section 2.4 of ACI 209R-92 (Recommended Creep and Shrinkage Equations for Standard Conditions). An alternative creep coefficient is also calculated using Section 2.8.1 of ACI 209R-92, which is for massive structures that retain their moisture during their lifetime. The final creep coefficient and shrinkage strains for use in FEA is selected in Section D8.0

All equation and section references are to ACI 209R-92 [D1] unless otherwise noted

D7.0 Computations

Computation contents are listed below.

- 7.1. Specify Input Parameters
- 7.2. Define Creep and Shrinkage Calculation Functions
- 7.3. Define Functions for Calculation of Creep Correction Factors
- 7.4. Define Functions for Calculation of Shrinkage Correction Factors
- 7.5. Calculate Creep Coefficient for use in FE Model
- 7.6. Calculate Shrinkage Strain for use in FE Model

All equation and section references are to ACI 209R-92 [D1] unless otherwise noted

D7.1 Specify Input Parameters

(Section 2.4, take $\psi=0.60$) $\psi := 0.60$

(Section 2.4, take $d=10$ days) $d := 10\text{day}$

(Section 2.4, take $\alpha=1$) $\alpha := 1$

(Section 2.4, take $v_{ub} = 2.35$) $v_{ub} := 2.35$

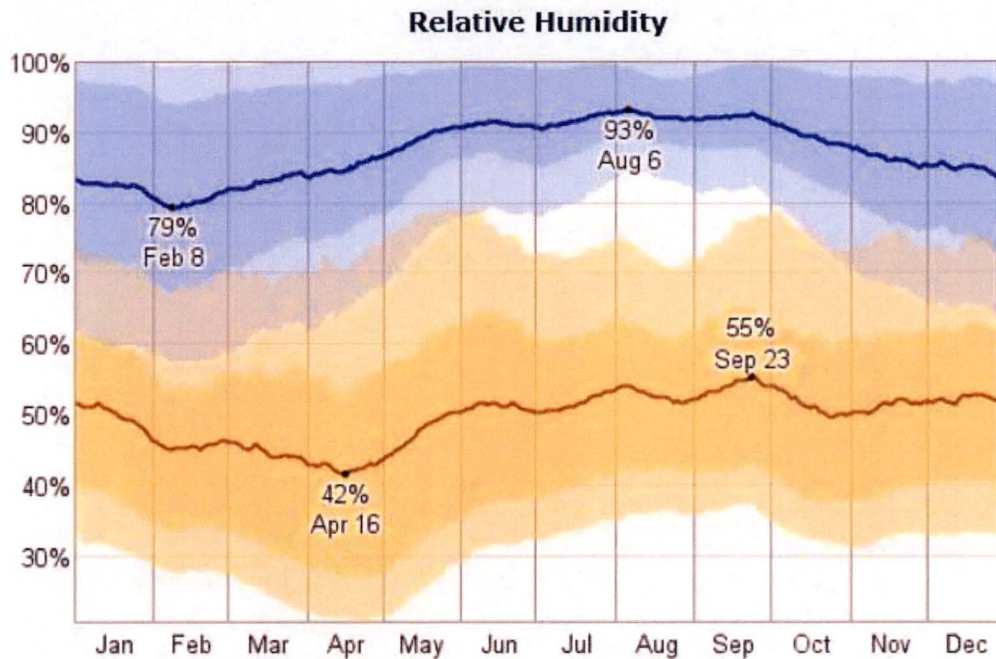
(Section 2.4, take $\varepsilon_{shub} = 780.0 \cdot 10^{-6}$) $\varepsilon_{shub} := 780 \cdot 10^{-6}$

(Section 2.4, take $f=35$ days) $f := 35\text{day}$

Duration of initial moist curing $t_{cp} := 7\text{day}$

Age of concrete at initial loading $t_{la} := 7\text{day}$

Average Relative Humidity $\psi := 0.65$ (See climate information below)



The average daily high (blue) and low (brown) relative humidity with percentile bands (inner bands from 25th to 75th percentile, outer bands from 10th to 90th percentile).

Plot and caption above are taken from www.weatherspark.com [D5] for Portsmouth, NH.

D7.1 Specify Input Parameters (Continued)

Volume to surface ratio
(varies w/ thickness of
CEB wall)

$$v_{sr_36in} := \frac{36in}{2}$$

$$v_{sr_27in} := \frac{18in}{2}$$

$$v_{sr_15in} := \frac{15in}{2}$$

Slump

$$slump := 3.25in$$

Slump of 3.25" is based on information provided in 17 April 2015 email from Ted Vassallo [D3].

Fine Aggregate Content
(decimal)

$$f_a := 0.422$$

Fine aggregate content of 0.422 is based on information provided in 20 April 2014 email from Ted Vassallo [D4].

Air Content (decimal)

$$c := 0.06$$

Air content of 0.06 is based on information provided in 17 April 2015 email from Ted Vassallo [D3].

Cement content (lb/yd³)

$$c := 560 \frac{lb}{yd^3}$$

Cement content of 560 lbf/yd³ is based on information provided in 20 April 2014 email from Ted Vassallo [D4].

D7.2 Define Creep and Shrinkage Calculation Functions

(Eqn 2-6)
Function for
creep coefficient

$$v_t(t, d, \psi, v_u) := \frac{\left(\frac{t}{\text{day}}\right)^{-\psi}}{\left[\frac{d}{\text{day}} + \left(\frac{t}{\text{day}}\right)^{-\alpha}\right]} \cdot v_u$$

(Eqn 2-7)
Function for
shrinkage strain

$$sht(t, f, \epsilon_{shu}) := \frac{\left(\frac{t}{\text{day}}\right)^{-\psi}}{\frac{f}{\text{day}} + \left(\frac{t}{\text{day}}\right)^{-\alpha}} \cdot \epsilon_{shu}$$

Normal ranges of the constants in Eqs. (2-6) and (2-7) were found to be:^{6,7}

$$\begin{aligned} \psi &= 0.40 \text{ to } 0.80, \\ d &= 6 \text{ to } 30 \text{ days}, \\ v_u &= 1.30 \text{ to } 4.15, \\ \alpha &= 0.90 \text{ to } 1.10, \\ f &= 20 \text{ to } 130 \text{ days}, \\ (\epsilon_{sh})_u &= 415 \times 10^{-6} \text{ to } 1070 \times 10^{-6} \text{ in./in. (m/m)} \end{aligned}$$

Recommended creep and shrinkage constants under "standard conditions" (Section 2.4)

$\psi=0.60$, $d= 10$ days, $\alpha = 1$, $f = 35$ days, $v_u = 2.35$, $\epsilon_{shu} = 780 \times 10^{-6}$

D7.3 Define Functions for Calculation of Creep Correction Factors

Section 2.5.1: Loading Age

(Eqn 2-11)

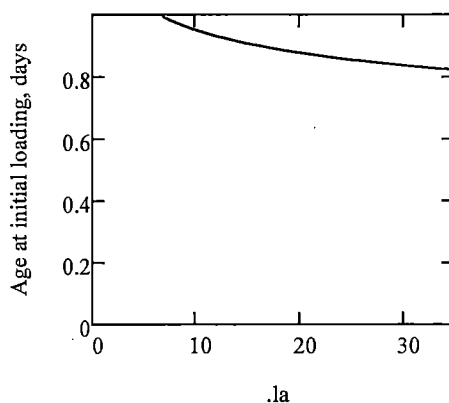
Function for adjustment factor for loading age.

Input parameter t_{la} is the age of loading in days.

$$i_a(t_{la}) := \begin{cases} \left[1.25 \cdot \left(\frac{t_{la}}{\text{day}} \right)^{-0.118} \right] & \text{if } t_{la} > 7 \text{ day} \\ 1.0 & \text{otherwise} \end{cases}$$

Notes:

The value of i_a is less than 1.0 if a t_{la} greater than 7 days is used. This correction factor causes the ultimate creep coefficient to decrease because the concrete has cured prior to application of the load.



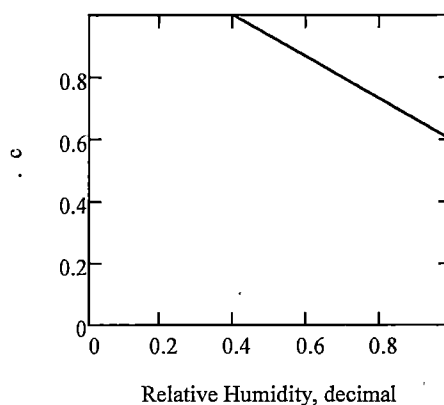
Section 2.5.4: Ambient Relative Humidity

(Eqn 2-14)

Function for adjustment factor for ambient relative humidity.

Input parameter λ is relative humidity as decimal.

$$c(\lambda) := \begin{cases} 1.0 & \text{if } \lambda \leq 0.4 \\ (1.27 - 0.67 \cdot \lambda) & \text{if } \lambda > 0.40 \\ \text{"ERROR"} & \text{otherwise} \end{cases}$$



D7.3 Define Functions for Calculation of Creep Correction Factors (Continued)

Section 2.5.5b: Member Size (Volume-surface ratio method)

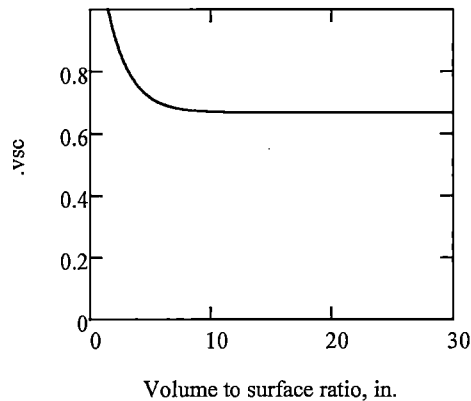
Note: Section 2.5.5a (Member thickness method) is not implemented because it is not supported for members thicker than 15 in.

(Eqn 2-21)

Function for adjustment factor
for volume to surface ratio.

Input parameter vsr is the
volume to surface ratio in
inches.

$$vsc_vsr := \left(\frac{2}{3}\right) \cdot \left[1 + 1.13 \cdot e^{\left(-0.54 \cdot \frac{vsr}{in}\right)}\right]$$



Section 2.5.6: Temperature

ACI 209R-92 recognizes temperature as a significant factor effecting creep, but does not provide correction factors to account for temperatures other than 70 degrees F.

The text of ACI 209R-92 states that creep strains can be approximately two to three times greater at 122 degrees F than at 70 degrees F.

D7.3 Define Functions for Calculation of Creep Correction Factors (Continued)

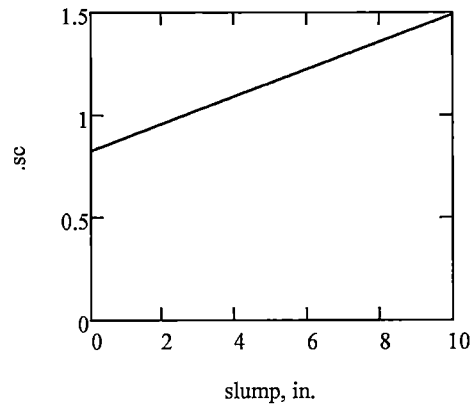
Section 2.6.1: Slump

(Eqn 2-23)

Function for slump correction factor.

Slump is input in inches.

$$sc(\text{slump}) := 0.82 + 0.067 \cdot \frac{\text{slump}}{\text{in}}$$



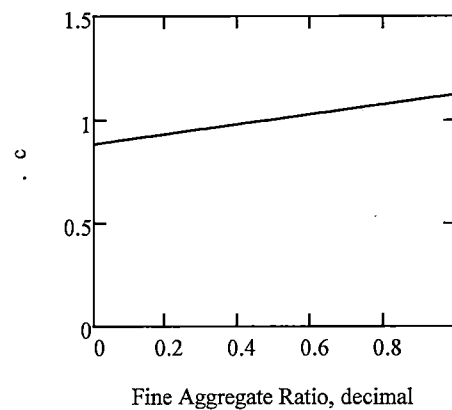
Section 2.6.2: Fine Aggregate Percentage

(Eqn 2-25)

Function for fine aggregate percentage.

ψ is the ratio of fine aggregate to total aggregate by weight expressed as a decimal.

$$c(\psi) := 0.88 + 0.24 \cdot \psi$$



D7.3 Define Functions for Calculation of Creep Correction Factors (Continued)

Section 2.6.3: Cement Content

According to ACI 209R-92 Section 2.6.3, cement content has a negligible effect on creep coefficient.

$$c_c := 1$$

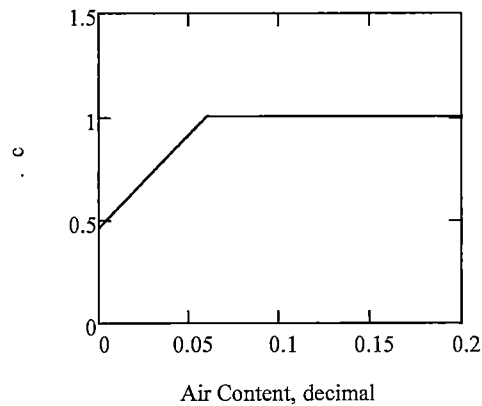
Section 2.6.4: Air Content

(Eqn 2-29)

Function for air content
correction factor.

α_c is the air content as
a decimal.

$$c(\alpha_c) := \min(1.0, 0.46 + 9\alpha_c)$$



D7.4 Define Functions for Calculation of Shrinkage Correction Factors

Section 2.5.3: Duration of Initial Moist Curing

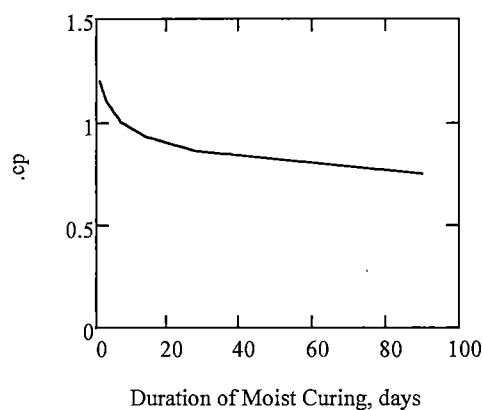
(Table 2.5.3)

Allow linear interpolation
between table values.
Do not permit extrapolation.

table253x :=	$\begin{pmatrix} 1 \\ 3 \\ 7 \\ 14 \\ 28 \\ 90 \end{pmatrix}$	day	table253y :=	$\begin{pmatrix} 1.2 \\ 1.1 \\ 1.0 \\ 0.93 \\ 0.86 \\ 0.75 \end{pmatrix}$
--------------	---	-----	--------------	---

Function for adjustment factor
for duration of moist curing,
based on Table 2.5.3.

$$cp(_t_{cp}) := \begin{cases} \text{interp}(\text{table253x}, \text{table253y}, _t_{cp}) & \text{if } 1 \text{ day} \leq _t_{cp} \leq 90 \text{ day} \\ \text{"ERROR"} & \text{otherwise} \end{cases}$$

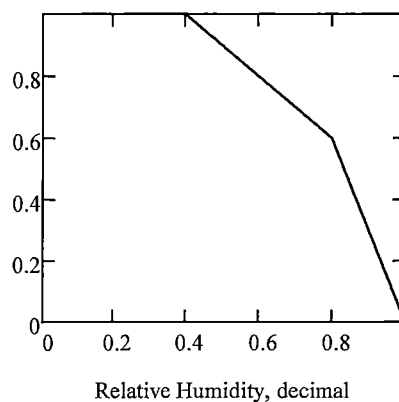


Section 2.5.4: Ambient Relative Humidity

(Eqn 2-14)

Function for adjustment factor
for ambient relative humidity.
Input parameter λ is relative
humidity as decimal.

$$s(_) := \begin{cases} 1.0 & \text{if } _ < 0.4 \\ (1.4 - 1.0 _) & \text{if } 0.4 \leq _ \leq 0.8 \\ (3.0 - 3.0 _) & \text{if } 0.8 < _ \leq 1 \\ \text{"ERROR"} & \text{otherwise} \end{cases}$$



D7.4 Define Functions for Calculation of Shrinkage Correction Factors (Continued)

Section 2.5.5b: Member Size (Volume-surface ratio method)

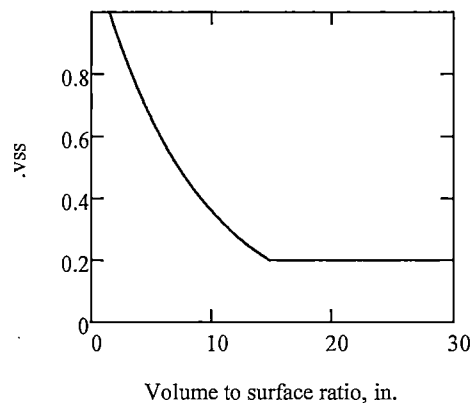
Note: Section 2.5.5a (Member thickness method) is not implemented because it is not supported for members thicker than 15 in.

(Eqn 2-22)

Function for adjustment factor
for volume to surface ratio.

Input parameter vsr is the
volume to surface ratio in
inches.

$$vss(\text{vsr}) := \max \left[1.20 \cdot e^{\left(-0.12 \cdot \frac{\text{vsr}}{\text{in}} \right)}, 0.2 \right]$$



Section 2.5.6: Temperature

ACI 209R-92 recognizes temperature as a significant factor effecting shrinkage, but does not provide correction factors to account for temperatures other than 70 degrees F.

D7.4 Define Functions for Calculation of Shrinkage Correction Factors (Continued)

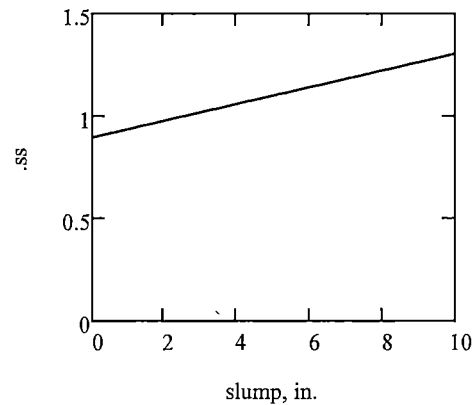
Section 2.6.1: Slump

(Eqn 2-24)

Function for slump correction factor.

Slump is input in inches.

$$ss(\text{slump}) := 0.89 + 0.041 \cdot \frac{\text{slump}}{\text{in}}$$



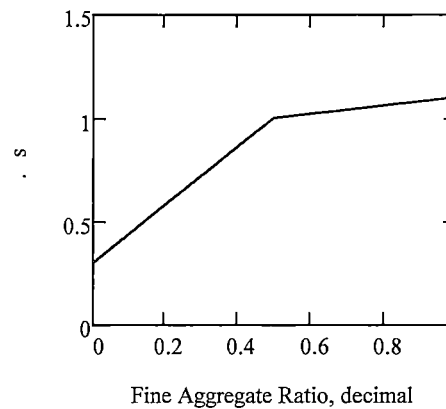
Section 2.6.2: Fine Aggregate Percentage

(Eqn 2-26 and 2-27)

Function for fine aggregate percentage.

ψ is the ratio of fine aggregate to total aggregate by weight expressed as a decimal.

$$s(\psi) := \begin{cases} (0.30 + 1.4 \cdot \psi) & \text{if } \psi \leq 0.5 \\ (0.90 + 0.2 \cdot \psi) & \text{otherwise} \end{cases}$$



D7.4 Define Functions for Calculation of Shrinkage Correction Factors (Continued)

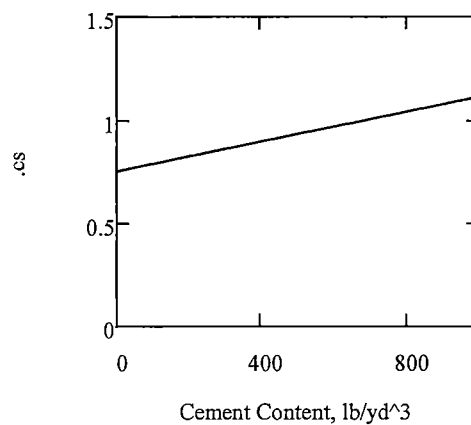
Section 2.6.3: Cement Content

(Eqn 2-28)

Function for cement content correction factor.

Cement content, c , in lb/yd^3

$$cs(_c) := 0.75 + 0.00036 \cdot \frac{c}{\left(\frac{\text{lbf}}{\text{yd}^3}\right)}$$



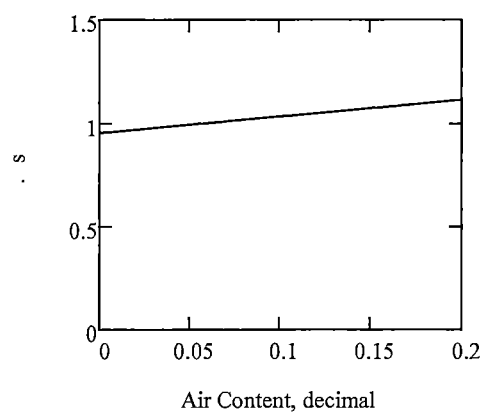
Section 2.6.4: Air Content

(Eqn 2-29)

Function for air content correction factor.

α_c is the air content as a decimal.

$$s(_c) := 0.95 + 0.8 _c$$



D7.5 Calculate Creep Coefficients for use in FE Model

Correction factor:
Loading Age

$$l_a(t_{la}) = 1$$

Correction factor:
Relative Humidity

$$c_r = 0.835$$

Correction factor:
Volume to surface ratio

$$v_{sc}(v_{sr_36in}) = 0.667$$

$$v_{sc}(v_{sr_27in}) = 0.673$$

$$v_{sc}(v_{sr_15in}) = 0.68$$

Note: Volume-to-surface ratio correction factor is around 0.67 for all wall thicknesses in consideration. Moving forward, use $v_{vs} = 0.673$.

Correction factor:
Slump

$$s_c(\text{slump}) = 1.038$$

Correction factor:
Fine Aggregate Percentage

$$c_{fa} = 0.981$$

Correction factor:
Cement Content

$$c_c = 1$$

Correction factor:
Air Content

$$c_a = 1$$

Cumulative correction factor

$$c_{creep} := l_a(t_{la}) \cdot c_r \cdot v_{sc}(v_{sr_27in}) \cdot s_c(\text{slump}) \cdot c_{fa} \cdot c_c \cdot c_a$$

$$c_{creep} = 0.571$$

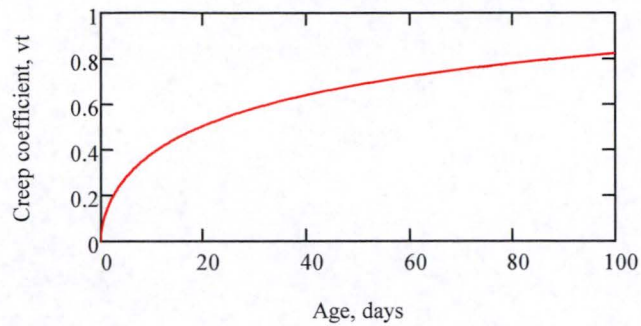
Ultimate creep coefficient

$$v_u := v_{ub} \cdot c_{creep}$$

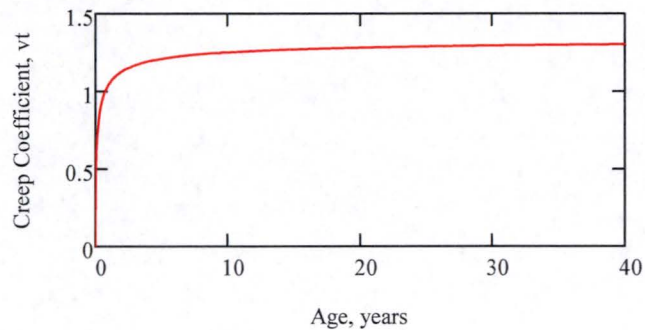
$$v_u = 1.343$$

D7.5 Calculate Creep Coefficients for use in FE Model (Continued)

Creep strain per unit of elastic strain (first 100 days)



Creep strain per unit of elastic strain (first 30 years)



$$v_t @ 1 \text{ yr: } v_t(1 \text{ yr}, d, \nu_u) = 1.041$$

$$v_t @ 5 \text{ yrs: } v_t(5 \text{ yr}, d, \nu_u) = 1.209$$

$$v_t @ 10 \text{ yrs: } v_t(10 \text{ yr}, d, \nu_u) = 1.252$$

$$v_t @ 25 \text{ yrs: } v_t(25 \text{ yr}, d, \nu_u) = 1.289$$

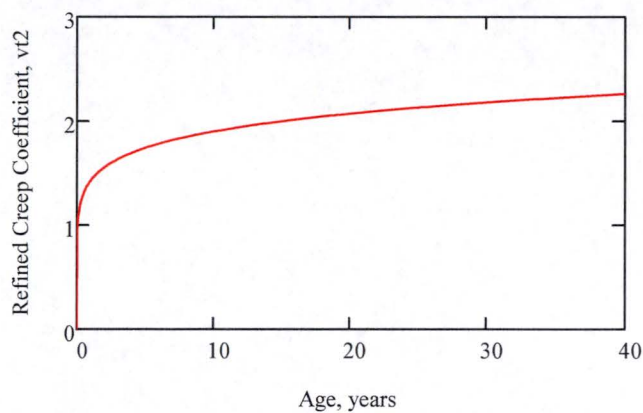
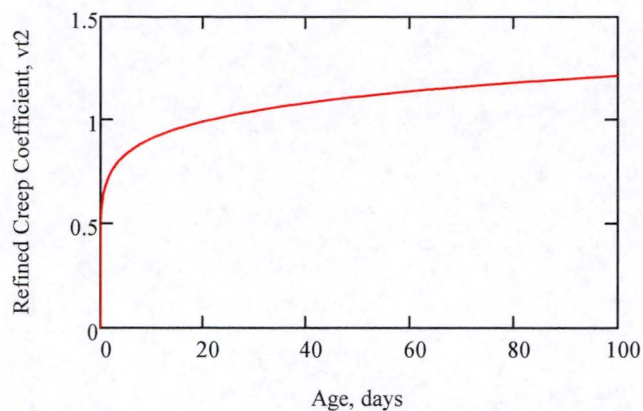
$$v_t @ 35 \text{ yrs: } v_t(35 \text{ yr}, d, \nu_u) = 1.298$$

$$\epsilon_{creep} = \frac{v_t}{E_0} \sigma_D \quad (\text{Eqn 1-1})$$

D7.5 Calculate Creep Coefficients for use in FE Model (Continued)

(Eqn 2-33)
Refined creep coefficient
for massive structures

$$v_{t2}(-v_u, -t_{la}, -t) := 0.97 \cdot v_u \cdot \left(\frac{-t_{la}}{\text{day}} \right)^{\left(\frac{-1}{3} \right)} \cdot \left(\frac{-t}{\text{day}} \right)^{\frac{1}{8}}$$



vt2 @ 1 yr: $v_{t2}(v_u, t_{la}, 1\text{yr}) = 1.424$

vt2 @ 5 yrs: $v_{t2}(v_u, t_{la}, 5\text{yr}) = 1.741$

vt2 @ 10 yrs: $v_{t2}(v_u, t_{la}, 10\text{yr}) = 1.899$

vt2 @ 25 yrs: $v_{t2}(v_u, t_{la}, 25\text{yr}) = 2.129$

vt2 @ 35 yrs: $v_{t2}(v_u, t_{la}, 35\text{yr}) = 2.221$

$$\epsilon_{\text{creep}} = \frac{v_t}{E_0} \sigma_D \quad (\text{Eqn 1-1})$$

D7.6 Calculate Shrinkage Strain for use in FE Model

Correction factor:
Initial Moist Cure Duration $cp(t_{cp}) = 1$

Correction factor:
Relative Humidity $s(\) = 0.75$

Correction factor:
Volume to surface ratio $vss(vsr_{36in}) = 0.2$
 $vss(vsr_{27in}) = 0.408$
 $vss(vsr_{15in}) = 0.488$

Correction factor:
Slump $ss(slump) = 1.023$

Correction factor:
Fine Aggregate Percentage $s(fa) = 0.891$

Correction factor:
Cement Content $cs(c) = 0.952$

Correction factor:
Air Content $s(c) = 0.998$

Cumulative correction
factor for shrinkage strain
of 36 in. thick walls $shrinkage_{36} := cp(t_{cp}) \cdot s(\) \cdot vss(vsr_{36in}) \cdot ss(slump) \cdot s(fa) \cdot cs(c) \cdot s(c)$
 $shrinkage_{36} = 0.13$

Cumulative correction
factor for shrinkage strain
of 27 in. thick walls $shrinkage_{27} := cp(t_{cp}) \cdot s(\) \cdot vss(vsr_{27in}) \cdot ss(slump) \cdot s(fa) \cdot cs(c) \cdot s(c)$
 $shrinkage_{27} = 0.265$

Cumulative correction
factor for shrinkage strain
of 15 in. thick walls $shrinkage_{15} := cp(t_{cp}) \cdot s(\) \cdot vss(vsr_{15in}) \cdot ss(slump) \cdot s(fa) \cdot cs(c) \cdot s(c)$
 $shrinkage_{15} = 0.317$

D7.6 Calculate Shrinkage Strain for use in FE Model (Continued)

Ultimate shrinkage strain
for 36 in. thick walls

$shu_{36} := shub \cdot shrinkage_{36}$

$$shu_{36} = 1.013 \times 10^{-4}$$

Ultimate shrinkage strain
for 27 in. thick walls

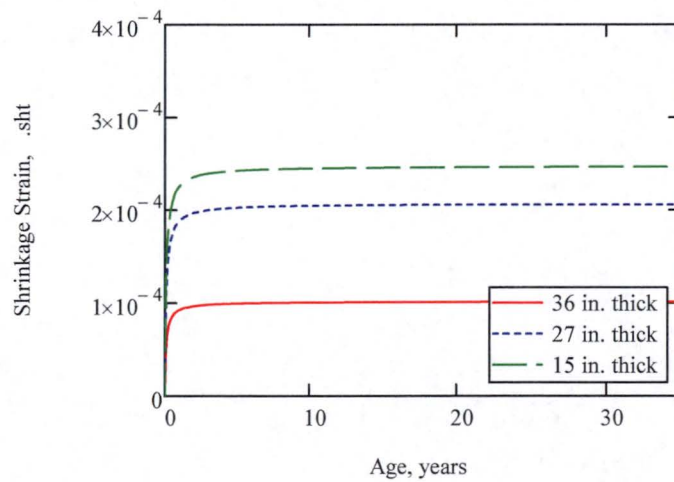
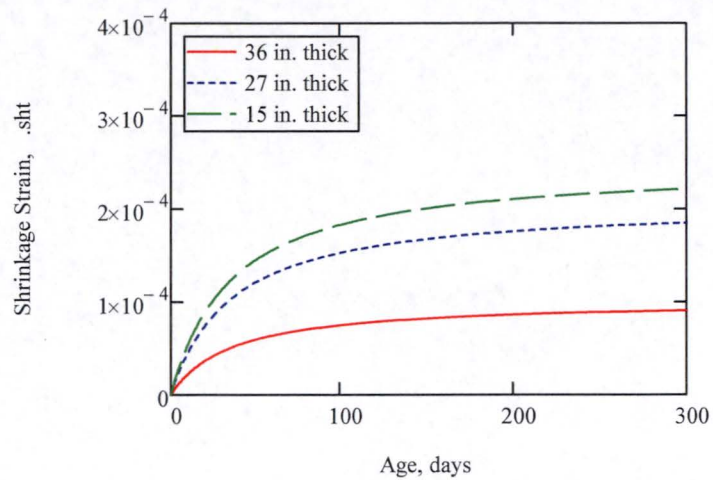
$shu_{27} := shub \cdot shrinkage_{27}$

$$shu_{27} = 2.064 \times 10^{-4}$$

Ultimate shrinkage strain
for 15 in. thick walls

$shu_{15} := shub \cdot shrinkage_{15}$

$$shu_{15} = 2.471 \times 10^{-4}$$



D7.6 Calculate Shrinkage Strain for use in FE Model (Continued)

For 36 in. thick walls:

$$\begin{aligned}\epsilon_{\text{sht}} @ 1 \text{ yr:} & \quad \text{sht}(1\text{yr}, ,f, \text{shu}_{36}) = 9.243 \times 10^{-5} \\ \epsilon_{\text{sht}} @ 5 \text{ yrs:} & \quad \text{sht}(5\text{yr}, ,f, \text{shu}_{36}) = 9.938 \times 10^{-5} \\ \epsilon_{\text{sht}} @ 10 \text{ yrs:} & \quad \text{sht}(10\text{yr}, ,f, \text{shu}_{36}) = 1.003 \times 10^{-4} \\ \epsilon_{\text{sht}} @ 25 \text{ yrs:} & \quad \text{sht}(25\text{yr}, ,f, \text{shu}_{36}) = 1.009 \times 10^{-4} \\ \epsilon_{\text{sht}} @ 35 \text{ yrs:} & \quad \text{sht}(35\text{yr}, ,f, \text{shu}_{36}) = 1.01 \times 10^{-4}\end{aligned}$$

For 27 in. thick walls:

$$\begin{aligned}\epsilon_{\text{sht}} @ 1 \text{ yr:} & \quad \text{sht}(1\text{yr}, ,f, \text{shu}_{27}) = 1.883 \times 10^{-4} \\ \epsilon_{\text{sht}} @ 5 \text{ yrs:} & \quad \text{sht}(5\text{yr}, ,f, \text{shu}_{27}) = 2.025 \times 10^{-4} \\ \epsilon_{\text{sht}} @ 10 \text{ yrs:} & \quad \text{sht}(10\text{yr}, ,f, \text{shu}_{27}) = 2.044 \times 10^{-4} \\ \epsilon_{\text{sht}} @ 25 \text{ yrs:} & \quad \text{sht}(25\text{yr}, ,f, \text{shu}_{27}) = 2.056 \times 10^{-4} \\ \epsilon_{\text{sht}} @ 35 \text{ yrs:} & \quad \text{sht}(35\text{yr}, ,f, \text{shu}_{27}) = 2.058 \times 10^{-4}\end{aligned}$$

For 15 in. thick walls:

$$\begin{aligned}\epsilon_{\text{sht}} @ 1 \text{ yr:} & \quad \text{sht}(1\text{yr}, ,f, \text{shu}_{15}) = 2.255 \times 10^{-4} \\ \epsilon_{\text{sht}} @ 5 \text{ yrs:} & \quad \text{sht}(5\text{yr}, ,f, \text{shu}_{15}) = 2.424 \times 10^{-4} \\ \epsilon_{\text{sht}} @ 10 \text{ yrs:} & \quad \text{sht}(10\text{yr}, ,f, \text{shu}_{15}) = 2.447 \times 10^{-4} \\ \epsilon_{\text{sht}} @ 25 \text{ yrs:} & \quad \text{sht}(25\text{yr}, ,f, \text{shu}_{15}) = 2.461 \times 10^{-4} \\ \epsilon_{\text{sht}} @ 35 \text{ yrs:} & \quad \text{sht}(35\text{yr}, ,f, \text{shu}_{15}) = 2.464 \times 10^{-4}\end{aligned}$$

D8.0 Conclusions

Creep coefficients of approx. 1.3 and 2.3 are computed in this appendix. The use of a lower creep coefficient is most conservative for this calculation because it causes less of the CEB deformation to be attributed to creep (and therefore more CEB deformation is attributed to other self-straining loads such as ASR expansion). In design confirmation FEA, use creep coefficient of $v_t = 1.3$. Creep strains will be calculated using the equation below. σ_D is the sustained dead load. E_0 is the initial concrete modulus of elasticity.

$$\epsilon_{creep} = \frac{v_t}{E_0} \sigma_D$$

In design confirmation FEA, use the following shrinkage strains:

- $\epsilon_{sh} = 1.0 \times 10^{-4}$ for 36 in. thick walls
- $\epsilon_{sh} = 2.0 \times 10^{-4}$ for 27 in. thick walls
- $\epsilon_{sh} = 2.5 \times 10^{-4}$ for 15 in. thick walls.

D9.0 References

- [D1] ACI Committee 209, Prediction of Creep, Shrinkage, and Temperature Effects in Concrete Structures, ACI 209R-92, Reapproved 1997.
- [D2] Vassallo, T. "CEB Concrete Mix." 8 April 2015. E-mail.
- [D3] Vassallo, T. "CEB Concrete Slump." 17 April 2015. E-mail.
- [D4] Vassallo, T. "CEB Concrete Mix." 20 April 2015. E-mail.
- [D5] WeatherSpark, "Average Weather For Portsmouth, New Hampshire, USA." Accessed 20 April 2015. <https://weatherspark.com/averages/31310/Portsmouth-New-Hampshire-United-States>.



Appendix E Computation of PM Interaction using spColumn

E1. REVISION HISTORY

Revision 0

Initial document.

E2. OBJECTIVE

The objective of this calculation is to compute axial-moment (PM) interaction curves for the CEB wall.

E3. RESULTS AND CONCLUSIONS

PM interaction capacity curves are used in the element-by-element evaluation of the CEB. Plots and spColumn output data for all PM interaction capacity curves are available on 150252-CA-02-CD-01. A selection of PM interaction capacity curves and spColumn output data are shown in this appendix for information.

E4. DESIGN DATA / CRITERIA

Wall geometry, reinforcement layout, and material properties are based on the structural drawings listed in the project Criteria Document 150252-CD-03 [E-1].

E5. ASSUMPTIONS

Justified Assumptions

There are no justified assumptions.

Unverified Assumptions

There are no unverified assumptions.

E6. METHODOLOGY

The wall is divided into 12 in. wide strips along the hoop and meridional directions to facilitate computation of PM interaction curves. Interaction capacity curves are generated using



spColumn Version 4.81 [E-2], which has been verified and validated in accordance with the SGH QANF program [E-3, E-4].

Based on ACI 318-71, strength reduction (ϕ) factors of 0.9 for tension-controlled failure and 0.7 for compression-controlled failure are specified in the spColumn software. However, spColumn transitions between these ϕ factors linearly between the points where the tensile reinforcement strain is 0.005 and 0.002 (this conforms to the modern ACI 318 building code). The ACI 318-71 building code specifies that the ϕ factor should transition between the point of zero axial load and the lesser of the balanced point (point with 0.002 tensile reinforcement strain) or the point at which axial load is $0.1f'_cA_g$ (where A_g is the gross area of the section). Due to this difference in transition points, the PM interaction curves computed by spColumn are modified by the project-specific routine "SR_correctPM_PhiFactor_r0." This routine modifies the PM interaction capacity curves output by spColumn to meet the ϕ factor transition specified by ACI 318-71. The functionality of this routine is demonstrated in the interaction diagrams presented in Section E7.

E7. COMPUTATIONS

Plots and spColumn output data for all PM interaction capacity curves are available on 150252-CA-02-CD-01. PM interaction capacity curves and spColumn output data for the wall sections listed below are shown in this appendix for information purposes. Only the second page of the three-page spColumn output files is shown because p. 1 contains header information and p. 3 is blank. The full spColumn output files are provided on 150252-CA-02-CD-01.

- 15 in. thick wall segment with #8@12 in. on each face (EF) hoop reinforcement:
 - PM Interaction Capacity Curve: Figure E1
 - spColumn Output: Table E1
- 36 in. thick wall segment with one layer #11@6 in. inside face (IF) and two layers of #11@6 in. outside face (OF) meridional reinforcement:
 - PM Interaction Capacity Curve: Figure E2
 - spColumn Output: Table E2

PROJECT NO: 150252DATE: July 2016CLIENT: NextEra Energy Seabrook BY: R.M. MonesSUBJECT: Evaluation and Design Confirmation of As-Deformed CEB VERIFIER: A.T. Sarawit**E8. REFERENCES**

- [E-1] Simpson Gumpertz & Heger Inc., *Criteria Document for Evaluation of As-Deformed Containment Enclosure Building at Seabrook Station in Seabrook, NH*, 150252-CD-03, Revision 0, Waltham, MA, 27 July 2016.
- [E-2] Structure Point, *spColumn v4.81 Software*, 2013.
- [E-3] Simpson Gumpertz & Heger Inc, *spColumn v4.81 Commercial Grade Software Dedication Plan/Report*, Revision 0, Waltham, MA, July 2014.
- [E-4] Simpson Gumpertz & Heger Inc., *Quality Assurance Manual for Nuclear Facility Work*, Revision 7, Waltham, MA, 1 Dec. 2013.

```

Line  spColumn Text Output
53  STRUCTUREPOINT - spColumn v4.81 (TM)
54  Licensed to: Simpson Gumpertz & Heger Inc. License ID: 63848-1047578-4-1ED95-1A93A
55  h_15_604_704.cti
56
57
58  General Information:
59  _____
60  File Name: h_15_604_704.cti
61  Project: 150252.12 Seabrook
62  Column: 15_604_704
63  Code: ACI 318-08
64
65  Run Option: Investigation
66  Run Axis: X-axis
67
68  Material Properties:
69  _____
70  f'c = 4 ksi
71  Ec = 3605 ksi
72  Ultimate strain = 0.003 in/in
73  Beta1 = 0.85
74
75  Section:
76  _____
77  Rectangular: Width = 12 in
78
79  Gross section area, Ag = 180 in^2
80  Ix = 3375 in^4
81  rx = 4.33013 in
82  Xo = 0 in
83
84  Reinforcement:
85  _____
86  Bar Set: User-defined
87  Size Diam (in) Area (in^2) Size Diam (in) Area (in^2) Size Diam (in) Area (in^2)
88
89  # 0 0.00 0.00 # 1 0.00 0.00 # 2 0.00 0.00
90  # 3 0.00 0.00 # 4 0.50 0.20 # 5 0.63 0.31
91  # 6 0.75 0.44 # 7 0.88 0.60 # 8 1.00 0.79
92  # 9 1.13 1.00 # 10 1.27 1.27 # 11 1.41 1.56
93  # 12 0.00 0.00 # 13 0.00 0.00 # 14 1.69 2.25
94  # 15 0.00 0.00 # 16 0.00 0.00 # 17 0.00 0.00
95  # 18 2.26 4.00 # 19 0.00 0.00
96
97  Confinement: Other; #1 ties with #7 bars, #1 with larger bars.
98  phi(a) = 0.7, phi(b) = 0.9, phi(c) = 0.7
99
100  Pattern: Irregular
101  Total steel area: As = 1.58 in^2 at rho = 0.88% (Note: rho < 1.0%)

```



Table E1 – spColumn Output for 15 in. Thick Wall Segment with #8@12EF Hoop Reinforcement

Line	spColumn Text Output									
102	Minimum clear spacing = 0.00 in									
103										
104	Area in^2	X (in)	Y (in)	Area in^2	X (in)	Y (in)	Area in^2	X (in)	Y (in)	
105										
106	0.79	0.0	-5.0	0.79	0.0	4.0	0.00	0.0	0.0	
107	0.00	0.0	0.0	0.00	0.0	0.0	0.00	0.0	0.0	
108	0.00	0.0	0.0	0.00	0.0	0.0	0.00	0.0	0.0	
109	0.00	0.0	0.0	0.00	0.0	0.0	0.00	0.0	0.0	
110										
111	Control Points:									
112										
113				Axial Load P	X-Moment	Y-Moment	NA depth	Dt depth	eps_t	Phi
114	Bending about			kip	k-ft	k-ft	in	in		
115										
116	X @ Max compression			491.0	2.61	-0.00	37.06	11.50	-0.00207	0.700
117	@ Allowable comp.			343.7	65.67	0.00	12.68	11.50	-0.00028	0.700
118	@ fs = 0.0			310.5	73.82	0.00	11.50	11.50	0.00000	0.700
119	@ fs = 0.5*fy			222.3	85.45	-0.00	8.55	11.50	0.00103	0.700
120	@ Balanced point			160.6	86.40	0.00	6.81	11.50	0.00207	0.700
121	@ Tension control			115.5	87.61	-0.00	4.31	11.50	0.00500	0.900
122	@ Pure bending			-0.0	40.44	-0.00	1.94	11.50	0.01479	0.900
123	@ Max tension			-85.3	-3.55	0.00	0.00	11.50	9.99999	0.900
124										
125	-X @ Max compression			491.0	2.61	-0.00	40.28	12.50	-0.00207	0.700
126	@ Allowable comp.			343.7	-63.14	0.00	12.82	12.50	-0.00007	0.700
127	@ fs = 0.0			334.7	-65.75	0.00	12.50	12.50	0.00000	0.700
128	@ fs = 0.5*fy			237.2	-83.03	0.00	9.29	12.50	0.00103	0.700
129	@ Balanced point			169.9	-86.84	0.00	7.40	12.50	0.00207	0.700
130	@ Tension control			116.9	-89.34	0.00	4.69	12.50	0.00500	0.900
131	@ Pure bending			-0.0	-47.24	0.00	2.34	12.50	0.01300	0.900
132	@ Max tension			-85.3	-3.55	0.00	0.00	12.50	9.99999	0.900
133										
134										
135	*** End of output ***									
136										


Table E2 – spColumn Output for 36 in. Thick Wall Segment with 1#11@6" IF and 2#11@6" OF Meridional Reinforcement

Line	spColumn Text Output	
53	STRUCTUREPOINT - spColumn v4.81 (TM)	Page 2
54	Licensed to: Simpson Gumpertz & Heger Inc. License ID: 63848-1047578-4-1ED95-1A93A	06/06/16
55	m_36_616_709.cti	09:15 AM
56		
57		
58	General Information:	
59		
60	File Name: m_36_616_709.cti	
61	Project: 150252.12 Seabrook	
62	Column: 36_616_709	Engineer: RMMones
63	Code: ACI 318-08	Units: English
64		
65	Run Option: Investigation	Slenderness: Not considered
66	Run Axis: X-axis	Column Type: Structural
67		
68	Material Properties:	
69		
70	f'c = 4 ksi	fy = 60 ksi
71	Ec = 3605 ksi	Es = 29000 ksi
72	Ultimate strain = 0.003 in/in	
73	Betal = 0.85	
74		
75	Section:	
76		
77	Rectangular: Width = 12 in	Depth = 36 in
78		
79	Gross section area, Ag = 432 in^2	
80	Ix = 46656 in^4	Iy = 5184 in^4
81	rx = 10.3923 in	ry = 3.4641 in
82	Xo = 0 in	Yo = 0 in
83		
84	Reinforcement:	
85		
86	Bar Set: User-defined	
87	Size Diam (in) Area (in^2)	Size Diam (in) Area (in^2) Size Diam (in) Area (in^2)
88		
89	# 0 0.00 0.00	# 1 0.00 0.00 # 2 0.00 0.00
90	# 3 0.00 0.00	# 4 0.50 0.20 # 5 0.63 0.31
91	# 6 0.75 0.44	# 7 0.88 0.60 # 8 1.00 0.79
92	# 9 1.13 1.00	# 10 1.27 1.27 # 11 1.41 1.56
93	# 12 0.00 0.00	# 13 0.00 0.00 # 14 1.69 2.25
94	# 15 0.00 0.00	# 16 0.00 0.00 # 17 0.00 0.00
95	# 18 2.26 4.00	# 19 0.00 0.00
96		
97	Confinement: Other; #1 ties with #7 bars, #1 with larger bars.	
98	phi(a) = 0.7, phi(b) = 0.9, phi(c) = 0.7	
99		
100	Pattern: Irregular	
101	Total steel area: As = 9.36 in^2 at rho = 2.17%	

(Output continued on next page)


Table E2 – spColumn Output for 36 in. Thick Wall Segment with 1#11@6" IF and 2#11@6" OF Meridional Reinforcement

Line

spColumn Text Output

102	Minimum clear spacing = 0.00 in								
103									
104	Area in^2	X (in)	Y (in)	Area in^2	X (in)	Y (in)	Area in^2	X (in)	Y (in)
105									
106	1.56	-3.0	-14.3	1.56	3.0	-14.3	1.56	-3.0	-11.5
107	1.56	3.0	-11.5	1.56	-3.0	15.3	1.56	3.0	15.3
108	0.00	0.0	0.0	0.00	0.0	0.0	0.00	0.0	0.0
109	0.00	0.0	0.0	0.00	0.0	0.0	0.00	0.0	0.0
110									
111	Control Points:								
112									
113		Axial Load P	X-Moment	Y-Moment	NA depth	Dt depth	eps_t	Phi	
114	Bending about	kip	k-ft	k-ft	in	in			
115									
116	X @ Max compression	1399.0	107.91	-0.00	107.28	33.29	-0.00207	0.700	
117	@ Allowable comp.	979.3	591.20	-0.00	30.79	33.29	0.00024	0.700	
118	@ fs = 0.0	1055.5	524.76	-0.00	33.29	33.29	0.00000	0.700	
119	@ fs = 0.5*fy	782.7	723.51	-0.00	24.76	33.29	0.00103	0.700	
120	@ Balanced point	590.6	812.41	-0.00	19.71	33.29	0.00207	0.700	
121	@ Tension control	487.2	918.69	-0.00	12.49	33.29	0.00500	0.900	
122	@ Pure bending	-0.0	449.31	-0.00	5.26	33.29	0.01598	0.900	
123	@ Max tension	-505.4	-147.07	-0.00	0.00	33.29	9.99999	0.900	
124									
125	-X @ Max compression	1399.0	107.91	-0.00	104.06	32.30	-0.00207	0.700	
126	@ Allowable comp.	979.3	-370.51	0.00	33.87	32.30	-0.00014	0.700	
127	@ fs = 0.0	924.2	-420.96	0.00	32.30	32.30	0.00000	0.700	
128	@ fs = 0.5*fy	597.9	-655.56	0.00	24.01	32.30	0.00103	0.700	
129	@ Balanced point	353.6	-794.06	0.00	19.11	32.30	0.00207	0.700	
130	@ Tension control	200.0	-969.25	0.00	12.11	32.30	0.00500	0.900	
131	@ Pure bending	0.0	-790.17	0.00	6.52	32.30	0.01186	0.900	
132	@ Max tension	-505.4	-147.07	-0.00	0.00	32.30	9.99999	0.900	
133									
134									
135	*** End of output ***								
136									

E10. FIGURES

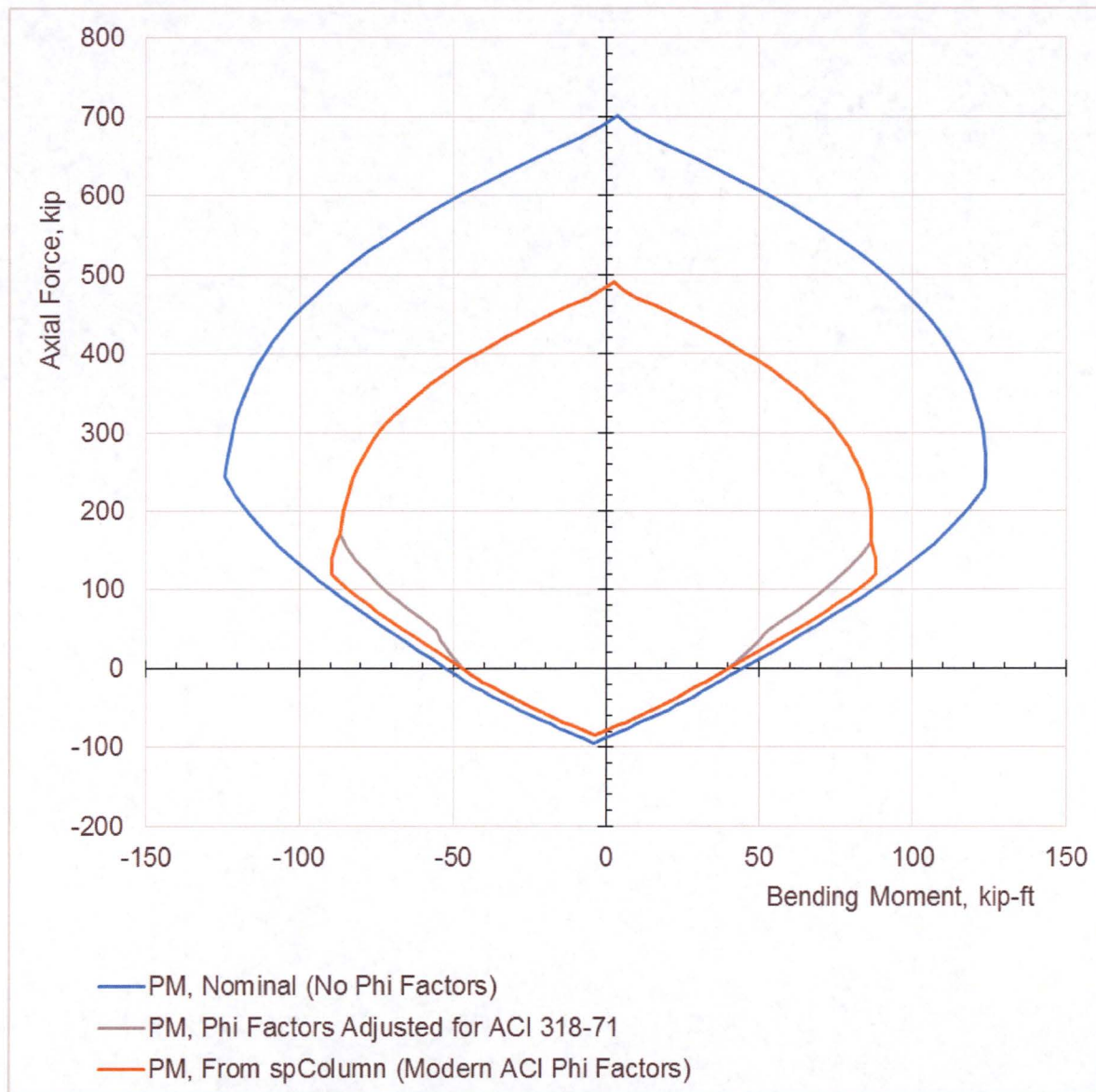


Figure E1 – PM Interaction Capacity Curve for 15 in. Thick Wall Section with #8@12EF in Hoop Direction

Notes:

Compression is positive in this diagram (this does not follow the sign convention generally used in this calculation). Compression capacity is not reduced for accidental eccentricity in this diagram; this is done during the element-by-element evaluation in a separate axial compression check as described in Section 7.1.1 in the main body of this calculation.

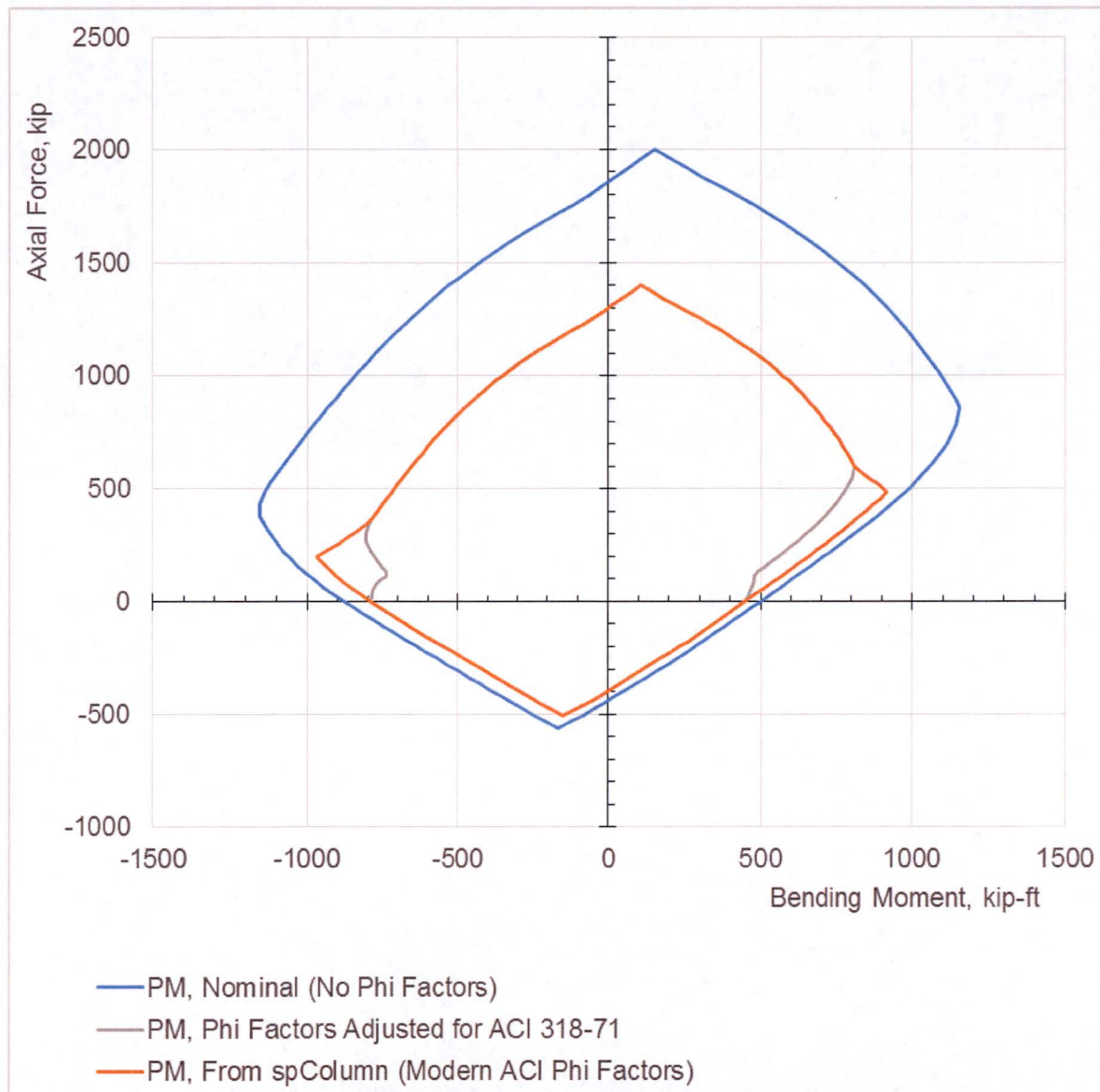


Figure E2 – PM Interaction Capacity Curve for 36 in. Thick Wall Section with One layer #11@6IF and Two Layer #11@6OF in Meridional Direction

Notes:

Compression is positive in this diagram (this does not follow the sign convention generally used in this calculation). Compression capacity is not reduced for accidental eccentricity in this diagram; this is done during the element-by-element evaluation in a separate axial compression check as described in Section 7.1.1 in the main body of this calculation.



Appendix F

Input Seismic Accelerations for 3D Analysis

F1. REVISION HISTORY

Revision 0

Initial document.

F2. OBJECTIVE OF CALCULATION

The objective of this calculation is to evaluate the impact of alkali-silica reaction (ASR) expansion, swelling, shrinkage, and creep on the Containment Enclosure Building (CEB) structural dynamic properties, and determine whether the same input seismic accelerations for the 3D analyses for an assumed structure without ASR expansion, swelling, shrinkage, and creep effects can be used for the actual structure with the effects.

F3. RESULTS AND CONCLUSIONS

This study shows that ASR expansion, swelling, shrinkage, and creep have a negligible impact on the CEB structural dynamic properties; therefore, the same input seismic accelerations for the 3D analyses can be used for the CEB structure, either with or without the effects.

It is beyond the scope of this work to recompute seismic accelerations for the as-deformed CEB structure. However, since this study shows that the as-deformed condition of the CEB does not impact the dynamic properties, it is concluded that the original design seismic accelerations computed by United Engineers & Constructors Inc. (UE) in their calculation SBSAG-4CE [F-1] may reasonably be used in the seismic analyses in this calculation (see Section F5 for more information).

F4. DESIGN DATA / CRITERIA

The finite element mesh and wall section properties of the CEB finite element model described in the main body of the calculation for the (1) undeformed condition, (2) as-deformed condition of the Standard Analysis Case, and (3) as-deformed condition of the Standard-Plus Analysis Case are used as input to this calculation to compute the following CEB structure cross-section properties:



- AREA – Area value
- IYY, IYZ, IZZ – Moments of inertia
- WARP – Warping constant
- TORS – Torsion constant
- CGY, CGZ – Y or Z coordinate center of gravity
- SHCY, SHCZ – Y or Z coordinate shear center
- SCYY, SCYZ, SCZZ – Shear correction factors

where Y and Z are local cross-section axes pointing toward east and north directions. Note that this local coordinate system is unique to the computations documented in this appendix.

The following criteria are used to determine if the cross-section properties of the undeformed (structure without the effects) and deformed (due to the effects) are significantly different.

- If fractional difference is less than or equal to 5% then the property value is considered to not significantly have changed. If the fractional difference is more than 5% then check the absolute difference where:

$$\text{Fractional Difference} = \frac{|A - B|}{\max(|A|, |B|)}$$

$$\text{Absolute Difference} = |A - B|$$

- If the absolute difference is determined to be small by engineering judgment then the property value is considered to not significantly have changed. If the fractional difference is more than 5% and the absolute difference is large then the property value is considered to have significantly changed.

F5. ASSUMPTIONS

Justified Assumptions

- The input seismic accelerations for the 3D analysis if computed using the dynamic properties calculated in this study, and using boundary condition assumptions accounting for SSI effects, could be somewhat different from the original design accelerations provided by UE; further seismic analysis study could be performed to evaluate this; however, it is beyond the current scope of this work.
- The modulus of elasticity of reinforced concrete is not significantly changed due to ASR expansion, shrinkage, or creep [F-3].



- Cracked section properties do not affect the global seismic response of the CEB. This assumption is justified because the global response of the CEB to seismic motion primarily causes in-plane shear and overturning stresses; both are resisted by the membrane stiffnesses of the CEB wall that are not impacted by cracking.

Unverified Assumptions

There are no unverified assumptions.

F6. METHODOLOGY

The input seismic accelerations for 3D analysis are a function of structural dynamic properties, structure boundary conditions, and seismic ground motion. The structural dynamic properties are mass, stiffness, and damping. For the purpose of this calculation the structural dynamic properties are considered to not change if the cross-section properties of the CEB have not changed due to ASR expansion, swelling, shrinkage, and creep effects. Note that as part of an assumption to this calculation, the modulus of elasticity of reinforced concrete is deemed to have not changed significantly due to ASR expansion, swelling, shrinkage, or creep effects.

The cross-section properties of the CEB are computed at multiple elevations for the (1) undeformed condition, (2) as-deformed condition of the Standard Analysis Case, and (3) as-deformed condition of the Standard-Plus Analysis Case. Assumptions associated with these various configurations are described in the main body of the calculation. The cross-section properties of these three cases are compared, and determination is made whether they are significantly different per the criteria described in Section F4.

F7. COMPUTATIONS

Eight elevations along the height of the CEB structure as shown in Figure F1 were selected for computing the cross-section properties. Elevations were selected at sections with major differences in openings and wall thicknesses, and at various heights along the cylinder section of the CEB. Elevations in the dome region were not selected for this study because the finite element mesh in this region is irregular, and it would have required significant additional calculations to interpolate the mesh geometry to a common elevation. The deformation in the dome section is not more than the cylinder section, and therefore, for the purpose of this study, additional evaluation in this region is not needed.



The cross-section properties are computed using ANSYS finite element software [F-2] for the (1) undeformed condition, (2) as-deformed condition of the Standard Analysis Case, and (3) as-deformed condition of the Standard-Plus Analysis Case; the results are summarized in Tables F.1 through F.3, respectively. The elevations at which cross-section properties are computed are shown in Figure F.1. Plots of the cross-sections including its properties of the undeformed structure are shown in Figures F.2 through F.10 for select elevations. ANSYS cannot compute properties of a section with multiple disconnected wall sections; thus, thin wall sections are used at the openings, which are deemed acceptable for comparing properties for the purpose of this study.

The fractional difference between the undeformed condition and the as-deformed conditions for each analysis case are computed; the results are summarized in Tables F.4 and F.6. Values highlighted in gray are those having differences higher than 5%. Where the fractional differences are higher than 5%, the absolute differences are computed; the results are summarized in Tables F.5 and F.7.

As can be seen from Tables F.4 through F.7, most of the properties have fractional differences of less than 5%, and where the fractional differences are more than 5%, the absolute differences are small and deemed not significant (i.e., the center of gravity and shear center moved less than 0.5 in., which is considered very small for a structure with an inside radius of 79 ft).

PROJECT NO: 150252DATE: July 2016CLIENT: NextEra Energy SeabrookBY: R.M. MonesSUBJECT: Evaluation and Design Confirmation of As-Deformed CEBVERIFIER: A.T. Sarawit**F8. REFERENCES**

- [F-1] United Engineers & Constructors Inc., *Enclosure Building 3-D Structural Analysis/Floor Response Spectra/A.R.S*, Calc. Set No. SBSAG-4CE, Dec. 1977.
- [F-2] ANSYS Release 15.0, ANSYS Inc.
- [F-3] MPR Associates, Seabrook Station – Implications of Large-Scale Test Program Results on Reinforced Concrete Affected by Alkali-Silica Reaction, MPR-4273 Revision Draft, Apr. 2016.


F9. TABLES
Table F.1 – Cross-Section Properties of the Undeformed CEB

EL. (ft)	Area (x10 ³ in. ²)	IYY (x10 ⁹ in. ⁴)	IYZ (x10 ⁹ in. ⁴)	IZZ (x10 ⁹ in. ⁴)	WARP (x10 ¹⁵ in. ⁶)	TORS (x10 ⁹ in. ⁹)
108.8	90.1	41.1	0.0	41.1	0.0	82.2
86.3	90.1	41.1	0.0	41.1	0.0	82.2
61.3	90.1	41.2	0.0	41.1	0.0	82.3
35.4	156.7	70.8	2.6	73.9	17.7	94.9
12.8	138.9	62.1	-0.2	65.1	8.2	48.1
-1.5	123.9	58.2	1.7	51.7	4.5	37.9
-15.1	164.1	77.6	2.6	68.8	6.2	46.0
-30	167.5	80.1	3.3	69.0	7.8	48.8

EL. (ft)	CGY (in.)	CGZ (in.)	SHCY (in.)	SHCZ (in.)	SCYY	SCYZ	SCZZ
108.8	0.0	0.0	0.0	0.0	0.50	0.00	0.50
86.3	0.0	0.0	0.0	0.0	0.50	0.00	0.50
61.3	0.5	-0.8	0.3	-0.5	0.50	0.00	0.50
35.4	-19.2	34.0	-349.6	618.0	0.35	-0.09	0.47
12.8	-9.2	-94.4	-6.8	-659.5	0.24	0.00	0.18
-1.5	172.2	-87.3	788.0	-424.3	0.20	0.06	0.25
-15.1	180.0	-93.6	819.8	-447.9	0.19	0.06	0.24
-30	174.8	-111.4	851.1	-598.1	0.26	0.10	0.26

Notes:

EL. – Elevation

AREA – Area value

IYY, IYZ, IZZ – Moments of inertia

WARP – Warping constant

TORS – Torsion constant

CGY, CGZ – Y or Z coordinate center of gravity

SHCY, SHCZ – Y or Z coordinate shear center

SCYY, SCYZ, SCZZ – Shear correction factors


Table F.2 – Cross-Section Properties of Deformed CEB for the Standard Analysis Case

EL. (ft)	Area ($\times 10^3 \text{ in.}^2$)	IYY ($\times 10^9 \text{ in.}^4$)	IYZ ($\times 10^9 \text{ in.}^4$)	IZZ ($\times 10^9 \text{ in.}^4$)	WARP ($\times 10^{15} \text{ in.}^6$)	TORS ($\times 10^9 \text{ in.}^9$)
108.8	90.0	41.1	0.0	41.1	0.0	82.2
86.3	90.0	41.1	0.0	41.1	0.0	82.2
61.3	90.1	41.2	-0.1	41.1	0.0	82.3
35.4	156.7	70.8	2.6	73.9	17.7	94.9
12.8	138.8	62.1	-0.2	65.0	8.2	48.0
-1.5	123.8	58.1	1.7	51.7	4.4	37.9
-15.1	164.1	77.5	2.6	68.8	6.2	46.0
-30	167.5	80.1	3.3	69.0	7.8	48.8

EL. (ft)	CGY (in.)	CGZ (in.)	SHCY (in.)	SHCZ (in.)	SCYY	SCYZ	SCZZ
108.8	-0.1	0.4	-0.1	0.4	0.50	0.00	0.50
86.3	-0.1	0.4	-0.1	0.4	0.50	0.00	0.50
61.3	0.3	-0.5	0.1	-0.1	0.50	0.00	0.50
35.4	-19.4	34.4	-349.8	618.2	0.35	-0.09	0.47
12.8	-9.4	-94.2	-7.1	-658.8	0.24	0.00	0.18
-1.5	172.2	-87.2	788.0	-424.0	0.20	0.06	0.25
-15.1	179.9	-93.4	819.7	-447.7	0.19	0.06	0.24
-30	174.7	-111.3	851.2	-598.0	0.26	0.10	0.26

Notes:

EL. – Elevation

AREA – Area value

IYY, IYZ, IZZ – Moments of inertia

WARP – Warping constant

TORS – Torsion constant

CGY, CGZ – Y or Z coordinate center of gravity

SHCY, SHCZ – Y or Z coordinate shear center

SCYY, SCYZ, SCZZ – Shear correction factors


Table F.3 – Cross-Section Properties of Deformed CEB for the Standard-Plus Analysis Case

EL. (ft)	Area ($\times 10^3$ in. ²)	IYY ($\times 10^9$ in. ⁴)	IYZ ($\times 10^9$ in. ⁴)	IZZ ($\times 10^9$ in. ⁴)	WARP ($\times 10^{15}$ in. ⁶)	TORS ($\times 10^9$ in. ⁹)
108.8	90.0	41.1	0.0	41.1	0.0	82.2
86.3	90.0	41.1	0.0	41.1	0.0	82.2
61.3	90.1	41.2	-0.1	41.1	0.0	82.3
35.4	156.7	70.8	2.6	73.9	17.7	94.9
12.8	138.8	62.1	-0.2	65.0	8.2	48.0
-1.5	123.9	58.1	1.7	51.7	4.4	37.9
-15.1	164.1	77.5	2.6	68.8	6.2	46.0
-30	167.5	80.1	3.3	69.0	7.8	48.8

EL. (ft)	CGY (in.)	CGZ (in.)	SHCY (in.)	SHCZ (in.)	SCYY	SCYZ	SCZZ
108.8	-0.1	0.3	-0.1	0.3	0.50	0.00	0.50
86.3	-0.2	0.3	-0.2	0.3	0.50	0.00	0.50
61.3	0.3	-0.5	0.1	-0.2	0.50	0.00	0.50
35.4	-19.4	34.3	-349.8	618.2	0.35	-0.09	0.47
12.8	-9.4	-94.3	-7.2	-658.9	0.24	0.00	0.18
-1.5	172.1	-87.2	787.9	-424.0	0.20	0.06	0.25
-15.1	179.9	-93.5	819.7	-447.6	0.19	0.06	0.24
-30	174.7	-111.3	851.2	-598.0	0.26	0.10	0.26

Notes:

EL. – Elevation

AREA – Area value

IYY, IYZ, IZZ – Moments of inertia

WARP – Warping constant

TORS – Torsion constant

CGY, CGZ – Y or Z coordinate center of gravity

SHCY, SHCZ – Y or Z coordinate shear center

SCYY, SCYZ, SCZZ – Shear correction factors

Table F.4 – Fractional Differences between Cross-Section Properties of Undeformed and Deformed Standard Model

EL. (ft)	Area	IYY	IYZ	IZZ	WARP	TORS
108.8	0.0%	0.1%	99.8%	0.1%	100.0%	0.1%
86.3	0.0%	0.1%	100.1%	0.0%	100.0%	0.1%
61.3	0.0%	0.1%	14.0%	0.0%	40.8%	0.0%
35.4	0.0%	0.1%	0.7%	0.0%	0.0%	0.0%
12.8	0.0%	0.1%	7.9%	0.0%	0.1%	0.0%
-1.5	0.0%	0.1%	0.4%	0.1%	0.1%	0.1%
-15.1	0.0%	0.1%	0.1%	0.1%	0.0%	0.0%
-30	0.0%	0.0%	0.1%	0.0%	0.1%	0.1%

EL. (ft)	CGY	CGZ	SHCY	SHCZ	SCYY	SCYZ	SCZZ
108.8	100.3%	100.2%	100.3%	100.2%	0.0%	99.8%	0.0%
86.3	100.3%	100.2%	100.3%	100.2%	0.0%	100.1%	0.0%
61.3	58.4%	75.7%	147.7%	236.3%	0.0%	13.0%	0.0%
35.4	1.0%	1.1%	0.1%	0.0%	0.0%	0.1%	0.0%
12.8	2.0%	0.2%	3.8%	0.1%	0.1%	20.9%	0.1%
-1.5	0.0%	0.2%	0.0%	0.1%	0.0%	0.3%	0.0%
-15.1	0.1%	0.1%	0.0%	0.0%	0.0%	0.2%	0.0%
-30	0.1%	0.1%	0.0%	0.0%	0.0%	0.1%	0.0%

Notes:

EL. – Elevation

AREA – Area value

IYY, IYZ, IZZ – Moments of inertia

WARP – Warping constant

TORS – Torsion constant

CGY, CGZ – Y or Z coordinate center of gravity

SHCY, SHCZ – Y or Z coordinate shear center

SCYY, SCYZ, SCZZ – Shear correction factors

Table F.5 – Absolute Differences between Cross-Section Properties of Undeformed and Deformed Standard Model

EL. (ft)	Area ($\times 10^3$ in. ²)	IYY ($\times 10^9$ in. ⁴)	IYZ ($\times 10^9$ in. ⁴)	IZZ ($\times 10^9$ in. ⁴)	WARP ($\times 10^{15}$ in. ⁶)	TORS ($\times 10^9$ in. ⁹)
108.8	-	-	0.0	-	0.0	-
86.3	-	-	0.0	-	0.0	-
61.3	-	-	0.0	-	0.0	-
35.4	-	-	-	-	-	-
12.8	-	-	0.0	-	-	-
-1.5	-	-	-	-	-	-
-15.1	-	-	-	-	-	-
-30	-	-	-	-	-	-

EL. (ft)	CGY (in.)	CGZ (in.)	SHCY (in.)	SHCZ (in.)	SCYY	SCYZ	SCZZ
108.8	-0.1	0.4	-0.1	0.4	-	0.0	-
86.3	-0.1	0.4	-0.1	0.4	-	0.0	-
61.3	-0.2	0.3	-0.2	0.4	-	0.0	-
35.4	-	-	-	-	-	-	-
12.8	-	-	-0.3	-	-	0.0	-
-1.5	-	-	-	-	-	-	-
-15.1	-	-	-	-	-	-	-
-30	-	-	-	-	-	-	-

Notes:

EL. – Elevation

AREA – Area value

IYY, IYZ, IZZ – Moments of inertia

WARP – Warping constant

TORS – Torsion constant

CGY, CGZ – Y or Z coordinate center of gravity

SHCY, SHCZ – Y or Z coordinate shear center

SCYY, SCYZ, SCZZ – Shear correction factors

Table F.6 – Fractional Differences between Cross-Section Properties of Undeformed and Deformed Standard-Plus Model

EL. (ft)	Area	IYY	IYZ	IZZ	WARP	TORS
108.8	0.0%	0.1%	99.4%	0.1%	100.0%	0.1%
86.3	0.0%	0.1%	100.2%	0.0%	100.0%	0.1%
61.3	0.0%	0.1%	5.6%	0.0%	37.1%	0.0%
35.4	0.0%	0.1%	0.2%	0.0%	0.0%	0.0%
12.8	0.0%	0.1%	1.2%	0.0%	0.1%	0.0%
-1.5	0.0%	0.1%	0.2%	0.1%	0.1%	0.1%
-15.1	0.0%	0.1%	0.2%	0.1%	0.0%	0.0%
-30	0.0%	0.0%	0.1%	0.0%	0.1%	0.1%

EL. (ft)	CGY	CGZ	SHCY	SHCZ	SCYY	SCYZ	SCZZ
108.8	100.3%	100.2%	100.3%	100.2%	0.0%	99.4%	0.0%
86.3	100.3%	100.2%	100.3%	100.2%	0.0%	100.2%	0.0%
61.3	62.8%	55.5%	167.4%	141.0%	0.0%	5.4%	0.0%
35.4	1.1%	0.9%	0.1%	0.0%	0.0%	0.0%	0.0%
12.8	2.3%	0.1%	4.8%	0.1%	0.1%	10.3%	0.1%
-1.5	0.1%	0.1%	0.0%	0.1%	0.0%	0.2%	0.0%
-15.1	0.1%	0.1%	0.0%	0.1%	0.0%	0.2%	0.0%
-30	0.1%	0.1%	0.0%	0.0%	0.0%	0.1%	0.0%

Notes:

EL. – Elevation

AREA – Area value

IYY, IYZ, IZZ – Moments of inertia

WARP – Warping constant

TORS – Torsion constant

CGY, CGZ – Y or Z coordinate center of gravity

SHCY, SHCZ – Y or Z coordinate shear center

SCYY, SCYZ, SCZZ – Shear correction factors

Table F.7 – Absolute Differences between Cross-Section Properties of Undeformed and Deformed Standard-Plus Model

EL. (ft)	Area ($\times 10^3$ in. ²)	IYY ($\times 10^9$ in. ⁴)	IYZ ($\times 10^9$ in. ⁴)	IZZ ($\times 10^9$ in. ⁴)	WARP ($\times 10^{15}$ in. ⁶)	TORS ($\times 10^9$ in. ⁹)
108.8	-	-	0.0	-	0.0	-
86.3	-	-	0.0	-	0.0	-
61.3	-	-	0.0	-	0.0	-
35.4	-	-	-	-	-	-
12.8	-	-	-	-	-	-
-1.5	-	-	-	-	-	-
-15.1	-	-	-	-	-	-
-30	-	-	-	-	-	-

EL. (ft)	CGY (in.)	CGZ (in.)	SHCY (in.)	SHCZ (in.)	SCYY	SCYZ	SCZZ
108.8	-0.1	0.3	-0.1	0.3	-	0.0	-
86.3	-0.2	0.3	-0.2	0.3	-	0.0	-
61.3	-0.2	0.3	-0.2	0.3	-	0.0	-
35.4	-	-	-	-	-	-	-
12.8	-	-	-	-	-	0.0	-
-1.5	-	-	-	-	-	-	-
-15.1	-	-	-	-	-	-	-
-30	-	-	-	-	-	-	-

Notes:

EL. – Elevation

AREA – Area value

IYY, IYZ, IZZ – Moments of inertia

WARP – Warping constant

TORS – Torsion constant

CGY, CGZ – Y or Z coordinate center of gravity

SHCY, SHCZ – Y or Z coordinate shear center

SCYY, SCYZ, SCZZ – Shear correction factors

F10. FIGURES

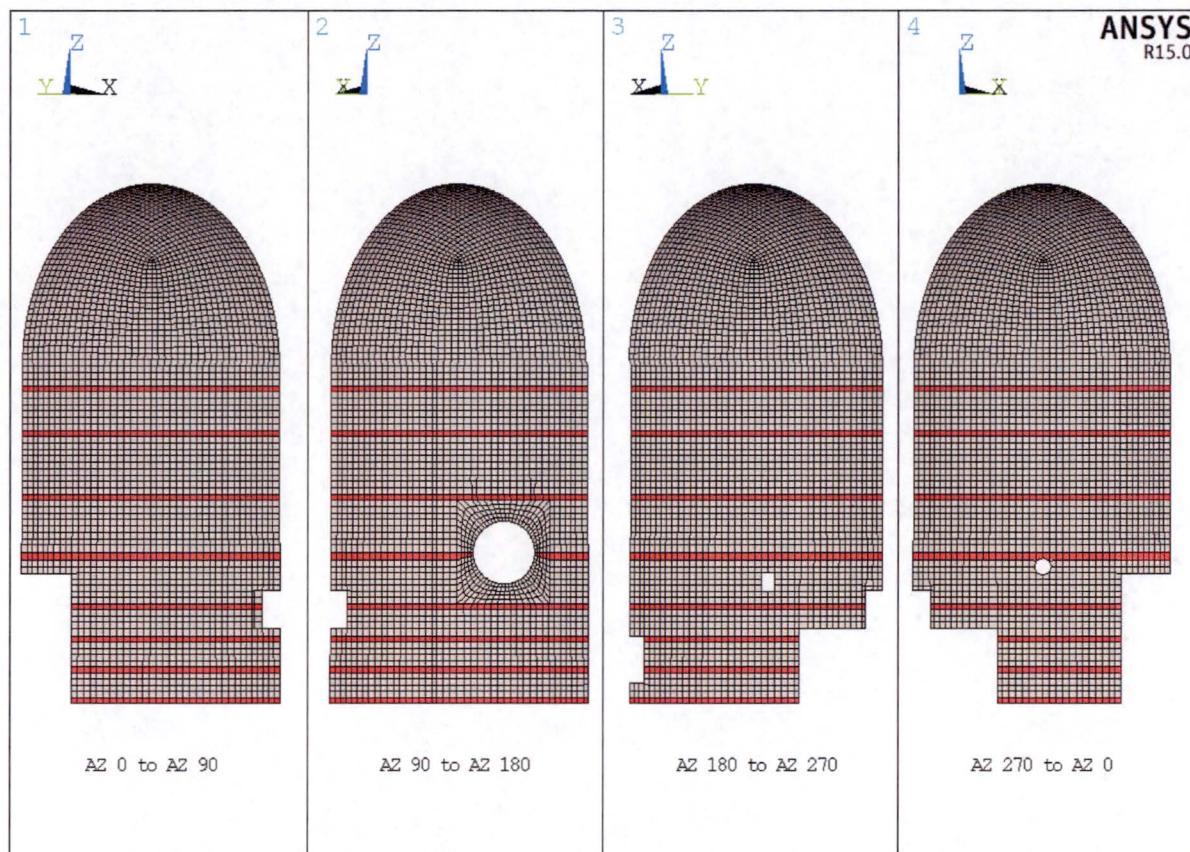
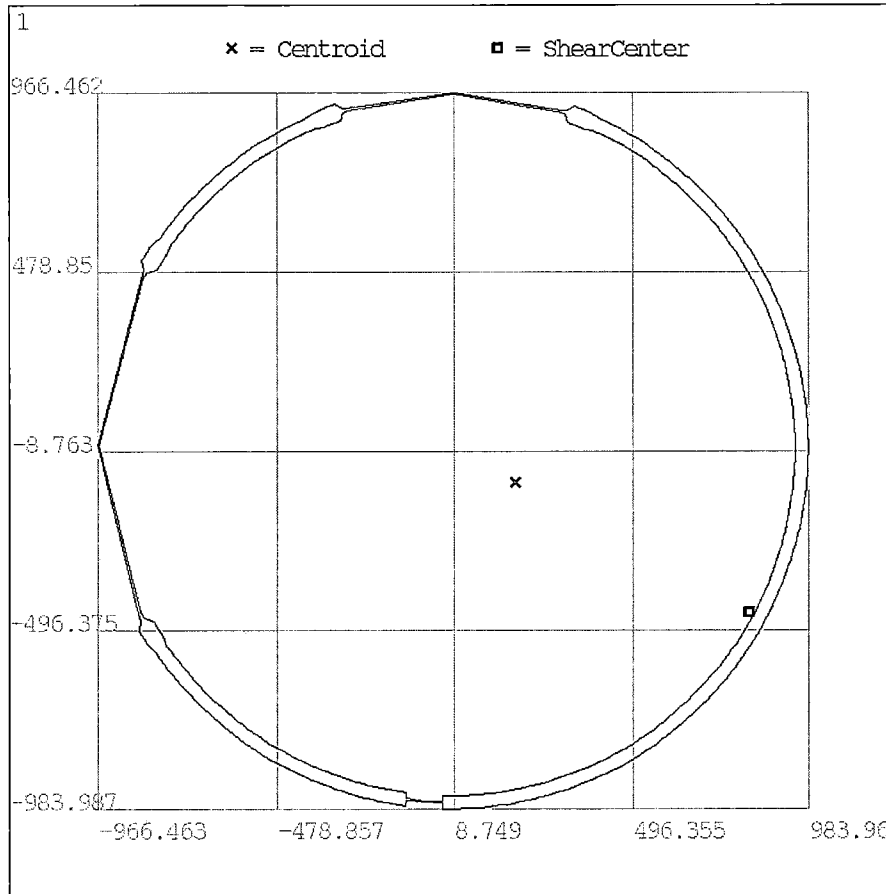


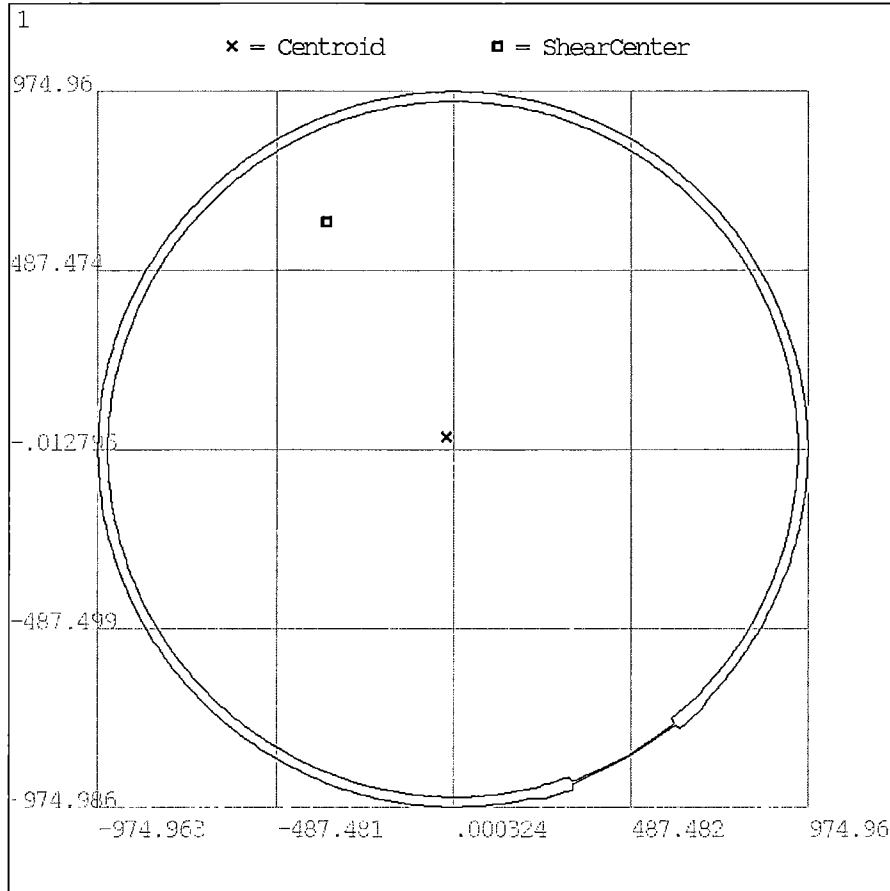
Figure F.1 – Elevations where Cross-Section Properties Are Computed



SECTION ID 2
DATA SUMMARY

Section Name
= n015d1
Area
= 164050
Iyy
= .776E+11
Iyz
= .256E+10
Izz
= .688E+11
Warping Constant
= .624E+16
Torsion Constant
= .460E+11
Centroid Y
= 180.037
Centroid Z
= -93.5753
Shear Center Y
= 819.787
Shear Center Z
= -447.898
Shear Corr. YY
= .18588
Shear Corr. YZ
= .05896
Shear Corr. ZZ
= .235502

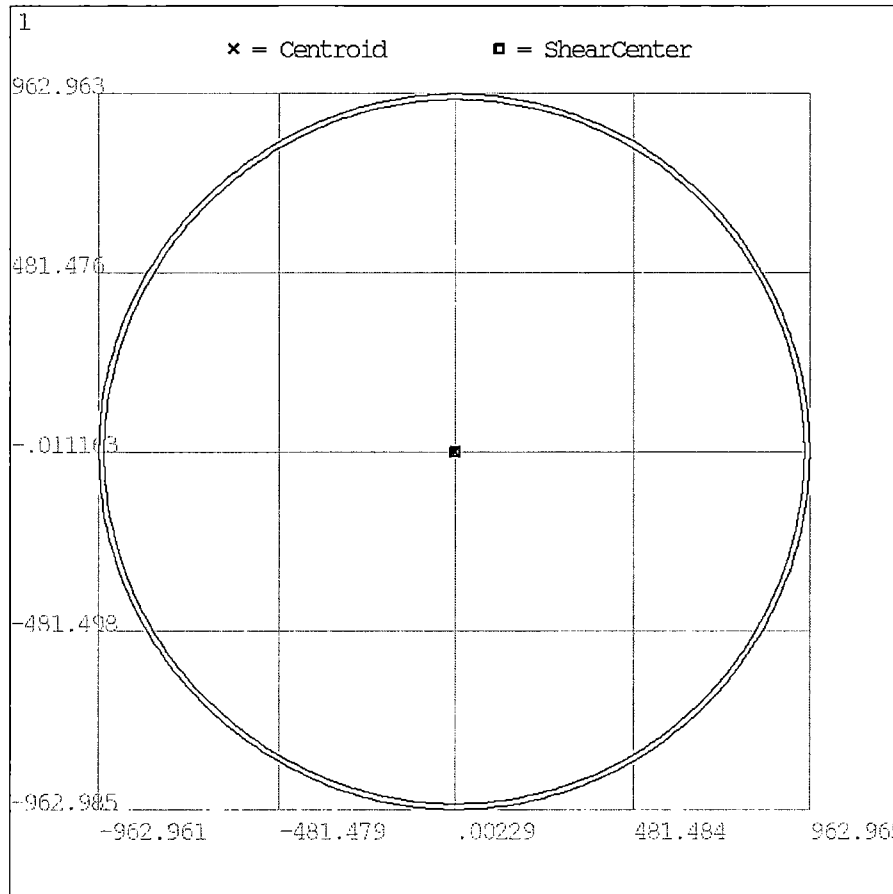
Figure F.2 – Cross-Section Properties (in. based units) of Undeformed CEB at EL = (-)15.1 ft



SECTION ID 5
DATA SUMMARY

Section Name
= p035d4
Area
= 156713
I_{yy}
= .708E+11
I_{yz}
= .261E+10
I_{zz}
= .739E+11
Warping Constant
= .177E+17
Torsion Constant
= .949E+11
Centroid Y
= -19.2296
Centroid Z
= 33.9943
Shear Center Y
= -349.578
Shear Center Z
= 617.961
Shear Corr. YY
= .352965
Shear Corr. YZ
= -.093887
Shear Corr. ZZ
= .465828

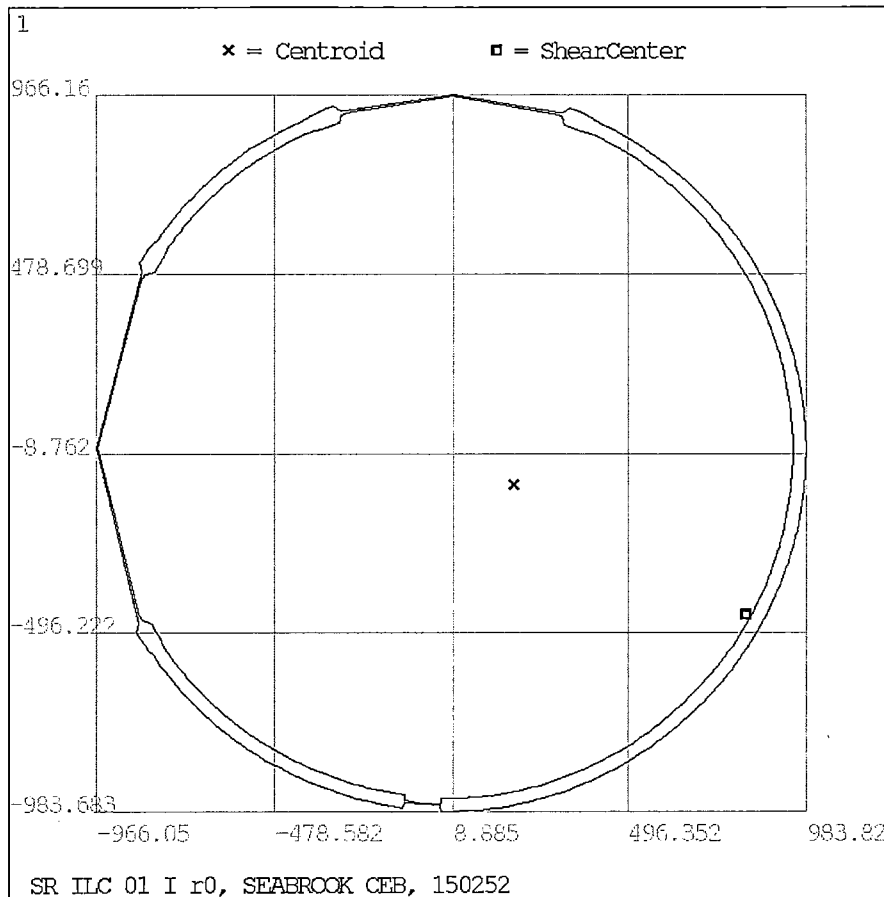
Figure F.3 – Cross-Section Properties (in. based units) of Undeformed CEB at EL = 35.4 ft



SECTION ID 8
DATA SUMMARY

Section Name
= p108d8
Area
= 90053.8
Iyy
= .411E+11
Iyz
= -7017.86
Izz
= .411E+11
Warping Constant
= 9497.03
Torsion Constant
= .822E+11
Centroid Y
= .406E-03
Centroid Z
= -.622E-03
Shear Center Y
= .406E-03
Shear Center Z
= -.620E-03
Shear Corr. YY
= .500051
Shear Corr. YZ
= -.856E-07
Shear Corr. ZZ
= .500051

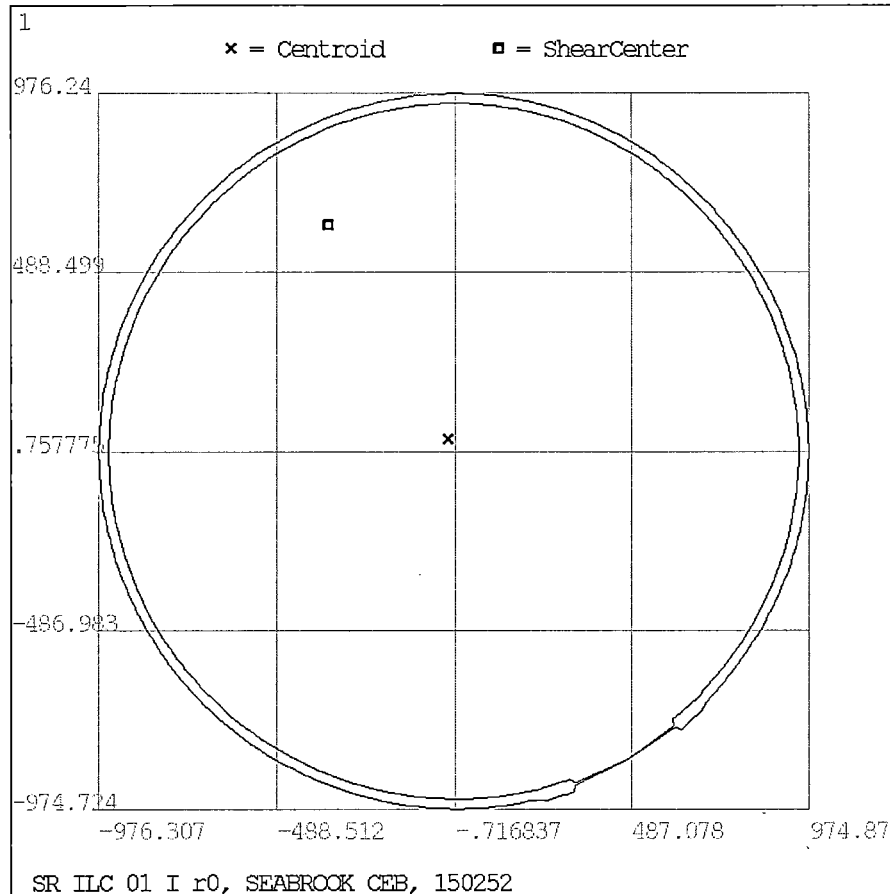
Figure F.4 – Cross-Section Properties (in. based units) of Undeformed CEB at EL = 108.8 ft



SECTION ID 2
DATA SUMMARY

Section Name
= n015dl
Area
= 164056
I_{yy}
= .775E+11
I_{yz}
= .256E+10
I_{zz}
= .688E+11
Warping Constant
= .624E+16
Torsion Constant
= .460E+11
Centroid Y
= 179.908
Centroid Z
= -93.4436
Shear Center Y
= 819.743
Shear Center Z
= -447.691
Shear Corr. YY
= .185936
Shear Corr. YZ
= .058851
Shear Corr. ZZ
= .235512

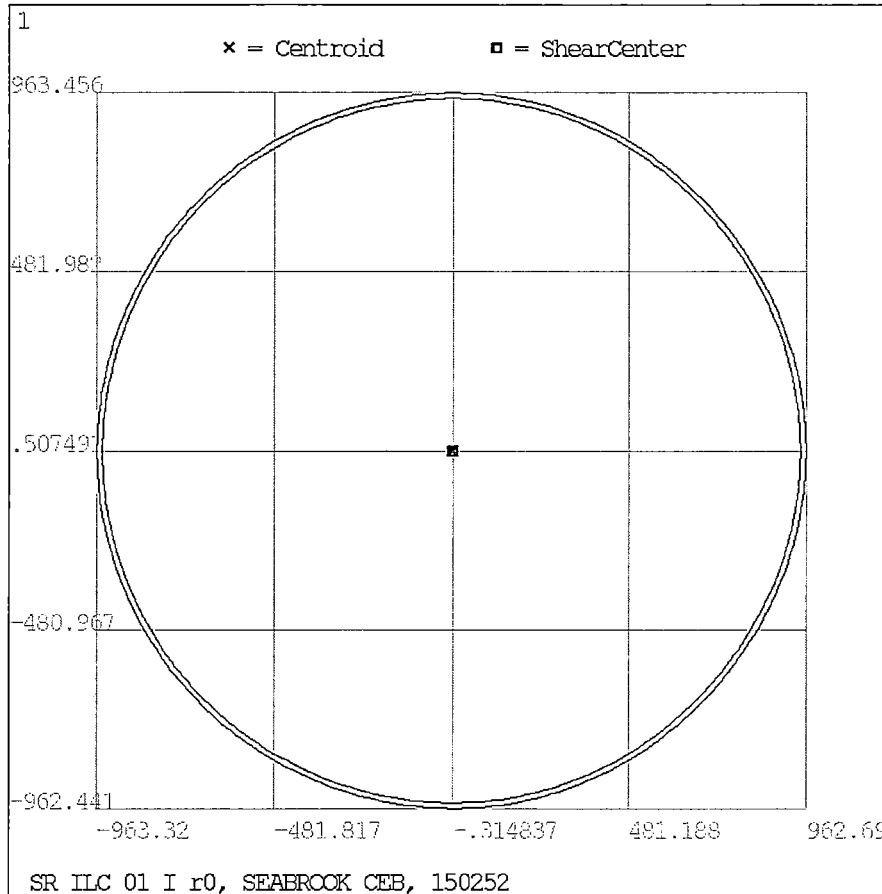
**Figure F.5 – Cross-Section Properties (in. based units) of Deformed CEB
from Standard Analysis Case at EL = (-)15.1 ft**



**SECTION ID 5
DATA SUMMARY**

Section Name
= p035d4
Area
= 156697
I_{yy}
= .708E+11
I_{yz}
= .260E+10
I_{zz}
= .739E+11
Warping Constant
= .177E+17
Torsion Constant
= .949E+11
Centroid Y
= -19.4305
Centroid Z
= 34.3604
Shear Center Y
= -349.834
Shear Center Z
= 618.215
Shear Corr. YY
= .35306
Shear Corr. YZ
= -.093971
Shear Corr. ZZ
= .465744

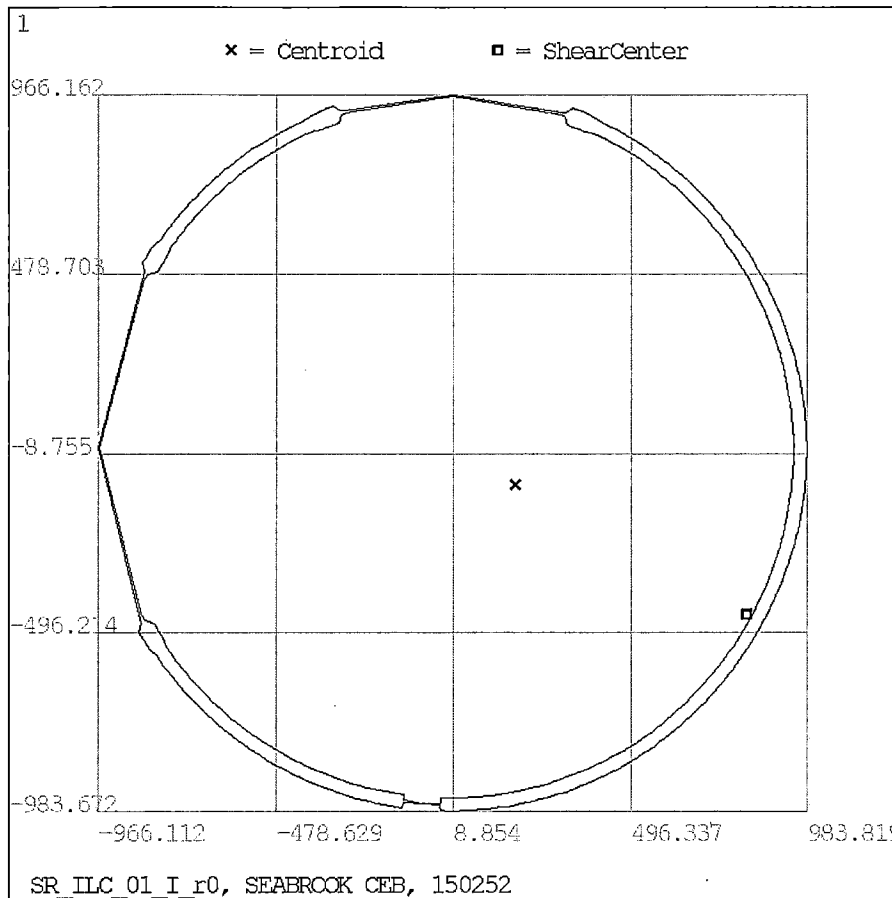
**Figure F.6 – Cross-Section Properties (in. based units) of Deformed CEB
from Standard Analysis Case at EL = 35.4 ft**



SECTION ID 8
DATA SUMMARY

Section Name
= p108d8
Area
= 90033
Iyy
= .411E+11
Iyz
= -.394E+07
Izz
= .411E+11
Warping Constant
= .563E+09
Torsion Constant
= .822E+11
Centroid Y
= -.123875
Centroid Z
= .355523
Shear Center Y
= -.123025
Shear Center Z
= .355103
Shear Corr. YY
= .500097
Shear Corr. YZ
= -.478E-04
Shear Corr. ZZ
= .500005

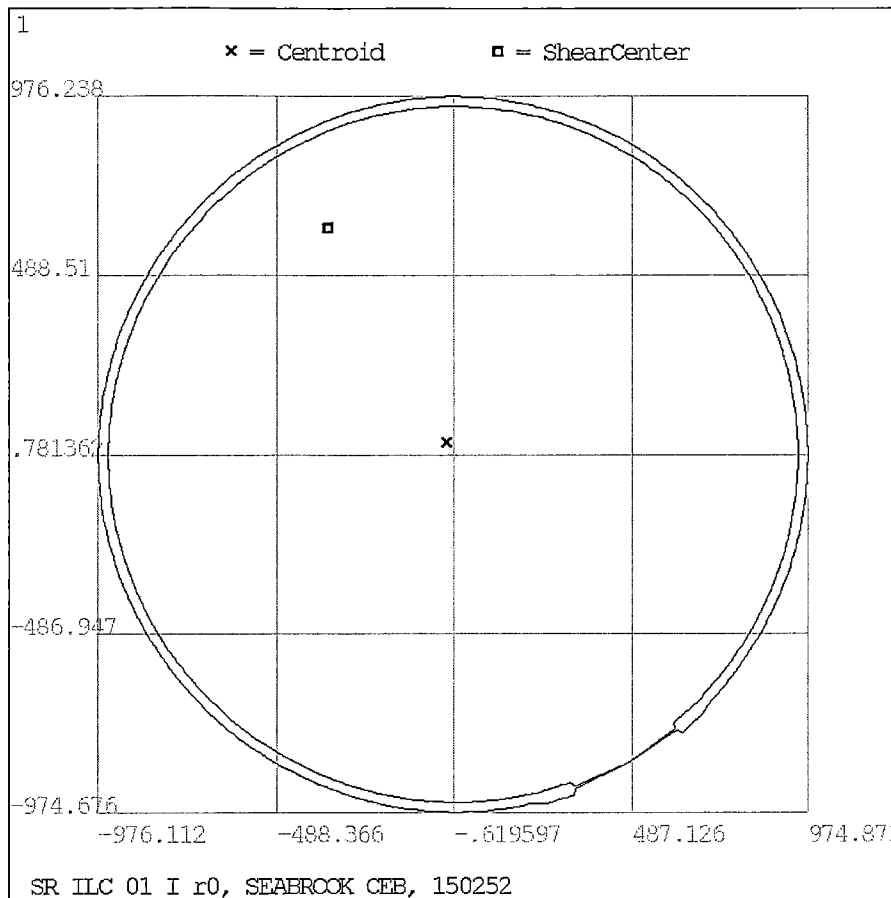
**Figure F.7 – Cross-Section Properties (in. based units) of Deformed CEB
from Standard Analysis Case at EL = 108.8 ft**



SECTION ID 2
DATA SUMMARY

Section Name
= n015d1
Area
= 164057
I_{yy}
= .775E+11
I_{yz}
= .257E+10
I_{zz}
= .688E+11
Warping Constant
= .624E+16
Torsion Constant
= .460E+11
Centroid Y
= 179.884
Centroid Z
= -93.4701
Shear Center Y
= 819.729
Shear Center Z
= -447.643
Shear Corr. YY
= .185938
Shear Corr. YZ
= .058859
Shear Corr. ZZ
= .235499

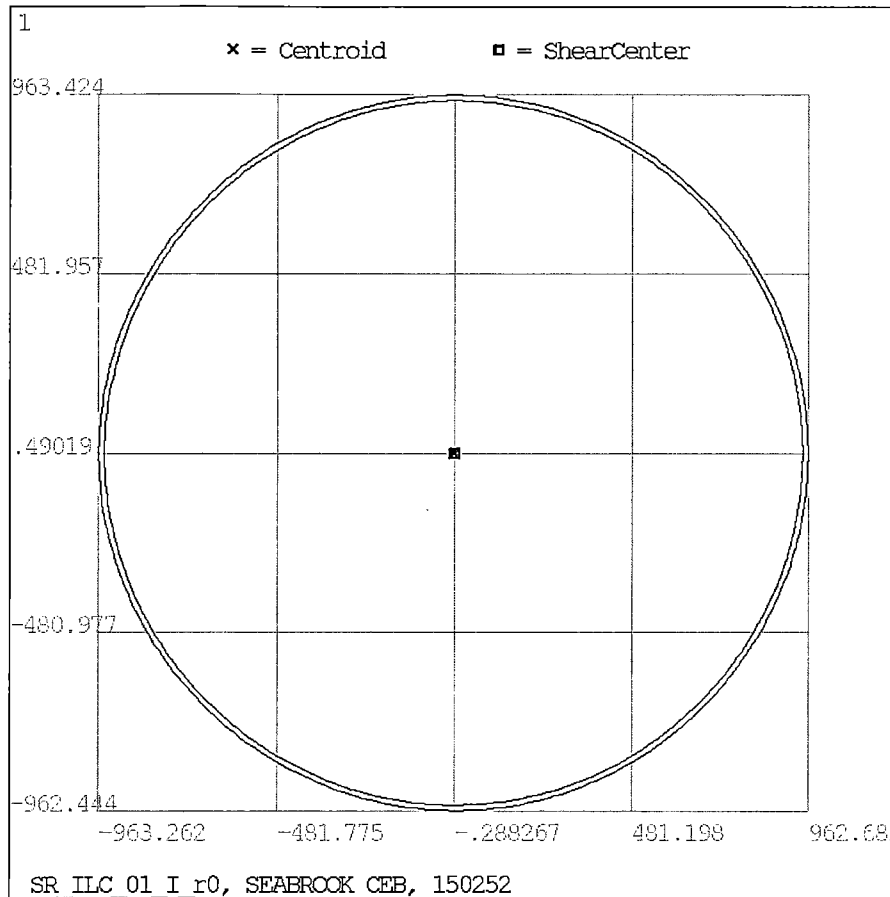
**Figure F.8 – Cross-Section Properties (in.-based units) of Deformed CEB
from Standard-Plus Analysis Case at EL = (-)15.1 ft**



SECTION ID 5
DATA SUMMARY

Section Name
= p035d4
Area
= 156696
I_{yy}
= .708E+11
I_{yz}
= .261E+10
I_{zz}
= .739E+11
Warping Constant
= .177E+17
Torsion Constant
= .949E+11
Centroid Y
= -19.4352
Centroid Z
= 34.3038
Shear Center Y
= -349.779
Shear Center Z
= 618.154
Shear Corr. YY
= .353034
Shear Corr. YZ
= -.09391
Shear Corr. ZZ
= .465745

**Figure F.9 – Cross-Section Properties (in. based units) of Deformed CEB
from Standard-Plus Analysis Case at EL = 35.4 ft**



SECTION ID 8
DATA SUMMARY

Section Name
= p108d8
Area
= 90033
I_{yy}
= .411E+11
I_{yz}
= -.113E+07
I_{zz}
= .411E+11
Warping Constant
= .532E+09
Torsion Constant
= .822E+11
Centroid Y
= -.135442
Centroid Z
= .293127
Shear Center Y
= -.13469
Shear Center Z
= .292801
Shear Corr. YY
= .500092
Shear Corr. YZ
= -.136E-04
Shear Corr. ZZ
= .500009

**Figure F.10 – Cross-Section Properties (in. based units) of Deformed CEB
from Standard-Plus Analysis Case at EL = 108.8 ft**

**Appendix G****Evaluation Results for Load Combinations for Original Design Analysis Case without As-Deformed Condition Demands****G1. REVISION HISTORY****Revision 0:**

Initial document.

G2. OVERVIEW

This appendix contains evaluation results for the Original Design Analysis Case. The Original Design Analysis Case is performed with all loads defined in the original SD-66 structural criteria document, but does not include any self-straining loads (i.e., S_a and S_w in the load combinations in Table 5 in the main body of this calculation are zero). The contour plots presented in this appendix contain enveloped demand-to-capacity ratios (DCRs) for static and OBE combinations, as those are the combinations that generally control the design of the CEB.

The Original Design Analysis Case represents the original design requirements for the structure and are evaluated to demonstrate that the FEA model developed in this calculation gives reasonable evaluation results for the condition without self-straining loads.

G3. METHODOLOGY

The methodology for structural analysis is documented in Section 6 of the main body of this calculation. Evaluation methodology is documented in Section 7 of the main body of this calculation. Self-straining loads (i.e., ASR and concrete swelling) are excluded in this analysis case, and design loads are applied to the as-designed CEB instead of the as-deformed condition of the CEB.

**G4. RESULTS AND CONCLUSIONS**

The evaluation indicates that the CEB meets ACI 318-71 evaluation criteria for the Original Design Analysis Case.

Contour plots showing the results of the element-by-element evaluation for OBE and Static combinations are shown in Figures G1 through G14. In these enveloped contour plots, each element is colored based on its maximum DCR for all combinations of the given type (OBE or static). Therefore, the enveloped contour plots may show multiple areas of high DCR, but these areas with elevated demand may actually occur in different load combinations.

The evaluation of the Original Design Analysis Case is summarized in the list below.

- **Axial compression in the hoop direction.**

Enveloped contour plots of DCRs from the element-by-element evaluation results are shown in Figures G1 and G2 for the OBE and static combinations, respectively. No capacity exceedances are identified.

- **Axial compression in the meridional direction.**

Enveloped contour plots of DCRs from the element-by-element evaluation results are shown in Figures G3 and G4 for the OBE and static combinations, respectively. No capacity exceedances are identified.

- **In-plane shear.**

Enveloped contour plots of DCRs from the element-by-element evaluation results are shown in Figures G5 and G6 for the OBE and static combinations, respectively. No capacity exceedances are identified in the static combinations. In the OBE combinations, some minor in-plane shear capacity exceedances are identified at the reentrant corners of the Electrical and Mechanical Penetrations. These capacity exceedances are minor and localized, and are judged to be acceptable if consideration is given to local distribution of demands within the wall. Additionally, #8@6" diagonal reinforcement is provided at the reentrant corners of the large penetrations, which are not considered in the evaluation but would be effective at resisting these in-plane shear demands.



- **Out-of-plane shear.**

Enveloped contour plots of DCRs from the element-by-element evaluation results are shown in Figures G7 through G10 for the OBE and static combinations. No capacity exceedances are identified in the static combinations. In the OBE combinations, some minor out-of-plane shear capacity exceedances are identified at the reentrant corners of the Electrical and Mechanical Penetrations. These capacity exceedances are minor and localized, and are judged to be acceptable if consideration is given to local distribution of demands within the wall. Additionally, #6@6" transverse reinforcement are provided at the edges of the pilasters, which are not considered in the evaluation but would be effective at resisting these out-of-plane shear demands.

- **Axial-flexure interaction in the hoop direction.**

Enveloped contour plots of DCRs from the element-by-element evaluation results are shown in Figures G11 and G12 for the OBE and static combinations, respectively. The element-by-element evaluation identifies localized capacity exceedances for axial-flexure (PM) interaction on either side of the West Pipe Chase and near the reentrant corners of the West Pipe Chase. The exceedances are more severe in OBE combinations than static combinations. Section cut evaluation (Section Cut 19) is performed in the area to the south of the West Pipe Chase where the element-by-element evaluation identifies the most-severe capacity exceedances. The section cut evaluation shows that PM interaction does not exceed capacity (Figure G15). The location and properties of Section Cut 19 can be seen in Appendix N.

- **Axial-flexure interaction in the meridional direction.**

Enveloped contour plots of DCRs from the element-by-element evaluation results are shown in Figures G13 and G14 for the OBE and static combinations, respectively. No capacity exceedances are identified in the static combinations. The element-by-element evaluation of OBE combinations identifies localized capacity exceedances for axial-flexure (PM) interaction in the meridional direction on the pilasters on either side of the Electrical Penetration. Section cut evaluations (Section Cuts 8 and 11) are performed for the two pilasters. The section cut evaluations show that PM interaction does not exceed capacity (Figures G16 and G17). The location and properties of Section Cuts 8 and 11 can be seen in Appendix N.

G5. FIGURES

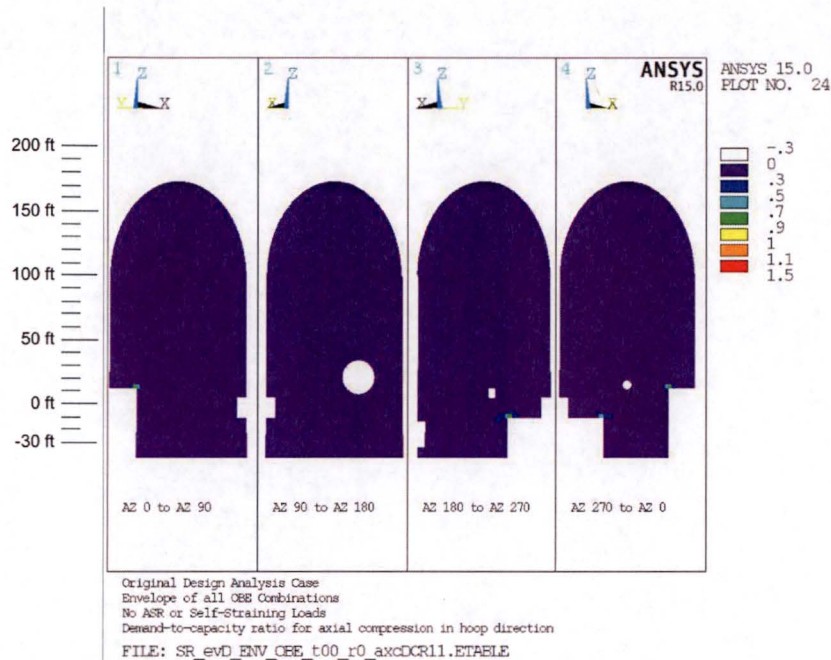


Figure G1 – DCR for Axial Compression in the Hoop Direction, Original Design Analysis Case, Envelope of All OBE Combinations

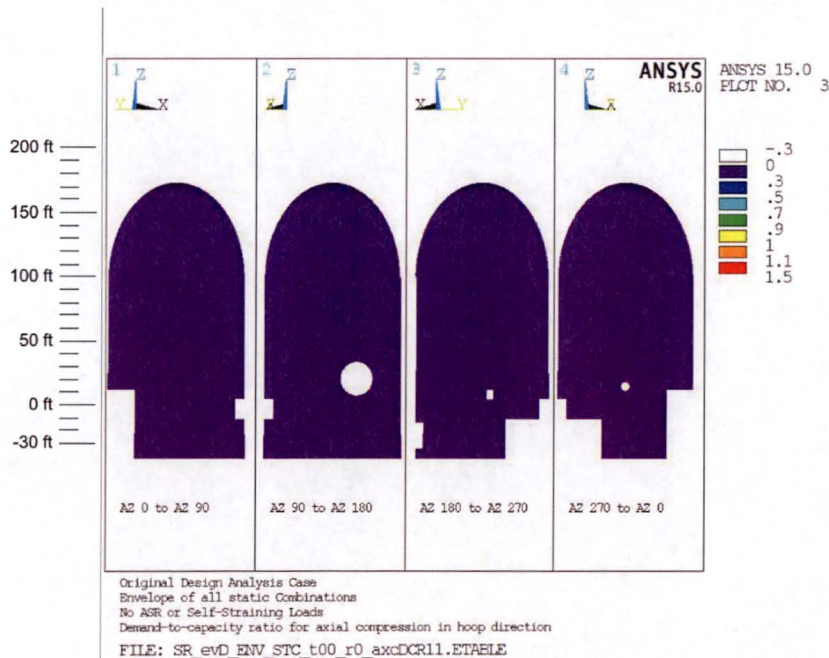


Figure G2 – DCR for Axial Compression in the Hoop Direction, Original Design Analysis Case, Envelope of All Static Combinations

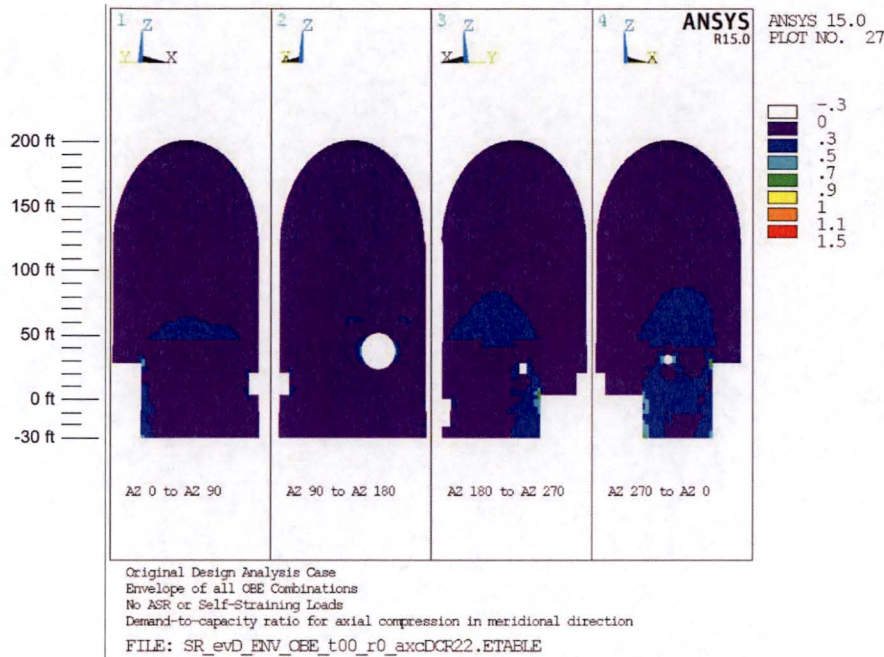


Figure G3 – DCR for Axial Compression in the Meridional Direction, Original Design Analysis Case, Envelope of All OBE Combinations

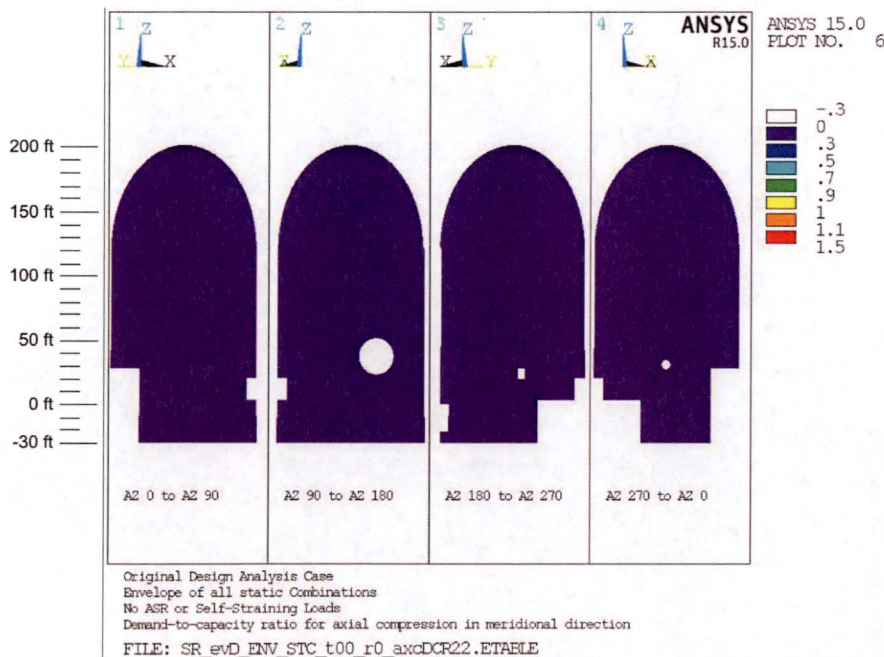
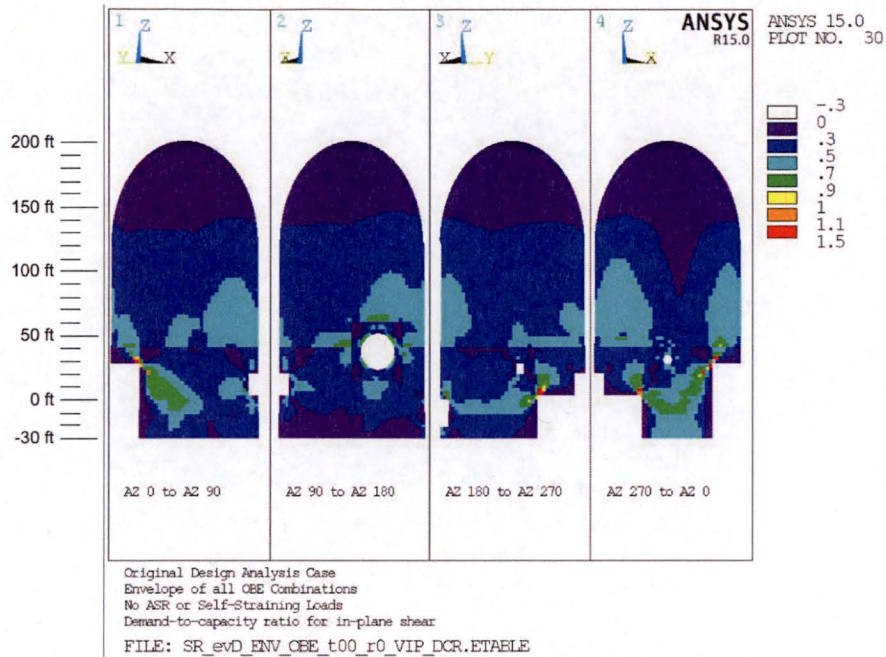
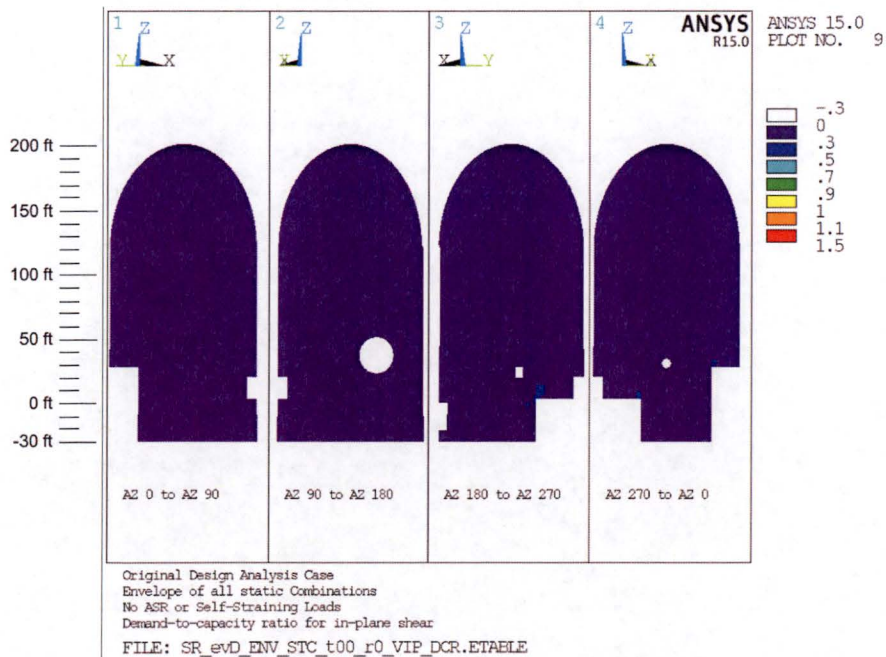


Figure G4 – DCR for Axial Compression in the Meridional Direction, Original Design Analysis Case, Envelope of All Static Combinations



**Figure G5 – DCR for In-Plane Shear,
Original Design Analysis Case, Envelope of All OBE Combinations**



**Figure G6 – DCR for In-Plane Shear,
Original Design Analysis Case, Envelope of All Static Combinations**

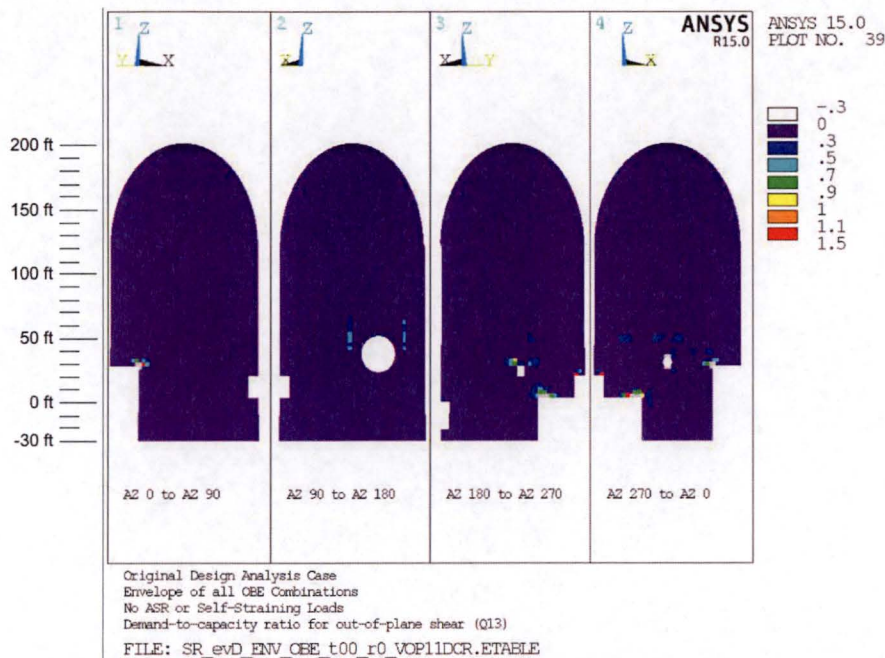


Figure G7 – DCR for Out-of-Plane Shear Acting on the Meridional-Radial Plane, Original Design Analysis Case, Envelope of All OBE Combinations

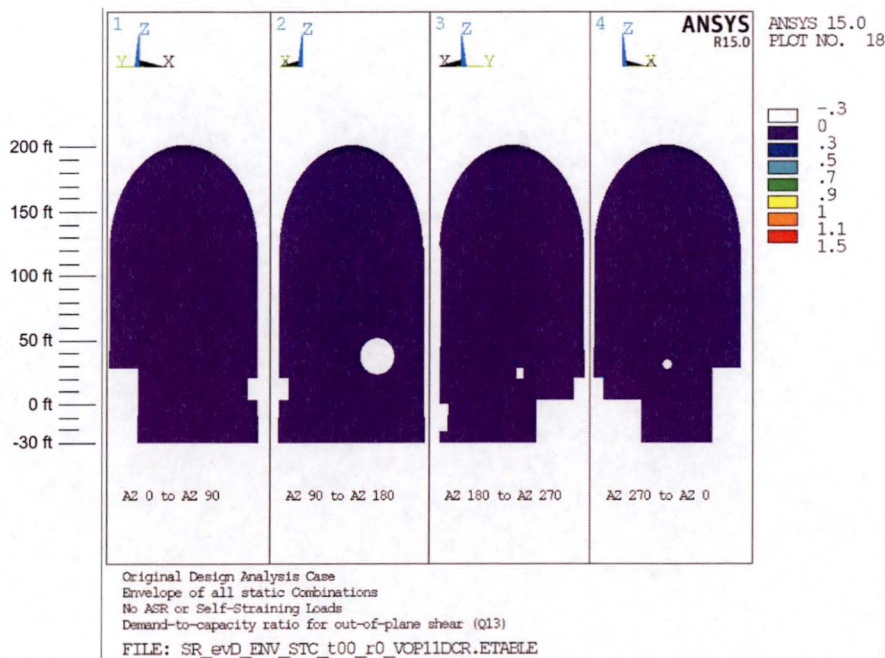


Figure G8 – DCR for Out-of-Plane Shear Acting on the Meridional-Radial Plane, Original Design Analysis Case, Envelope of All Static Combinations

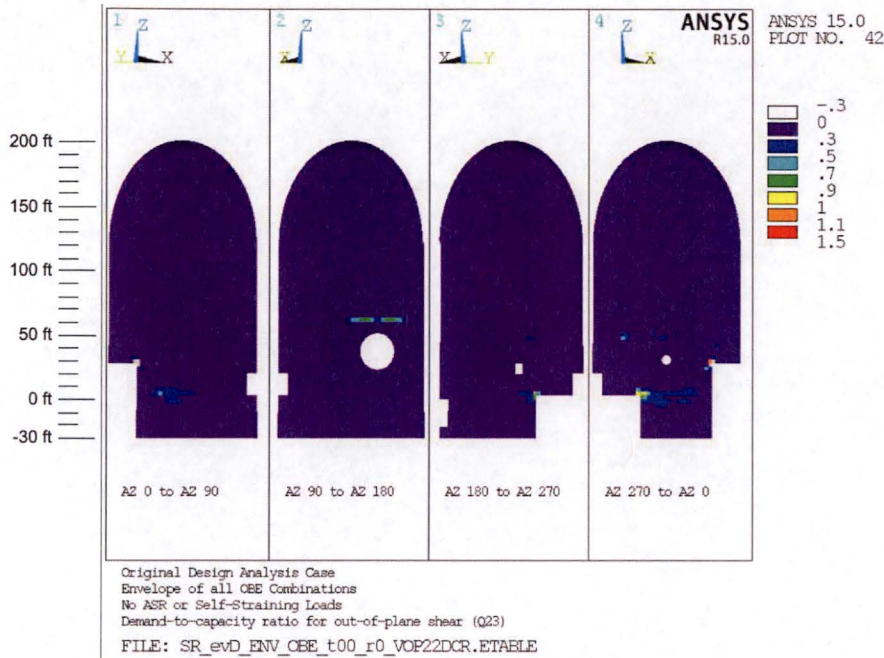


Figure G9 – DCR for Out-of-Plane Shear Acting on the Hoop-Radial Plane, Original Design Analysis Case, Envelope of All OBE Combinations

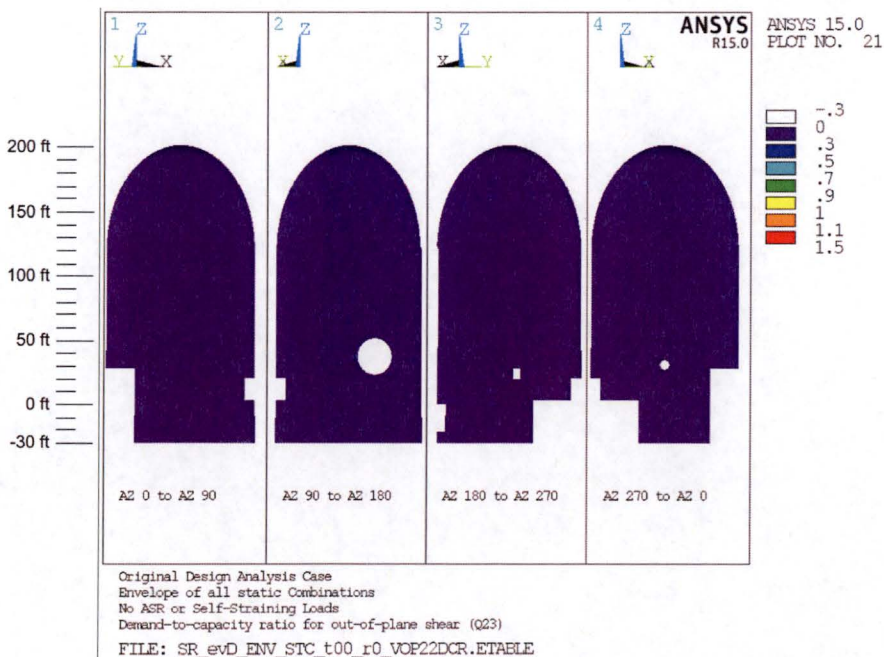


Figure G10 – DCR for Out-of-Plane Shear Acting on the Hoop-Radial Plane, Original Design Analysis Case, Envelope of All Static Combinations

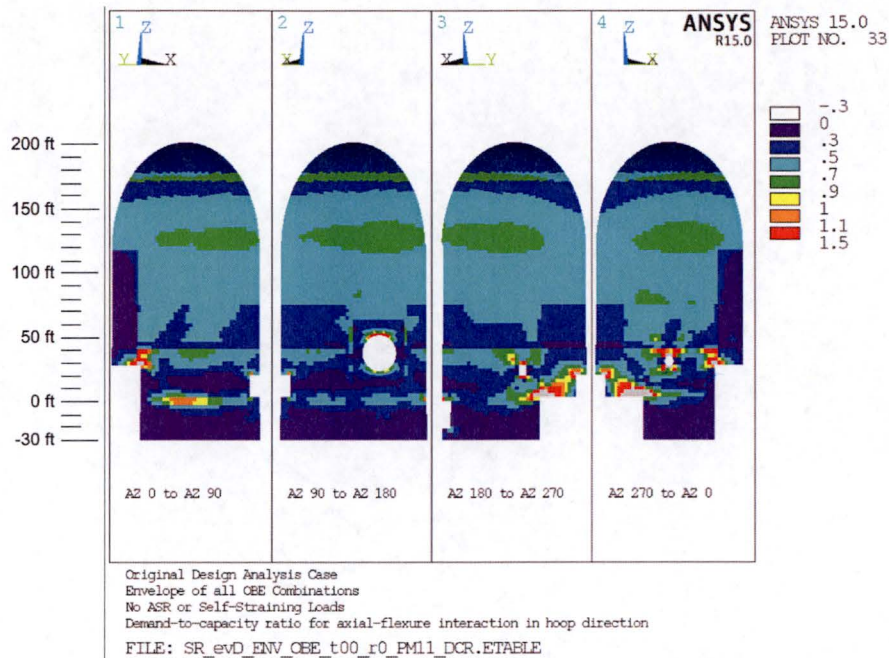


Figure G11 – DCR for Axial-Flexure Interaction in the Hoop Direction, Original Design Analysis Case, Envelope of All OBE Combinations

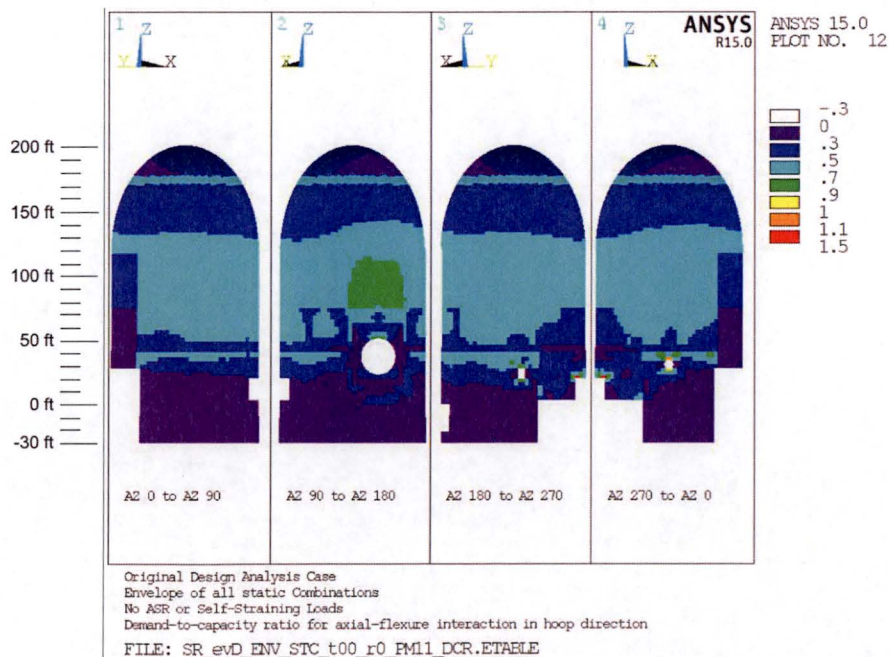


Figure G12 – DCR for Axial-Flexure Interaction in the Hoop Direction, Original Design Analysis Case, Envelope of All Static Combinations

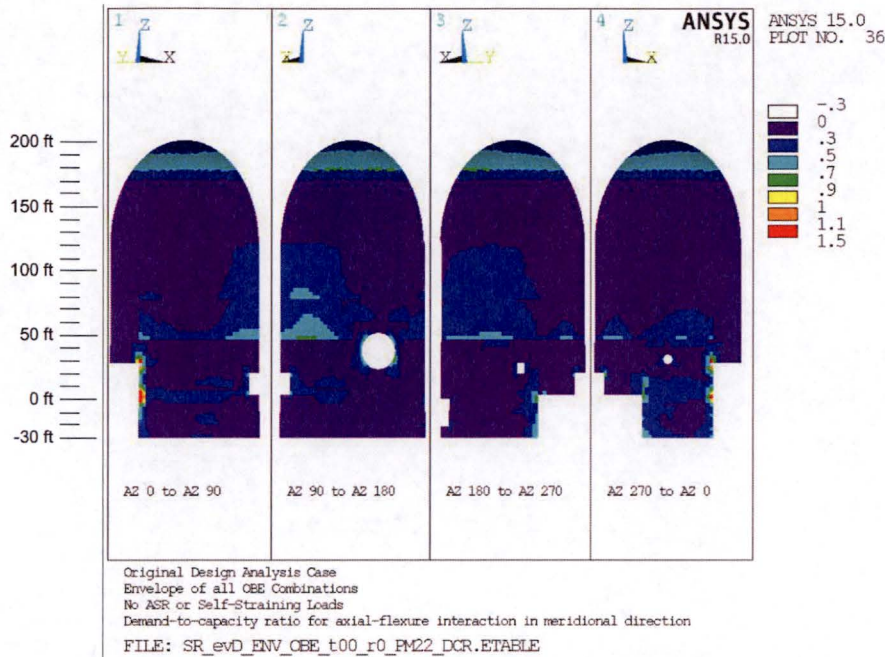


Figure G13 – DCR for Axial-Flexure Interaction in the Meridional Direction, Original Design Analysis Case, Envelope of All OBE Combinations

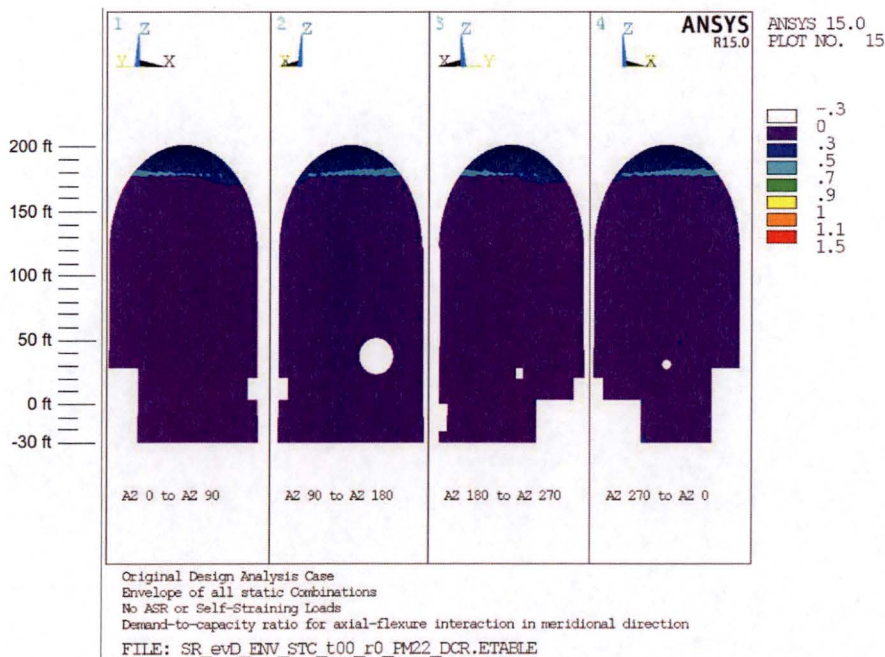
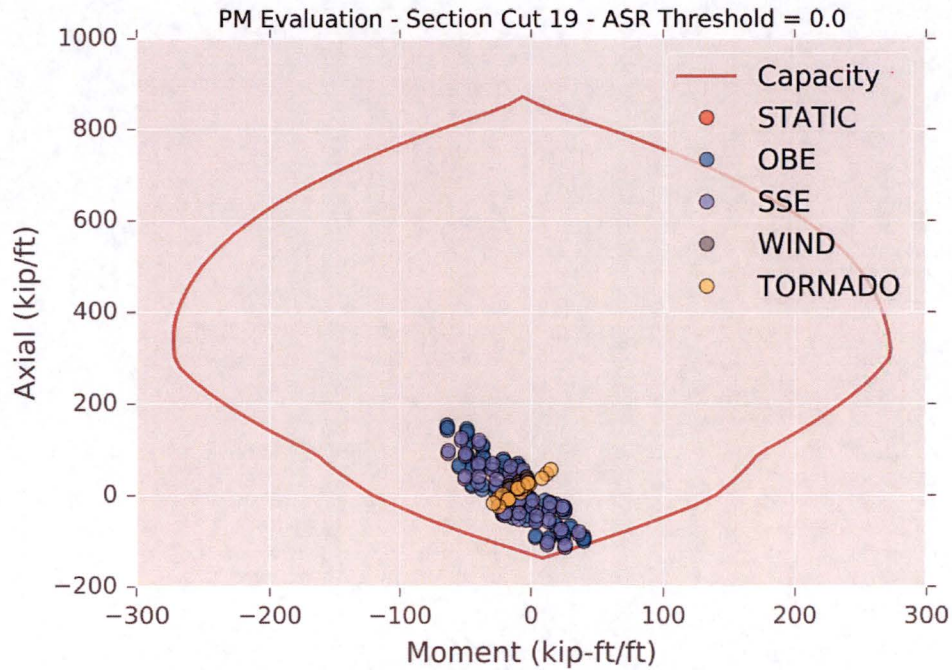
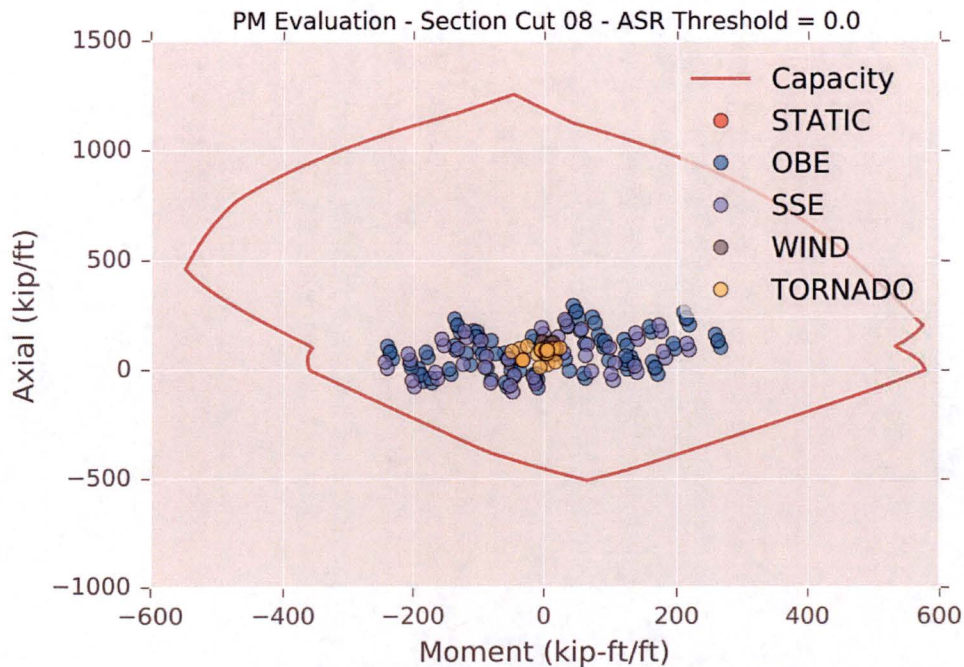


Figure G14 – DCR for Axial-Flexure Interaction in the Meridional Direction, Original Design Analysis Case, Envelope of All Static Combinations



**Figure G15 – Axial-Flexure Interaction for Section Cut 19,
Original Design Analysis Case**



**Figure G16 – Axial-Flexure Interaction for Section Cut 8,
Original Design Analysis Case**

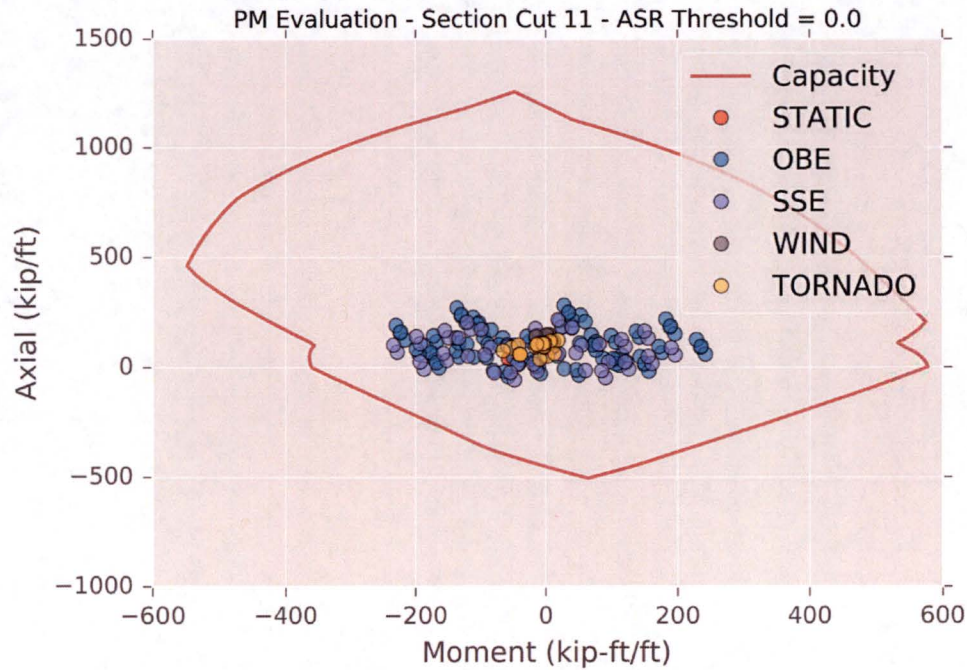


**Figure G17 – Axial-Flexure Interaction for Section Cut 11,
Original Design Analysis Case**



Appendix H Documentation of Moment Redistribution

H1. REVISION HISTORY

H1.1 Revisions 0

Initial Document

H2. OVERVIEW

In this appendix, the moment redistribution analyses performed on the CEB are documented. Moment redistribution is used to redistribute the moment in excess of axial-flexure (PM) interaction capacity to adjacent portions of the CEB. Moment redistribution is performed for the analysis cases and load combinations listed below.

- Static load combination NO_1 for the Standard Analysis Case
- Static load combination NO_1 for the Standard-Plus Analysis Case
- OBE load combination OBE_4 with excitation in the 100% West, 40% North, and 40% Vertical Down direction for the Standard-Plus Analysis Case

For both the Standard and Standard-Plus Analysis Cases, the static load combination NO_1 (as defined in Table 5 of the main body) generally controls PM interaction demands due to the large load factor on ASR demands. The OBE_4 combination with 100% excitation in the west direction, 40% excitation in the north direction, and 40% excitation in the vertical down direction generally controls for PM interaction among OBE combinations; however, there are many other OBE load combinations with similar demands due to the large number of OBE load combinations (consisting of different 100-40-40 directional orientations) evaluated.

The moment redistribution uses the approach defined and validated in Appendix L of this calculation. The moment redistribution procedure utilizes the linear elastic model to simulate the redistribution of moments that would occur when localized flexural plasticity occurs. The goal of the moment redistribution analyses is to reduce flexural demand at each region of exceedance such that it is approximately equivalent to the flexural capacity of the section at the given level of axial demand. An iterative procedure is used to redistribute the moments in the linear elastic model, as



moments redistributed from one region can potentially impact other regions. In some isolated locations, the demand point is slightly outside of the PM capacity curve after moment redistribution is completed; these occasions are deemed acceptable if the residual exceedance is small.

During moment redistributions, the connection between the wall and foundation (which typically is a fully-fixed connection capable of transferring moment, shear, and vertical forces) is modified when redistributing excess moment to a pinned connection capable of transferring shear and vertical forces only. This modification is made to prevent moment redistributions performed at the pilasters to transmit additional bending moments directly to the base of the wall, which is generally also near or beyond its own PM interaction capacity in such cases. Moment redistributions performed at the base of the wall are applied to the nodes at the base of the wall, rather than the elements, due to the nearby edge of the wall.

The ductility demand for areas where moment redistribution is performed is evaluated in Appendix O. This appendix shows that the maximum ductility (ratio of reinforcement strain to yield strain) is 3.5, occurring in Section Cut 22 for the Standard-Plus Analysis Case for static combination NO_1. All other section cuts have a maximum ductility of 2.5 or less.

H3. SECTION CUTS FOR EVALUATION OF PM INTERACTION

Section cut evaluations are performed at the locations identified in Appendix N. Section cuts 1, 2, 3, and 4 are long cuts that are located on the base of the CEB wall. These cuts are primarily intended for evaluation of in-plane and out-of-plane shear demands and are subdivided into smaller segments of length equal to about 8 wall thicknesses for evaluation of PM interaction. Section cut 7 is an 80 ft long cut between the Electrical and Mechanical Penetrations near El. +15 ft; this section cut is also used to evaluate shear demands and is not used to evaluate PM interaction.

Section Cuts 28, 29 and 30 are not evaluated in the Standard Analysis Case, but were added for evaluation of the Standard-Plus Analysis Case because potentially high demands in these areas are indicated by the element-by-element evaluations of the Standard-Plus case.



H4. MOMENT REDISTRIBUTION FOR STATIC COMBINATION OF THE STANDARD ANALYSIS CASE

Contour plots of DCRs for PM interaction for the hoop and meridional directions for the Static NO_1 load combination of the Standard Analysis Case are shown in Figures H1 and H2. Moment redistribution analyses are performed in the regions of exceedance identified in these figures. Other regions of exceedance, as indicated in these figures, are evaluated and shown to meet evaluation criteria using section cuts and do not require moment redistribution.

PM interaction diagrams before and after moment redistribution are provided in Figures H3 through H24 for the section cuts identified in Section H3. These figures show that all PM capacity exceedances are resolved through moment redistribution with the exception of Section Cuts 16 and 17. These cuts have DCR ratios near 1.0, and would be within capacity after a small adjustment to the quantity of moment redistribution applied to the region around the CEVA opening. The impact of such an adjustment is judged to be small, and therefore these PM interaction exceedances are judged to be acceptable.

The impact of the moment redistributions on membrane demands are shown in Figures H25 through H29. Redistribution of bending moments at the base of the wall cause additional hoop and meridional axial compression demands, as well as additional in-plane shear demands. DCRs for hoop compression generally remain below 0.7. The maximum meridional compression demand (evaluated at a section cut equal to 4 wall thicknesses at the north side of the Mechanical Penetration) is 65.4 kip/in, which is significantly smaller than the compressive capacity of $\phi P_n = 96.4$ kip/in computed in Section 7.5.2 of the calculation main body (DCR = 0.68). The element-by-element analysis indicates an increase to in-plane shear demands for the wall segment between the Electrical and Mechanical Penetrations; however the impact to the total in-plane shear demand for this wall segment (computed using a Section Cut 4) is very small (see Section 7.6.1 for a description of how in-plane shear demands are evaluated at the base of the wall). Out-of-plane shear demands acting on the meridional-radial plane are increased above the Personnel Hatch opening; however the out-of-plane shear capacity in this region is computed with significant conservatism because the transverse ties around the missile shield block are not considered in the element-by-element evaluation. Out-of-plane shear demands acting on the hoop-radial plane are increased at the base of the wall between AZ 270 and 360 as well as on the pilasters on either side



of the Electrical Penetration; however the out-of-plane shear DCRs remain below 0.9 in these regions based on the conservative element-by-element evaluation.

H5. MOMENT REDISTRIBUTION FOR STATIC COMBINATION OF THE STANDARD-PLUS ANALYSIS CASE

Contour plots of DCRs for PM interaction for the hoop and meridional directions for the static load combination NO_1 of the Standard-Plus Analysis Case are shown in Figures H30 and H31. Moment redistribution analyses are performed in the regions of exceedance identified in these figures. Other regions of exceedance, as indicated in these figures, are evaluated and shown to meet evaluation criteria using section cuts and do not require moment redistribution.

PM interaction diagrams before and after moment redistribution are provided in Figures H32 through H56 for the section cuts identified in Section H3. These figures show that all PM capacity exceedances are resolved through moment redistribution with the exception of Section Cuts 28, which is evaluated separately in Appendix M.

The impact of the moment redistributions on membrane demands are shown in Figures H57 through H61. Redistribution of bending moments at the base of the wall cause additional hoop and meridional axial compression demands, as well as additional in-plane shear demands. DCRs for hoop compression generally remain below 0.7. The maximum meridional compression demand (evaluated at a section cut equal to 4 wall thicknesses at the south side of the Mechanical Penetration) is 70.9 kip/in, which is significantly smaller than the compressive capacity of $\phi P_n = 96.4$ kip/in computed in Section 7.5.2 of the calculation main body (DCR = 0.74). The element-by-element analysis indicates an increase to in-plane shear demands for the wall segment between the Electrical and Mechanical Penetrations; however the impact to the total in-plane shear demand for this wall segment (computed using Section Cut 4) is very small (see Section 7.6.1 for a description of how in-plane shear demands are evaluated at the base of the wall). Out-of-plane shear demands acting on the meridional-radial plane are increased above the Personnel Hatch opening; however the out-of-plane shear capacity in this region is computed with significant conservatism because the transverse ties around the missile shield block are not considered in the element-by-element evaluation. Out-of-plane shear demands acting on the hoop-radial plane are increased at the base of the wall between AZ 270 and 360 as well as on the pilasters on either side



of the Electrical and Mechanical Penetrations; however the out-of-plane shear DCRs remain below 1.0 in these regions based on the conservative element-by-element evaluation.

H6. MOMENT REDISTRIBUTION FOR OBE COMBINATION OF THE STANDARD ANALYSIS CASE

The static load combination NO_1 (as defined in Table 5 of the calculation main body) generally controls the evaluation for PM interaction due to the large load factor assigned to ASR demands in that combination. Additionally, Sections H4 and H5 show that moment redistribution typically has a small impact on membrane demands. A moment redistribution analysis is performed for a controlling OBE load combination in this section to confirm that the redistribution does not result in a condition that controls over the static combination discussed in Section H5.

Contour plots of DCRs for PM interaction for the hoop and meridional directions for the seismic load combination OBE_4 of the Standard-Plus Analysis Case are shown in Figures H62 and H63. Moment redistribution analyses are performed in the regions of exceedance identified in these figures. Other regions of exceedance, as indicated in these figures, are evaluated and shown to meet evaluation criteria using section cuts and do not require moment redistribution.

PM interaction diagrams before and after moment redistribution are provided in Figures H64 through H85 for the section cuts identified in Section H3. These figures show that all PM capacity exceedances are resolved through moment redistribution.

The impact of the moment redistributions on membrane demands are shown in Figures H86 through H90. These figures show that the moment redistribution has a minor impact to membrane demands. By observation of DCR contour plots, the evaluation of in-plane shear between AZ 180 and 270 is most impacted by the moment redistribution; however, based on section cut evaluation, the DCR for in-plane shear in this region remains low (0.49) after moment redistribution.

H7. CONCLUSIONS

The results presented in this appendix show that the moment redistributions used in this calculation are effective at simulating localized plasticity. The moment redistributions generally have a small impact on other demands (axial and shear demands).

H8. FIGURES

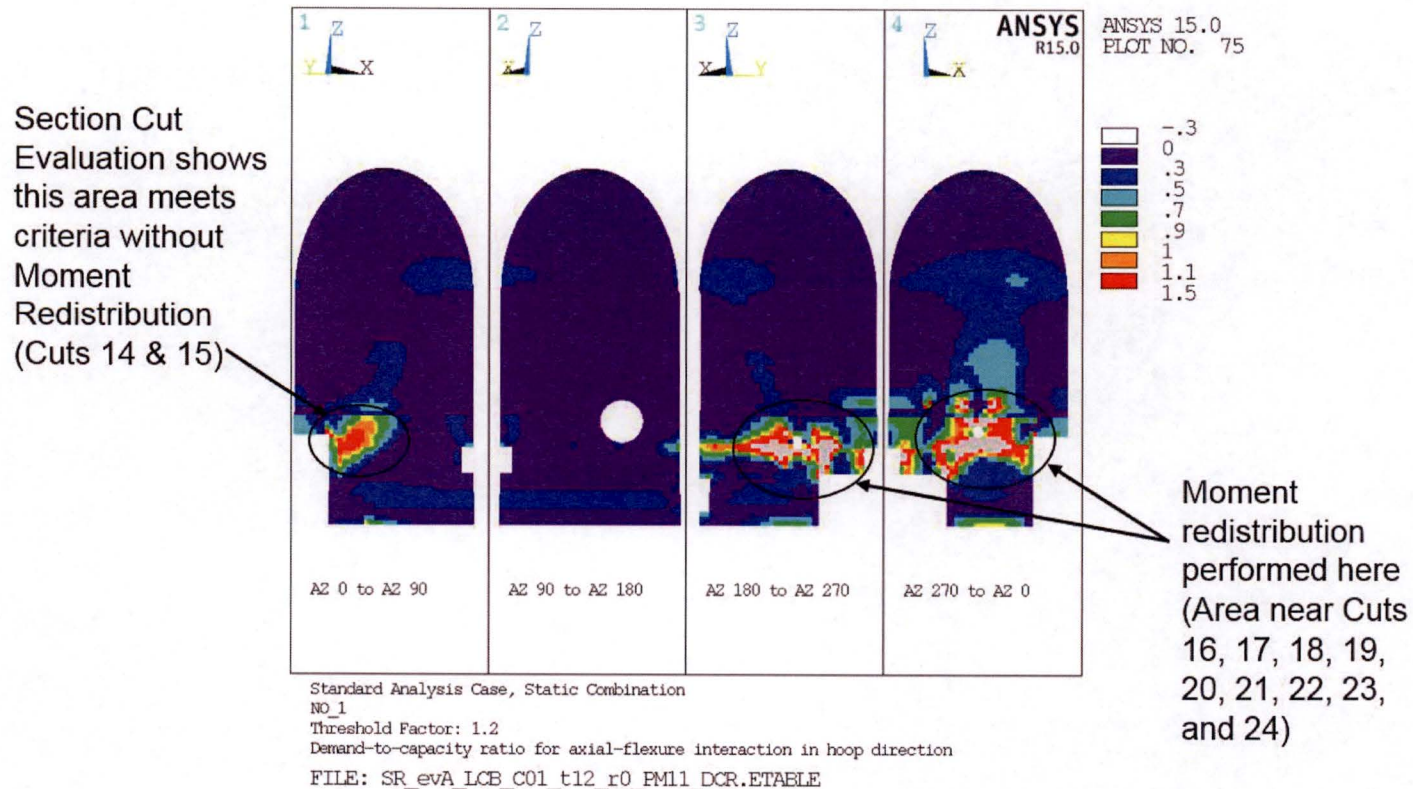


Figure H1. Contours of DCRs for PM Interaction in the Hoop Direction Prior to Moment Redistribution, Standard Analysis Case, Static Load Combination NO_1

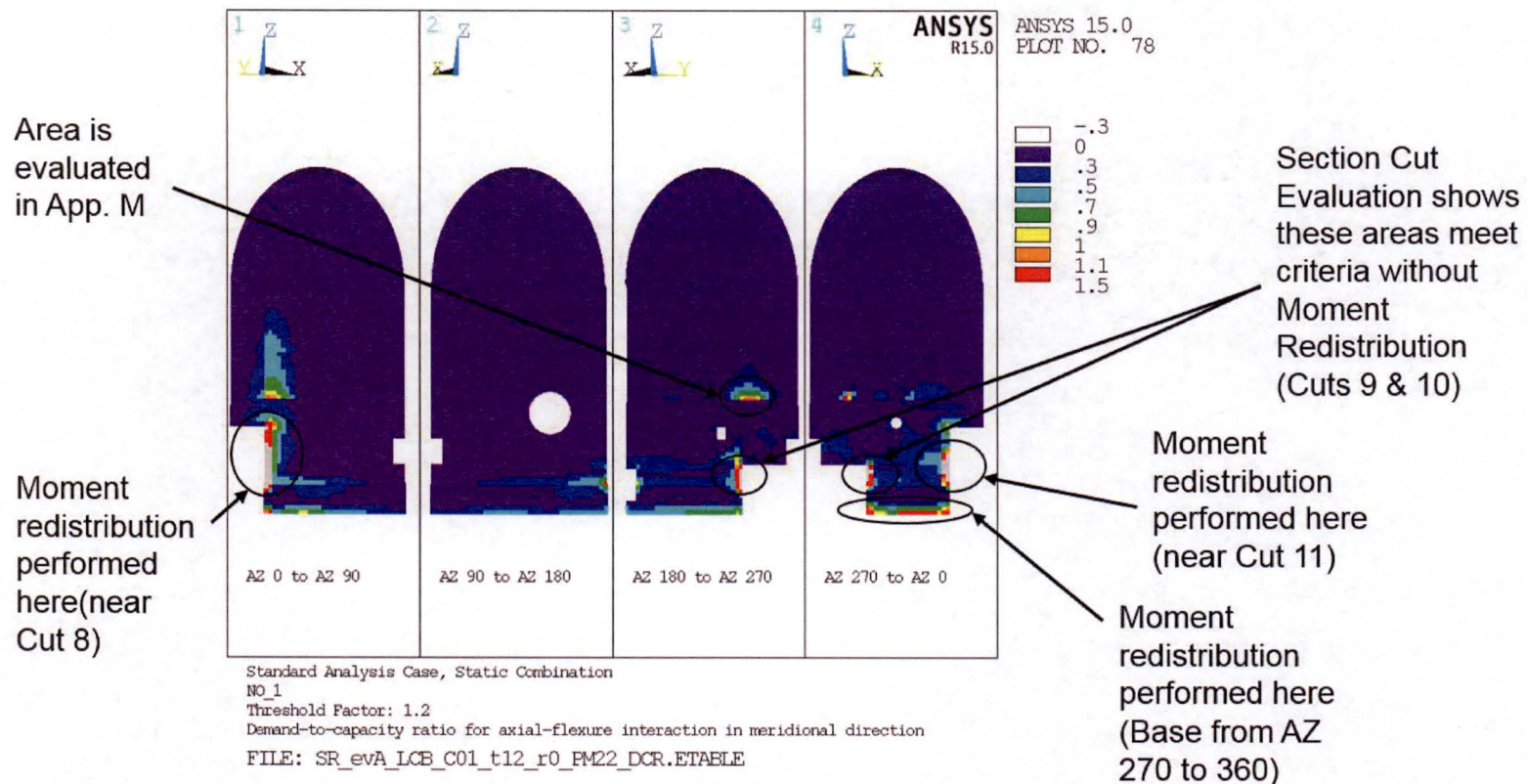


Figure H2. Contours of DCRs for PM Interaction in the Meridional Direction Prior to Moment Redistribution, Standard Analysis Case, Static Load Combination NO_1

SIMPSON GUMPERTZ & HEGER

Engineering of Structures
and Building Enclosures

CLIENT: NextEra Energy Seabrook

SUBJECT: Evaluation and Design Confirmation of As-Deformed CEB

PROJECT NO: 150252

DATE: July 2016

BY: R.M. Mones

VERIFIER: A.T. Sarawit

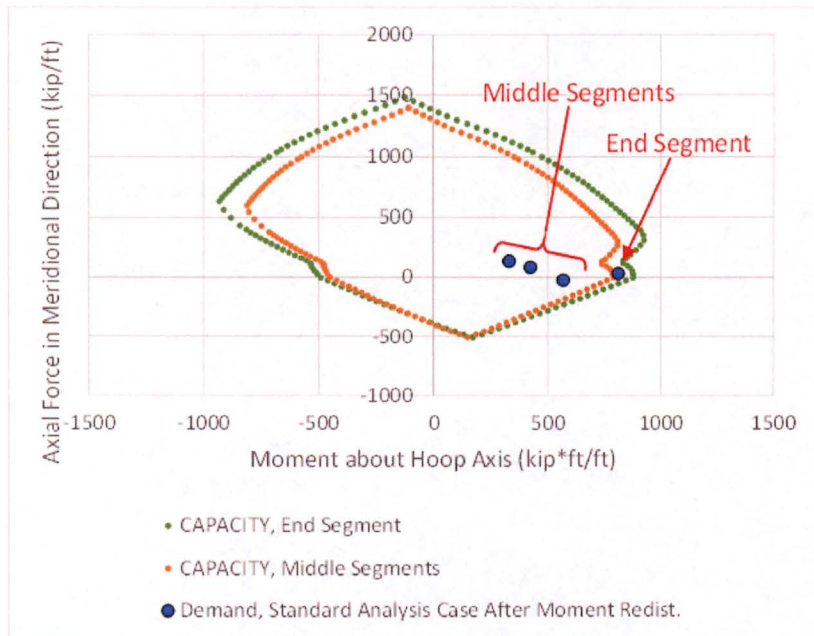
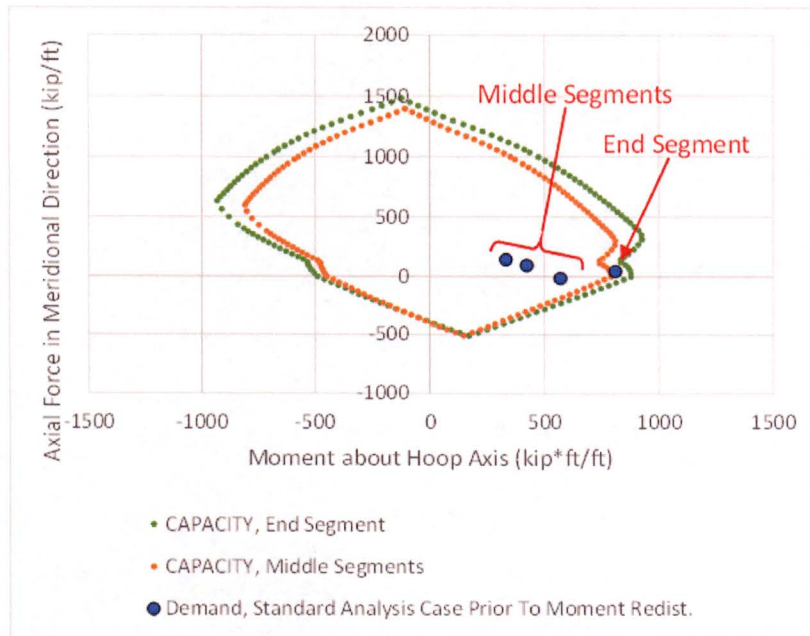


Figure H3. Comparison of PM Interaction Diagrams for Wall Segments along Base between AZ 0 and 90 Before (left) and After (right) Moment Redistribution, Standard Analysis Case, Static Load Combination NO_1

CLIENT: NextEra Energy Seabrook

SUBJECT: Evaluation and Design Confirmation of As-Deformed CEB

PROJECT NO: 150252

DATE: July 2016

BY: R.M. Mones

VERIFIER: A.T. Sarawit

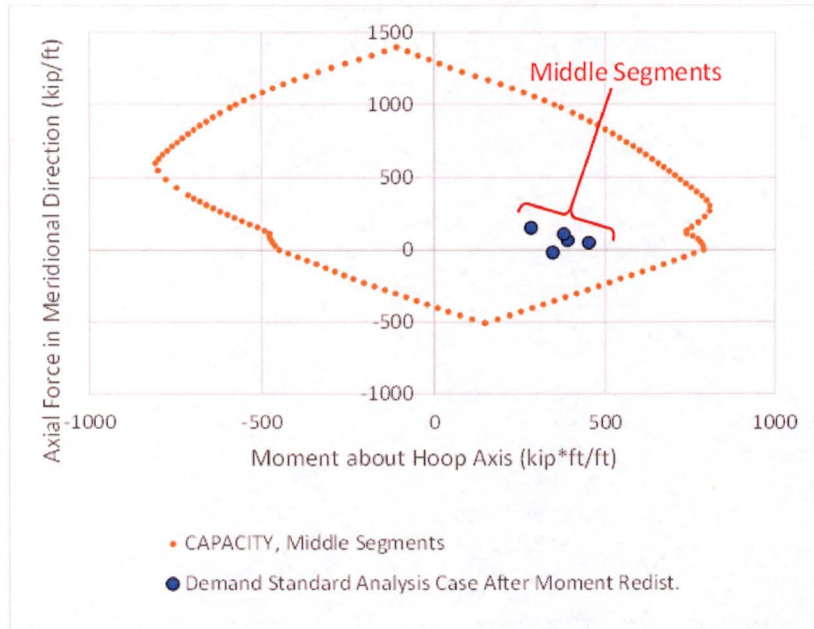
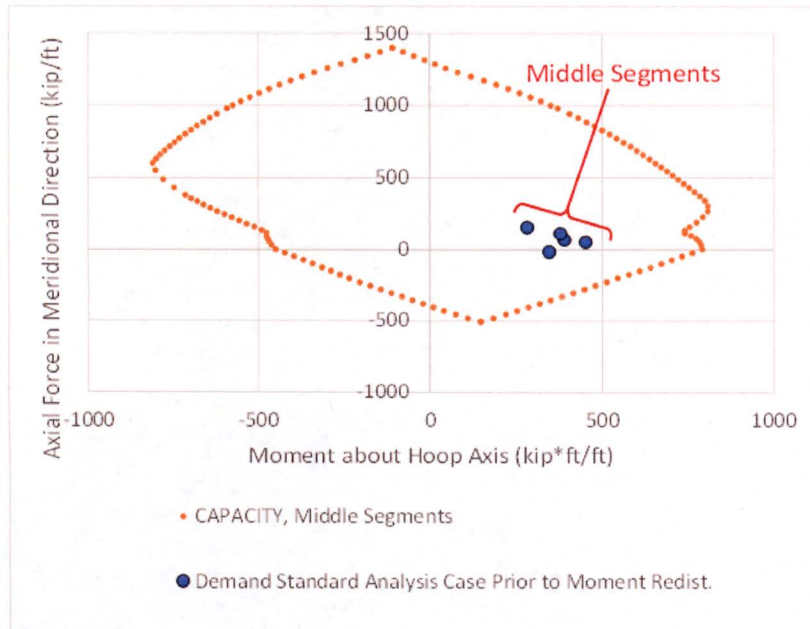


Figure H4. Comparison of PM Interaction Diagrams for Wall Segments along Base between AZ 90 and 180 Before (left) and After (right) Moment Redistribution, Standard Analysis Case, Static Load Combination NO_1

CLIENT: NextEra Energy Seabrook

SUBJECT: Evaluation and Design Confirmation of As-Deformed CEB

PROJECT NO: 150252

DATE: July 2016

BY: R.M. Mones

VERIFIER: A.T. Sarawit

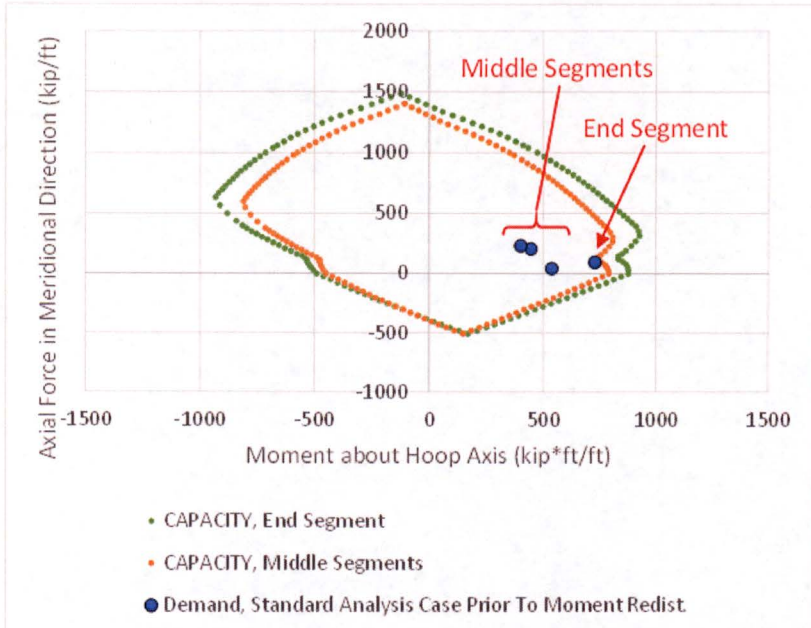
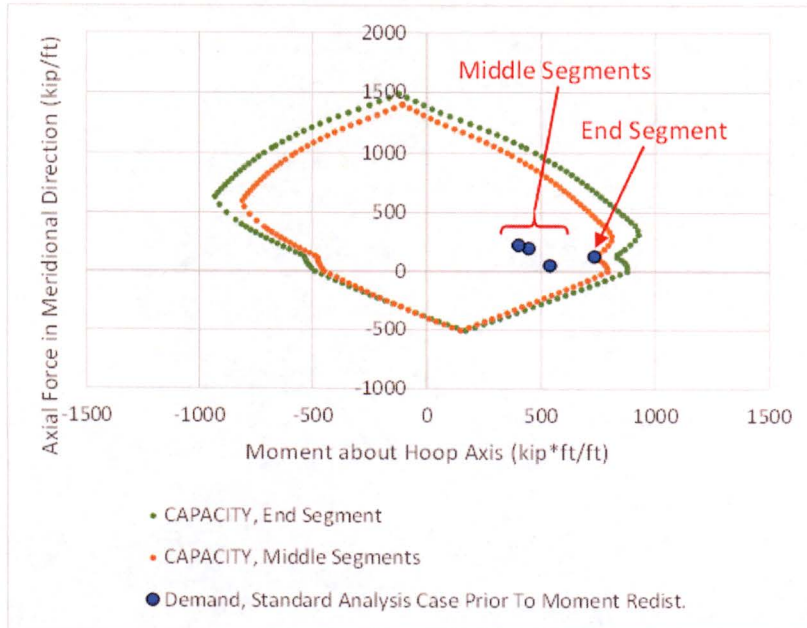


Figure H5. Comparison of PM Interaction Diagrams for Wall Segments along Base between AZ 180 and 270 Before (left) and After (right) Moment Redistribution, Standard Analysis Case, Static Load Combination NO_1

CLIENT: NextEra Energy Seabrook

SUBJECT: Evaluation and Design Confirmation of As-Deformed CEB

PROJECT NO: 150252

DATE: July 2016

BY: R.M. Mones

VERIFIER: A.T. Sarawit

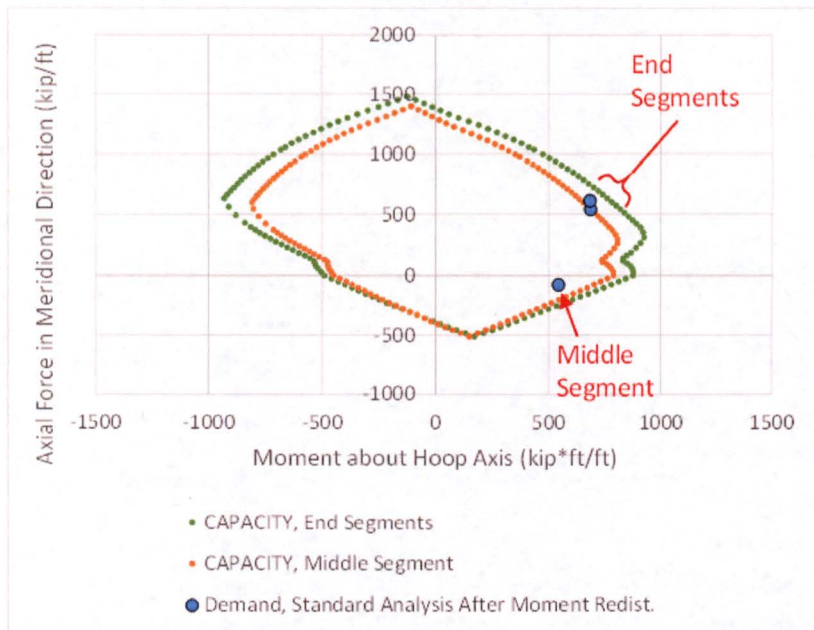
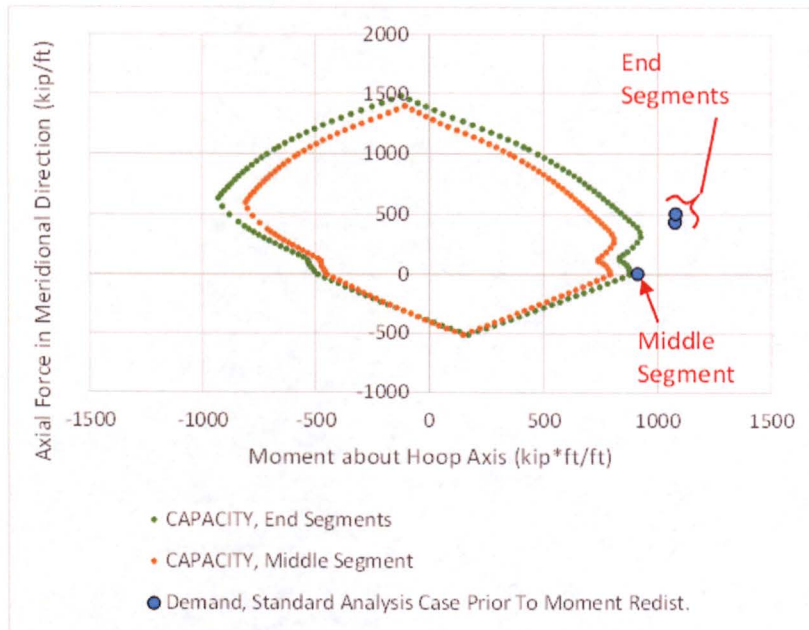


Figure H6. Comparison of PM Interaction Diagrams for Wall Segments along Base between AZ 270 and 360 Before (left) and After (right) Moment Redistribution, Standard Analysis Case, Static Load Combination NO_1

CLIENT: NextEra Energy Seabrook

SUBJECT: Evaluation and Design Confirmation of As-Deformed CEB

PROJECT NO: 150252

DATE: July 2016

BY: R.M. Mones

VERIFIER: A.T. Sarawit

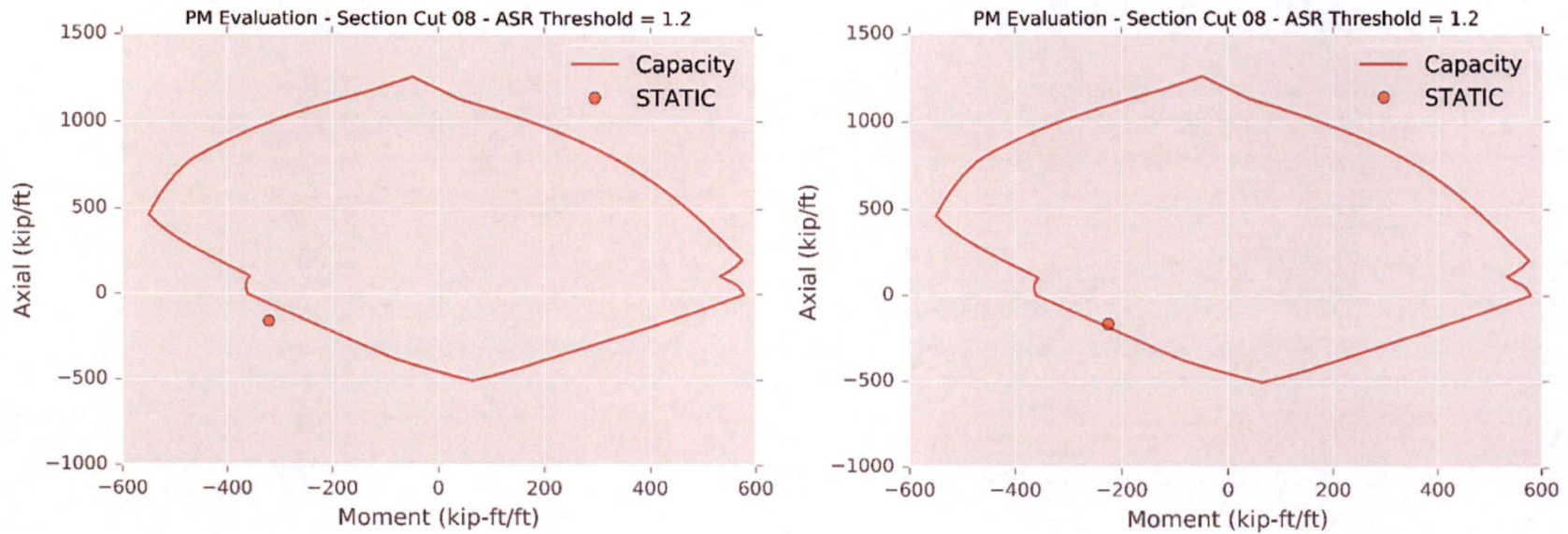


**Figure H7. Comparison of PM Interaction Diagrams for Section 8
Before (left) and After (right) Moment Redistribution,
Standard Analysis Case, Static Load Combination NO_1**



CLIENT: NextEra Energy Seabrook

SUBJECT: Evaluation and Design Confirmation of As-Deformed CEB

PROJECT NO: 150252

DATE: July 2016

BY: R.M. Mones

VERIFIER: A.T. Sarawit

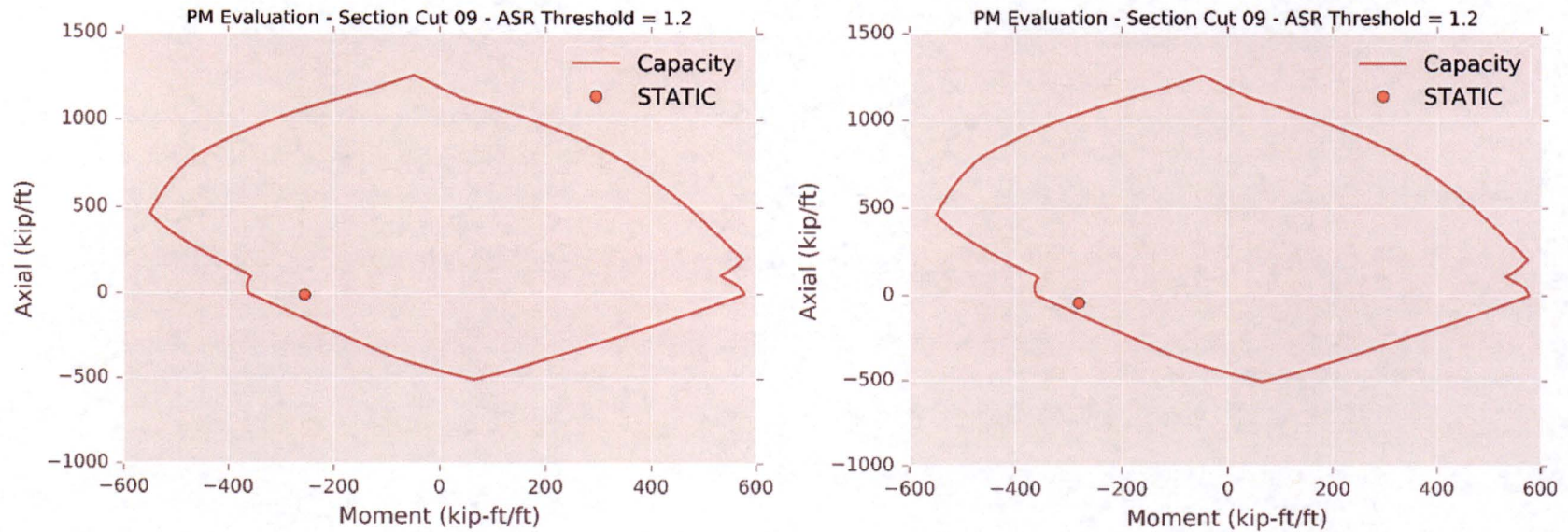


**Figure H8. Comparison of PM Interaction Diagrams for Section 9
Before (left) and After (right) Moment Redistribution,
Standard Analysis Case, Static Load Combination NO_1**

CLIENT: NextEra Energy Seabrook

SUBJECT: Evaluation and Design Confirmation of As-Deformed CEB

PROJECT NO: 150252

DATE: July 2016

BY: R.M. Mones

VERIFIER: A.T. Sarawit

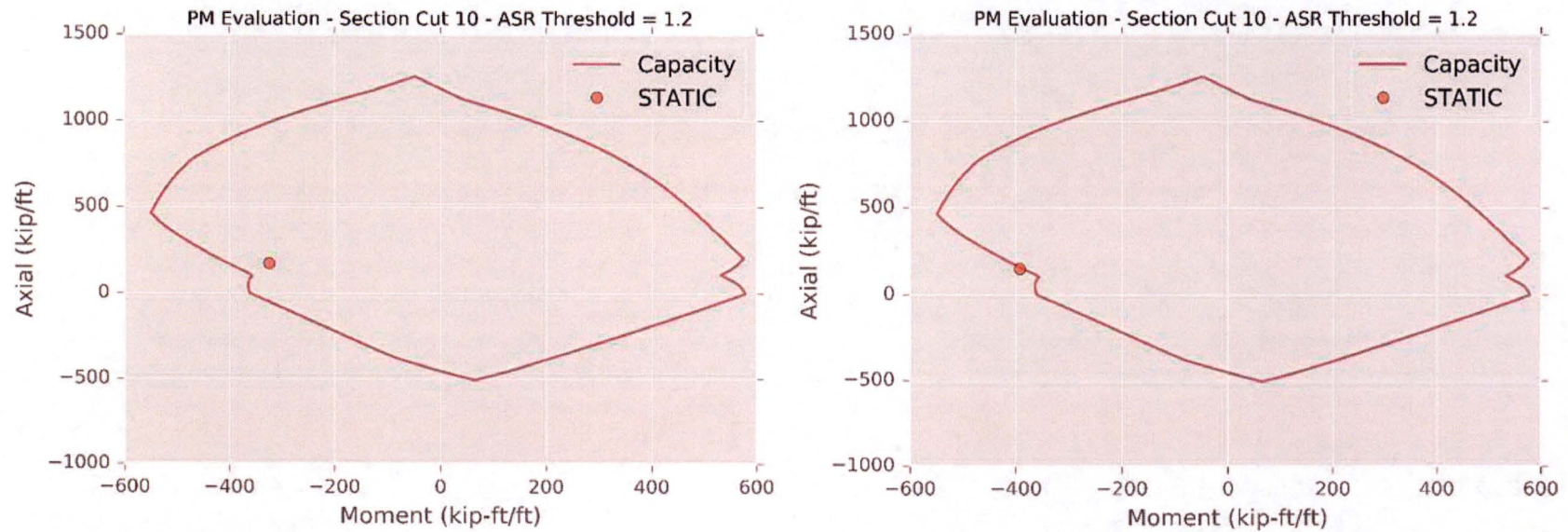


**Figure H9. Comparison of PM Interaction Diagrams for Section 10
Before (left) and After (right) Moment Redistribution,
Standard Analysis Case, Static Load Combination NO_1**

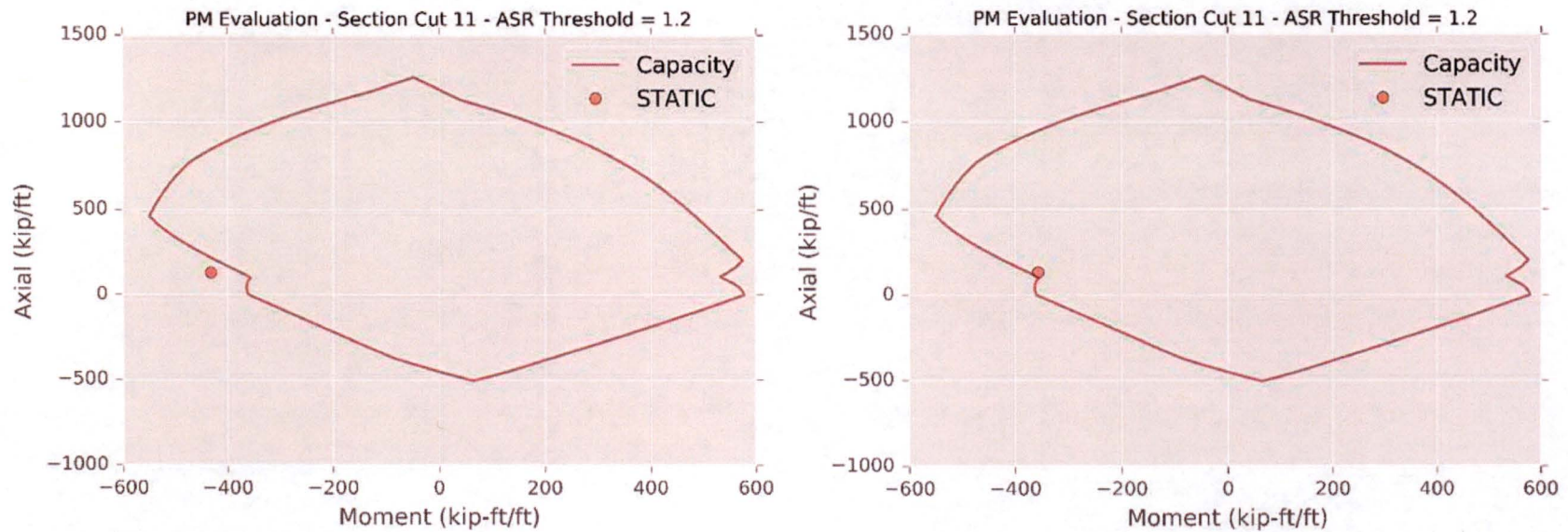


**Figure H10. Comparison of PM Interaction Diagrams for Section 11
Before (left) and After (right) Moment Redistribution,
Standard Analysis Case, Static Load Combination NO_1**

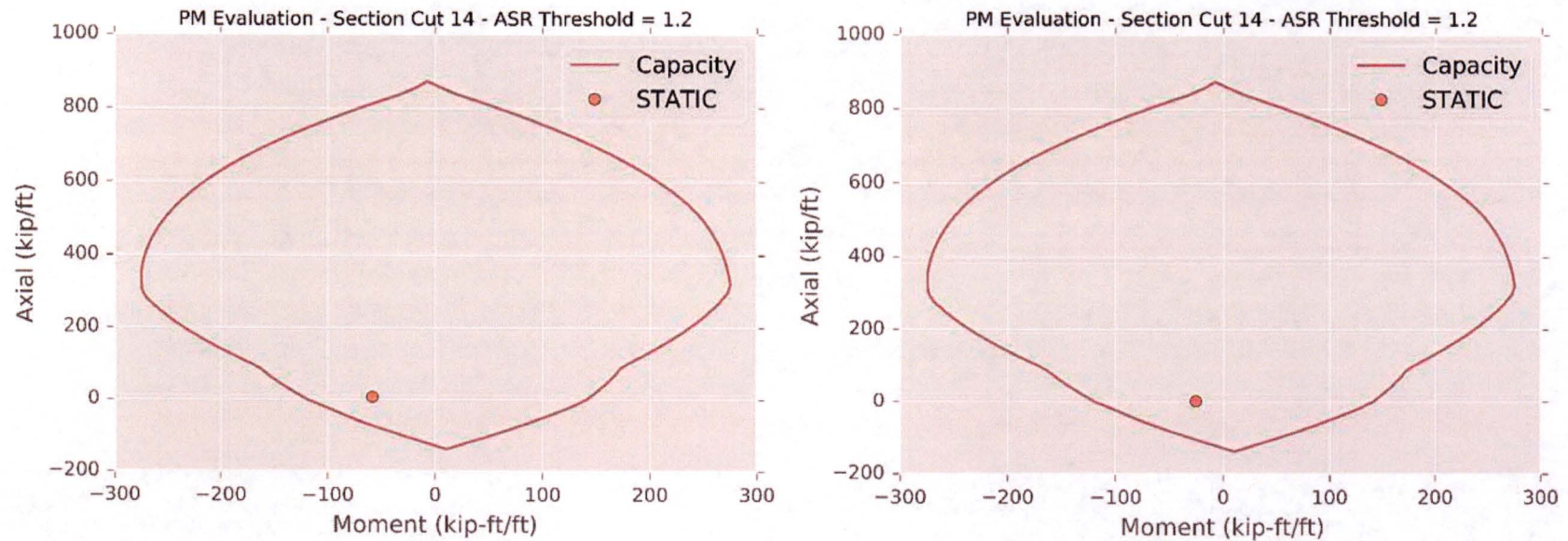


**Figure H11. Comparison of PM Interaction Diagrams for Section 14
Before (left) and After (right) Moment Redistribution,
Standard Analysis Case, Static Load Combination NO_1**

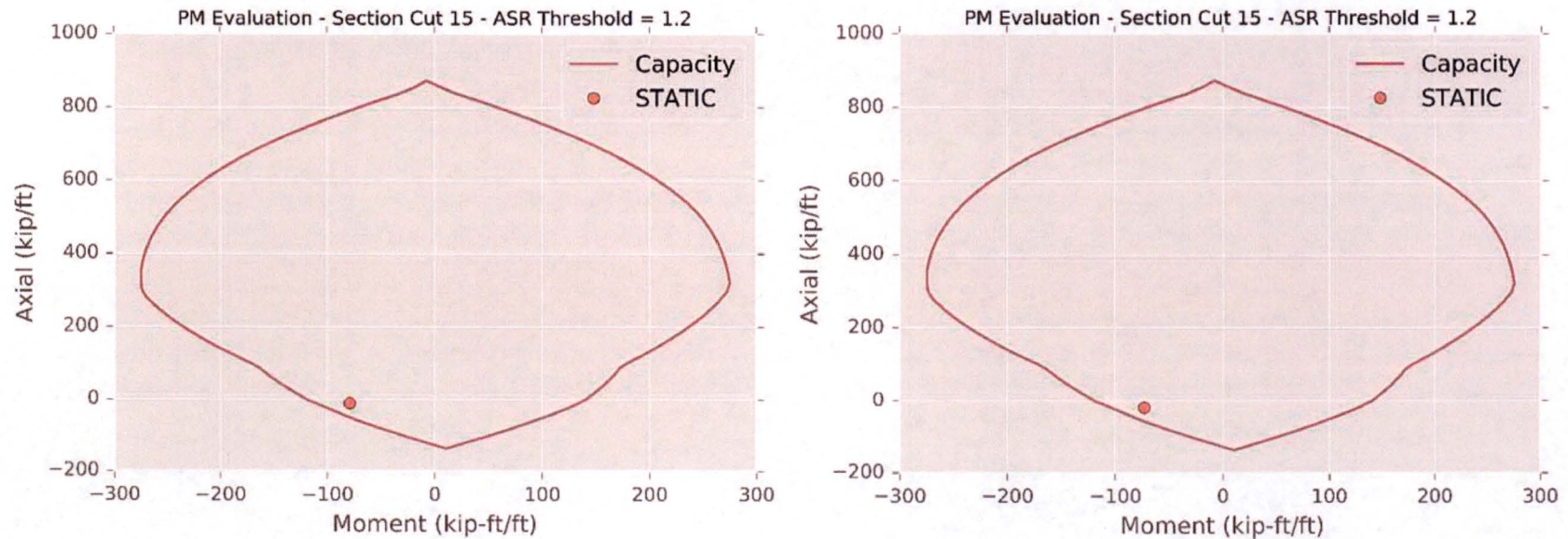


**Figure H12. Comparison of PM Interaction Diagrams for Section 15
Before (left) and After (right) Moment Redistribution,
Standard Analysis Case, Static Load Combination NO_1**



CLIENT: NextEra Energy Seabrook

SUBJECT: Evaluation and Design Confirmation of As-Deformed CEB

PROJECT NO: 150252

DATE: July 2016

BY: R.M. Mones

VERIFIER: A.T. Sarawit

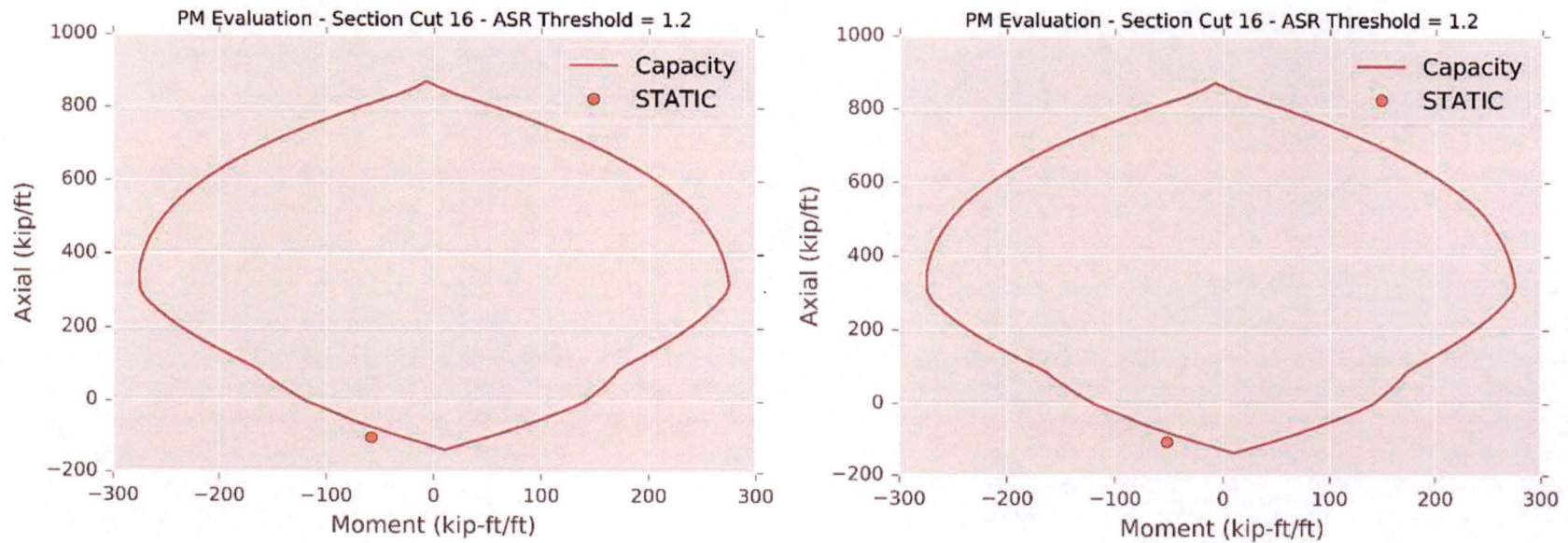


**Figure H13. Comparison of PM Interaction Diagrams for Section 16
Before (left) and After (right) Moment Redistribution,
Standard Analysis Case, Static Load Combination NO_1**

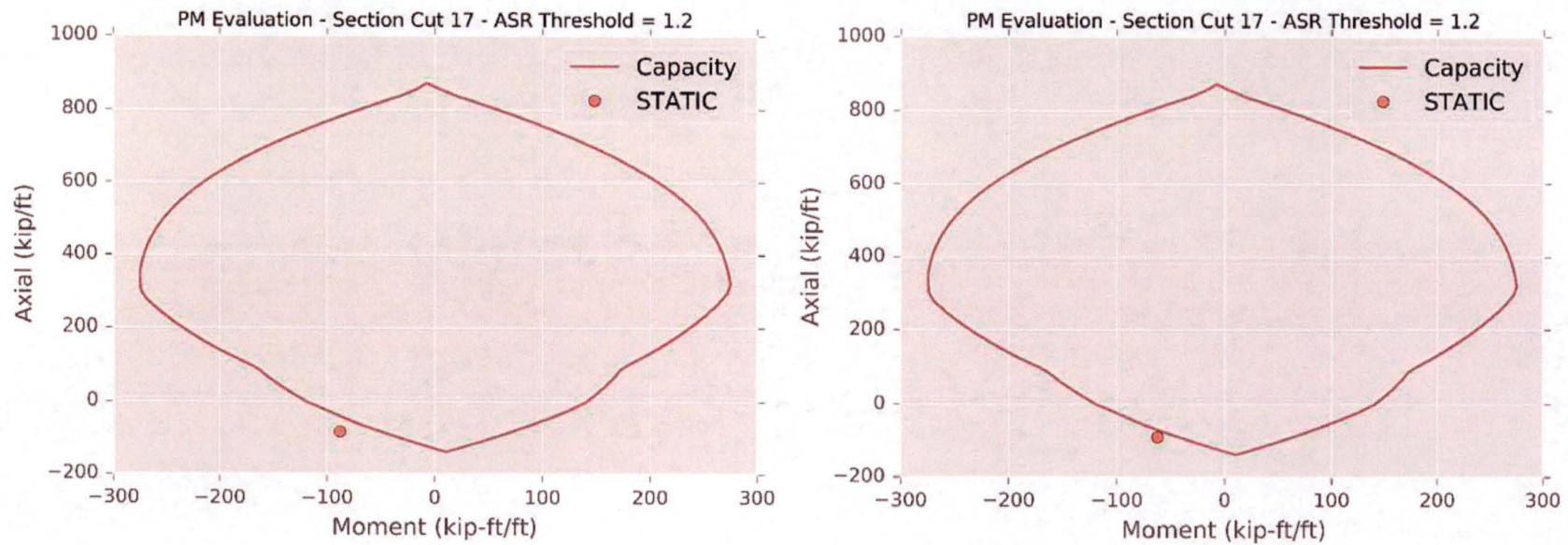


**Figure H14. Comparison of PM Interaction Diagrams for Section 17
Before (left) and After (right) Moment Redistribution,
Standard Analysis Case, Static Load Combination NO_1**

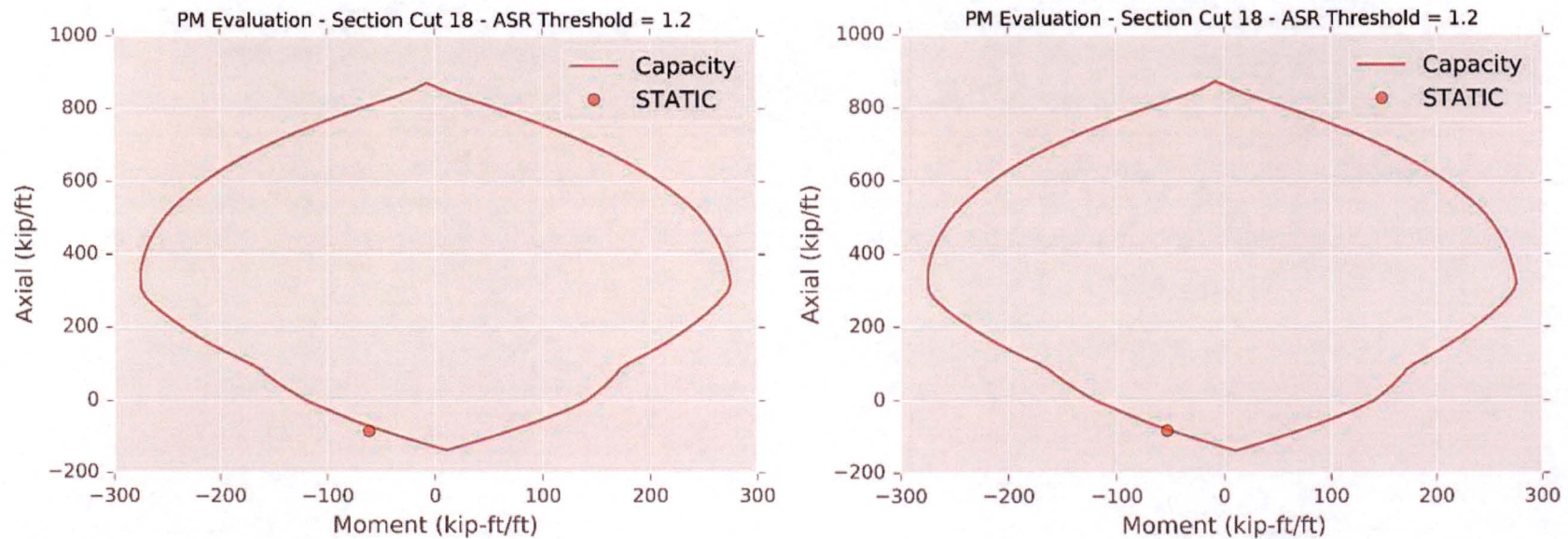


**Figure H15. Comparison of PM Interaction Diagrams for Section 18
Before (left) and After (right) Moment Redistribution,
Standard Analysis Case, Static Load Combination NO_1**

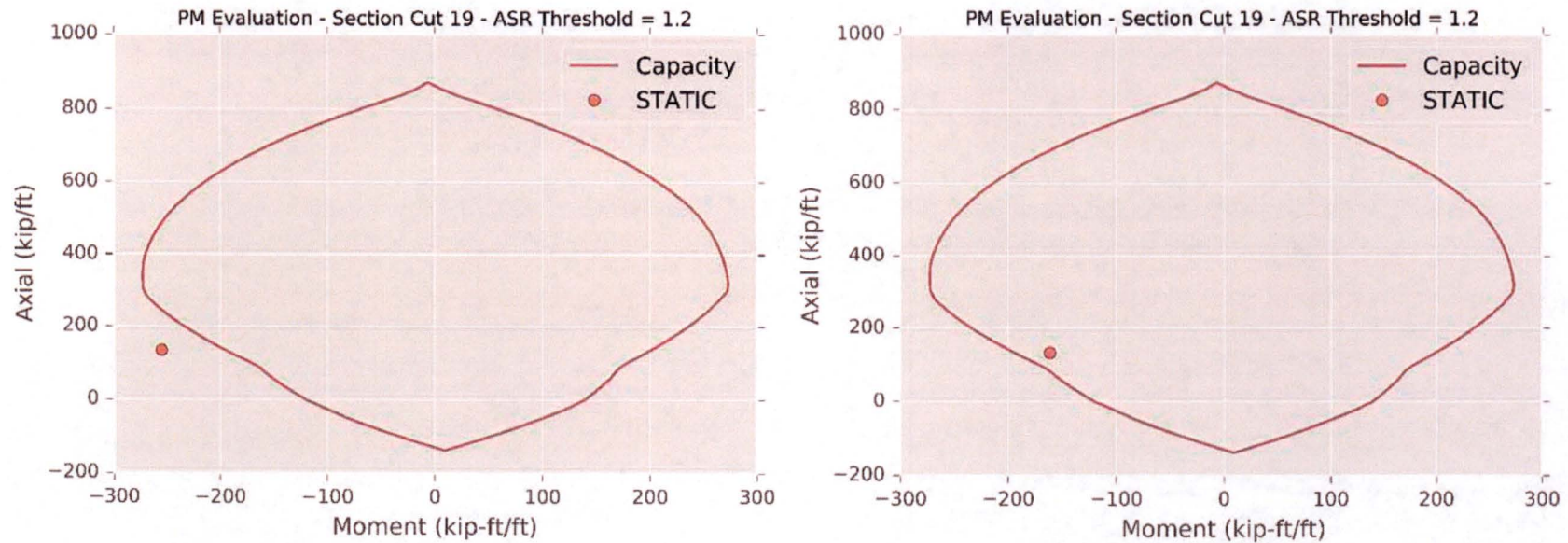


**Figure H16. Comparison of PM Interaction Diagrams for Section 19
Before (left) and After (right) Moment Redistribution,
Standard Analysis Case, Static Load Combination NO_1**

CLIENT: NextEra Energy Seabrook

SUBJECT: Evaluation and Design Confirmation of As-Deformed CEB

PROJECT NO: 150252

DATE: July 2016

BY: R.M. Mones

VERIFIER: A.T. Sarawit

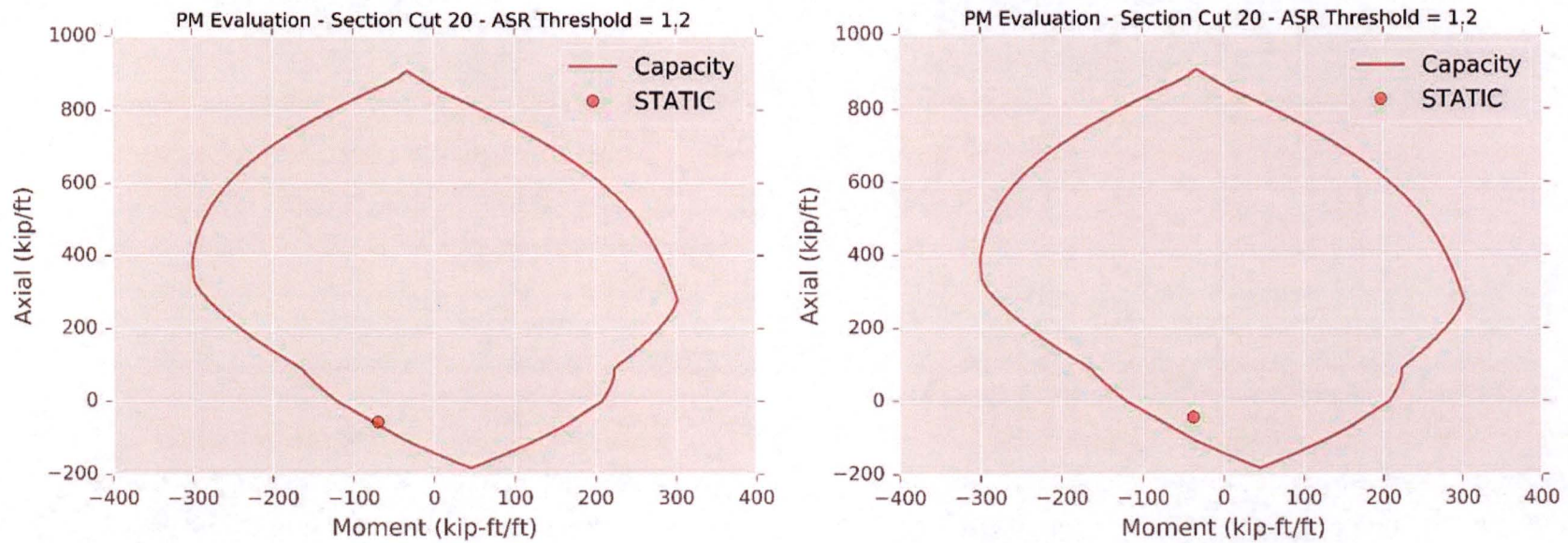


**Figure H17. Comparison of PM Interaction Diagrams for Section 20
Before (left) and After (right) Moment Redistribution,
Standard Analysis Case, Static Load Combination NO_1**

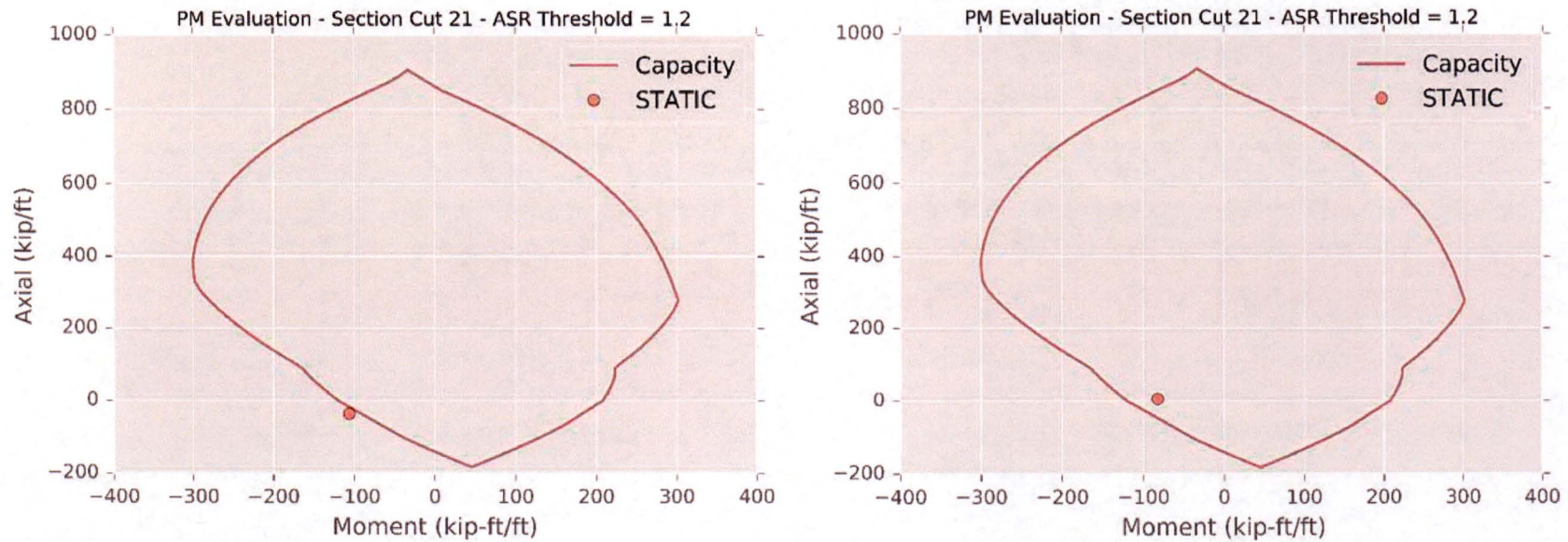


**Figure H18. Comparison of PM Interaction Diagrams for Section 21
Before (left) and After (right) Moment Redistribution,
Standard Analysis Case, Static Load Combination NO_1**

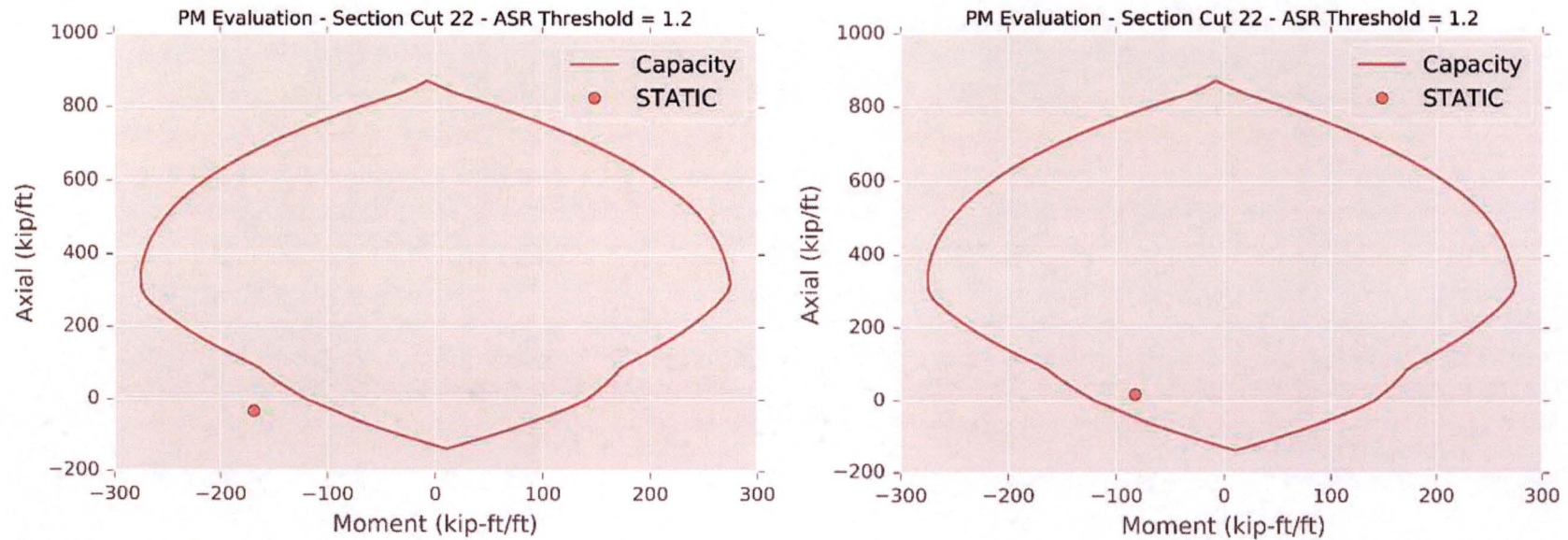


**Figure H19. Comparison of PM Interaction Diagrams for Section 22
Before (left) and After (right) Moment Redistribution,
Standard Analysis Case, Static Load Combination NO_1**

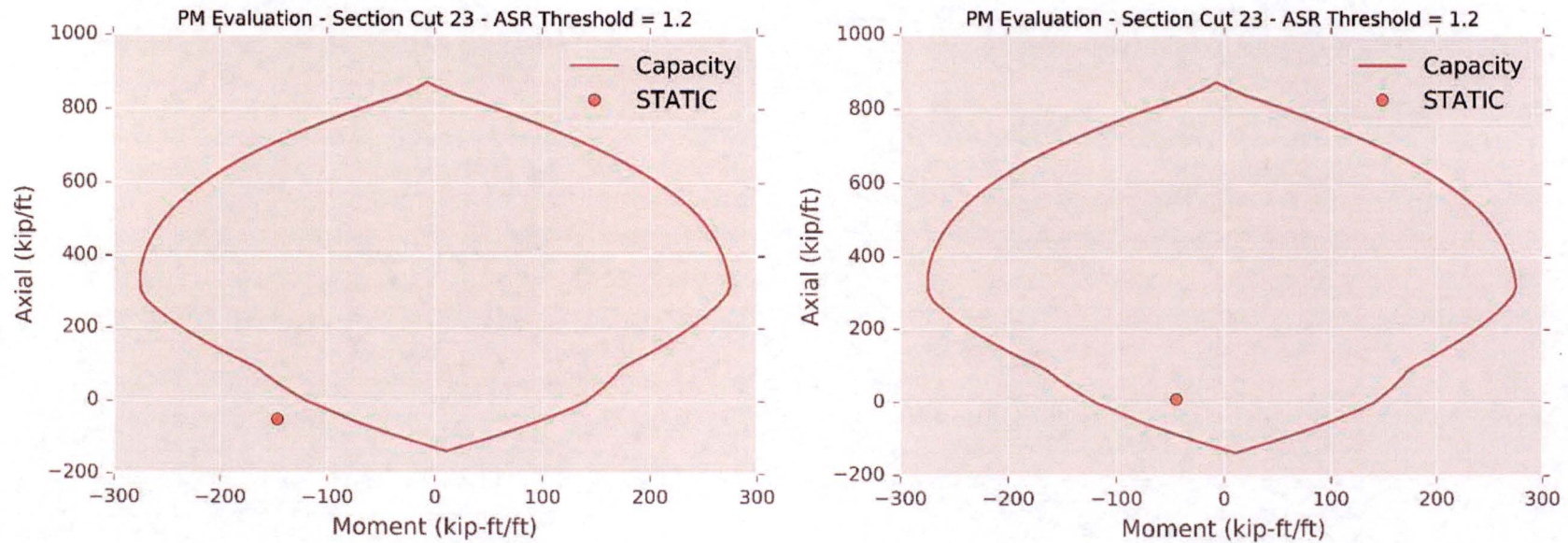


**Figure H20. Comparison of PM Interaction Diagrams for Section 23
Before (left) and After (right) Moment Redistribution,
Standard Analysis Case, Static Load Combination NO_1**

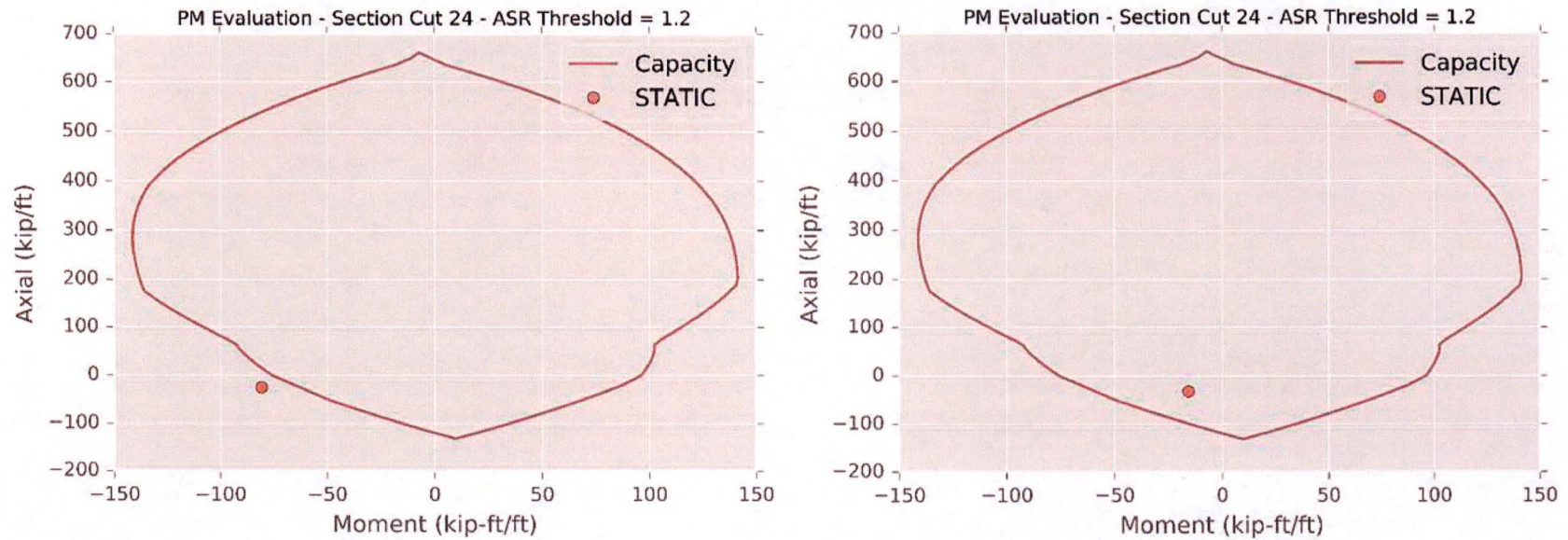


**Figure H21. Comparison of PM Interaction Diagrams for Section 24
Before (left) and After (right) Moment Redistribution,
Standard Analysis Case, Static Load Combination NO_1**

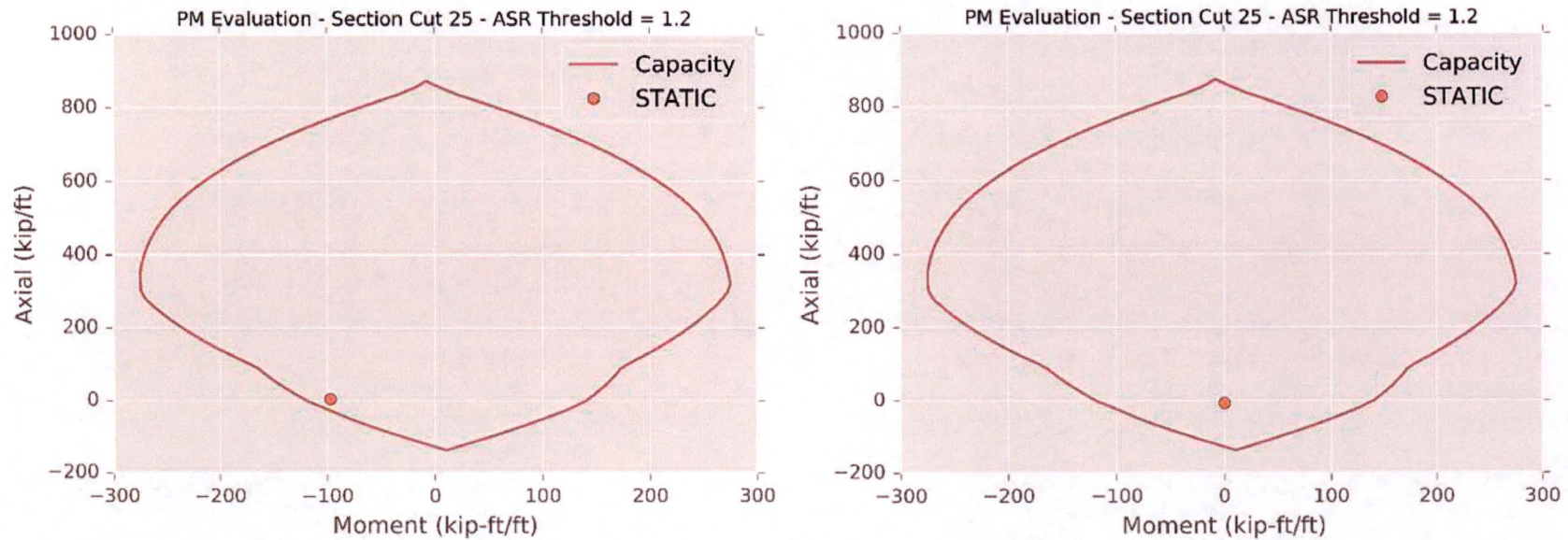


**Figure H22. Comparison of PM Interaction Diagrams for Section 25
Before (left) and After (right) Moment Redistribution,
Standard Analysis Case, Static Load Combination NO_1**

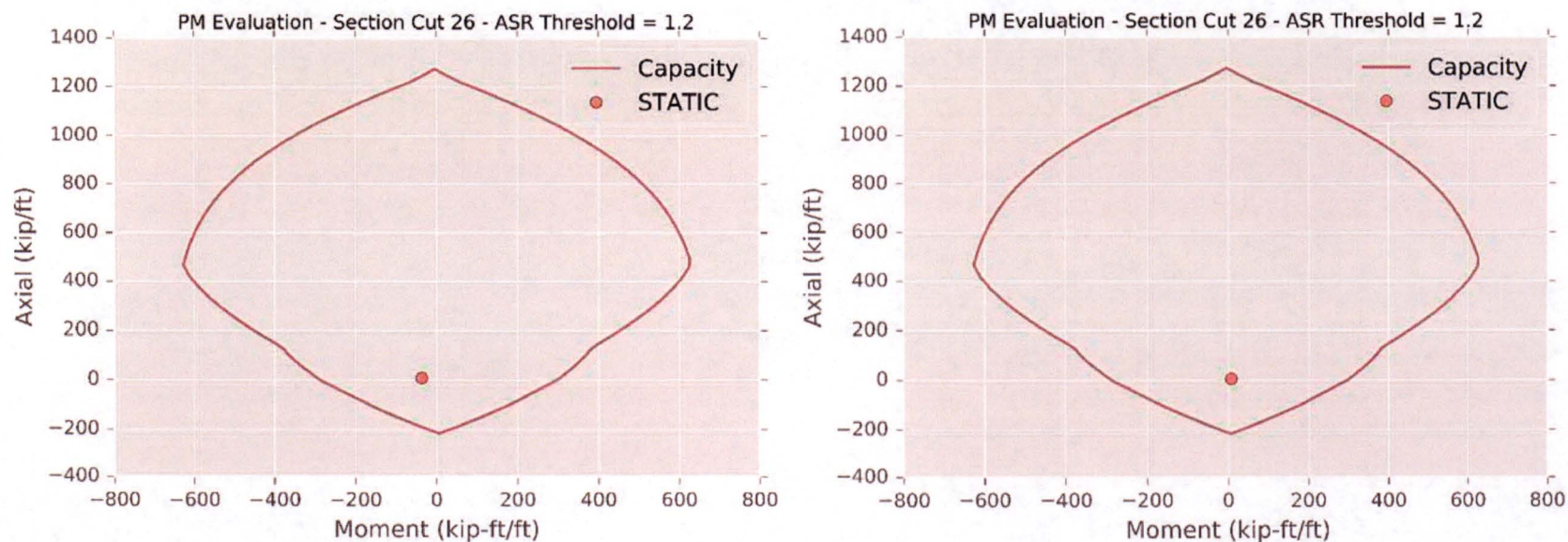


**Figure H23. Comparison of PM Interaction Diagrams for Section 26
Before (left) and After (right) Moment Redistribution,
Standard Analysis Case, Static Load Combination NO_1**

CLIENT: NextEra Energy Seabrook

SUBJECT: Evaluation and Design Confirmation of As-Deformed CEB

PROJECT NO: 150252

DATE: July 2016

BY: R.M. Mones

VERIFIER: A.T. Sarawit

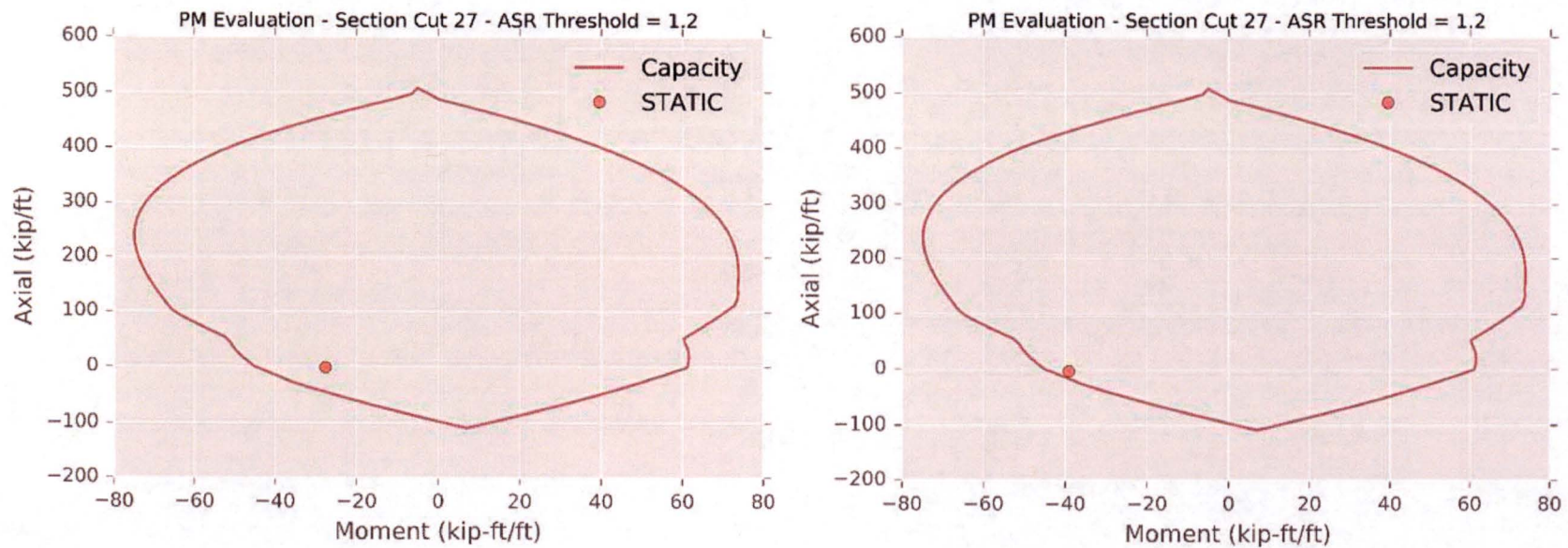


**Figure H24. Comparison of PM Interaction Diagrams for Section 27
Before (left) and After (right) Moment Redistribution,
Standard Analysis Case, Static Load Combination NO_1**

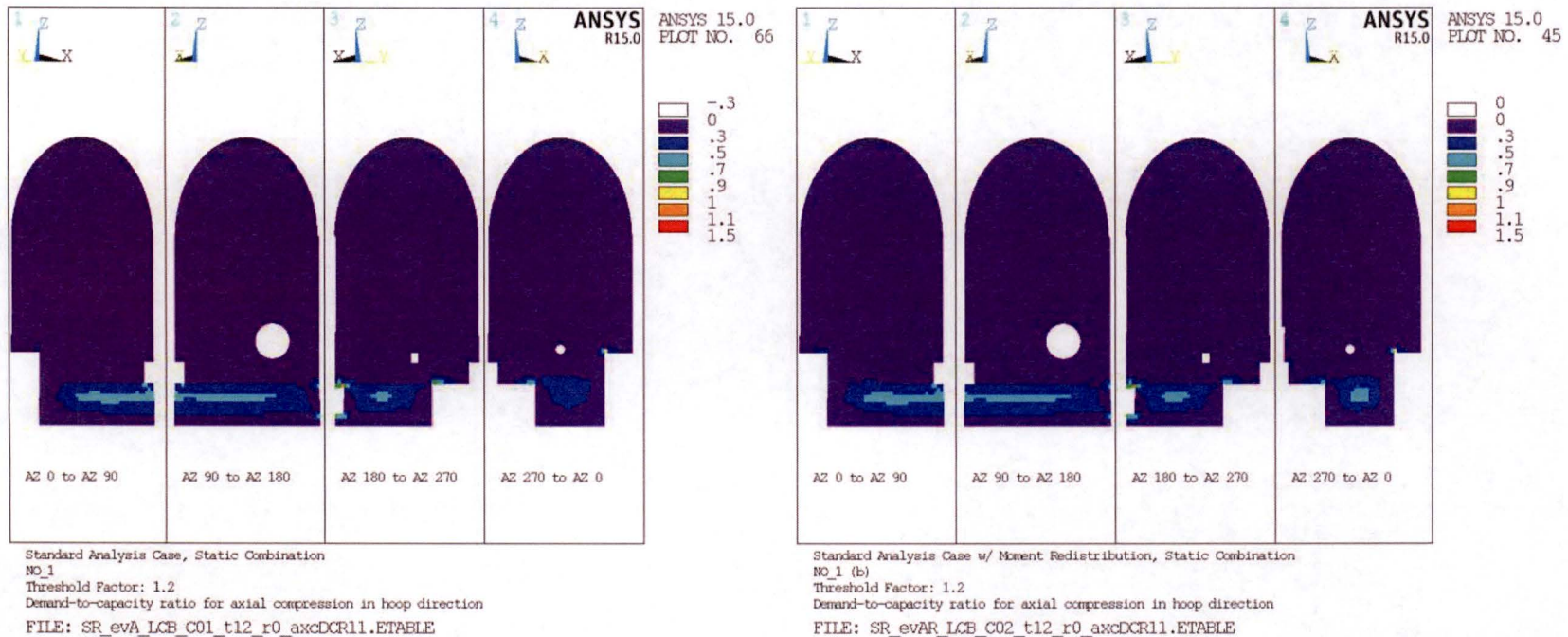
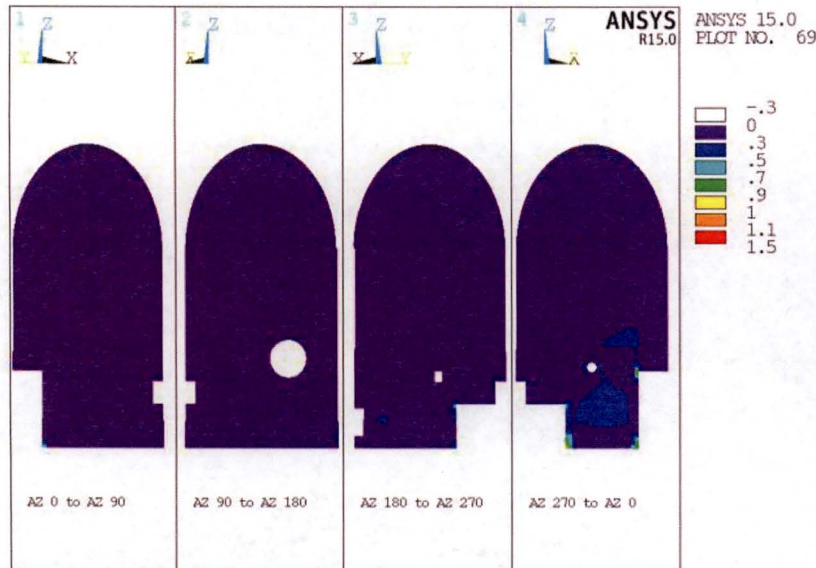
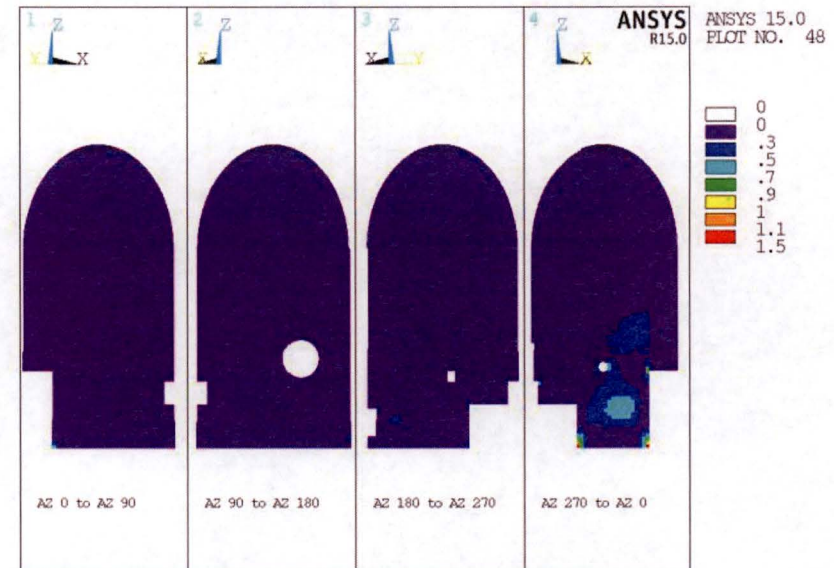


Figure H25. Comparison of DCRs for Axial Compression in the Hoop Direction Before (left) and After (right) Moment Redistribution, Standard Analysis Case, Static Load Combination NO_1



Standard Analysis Case, Static Combination
NO_1
Threshold Factor: 1.2
Demand-to-capacity ratio for axial compression in meridional direction
FILE: SR_evA_LCB_C01_t12_r0_axcDCR22.ETABLE



Standard Analysis Case w/ Moment Redistribution, Static Combination
NO_1 (b)
Threshold Factor: 1.2
Demand-to-capacity ratio for axial compression in meridional direction
FILE: SR_evAR_LCB_C02_t12_r0_axcDCR22.ETABLE

**Figure H26. Comparison of DCRs for Axial Compression in the Meridional Direction
Before (left) and After (right) Moment Redistribution,
Standard Analysis Case, Static Load Combination NO_1**

CLIENT: NextEra Energy Seabrook

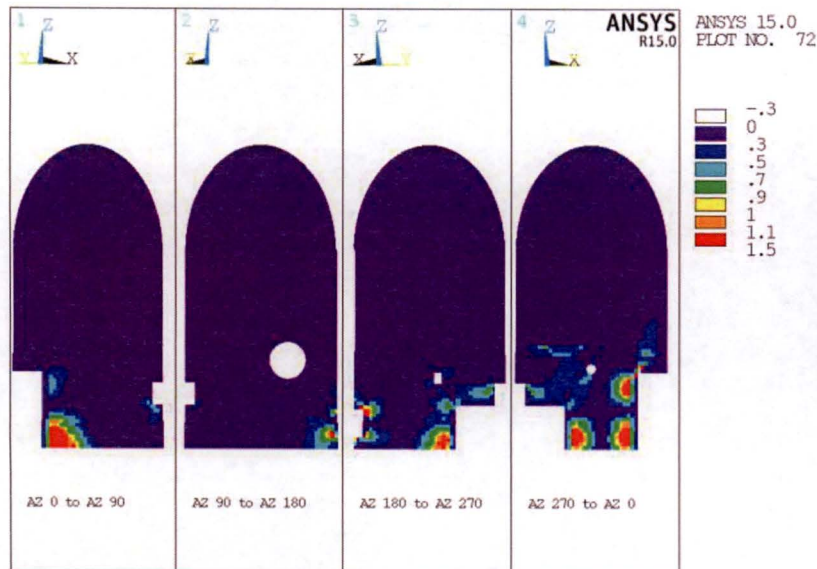
SUBJECT: Evaluation and Design Confirmation of As-Deformed CEB

PROJECT NO: 150252

DATE: July 2016

BY: R.M. Mones

VERIFIER: A.T. Sarawit



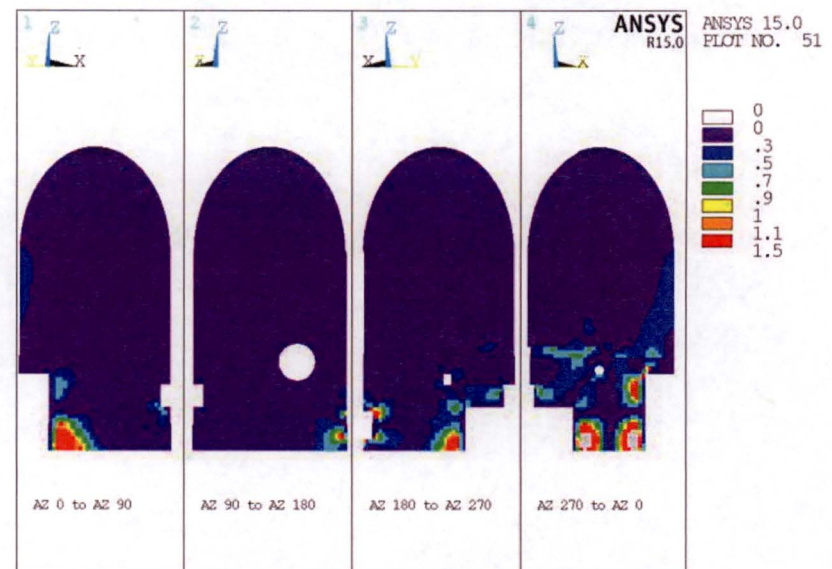
Standard Analysis Case, Static Combination

NO_1

Threshold Factor: 1.2

Demand-to-capacity ratio for in-plane shear

FILE: SR_eva_LCB_C01_t12_r0_VIP_DCR.ETABLE



Standard Analysis Case w/ Moment Redistribution, Static Combination

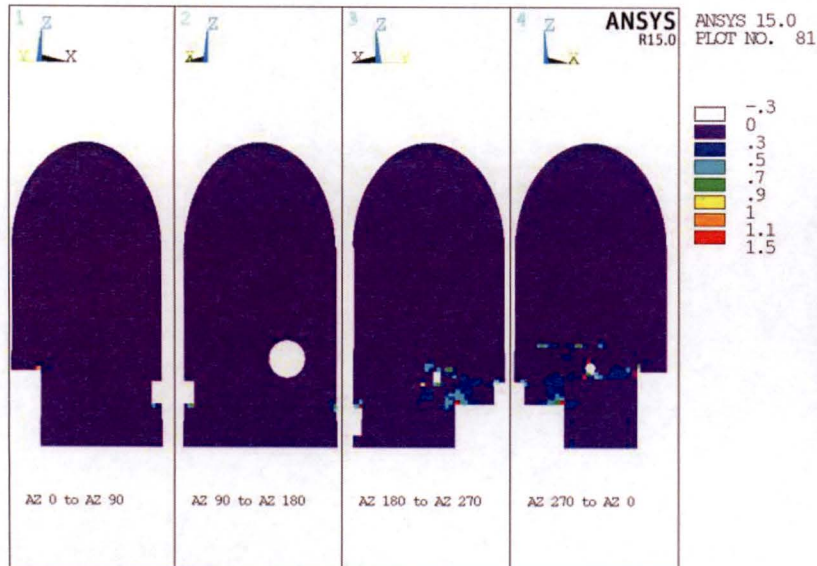
NO_1 (b)

Threshold Factor: 1.2

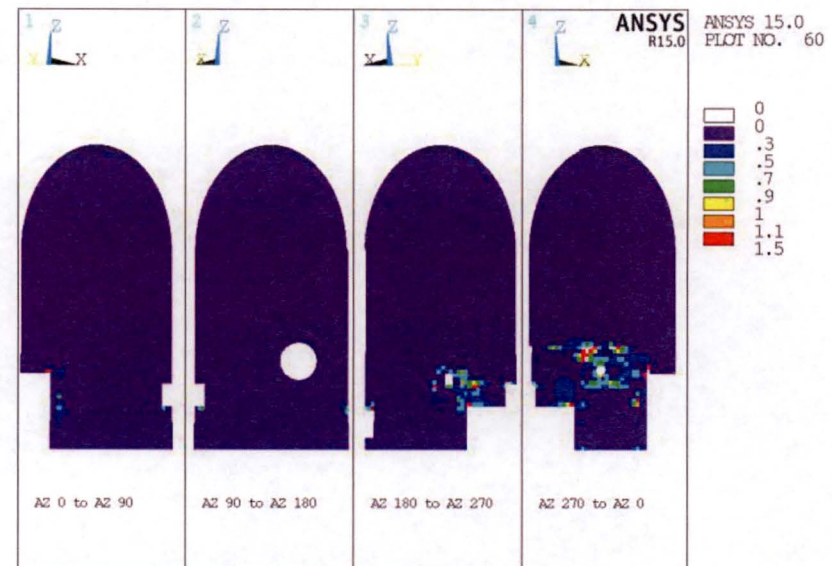
Demand-to-capacity ratio for in-plane shear

FILE: SR_eva_LCB_C02_t12_r0_VIP_DCR.ETABLE

**Figure H27. Comparison of DCRs for In-Plane Shear
Before (left) and After (right) Moment Redistribution,
Standard Analysis Case, Static Load Combination NO_1**

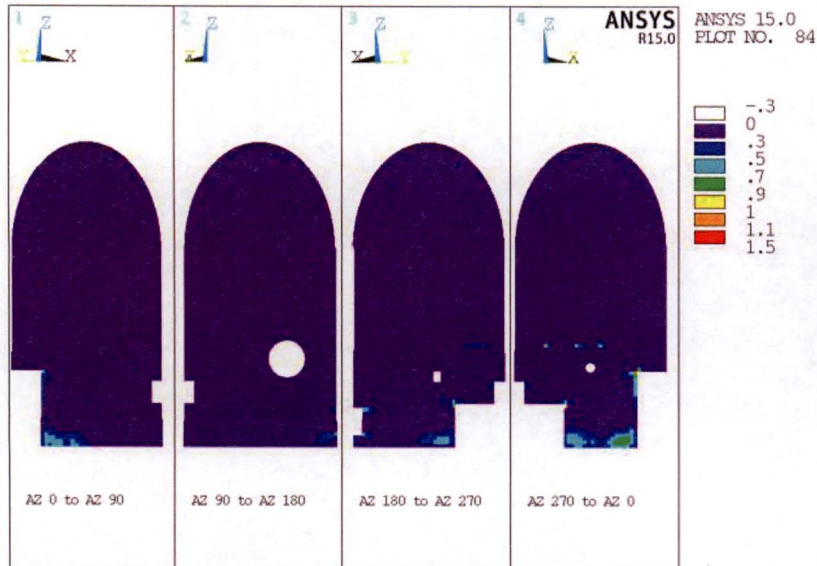


Standard Analysis Case, Static Combination
NO_1
Threshold Factor: 1.2
Demand-to-capacity ratio for out-of-plane shear (Q13)
FILE: SR_evA_LCB_C01_t12_r0_VOP11DCR.ETABLE

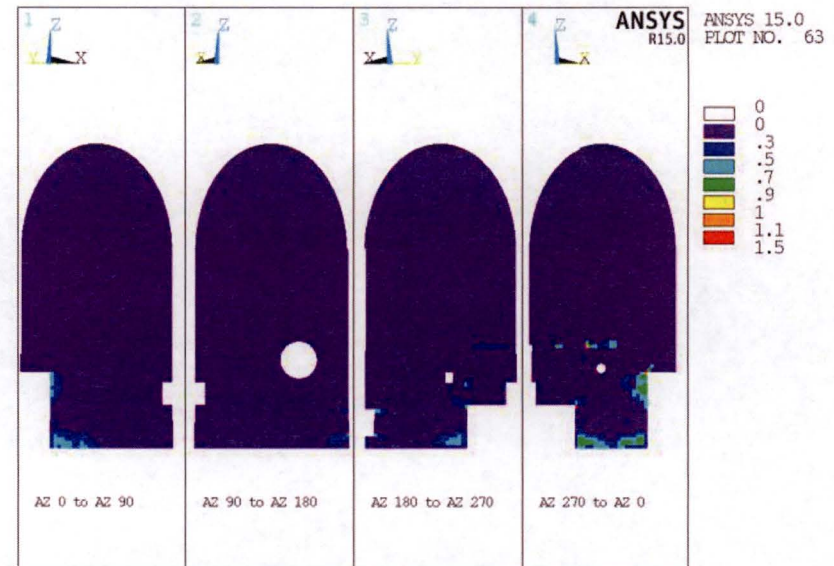


Standard Analysis Case w/ Moment Redistribution, Static Combination
NO_1 (b)
Threshold Factor: 1.2
Demand-to-capacity ratio for out-of-plane shear (Q13)
FILE: SR_evAR_LCB_C02_t12_r0_VOP11DCR.ETABLE

Figure H28. Comparison of DCRs for Out-Of-Plane Shear Acting on Meridional-Radial Plane Before (left) and After (right) Moment Redistribution, Standard Analysis Case, Static Load Combination NO_1



Standard Analysis Case, Static Combination
NO_1
Threshold Factor: 1.2
Demand-to-capacity ratio for out-of-plane shear (Q23)
FILE: SR_evA_LCB_C01_t12_r0_VOP22DCR.ETABLE



Standard Analysis Case w/ Moment Redistribution, Static Combination
NO_1 (b)
Threshold Factor: 1.2
Demand-to-capacity ratio for out-of-plane shear (Q23)
FILE: SR_evAR_LCB_C02_t12_r0_VOP22DCR.ETABLE

**Figure H29. Comparison of DCRs for Out-Of-Plane Shear Acting on Hoop-Radial Plane
Before (left) and After (right) Moment Redistribution,
Standard Analysis Case, Static Load Combination NO_1**

Section Cut
Evaluation shows
this area meets
criteria without
Moment
Redistribution
(Cuts 14 & 15)

This area is
evaluated in
Section 7.5.6
(Cuts 14 & 15)

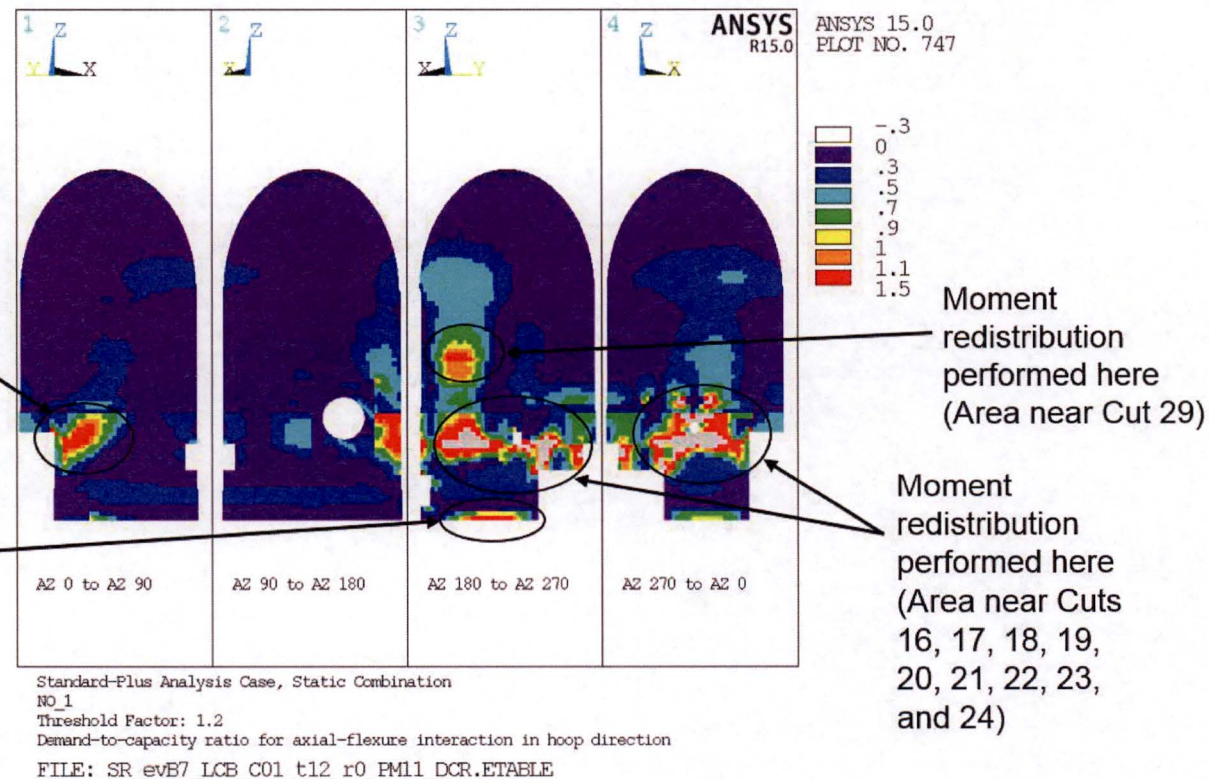


Figure H30. Contours of DCRs for PM Interaction in the Hoop Direction Prior to Moment Redistribution, Standard-Plus Analysis Case, Static Load Combination NO_1

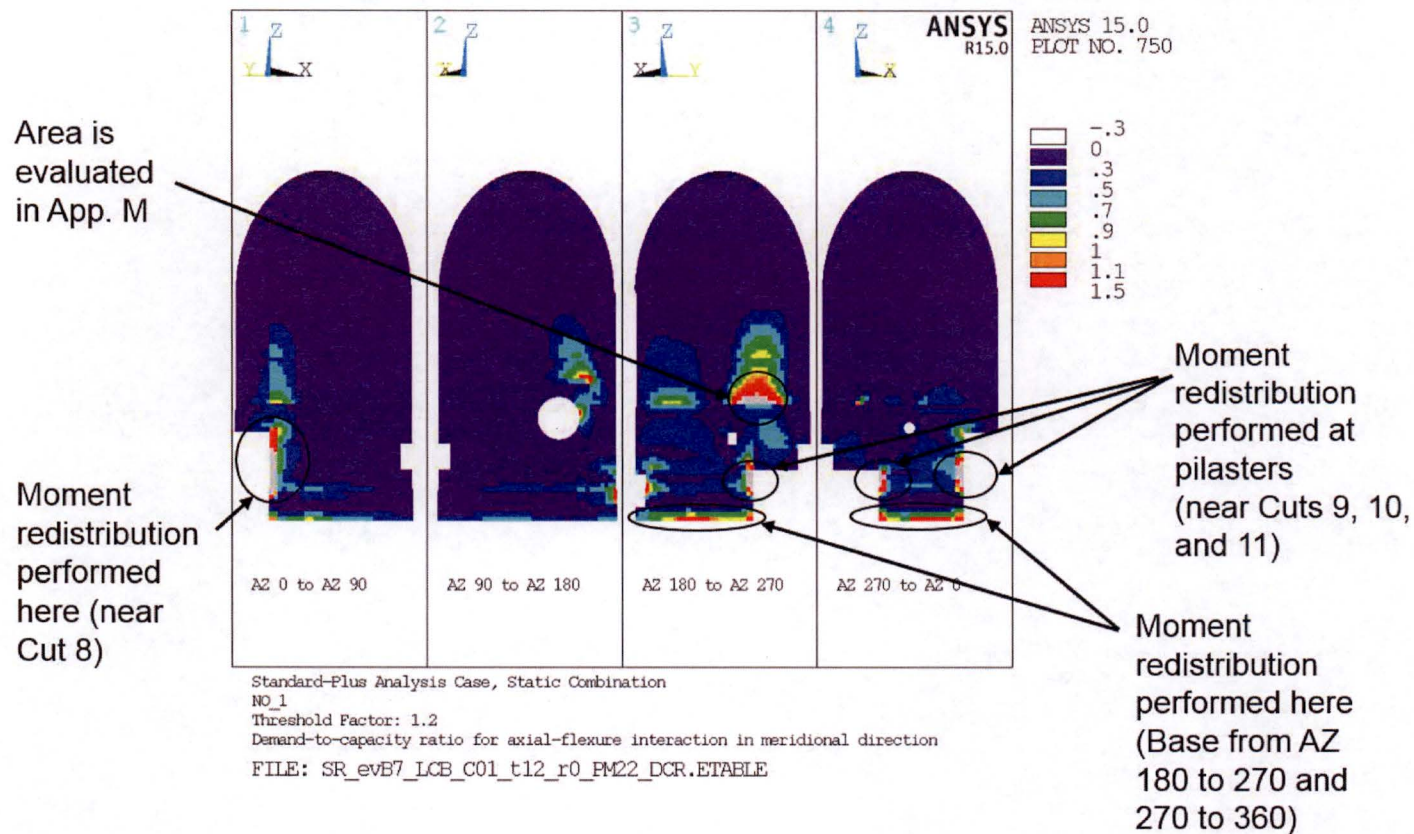


Figure H31. Contours of DCRs for PM Interaction in the Meridional Direction Prior to Moment Redistribution, Standard-Plus Analysis Case, Static Load Combination NO_1

CLIENT: NextEra Energy Seabrook

SUBJECT: Evaluation and Design Confirmation of As-Deformed CEB

PROJECT NO: 150252

DATE: July 2016

BY: R.M. Mones

VERIFIER: A.T. Sarawit

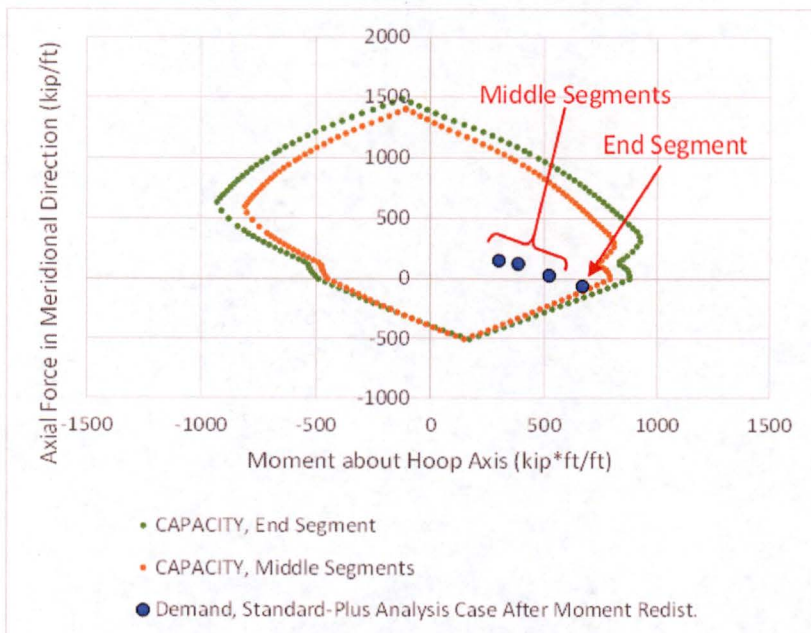
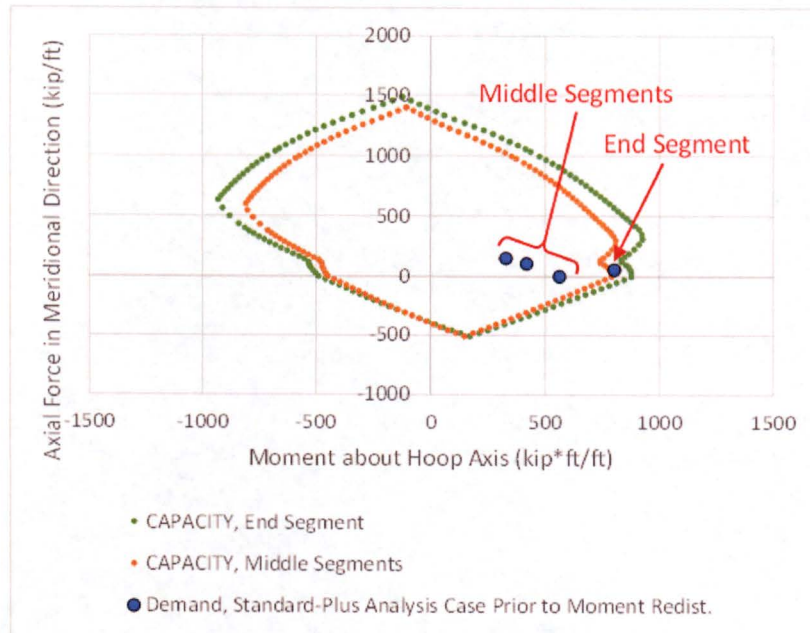


Figure H32. Comparison of PM Interaction Diagrams for Wall Segments along Base between AZ 0 and 90 Before (left) and After (right) Moment Redistribution, Standard-Plus Analysis Case, Static Load Combination NO_1

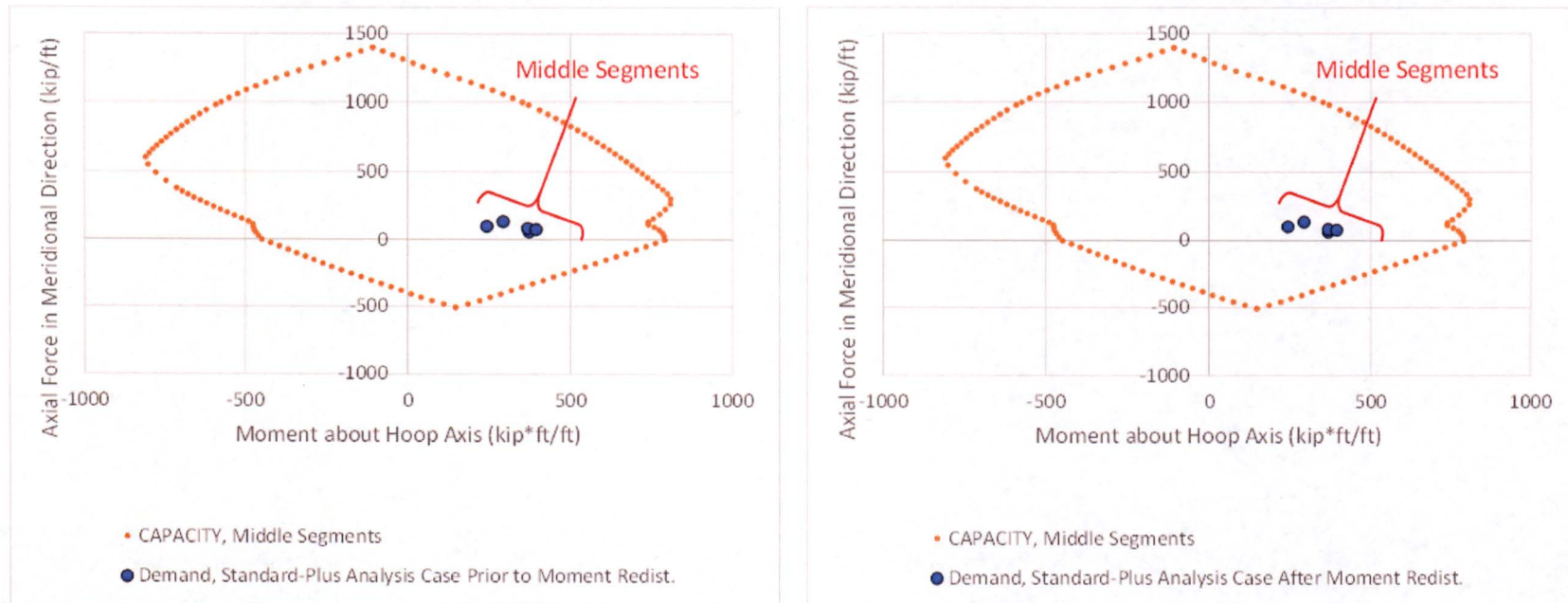


Figure H33. Comparison of PM Interaction Diagrams for Wall Segments along Base between AZ 90 and 180 Before (left) and After (right) Moment Redistribution, Standard-Plus Analysis Case, Static Load Combination NO_1

CLIENT: NextEra Energy Seabrook

SUBJECT: Evaluation and Design Confirmation of As-Deformed CEB

PROJECT NO: 150252

DATE: July 2016

BY: R.M. Mones

VERIFIER: A.T. Sarawit

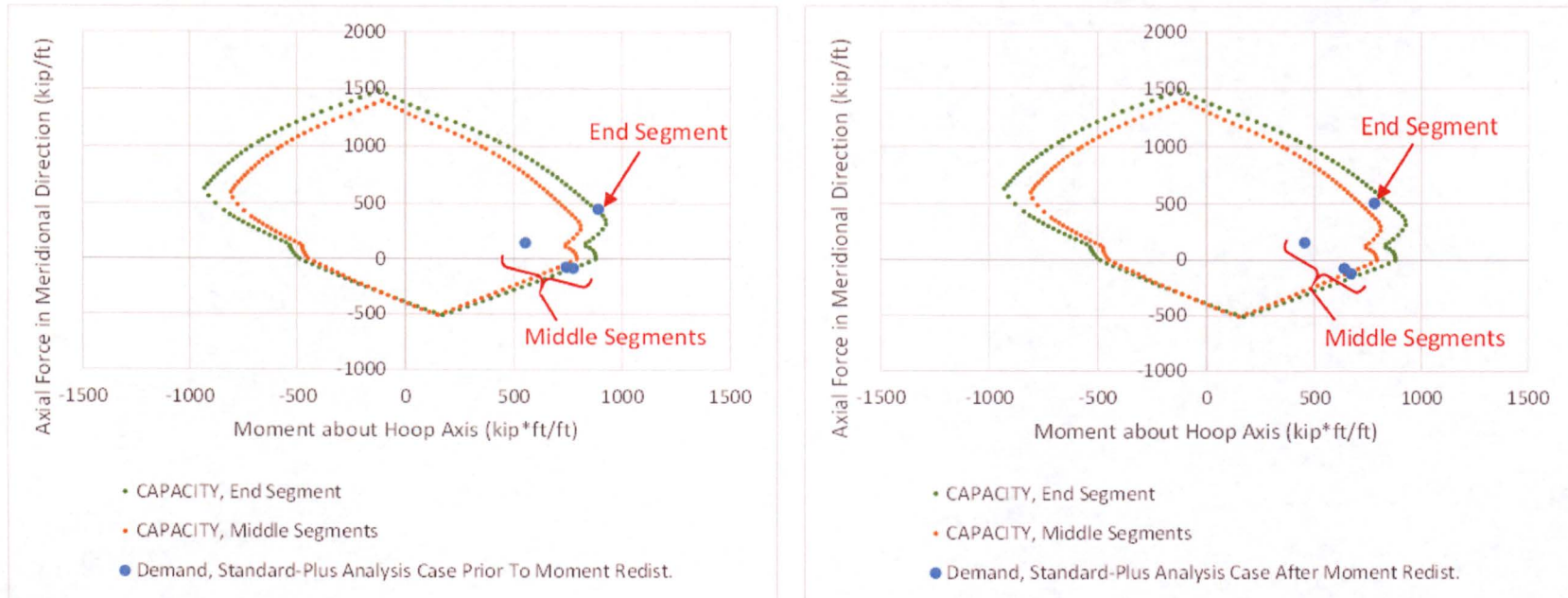


Figure H34. Comparison of PM Interaction Diagrams for Wall Segments along Base between AZ 180 and 270 Before (left) and After (right) Moment Redistribution, Standard-Plus Analysis Case, Static Load Combination NO_1

CLIENT: NextEra Energy Seabrook

SUBJECT: Evaluation and Design Confirmation of As-Deformed CEB

PROJECT NO: 150252

DATE: July 2016

BY: R.M. Mones

VERIFIER: A.T. Sarawit

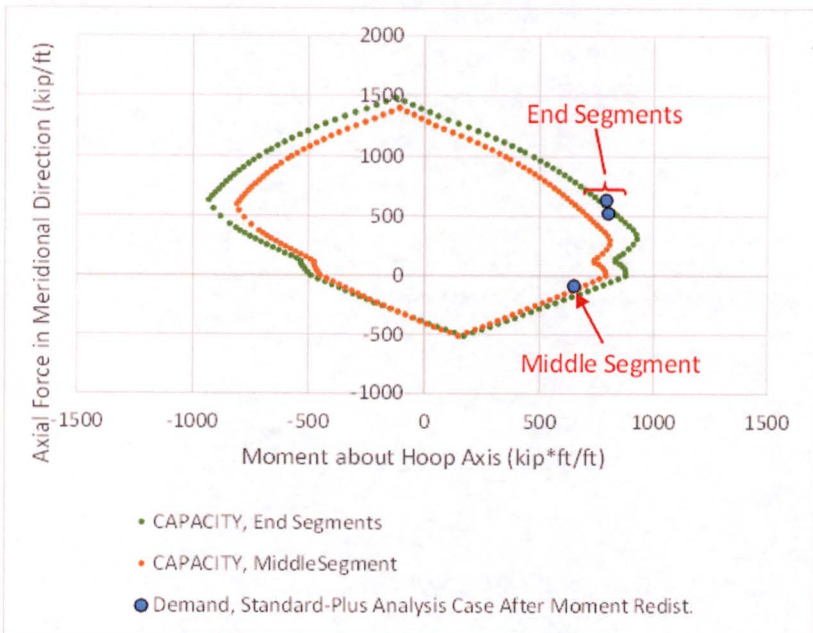
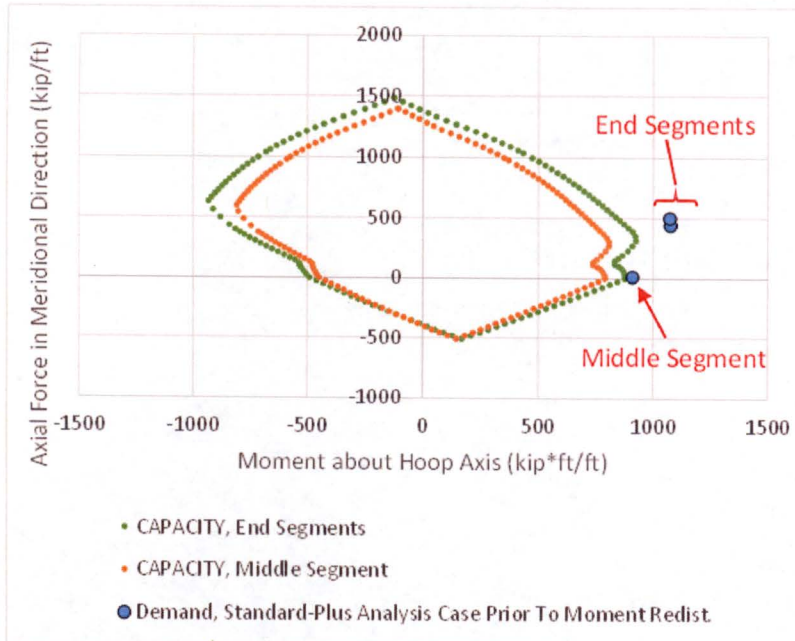


Figure H35. Comparison of PM Interaction Diagrams for Wall Segments along Base between AZ 270 and 360 Before (left) and After (right) Moment Redistribution, Standard-Plus Analysis Case, Static Load Combination NO_1

CLIENT: NextEra Energy Seabrook

SUBJECT: Evaluation and Design Confirmation of As-Deformed CEB

PROJECT NO: 150252

DATE: July 2016

BY: R.M. Mones

VERIFIER: A.T. Sarawit

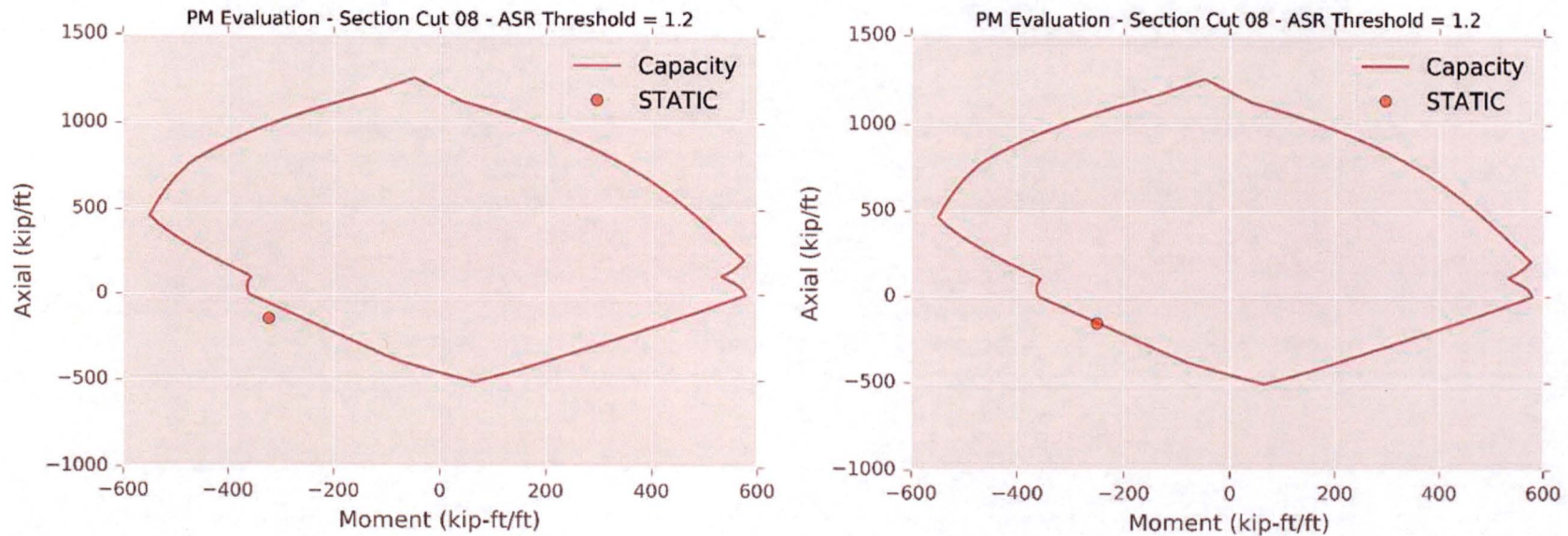


**Figure H36. Comparison of PM Interaction Diagrams for Section 8
Before (left) and After (right) Moment Redistribution,
Standard-Plus Analysis Case, Static Load Combination NO_1**

CLIENT: NextEra Energy Seabrook

SUBJECT: Evaluation and Design Confirmation of As-Deformed CEB

PROJECT NO: 150252

DATE: July 2016

BY: R.M. Mones

VERIFIER: A.T. Sarawit

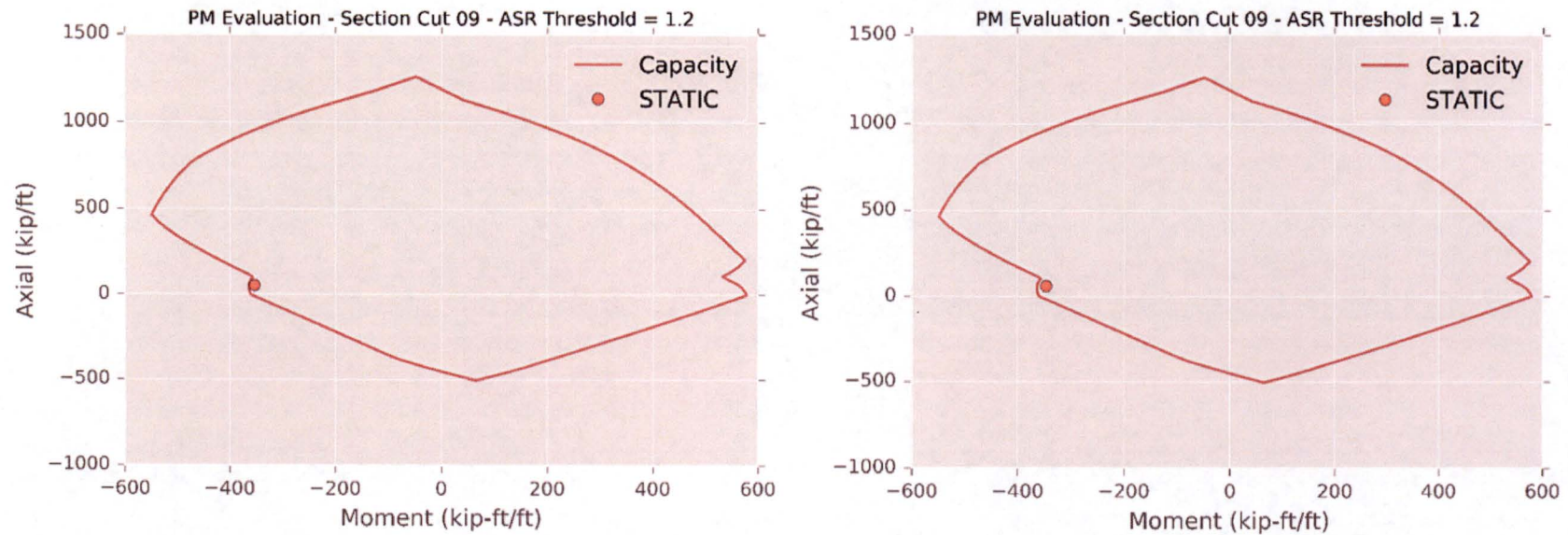


**Figure H37. Comparison of PM Interaction Diagrams for Section 9
Before (left) and After (right) Moment Redistribution,
Standard-Plus Analysis Case, Static Load Combination NO_1**

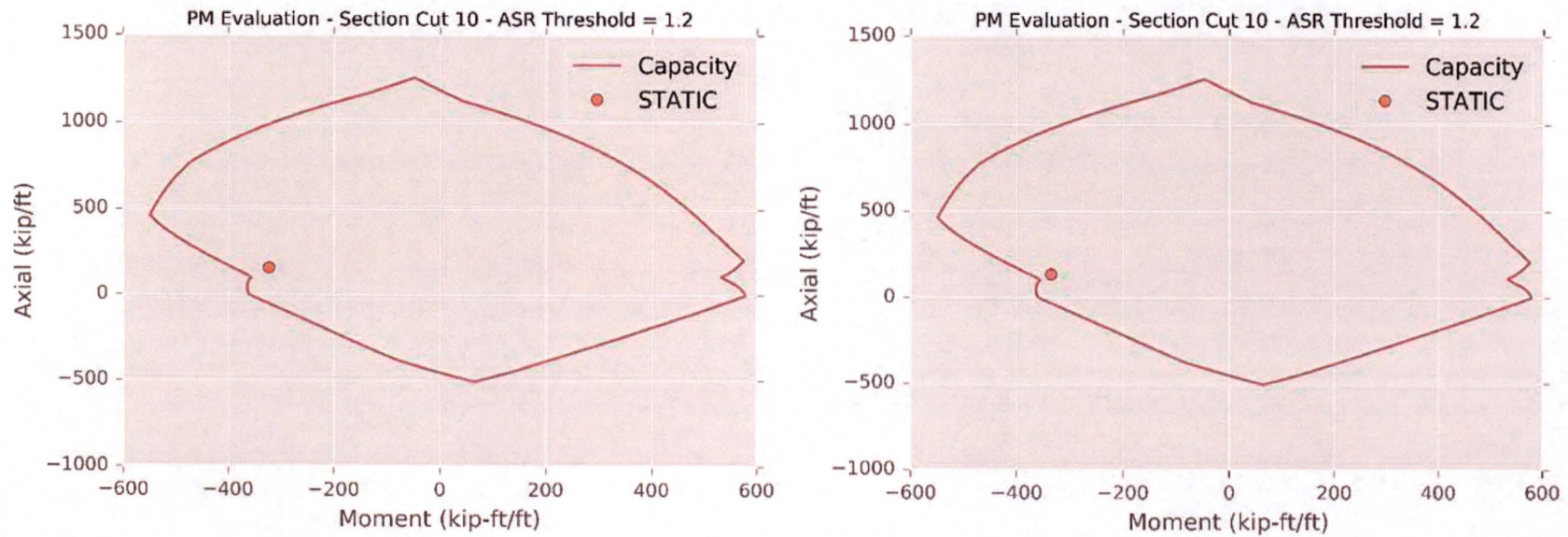


**Figure H38. Comparison of PM Interaction Diagrams for Section 10
Before (left) and After (right) Moment Redistribution,
Standard-Plus Analysis Case, Static Load Combination NO_1**

CLIENT: NextEra Energy Seabrook

SUBJECT: Evaluation and Design Confirmation of As-Deformed CEB

PROJECT NO: 150252

DATE: July 2016

BY: R.M. Mones

VERIFIER: A.T. Sarawit

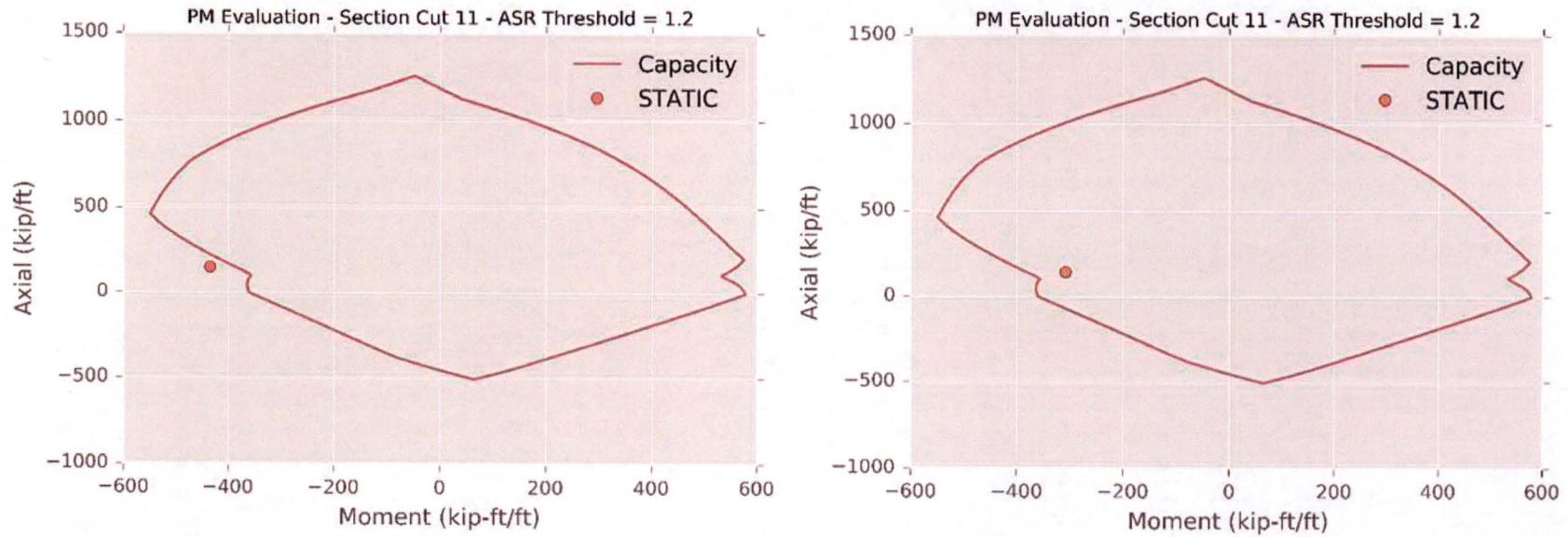


**Figure H39. Comparison of PM Interaction Diagrams for Section 11
Before (left) and After (right) Moment Redistribution,
Standard-Plus Analysis Case, Static Load Combination NO_1**

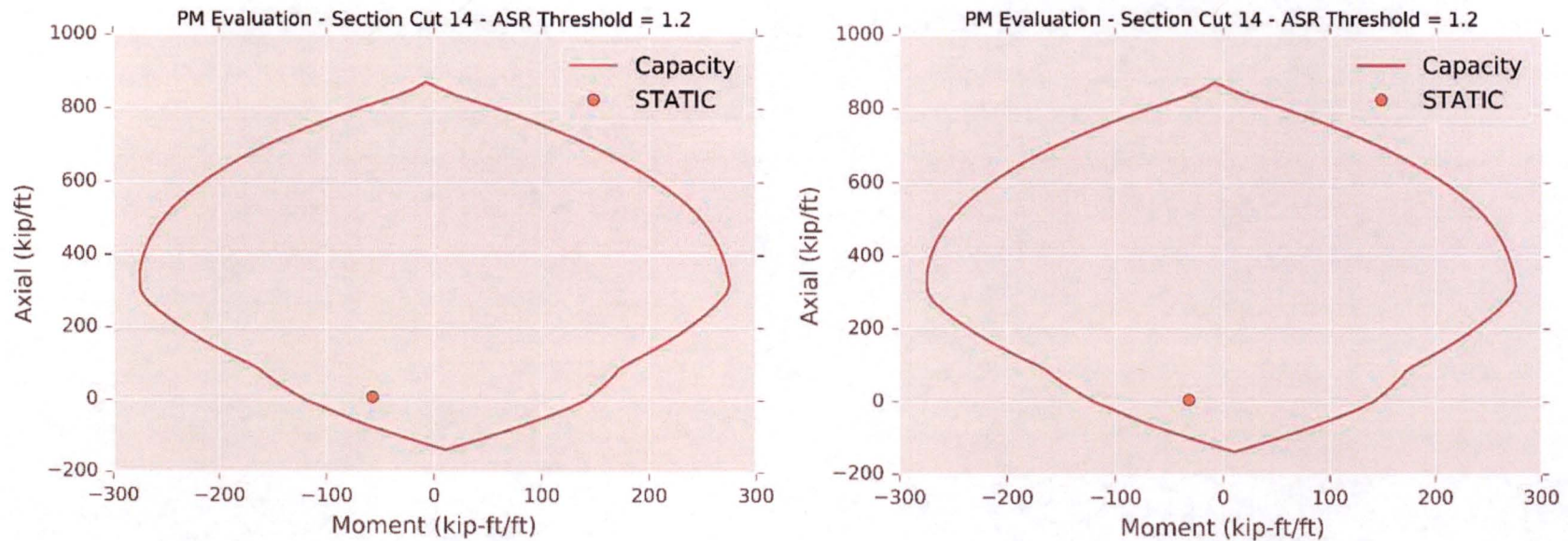


**Figure H40. Comparison of PM Interaction Diagrams for Section 14
Before (left) and After (right) Moment Redistribution,
Standard-Plus Analysis Case, Static Load Combination NO_1**

CLIENT: NextEra Energy Seabrook

SUBJECT: Evaluation and Design Confirmation of As-Deformed CEB

PROJECT NO: 150252

DATE: July 2016

BY: R.M. Mones

VERIFIER: A.T. Sarawit

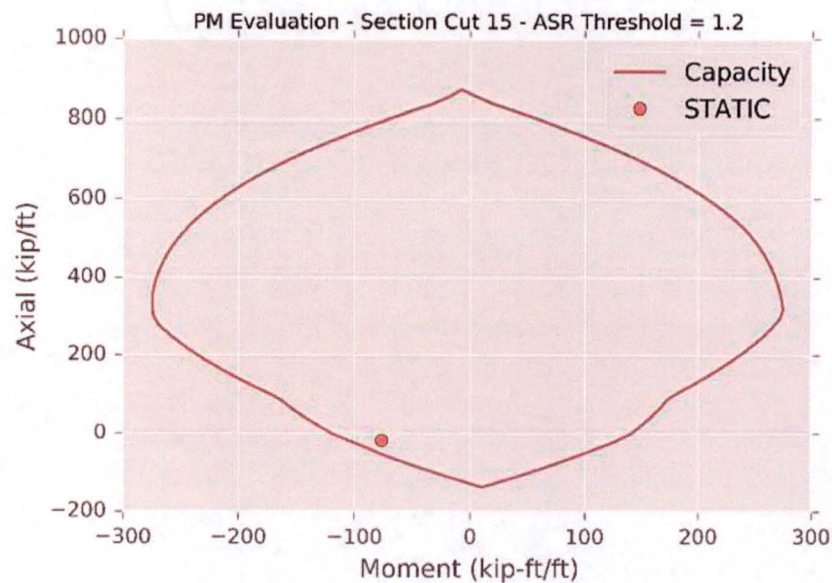
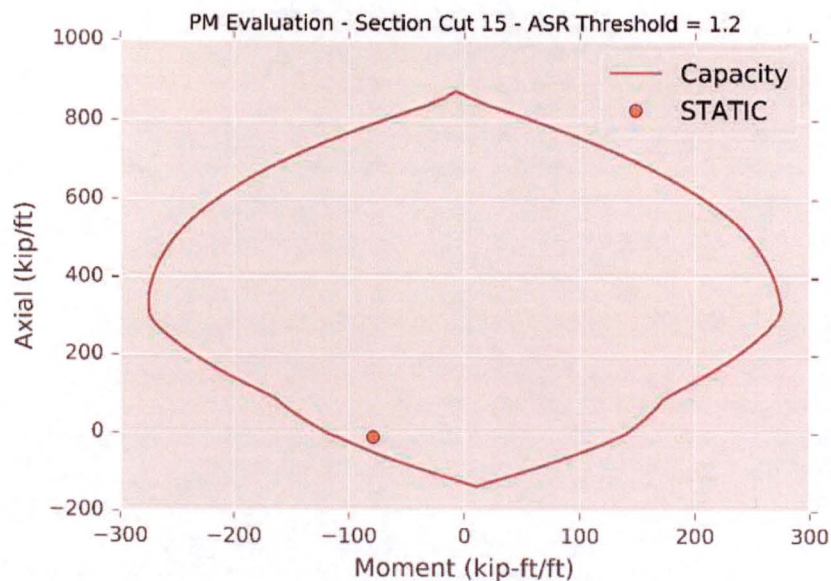


**Figure H41. Comparison of PM Interaction Diagrams for Section 15
Before (left) and After (right) Moment Redistribution,
Standard-Plus Analysis Case, Static Load Combination NO_1**

CLIENT: NextEra Energy Seabrook

SUBJECT: Evaluation and Design Confirmation of As-Deformed CEB

PROJECT NO: 150252

DATE: July 2016

BY: R.M. Mones

VERIFIER: A.T. Sarawit

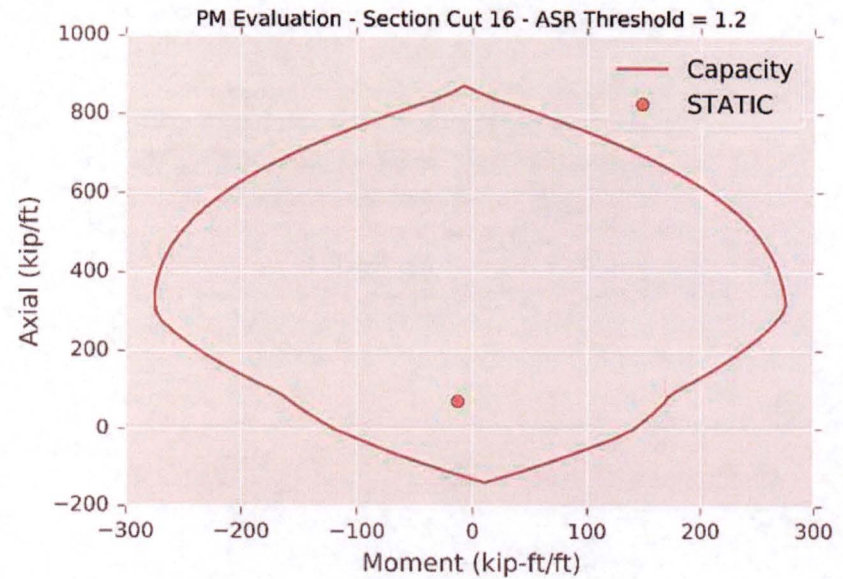
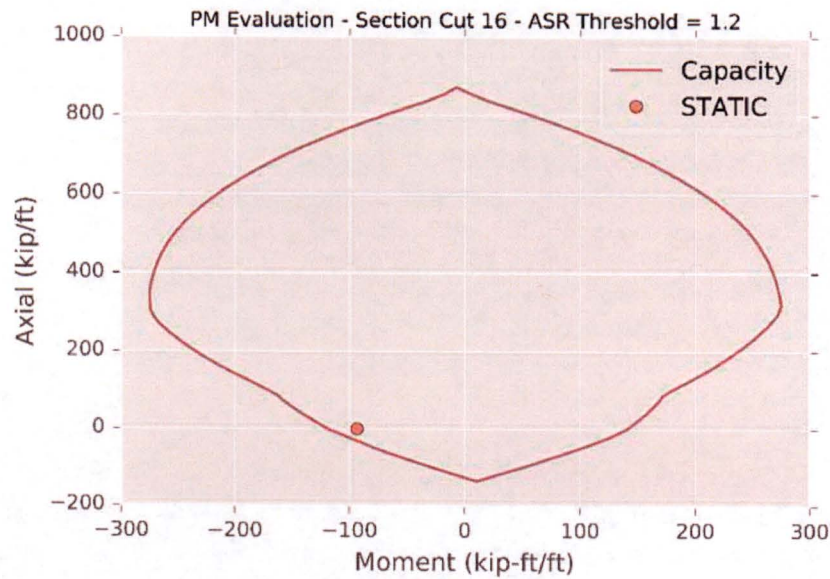


**Figure H42. Comparison of PM Interaction Diagrams for Section 16
Before (left) and After (right) Moment Redistribution,
Standard-Plus Analysis Case, Static Load Combination NO_1**

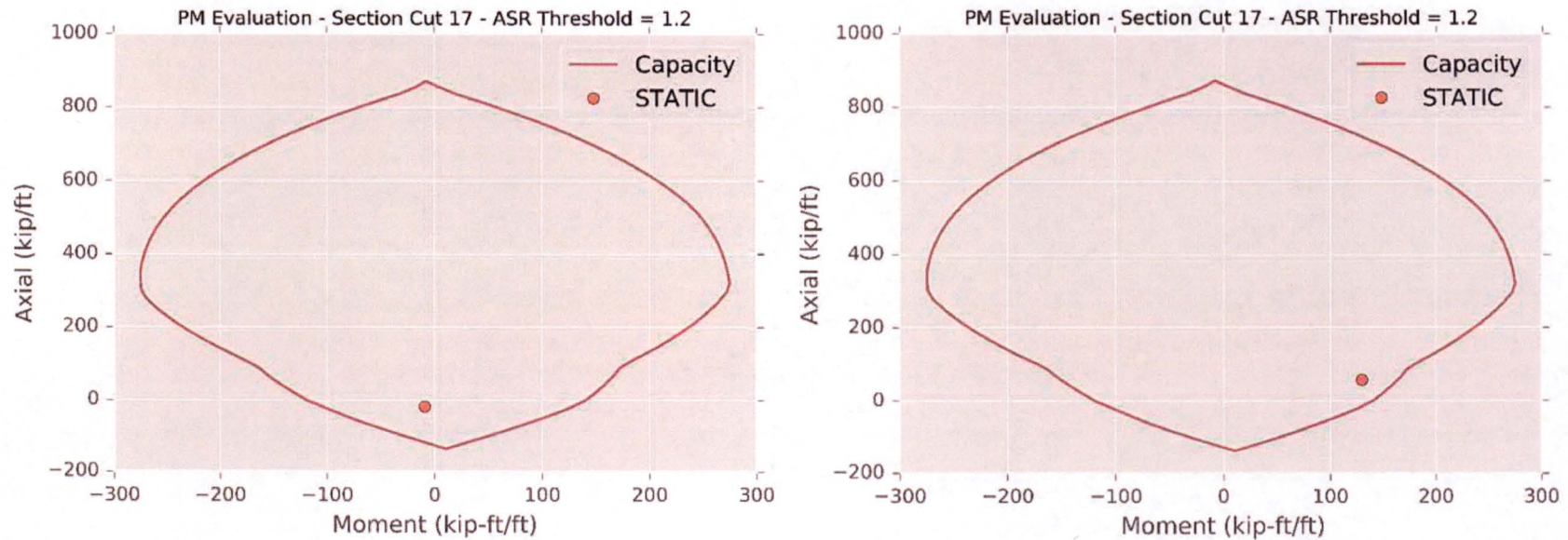


**Figure H43. Comparison of PM Interaction Diagrams for Section 17
Before (left) and After (right) Moment Redistribution,
Standard-Plus Analysis Case, Static Load Combination NO_1**

CLIENT: NextEra Energy Seabrook

SUBJECT: Evaluation and Design Confirmation of As-Deformed CEB

PROJECT NO: 150252

DATE: July 2016

BY: R.M. Mones

VERIFIER: A.T. Sarawit

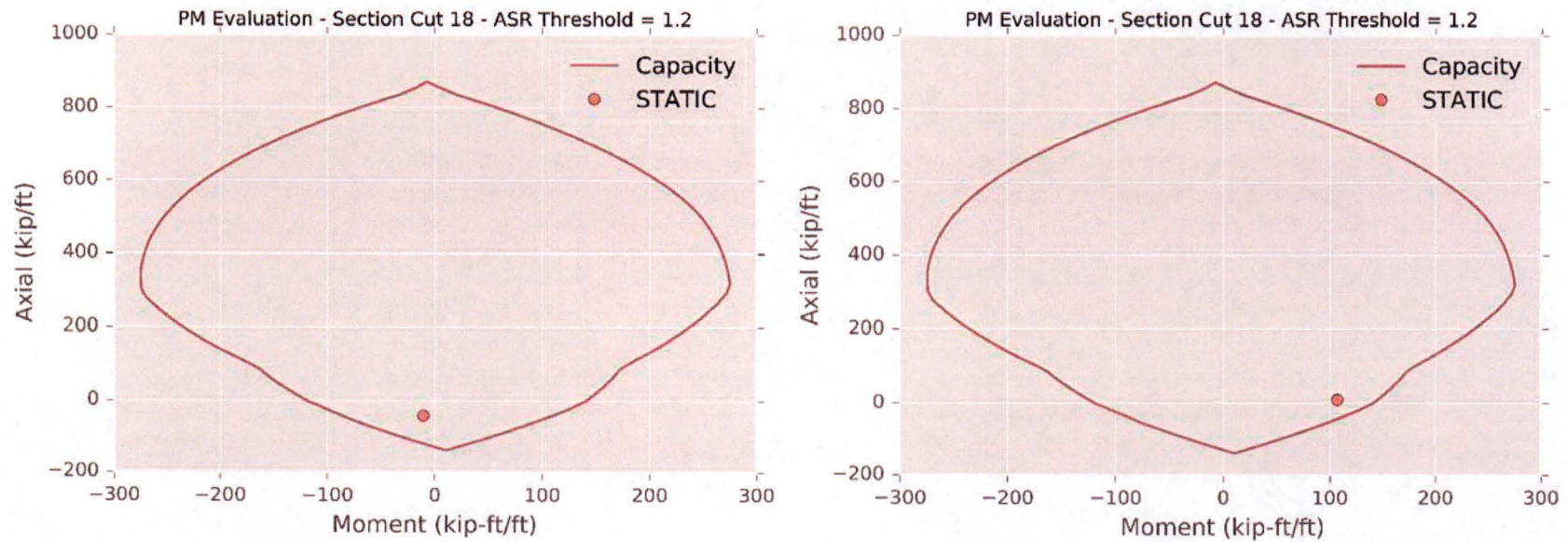


**Figure H44. Comparison of PM Interaction Diagrams for Section 18
Before (left) and After (right) Moment Redistribution,
Standard-Plus Analysis Case, Static Load Combination NO_1**

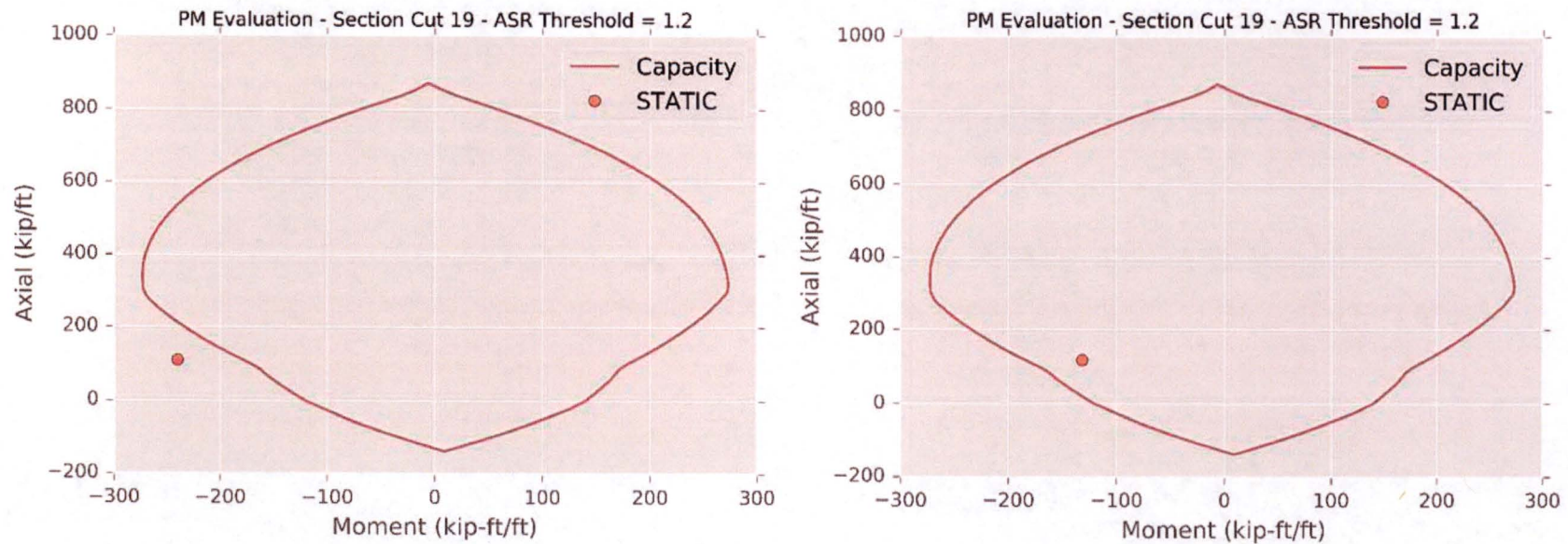


**Figure H45. Comparison of PM Interaction Diagrams for Section 19
Before (left) and After (right) Moment Redistribution,
Standard-Plus Analysis Case, Static Load Combination NO_1**

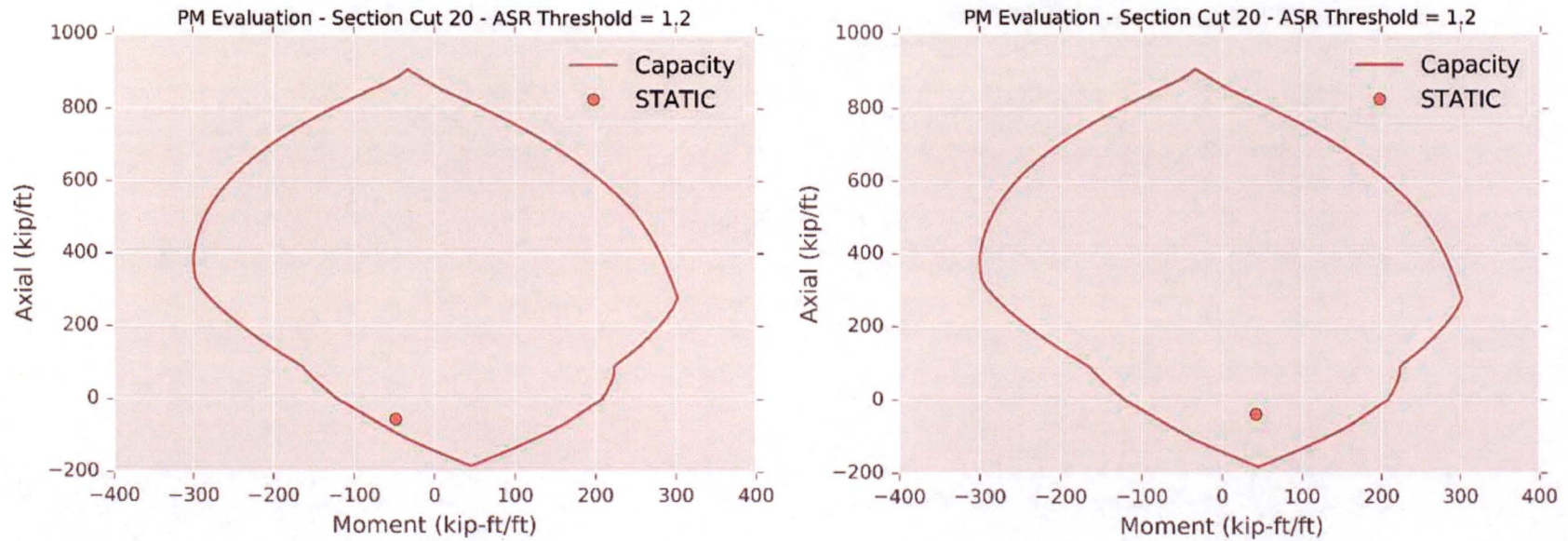


**Figure H46. Comparison of PM Interaction Diagrams for Section 20
Before (left) and After (right) Moment Redistribution,
Standard-Plus Analysis Case, Static Load Combination NO_1**

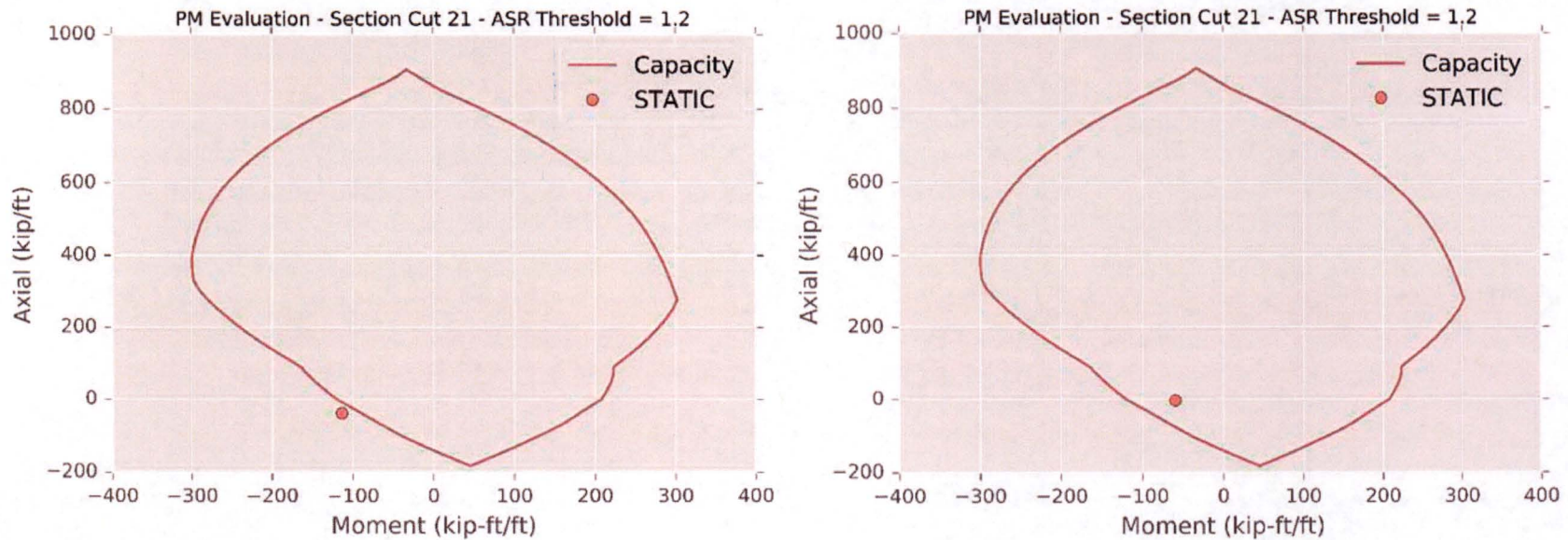


**Figure H47. Comparison of PM Interaction Diagrams for Section 21
Before (left) and After (right) Moment Redistribution,
Standard-Plus Analysis Case, Static Load Combination NO_1**

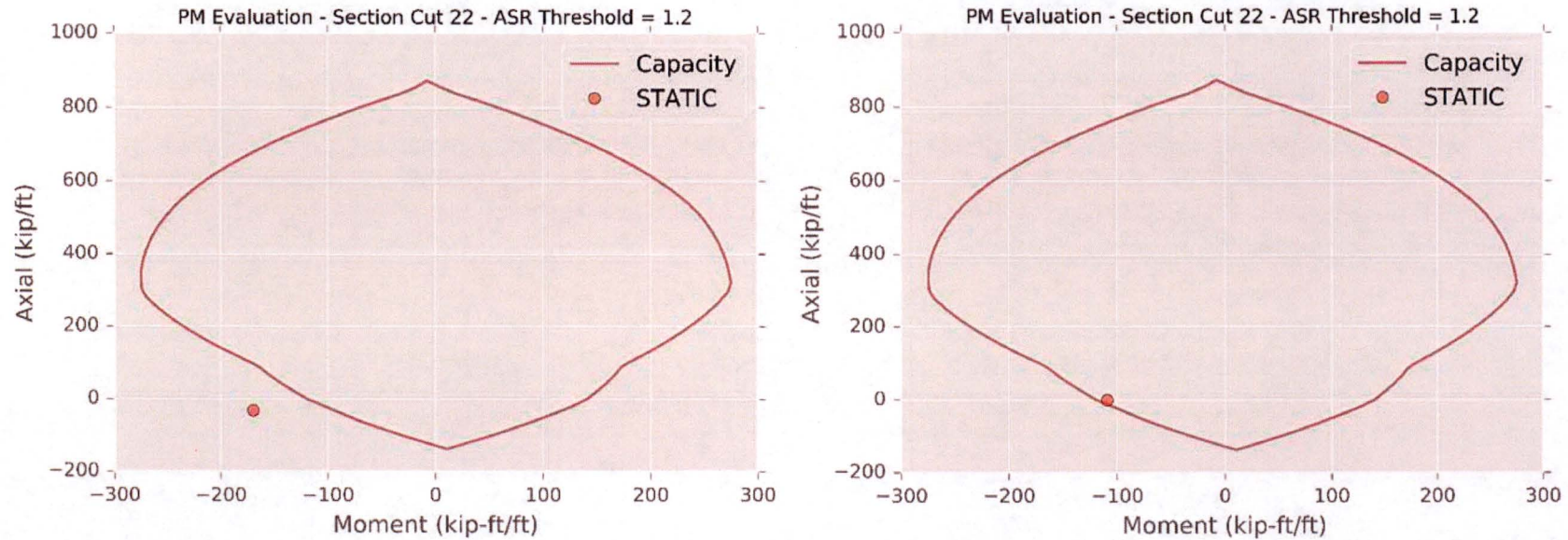


**Figure H48. Comparison of PM Interaction Diagrams for Section 22
Before (left) and After (right) Moment Redistribution,
Standard-Plus Analysis Case, Static Load Combination NO_1**

CLIENT: NextEra Energy Seabrook

SUBJECT: Evaluation and Design Confirmation of As-Deformed CEB

PROJECT NO: 150252

DATE: July 2016

BY: R.M. Mones

VERIFIER: A.T. Sarawit

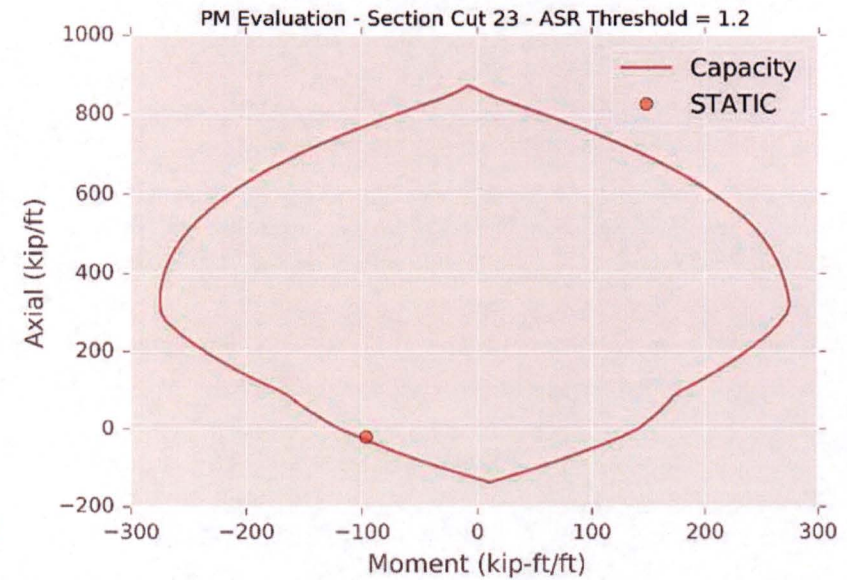
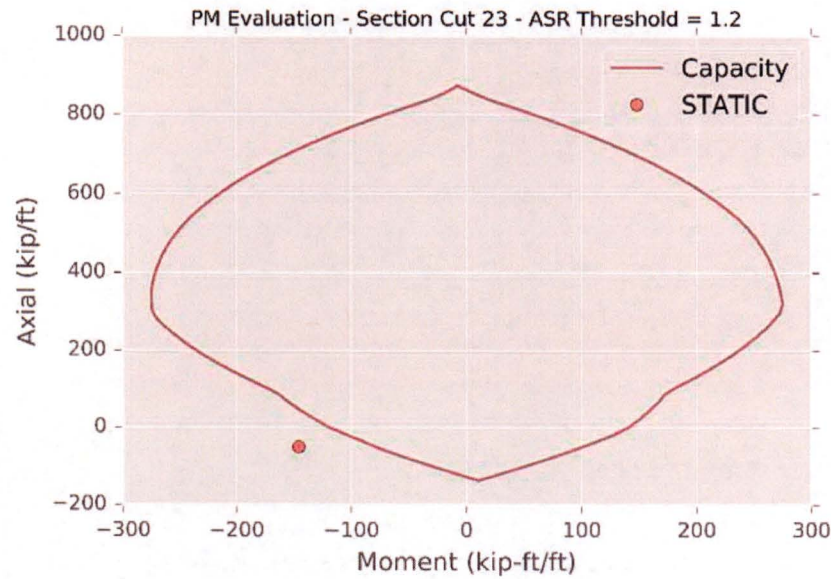


**Figure H49. Comparison of PM Interaction Diagrams for Section 23
Before (left) and After (right) Moment Redistribution,
Standard-Plus Analysis Case, Static Load Combination NO_1**

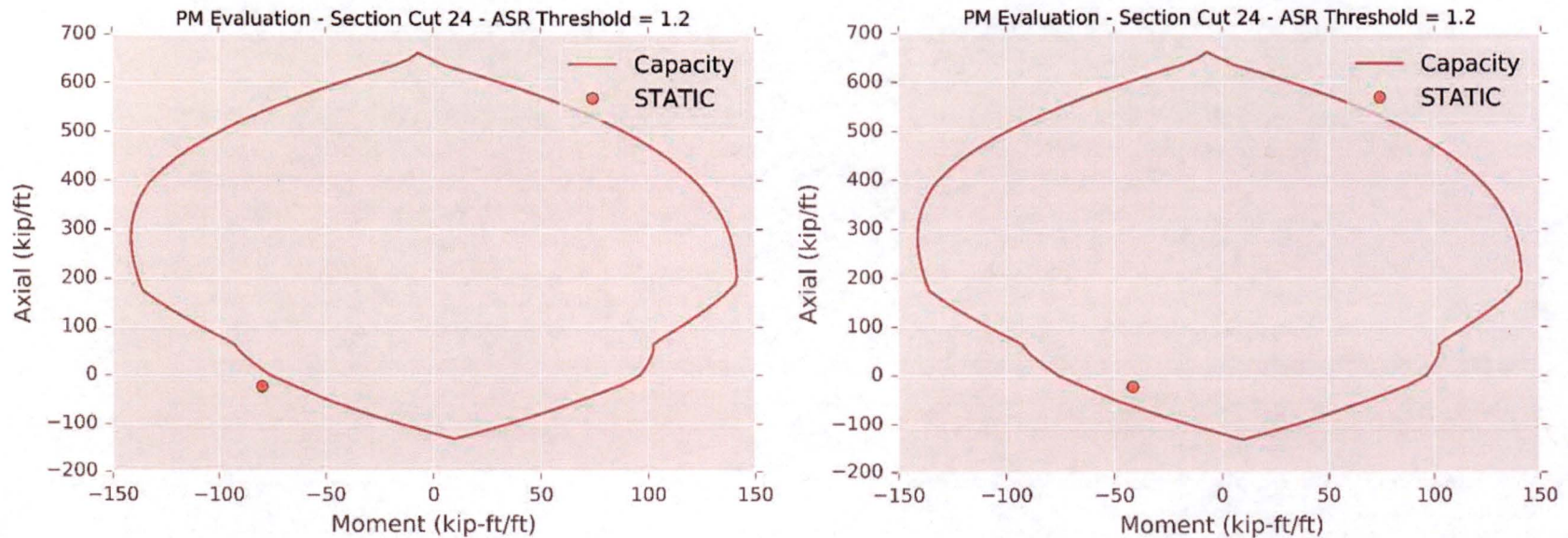


**Figure H50. Comparison of PM Interaction Diagrams for Section 24
Before (left) and After (right) Moment Redistribution,
Standard-Plus Analysis Case, Static Load Combination NO_1**

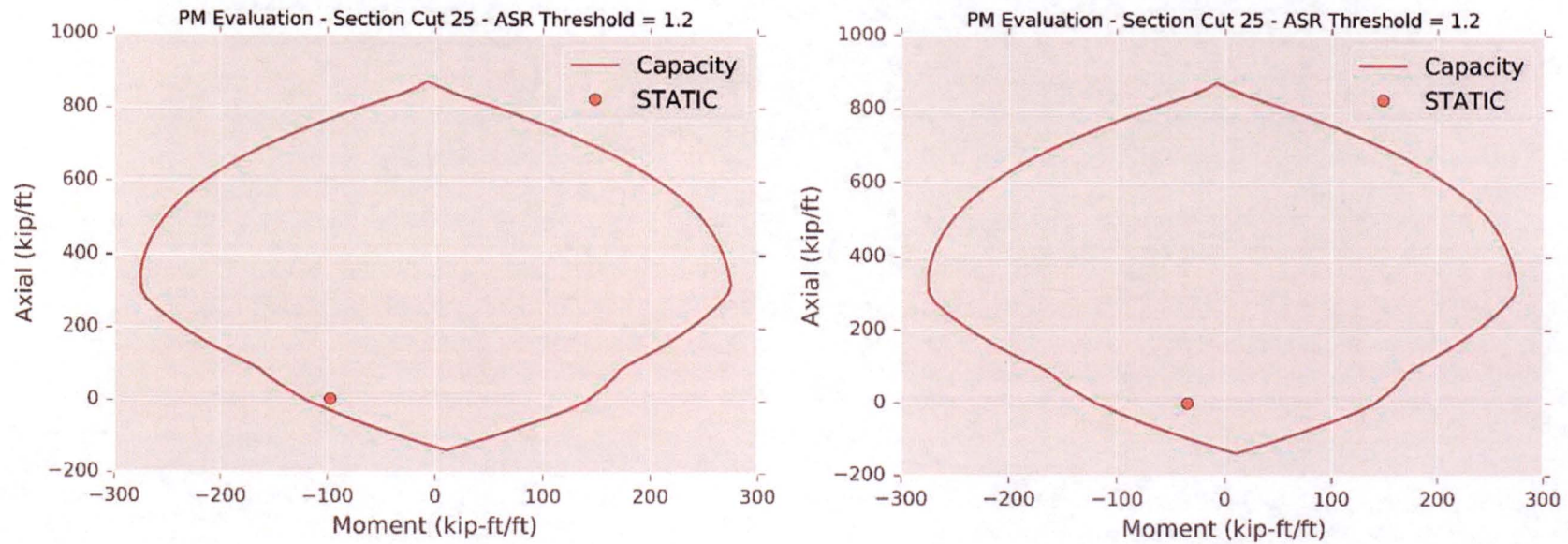


**Figure H51. Comparison of PM Interaction Diagrams for Section 25
Before (left) and After (right) Moment Redistribution,
Standard-Plus Analysis Case, Static Load Combination NO_1**

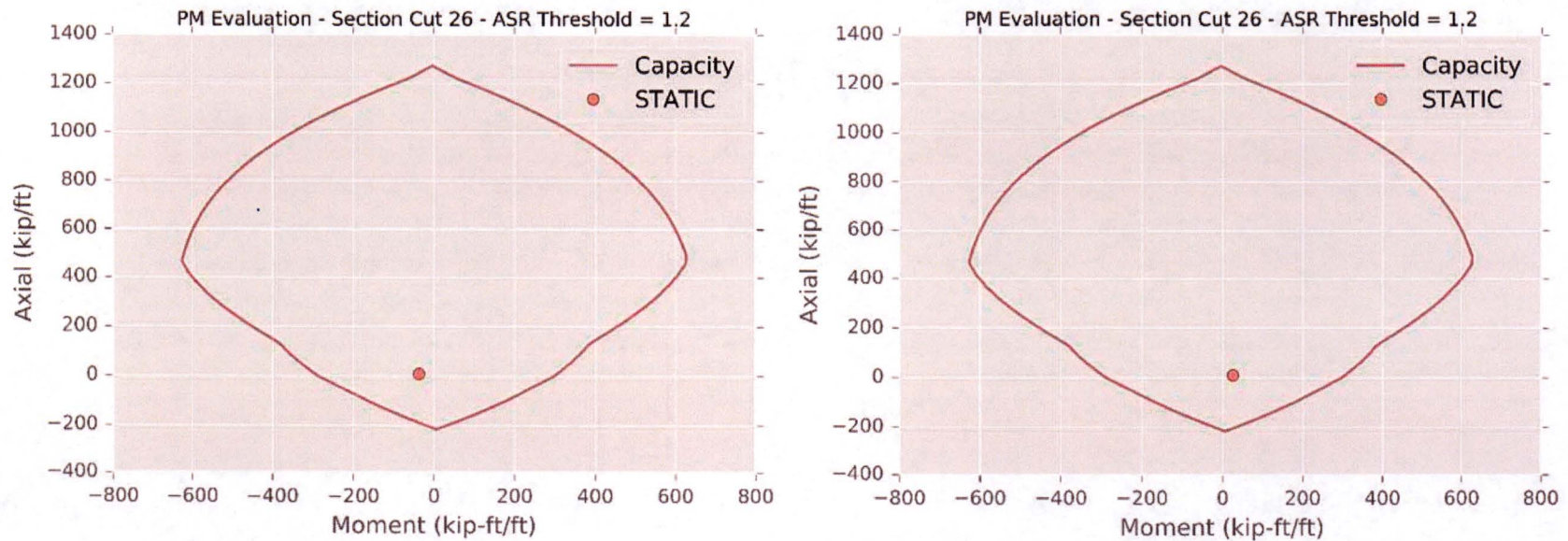


**Figure H52. Comparison of PM Interaction Diagrams for Section 26
Before (left) and After (right) Moment Redistribution,
Standard-Plus Analysis Case, Static Load Combination NO_1**

CLIENT: NextEra Energy Seabrook

SUBJECT: Evaluation and Design Confirmation of As-Deformed CEB

PROJECT NO: 150252

DATE: July 2016

BY: R.M. Mones

VERIFIER: A.T. Sarawit

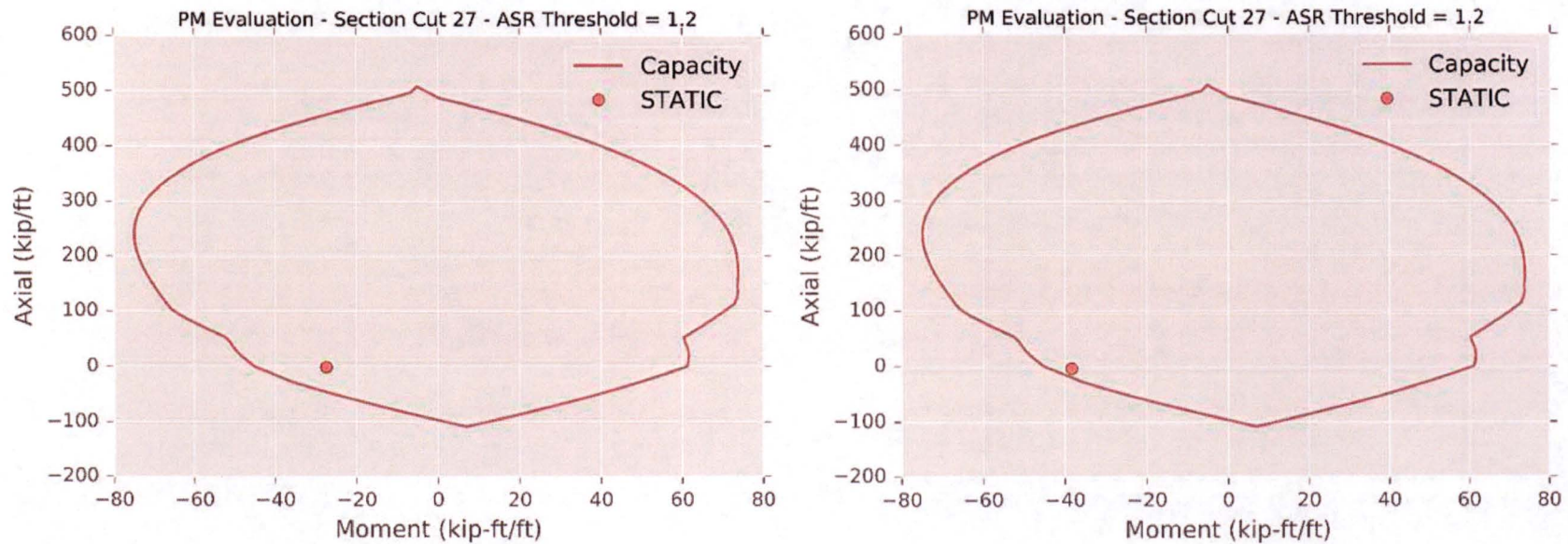
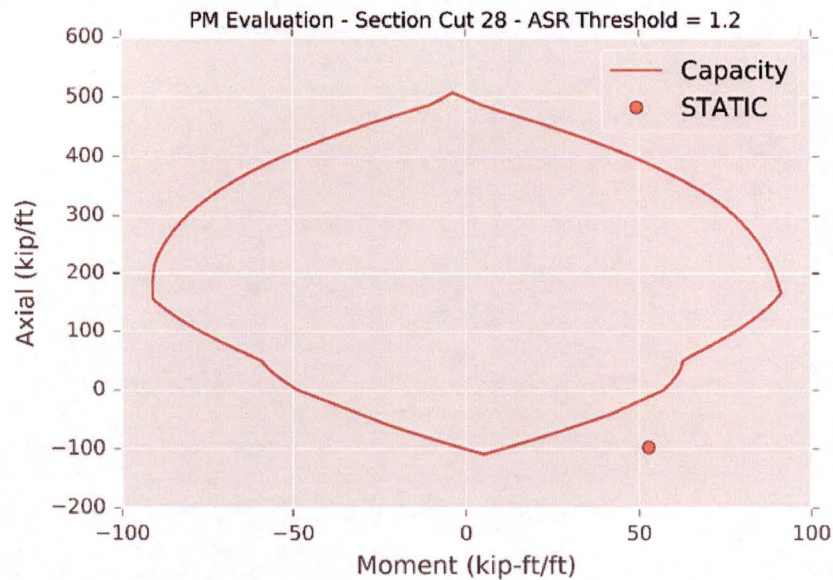


**Figure H53. Comparison of PM Interaction Diagrams for Section 27
Before (left) and After (right) Moment Redistribution,
Standard-Plus Analysis Case, Static Load Combination NO_1**



See Appendix M for
evaluation of this section cut

**Figure H54. Comparison of PM Interaction Diagrams for Section 28
Before (left) and After (right) Moment Redistribution,
Standard-Plus Analysis Case, Static Load Combination NO_1**

CLIENT: NextEra Energy Seabrook

SUBJECT: Evaluation and Design Confirmation of As-Deformed CEB

PROJECT NO: 150252

DATE: July 2016

BY: R.M. Mones

VERIFIER: A.T. Sarawit

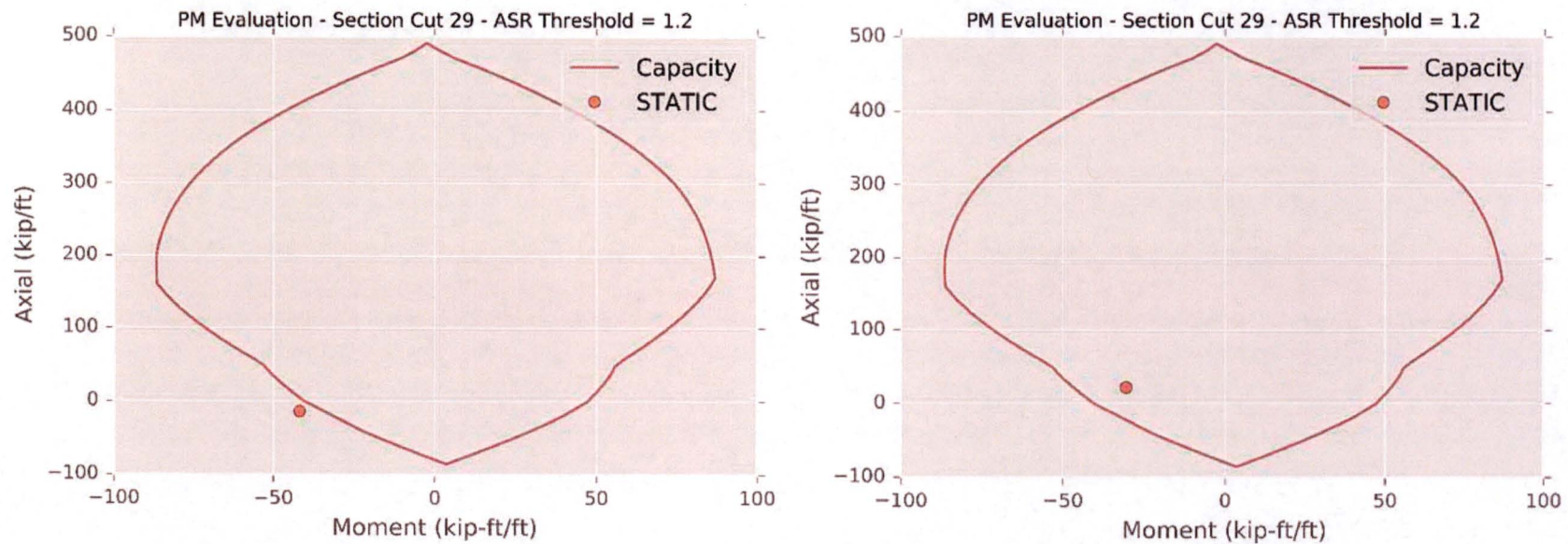


**Figure H55. Comparison of PM Interaction Diagrams for Section 29
Before (left) and After (right) Moment Redistribution,
Standard-Plus Analysis Case, Static Load Combination NO_1**

CLIENT: NextEra Energy Seabrook

SUBJECT: Evaluation and Design Confirmation of As-Deformed CEB

PROJECT NO: 150252

DATE: July 2016

BY: R.M. Mones

VERIFIER: A.T. Sarawit

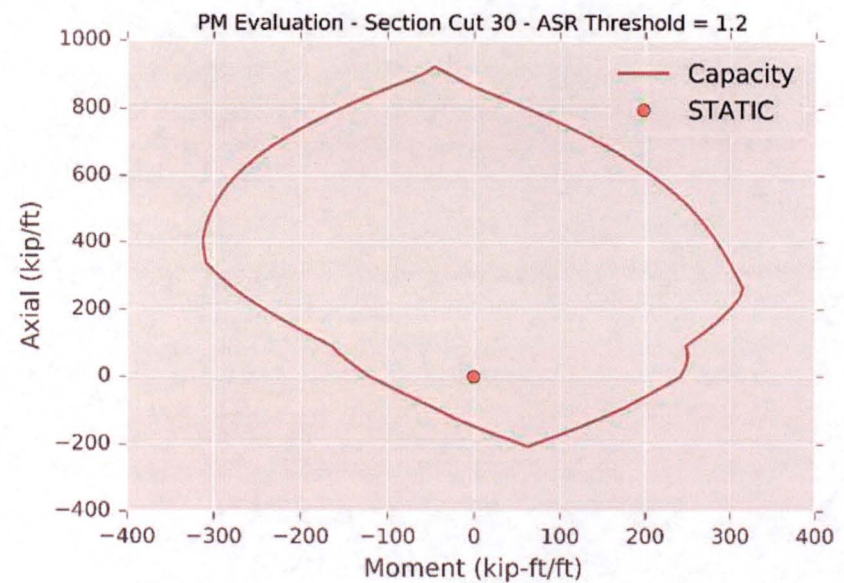
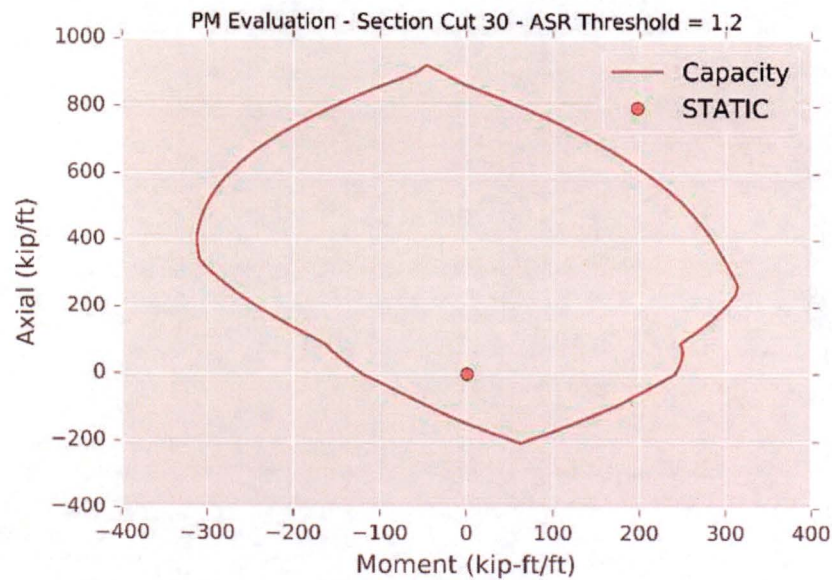


**Figure H56. Comparison of PM Interaction Diagrams for Section 30
Before (left) and After (right) Moment Redistribution,
Standard-Plus Analysis Case, Static Load Combination NO_1**

CLIENT: NextEra Energy Seabrook

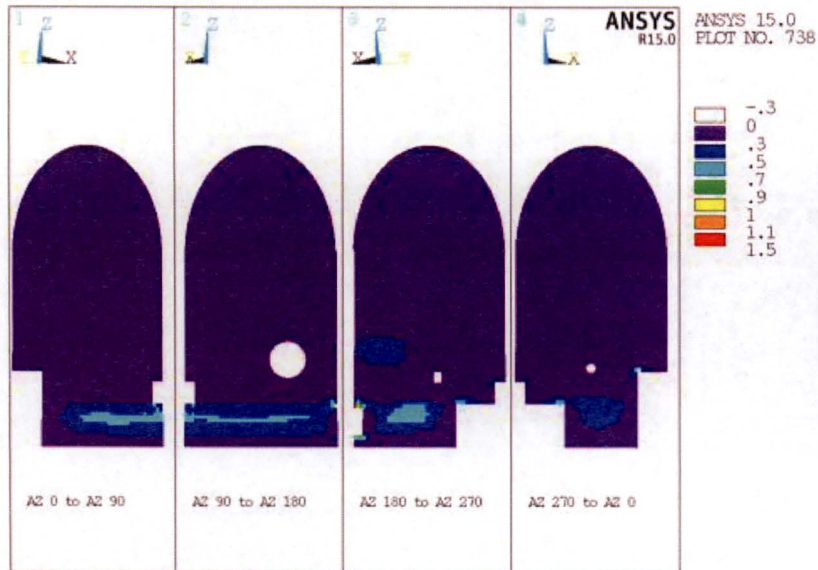
SUBJECT: Evaluation and Design Confirmation of As-Deformed CEB

PROJECT NO: 150252

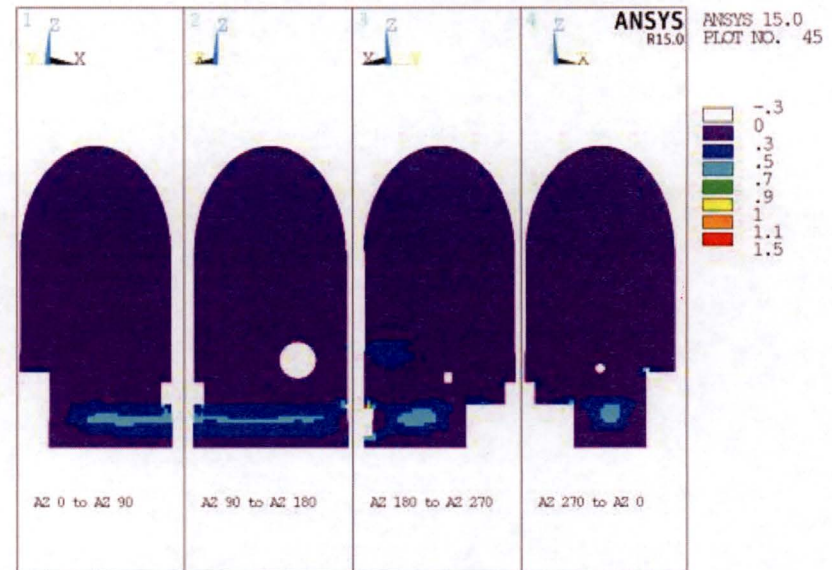
DATE: July 2016

BY: R.M. Mones

VERIFIER: A.T. Sarawit



Standard-Plus Analysis Case, Static Combination
NO_1
Threshold Factor: 1.2
Demand-to-capacity ratio for axial compression in hoop direction
FILE: SR_evE7_LCB_C01_t12_r0_axcDCR11.ETABLE



Standard-Plus Analysis Case w/ Moment Redist., Static Combination
NO_1 (b)
Threshold Factor: 1.2
Demand-to-capacity ratio for axial compression in hoop direction
FILE: SR_evE7_LCB_C02_t12_r0_axcDCR11.ETABLE

**Figure H57. Comparison of DCRs for Axial Compression in the Hoop Direction
Before (left) and After (right) Moment Redistribution,
Standard-Plus Analysis Case, Static Load Combination NO_1**

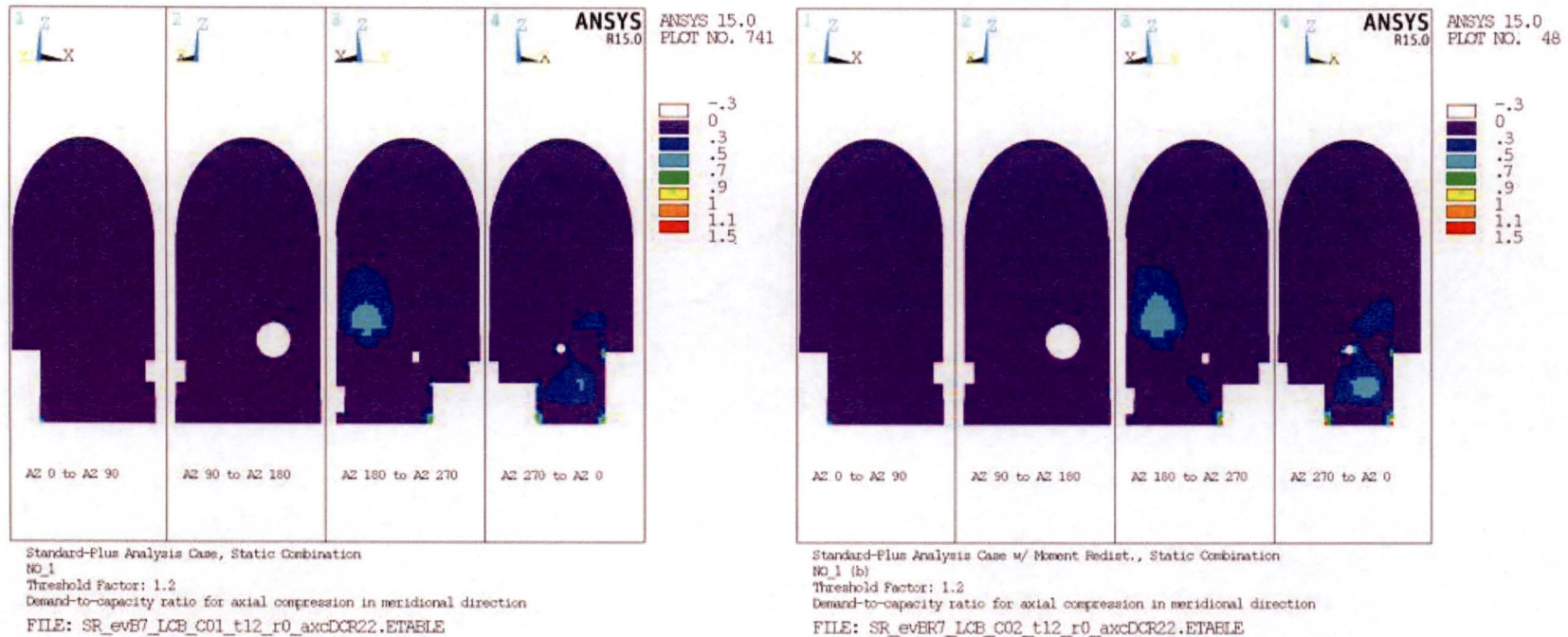


**Figure H58. Comparison of DCRs for Axial Compression in the Meridional Direction
Before (left) and After (right) Moment Redistribution,
Standard-Plus Analysis Case, Static Load Combination NO_1**

CLIENT: NextEra Energy Seabrook

SUBJECT: Evaluation and Design Confirmation of As-Deformed CEB

PROJECT NO: 150252

DATE: July 2016

BY: R.M. Mones

VERIFIER: A.T. Sarawit

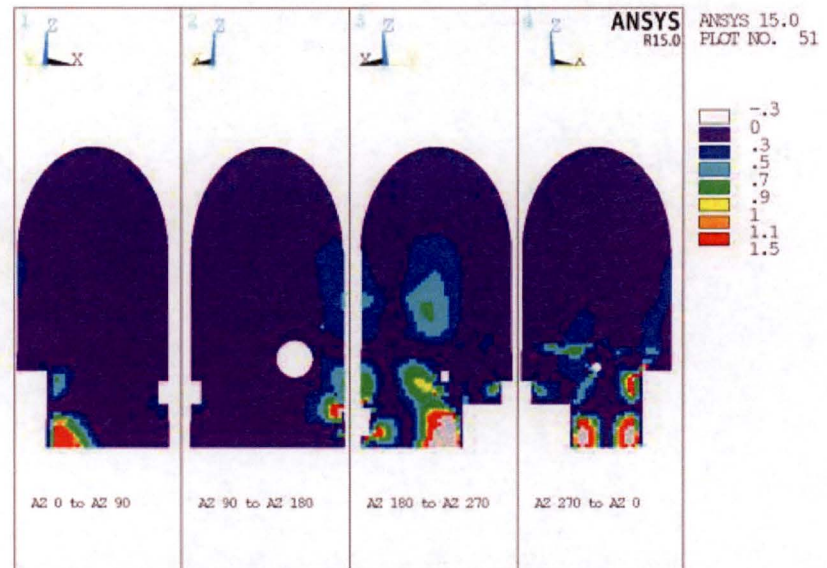
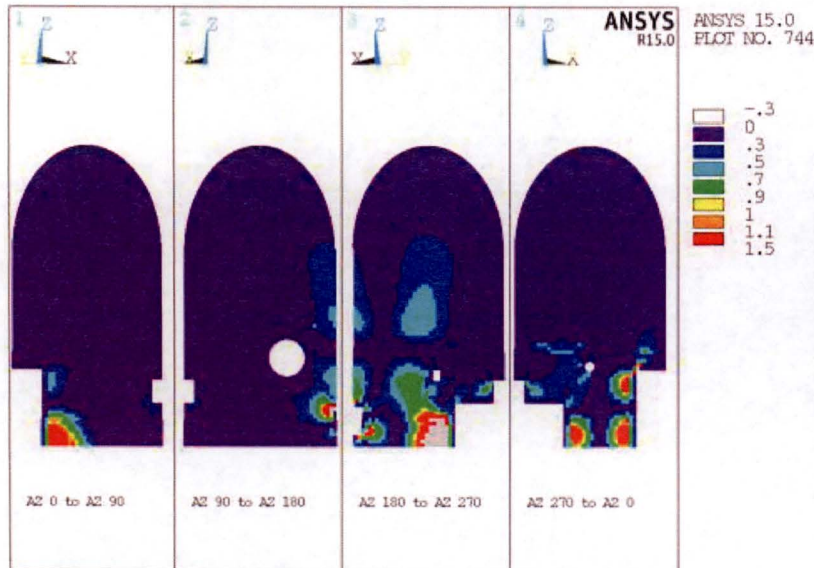


**Figure H59. Comparison of DCRs for In-Plane Shear
Before (left) and After (right) Moment Redistribution,
Standard-Plus Analysis Case, Static Load Combination NO_1**

CLIENT: NextEra Energy Seabrook

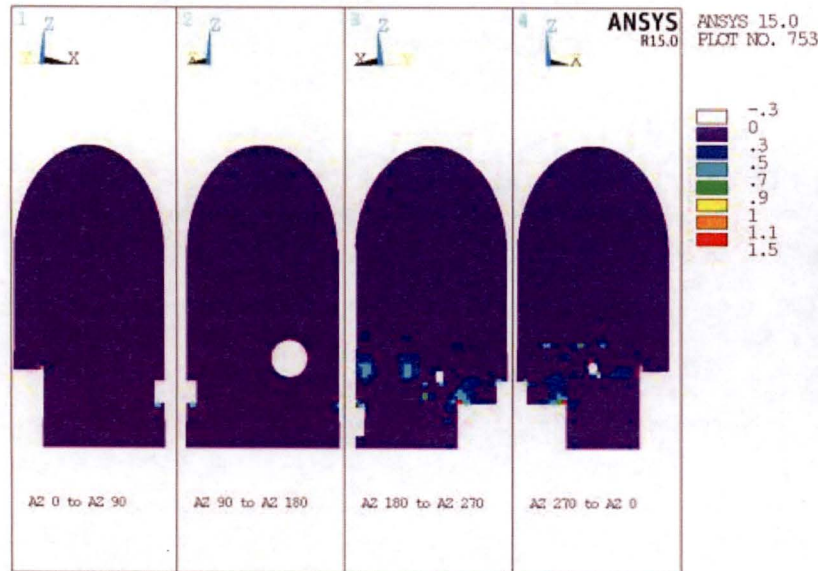
SUBJECT: Evaluation and Design Confirmation of As-Deformed CEB

PROJECT NO: 150252

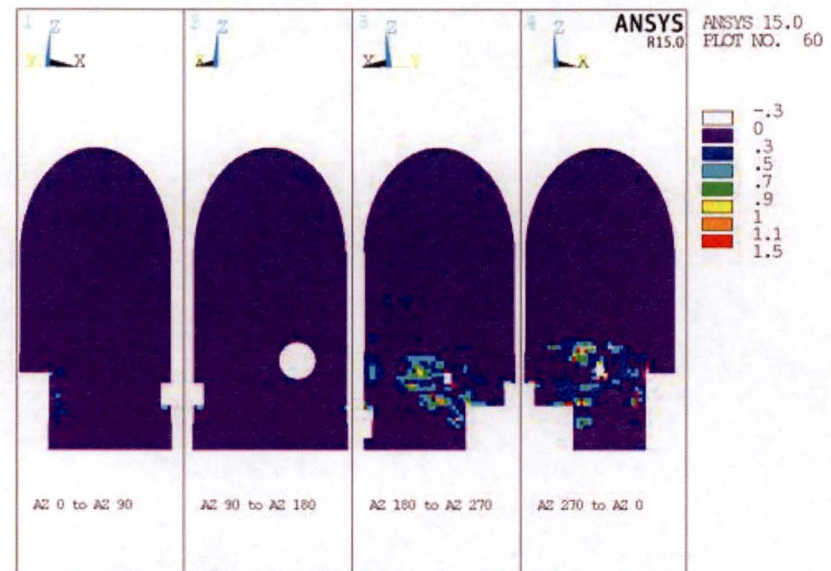
DATE: July 2016

BY: R.M. Mones

VERIFIER: A.T. Sarawit



Standard-Plus Analysis Case, Static Combination
NO_1
Threshold Factor: 1.2
Demand-to-capacity ratio for out-of-plane shear (Q13)
FILE: SR_evB7_LCB_C01_t12_r0_VOP11DCR.ETABLE



Standard-Plus Analysis Case w/ Moment Redist., Static Combination
NO_1 (b)
Threshold Factor: 1.2
Demand-to-capacity ratio for out-of-plane shear (Q13)
FILE: SR_evBR7_LCB_C02_t12_r0_VOP11DCR.ETABLE

**Figure H60. Comparison of DCRs for Out-Of-Plane Shear Acting on Meridional-Radial Plane
Before (left) and After (right) Moment Redistribution,
Standard-Plus Analysis Case, Static Load Combination NO_1**

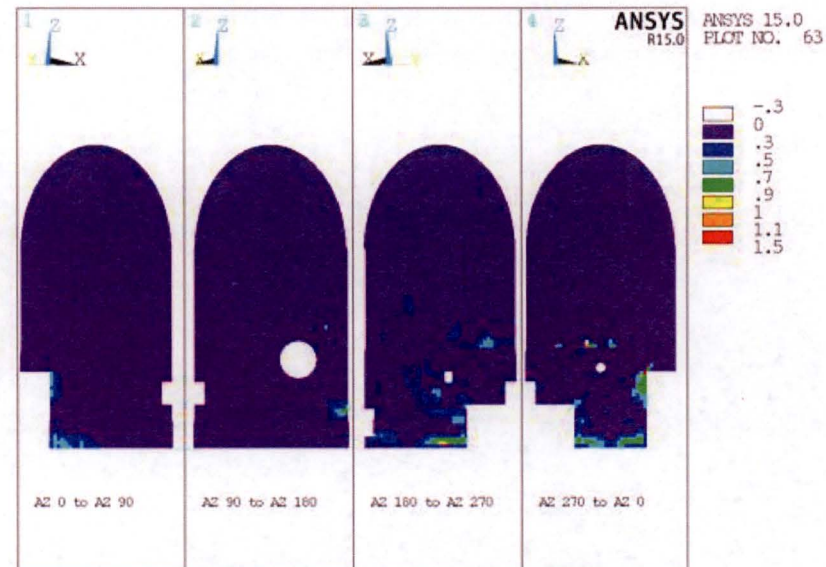
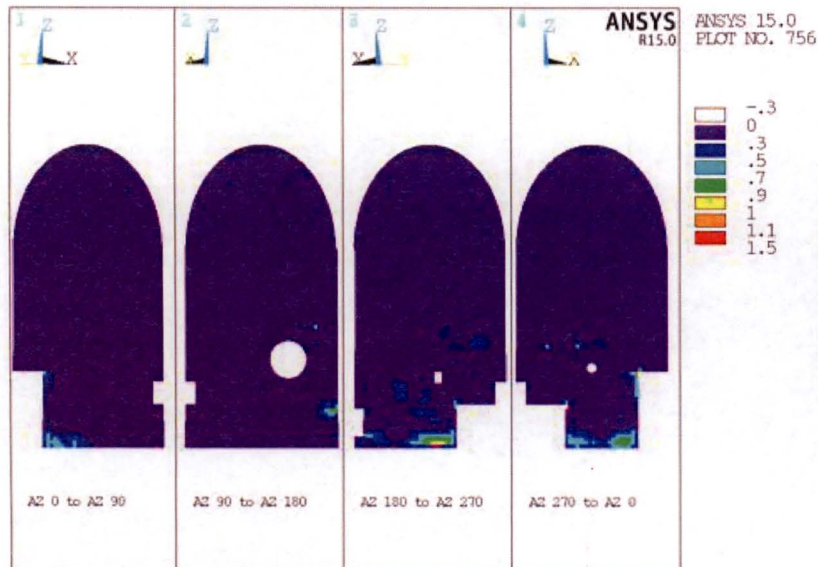
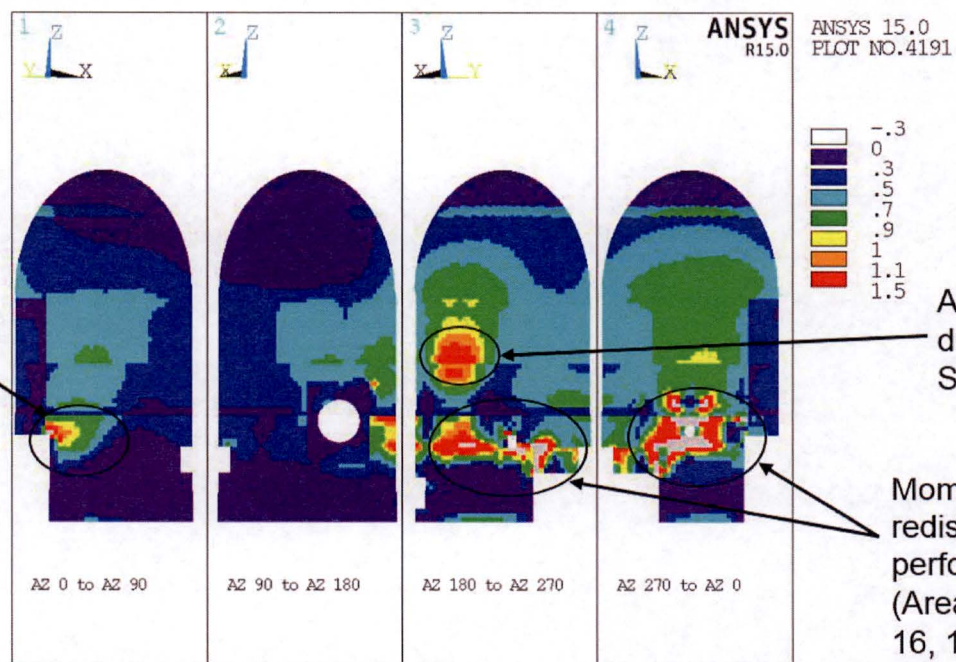


**Figure H61. Comparison of DCRs for Out-Of-Plane Shear Acting on Hoop-Radial Plane
Before (left) and After (right) Moment Redistribution,
Standard-Plus Analysis Case, Static Load Combination NO_1**

Section Cut
Evaluation shows
this area meets
criteria without
Moment
Redistribution
(Cuts 14 & 15)



Standard-Plus Analysis Case, OBE Combination
OBE_4, -100 +40 -40
Threshold Factor: 1.2
Demand-to-capacity ratio for axial-flexure interaction in hoop direction
FILE: SR_evB7_LCB_G07_t12_r0_PM11_DCR.ETABLE

Figure H62. Contours of DCRs for PM Interaction in the Hoop Direction Prior to Moment Redistribution, Standard-Plus Analysis Case, OBE Load Combination OBE_4

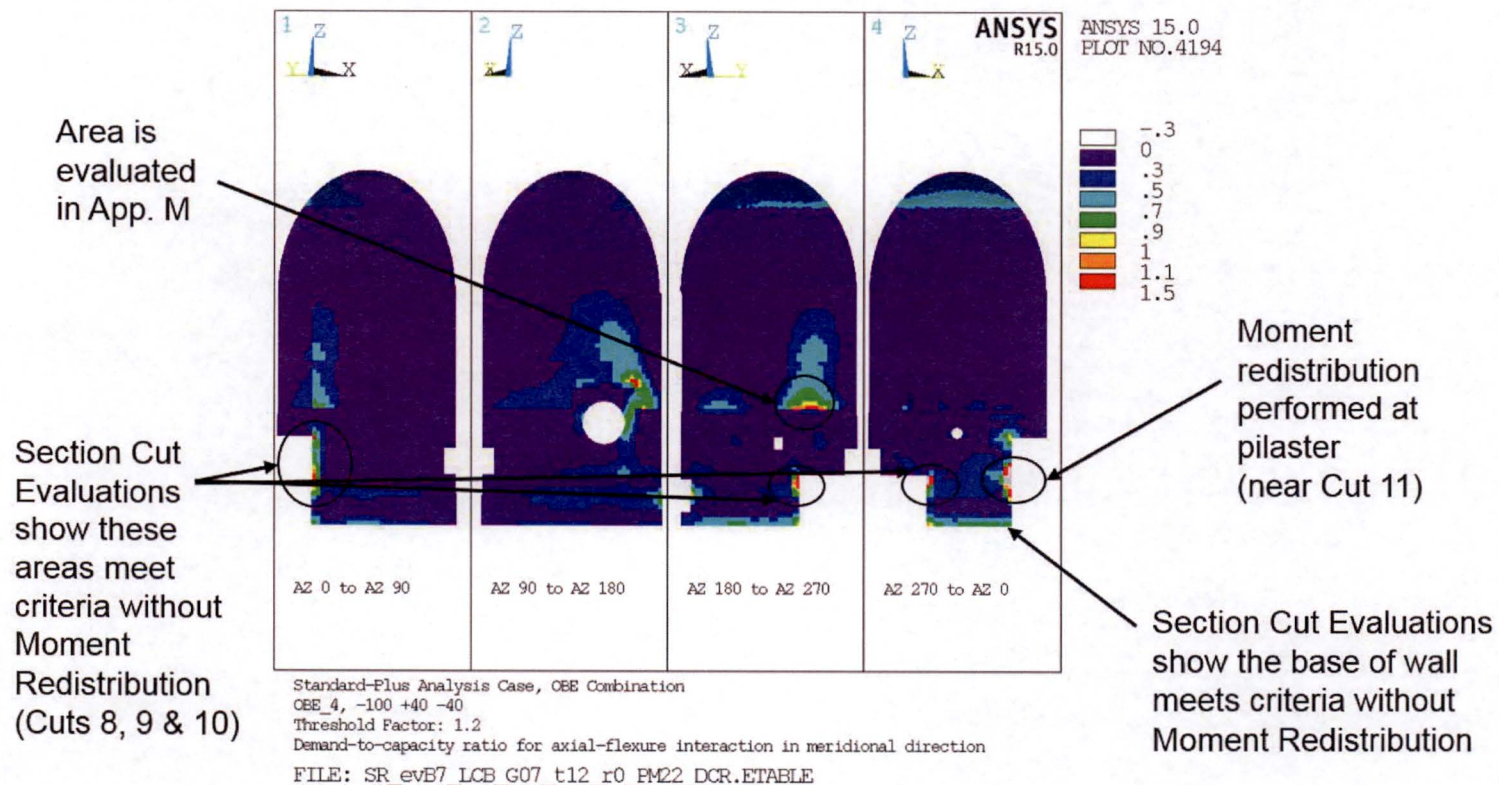


Figure H63. Contours of DCRs for PM Interaction in the Meridional Direction Prior to Moment Redistribution, Standard-Plus Analysis Case, OBE Load Combination OBE_4

CLIENT: NextEra Energy Seabrook

SUBJECT: Evaluation and Design Confirmation of As-Deformed CEB

PROJECT NO: 150252

DATE: July 2016

BY: R.M. Mones

VERIFIER: A.T. Sarawit

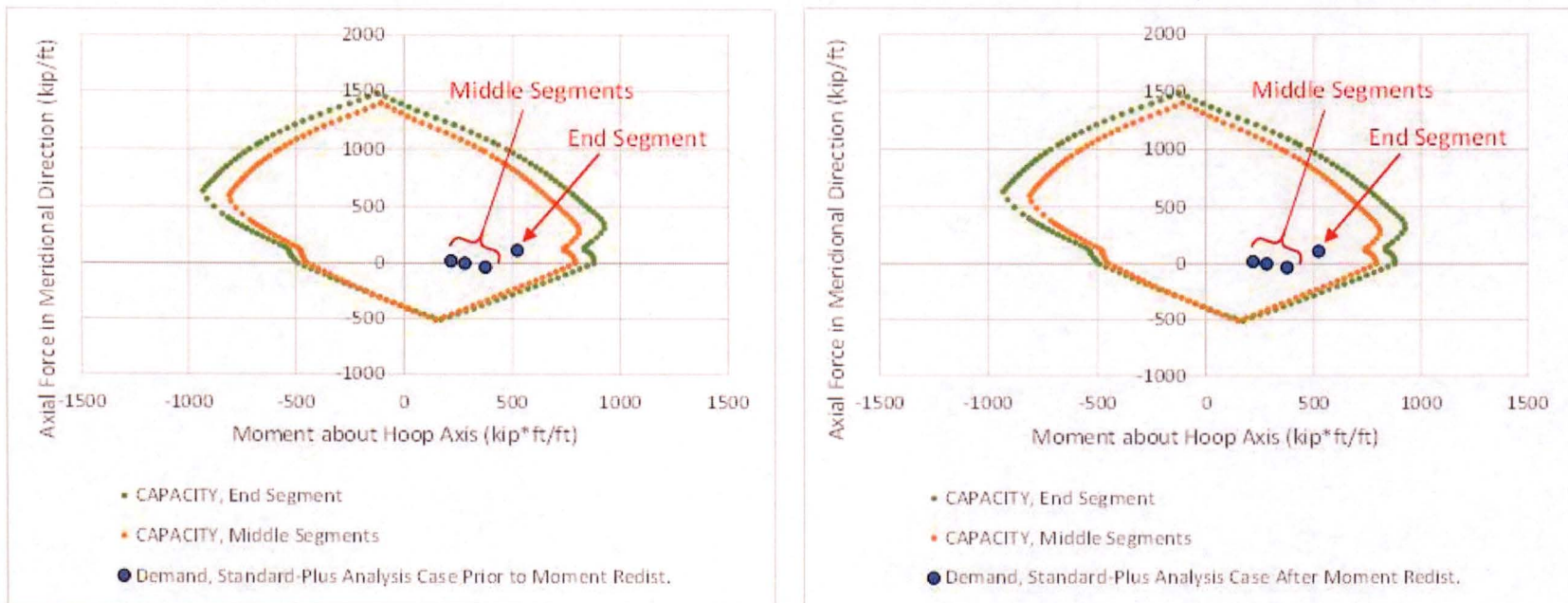


Figure H64. Comparison of PM Interaction Diagrams for Wall Segments along Base between AZ 0 and 90 Before (left) and After (right) Moment Redistribution, Standard-Plus Analysis Case, Seismic Load Combination OBE_4

CLIENT: NextEra Energy Seabrook

SUBJECT: Evaluation and Design Confirmation of As-Deformed CEB

PROJECT NO: 150252

DATE: July 2016

BY: R.M. Mones

VERIFIER: A.T. Sarawit

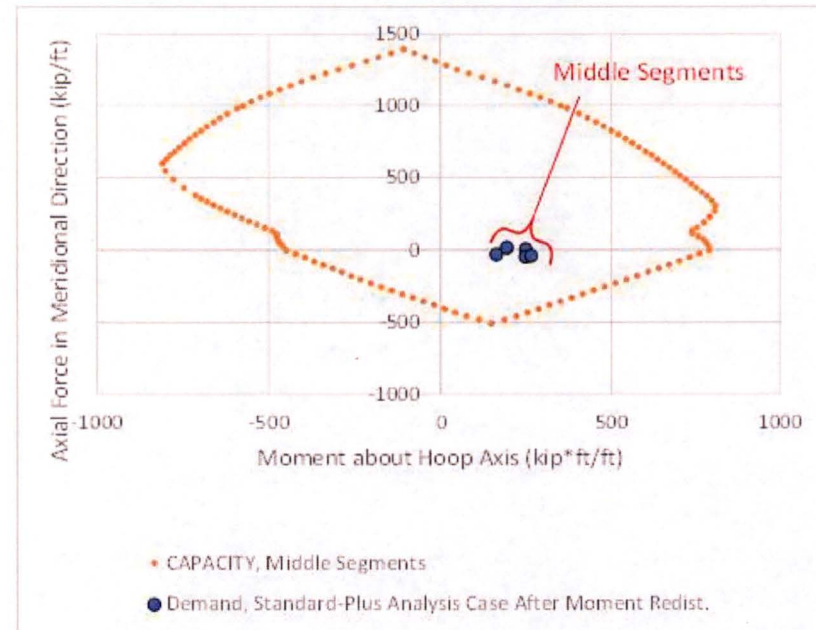
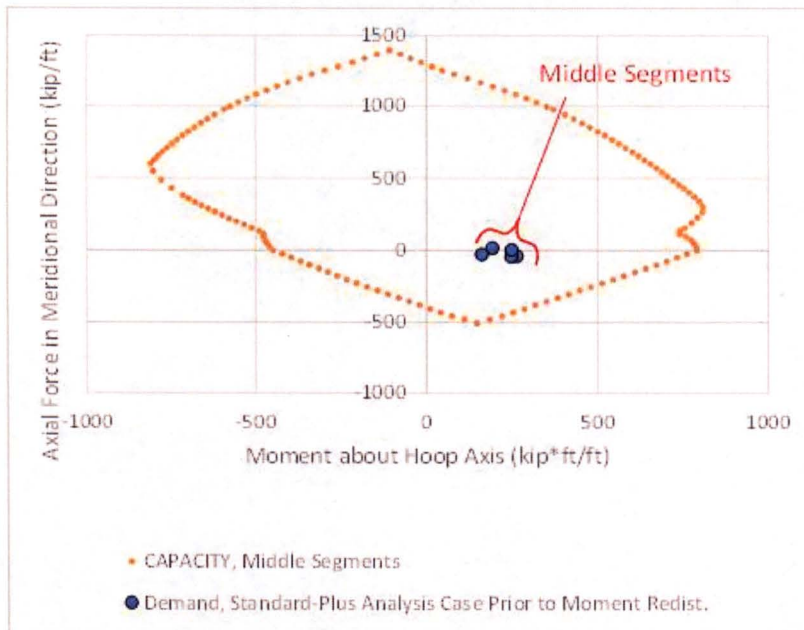


Figure H65. Comparison of PM Interaction Diagrams for Wall Segments along Base between AZ 90 and 180 Before (left) and After (right) Moment Redistribution, Standard-Plus Analysis Case, Seismic Load Combination OBE_4

CLIENT: NextEra Energy Seabrook

SUBJECT: Evaluation and Design Confirmation of As-Deformed CEB

PROJECT NO: 150252

DATE: July 2016

BY: R.M. Mones

VERIFIER: A.T. Sarawit

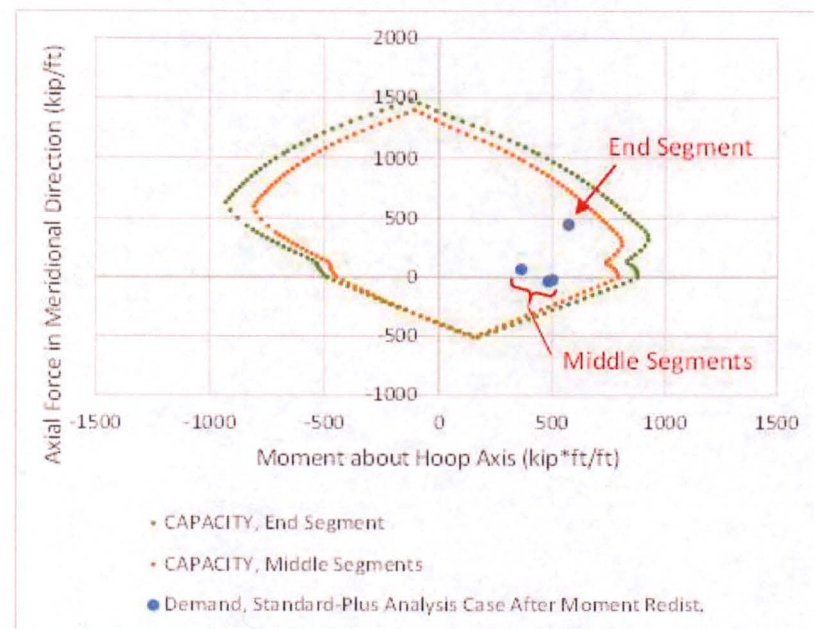
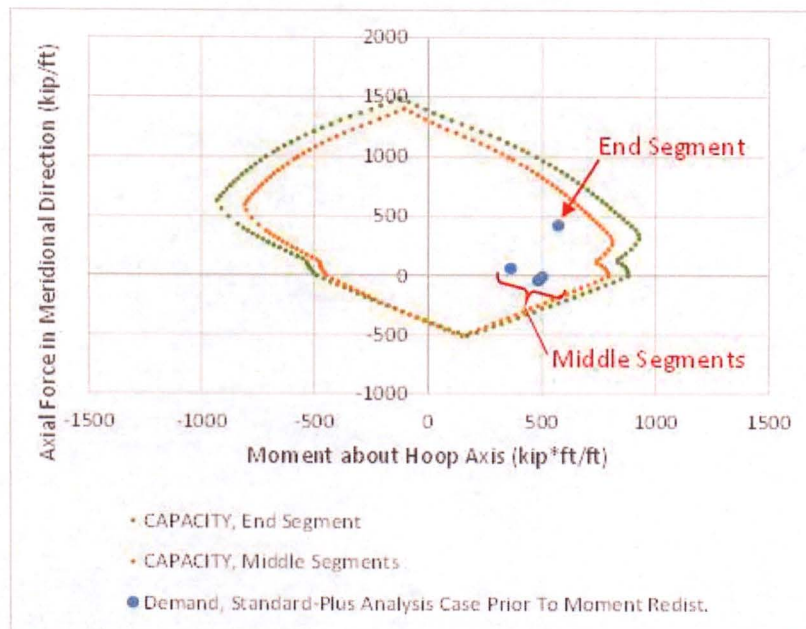


Figure H66. Comparison of PM Interaction Diagrams for Wall Segments along Base between AZ 180 and 270 Before (left) and After (right) Moment Redistribution, Standard-Plus Analysis Case, Seismic Load Combination OBE_4

CLIENT: NextEra Energy Seabrook

SUBJECT: Evaluation and Design Confirmation of As-Deformed CEB

PROJECT NO: 150252

DATE: July 2016

BY: R.M. Mones

VERIFIER: A.T. Sarawit

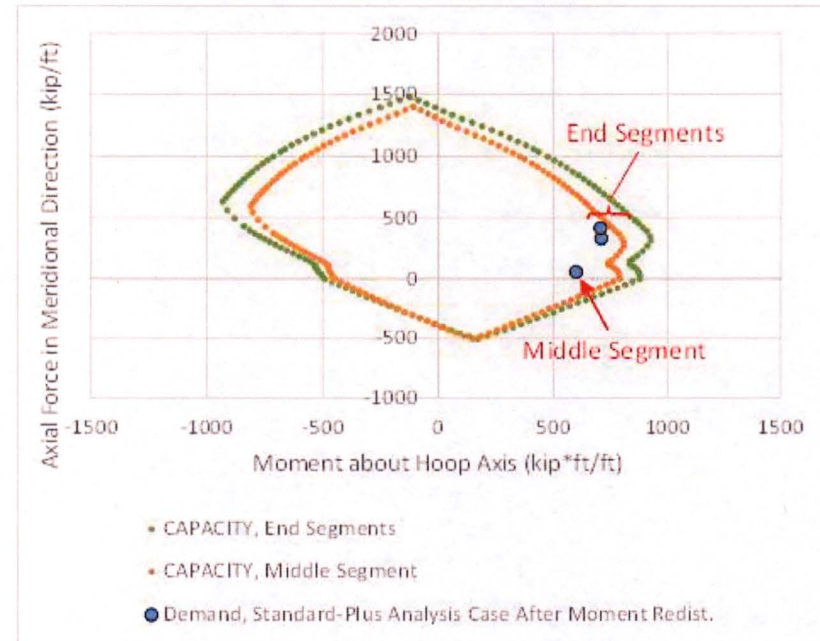
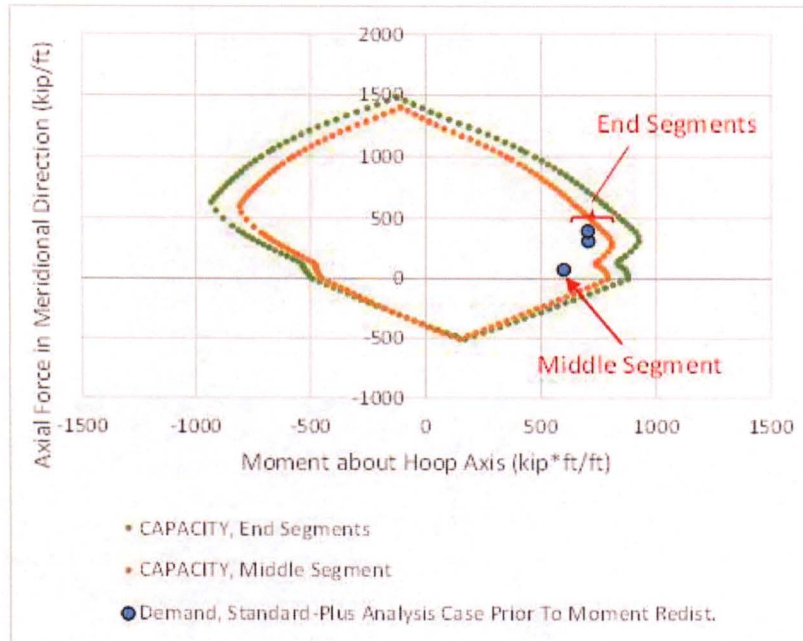


Figure H67. Comparison of PM Interaction Diagrams for Wall Segments along Base between AZ 270 and 360 Before (left) and After (right) Moment Redistribution, Standard-Plus Analysis Case, Seismic Load Combination OBE_4

CLIENT: NextEra Energy Seabrook

SUBJECT: Evaluation and Design Confirmation of As-Deformed CEB

PROJECT NO: 150252

DATE: July 2016

BY: R.M. Mones

VERIFIER: A.T. Sarawit

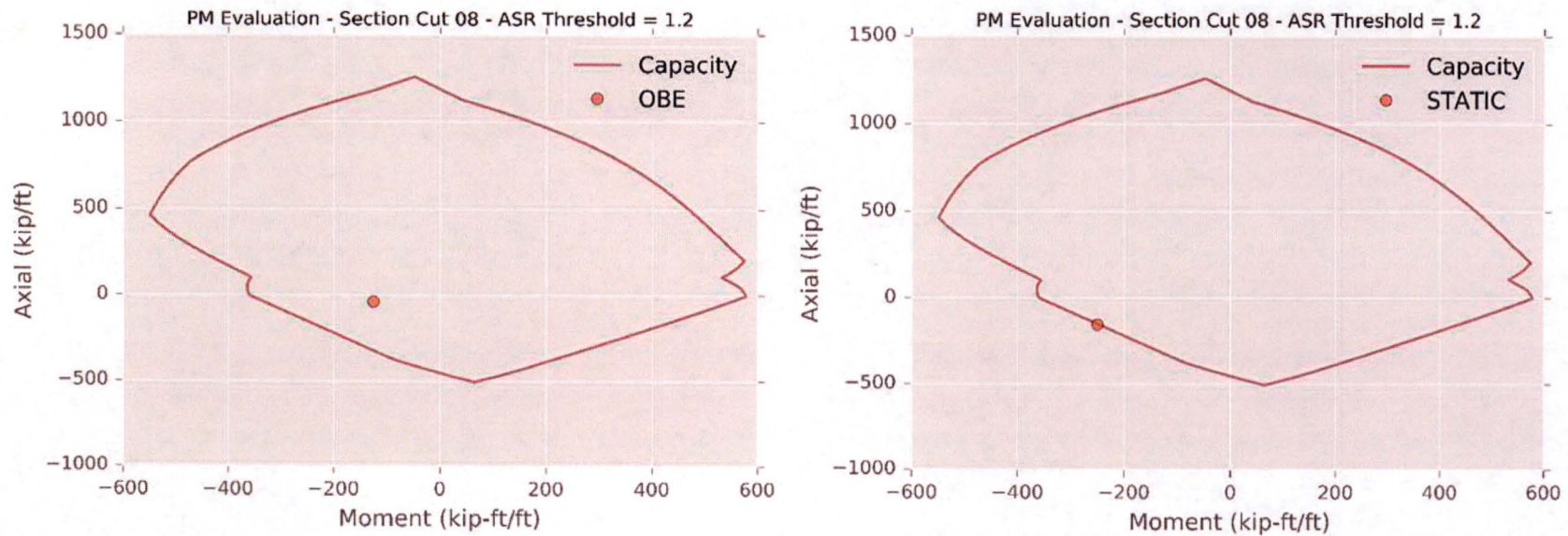


**Figure H68. Comparison of PM Interaction Diagrams for Section 8
Before (left) and After (right) Moment Redistribution,
Standard-Plus Analysis Case, Seismic Load Combination OBE_4**

CLIENT: NextEra Energy Seabrook

SUBJECT: Evaluation and Design Confirmation of As-Deformed CEB

PROJECT NO: 150252

DATE: July 2016

BY: R.M. Mones

VERIFIER: A.T. Sarawit

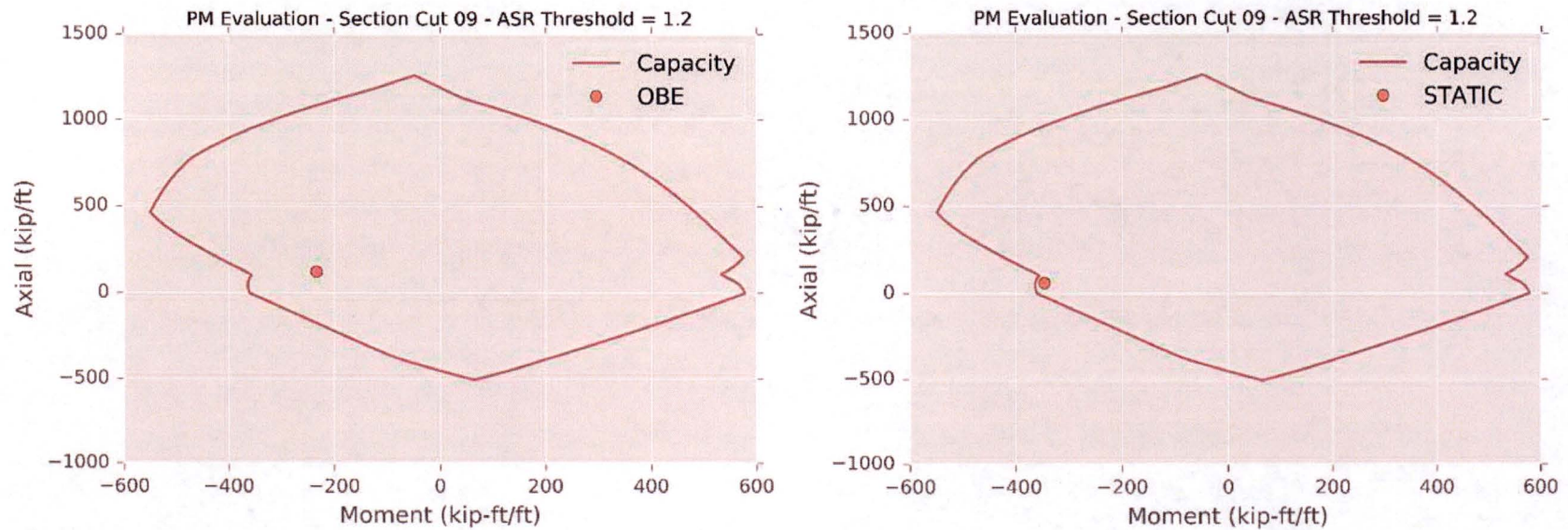


**Figure H69. Comparison of PM Interaction Diagrams for Section 9
Before (left) and After (right) Moment Redistribution,
Standard-Plus Analysis Case, Seismic Load Combination OBE_4**

CLIENT: NextEra Energy Seabrook

SUBJECT: Evaluation and Design Confirmation of As-Deformed CEB

PROJECT NO: 150252

DATE: July 2016

BY: R.M. Mones

VERIFIER: A.T. Sarawit

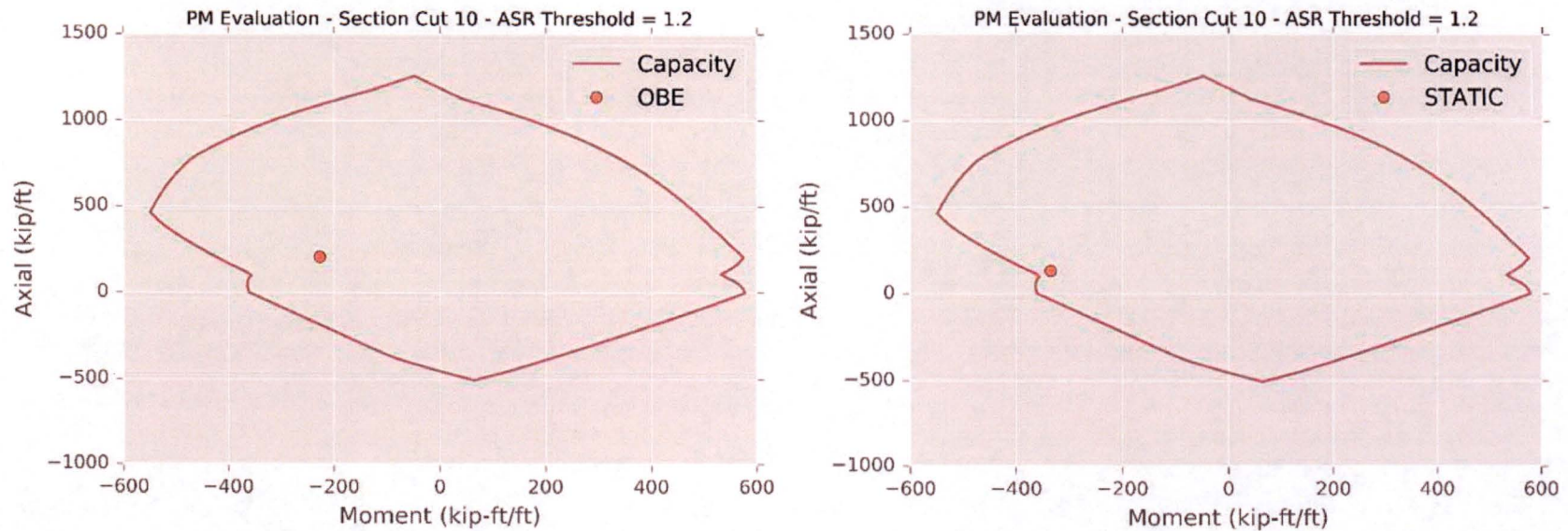


**Figure H70. Comparison of PM Interaction Diagrams for Section 10
Before (left) and After (right) Moment Redistribution,
Standard-Plus Analysis Case, Seismic Load Combination OBE_4**

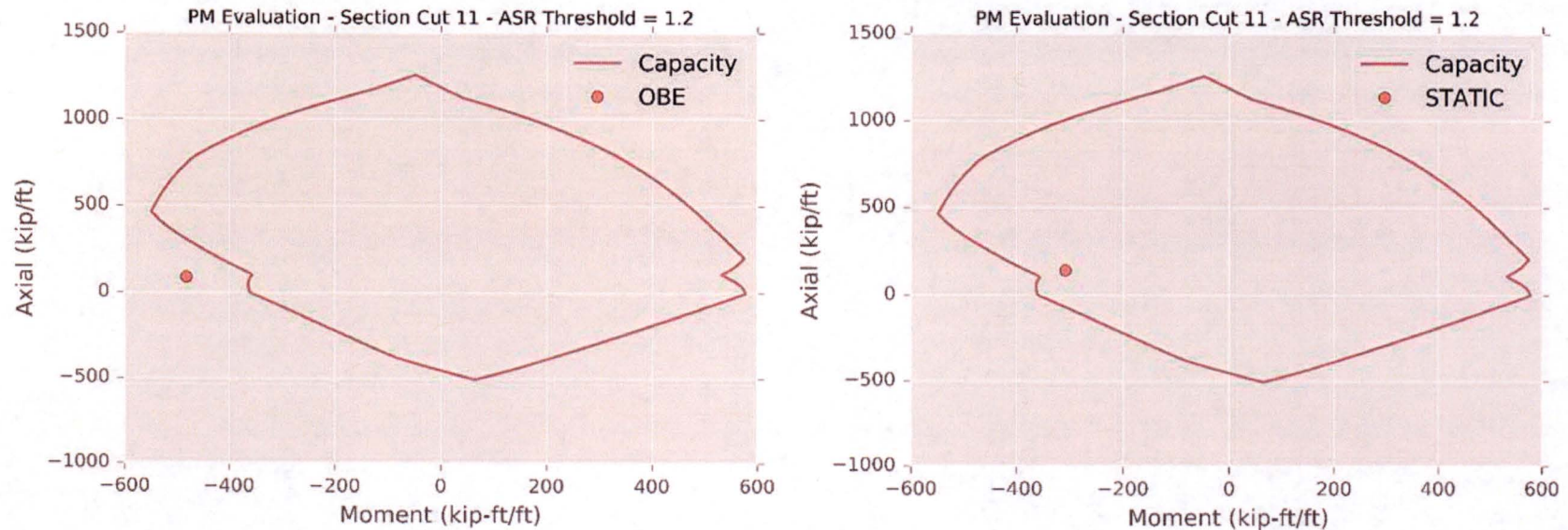


**Figure H71. Comparison of PM Interaction Diagrams for Section 11
Before (left) and After (right) Moment Redistribution,
Standard-Plus Analysis Case, Seismic Load Combination OBE_4**

CLIENT: NextEra Energy Seabrook

SUBJECT: Evaluation and Design Confirmation of As-Deformed CEB

PROJECT NO: 150252

DATE: July 2016

BY: R.M. Mones

VERIFIER: A.T. Sarawit

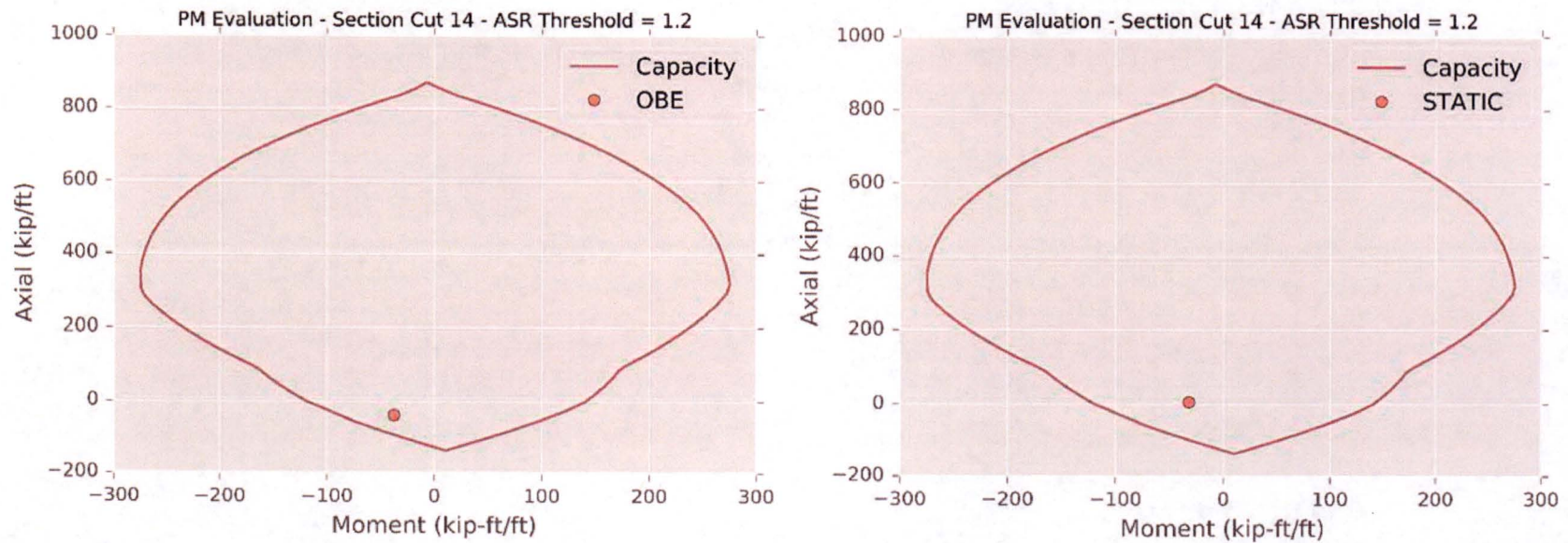


**Figure H72. Comparison of PM Interaction Diagrams for Section 14
Before (left) and After (right) Moment Redistribution,
Standard-Plus Analysis Case, Seismic Load Combination OBE_4**

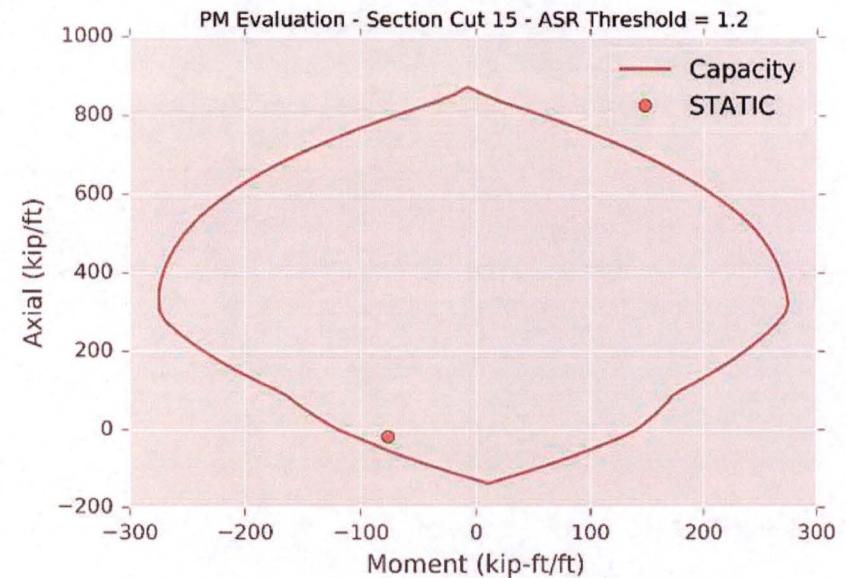
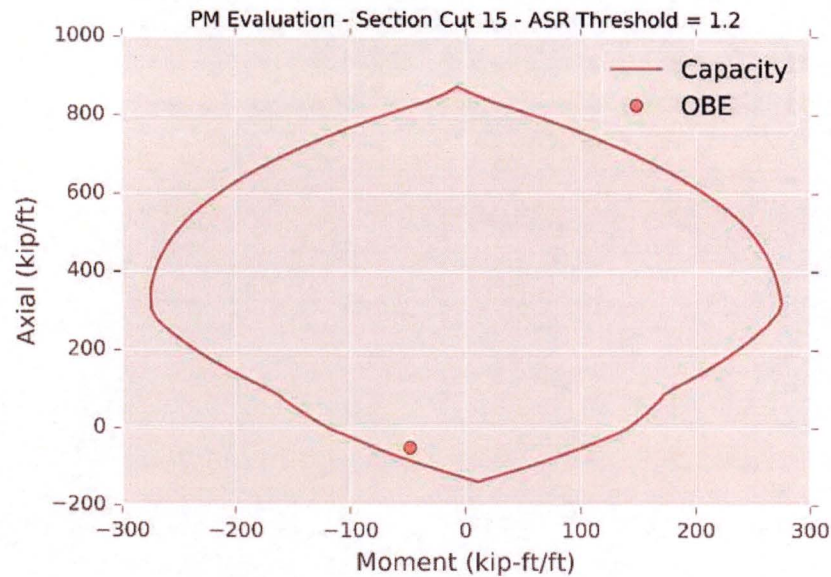


**Figure H73. Comparison of PM Interaction Diagrams for Section 15
Before (left) and After (right) Moment Redistribution,
Standard-Plus Analysis Case, Seismic Load Combination OBE_4**

CLIENT: NextEra Energy Seabrook

SUBJECT: Evaluation and Design Confirmation of As-Deformed CEB

PROJECT NO: 150252

DATE: July 2016

BY: R.M. Mones

VERIFIER: A.T. Sarawit

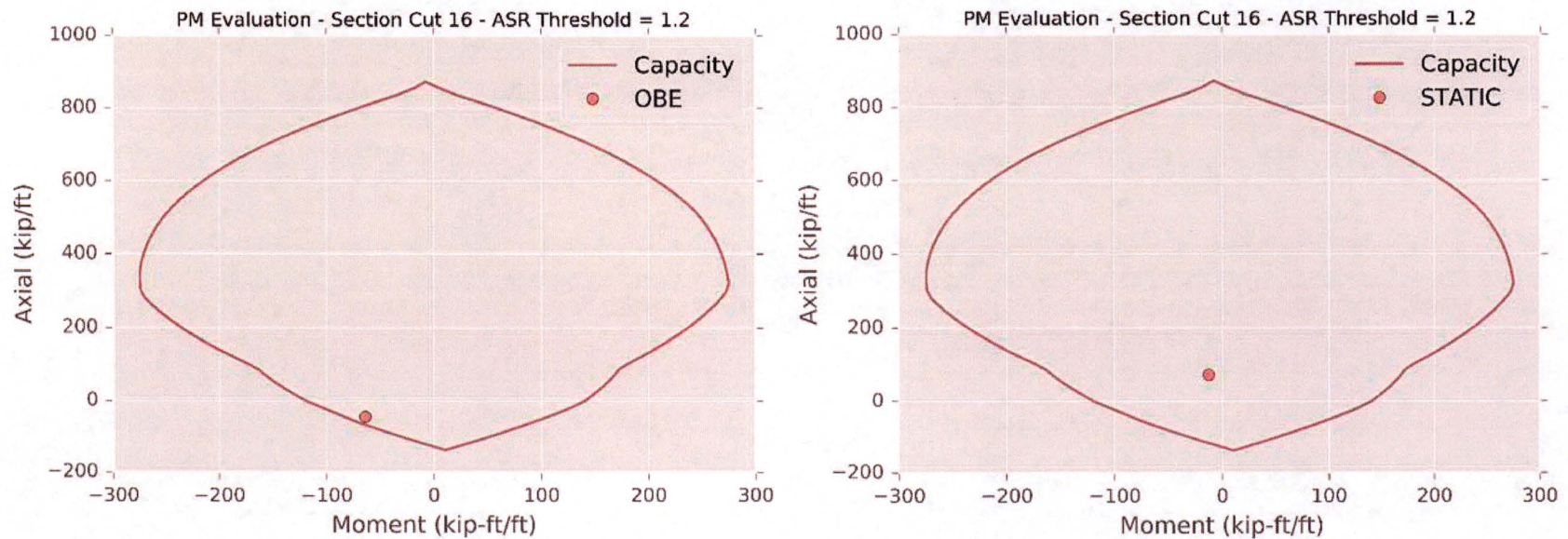


**Figure H74. Comparison of PM Interaction Diagrams for Section 16
Before (left) and After (right) Moment Redistribution,
Standard-Plus Analysis Case, Seismic Load Combination OBE_4**

CLIENT: NextEra Energy Seabrook

SUBJECT: Evaluation and Design Confirmation of As-Deformed CEB

PROJECT NO: 150252

DATE: July 2016

BY: R.M. Mones

VERIFIER: A.T. Sarawit

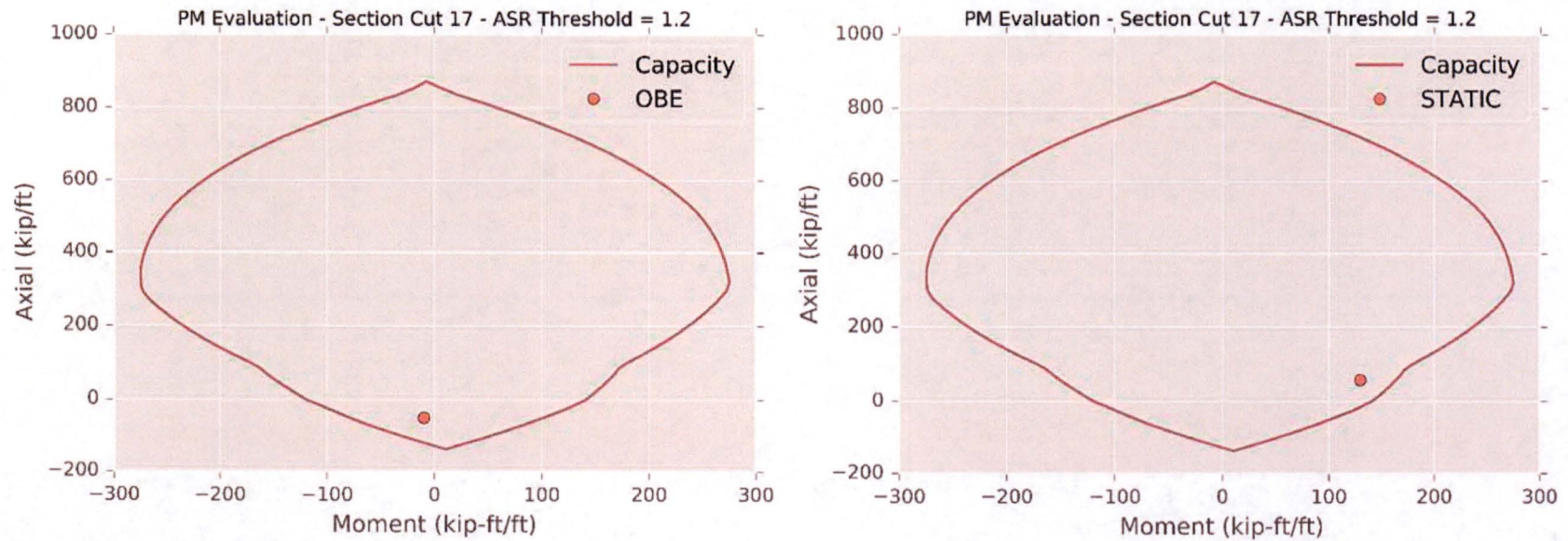


**Figure H75. Comparison of PM Interaction Diagrams for Section 17
Before (left) and After (right) Moment Redistribution,
Standard-Plus Analysis Case, Seismic Load Combination OBE_4**

CLIENT: NextEra Energy Seabrook

SUBJECT: Evaluation and Design Confirmation of As-Deformed CEB

PROJECT NO: 150252

DATE: July 2016

BY: R.M. Mones

VERIFIER: A.T. Sarawit

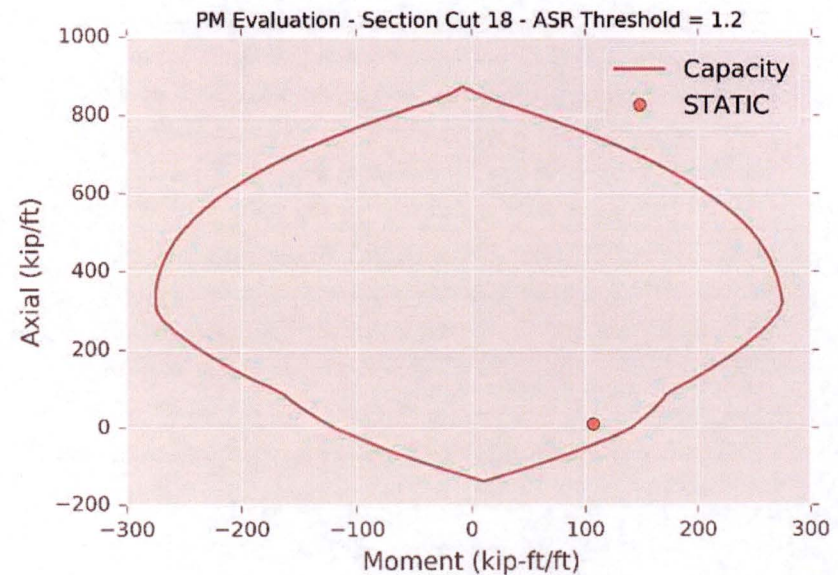
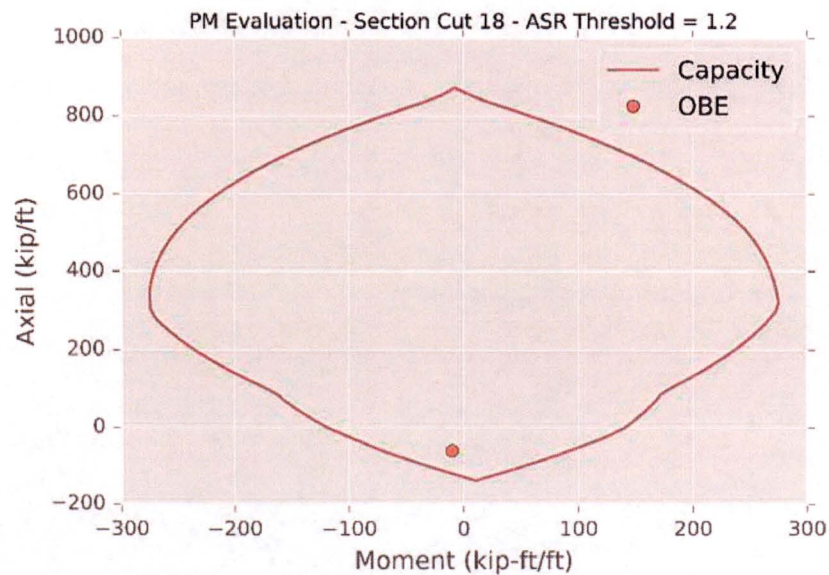


**Figure H76. Comparison of PM Interaction Diagrams for Section 18
Before (left) and After (right) Moment Redistribution,
Standard-Plus Analysis Case, Seismic Load Combination OBE_4**

CLIENT: NextEra Energy Seabrook

SUBJECT: Evaluation and Design Confirmation of As-Deformed CEB

PROJECT NO: 150252

DATE: July 2016

BY: R.M. Mones

VERIFIER: A.T. Sarawit

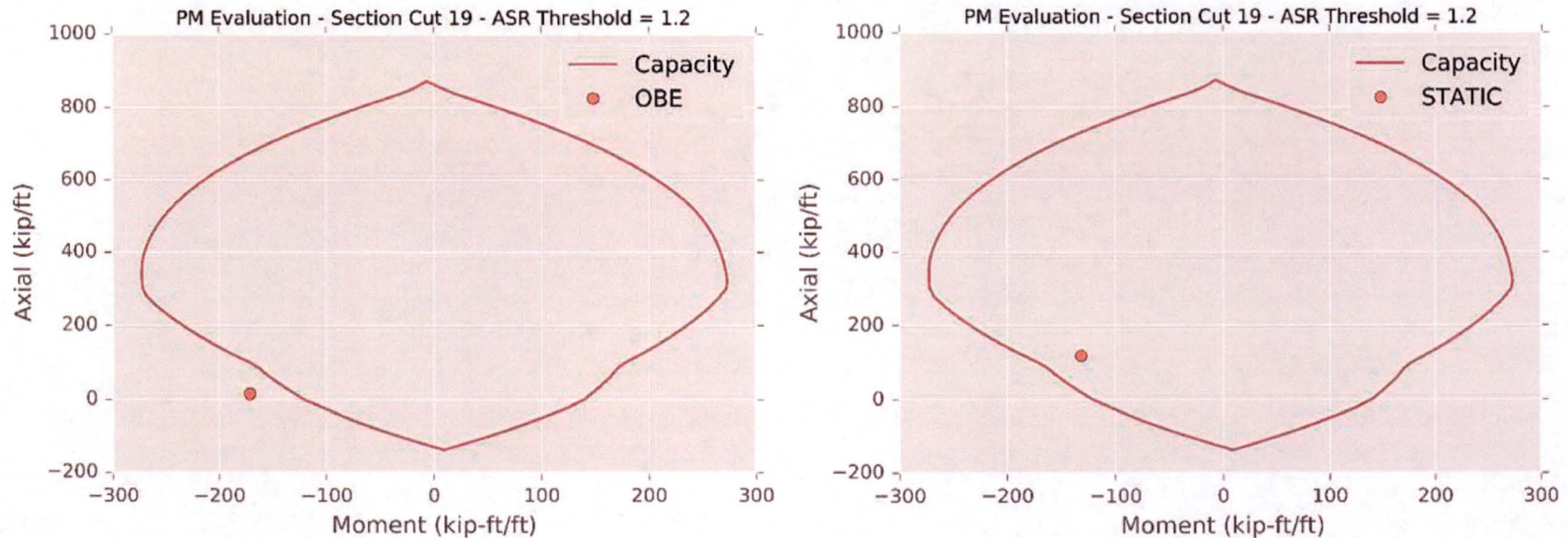


**Figure H77. Comparison of PM Interaction Diagrams for Section 19
Before (left) and After (right) Moment Redistribution,
Standard-Plus Analysis Case, Seismic Load Combination OBE_4**

CLIENT: NextEra Energy Seabrook

SUBJECT: Evaluation and Design Confirmation of As-Deformed CEB

PROJECT NO: 150252

DATE: July 2016

BY: R.M. Mones

VERIFIER: A.T. Sarawit

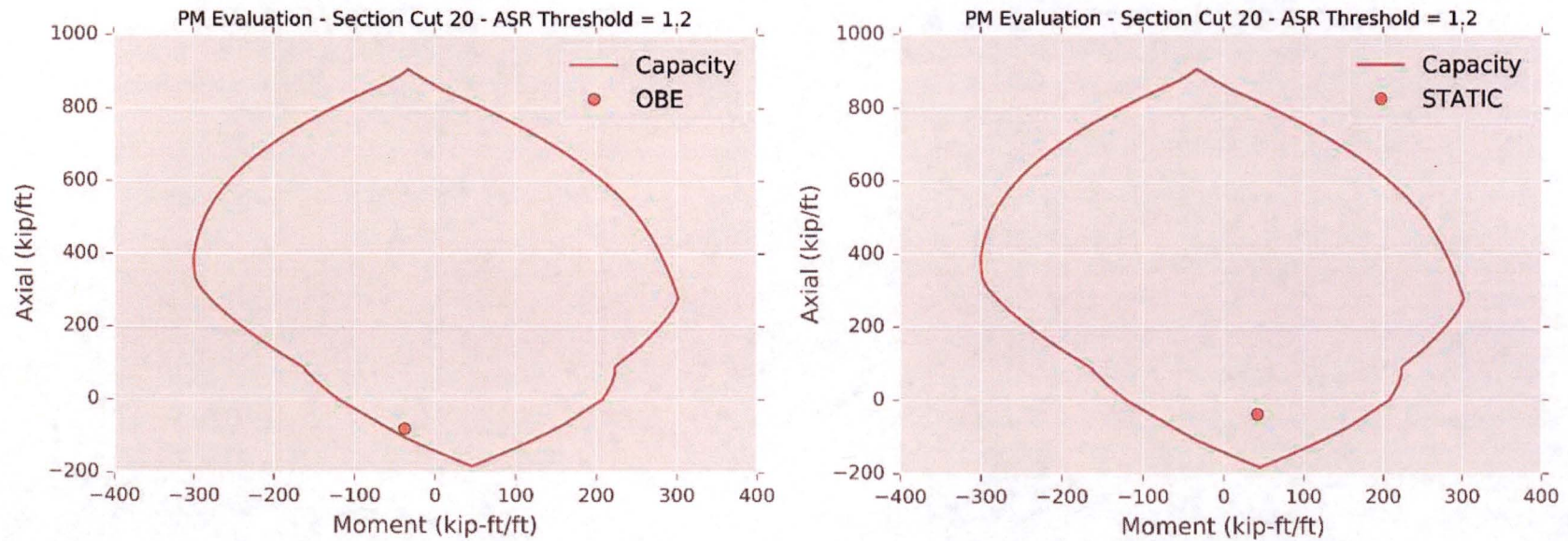


**Figure H78. Comparison of PM Interaction Diagrams for Section 20
Before (left) and After (right) Moment Redistribution,
Standard-Plus Analysis Case, Seismic Load Combination OBE_4**

CLIENT: NextEra Energy Seabrook

SUBJECT: Evaluation and Design Confirmation of As-Deformed CEB

PROJECT NO: 150252

DATE: July 2016

BY: R.M. Mones

VERIFIER: A.T. Sarawit

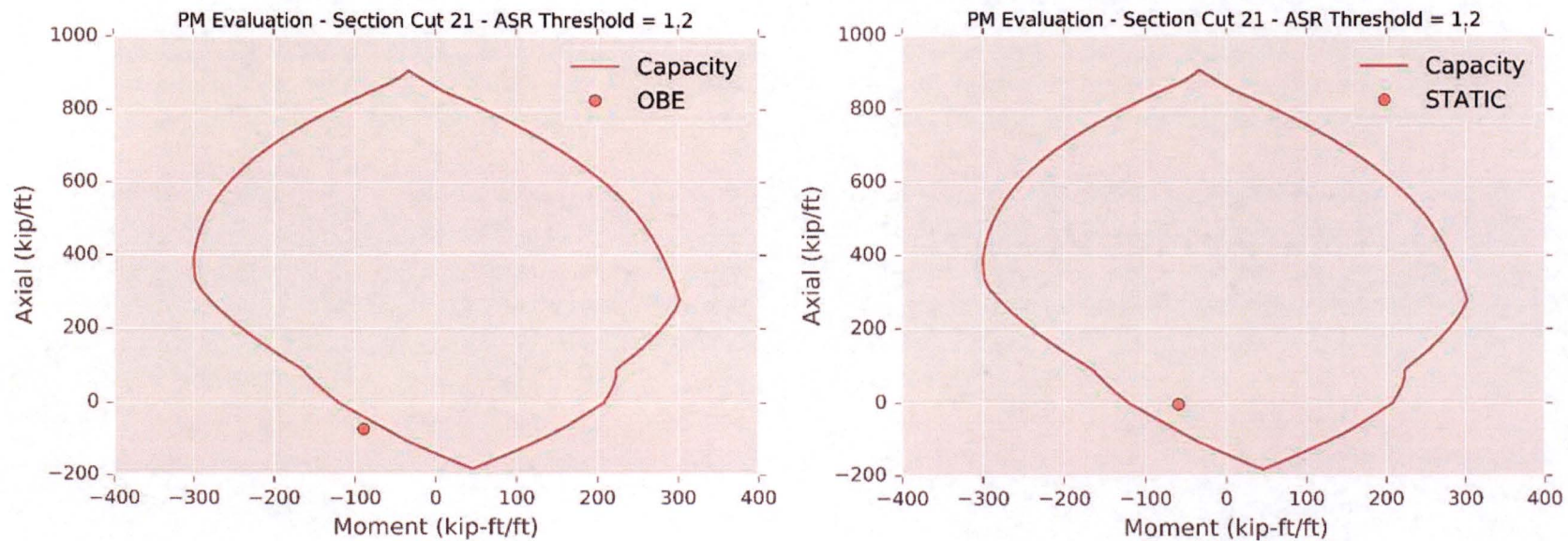


**Figure H79. Comparison of PM Interaction Diagrams for Section 21
Before (left) and After (right) Moment Redistribution,
Standard-Plus Analysis Case, Seismic Load Combination OBE_4**

CLIENT: NextEra Energy Seabrook

SUBJECT: Evaluation and Design Confirmation of As-Deformed CEB

PROJECT NO: 150252

DATE: July 2016

BY: R.M. Mones

VERIFIER: A.T. Sarawit

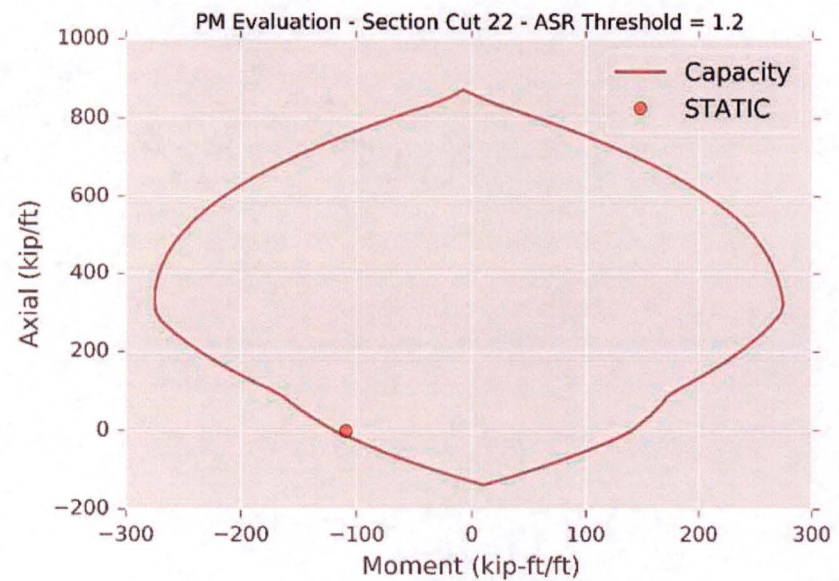
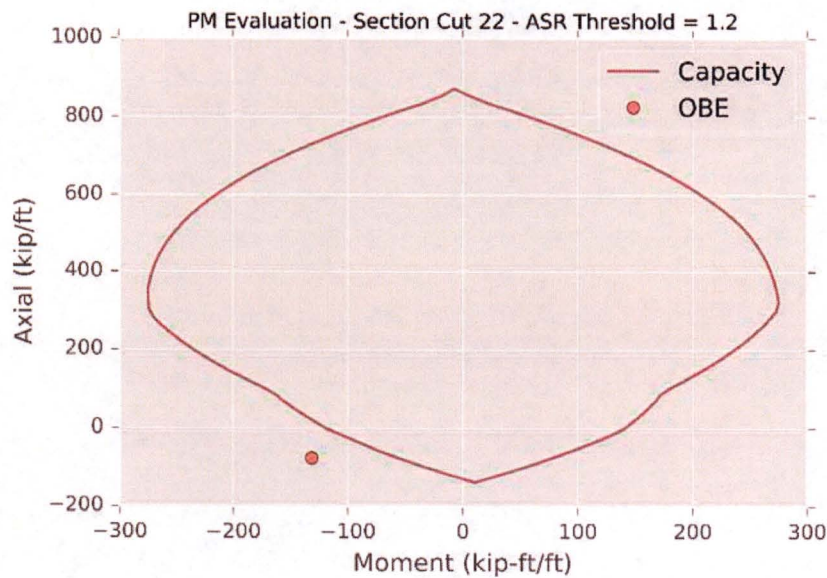


**Figure H80. Comparison of PM Interaction Diagrams for Section 22
Before (left) and After (right) Moment Redistribution,
Standard-Plus Analysis Case, Seismic Load Combination OBE_4**

CLIENT: NextEra Energy Seabrook

SUBJECT: Evaluation and Design Confirmation of As-Deformed CEB

PROJECT NO: 150252

DATE: July 2016

BY: R.M. Mones

VERIFIER: A.T. Sarawit

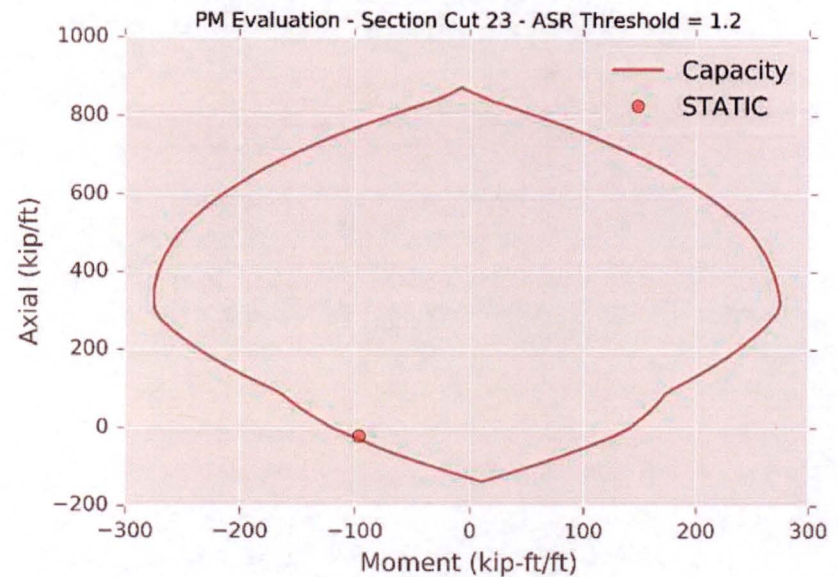
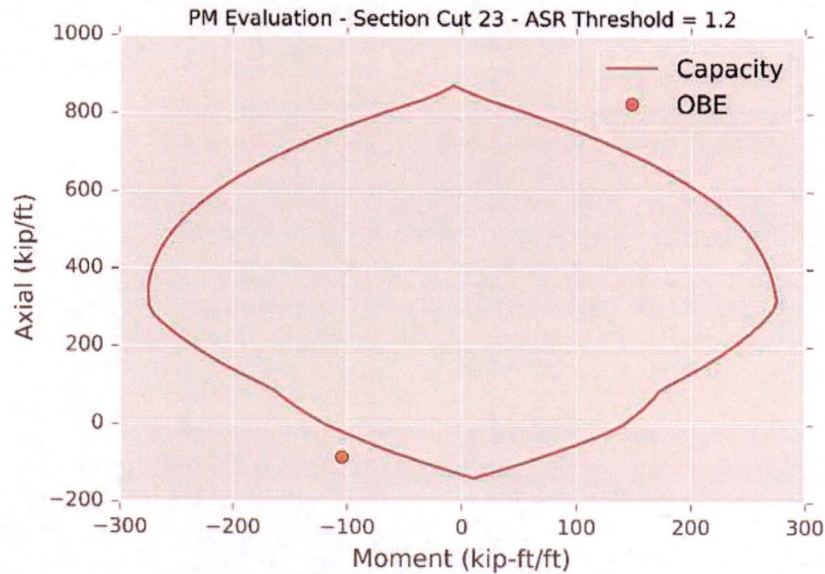


**Figure H81. Comparison of PM Interaction Diagrams for Section 23
Before (left) and After (right) Moment Redistribution,
Standard-Plus Analysis Case, Seismic Load Combination OBE_4**

CLIENT: NextEra Energy Seabrook

SUBJECT: Evaluation and Design Confirmation of As-Deformed CEB

PROJECT NO: 150252

DATE: July 2016

BY: R.M. Mones

VERIFIER: A.T. Sarawit

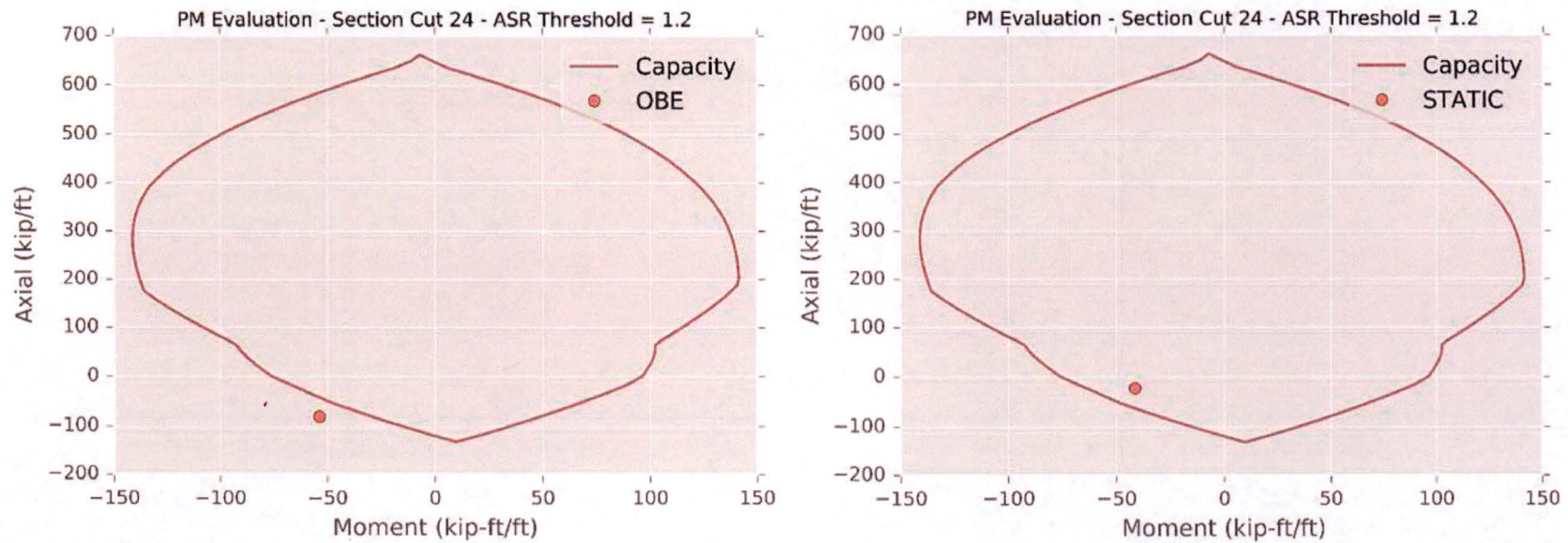


**Figure H82. Comparison of PM Interaction Diagrams for Section 24
Before (left) and After (right) Moment Redistribution,
Standard-Plus Analysis Case, Seismic Load Combination OBE_4**

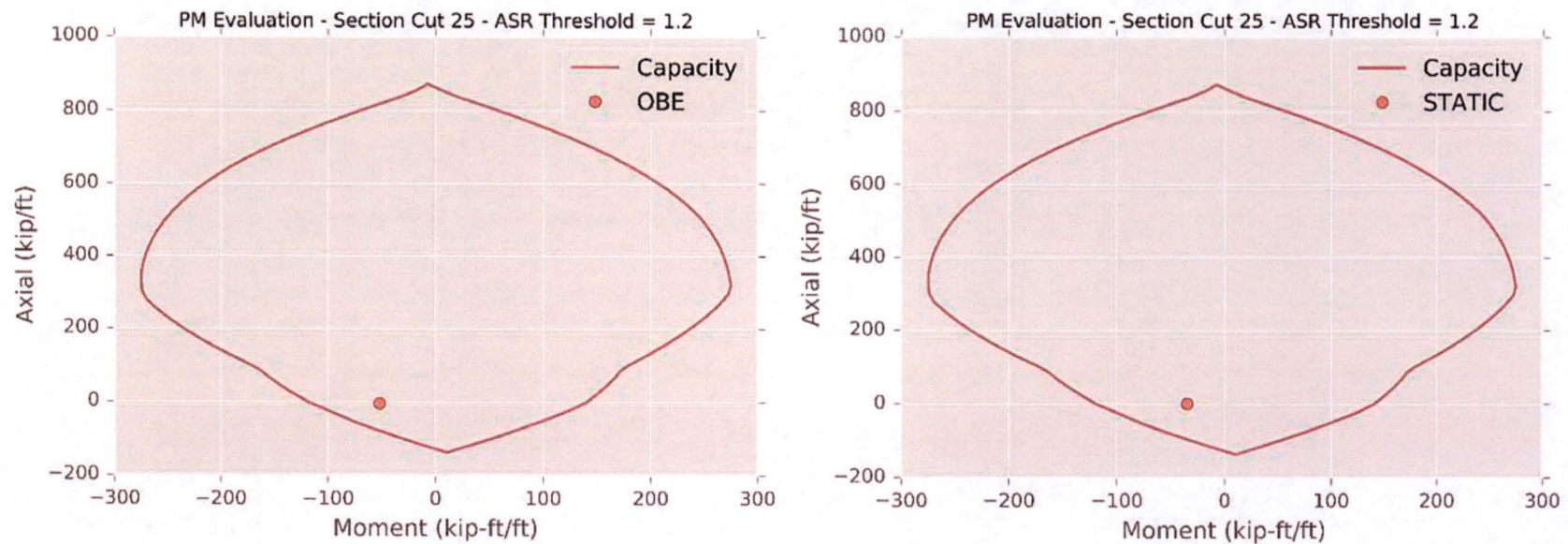


**Figure H83. Comparison of PM Interaction Diagrams for Section 25
Before (left) and After (right) Moment Redistribution,
Standard-Plus Analysis Case, Seismic Load Combination OBE_4**

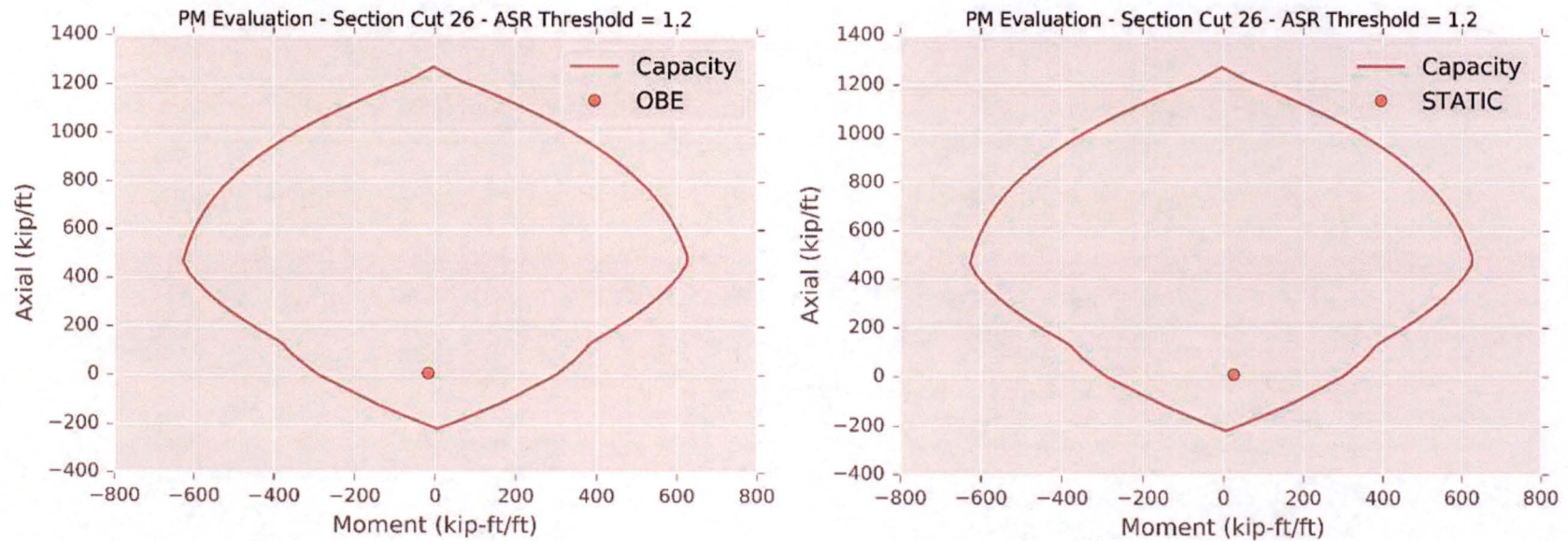


**Figure H84. Comparison of PM Interaction Diagrams for Section 26
Before (left) and After (right) Moment Redistribution,
Standard-Plus Analysis Case, Seismic Load Combination OBE_4**

CLIENT: NextEra Energy Seabrook

SUBJECT: Evaluation and Design Confirmation of As-Deformed CEB

PROJECT NO: 150252

DATE: July 2016

BY: R.M. Mones

VERIFIER: A.T. Sarawit

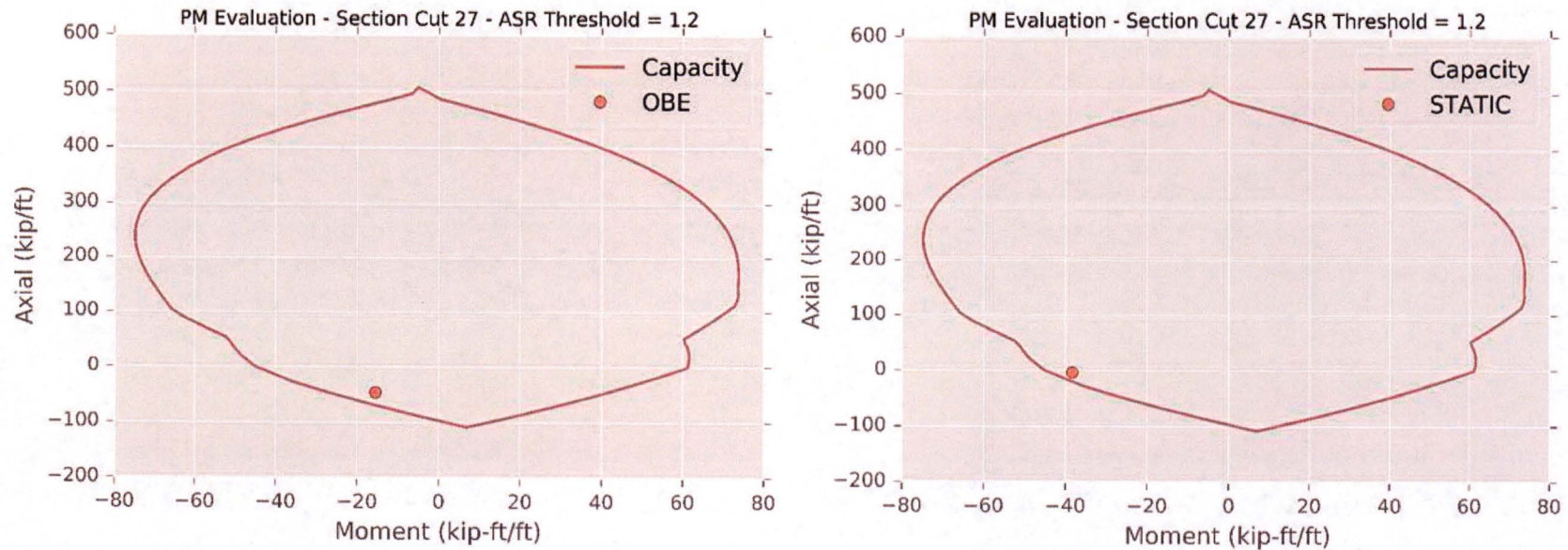


**Figure H85. Comparison of PM Interaction Diagrams for Section 27
Before (left) and After (right) Moment Redistribution,
Standard-Plus Analysis Case, Seismic Load Combination OBE_4**

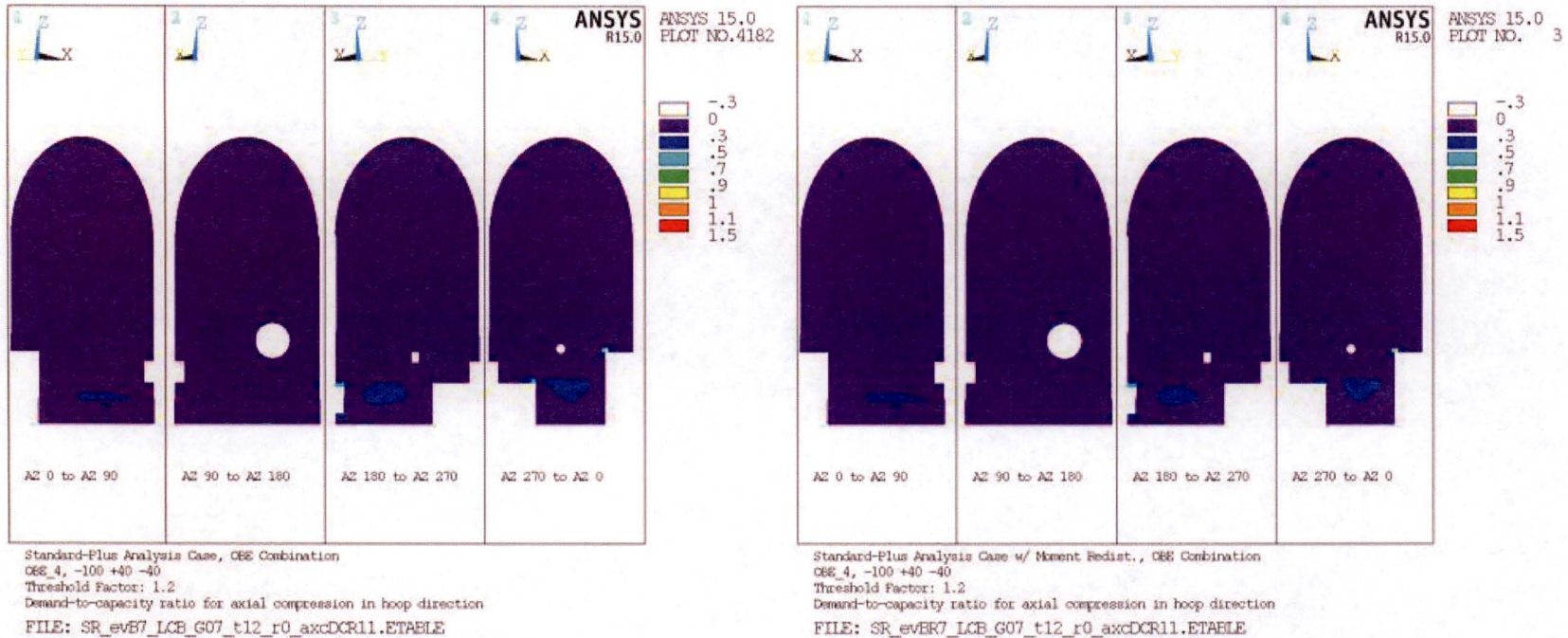


**Figure H86. Comparison of DCRs for Axial Compression in the Hoop Direction
Before (left) and After (right) Moment Redistribution,
Standard-Plus Analysis Case, Seismic Load Combination OBE_4**

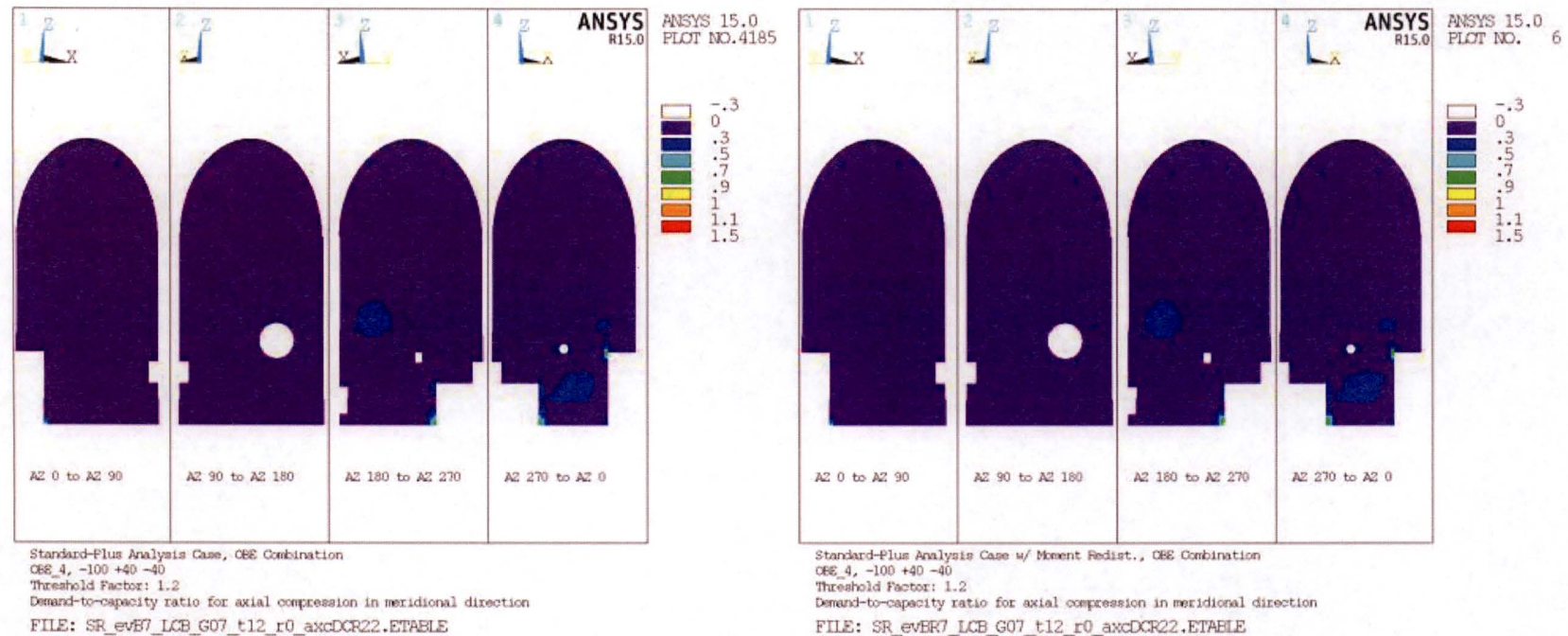


**Figure H87. Comparison of DCRs for Axial Compression in the Meridional Direction
Before (left) and After (right) Moment Redistribution,
Standard-Plus Analysis Case, Seismic Load Combination OBE_4**

CLIENT: NextEra Energy Seabrook

SUBJECT: Evaluation and Design Confirmation of As-Deformed CEB

PROJECT NO: 150252

DATE: July 2016

BY: R.M. Mones

VERIFIER: A.T. Sarawit

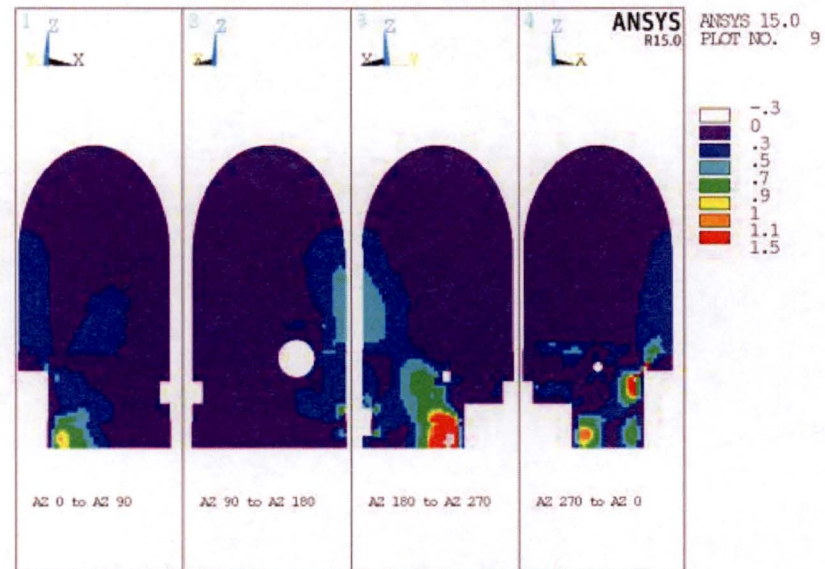
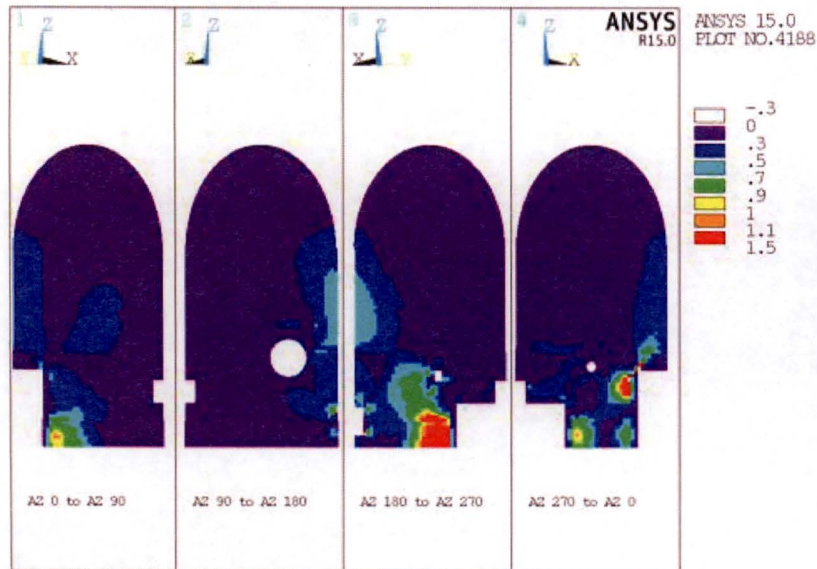


**Figure H88. Comparison of DCRs for In-Plane Shear
Before (left) and After (right) Moment Redistribution,
Standard-Plus Analysis Case, Seismic Load Combination OBE_4**

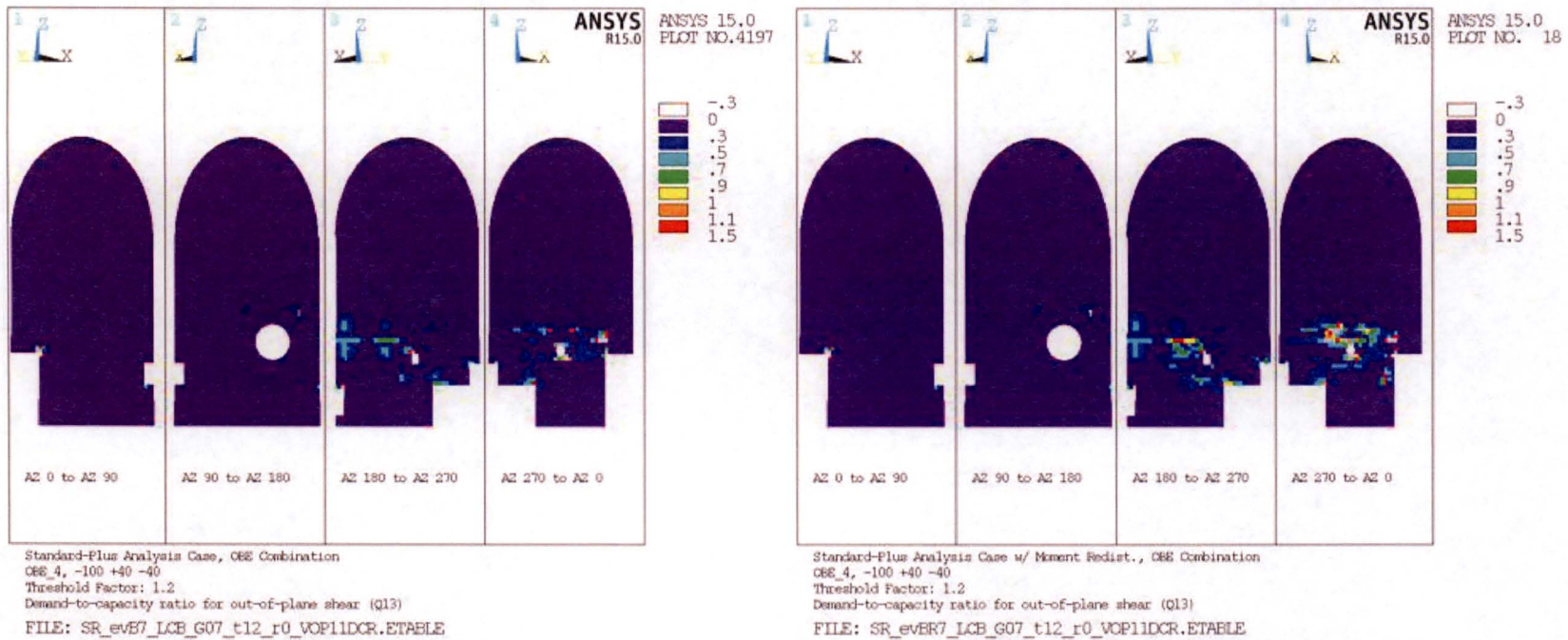


**Figure H89. Comparison of DCRs for Out-Of-Plane Shear Acting on Meridional-Radial Plane
Before (left) and After (right) Moment Redistribution,
Standard-Plus Analysis Case, Seismic Load Combination OBE_4**

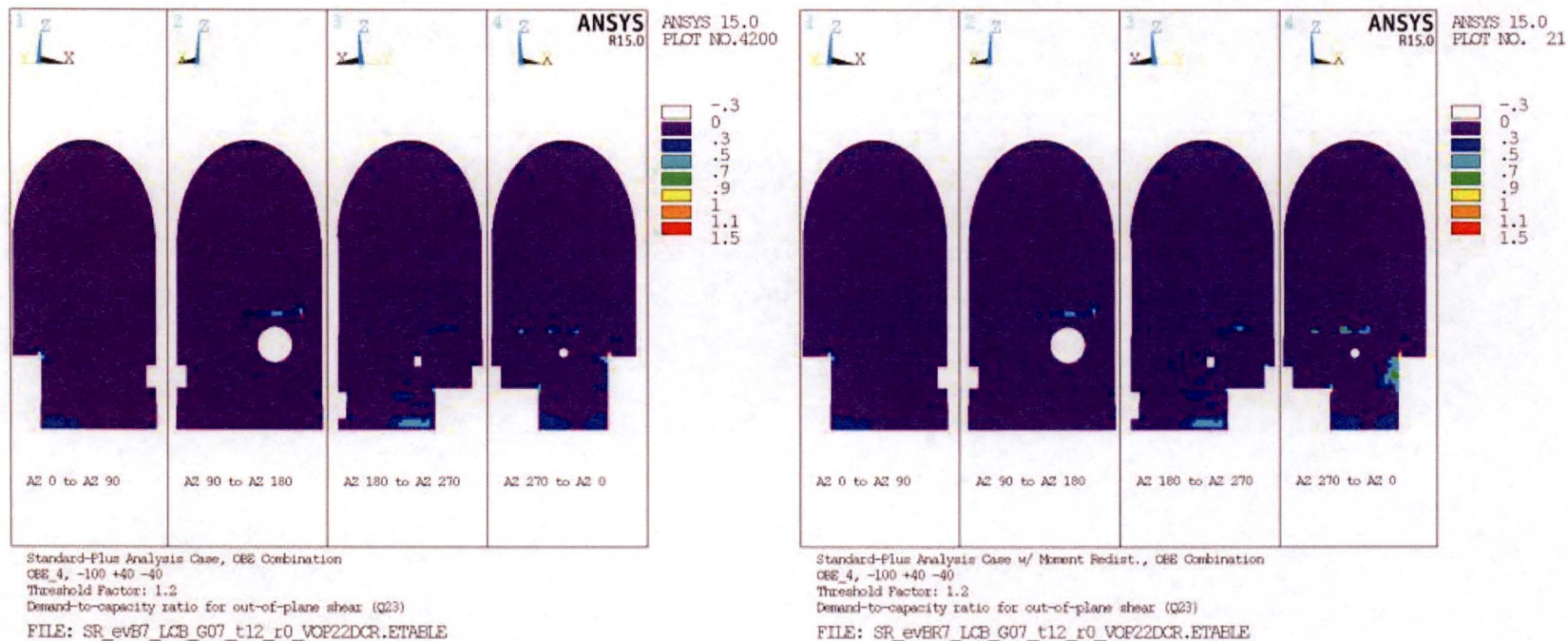


**Figure H90. Comparison of DCRs for Out-Of-Plane Shear Acting on Hoop-Radial Plane
Before (left) and After (right) Moment Redistribution,
Standard-Plus Analysis Case, Seismic Load Combination OBE_4**

CLIENT NextEra Energy SeabrookSUBJECT Evaluation and Design Confirmation of As-Deformed CEBPROJECT NO. 150252DATE July 2016BY R.W. KeeneCHECKED BY A.T. Sarawit

APPENDIX I

GLOBAL STABILITY OF CEB STRUCTURE

11. OBJECTIVE OF CALCULATION

The objective of this calculation is to determine the global stability of the CEB structure for sliding, overturning and buoyancy.

12. RESULTS AND CONCLUSIONS

Failure of the CEB ring wall foundation by sliding is not possible. The foundation is enclosed by concrete backfill and or bedrock, and the lateral load acting at the base of the foundation would get transferred from the CEB ring wall to the concrete backfill and or bedrock in bearing (Ref. I4). The CEB will not overturn or float based on calculations below.

13. DESIGN DATA / CRITERIA

The sliding and overturning criteria is per Section 5.4.1 of System Description for Structural Design Criteria for Public Service Company of New Hampshire, Seabrook Station, Unit Nos. 1 & 2, 19 October, 1976. The load combinations include:

- 1) $D+E_o+H+H_e$, minimum factor of safety of 1.5 for overturning and 1.5 for sliding
- 2) $D+E_{ss}+H+H_s$, minimum factor of safety of 1.1 for overturning and 1.1 for sliding
- 3) $D+F$ with hydrostatic load excluded, minimum factor of safety for flotation of 1.1

For overturning and sliding, we also add in the effects of ASR and self-straining forces.

14. ASSUMPTIONS

There are no assumptions in this calculation.

15. METHODOLOGY

We perform overturning calculations with overturning demand based on the sum of the moments of the reaction forces around the CEB. The total base shear in the North direction considers 100% of the reaction due to applied load in the North direction plus 40% of the reaction due to load applied in the East or West direction, whichever leads to a higher total demand. ASR loads include a threshold factor of 1.2. Resistance to overturning consists of dead load minus 40% of seismic vertical demand. Resistance is calculated using the distance from the toe of the CEB to the CG of the CEB calculated in the ANSYS analysis (Ref. I2). Resistance includes the effect of the rock support, consistent with the original design calculations.

17. REFERENCES

11. System Description for Structural Design Criteria for Public Service Company of New Hampshire, Seabrook Station, Unit No. 1 & 2, 19 October 1976.
12. ANSYS model output, SR_ILC_03_I_r0.out.
13. United Engineers, Stability Check for Enclosure Building, Revision 2, 1 September 1983.
14. Simpson Gumpertz & Heger, Document ID No. 150252-R-01, Geotechnical Assessment of the CEB, NextEra Energy Seabrook Facility, Seabrook, NH, Revision 0, 22 June 2015.
15. ANSYS model output, SR_ILC_##_I_r0_reactionsSorted.output where ## = 03 to 23.

18. COMPUTATIONS

Demands CENTER OF MASS (X,Y,Z)= 65.310 -59.058 644.63
(Ref. 15) (Ref. 12)

LC :=	LCID :=	FX :=	lbf	FY :=	lbf	FZ :=	lbf
0	"NA"	0		0		0	
1	"NA"	0		0		0	
2	"NA"	0		0		0	
3	"Self"	-200		110		32212245	
4	"Hydro"	805890		5345		53932	
5	"ASR_Wall"	8		29		3	
6	"ASR_Fill"	1201658		28		334525	
7	"Shrnk"	0		2		5	
8	"Swell"	-14		-5		2	
9	"Earth"	1145877		561383		-2439	
10	"OBE_EW"	-7220929		-58		-2	
11	"OBE_NS"	225		-7106265		0	
12	"OBE_V"	49		-29		-6126732	
13	"OBE_H_0"	72		550723		1	
14	"OBE_H_90"	658971		-129		0	
15	"OBE_H_180"	-15		-360485		0	
16	"OBE_H_270"	-237887		-12		0	
17	"SSE_EW"	-11871648		-110		-26	
18	"SSE_NS"	352		-11689648		-20	
19	"SSE_V"	85		-45		-10591091	
20	"SSE_H_0"	135		1028018		1	
21	"SSE_H_90"	1230083		-245		1	
22	"SSE_H_180"	-29		-672905		0	
23	"SSE_H_270"	-444057		-18		1	

LC =	(0)	("NA")	(0)	(0)
	1	"NA"	0	0
	2	"NA"	0	0
	3	"Self"	-175297	-158600
	4	"Hydro"	33112	-8556
	5	"ASR_Wall"	-47	-28
	6	"ASR_Fill"	81901	223518
	7	"Shrnk"	-15	-19
	8	"Swell"	-18	-11
	9	"Earth"	55152	-26918
	10	"OBE_EW"	-1092301	-10
	11	"OBE_NS"	15	1076529
	12	"OBE_V"	9214	12163
	13	"OBE_H_0"	3	-28154
	14	"OBE_H_90"	33723	4
	15	"OBE_H_180"	0	18467
	16	"OBE_H_270"	-12164	1
	17	"SSE_EW"	-1737678	-15
	18	"SSE_NS"	23	1710643
	19	"SSE_V"	17916	23121
	20	"SSE_H_0"	5	-52554
	21	"SSE_H_90"	62949	7
	22	"SSE_H_180"	0	34473
	23	"SSE_H_270"	-22706	1

MX :=

ft·kip

MY :=

ft·kip

Z-coordinate at center of gravity (SR_ILC_03_I_r0.out)	$Z_{c.cg} := 644.63\text{in}$	
Z-coordinate at base of foundation (SR_ILC_03_I_r0.out)	$Z_{c.b} := -480\text{in}$	
X-coordiante at center of gravity (SR_ILC_03_I_r0.out)	$X_{c.cg} := 65.310\text{in}$	$X_{c.cg} = 5.442\text{ ft}$
Y-coordinate at center of gravity ((SR_ILC_03_I_r0.out)	$Y_{c.cg} := -59.058\text{in}$	$Y_{c.cg} = -4.921\text{ ft}$
Radius of outside of CEB foundation (Drawing 9763-F-101451)	$R_{CEB} := 86\text{ft} + 9\text{in}$	
Radius of outside of CEB wall (Drawing 9763-F-101451)	$R_{CEB.o} := 82\text{ft}$	
Radius of inside of CEB wall (Drawing 9763-F-101451)	$R_{CEB.i} := R_{CEB.o} - 3\text{ft}$	
Friction coefficient, concrete on concrete	$:= 0.6$	
Total height of fluid (Ref. I3, page 21 or 30)	$H_f := 60\text{ft}$	
Total unit weight of water	$w := 62.4 \frac{\text{lbf}}{\text{ft}^3}$	
Rock resistance (Ref. I3, Sheet 27)	$w_r := 90 \frac{\text{kip}}{\text{ft}}$	
Length of wall between radioactive tunnel and electrical tunnel (Ref. I3, Sheet 25)	$L_r := 61.73\text{ft}$	
Moment arm for rock resistance (Ref. I3, Sheet 25)	$d_r := 168.4\text{ft}$	

Total base shear calculations

Sliding to East, OBE

$$V_{E,OBE} := 1.2 \cdot FX_5 + 1.2 \cdot FX_6 + FX_7 + FX_8 + FX_9 + FX_{10} - 0.4FX_{11} + FX_{16} + 0.4(\min(FX_{13}, FX_{15})) \quad V_{E,OBE} = -4871 \cdot \text{kip}$$

Sliding to West, OBE

$$V_{W,OBE} := 1.2 \cdot FX_5 + 1.2 \cdot FX_6 + FX_7 + FX_8 + FX_9 - FX_{10} + 0.4FX_{11} + FX_{14} + 0.4(\max(FX_{13}, FX_{15})) \quad V_{W,OBE} = 10468 \cdot \text{kip}$$

Sliding to North, OBE

$$V_{N,OBE} := 1.2 \cdot FY_5 + 1.2 \cdot FY_6 + FY_7 + FY_8 + FY_9 + FY_{11} + 0.4FY_{10} + FY_{15} + 0.4(\min(FY_{14}, FY_{16})) \quad V_{N,OBE} = -6905 \cdot \text{kip}$$

Sliding to South, OBE

$$V_{S,OBE} := 1.2 \cdot FY_5 + 1.2 \cdot FY_6 + FY_7 + FY_8 + FY_9 - FY_{11} - 0.4FY_{10} + FY_{13} + 0.4(\max(FY_{14}, FY_{16})) \quad V_{S,OBE} = 8218 \cdot \text{kip}$$

Sliding to East, SSE

$$V_{E,SSE} := 1.2 \cdot FX_5 + 1.2 \cdot FX_6 + FX_7 + FX_8 + FX_9 + FX_{17} - 0.4FX_{18} + FX_{23} + 0.4(\min(FX_{20}, FX_{22})) \quad V_{E,SSE} = -9728 \cdot \text{kip}$$

Sliding to West, SSE

$$V_{W,SSE} := 1.2 \cdot FX_5 + 1.2 \cdot FX_6 + FX_7 + FX_8 + FX_9 - FX_{17} + 0.4FX_{18} + FX_{21} + 0.4(\max(FX_{20}, FX_{22})) \quad V_{W,SSE} = 15690 \cdot \text{kip}$$

Sliding to North, SSE

$$V_{N,SSE} := 1.2 \cdot FY_5 + 1.2 \cdot FY_6 + FY_7 + FY_8 + FY_9 + FY_{18} + 0.4FY_{17} + FY_{22} + 0.4(\min(FY_{21}, FY_{23})) \quad V_{N,SSE} = -11801 \cdot \text{kip}$$

Sliding to South, SSE

$$V_{S,SSE} := 1.2 \cdot FY_5 + 1.2 \cdot FY_6 + FY_7 + FY_8 + FY_9 - FY_{18} - 0.4FY_{17} + FY_{20} + 0.4(\max(FY_{21}, FY_{23})) \quad V_{S,SSE} = 13279 \cdot \text{kip}$$

Buoyancy

Total uplift pressure

$$P_{up} := H_f \cdot w$$

$$P_{up} = 3.744 \cdot \text{ksf}$$

Area of base, deduct openings
due to radioactive tunnels and
elec. tunnels (Ref. 13, p. 21 of 30)

$$A_{base} := \left(R_{CEB.o}^2 - R_{CEB.i}^2 \right) \cdot \frac{262}{360}$$

$$A_{base} = 1104 \cdot \text{ft}^2$$

Total buoyant force

$$F_b := P_{up} \cdot A_{base}$$

$$F_b = 4135 \cdot \text{kip}$$

Total resistance to sliding

Sliding resistance, OBE

$$V_{R.OBE} := \left(FZ_3 + FZ_4 - 0.4 \cdot FZ_{12} - F_b \right) \quad V_{R.OBE} = 18349 \cdot \text{kip}$$

Sliding resistance, SSE

$$V_{R.SSE} := \left(FZ_3 + FZ_4 - 0.4 \cdot FZ_{19} - F_b \right) \quad V_{R.SSE} = 19421 \cdot \text{kip}$$

Evaluation of sliding

Factor of Safety

$$OBE_{s,lim} := 1.5$$

$$SSE_{s,lim} := 1.1$$

Sliding to East, OBE

$$FS_{E.OBE} := \frac{V_{R.OBE}}{|V_{E.OBE}|} \quad FS_{E.OBE} = 3.767$$

Sliding to West, OBE

$$FS_{W.OBE} := \frac{V_{R.OBE}}{|V_{W.OBE}|} \quad FS_{W.OBE} = 1.753$$

Sliding to North, OBE

$$FS_{N.OBE} := \frac{V_{R.OBE}}{|V_{N.OBE}|} \quad FS_{N.OBE} = 2.657$$

Sliding to South, OBE

$$FS_{S.OBE} := \frac{V_{R.OBE}}{|V_{S.OBE}|} \quad FS_{S.OBE} = 2.233$$

Sliding to East, SSE

$$FS_{E.SSE} := \frac{V_{R.SSE}}{|V_{E.SSE}|} \quad FS_{E.SSE} = 1.996$$

Sliding to West, SSE

$$FS_{W.SSE} := \frac{V_{R.SSE}}{|V_{W.SSE}|} \quad FS_{W.SSE} = 1.238$$

Sliding to North, SSE

$$FS_{N.SSE} := \frac{V_{R.SSE}}{|V_{N.SSE}|} \quad FS_{N.SSE} = 1.646$$

Sliding to South, SSE

$$FS_{S.SSE} := \frac{V_{R.SSE}}{|V_{S.SSE}|} \quad FS_{S.SSE} = 1.463$$

The factor of safety for sliding from OBE is greater than 1.5 in all cases; therefore sliding stability is OK for OBE.

The factor of safety for sliding from SSE is greater than 1.1 in all cases; therefore sliding stability is OK for SSE.

Overturning calculation

Distance from center of gravity to
toe of foundation

$$L_{cg} := R_{CEB} - \sqrt{X_{c.cg}^2 + Y_{c.cg}^2}$$

$$L_{cg} = 79.412 \text{ ft}$$

Overturning to East, OBE

$$M_{E.OBE} := 1.2 \cdot MX_5 + 1.2 \cdot MX_6 + MX_7 + MX_8 + MX_9 + MX_{10} - 0.4MX_{11} + MX_{16} + 0.4(\min(MX_{13}, MX_{15}))$$

$$M_{E.OBE} = -951127 \text{ ft}\cdot\text{kip}$$

Overturning to West, OBE

$$M_{W.OBE} := 1.2 \cdot MX_5 + 1.2 \cdot MX_6 + MX_7 + MX_8 + MX_9 - MX_{10} + 0.4MX_{11} + MX_{14} + 0.4(\max(MX_{13}, MX_{15}))$$

$$M_{W.OBE} = 1279375 \text{ ft}\cdot\text{kip}$$

Overturning to North, OBE

$$M_{N.OBE} := 1.2 \cdot MY_5 + 1.2 \cdot MY_6 + MY_7 + MY_8 + MY_9 + MY_{11} + 0.4MY_{10} + MY_{15} + 0.4(\min(MY_{14}, MY_{16}))$$

$$M_{N.OBE} = 1336232 \text{ ft}\cdot\text{kip}$$

Overturning to South, OBE

$$M_{S.OBE} := 1.2 \cdot MY_5 + 1.2 \cdot MY_6 + MY_7 + MY_8 + MY_9 - MY_{11} - 0.4MY_{10} + MY_{13} + 0.4(\max(MY_{14}, MY_{16}))$$

$$M_{S.OBE} = -863437 \text{ ft}\cdot\text{kip}$$

Overturning to East, SSE

$$M_{E.SSE} := 1.2 \cdot MX_5 + 1.2 \cdot MX_6 + MX_7 + MX_8 + MX_9 + MX_{17} - 0.4MX_{18} + MX_{23} + 0.4(\min(MX_{20}, MX_{22}))$$

$$M_{E.SSE} = -1607049 \text{ ft}\cdot\text{kip}$$

Overturning to West, SSE

$$M_{W.SSE} := 1.2 \cdot MX_5 + 1.2 \cdot MX_6 + MX_7 + MX_8 + MX_9 - MX_{17} + 0.4MX_{18} + MX_{21} + 0.4(\max(MX_{20}, MX_{22}))$$

$$M_{W.SSE} = 1953982 \text{ ft}\cdot\text{kip}$$

Overturning to North, SSE

$$M_{N.SSE} := 1.2 \cdot MY_5 + 1.2 \cdot MY_6 + MY_7 + MY_8 + MY_9 + MY_{18} + 0.4MY_{17} + MY_{22} + 0.4(\min(MY_{21}, MY_{23}))$$

$$M_{N.SSE} = 1986350 \text{ ft}\cdot\text{kip}$$

Overturning to South, SSE

$$M_{S.SSE} := 1.2 \cdot MY_5 + 1.2 \cdot MY_6 + MY_7 + MY_8 + MY_9 - MY_{18} - 0.4MY_{17} + MY_{20} + 0.4(\max(MY_{21}, MY_{23}))$$

$$M_{S.SSE} = -1521948 \text{ ft}\cdot\text{kip}$$

Total resistance to overturning

Overturning resistance, OBE $M_{R,OBE} := (FZ_3 + FZ_4 + 0.4 \cdot FZ_{12} - F_b) \cdot L_{cg} + w_r \cdot L_r \cdot d_r$ $M_{R,OBE} = 2974959 \text{ ft} \cdot \text{kip}$

Overturning resistance, SSE $M_{R,SSE} := (FZ_3 + FZ_4 + 0.4 \cdot FZ_{19} - F_b) \cdot L_{cg} + w_r \cdot L_r \cdot d_r$ $M_{R,SSE} = 2833149 \text{ ft} \cdot \text{kip}$

Evaluation of overturning

Factor of Safety $OBE_{o.lim} := 1.5$

$$SSE_{o.lim} := 1.1$$

Overturning to East, OBE $FS_{E,OBE} := \left| \frac{M_{R,OBE}}{M_{E,OBE}} \right|$ $FS_{E,OBE} = 3.128$

Overturning to West, OBE $FS_{W,OBE} := \left| \frac{M_{R,OBE}}{M_{W,OBE}} \right|$ $FS_{W,OBE} = 2.325$

Overturning to North, OBE $FS_{N,OBE} := \left| \frac{M_{R,OBE}}{M_{N,OBE}} \right|$ $FS_{N,OBE} = 2.226$

Overturning to South, OBE $FS_{S,OBE} := \left| \frac{M_{R,OBE}}{M_{S,OBE}} \right|$ $FS_{S,OBE} = 3.445$

Factor of safety for OBE overturning is greater than 1.5 for all cases, therefore the CEB will not overturn for OBE loads.

Overturning to East, SSE $FS_{E,O,SSE} := \left| \frac{M_{R,SSE}}{M_{E,SSE}} \right|$ $FS_{E,O,SSE} = 1.763$

Overturning to West, SSE $FS_{W,O,SSE} := \left| \frac{M_{R,SSE}}{M_{W,SSE}} \right|$ $FS_{W,O,SSE} = 1.45$

Overturning to North, SSE $FS_{N,O,SSE} := \left| \frac{M_{R,SSE}}{M_{N,SSE}} \right|$ $FS_{N,O,SSE} = 1.426$

Overturning to South, SSE $FS_{S,O,SSE} := \left| \frac{M_{R,SSE}}{M_{S,SSE}} \right|$ $FS_{S,O,SSE} = 1.862$

Factor of safety for SSE overturning is greater than 1.1 for all cases, therefore the CEB will not overturn for SSE loads.

Evaluation of buoyancy

$$F_{lim} := 1.1$$

Factor of safety for flotation $FS_F := \frac{FZ_3}{F_b}$ $FS_F = 7.791$

Factor of safety for flotation is greater than 1.1, therefore the CEB will not float.



Appendix J Parametric Studies

J1. REVISION HISTORY

J1.1. Revision 0

Initial document.

J2. OVERVIEW

Parametric studies supporting the analyses and evaluations performed in this calculation are documented in this appendix. The purpose and conclusions of each parametric study is provided individually in the subsequent sections. A list of parametric studies is below.

- Parametric Study One: Study impact of reduced concrete elastic modulus (Section J3)
- Parametric Study Two: Study impact of ASR expansion applied at springline (Section J4)
- Parametric Study Three: Study impact of concrete fill ASR expansion on CEB deformation (Section J5)

J2.1. PARAMETRIC STUDY ONE: STUDY IMPACT OF REDUCED CONCRETE ELASTIC MODULUS

J2.2. Purpose and Description

This parametric study is performed to assess the impact of modeling the concrete of the CEB with a reduced elastic modulus. Physical testing, as noted in main body of this calculation, of concrete cores affected by ASR removed from in-situ conditions have indicated a reduction in elastic modulus. This parametric study is performed by reducing the elastic modulus of the concrete by 50% (referred to as Analysis Set H in this appendix) and compares resulting computed demands due to ASR expansion of the CEB wall to a case performed without a reduction in elastic modulus (referred to as Analysis Set A in this appendix). This parametric study was performed on a development version of the CEB model, which has small differences in geometry and ASR expansion profile than the CEB model documented in this calculation. However, since the conclusions of this study are based on comparison with a corresponding development model, the use of a development model in this study is judged to be inconsequential.

**J2.3. Results and Conclusions**

The elastic modulus has negligible impact on the radial deformations due to ASR of the CEB wall (Table J-1). This is because ASR strains are a prescribed value. The reinforcement and concrete stresses are consistently larger in Set A, indicating that it is conservative to use the concrete elastic modulus without reduction. For this reason, no reduction will be applied to the concrete elastic modulus in the CEB model.

J3. PARAMETRIC STUDY TWO: STUDY IMPACT OF ASR EXPANSION APPLIED AT SPRINGLINE**J3.1. Purpose and Description**

CI measurements recorded at the springline indicate strains of about 0.1% in the hoop direction and about 0.05% in the vertical direction. As noted in Section 6.3.1 of the main body of the calculation, the orientation and pattern of cracks at the springline elevation indicate that cracking is at least partially related to structural demands rather than ASR expansion alone. ASR cracking typically has a map pattern, which is generally less apparent at the springline elevation than at other ASR monitoring locations. Structural cracking at the springline may be related to thrust forces from the transition between the CEB dome and shell. The cracks may have initiated during construction of the CEB, when the dome concrete was curing; at that time the eccentric weight of the dome was present, but the stiffness and strength of the dome were not yet developed. Nevertheless, this parametric study is carried out with a conservative assumption that the cracks at the springline are due to ASR to assess its impact on the CEB structure. This parametric study was performed on a development version of the CEB model, which has some differences in ASR expansion profile in comparison to the CEB model documented in the main body of this calculation. However, since the conclusions of this study are based on comparison with a corresponding development model, the use of a development model in this study is judged to be inconsequential.

J3.2. Results and Conclusions

In this study, the Standard-Plus analysis case subject to load combination NO_1 is used as a baseline for comparison with the case study with additional ASR at the springline. The concrete surface strains in the Hoop and Meridional directions due to application of ASR in CEB wall alone for Standard-Plus analysis case are shown in Figures J1 and J3, respectively. Additional ASR at



the springline are applied to this analysis case to simulate recent field measurements of cracks found at the springline. The concrete surface strains in the Hoop and Meridional directions due to application of ASR in CEB wall alone for Standard-Plus analysis case plus additional ASR at the springline are shown in Figure J2 and J4, respectively. As can be seen from these figures, there is a narrow band of additional ASR strain of 0.8% at the springline in both the Hoop and Meridional directions. Comparison of the demand-to-capacity ratios (DCRs) of the Standard-Plus analysis case with and without additional ASR at the springline are shown in Figures J5 through J16, for axial compression, in-plane shear, out-of-plane shear, and axial-flexure interaction. As can be seen from these figures, all DCRs except the in-plane shear have increased at the springline. The additional ASR at the springline does not cause the DCRs for in-plane shear or for axial compression in the hoop direction, or meridional direction to exceed 1.0. There is little to no change to the DCRs away from the springline, which suggest the high strain measurements at the springline regardless of whether they are caused by ASR or are from construction do not significantly affect the CEB structural performance in other regions away from the springline.

J4. PARAMETRIC STUDY THREE: STUDY IMPACT OF CONCRETE FILL ASR EXPANSION ON CEB DEFORMATION

J4.1. Purpose and Description

The purpose of this parametric study is to evaluate the impact of concrete fill ASR expansion on the CEB deformation, and to select a case for further structural evaluation. The selected case is to provide an improved simulation of deformation measurements near AZ 230° over the "Standard" case by assuming that the concrete fill in the wedge region near AZ 230° is in contact with the CEB, which does not conform to design drawings. The following three cases were considered in this parametric study:

Case 1: Concrete fill ASR expansion corresponding to 100% of the overburden pressure in the wedge only (above EL. 19 ft) and 50% below EL. 19 ft; see Figure J19.

Case 2: Concrete fill ASR expansion corresponding to 100% of the overburden pressure in the wedge only (above EL. 19 ft), 50% below EL. 0 ft, and 0% between EL. 0 ft and 19 ft; see Figure J20.



Case 3: Concrete fill ASR expansion corresponding to 50 to 100% of the overburden pressure at EL. 19 ft applied as gradient over wedge height, 50% below EL. 0 ft, and 0% between EL. 0 ft and 19 ft; see Figure J21.

J4.2. Results and Conclusions

Comparison of CEB deformation between Cases 1 and 2 at EL. 5.96 ft, 22.25 ft, 51.08 ft, and 119 ft are shown in Figures J22, J23, J24, and J25, respectively. Available field measurements at EL. 5.96 ft, 22.25 ft, and 119 ft are also included in the figures for comparison. There are no field measurements at elevation 51.08 ft. Results show Case 2 having less deformation than Case 1 in the wedge region near AZ 230°, and that both cases have less deformation than field measurements. The concrete fill ASR expansion pressure on CEB wall of Cases 1 and 2 are the same except that Case 2 has no pressure between elevation 0 to 19 ft near AZ 230°, and therefore resulted in less deformation in that region. Comparison of CEB deformation between Cases 1 and 3 at EL. 5.96 ft, 22.25 ft, 51.08 ft, and 119 ft are shown in Figures J26, J27, J28, and J29, respectively. As can be seen from these figures, the increase in concrete fill ASR expansion pressure in the wedge region from Case 2 to 3 resulted in deformation more similar to Case 1. Deformations for all three cases are similar at EL. 119 ft. Case 3 provides an improved simulation of deformation measurements near AZ 230° over the "Standard" and therefore is selected for further structural evaluation. Case 3 is referred elsewhere in the calculation as the "Standard-Plus" case.



J5. TABLES

Table J-1 – Comparison of Radial Deformations (in.) from ASR of Wall Independent Load Case (ILC) With and Without 50% Reduction in Concrete Elastic Modulus

FEA Node Number:	2203765	2200000	2203828	2200049	2200149	2212091	2101474	2200074	2212193	2206286	2202603
Approximate Azimuth:	AZ 210	AZ 270	AZ 330	AZ 270	AZ 280	AZ 100	AZ 340	AZ 270	AZ 90	AZ 0	AZ 315
Approximate Elevation:	EL +22ft	EL +22ft	EL +22ft	EL +50ft	EL +3ft	EL +13ft	EL 0ft	EL +119ft	EL +119ft	EL +28ft	EL +50
Description:	CEVA Area	Top of W. Pipe Chase Projection	Personnel Hatch Area	Radiation Shield Above W. Pipe Chase	Bottom of W. Pipe Chase Projection	East Pipe Chase	Side of Electrical Penetration	Spring Line, West	Spring Line, East	Top of Electrical Penetration	Above Personnel Hatch, on Rad Shield
ASR of Wall ILC - Parametric Analysis Set A	-0.41	1.36	0.01	1.01	1.65	-0.25	0.01	0.54	-0.45	1.17	-0.03
ASR of Wall ILC - Parametric Analysis Set H	-0.40	1.33	0.02	0.99	1.61	-0.25	0.00	0.53	-0.44	1.14	-0.02

J6. FIGURES

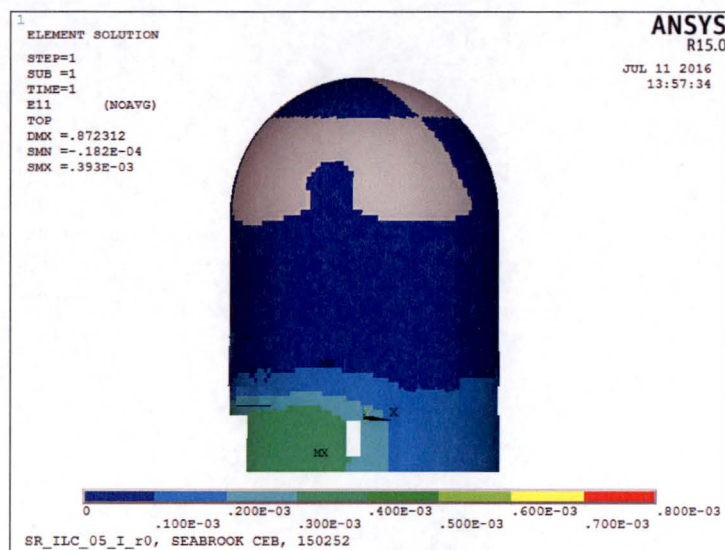


Figure J1. Concrete Surface Strains in the Hoop Direction due to Application of ASR in CEB Wall for Standard-Plus Analysis Case.

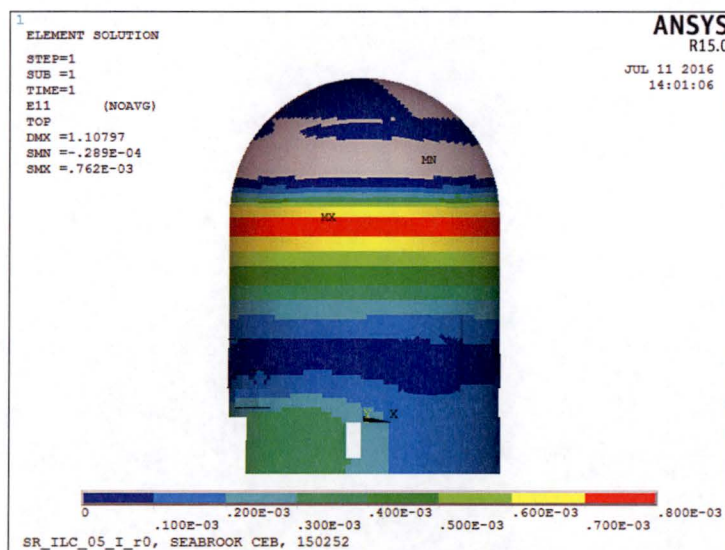


Figure J2. Concrete Surface Strains in the Hoop Direction due to Application of ASR in CEB Wall for Standard-Plus Analysis Case Plus Additional ASR at the Springline.

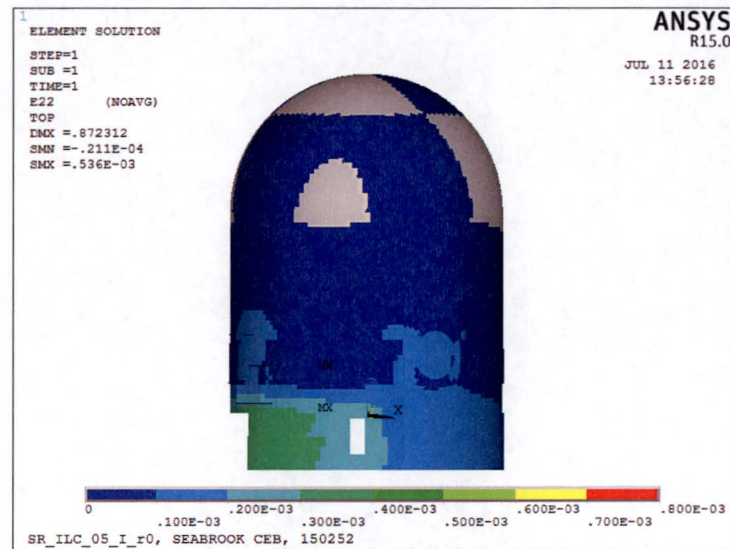


Figure J3. Concrete Surface Strains in the Meridional Direction due to Application of ASR in CEB Wall for Standard-Plus Analysis Case.

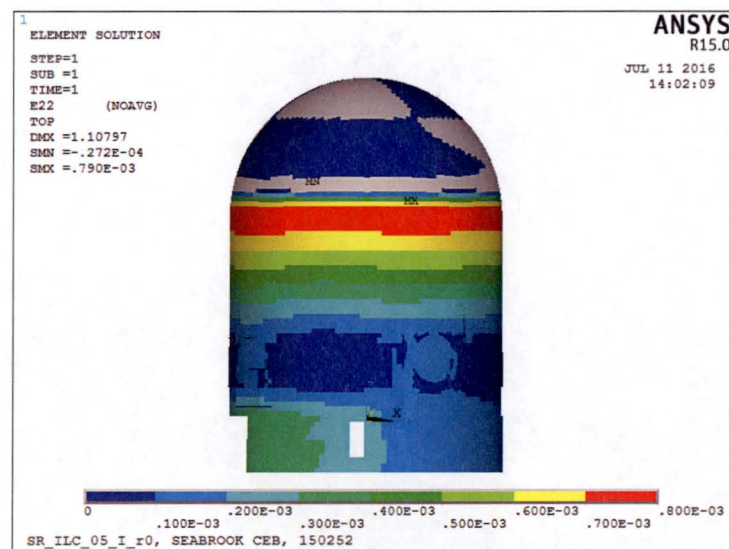


Figure J4. Concrete Surface Strains in the Meridional Direction due to Application of ASR in CEB Wall for Standard-Plus Analysis Case Plus Additional ASR at the Springline

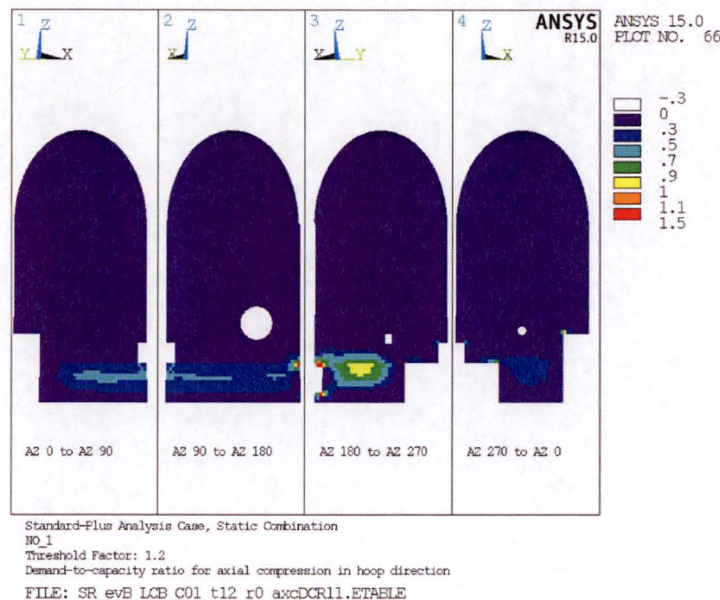


Figure J5. DCRs for Axial Compression in the Hoop Direction for Combination NO_1 for the Standard-Plus Analysis Case

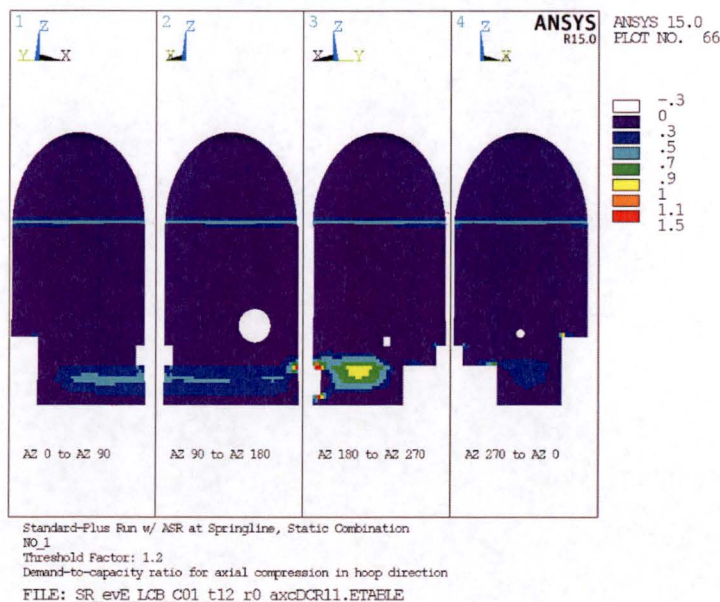


Figure J6. DCRs for Axial Compression in the Hoop Direction for Combination NO_1 for the Standard-Plus Analysis Case Plus Additional ASR at the Springline

CLIENT: NextEra Energy Seabrook

SUBJECT: Evaluation and Design Confirmation of As-Deformed CEB

PROJECT NO: 150252

DATE: July 2016

BY: R.M. Mones

VERIFIER: A.T. Sarawit

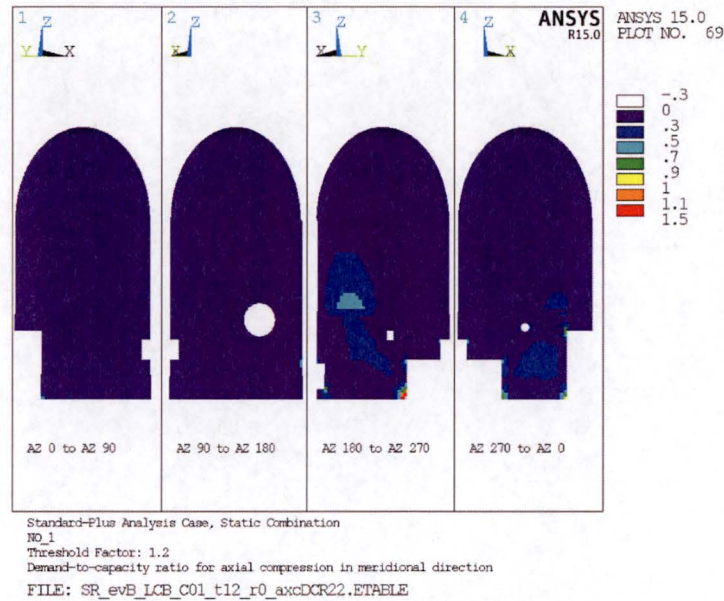


Figure J7. DCRs for Axial Compression in the Meridional Direction for Combination NO_1 for the Standard-Plus Analysis Case

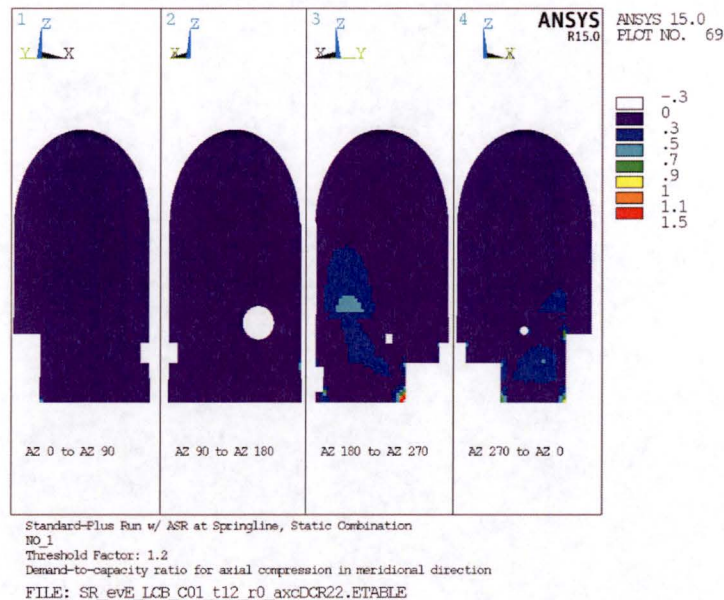


Figure J8. DCRs for Axial Compression in the Meridional Direction for Combination NO_1 for the Standard-Plus Analysis Case Plus Additional ASR at the Springline

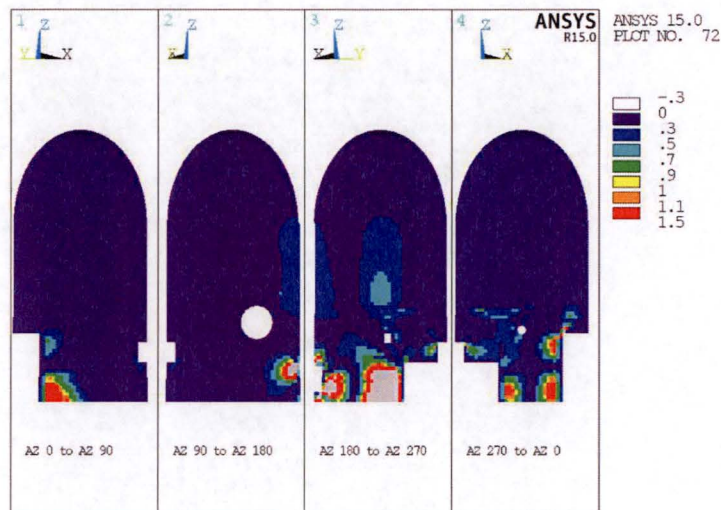


Figure J9. DCRs for In-Plane Shear for Combination NO_1 for the Standard-Plus Analysis Case

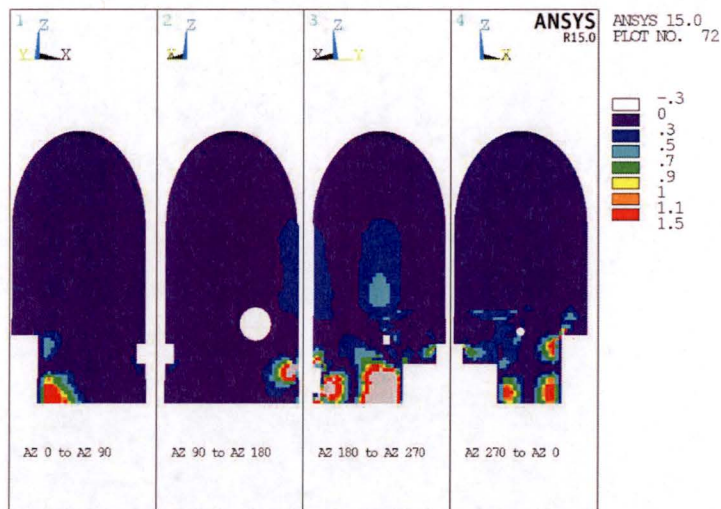


Figure J10. DCRs for In-Plane Shear for Combination NO_1 for the Standard-Plus Analysis Case Plus Additional ASR at the Springline

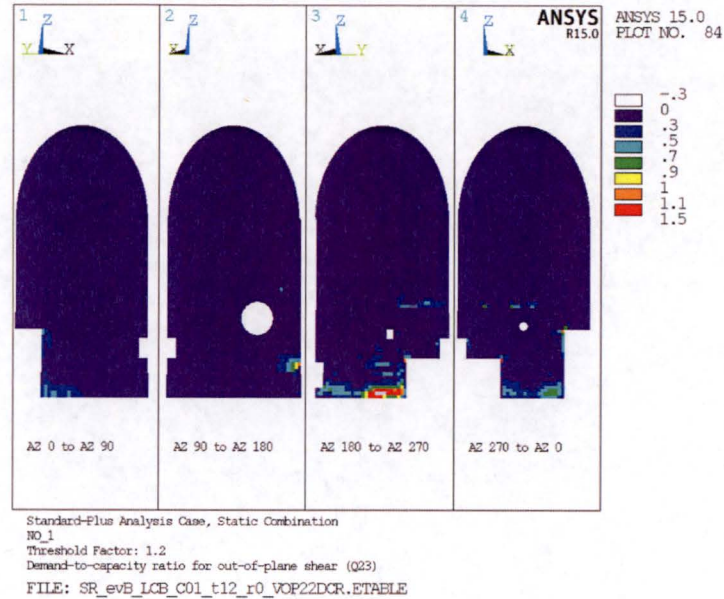


Figure J11. DCRs for Out-of-Plane Shear (acting on hoop-radial plane) for Combination NO_1 for the Standard-Plus Analysis Case

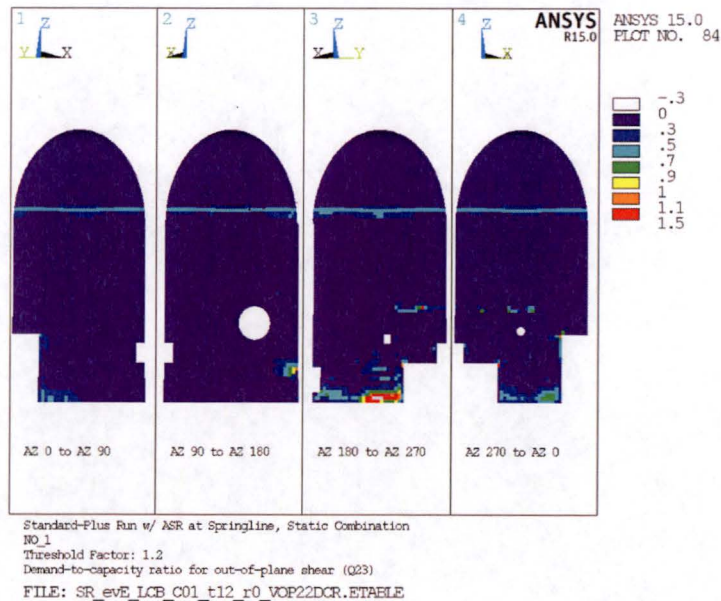


Figure J12. DCRs for Out-of-Plane Shear (acting on hoop-radial plane) for Combination NO_1 for the Standard-Plus Analysis Case Plus Additional ASR at the Springline

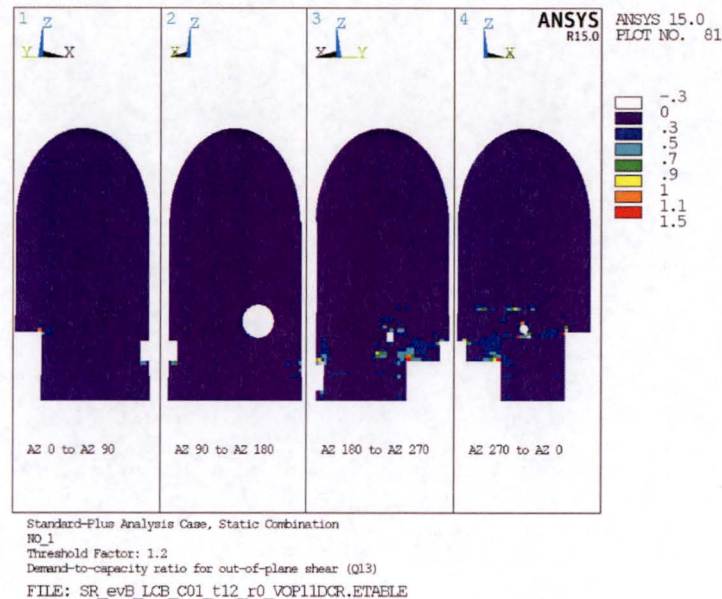


Figure J13. DCRs for Out-of-Plane Shear (acting on meridional-radial plane) for Combination NO_1 for the Standard-Plus Analysis Case

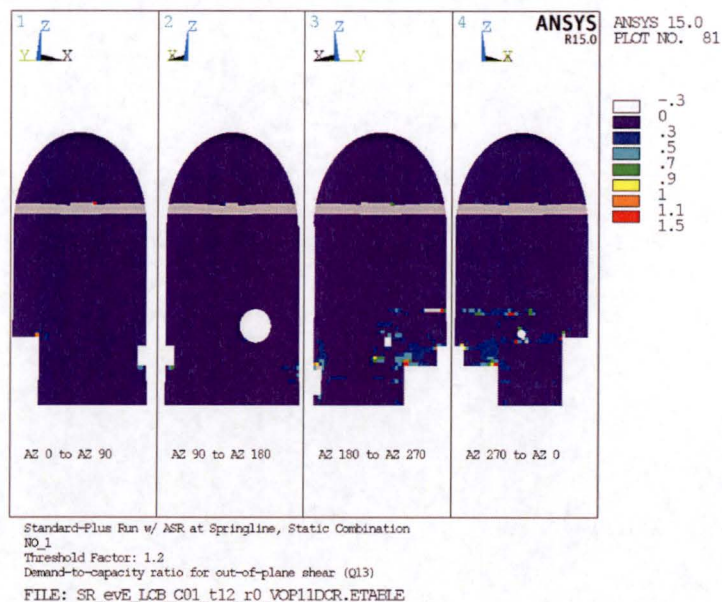


Figure J14. DCRs for Out-of-Plane Shear (acting on meridional-radial plane) for Combination NO_1 for the Standard-Plus Analysis Case Plus Additional ASR at Springline

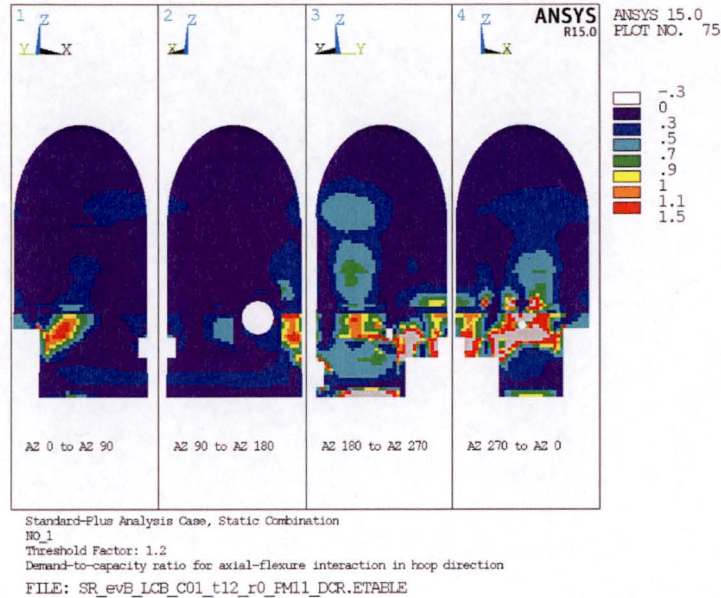


Figure J15. DCRs for Axial-Flexure Interaction in the Hoop Direction for Combination NO_1 for the Standard-Plus Analysis Case

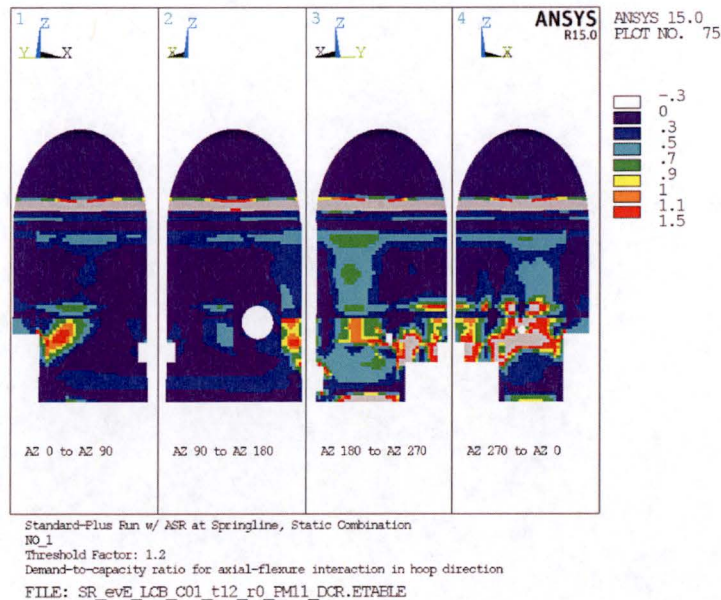


Figure J16. DCRs for Axial-Flexure Interaction in the Hoop Direction for Combination NO_1 for the Standard-Plus Analysis Case Plus Additional ASR at the Springline

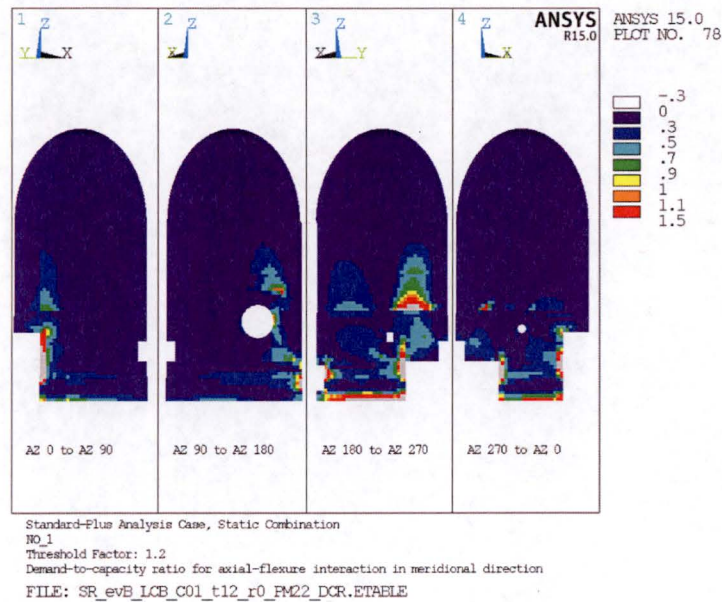


Figure J17. DCRs for Axial-Flexure Interaction in the Meridional Direction for Combination NO_1 for the Standard-Plus Analysis Case

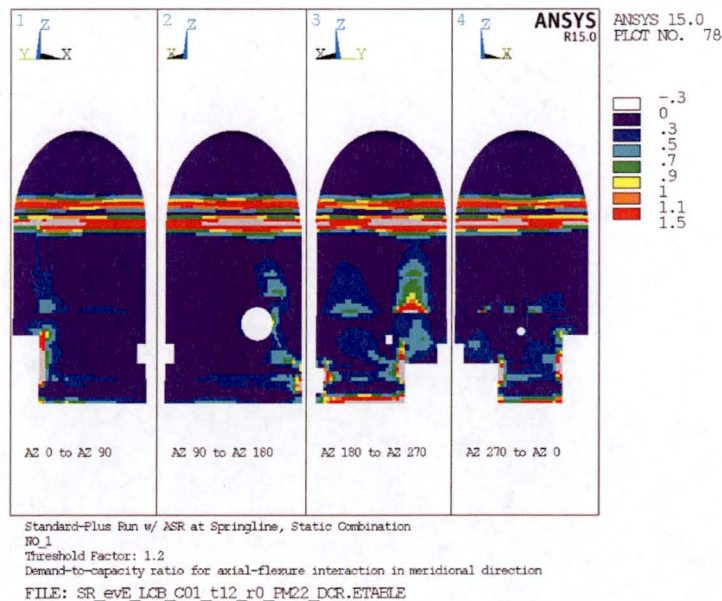


Figure J18. DCRs for Axial-Flexure Interaction in the Meridional Direction for Combination NO_1 for the Standard-Plus Analysis Case Plus Additional ASR at the Springline

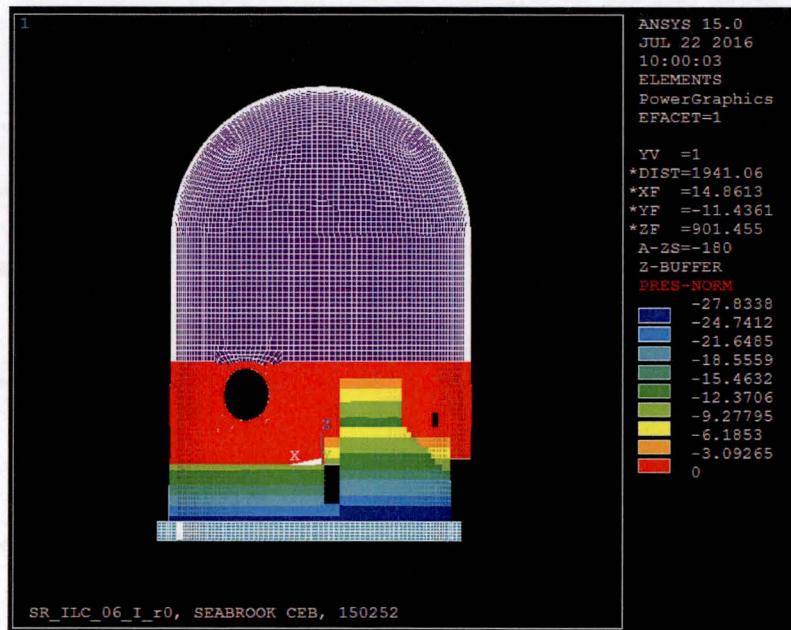


Figure J19. Concrete fill pressure on CEB wall for Case 1: Concrete fill ASR expansion corresponding to 100% of the overburden pressure in the wedge only (above EL. 19 ft) and 50% below EL. 19 ft (looking from inside CEB).

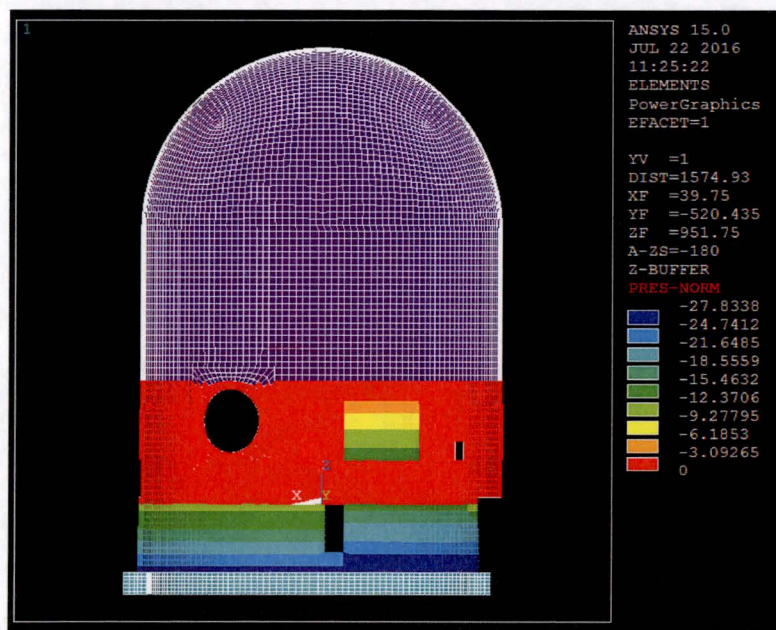


Figure J20. Concrete fill pressure on CEB wall for Case 2: Concrete fill ASR expansion corresponding to 100% of the overburden pressure in the wedge only (above EL. 19 ft), 50% below EL. 0 ft, and 0% between EL. 0 ft and 19 ft (looking from inside CEB).

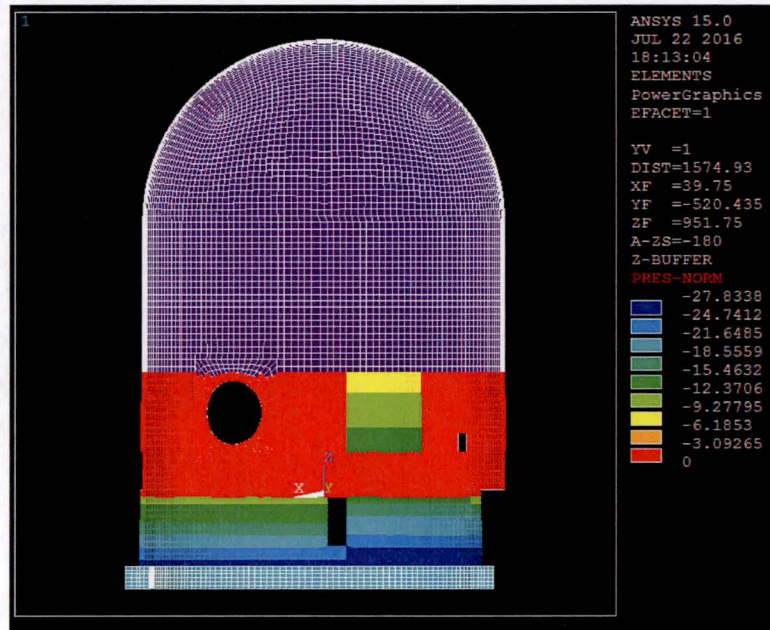


Figure J21. Concrete fill pressure on CEB wall for Case 3: Concrete fill ASR expansion corresponding to 50 to 100% of the overburden pressure at E. 19 ft applied as gradient over wedge height, 50% below EL. 0 ft, and 0% between EL. 0 ft and 19 ft (looking from inside CEB).

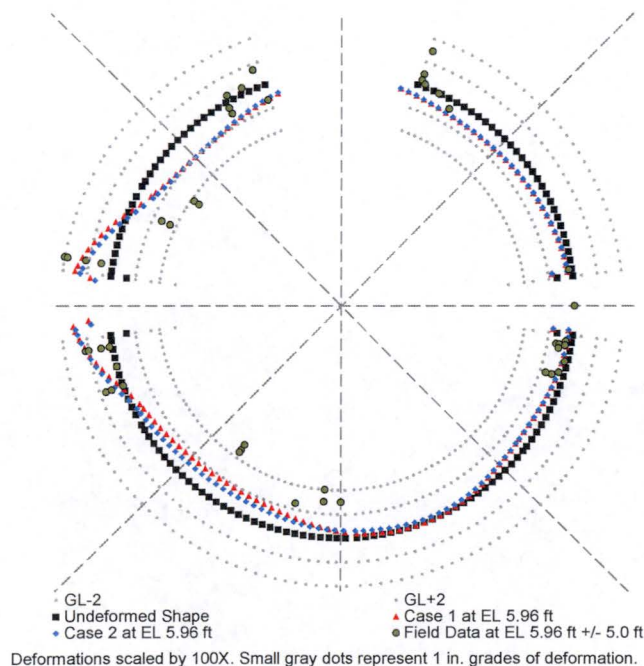


Figure J22. Deformation comparison between Cases 1 and 2, and Field Data at EL. 5.96 ft

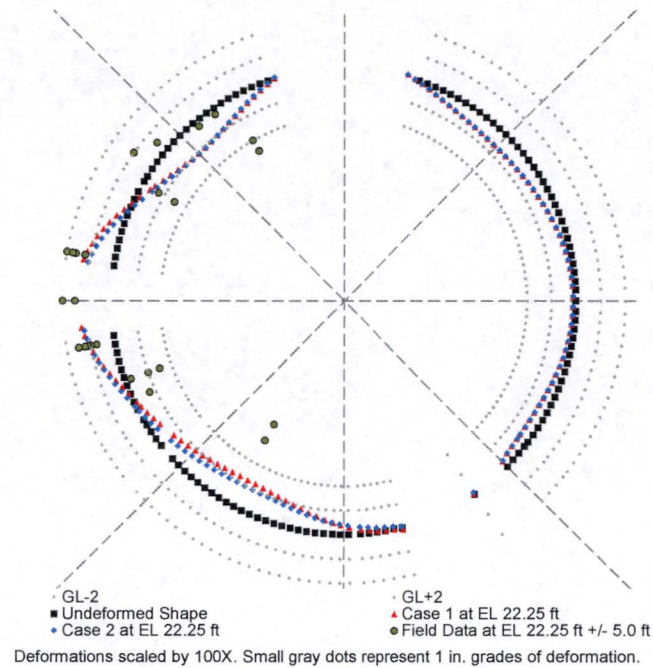


Figure J23. Deformation comparison between Cases 1 and 2, and Field Data at EL. 22.25 ft

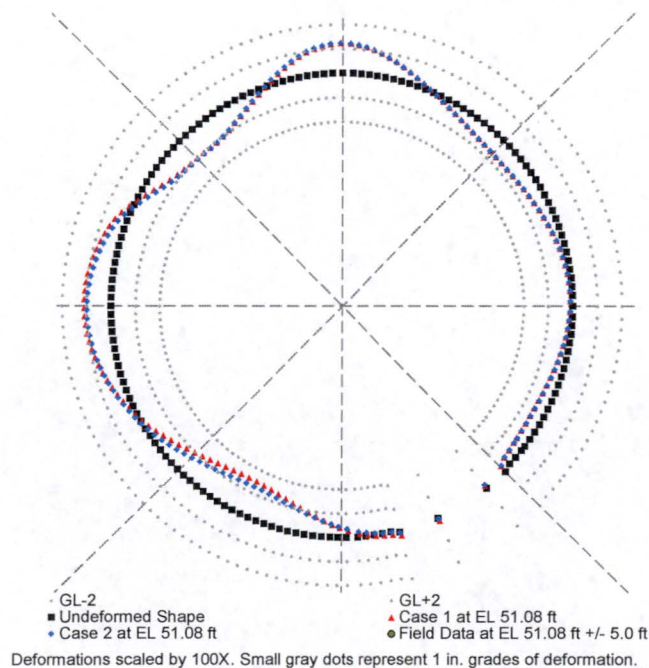


Figure J24. Deformation comparison between Cases 1 and 2, and Field Data at EL. 51.08 ft

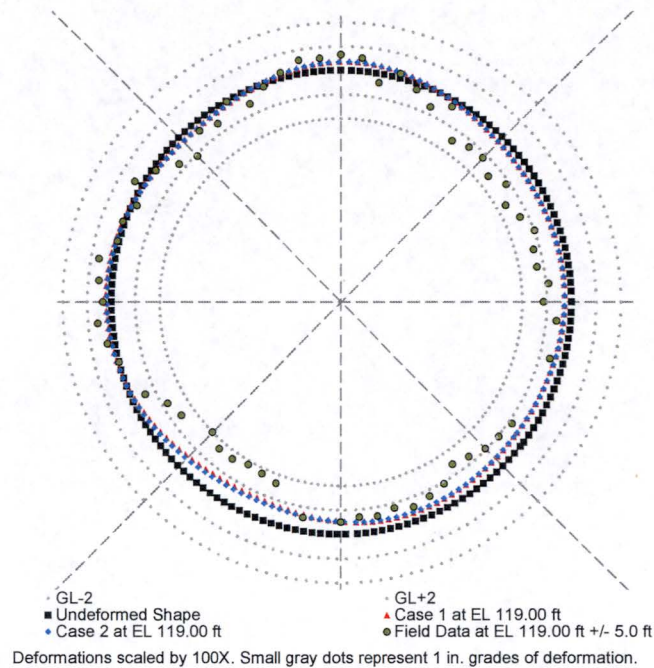


Figure J25. Deformation comparison between Cases 1 and 2, and Field Data at EL. 119.00 ft

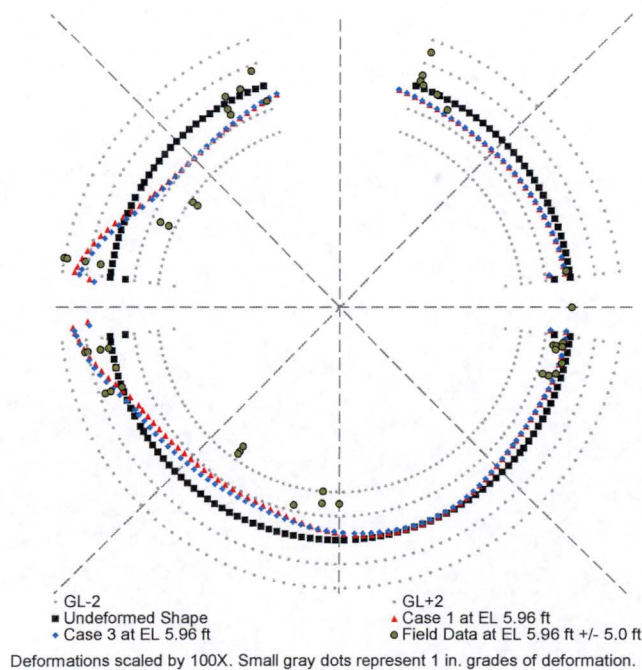


Figure J26. Deformation comparison between Cases 1 and 3, and Field Data at EL. 5.96 ft

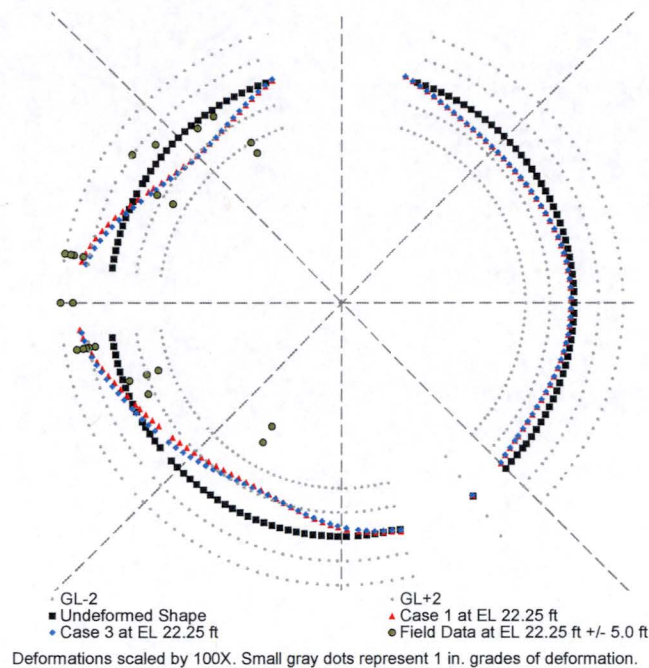


Figure J27. Deformation comparison between Cases 1 and 3, and Field Data at EL. 22.25 ft

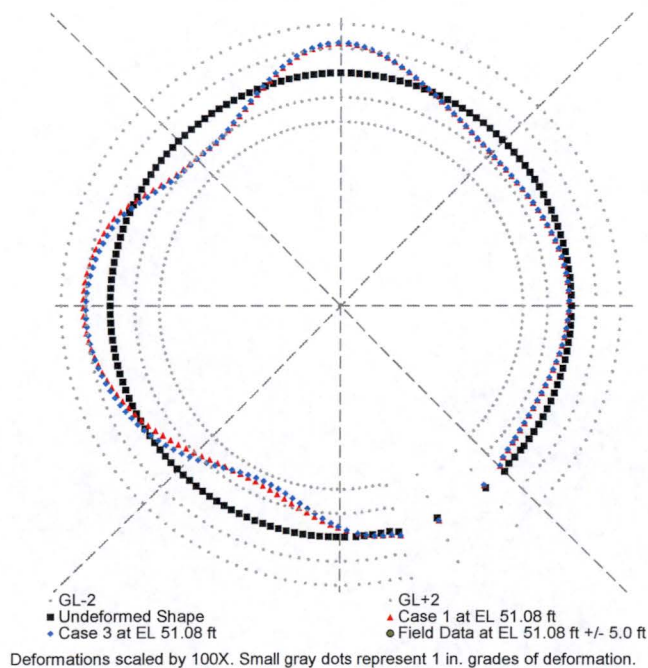


Figure J28. Deformation comparison between Cases 1 and 3, and Field Data at EL. 51.08 ft

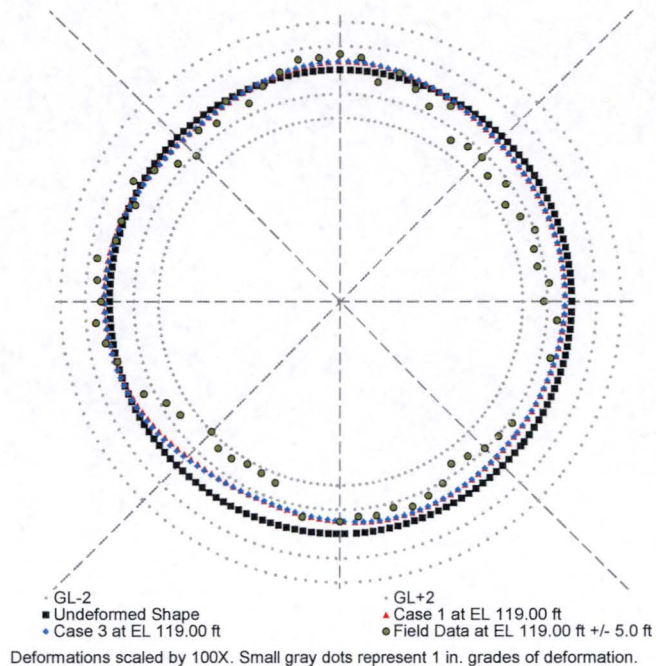


Figure J29. Deformation comparison between Cases 1 and 3, and Field Data at EL. 119.00 ft

PROJECT NO: 150252DATE: July 2016CLIENT: NextEra Energy SeabrookBY: R.M. MonesSUBJECT: Evaluation and Design Confirmation of As-Deformed CEBVERIFIER: A.T. Sarawit

Appendix K Evaluation Examples

K1. REVISION HISTORY

K1.1. Revision 0

Initial document.

K2. OVERVIEW

Provide example computation demonstrating the element-by-element evaluation methodology.
Element-by-element evaluation example is provided in Table K1.

Table K1. Demonstration of Element-By-Element Evaluation for One Element

Define Notation For Element Forces and Moments

Axis 1 is in hoop direction; Axis 2 is in meridional direction; Axis 3 is in radial direction

N11 = Axial force in hoop direction, kip/ft

N22 = Axial force in meridional direction, kip/ft

N12 = In-plane shear force, kip/ft

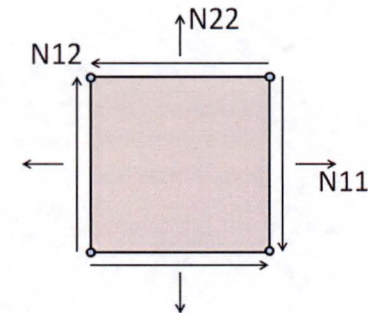
M11 = Bending moment about axis 2 (stresses rebars aligned with axis 1), kip-ft/ft

M22 = Bending moment about axis 1 (stresses rebars aligned with axis 2), kip-ft/ft

M12 = Torsional Bending Moment, kip-ft/ft

Q13 = Out-of-plane shear along hoop axis, kip/ft

Q23 = Out-of-plane shear along meridional axis, kip/ft



All forces and moments are given two subscripts:

First Subscript:

- Subscript C is given to all forces and moments extracted from the concrete element and
- Subscript S is given to all forces and moments extracted from the steel reinforcement membrane element.

Second Subscript:

- Subscript A is given to all forces and moments from self-straining loads,
- Subscript D is given to all forces and moments associated with original SD-66 loads.

For example, N11_{CA} is the total hoop axial force in the concrete due to self-straining loads

Element and Loading Information

Concrete Element Number: 2100117

Hoop/Meridional Reinforcement Element Number: 6100117/7100117

Element Description: El. -17 ft, AZ 218°

South of Mechanical Penetration near base of CEB

Thickness: 36 in.

Reinforcement in Hoop Direction: #11@12" Each Face

Reinforcement in Meridional Direction:

One #11@6" Inside Face and Two Layers #11@6 Outside Face

Analysis Case: Standard Analysis Case

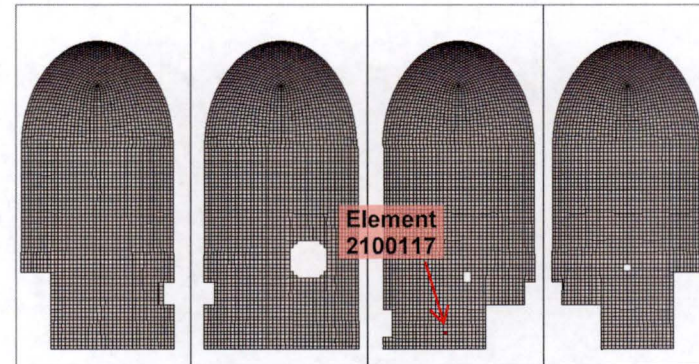
Loads: Combination OBE_1 with seismic excitation 100% East, 40%

North, and 40% Vertical Up. Threshold factor of 1.2 on ASR loads.

$(1.3 \times 1.2)S_a + 1.4S_w + 1.4D + 1.7L + 1.9E_o + 1.7H + 1.9H_e$

Evaluation results saved with the file name: SR_evA_LCB_D01_t12_r0

Element Location:



AZ 0° to 90°

AZ 90° to 180°

AZ 180° to 270°

AZ 270° to 0°



Table K1. Demonstration of Element-By-Element Evaluation for One Element

Analysis Step One

Compute as-deformed shape due to Independent Load Cases (ILCs) 3, 4, 5, 6, 7, 8, and 9 without load factors. Account for creep by multiplying deformations due to ILC 3, 4, and 9 by a factor of $(1.3 + 1.0)$, where 1.3 is the creep coefficient and the added 1.0 accounts for instantaneous deformations.

Also in Analysis Step One, compute the demands due to self-straining loads (ILC 5, 6, and 8 only, conservatively neglect all other self-straining loads):

Demands for Concrete Element (Element 2100117)

ILC	N11	N22	N12	M11	M22	M12	Q13	Q23
5	-35.03	-99.25	19.26	5.67	0.37	0.54	0.00	-1.52
6	-81.36	16.61	-37.87	-5.74	-29.72	-14.68	0.58	-9.26
8	-42.42	-29.12	25.23	1.21	0.70	0.40	0.00	-0.20

Demands for Hoop Reinforcement Element (Element 6100117)

ILC	N11	N22	N12	M11	M22	M12	Q13	Q23
5	35.02	0.0	0.0	0.0	0.0	0.0	0.0	0.0
8	6.84	0.0	0.0	0.0	0.0	0.0	0.0	0.0

Demands for Meridional Reinforcement Element (Element 7100117)

ILC	N11	N22	N12	M11	M22	M12	Q13	Q23
5	0.0	92.19	0.0	0.0	0.0	0.0	0.0	0.0
8	0.0	23.18	0.0	0.0	0.0	0.0	0.0	0.0

Combined and Factored Demands (Concrete)

	N11 _{CA}	N22 _{CA}	N12 _{CA}	M11 _{CA}	M22 _{CA}	M12 _{CA}	Q13 _{CA}	Q23 _{CA}
Conc.	-240.96	-169.68	6.29	1.58	-44.81	-21.51	0.91	-17.10

Combined and Factored Demands (Steel)

	N11 _{SA}	N22 _{SA}	N12 _{SA}	M11 _{SA}	M22 _{SA}	M12 _{SA}	Q13 _{SA}	Q23 _{SA}
Steel	64.21	176.27	0.00	0.00	0.00	0.00	0.00	0.00

Commentary

Loads from each independent load case are listed in this section.

Each ILC used in this example problem is briefly described below:

- ILC 3 = Self Weight
- ILC 4 = Hydrostatic Pressure
- ILC 5 = ASR of Wall
- ILC 6 = ASR of Fill
- ILC 7 = Shrinkage
- ILC 8 = Swelling
- ILC 9 = Static Earth Pressure
- ILC 10 = OBE Accelerations in East/West
- ILC 11 = OBE Accelerations in North/South
- ILC 12 = OBE Accelerations in Vertical
- ILC 15 = OBE Dynamic Soil Pressures Pushing North
- ILC 16 = OBE Dynamic Soil Pressures Pushing East
- ILC 24 = Live (Snow) Loads

Sign conventions and units are listed below:

- Positive axial loads are tensile.
- Positive bending moments cause tensile stress on the outside face of the CEB wall.
- Forces shown are in units of kip/ft
- Moments shown are in units of kip-ft/ft

Note: Reinforcement elements are active only in ILC 5 and 8, and therefore do not have output in all other ILCs.

Note: ASR demands (ILC 5 and 6) are factored by 1.3×1.2 (load factor and threshold factor). Swelling demands (ILC 8) are factored by 1.4 (same as dead load).



Table K1. Demonstration of Element-By-Element Evaluation for One Element

Analysis Step Two

Demands for Concrete Element (Element 2100117)

ILC	N11	N22	N12	M11	M22	M12	Q13	Q23
3	-11.92	-79.43	3.08	-0.08	-0.53	-0.07	0.00	-0.10
4	-1.89	-0.75	-0.84	-1.20	-1.70	0.92	0.13	0.17
9	-1.37	-2.22	-2.76	-0.01	-0.02	-0.04	0.00	0.00
10	7.98	57.90	23.94	0.05	0.41	0.54	0.00	0.07
11	17.97	39.21	-29.38	0.16	0.35	-0.54	-0.01	0.06
12	2.89	18.74	-0.74	0.02	0.13	0.02	0.00	0.02
15	-0.27	-0.65	-1.21	0.00	-0.01	-0.02	0.00	0.00
16	0.01	0.35	0.09	0.00	0.00	0.00	0.00	0.00
24	-0.85	-5.58	0.23	-0.01	-0.04	-0.01	0.00	-0.01

Combined and Factored Demands (excludes self-straining demands):

	N11 _{CD}	N22 _{CD}	N12 _{CD}	M11 _{CD}	M22 _{CD}	M12 _{CD}	Q13 _{CD}	Q23 _{CD}
Conc.	7.72	28.70	20.69	-1.60	-2.10	1.72	0.18	0.28

Commentary

In Analysis Step Two, demands from non-self-straining ILCs are computed. Reinforcement elements are not active in any of these ILCs, therefore only demands on the concrete element are presented in the tables in this section.

Non-self-straining loads are factored and combined as shown below for this combination:

$$1.4D + 1.7L + 1.9E_o + 1.7H + 1.9H_e$$

Note: Demands from self-straining loads are computed during Analysis Step One and are combined with Analysis Step Two demands during evaluation.



Table K1. Demonstration of Element-By-Element Evaluation for One Element

Element-by-Element Evaluation (Element 2100117)	Commentary
<p>Define other parameters for Evaluation:</p> <p>E_c = Concrete elastic modulus = 3605 ksi E_s = Steel elastic modulus = 29000 ksi t = Thickness of wall = 36 in. = 3 ft As_{11} = Area of steel per foot in hoop direction = 3.12 in²/ft As_{22} = Area of steel per foot in meridional direction = 9.36 in²/ft ϵ_{cc} = Compressive strain capacity of concrete = -0.003 f'_c = Design compressive strength of concrete = 4 ksi f_y = Yield strength of reinforcement = 60 ksi</p> <p><u>Evaluate Axial Compression:</u></p> <p>Total axial demand:</p> $Pu_{11} = N_{11_{CA}} + N_{11_{SA}} + N_{11_{CD}}$ $Pu_{11} = (-241.0 + 64.2 + 7.7)kip/ft = -169.1 kip/ft$ $Pu_{22} = N_{22_{CA}} + N_{22_{SA}} + N_{22_{CD}}$ $Pu_{22} = (-169.7 + 176.3 + 28.7)kip/ft = 35.3 kip/ft$ <p>Compute axial strain in concrete due to as-deformed condition:</p> $\epsilon_{11_{CA}} = \frac{N_{11_{CA}}}{t \times E_c} = \frac{-241.0kip/ft}{3ft \times 3605ksi \times 144in^2/ft^2} = -0.000155$ $\epsilon_{22_{CA}} = \frac{N_{22_{CA}}}{t \times E_c} = \frac{-169.7kip/ft}{3ft \times 3605ksi \times 144in^2/ft^2} = -0.000109$ <p>Compute axial strain in reinforcement due to as-deformed condition:</p> $\epsilon_{11_{SA}} = \frac{N_{11_{SA}}}{As_{11} \times E_s} = \frac{64.2kip/ft}{3.12in^2/ft \times 29000 ksi} = 0.000710$ $\epsilon_{22_{SA}} = \frac{N_{22_{SA}}}{As_{22} \times E_s} = \frac{176.3kip/ft}{9.36in^2/ft \times 29000 ksi} = 0.000649$	<p>Axial demands in the concrete and steel elements from the as-deformed condition (computed in Analysis Step One) are combined with axial demands from the factored original SD-66 loads (computed in Analysis Step Two)</p>



Table K1. Demonstration of Element-By-Element Evaluation for One Element

Evaluate Axial Compression (Continued):	Commentary
<p>Compute strain in steel when concrete crushing occurs:</p> $\epsilon_{sc11} = \epsilon_{11_{SA}} + \epsilon_{cc} - \epsilon_{11_{CA}} = 0.000710 - 0.003 + 0.000155 = -0.00214$ $\epsilon_{sc22} = \epsilon_{22_{SA}} + \epsilon_{cc} - \epsilon_{22_{CA}} = 0.000649 - 0.003 + 0.000109 = -0.00224$ <p>Since the strain ϵ_{sc} is more compressive than the yield strain for steel (-0.002) in both directions, the yield strength of the steel can be used to compute compressive capacity.</p> <p>Compute the axial compressive capacity per ft of wall:</p> $\phi P_{n11} = \phi \times -0.80 \left[0.85 f'_c (A_c - A_{s11}) + f_y A_{s11} \right]$ $= 0.70 \times -0.80 \left[0.85 \cdot 4 \text{ksi} \left(36 \text{in} - \frac{3.12 \text{in}^2/\text{ft}}{12 \text{in}/\text{ft}} \right) \cdot \frac{12 \text{in}}{\text{ft}} + 60 \text{ksi} \cdot 3.12 \text{in}^2/\text{ft} \right]$ $= 0.7 \times -0.80 (1645 \text{ kip}/\text{ft}) = -921 \text{ kip}/\text{ft}$ $\phi P_{n22} = \phi \times -0.80 \left[0.85 f'_c (A_c - A_{s22}) + f_y A_{s22} \right]$ $= 0.70 \times -0.80 \left[0.85 \cdot 4 \text{ksi} \left(36 \text{in} - \frac{9.36 \text{in}^2/\text{ft}}{12 \text{in}/\text{ft}} \right) \cdot \frac{12 \text{in}}{\text{ft}} + 60 \text{ksi} \cdot 9.36 \text{in}^2/\text{ft} \right]$ $= 0.7 \times -0.80 (1999 \text{ kip}/\text{ft}) = -1119 \text{ kip}/\text{ft}$ <p>Compute Axial Compression DCR:</p> $DCR_{11} = \frac{-169.1 \text{ kip}/\text{ft}}{-921 \text{ kip}/\text{ft}} = 0.18$ $DCR_{22} = \frac{35.3 \text{ kip}/\text{ft}}{-1119 \text{ kip}/\text{ft}} = -0.03 \rightarrow 0.0$	<p>See Section 7.1.1 for discussion on this equation.</p> <p>Based on ACI 318-71 Chapter 10 with modification as discussed in Section 7.1.1.</p> <p>Note that DCR22 for axial compression is expressed as zero because the net demand is tensile.</p>

Table K1. Demonstration of Element-By-Element Evaluation for One Element

Evaluate Axial-Flexure Interaction:

Total axial demand:

$$Pu11 = -169.1 \text{ kip/ft} \quad Pu22 = 35.3 \text{ kip/ft}$$

Total flexural demand:

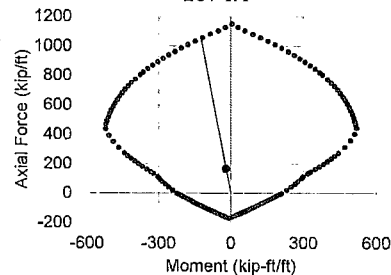
$$\begin{aligned} Mu11 &= (M11_{CA} + M11_{CD}) \pm (M12_{CA} + M12_{CD}) \\ Mu11 &= (1.58 - 1.60) \text{ kipft/ft} \pm (-21.51 + 1.72) \text{ kipft/ft} \\ Mu11 &= -19.81 \text{ kipft/ft}, 19.77 \text{ kipft/ft} \end{aligned}$$

$$\begin{aligned} Mu22 &= (M22_{CA} + M22_{CD}) \pm (M12_{CA} + M12_{CD}) \\ Mu22 &= (-44.8 - 2.1) \text{ kipft/ft} \pm (-21.51 + 1.72) \text{ kipft/ft} \\ Mu22 &= -66.69 \text{ kipft/ft}, -27.11 \text{ kipft/ft} \end{aligned}$$

Axial-flexure (PM) interaction computed using spColumn as described in App. E. DCR calculated as the ratio of the demand radius to the capacity radius.

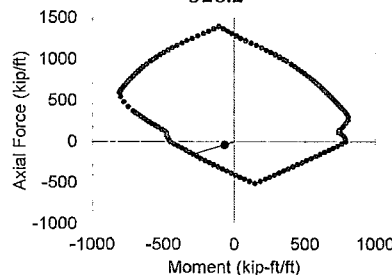
Bending About Meridional Axis

$$\begin{aligned} ru11 &= \sqrt{-169.1^2 + -19.81^2} = 170.25 \\ rn11 &= \sqrt{-1067.0^2 + -125.0^2} = 1074.4 \\ DCR11 &= \frac{170.25}{1074.4} = 0.16 \end{aligned}$$



Bending About Hoop Axis

$$\begin{aligned} ru22 &= \sqrt{35.3^2 + -66.7^2} = 75.5 \\ rn22 &= \sqrt{290.0^2 + -153.5^2} = 328.2 \\ DCR22 &= \frac{75.5}{328.2} = 0.23 \end{aligned}$$



Commentary

$Pu11$ and $Pu22$ values were calculated previously.

Torsional moments, $M12$, are conservatively added and subtracted from bending moments $M11$ and $M22$. See Section 7.1.2 for more information.

The unusual shape of PM capacity curves makes it difficult to establish a single function to compute DCR. The approach described here approximates DCR for a given case.

The demand radius is calculated as the straight line distance from the factored axial-flexure demand point to the origin (0,0). The line from the origin through the demand point is extended until it intersects with the factored PM capacity curve. The capacity radius is calculated as the straight line distance from the origin to the PM point closest to the intersection.

PM interaction curves include Phi factors. Axial tension is negative in PM plots (opposite sign from rest of calculation).



Table K1. Demonstration of Element-By-Element Evaluation for One Element

Evaluate In-Plane Shear:

Total in-plane shear demand:

$$Vu = Vu_B = 56.0 \text{ kip/ft} \quad (\text{see commentary})$$

Axial load on section:

$$Pu11 = N11_{cd} + \max(N11_{ca} + N11_{sa}, 0.0)$$

$$Pu11 = 7.7 \text{ kip/ft} + \max(-240.9 + 64.2, 0.0) \text{ kip/ft}$$

$$Pu11 = 7.7 \text{ kip/ft} = 643.2 \text{ lbf/in}$$

Concrete shear strength:

$$v_{ca} = 2 \left(1 + 0.0005 \frac{Pu11}{t} \right) \sqrt{f'_c}$$

$$v_{ca} = 2 \left(1 + 0.0005 \frac{643.2 \text{ lbf/in}}{36 \text{ in}} \right) \sqrt{4000 \text{ psi}} = 127 \text{ psi}$$

$$v_{cb} = 3.5 \sqrt{f'_c} \sqrt{1 + 0.002 \frac{Pu11}{t}}$$

$$v_{cb} = 3.5 \sqrt{4000 \text{ psi}} \sqrt{1 + 0.002 \frac{643.2 \text{ lbf/in}}{36 \text{ in}}} = 225 \text{ psi}$$

$$v_c = \min(v_{ca}, v_{cb}) = 127 \text{ psi}$$

Steel shear strength:

$$v_s = \frac{A_v f_y}{b_w s} = \frac{3.12 \text{ in}^2/\text{ft} \times 60000 \text{ psi}}{36 \text{ in} \times 12 \text{ in/ft}} = 433 \text{ psi}$$

Commentary

Since the element-by-element evaluation is a conservative screening, in-plane shear demand is computed as the maximum of the following four sums:

- $Vu_A = |N12_{cd}|$
- $Vu_B = |N12_{cd} + N12_{c,swell}|$
- $Vu_C = |N12_{cd} + N12_{c,ASR}|$
- $Vu_D = |N12_{cd} + N12_{c,swell} + N12_{c,ASR}|$

Where $N12_{c,swell}$ is the $N12$ (in-plane shear) demand from the swelling load case (ILC 8) multiplied by the load factor for swelling, and $N12_{c,ASR}$ is the $N12$ (in-plane shear) demand from the ASR load cases (ILC 5 and 6) multiplied by the load factor and threshold factor for ASR.

Design in-plane shear demands are combined with self-straining in-plane shear demands using algebraic sum because seismic loads are input in all directions (using the 100-40-40 approach).

Net axial compression on the section increases shear capacity. To evaluate conservatively, axial demand due to self-straining loads are excluded if they are compressive.

Concrete shear strength is based on:

ACI 318-71 Equation 11-6 and Equation 11-7 (for sections in axial compression)

Note: **Pu11** must be positive for compression in above equations.

Steel shear strength equation is based on ACI 318-71 Equation 11-13. Terms have been rearranged so v_s can be computed based on a given quantity of steel.



Table K1. Demonstration of Element-By-Element Evaluation for One Element

<p><u>Evaluate In-Plane Shear (Continued):</u></p> <p>Combine concrete and steel shear strength and apply Phi:</p> $\phi V_n = \phi(v_c + v_s) \times t = 0.85(127\text{psi} + 433\text{psi}) \times 36\text{in}$ $\phi V_n = 17136\text{ lbf/in} = 205.4\text{ kip/ft}$ <p>Check maximum in-plane shear strength:</p> $\phi V_{n,max} = \phi 10 \times t \sqrt{f'_c} = 0.85 \times 10 \times 36\text{in} \times \sqrt{4000\text{psi}}$ $= 232.2\text{ kip/ft}$ <p>Compute in-plane shear DCR:</p> $DCR = \left \frac{Vu}{\phi V_n} \right = \left \frac{56.0\text{ kip/ft}}{205.4\text{ kip/ft}} \right = 0.27$	<p><u>Commentary</u></p> <p>ACI 318-71 Section 11.16.5</p>
<p><u>Evaluate Out-Of-Plane Shear:</u></p> <p>Total out-of-plane shear demand:</p> $V_n = Q23_{CA} + Q23_{CD} = (-17.1 + 0.3)\text{kip/ft} = -16.8\text{kip/ft}$ <p>Axial load on section (calculated previously)</p> $Pu22 = 35.3\text{kip/ft} = 2942\text{lbf/in}$ <p>Concrete shear strength:</p> $v_c = 2 \left(1 + 0.002 * \frac{Pu22}{t} \right) \sqrt{f'_c}$ $v_c = 2 \left(1 + 0.002 * \frac{-2942\text{lb/in}}{36\text{in}} \right) \sqrt{4000\text{psi}} = 106\text{psi}$	<p><u>Commentary</u></p> <p>Out-of-plane shear is evaluated for a horizontal section in this example. In the element-by-element evaluation, out-of-plane shear is evaluated for both horizontal and vertical sections.</p> <p>ACI 318-71 Equation 11-8</p> <p>Note: Pu22 is negative in tension in the equation</p>



Table K1. Demonstration of Element-By-Element Evaluation for One Element

Evaluate Out-Of-Plane Shear:

Steel shear strength:

$$v_s = \frac{A_v f_y}{b_w s}$$

$$V_s = v_s b_w (0.8 \cdot d) = \frac{A_v f_y (0.8 \cdot d)}{s}$$

$$V_s = \frac{0.79 \text{ in}^2/\text{ft} \times 0.72 \times 60 \text{ ksi} \times (0.8 \cdot 36 \text{ in})}{12 \text{ in}} = 81.9 \text{ kip/ft}$$

Combine concrete and steel shear strength and apply Phi:

$$\phi V_n = \phi (v_c t + V_s)$$

$$\phi V_n = 0.85 \left(106 \text{ psi} \cdot 36 \text{ in} \cdot \frac{1 \text{ kip}}{1000 \text{ lbf}} \cdot \frac{12 \text{ in}}{1 \text{ ft}} + 81.9 \text{ kip/ft} \right)$$

$$= 127.7 \text{ kip/ft}$$

Compute out-of-plane shear DCR:

$$DCR_a = \frac{|V_n|}{\phi V_n} = \frac{16.8 \text{ kip/ft}}{127.7 \text{ kip/ft}} = 0.13$$

As an alternative approach, compute DCR using shear-friction.

If section is in axial tension, compute area of steel required to carry factored tensile demand.

$$RA_{st} = \frac{Pu_{22}}{\phi f_y} = \frac{35.3 \text{ kip/ft}}{0.9 \times 60 \text{ ksi}} = 0.654 \text{ in}^2/\text{ft}$$

Commentary

Based on ACI 318-71 Equation 11-13. Terms have been rearranged so v_s can be computed based on a given quantity of steel. Convert to units of force per length by multiplying by $b_w(0.8 \cdot d)$, where b_w is the theoretical strip width of the section under evaluation and d is the depth of the section.

Note: #8 steel stirrups are provided at this location spaced at 12 in. With the configuration provided, a #8 bar is unable to fully develop within a 36 in. thick wall section, therefore the strength of the bar is reduced by a factor of 0.72 to represent the fraction of development (Sheet B5 of the reference below).

United Engineers & Constructors Inc., *Containment-Enclosure Building (019)*, CE-4 (Rev. 6), Mar 1977 to Aug. 1983.

If section in axial compression, then RA_{st} is taken as zero. See Section 7.1.5.



Table K1. Demonstration of Element-By-Element Evaluation for One Element

<p><u>Evaluate Out-Of-Plane Shear (continued):</u></p> <p>Compute area of steel required to carry factored out-of-plane shear demand:</p> $RA_{sv} = \frac{ Vn }{\phi\mu f_y} = \frac{16.8kip/ft}{0.85 \times 1.0 \times 60ksi} = 0.329in^2/ft$	<p><u>Commentary</u></p> <p>See Section 7.1.5.</p>																								
<p><u>Evaluate Out-Of-Plane Shear (Continued):</u></p> <p>Compute DCR by dividing total required steel area by steel area provided:</p> $DCR_b = \frac{RA_{st} + RA_{sv}}{As22} = \frac{(0.654 + 0.329)in^2/ft}{9.36in^2/ft} = 0.11$ <p>Use lesser of DCR_a and DCR_b as final DCR for out-of-plane shear for this element:</p> $DCR = \min(DCR_a, DCR_b) = 0.11$	<p><u>Commentary</u></p>																								
<p><u>Compare DCR Values Computed in this Table to Those Extracted from Element-by-Element Evaluation:</u></p> <table><tr><td></td><td>DCR Computed in This Table</td><td>DCR Computed by Element-by-Element Evaluation</td></tr><tr><td>Hoop Compression</td><td>0.18</td><td>0.18</td></tr><tr><td>Meridional Compression</td><td>0.0</td><td>0.0</td></tr><tr><td>PM Interaction (Hoop Direction)</td><td>0.16</td><td>0.16</td></tr><tr><td>PM Interaction (Meridional Direction)</td><td>0.23</td><td>0.23</td></tr><tr><td>In-Plane Shear</td><td>0.27</td><td>0.27</td></tr><tr><td>Out-of-Plane Shear (for horizontal section)</td><td>0.11</td><td>0.12</td></tr><tr><td>Out-of-Plane Shear (for vertical section)</td><td>Not computed here</td><td>0.01</td></tr></table>			DCR Computed in This Table	DCR Computed by Element-by-Element Evaluation	Hoop Compression	0.18	0.18	Meridional Compression	0.0	0.0	PM Interaction (Hoop Direction)	0.16	0.16	PM Interaction (Meridional Direction)	0.23	0.23	In-Plane Shear	0.27	0.27	Out-of-Plane Shear (for horizontal section)	0.11	0.12	Out-of-Plane Shear (for vertical section)	Not computed here	0.01
	DCR Computed in This Table	DCR Computed by Element-by-Element Evaluation																							
Hoop Compression	0.18	0.18																							
Meridional Compression	0.0	0.0																							
PM Interaction (Hoop Direction)	0.16	0.16																							
PM Interaction (Meridional Direction)	0.23	0.23																							
In-Plane Shear	0.27	0.27																							
Out-of-Plane Shear (for horizontal section)	0.11	0.12																							
Out-of-Plane Shear (for vertical section)	Not computed here	0.01																							



Appendix L Moment Redistribution Validation Examples

L1. REVISION HISTORY

L1.1. Revision 0

Initial document.

L2. OBJECTIVE

Validate the simplified moment redistribution approach used in 150252-CA-02 with a more detailed approach consisting of nonlinear spring elements using the following two example problems:

- A cylindrical structure with diameter and wall thickness similar to Seabrook CEB
- The Seabrook CEB model

L3. CONCLUSIONS

The simplified moment redistribution approach provides demands that are reasonable when compared to those computed using a detailed approach with nonlinear spring elements.

L4. DESCRIPTION OF VALIDATION EXAMPLE PROBLEMS

The moment redistribution approach is validated using two example problems. The first example problem consists of a cylindrical structure with diameter and wall thickness that are similar to the Seabrook CEB. This is a simplified model that allows the effects of moment redistribution to be studied without complexities caused by large penetrations and changes in wall thickness. The second example problem uses the full Seabrook CEB model.

L4.1. Description of Cylindrical Model Example Problem

The cylindrical model has a diameter of 80 ft and a height of 150 ft. The entire cylindrical model consists of SHELL181 elements with thickness of 27 in. Both ends of the cylinder wall (i.e., bottom and top) have fully fixed boundary conditions. All elements in this cylindrical model are approximately 3 ft by 3 ft in size. The entire cylindrical model uses concrete material with an elastic modulus of 3,605,000 psi and Poisson's ratio of 0.15.



A single load case (referred to as "Case L") consisting of a unit out-of-plane surface pressure (1 psi) on a patch of eight elements is used to generate out-of-plane flexural demands on the cylinder wall. This unit pressure load case generates a peak out-of-plane moment of 1.51 kip-ft/ft in the hoop direction (i.e., about the meridional axis). This load case is multiplied by a factor of 100 to produce a total moment demand of 151 kip-ft/ft in the hoop direction. In this example problem, the wall is assigned a nominal flexural capacity of 100 kip-ft/ft (therefore requiring 51 kip-ft/ft to be redistributed).

The simplified moment redistribution is performed in a separate load case (referred to as "Case R") that uses the INISTATE command in ANSYS APDL to prescribe a hoop bending moment in the elements that have their flexural capacity exceeded. The ANSYS FEA software redistributes the initial stresses to reach a stress profile that satisfies static equilibrium. Since the INISTATE command is only capable of prescribing initial stresses (and cannot prescribe moments directly), it is used to prescribe an initial stress gradient of ± 100 psi on the extreme fibers of the section. After redistribution, this initial state results in a hoop bending moment of 5.3 kip-ft/ft at the location of moment exceedance. To redistribute 51 kip-ft/ft, this moment redistribution load case is scaled by a factor of 9.6.

The comparison nonlinear case (referred to as "Case N") is performed by disconnecting the elements in the region of moment exceedance, and then reconnecting them using coincident spring elements to transfer forces in all degrees of freedom. All reconnecting spring elements are linear (COMBIN14) with high stiffness except for the springs transferring hoop bending moments, which have nonlinear moment-curvature behavior (COMBIN39). The nonlinear springs are configured to be very stiff prior to yield, and then have near-zero bending stiffness after yielding. An out-of-plane pressure large enough to cause 151 kip-ft/ft (if the model were linear elastic) is applied to the same patch of elements as previously used for loading.

To assess the performance of the simplified moment redistribution approach, the superposition of "Case L" scaled by 100 and "Case R" scaled by 9.6 is compared to the nonlinear "Case N". The results of this comparison are presented in Section L5.1.



L4.2. Description of Full Model Example Problem

The full Seabrook CEB model is used to perform a second validation example. The full Seabrook CEB model has more complex geometry than the cylinder model presented in Section L4.1. The geometry of the CEB is defined in detail in the main body of this calculation. A development version of the CEB model is used in this example. The development model is identical to the production model used in the main body of this calculation, except the personnel hatch and equipment hatch are modeled using square openings (whereas the production model has approximately circular openings). Since the purpose of this validation example is to compare moment redistribution demands between the simplified and detailed approaches, the use of the development model for this exercise is not consequential.

Flexural demands are generated by applying ASR expansion, self-weight, hydrostatic pressure, earth pressure, OBE acceleration, and OBE dynamic soil pressures loads to the CEB model. The sum of these demands is referred to as "Case D." It must be noted that "Case D" consists of development loads, which are not equivalent to the loads used and documented in the main body of this calculation. However, this is judged to be inconsequential to this validation example since both the simplified and detailed approaches use the same loads. The region at AZ 315° and El. 30 ft (directly above and below the Personnel Hatch) is selected to serve as the region of theoretical hoop bending moment exceedance for this example problem. Hoop bending demands of "Case D" are approximately 110 kip-ft/ft at this location.

In the simplified method, hoop bending moments are redistributed by using the INISTATE command similarly to the cylindrical model in Section L4.1. The INISTATE stresses are applied to a patch of eight elements in a two by four grid at the location of moment exceedance. A theoretical hoop bending capacity of 50 kip-ft/ft is selected at this location, which accounts for hoop tensile stresses acting around the Personnel Hatch opening. After redistribution of INISTATE stresses, the initial state case (referred to as "Case M") results in a hoop bending moment of 4.9 kip-ft/ft at the location of moment exceedance. To redistribute 60 kip-ft/ft, this moment redistribution load case is scaled by a factor of 12.2.

The comparison nonlinear case (referred to as "Case K") is performed by disconnecting the elements in the region of moment exceedance, and then reconnecting them using spring elements to transfer forces in all degrees of freedom. All reconnecting spring elements are



linear (COMBIN14) with high stiffness except for the springs transferring hoop bending moments, which have nonlinear moment-curvature behavior (COMBIN39). The nonlinear springs are configured to be very stiff prior to yield and then have near-zero bending stiffness after yielding. The same loads as Case D are applied to the model with nonlinear springs.

To assess the performance of the simplified moment redistribution approach, the superposition of "Case D" and "Case M" scaled by a factor of 12.2 is compared to the nonlinear "Case K." The results of this comparison are presented in Section L5.2.

L5. VALIDATION EXAMPLE PROBLEM RESULTS

Demands computed using the simplified moment redistribution approach are compared to those computed using the detailed approach in this section. Flexural demands in the hoop direction (about the meridional axis) and in the meridional direction (about the hoop axis) are compared for the two approaches for section cuts taken at several different locations.

L5.1. Results of Cylindrical Model Example Problem

Hoop bending moments are compared at the elevation of moment exceedance in Figure L1. This comparison shows that the simplified approach is able to accurately limit the moment demand carried at the location of exceedance. At this cut location, the moment redistribution affects only a limited region of the cylinder (about 30° on either side of the exceedance). Figure L2 shows a zoomed view of the moment diagram in Figure L1; it can be seen that both redistribution approaches result in slightly increased negative moment on either side of the exceedance. Hoop bending moments are compared at an elevation 15 ft below the location of the exceedance in Figure L3. The simplified and detailed approaches show very little variation at this elevation; both locations indicate a small increase to hoop bending moments.

Meridional bending moments are compared at the azimuth of moment exceedance in Figure L4. Both the simplified and detailed approaches compute increased meridional bending moments at this cut due to the distribution of hoop moments. The simplified approach provides more-conservative demands, although the impact is limited to only the immediate area of the moment exceedance. Meridional bending moments are compared at a cut about 25° away from the location of moment exceedance in Figure L5. Meridional bending moments are small at this cut, and the impact of the moment redistribution is minor.

**L5.2. Results of Full Model Example Problem**

Hoop bending moments are compared at the elevation of moment exceedance in Figure L6. The simplified redistribution approach is effective at limiting bending moments at the location of exceedance to 50 kip-ft/ft. The simplified and detailed approaches result in very similar hoop bending demands along this elevation. This is also seen in the comparison of hoop bending moments along a cut about 15 ft above the elevation of moment exceedance (Figure L7). The distribution of meridional bending moments is compared for the two approaches in Figure L8.

L6. FIGURES

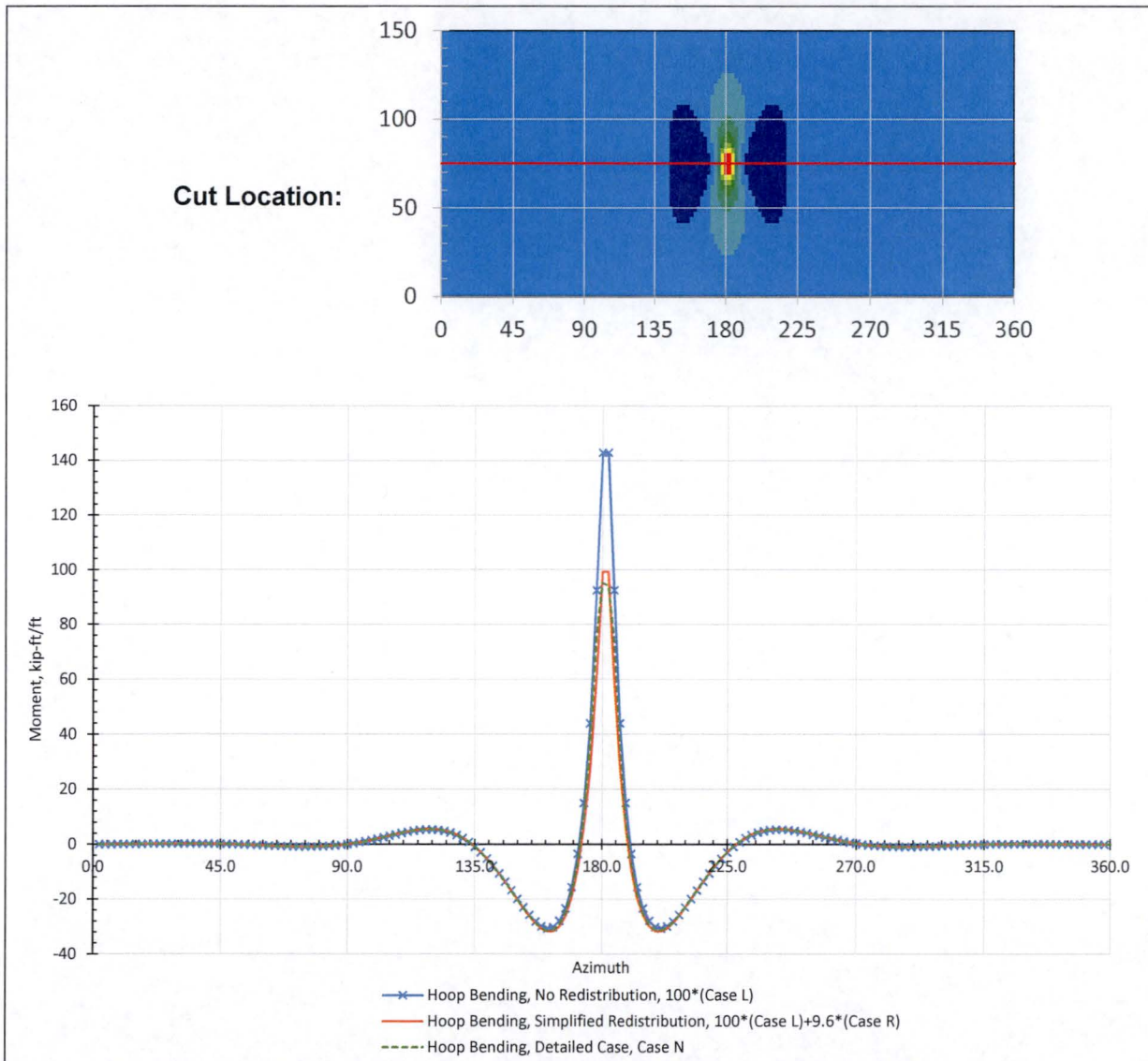


Figure L1 – Comparison of Hoop Bending Moments at El. 75 ft for Cylinder Model

Notes:

Cut is taken through region of moment exceedance at El. 75 ft (cut is shown as a red line in upper image).

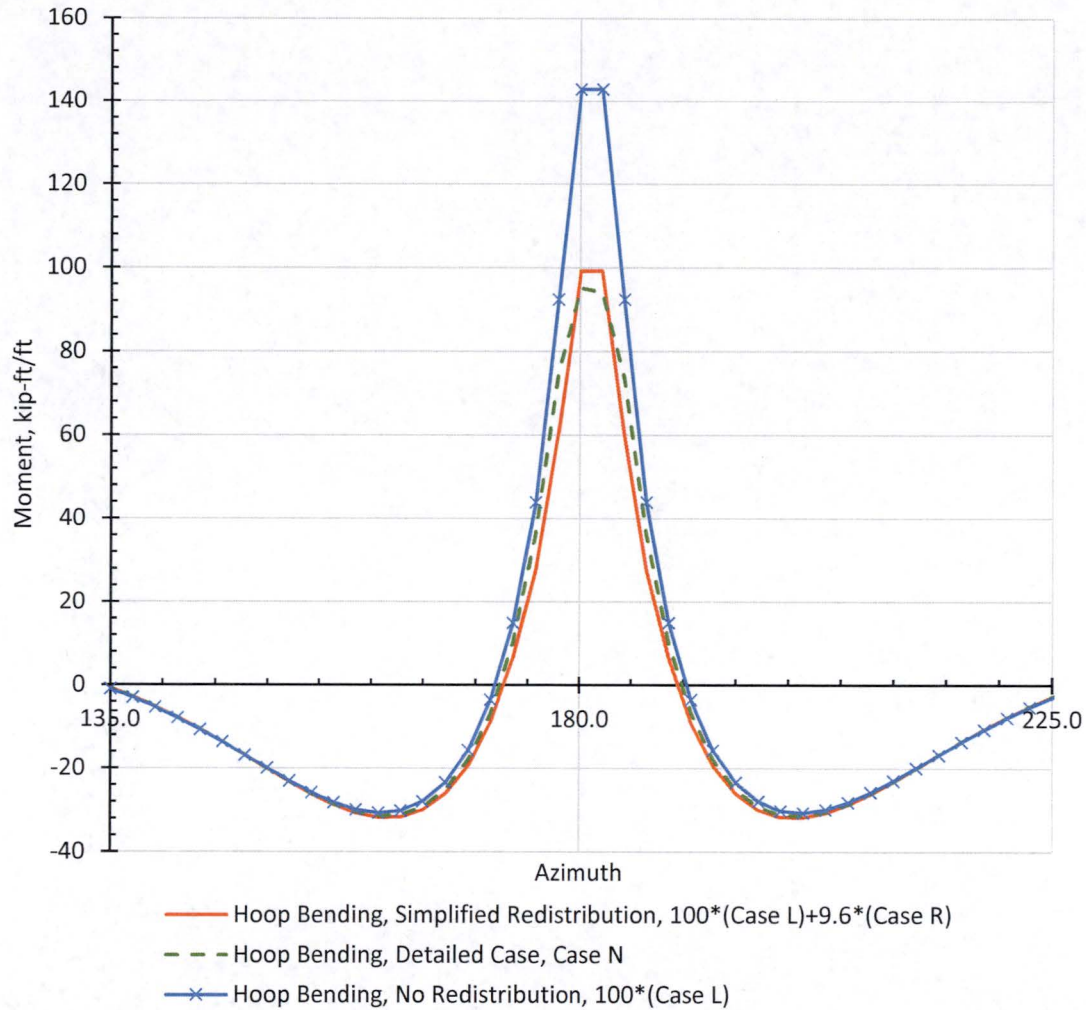


Figure L2 – Comparison of Hoop Bending Moments at El. 75 ft for Cylinder Model, Zoomed View from AZ 135° to AZ 225°

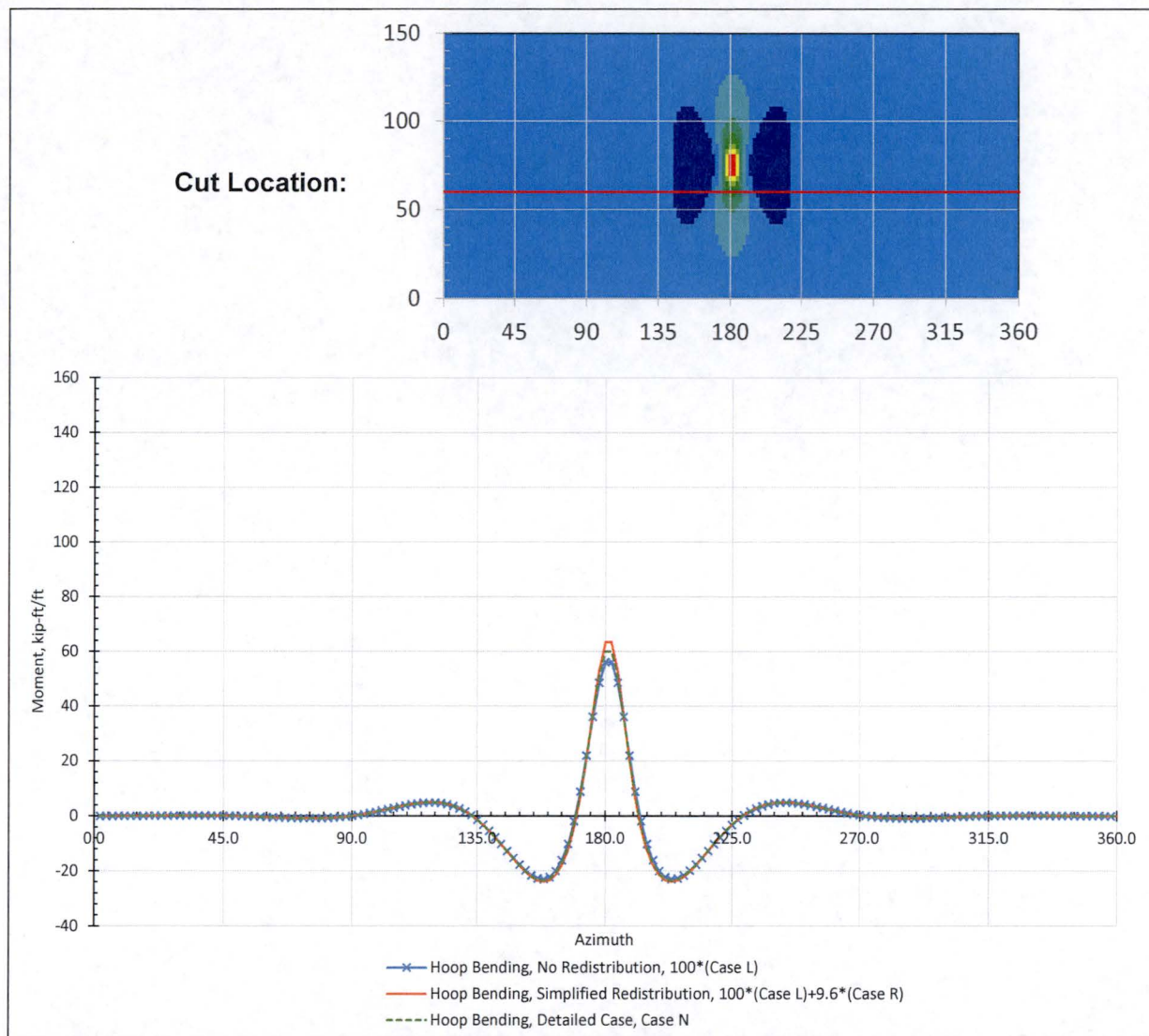


Figure L3 – Comparison of Hoop Bending Moments at El. 60 ft for Cylinder Model

Notes:

Cut is taken 15 ft below the location of moment exceedance (cut is shown as a red line in upper image).

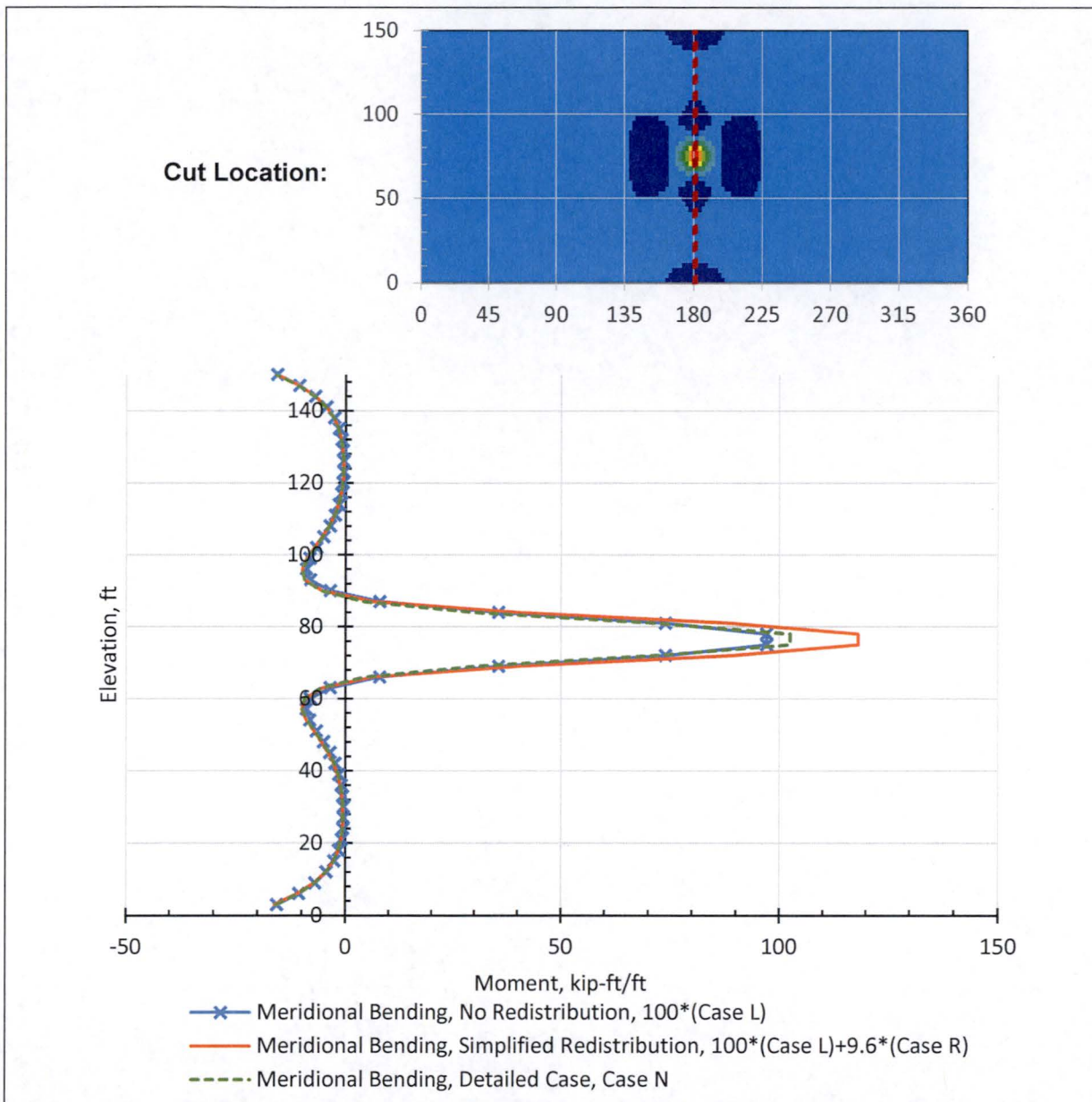


Figure L4 – Comparison of Meridional Bending Moments at AZ 180° for Cylinder Model

Notes:

Cut is taken through region of moment exceedance at AZ 180° (cut is shown as a red line in upper image).

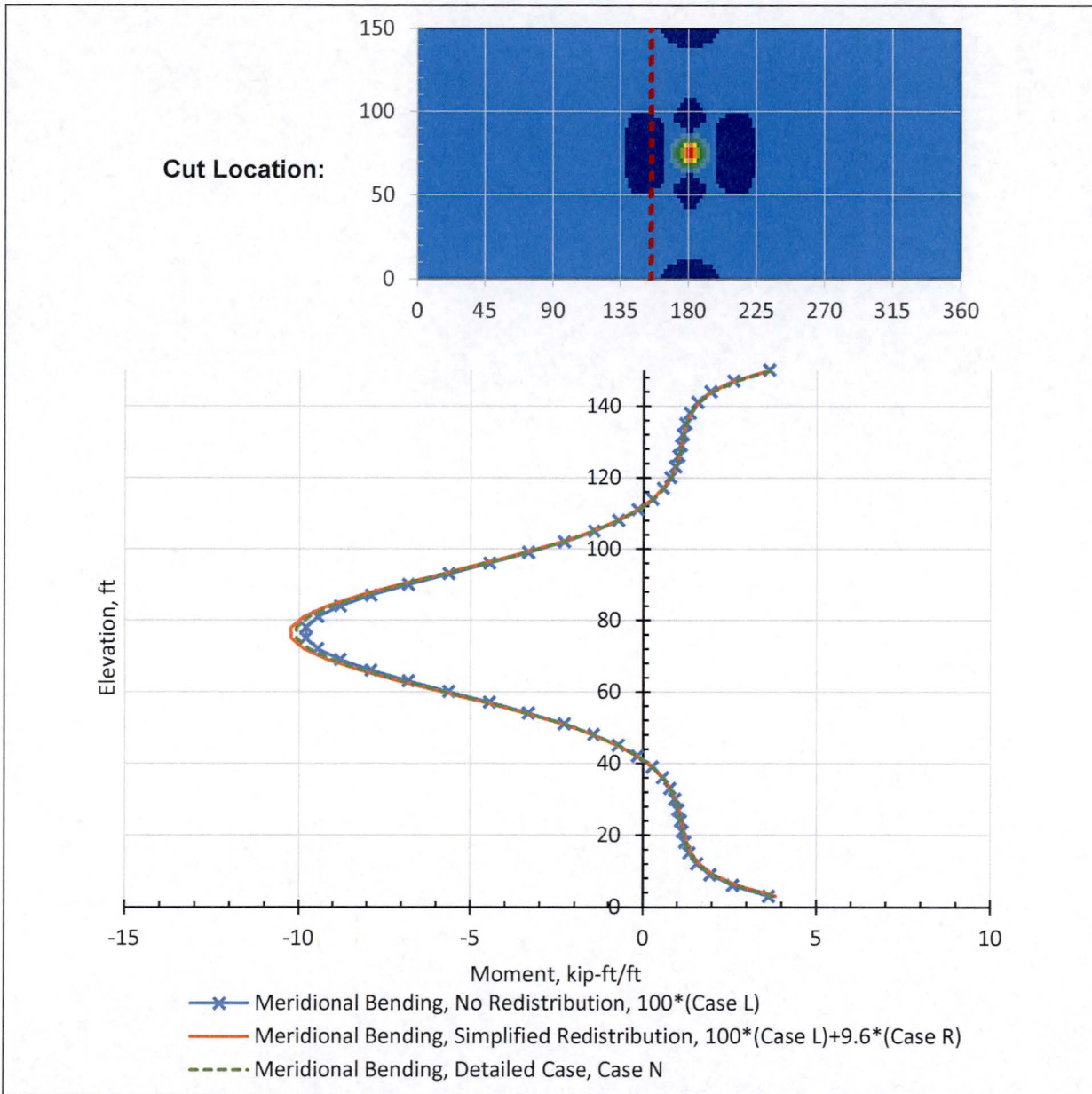


Figure L5 – Comparison of Meridional Bending Moments at AZ 155° for Cylinder Model

Notes:

Cut is taken at AZ 155° (cut is shown as a red line in upper image).

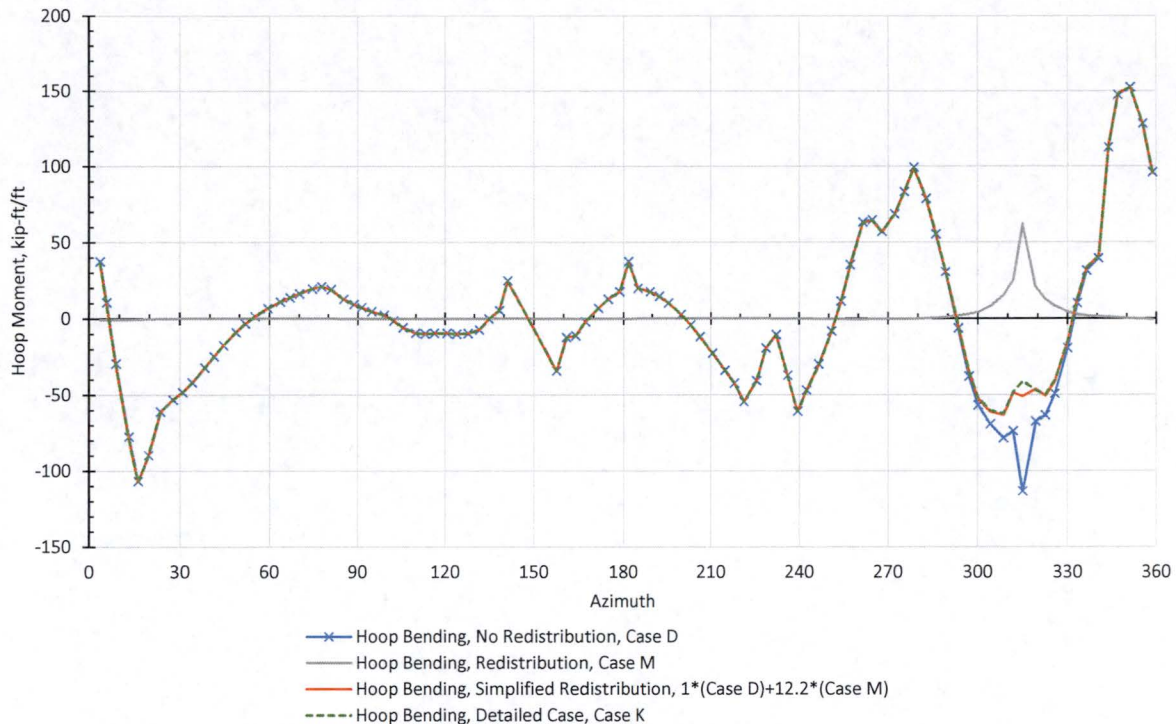


Figure L6 – Comparison of Hoop Bending Moments at El. 30 ft for Full Model

Note: Each data point shown in the above plot represents average demands for an approximately 12 ft long vertical section cut (equal to about eight wall thicknesses or about six element widths).

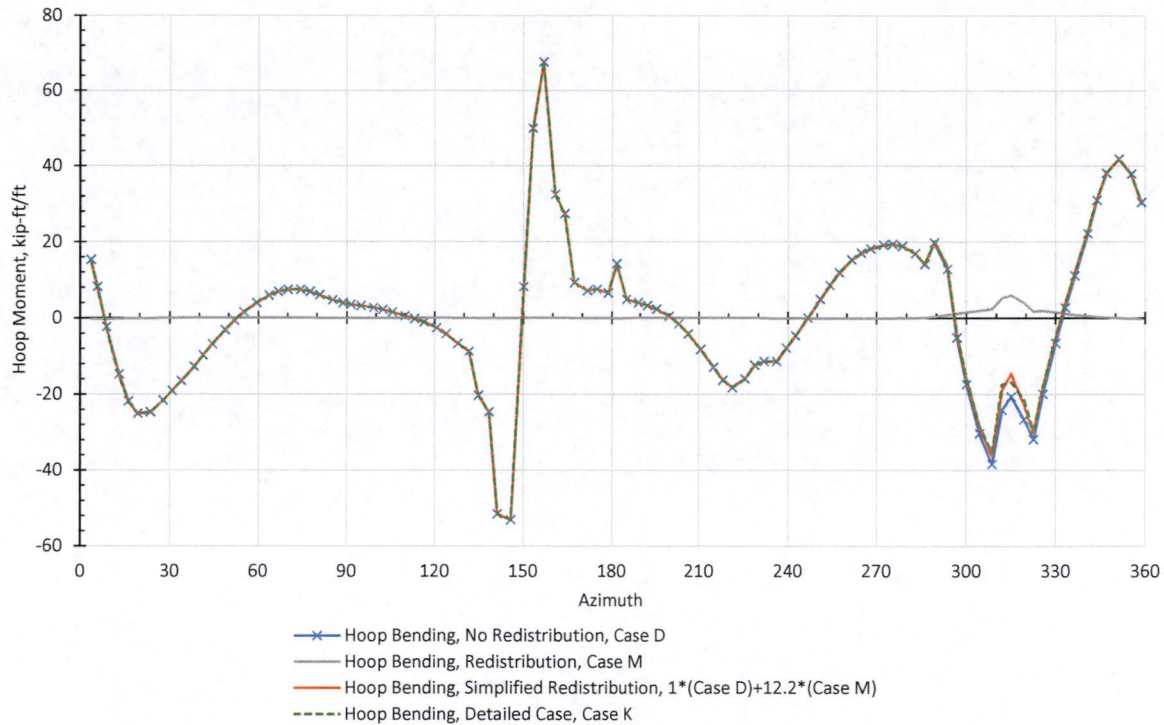


Figure L7 – Comparison of Hoop Bending Moments at El. 45 ft for Full Model

Note: Each data point shown in the above plot represents average demands for an approximately 12 ft long vertical section cut (equal to about eight wall thicknesses or about six element widths).

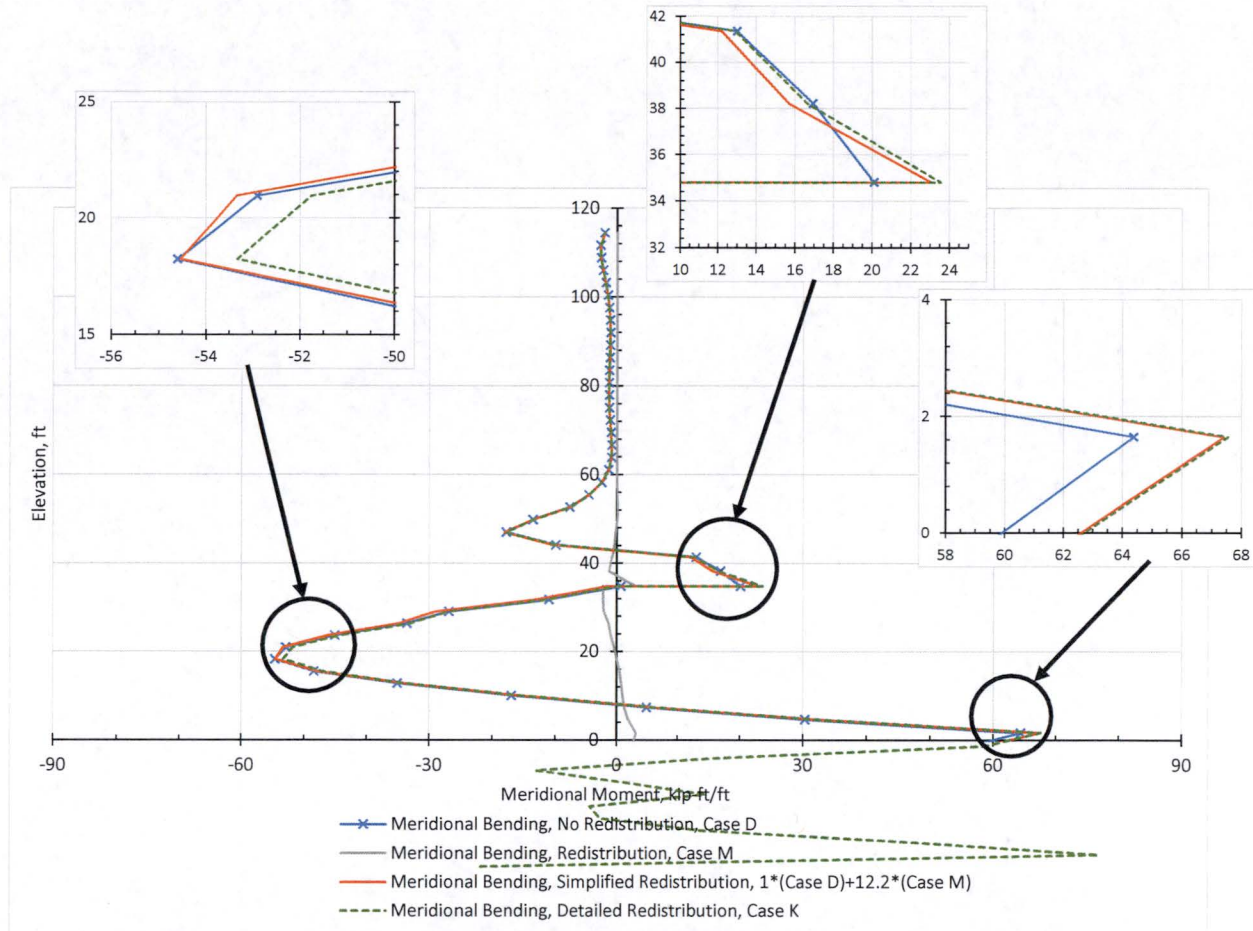


Figure L8 – Comparison of Meridional Bending Moments at AZ 315° for Full Model

Note: Each data point shown in the above plot represents average demands for an approximately 12 ft long horizontal section cut (equal to about eight wall thicknesses or about six element widths).



Appendix M

Analysis and Evaluation of Meridional Demands at El. +45.5 ft

M1. REVISION HISTORY

Revision 0:

Initial document.

M2. OVERVIEW

Evaluation of axial-flexure (PM) interaction in the meridional direction for the Standard-Plus Analysis Case shows a region of capacity exceedance above El. +45.5 ft at AZ 240°. The static load combination NO_1 is reevaluated using reduced stiffness properties in this region to simulate concrete cracking. The adjusted stiffness properties are shown to reduce tensile demands acting on this section.

M3. DESCRIPTION OF DEMANDS

Evaluation of axial-flexure (PM) interaction in the meridional direction for the Standard-Plus Analysis Case shows a region of capacity exceedance above El. +45.5 ft at AZ 240°. Unlike other PM interaction exceedances which are primarily governed by flexural demands, initial evaluations of the controlling static combination (NO_1 as defined in Table 5) show that the tensile capacity of the wall is almost exceeded at this location, as illustrated in Figure M1. The transition in wall thickness from 27 to 15 in. between El. +45 and +45.5 ft causes the wall's centerline to shift by 6 in., which causes the tensile demands to impart a bending moment on the wall about the hoop axis (Figure M2).

Tensile demands at this location are caused by the mechanisms described below.

- **Differential ASR expansion quantities acting vertically at the base of the wall**

ASR expansion applied to the CEB wall is based on measurements of crack index (CI) as described in Section 6.3.1 of the calculation main body. The magnitude of below-grade ASR expansion in the vertical direction varies at different azimuths. From AZ 0° to 180°, 0.015% expansion is applied. From AZ 180° to 270°, 0.04% is applied, and from AZ 270° to 360°, 0.06% is applied. The magnitude of vertical ASR expansion gradually tapers between adjacent wall segments. The differences in vertical ASR expansions in adjacent segments of wall cause meridional tensile demands in the regions between the segments.



- **Out-of-plane pressures acting on the wall**

The additional out-of-plane pressures modeled in the Standard-Plus Analysis Case between AZ 180° and 270° also cause meridional tensile demands at AZ 240°.

M4. ANALYSIS AND EVALUATION METHODOLOGY

The static load combination NO_1 for the Standard-Plus Analysis Case is reevaluated in this appendix with reduced stiffness in a horizontal strip of elements at El. +45.5 and AZ 240° to simulate localized concrete cracking where axial meridional tensile stress exceeds the modulus of rupture of concrete as defined in ACI 318-71 Section 9.5.2.2. These elements are highlighted in Figure M3. The reduced stiffness applied to these elements is equivalent to the stiffness of the meridional reinforcement, $A_s E_s$, where A_s is the area of steel (#9@12EF) and E_s is the elastic modulus of steel (29,000 ksi). The reduced stiffness is used for cases where ASR loads are applied to the structure; all other load cases (self-weight, seismic, etc.) use unreduced stiffness equivalent to the gross concrete section.

The stiffness reduction is applied by modifying the elastic modulus of the cracked elements in the CEB model. This reduction effectively reduces the stiffness of the concrete in both hoop and meridional directions, as well as the shear and bending stiffness of the concrete in this localized cracked region. The impacts of this modeling approach are assessed by analyzing membrane and shear forces and PM interaction close to this area.

Demands are computed at Section Cut 28 as defined in Appendix N. Capacity for this section cut is computed using spColumn as documented in Figure M4. The spColumn capacity shown in Figure M4 takes into consideration additional strength of the section due to the curvature of the wall, which the PM interaction diagram in Figure M1 (and generally used throughout this calculation) conservatively ignore. Since the cross-section is in tension, the adjustment to spColumn outputs to account for the difference in modern phi factors and ACI 318-71 phi factors in the compression regions of the interaction diagram is not needed (see Appendix E for additional information on this adjustment).

M5. DISCUSSION OF RESULTS AND CONCLUSIONS

The adjustment in stiffness to account for concrete cracking at El. +45.5 and AZ 240° reduces the tension demands caused by ASR loads through two mechanisms:



- Since tensile demands El. +45.5 are partially caused by differential vertical expansion of the below-grade wall, a portion of the tension demands are displacement-controlled. This means that the reduction in meridional stiffness allows the imposed below-grade displacements due to ASR to occur with less resistance from the above-grade portion of the structure at this location.
- The reduction of stiffness simulating concrete cracking causes additional demands to use other stiffer load paths within the structure.

Results of PM interaction evaluation after adjustment of stiffness is shown in Figure M5, which shows that PM interaction demands are less than capacity.

Comparisons of axial hoop forces, bending moments about the vertical axis, and out-of-plane shear forces at the location where cracking was modeled is provided in Figures M6 through M8. These comparisons show that this localized cracking has a negligible effect on other demands within the structure.

M6. FIGURES

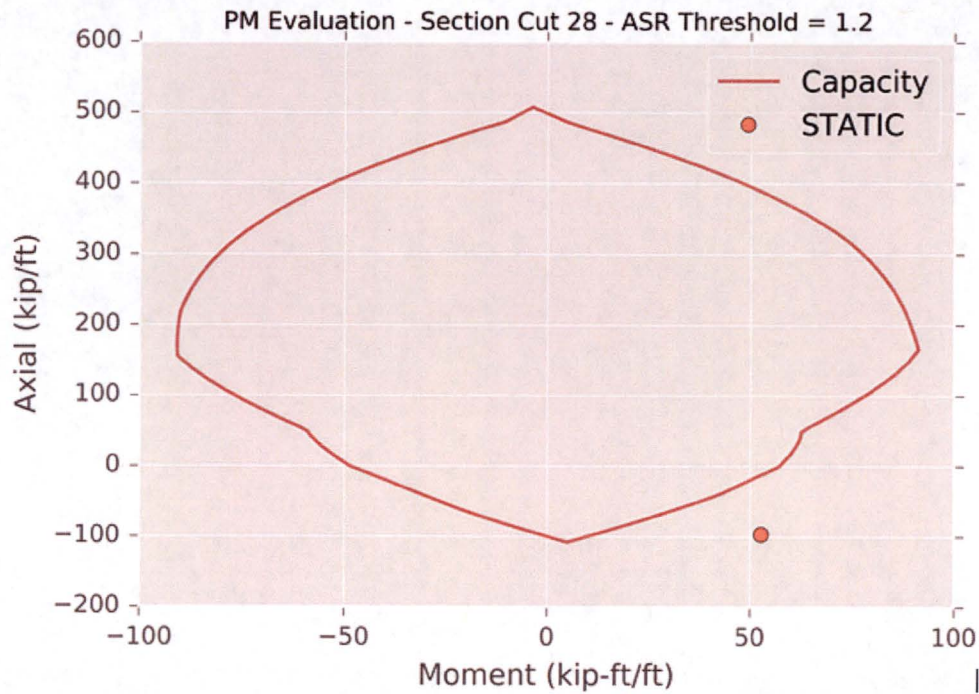


Figure M1. PM Interaction of Section Cut 28 for Standard-Plus Analysis Case for Load Combination NO_1 Before Reduction of Stiffness to Simulate Concrete Cracking

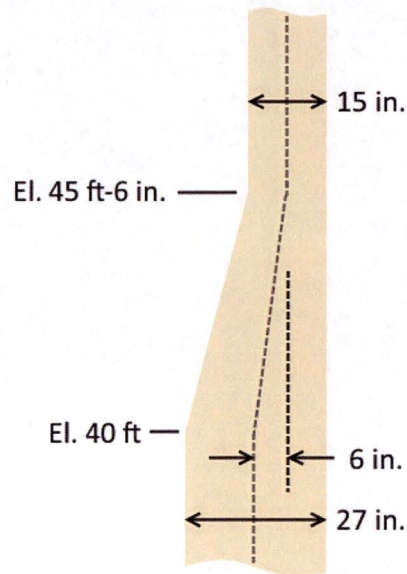


Figure M2. Eccentricity in Wall due to Thickness Reduction from 27 in. to 15 in.

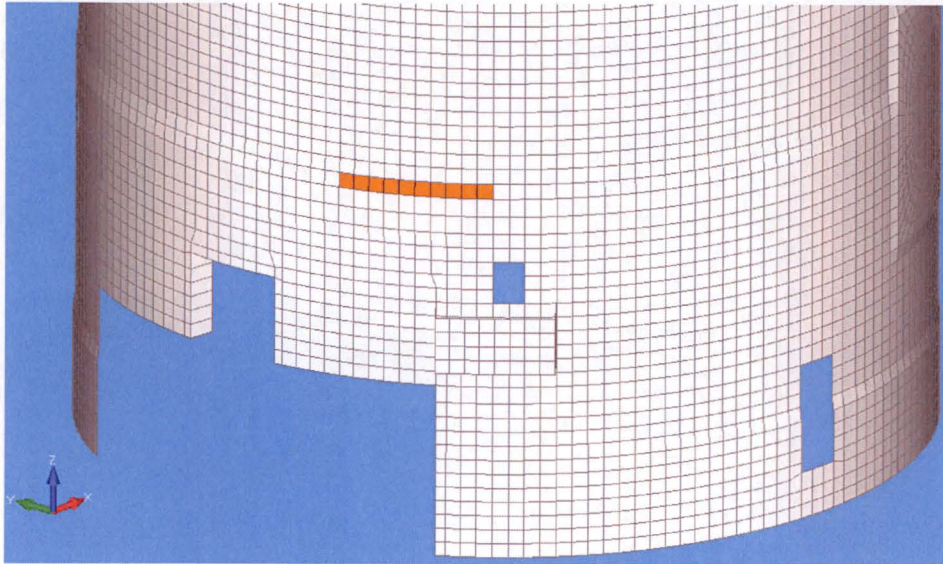


Figure M3. Elements Selected for Stiffness Adjustment to Simulate Concrete Cracking

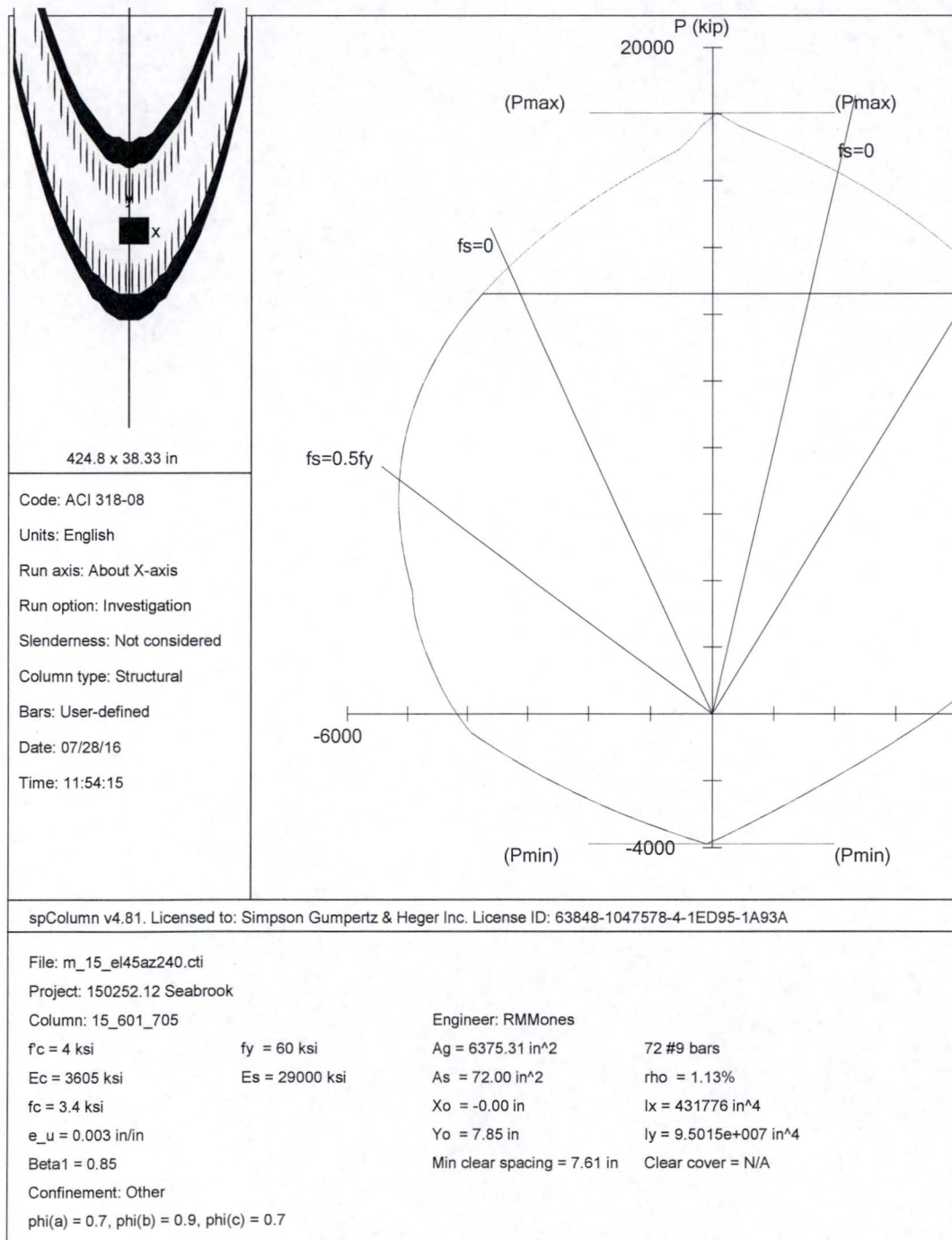


Figure M4. Axial-Flexure Interaction Capacity for Section Cut 28

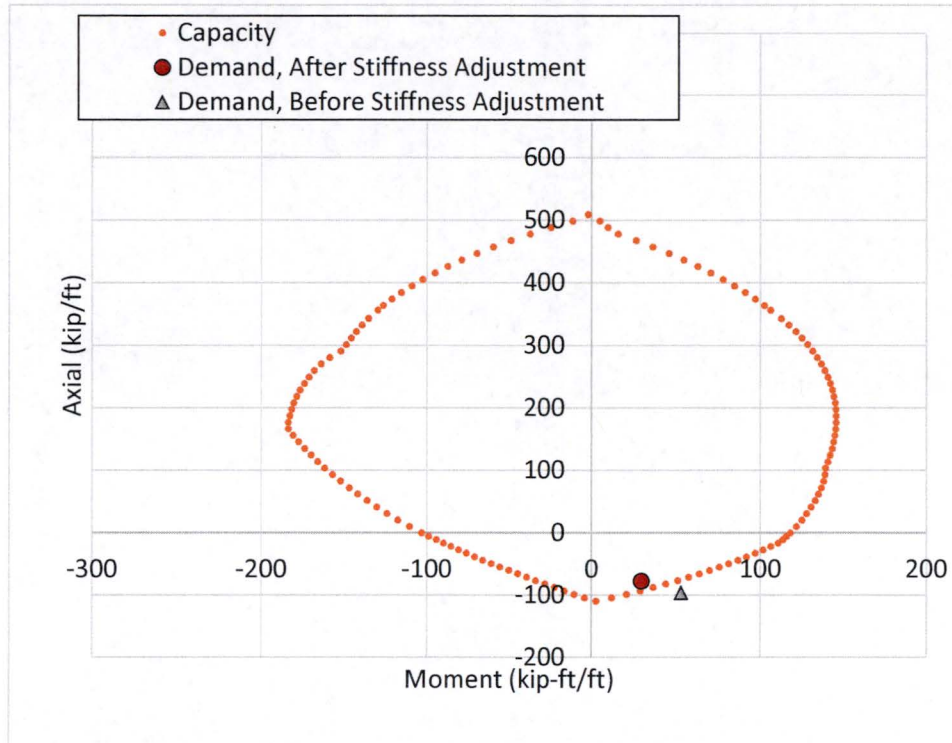


Figure M5. PM Interaction of Section Cut 28 for Standard-Plus Analysis Case for Load Combination NO_1 After Reduction of Stiffness to Simulate Concrete Cracking

Note: Capacity curve is from spColumn as shown in Figure M4.

CLIENT: NextEra Energy Seabrook

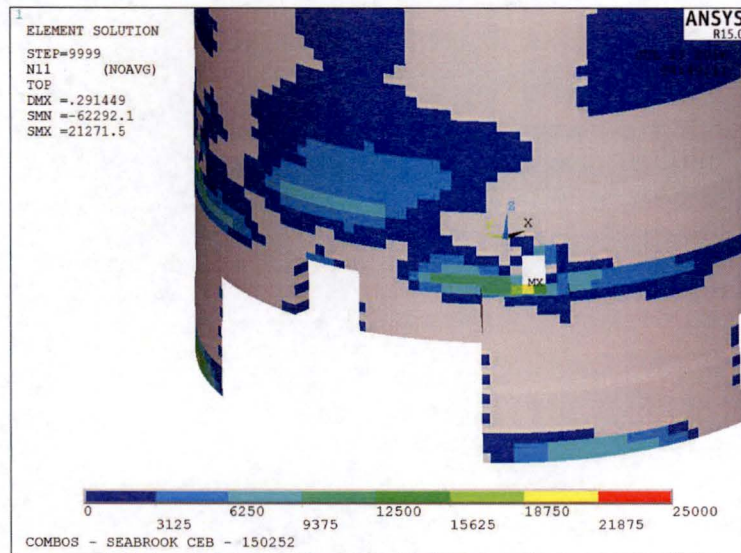
SUBJECT: Evaluation and Design Confirmation of As-Deformed CEB

PROJECT NO: 150252

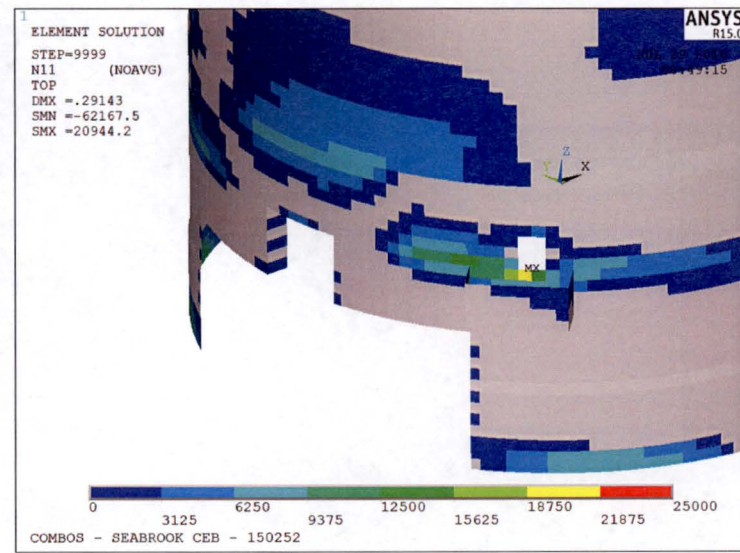
DATE: July 2016

BY: R.M. Mones

VERIFIER: A.T. Sarawit



Before Localized Cracking



After Localized Cracking

Figure M6. Comparison of Axial Forces in Hoop Direction (lb/in.) Around Location of Stiffness Reduction to Simulate Concrete Cracking

CLIENT: NextEra Energy Seabrook

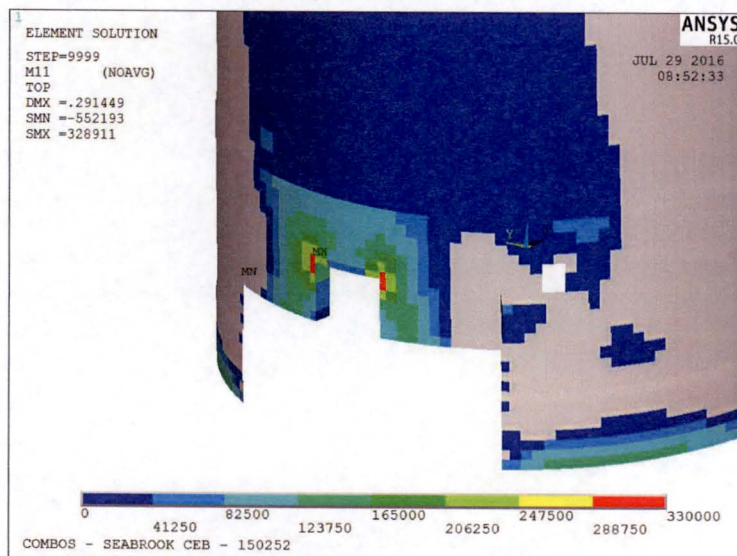
SUBJECT: Evaluation and Design Confirmation of As-Deformed CEB

PROJECT NO: 150252

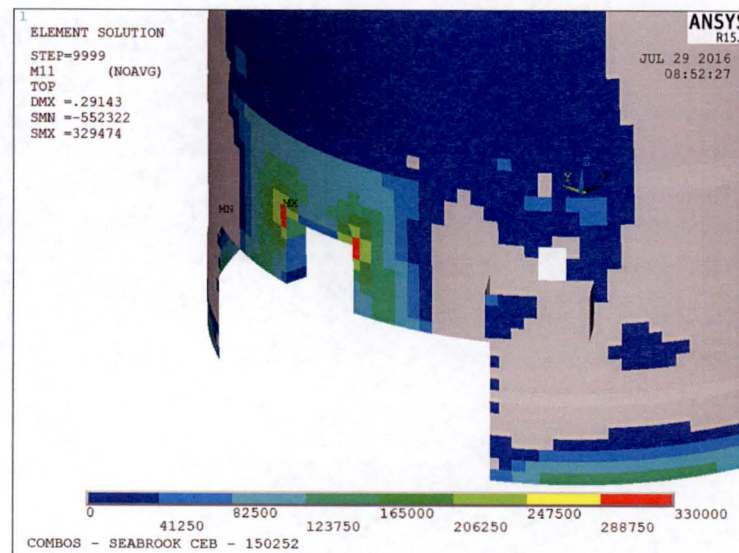
DATE: July 2016

BY: R.M. Mones

VERIFIER: A.T. Sarawit



Before Localized Cracking



After Localized Cracking

Figure M7. Comparison of Bending Moments about Meridional Axis (lbf-in/in) Around Location of Stiffness Reduction to Simulate Concrete Cracking

CLIENT: NextEra Energy Seabrook

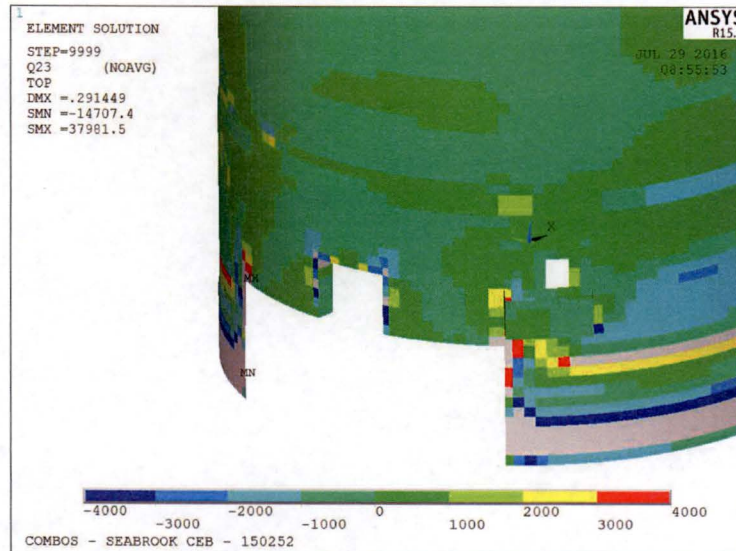
SUBJECT: Evaluation and Design Confirmation of As-Deformed CEB

PROJECT NO: 150252

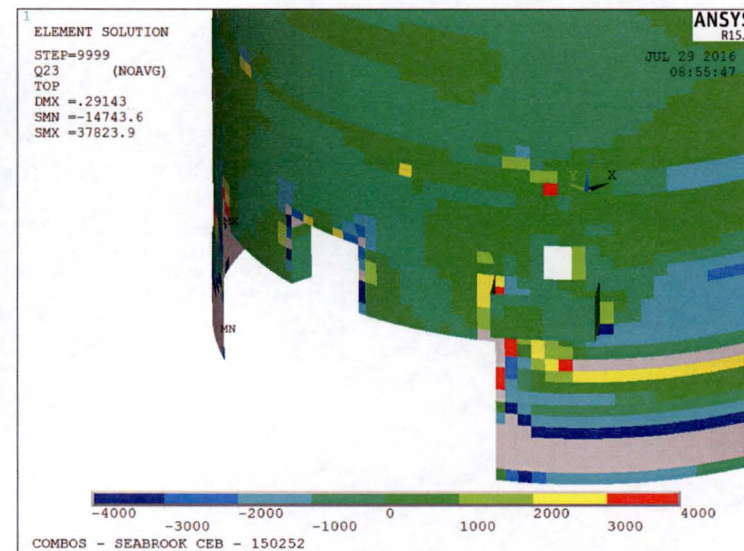
DATE: July 2016

BY: R.M. Mones

VERIFIER: A.T. Sarawit



Before Localized Cracking



After Localized Cracking

Figure M8. Comparison of Out-Of-Plane Forces Acting on the Hoop-Radial Plane (lbf/in) Around Location of Stiffness Reduction to Simulate Concrete Cracking

Appendix N Section Cut Properties

N1. REVISION HISTORY

Revision 0

Initial document.

N2. OBJECTIVE

The objective of this calculation is to document the locations and section properties of section cuts used in the CEB evaluation.

N3. RESULTS AND CONCLUSIONS

The result of this calculation is the documented locations and section properties of section cuts used in the CEB evaluation. Section cut properties are summarized in Table N-1. Section cut lengths are limited to eight times the wall thickness. The allowable number of elements per cut is summarized in Figure N-1. The elements used for each section are shown beginning with Figure N-2.

N4. DESIGN DATA / CRITERIA

Wall geometry, reinforcement layout, and material properties are based on the structural drawings listed in the project Criteria Document 150252-CD-03 [N-1].

N5. REFERENCES

- [N-1] Simpson Gumpertz & Heger Inc., *Criteria Document for Evaluation of As-Deformed Containment Enclosure Building at Seabrook Station in Seabrook, NH*, 150252-CD-03, Revision 0, Waltham, MA, 27 July 2016.

N6. TABLES

Table N-1 – Section Cut Properties

Cut	Arc Length	Chord Length	Elevation (centroid)	Orient-ation	Thick-ness	As, Inner, Hoop	As, Outer, Hoop	As, Inner, Merid-ional	As, Outer, Merid-ional	Cover, Inner, Hoop	Cover, Outer, Hoop	Cover, Inner, Merid-ional	Cover, Outer, Merid-ional	As/in, perpend-icular	As/in, parallel
-	in.	in.	in.	-	in.	in. ² /in.	in. ² /in.	in. ² /in.	in. ² /in.	in.	in.	in.	in.	in. ² /in.	in. ² /in.
1	1190.2	1116.3	-360	HOR	36.7	0.16	0.16	0.27	0.57	4.2	5.2	2.8	5.2	0.84	0.31
2	1532.8	1377.0	-360	HOR	36.0	0.13	0.13	0.26	0.52	4.1	5.1	2.8	5.1	0.78	0.26
3	985.5	943.3	-360	HOR	36.9	0.14	0.14	0.26	0.52	4.1	5.1	2.8	5.1	0.78	0.27
4	673.8	660.2	-360	HOR	38.5	0.28	0.28	0.26	0.59	4.1	5.2	2.8	5.2	0.85	0.55
7	1062.6	1009.3	169	HOR	28.6	0.12	0.11	0.26	0.29	4.0	3.8	2.8	5.0	0.55	0.23
8	211.8	211.3	0	HOR	31.0	0.13	0.13	0.26	0.52	4.0	5.0	2.8	5.0	0.78	0.26
9	199.6	199.2	-67	HOR	31.0	0.13	0.13	0.26	0.52	4.0	5.0	2.8	5.0	0.78	0.26
10	204.0	203.6	-67	HOR	31.0	0.24	0.24	0.26	0.52	4.0	5.0	2.8	5.0	0.78	0.47
11	215.4	214.9	0	HOR	31.0	0.24	0.24	0.26	0.52	4.0	5.0	2.8	5.0	0.78	0.47
14	195.4	195.4	234	VER	27.0	0.11	0.11	0.26	0.26	4.0	3.6	2.8	5.0	0.21	0.52
15	195.4	195.4	300	VER	27.0	0.11	0.11	0.26	0.26	4.0	3.6	2.8	5.0	0.21	0.52
16	195.4	195.4	267	VER	27.0	0.11	0.11	0.26	0.26	4.0	3.6	2.8	5.0	0.21	0.52
17	195.4	195.4	202	VER	27.0	0.11	0.11	0.26	0.26	4.0	3.6	2.8	5.0	0.21	0.52
18	195.4	195.4	234	VER	27.0	0.11	0.11	0.26	0.26	4.0	3.6	2.8	5.0	0.21	0.52
19	195.4	195.4	137	VER	27.0	0.11	0.11	0.26	0.30	4.0	3.9	2.8	5.0	0.21	0.56
20	195.4	195.4	267	VER	27.0	0.11	0.18	0.26	0.26	4.0	3.6	2.8	5.0	0.28	0.52

PROJECT NO: 150252

DATE: July 2016

CLIENT: NextEra Energy Seabrook

BY: J.B. Deaton

SUBJECT: Evaluation and Design Confirmation of As-Deformed CEB

VERIFIER: A.T. Sarawit

Table N-1 – Section Cut Properties (continued)

Cut	Arc Length	Chord Length	Elevation (centroid)	Orient -ation	Thick -ness	As, Inner, Hoop	As, Outer, Hoop	As, Inner, Merid -ional	As, Outer, Merid -ional	Cover, Inner, Hoop	Cover, Outer, Hoop	Cover, Inner, Merid -ional	Cover, Outer, Merid -ional	As/in, perpend -icular	As/in, parallel
-	in.	in.	in.	-	in.	in. ² /in.	in. ² /in.	in. ² /in.	in. ² /in.	in.	in.	in.	in.	in. ² /in.	in. ² /in.
21	195.4	195.4	267	VER	27.0	0.11	0.18	0.26	0.26	4.0	3.6	2.8	5.0	0.28	0.52
22	197.4	197.4	235	VER	27.0	0.11	0.11	0.26	0.26	4.0	3.6	2.8	5.0	0.21	0.52
23	203.6	203.6	336	VER	27.0	0.11	0.11	0.26	0.26	4.0	3.6	2.8	5.0	0.21	0.52
24	185.9	185.9	488	VER	19.8	0.10	0.10	0.22	0.22	4.0	3.6	2.7	4.9	0.20	0.45
25	195.4	195.4	234	VER	27.0	0.11	0.11	0.26	0.26	4.0	3.6	2.8	5.0	0.21	0.52
26	195.4	195.4	169	VER	39.0	0.17	0.17	0.26	0.48	4.0	4.8	2.8	5.0	0.33	0.74
27	134.9	134.9	783	VER	15.0	0.08	0.08	0.08	0.08	3.7	3.6	2.5	4.7	0.17	0.17
28	425	421	547	HOR	15.0	0.08	0.08	0.08	0.08	3.69	3.56	2.50	4.69	0.17	0.17
29	236	236	867	VER	15.0	0.08	0.08	0.08	0.08	3.64	3.55	2.47	4.64	0.16	0.16
30	216	216	372	VER	27.0	0.11	0.21	0.26	0.26	4.05	3.64	2.78	4.98	0.32	0.52

N7. FIGURES

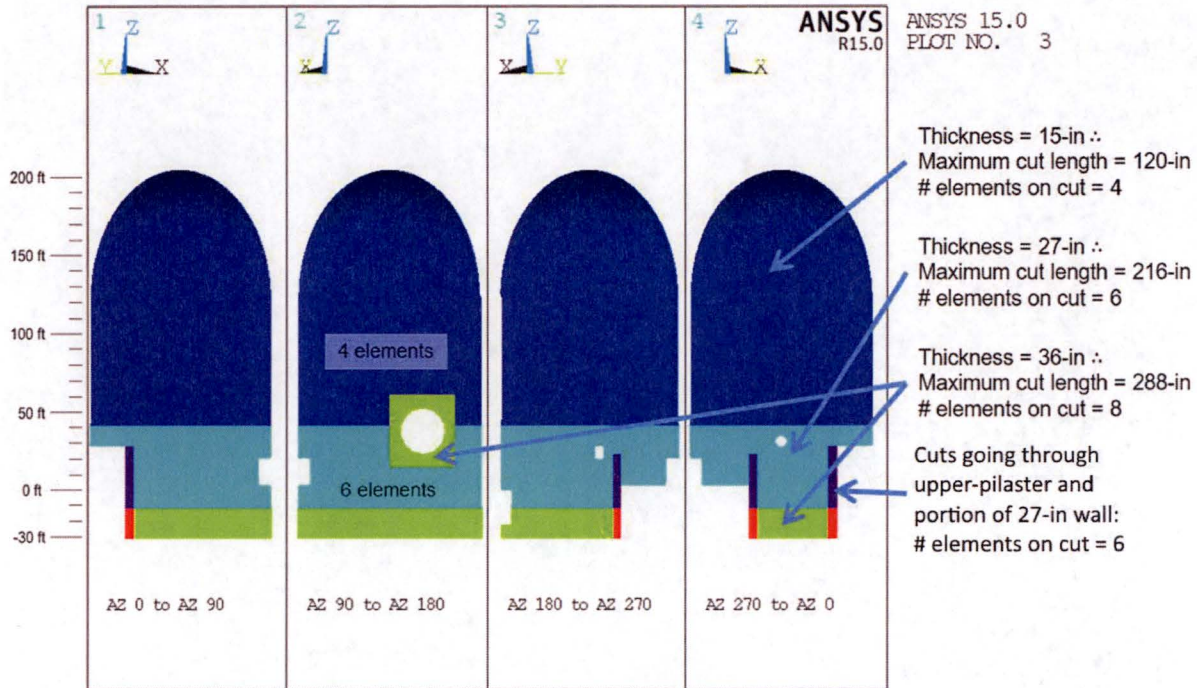
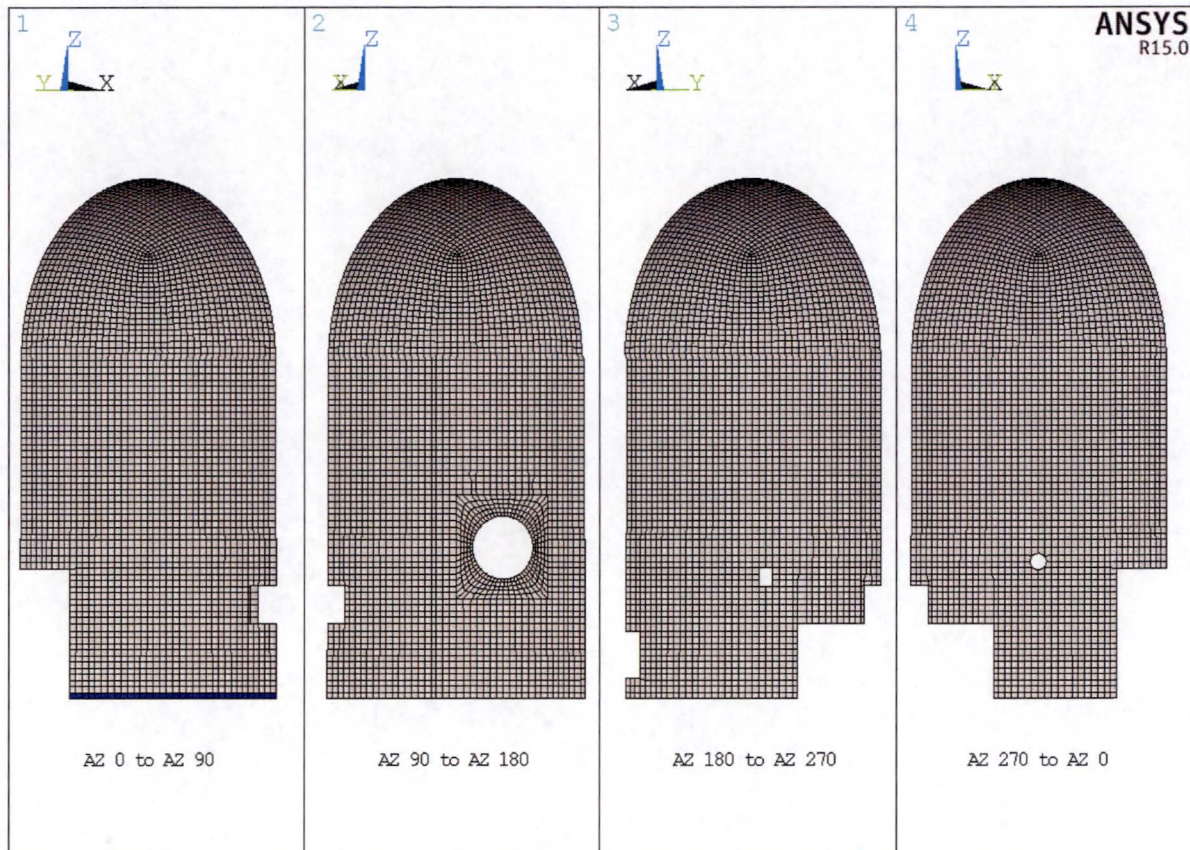


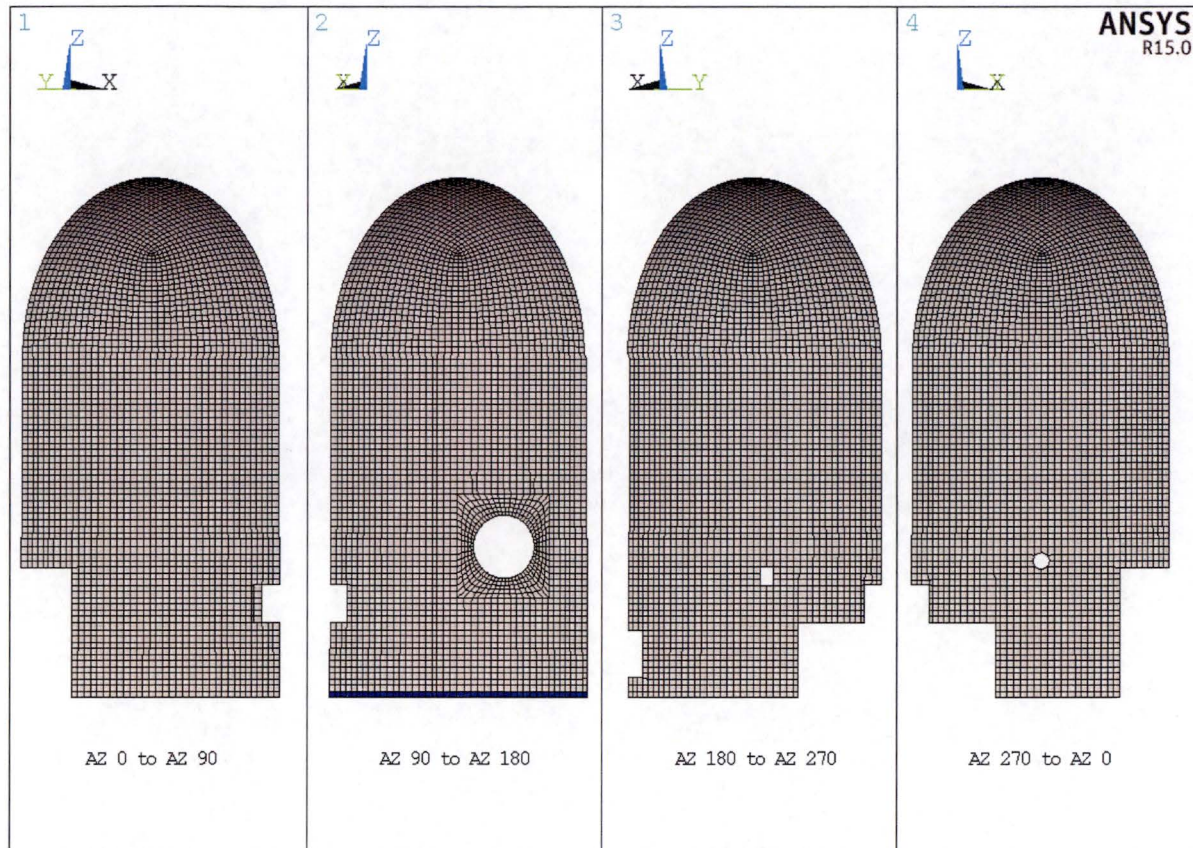
Figure N-1 – Allowable Number of Elements per Section Cut Based on 8x Wall Thickness

Note: Cut lengths in above figure are for evaluation of axial-flexure interaction. Out-of-plane shear acting at the base of the structure and in-plane shear acting throughout the structure are evaluated using section cuts up to 90 degrees or approximately 125 ft in length.



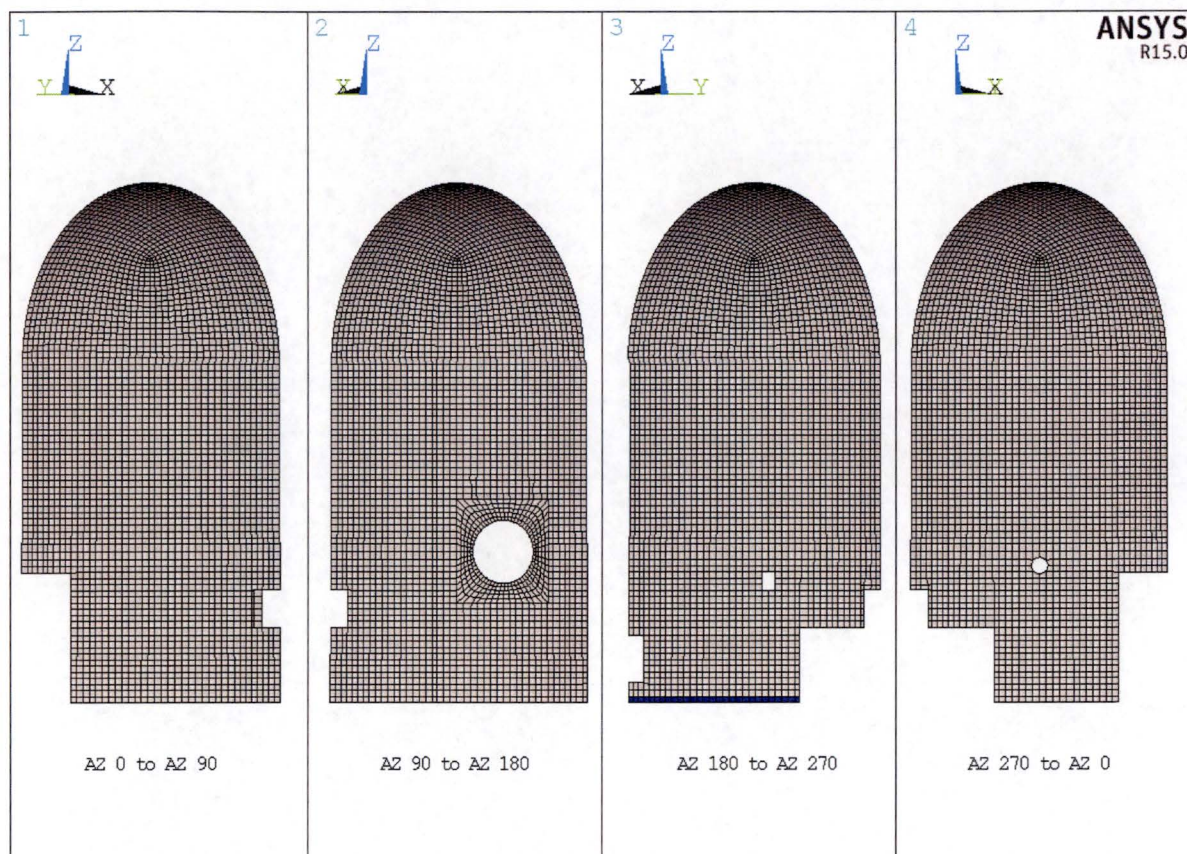
Section Cut Number 01

Figure N-2 – Elements Comprising Section Cut 1



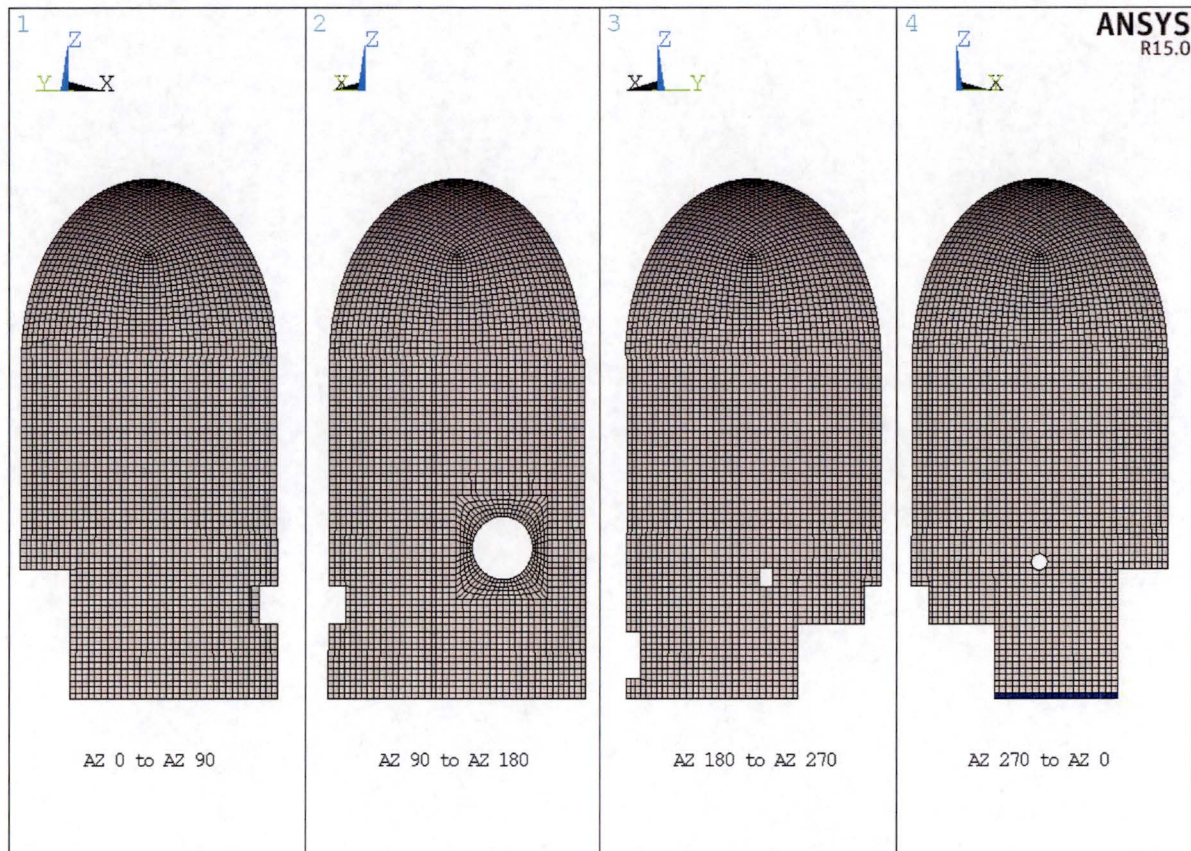
Section Cut Number 02

Figure N-3 – Elements Comprising Section Cut 2



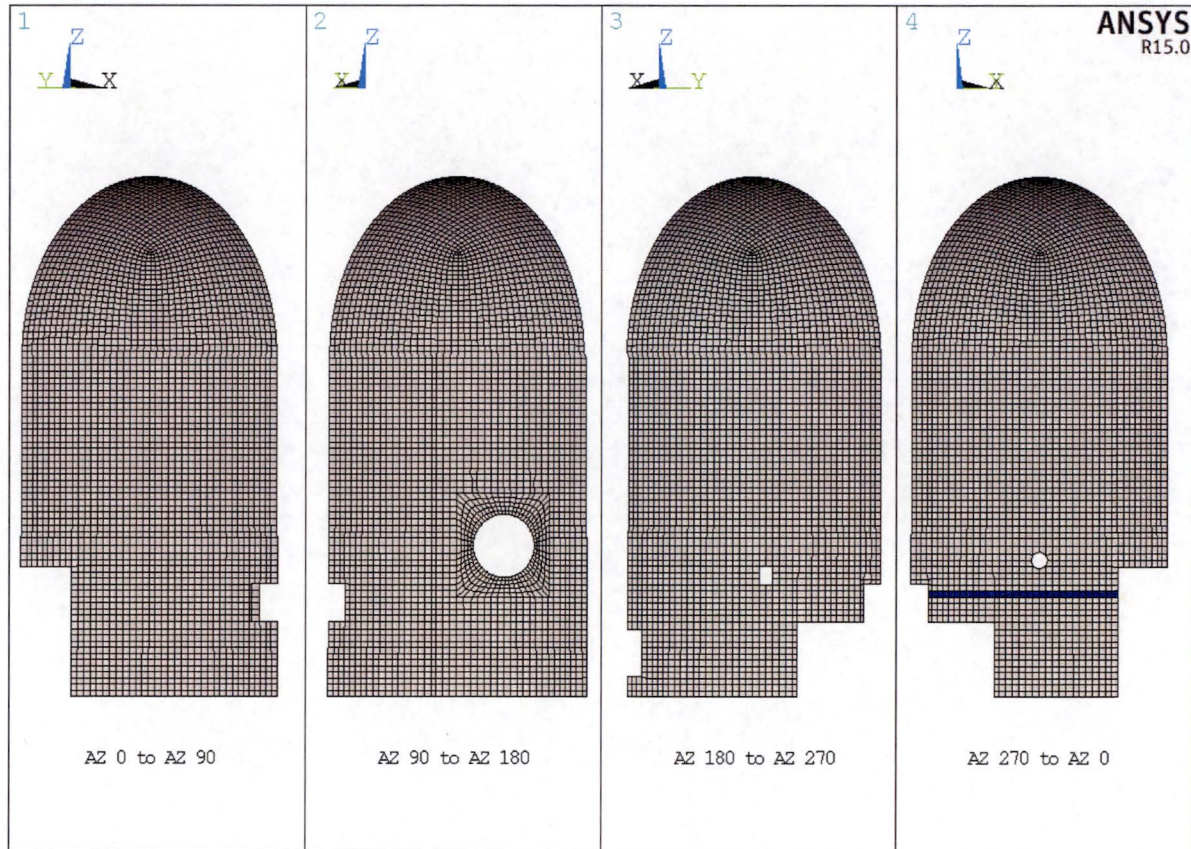
Section Cut Number 03

Figure N-4 – Elements Comprising Section Cut 3



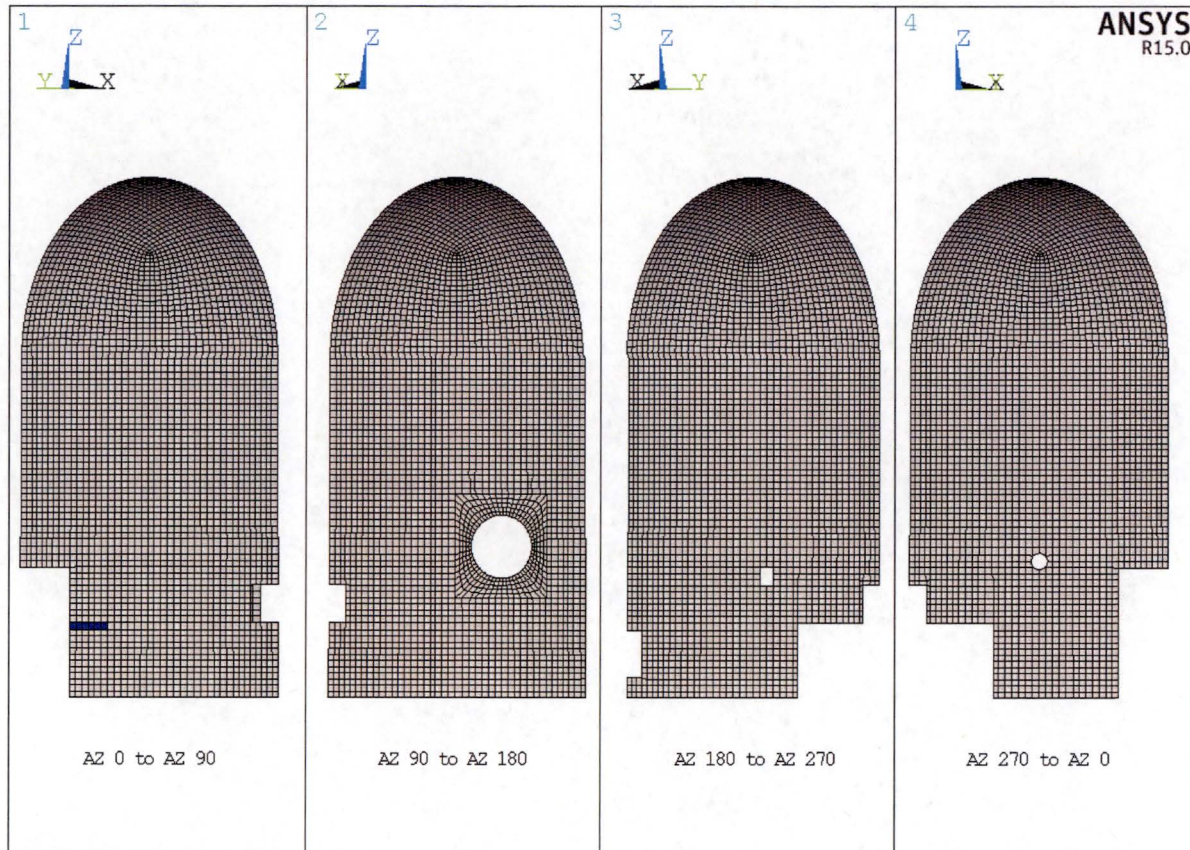
Section Cut Number 04

Figure N-5 – Elements Comprising Section Cut 4



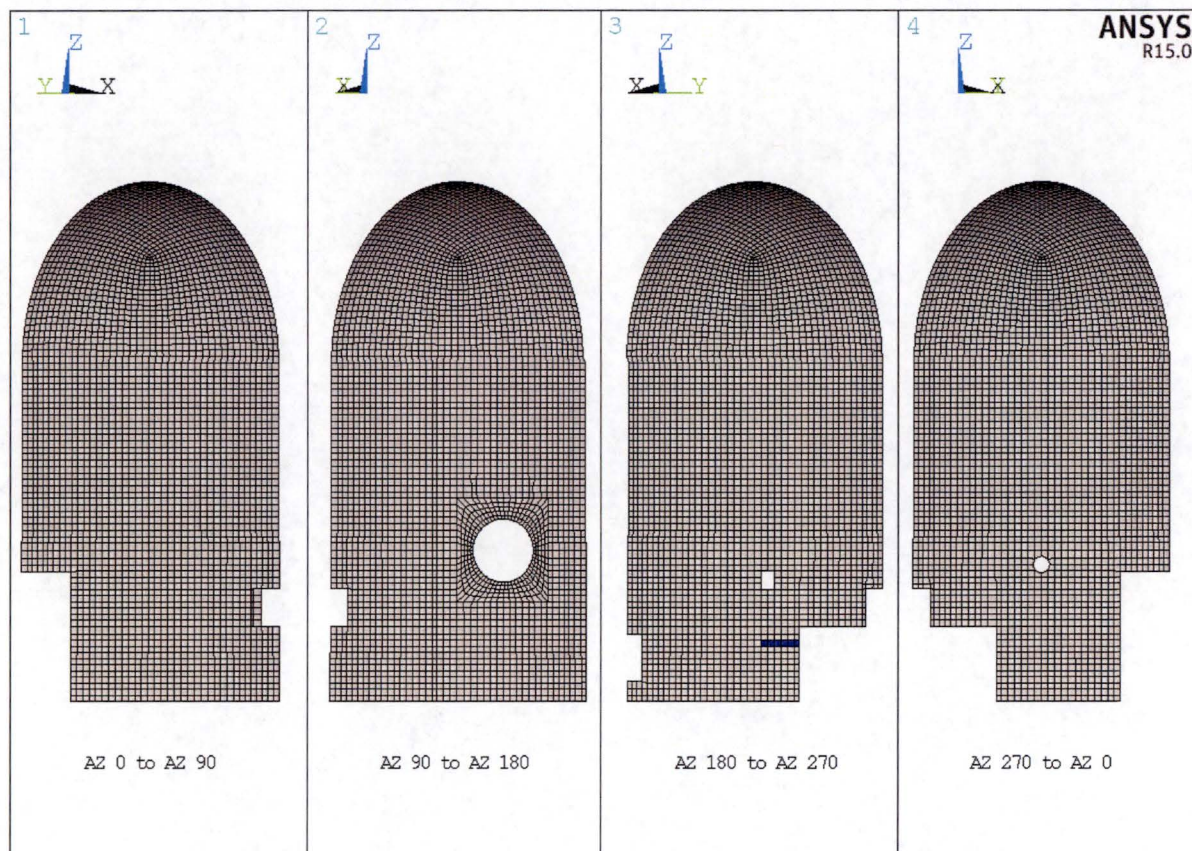
Section Cut Number 07

Figure N-6 – Elements Comprising Section Cut 7



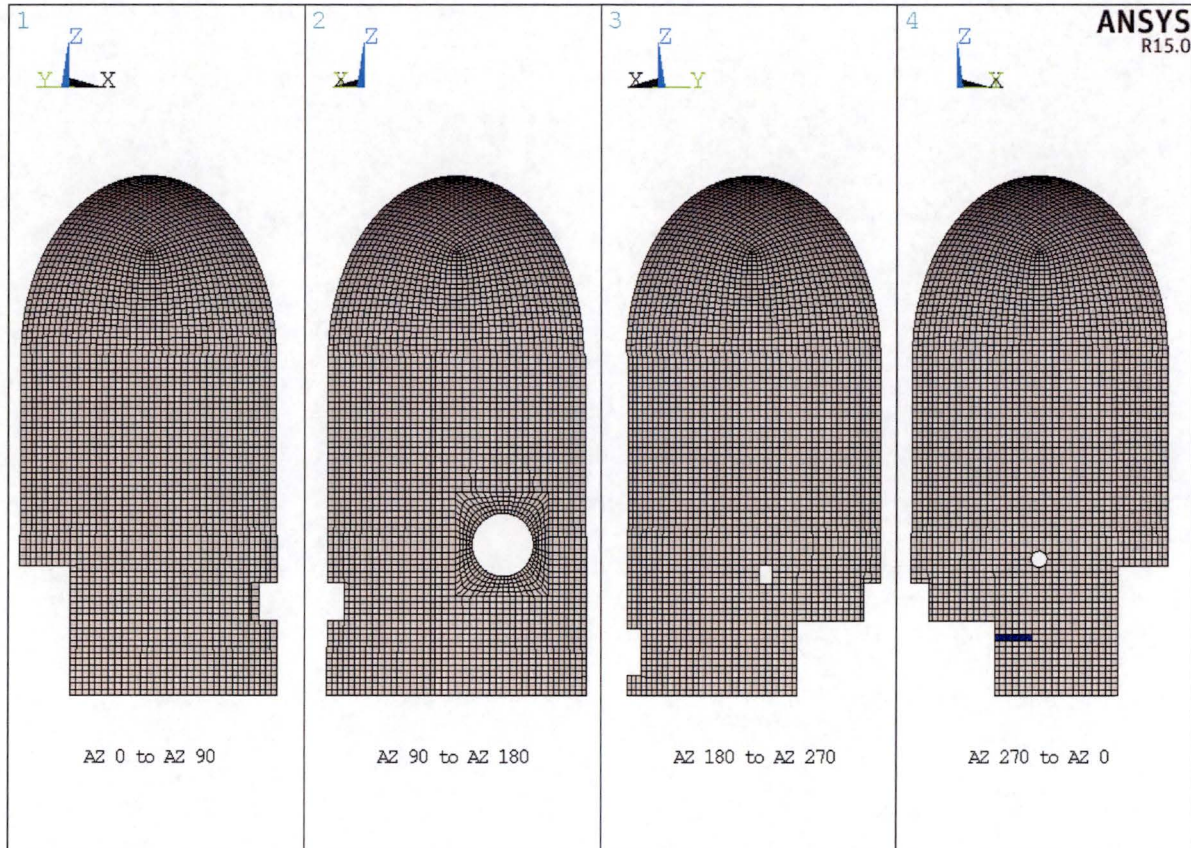
Section Cut Number 08

Figure N-7 – Elements Comprising Section Cut 8



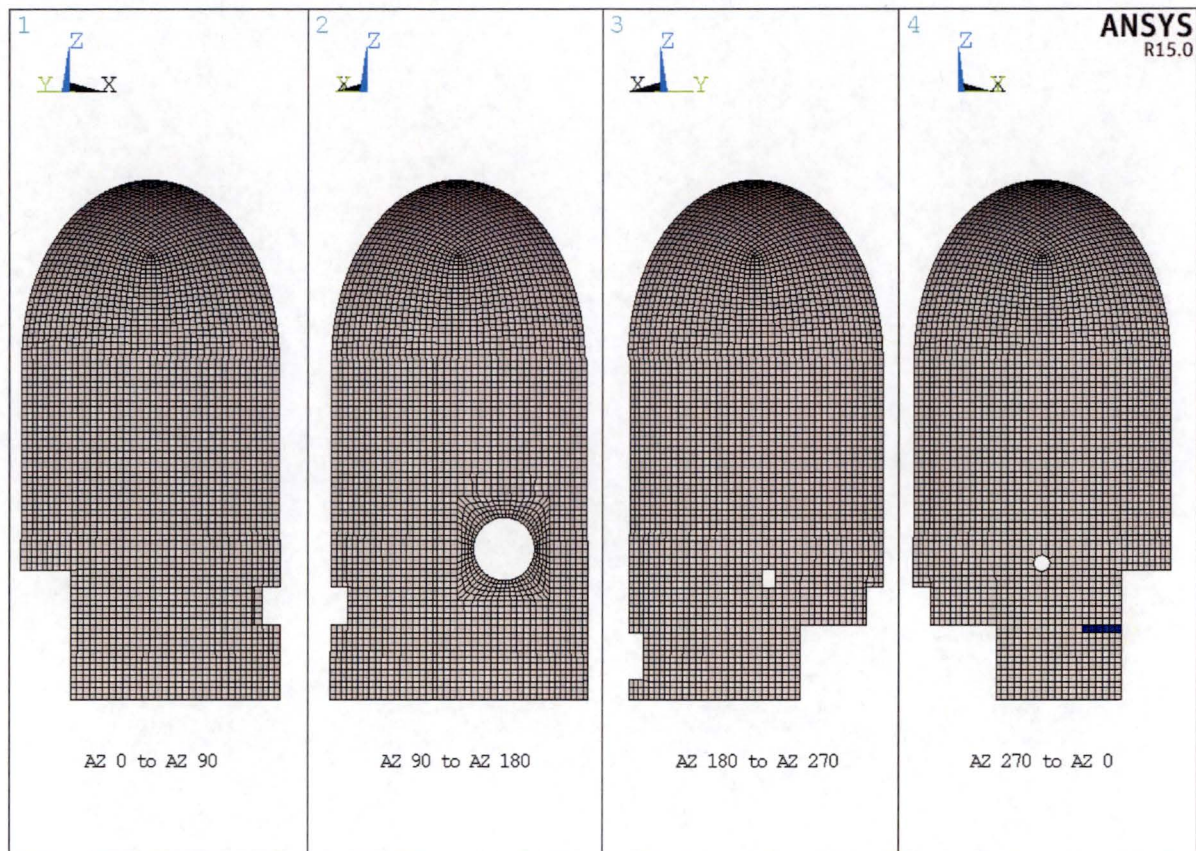
Section Cut Number 09

Figure N-8 – Elements Comprising Section Cut 9



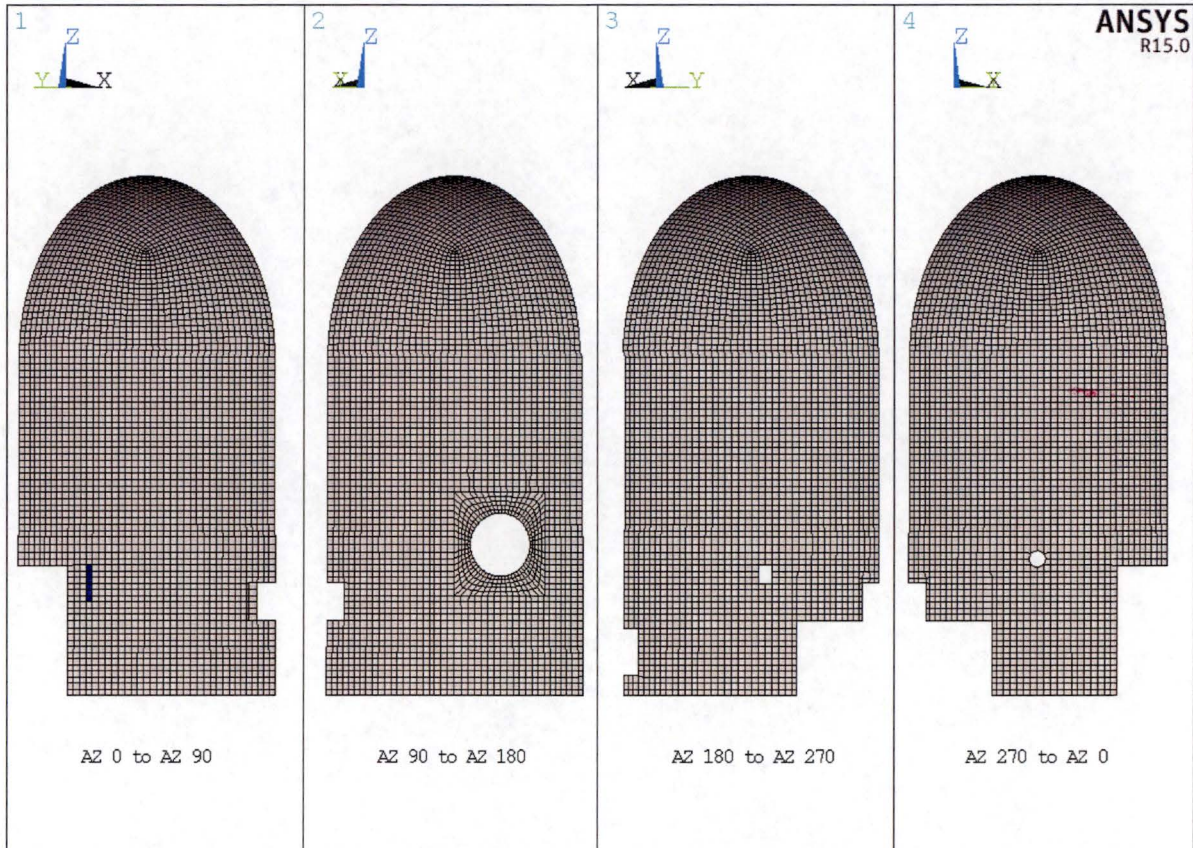
Section Cut Number 10

Figure N-9 – Elements Comprising Section Cut 10



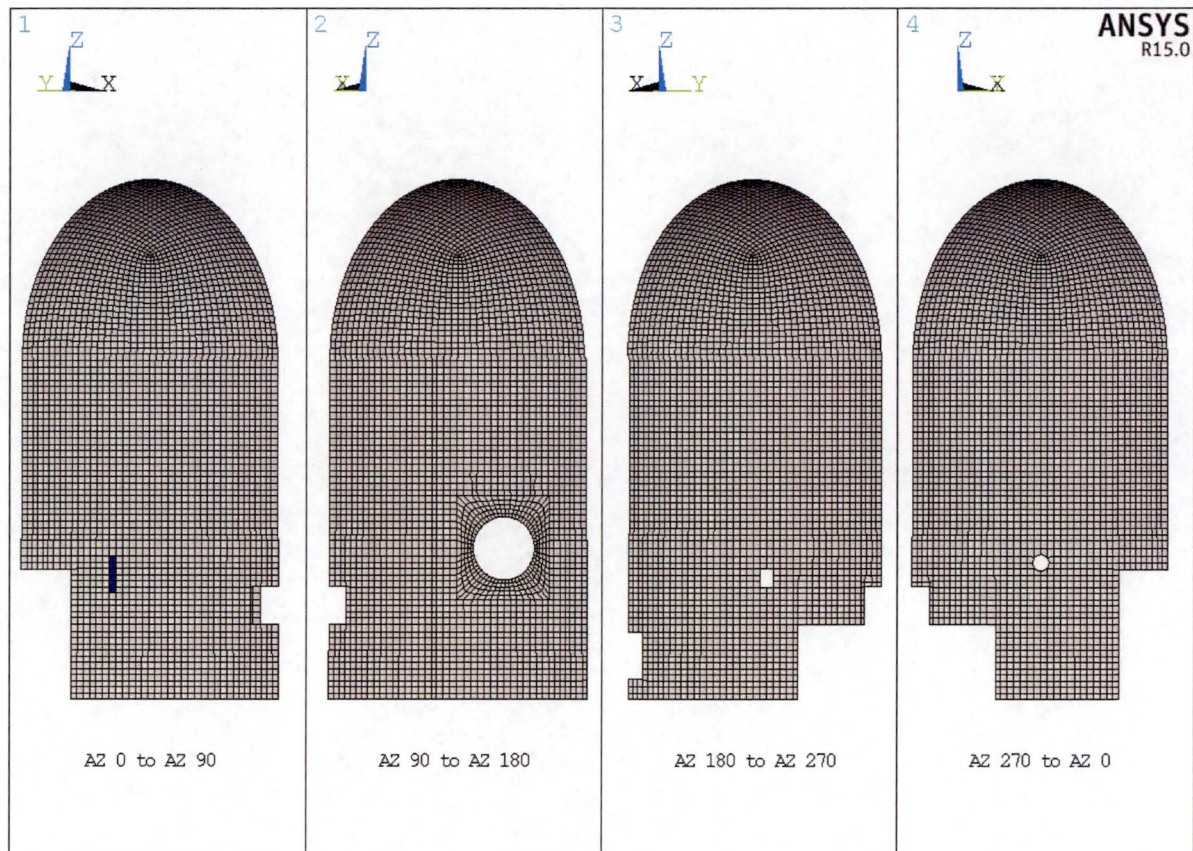
Section Cut Number 11

Figure N-10 – Elements Comprising Section Cut 11



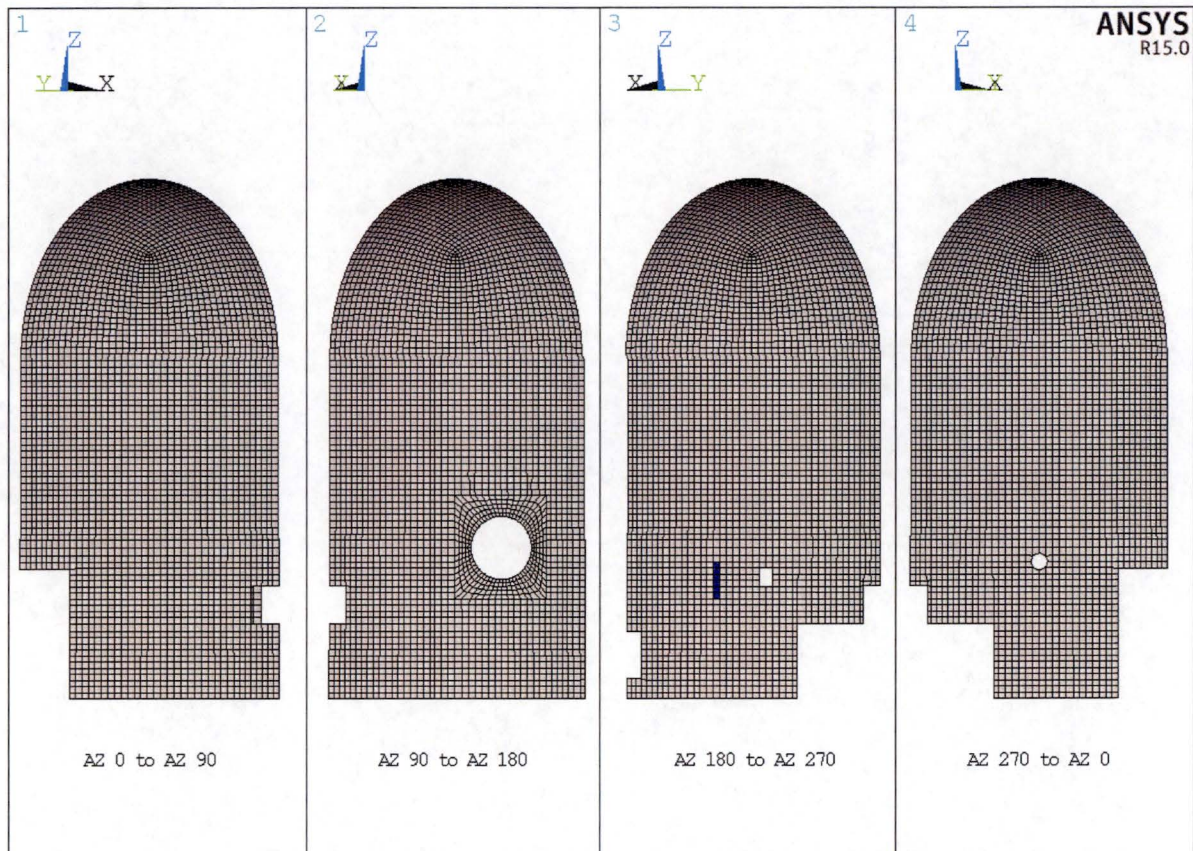
Section Cut Number 14

Figure N-11 – Elements Comprising Section Cut 14



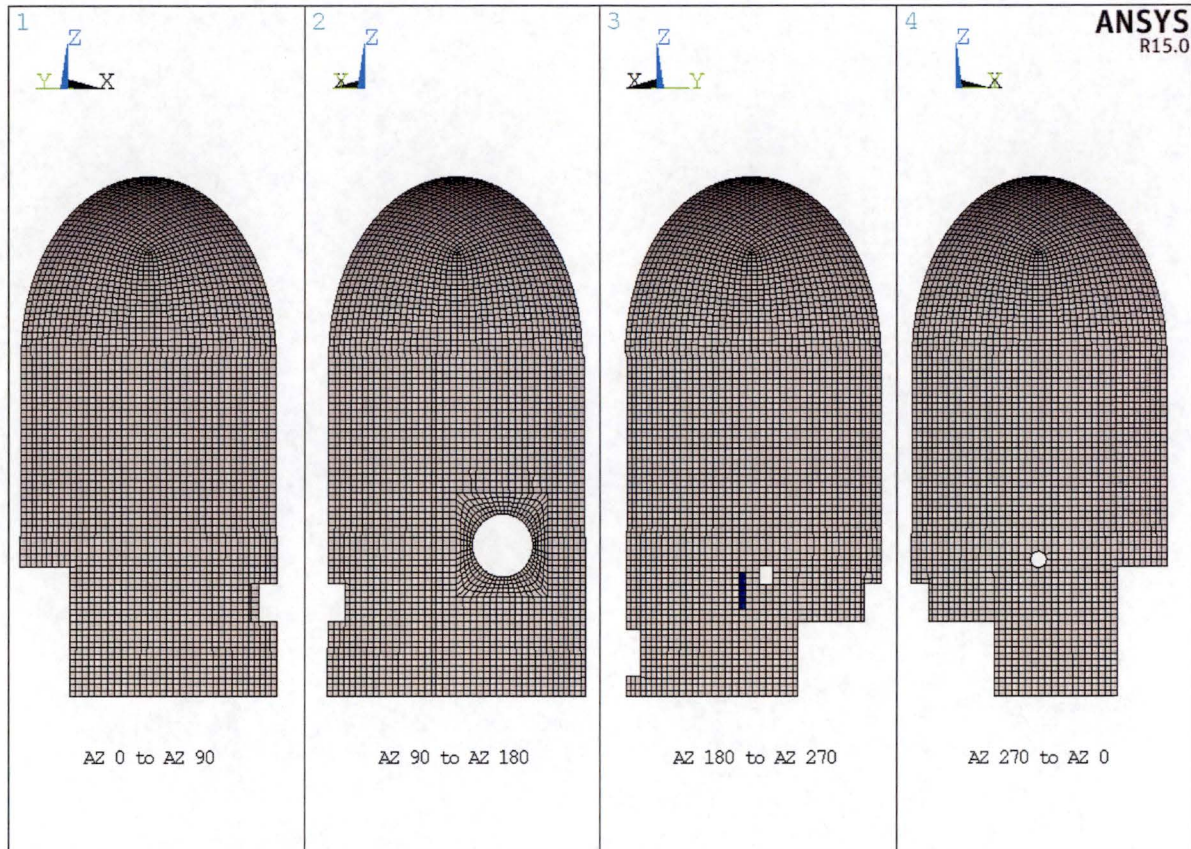
Section Cut Number 15

Figure N-12 – Elements Comprising Section Cut 15



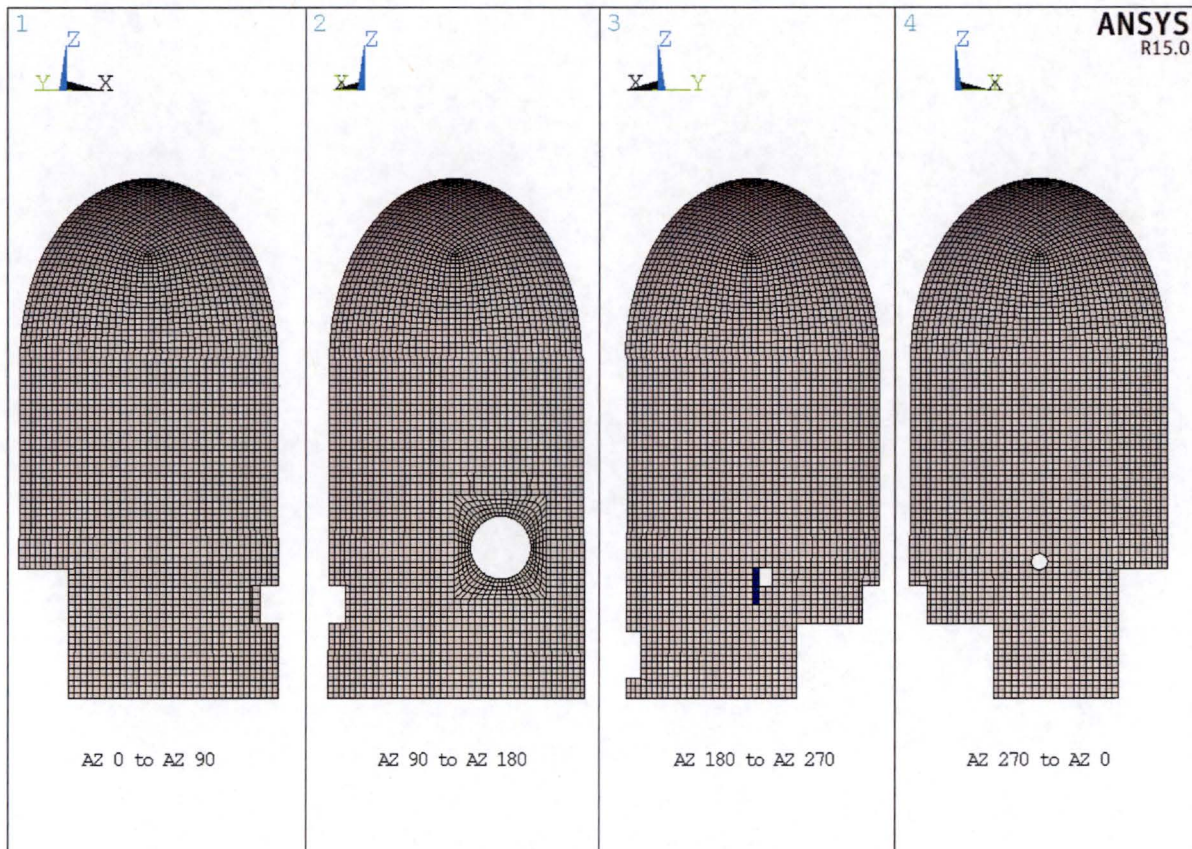
Section Cut Number 16

Figure N-13 – Elements Comprising Section Cut 16



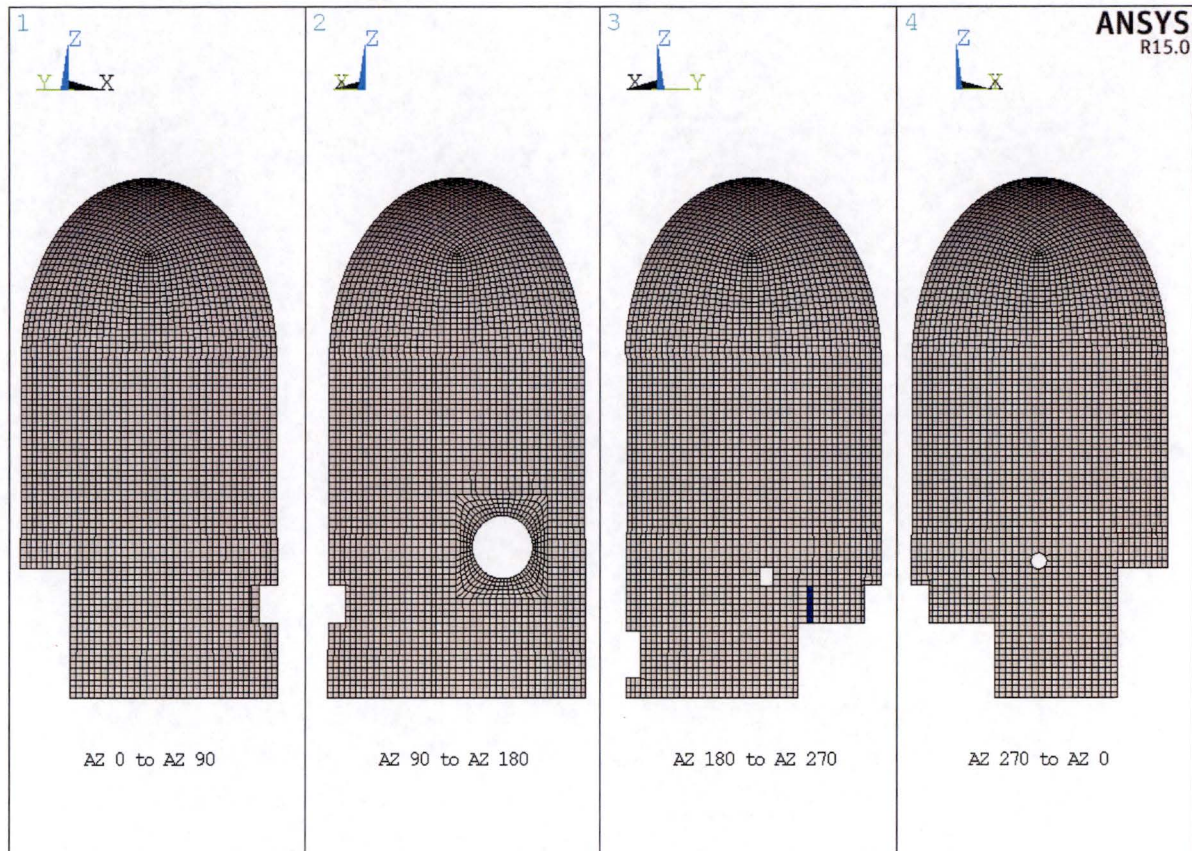
Section Cut Number 17

Figure N-14 – Elements Comprising Section Cut 17



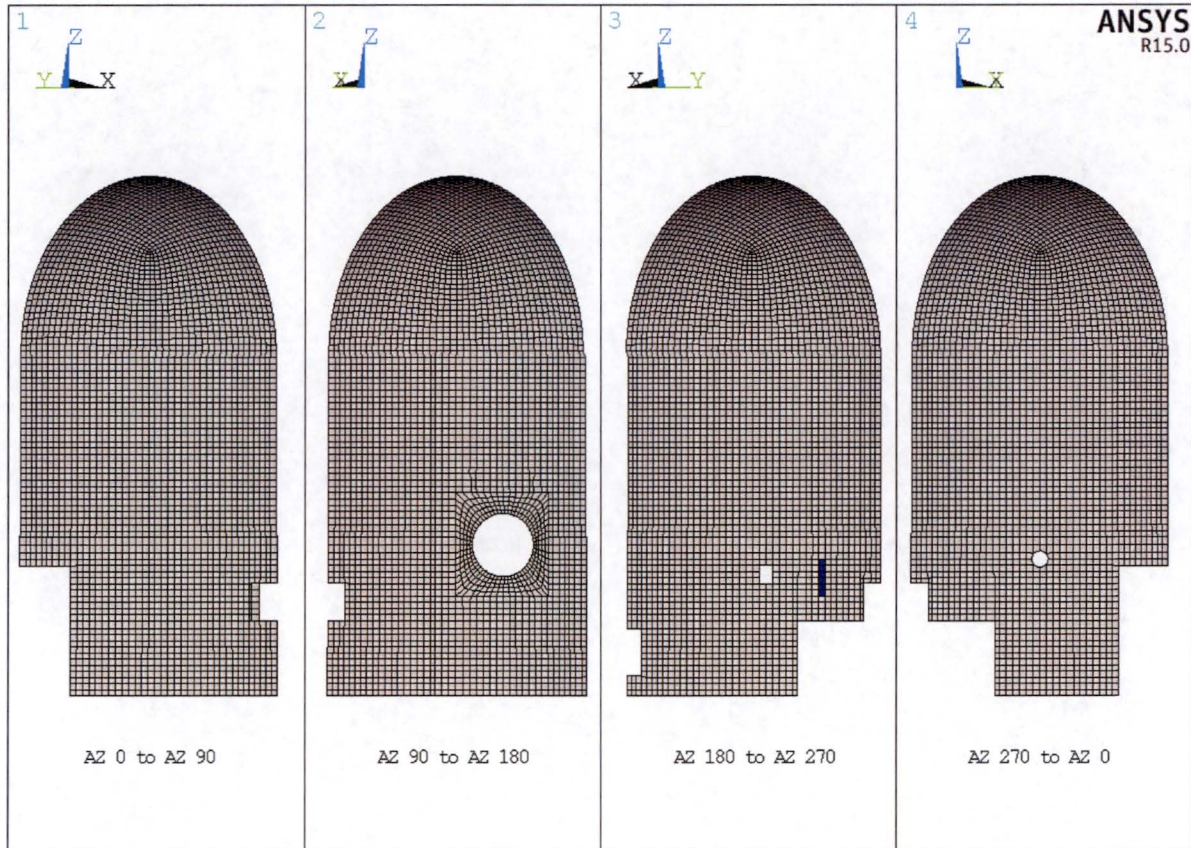
Section Cut Number 18

Figure N-15 – Elements Comprising Section Cut 18



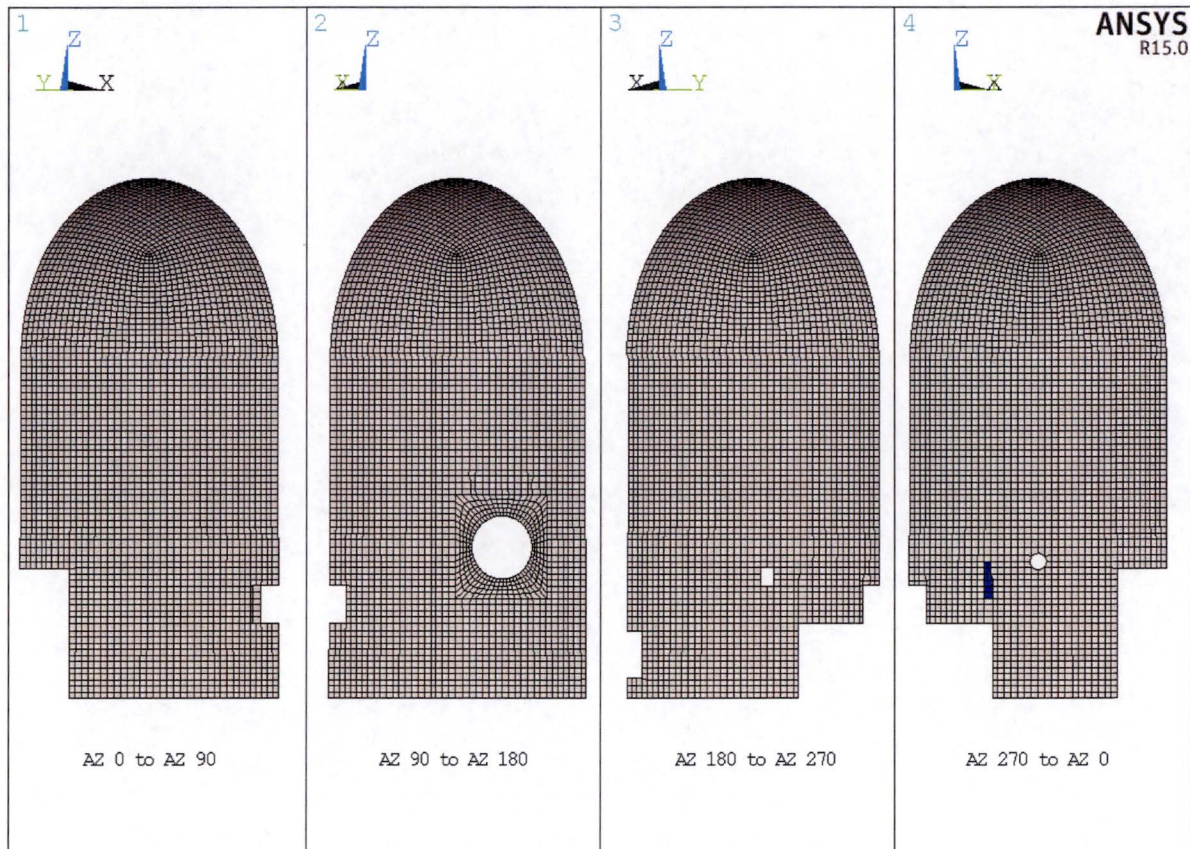
Section Cut Number 19

Figure N-16 – Elements Comprising Section Cut 19



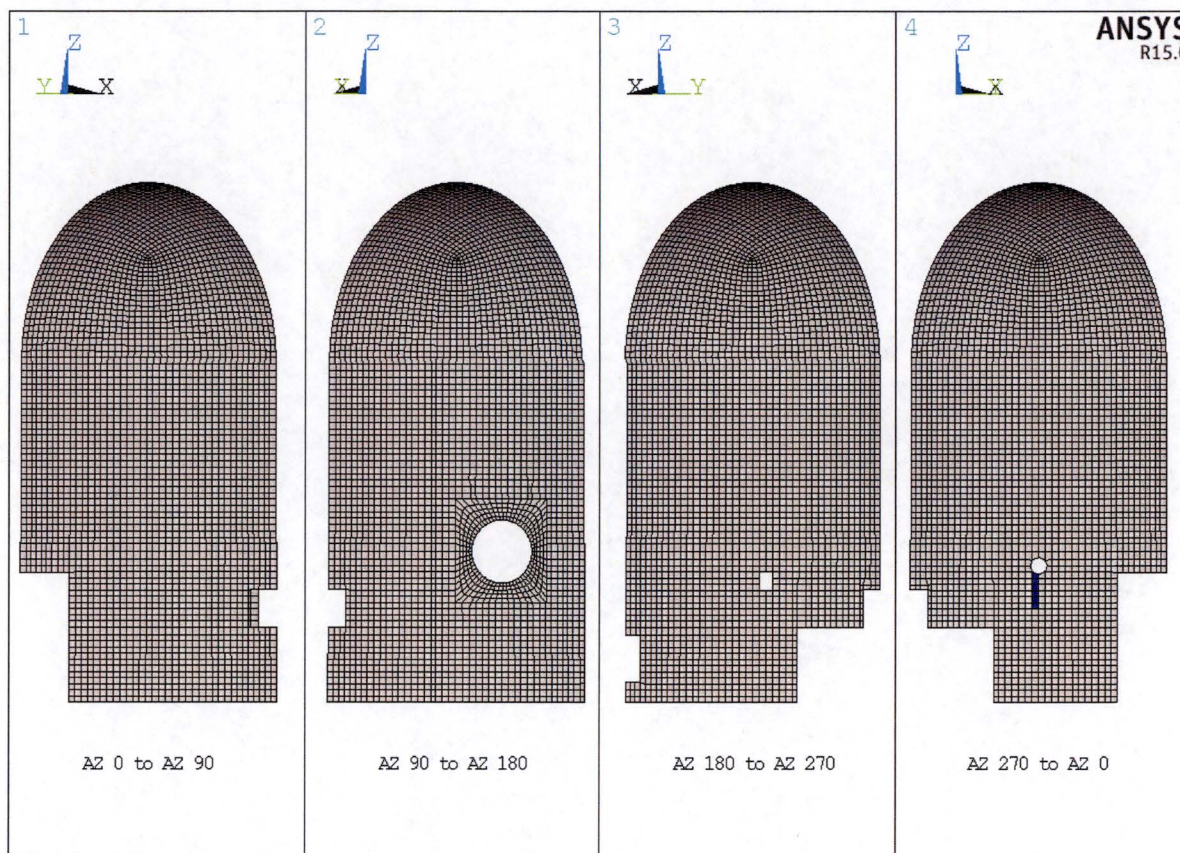
Section Cut Number 20

Figure N-17 – Elements Comprising Section Cut 20



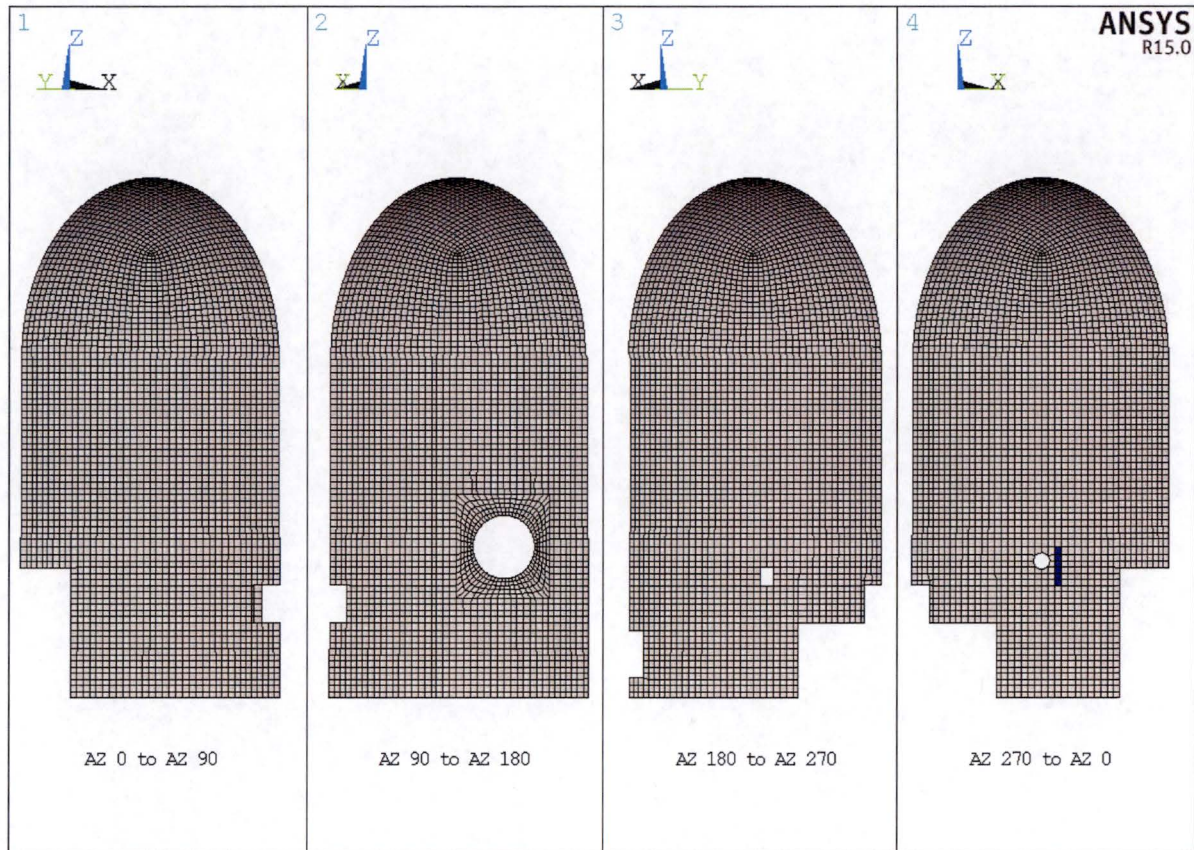
Section Cut Number 21

Figure N-18 – Elements Comprising Section Cut 21



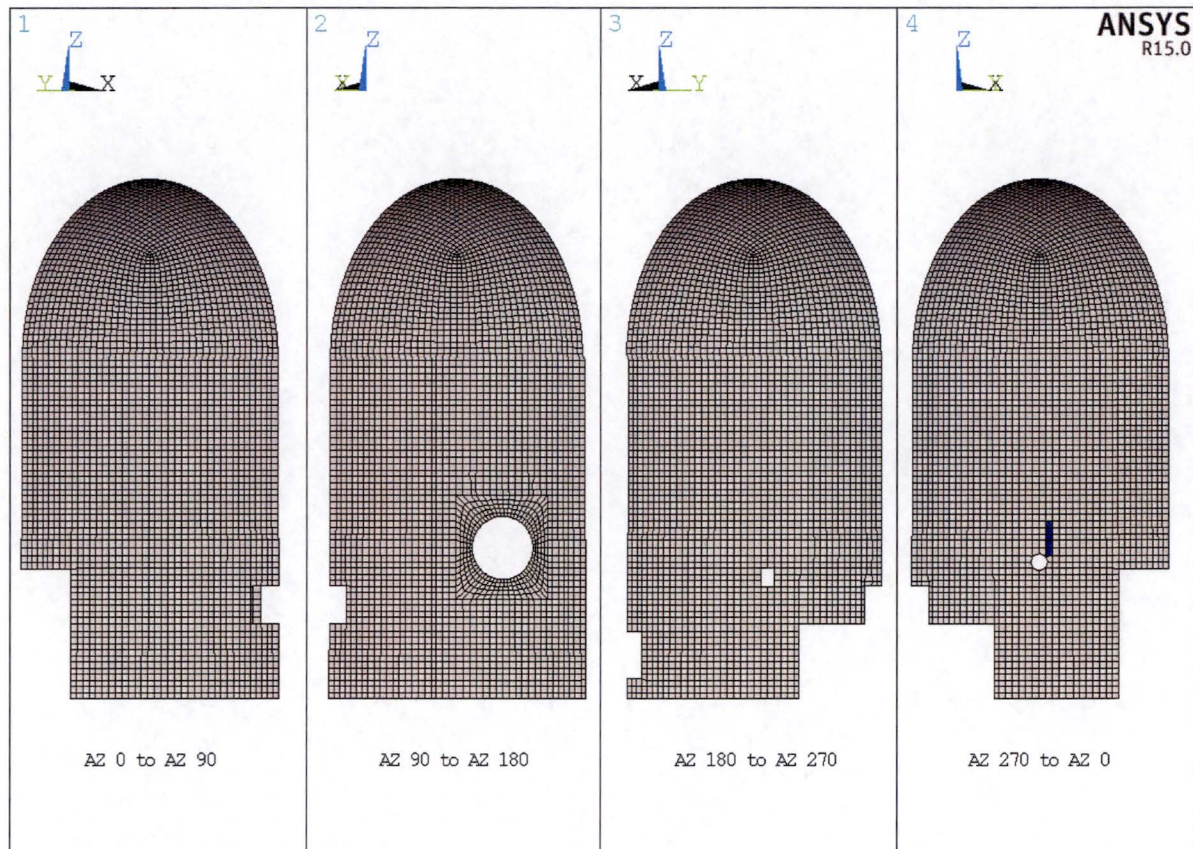
Section Cut Number 22

Figure N-19 – Elements Comprising Section Cut 22



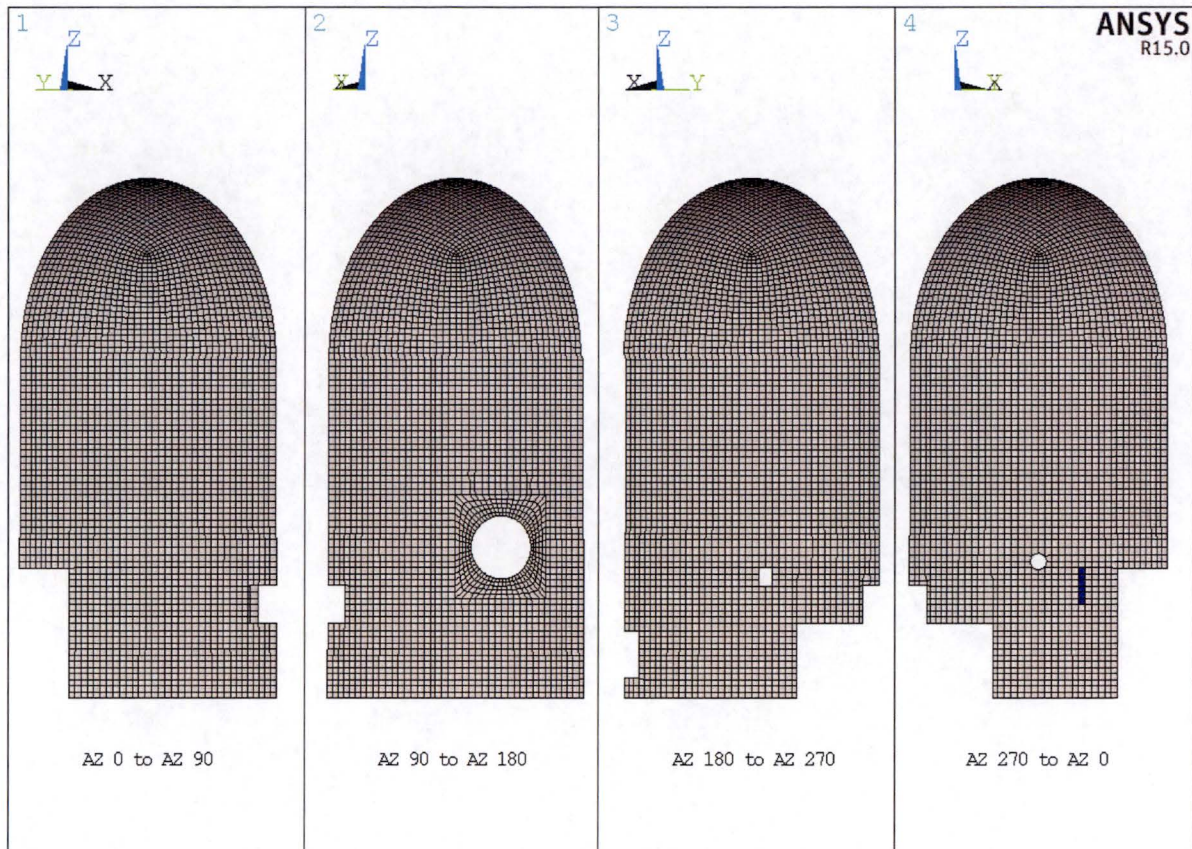
Section Cut Number 23

Figure N-20 – Elements Comprising Section Cut 23



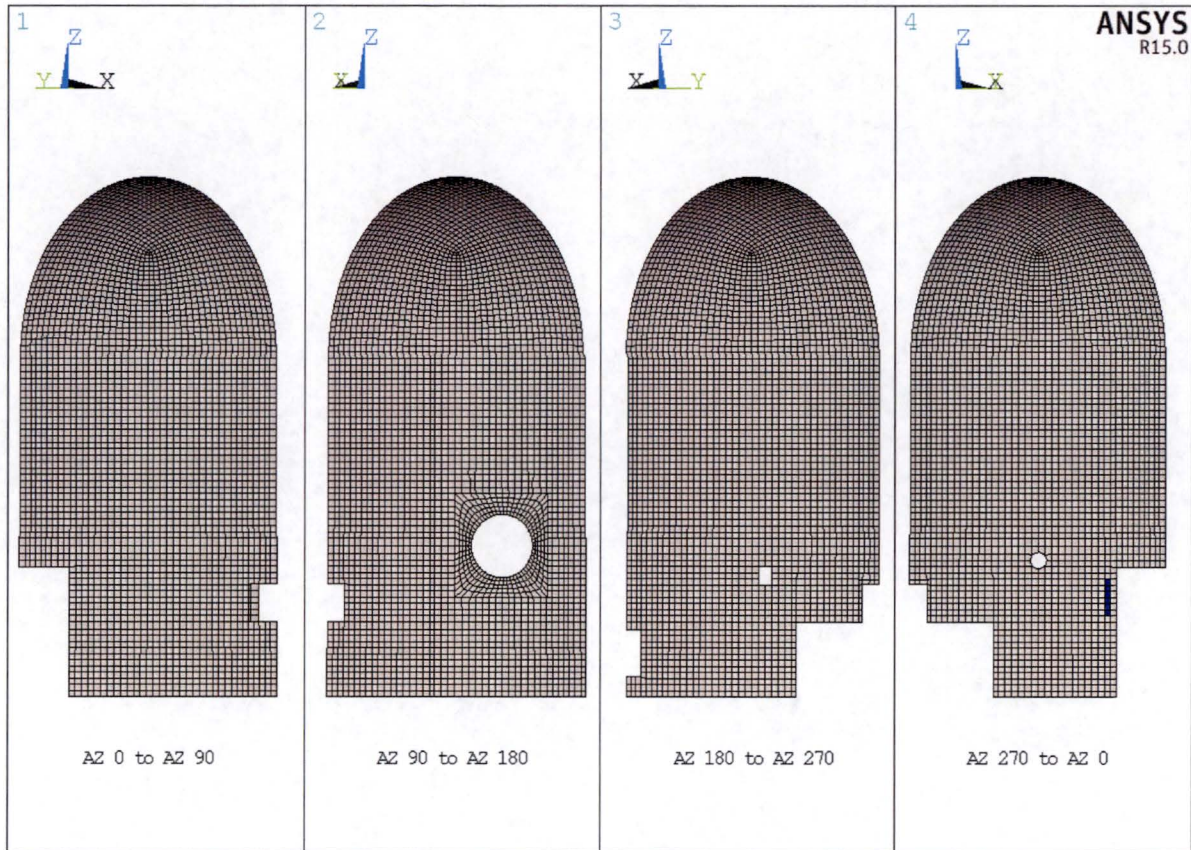
Section Cut Number 24

Figure N-21 – Elements Comprising Section Cut 24



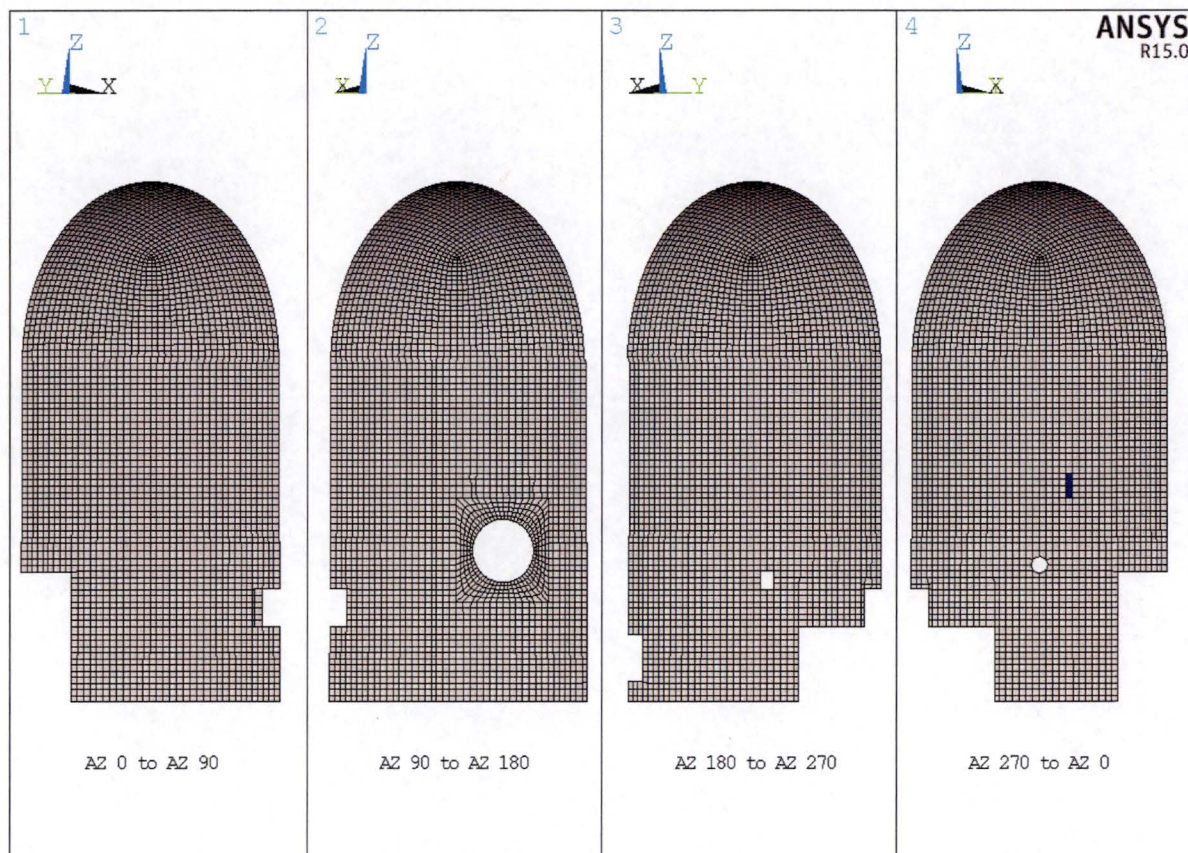
Section Cut Number 25

Figure N-22 – Elements Comprising Section Cut 25



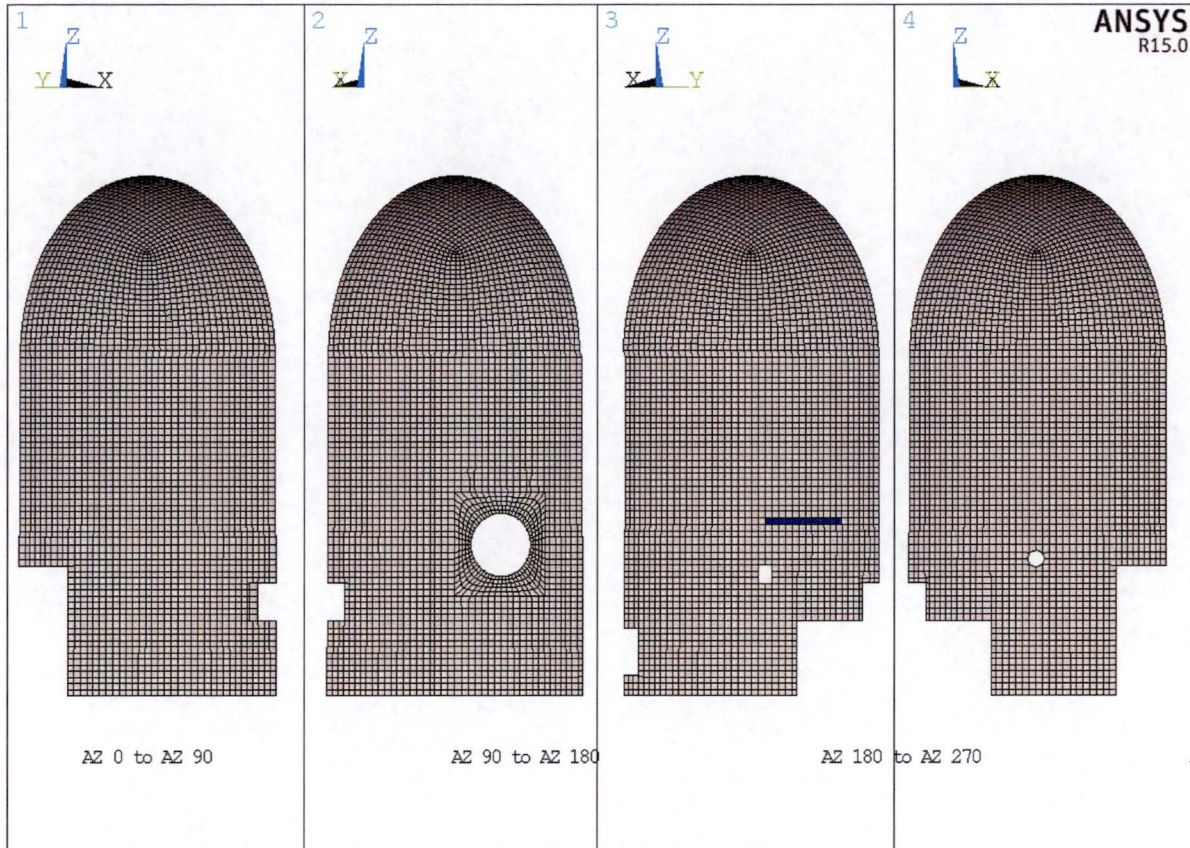
Section Cut Number 26

Figure N-23 – Elements Comprising Section Cut 26



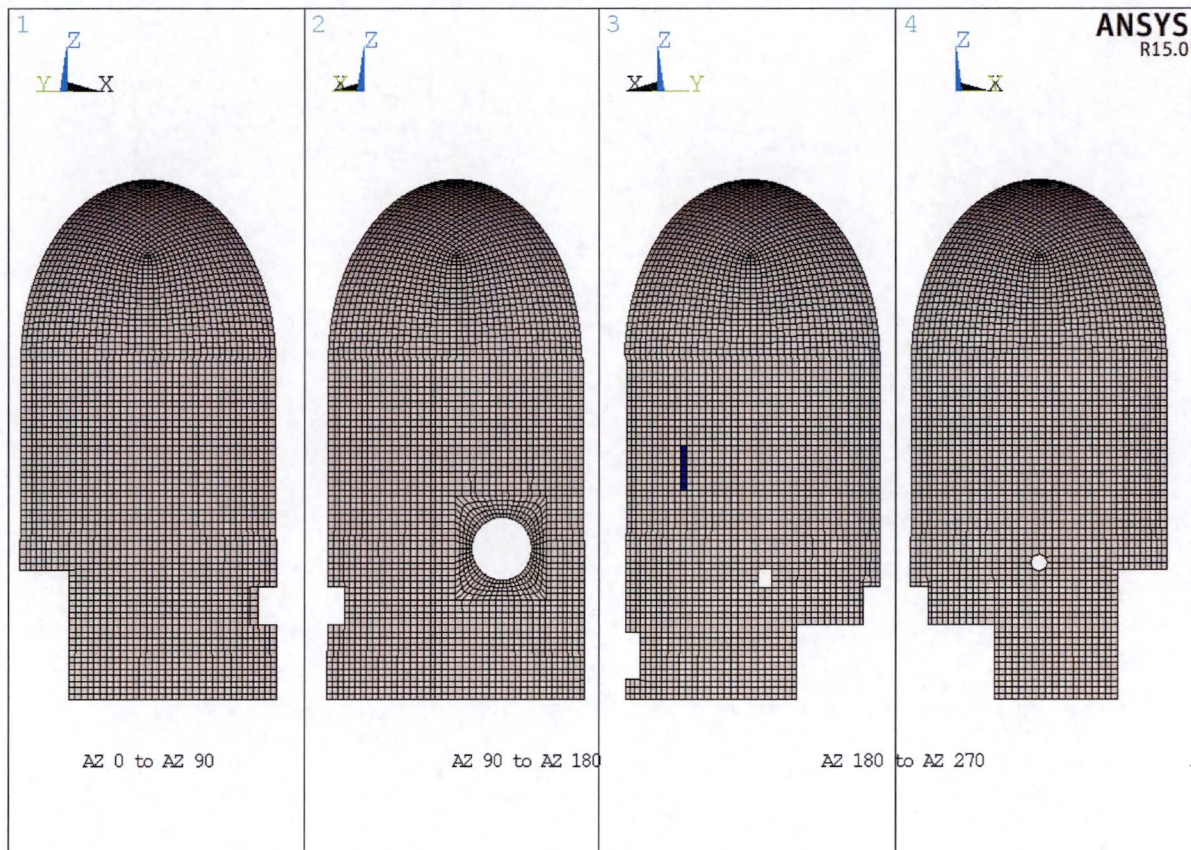
Section Cut Number 27

Figure N-24 – Elements Comprising Section Cut 27



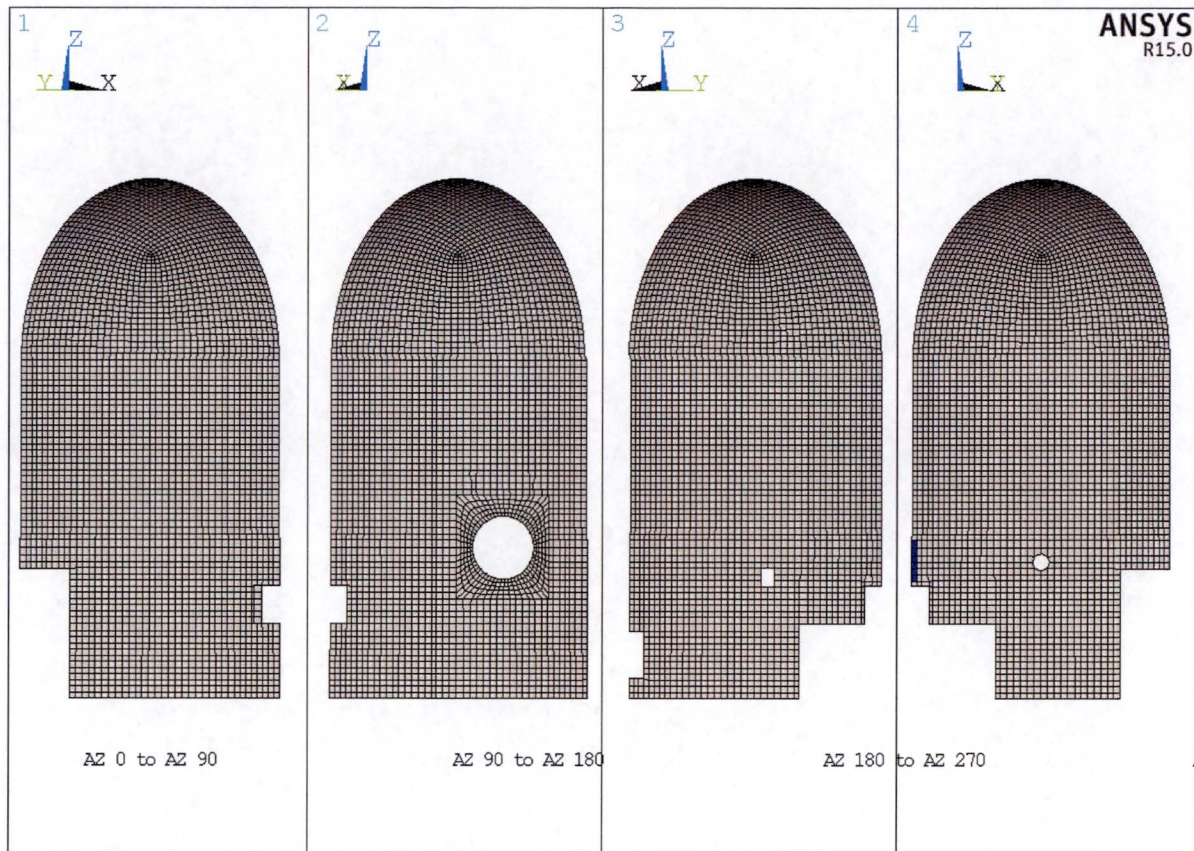
Section Cut Number 28

Figure N-25 – Elements Comprising Section Cut 28



Section Cut Number 29

Figure N-26 – Elements Comprising Section Cut 29



Section Cut Number 30

Figure N-27 – Elements Comprising Section Cut 30

Appendix O EVALUATION OF REINFORCED CONCRETE SECTION DUCTILITY DEMAND

01. REVISION HISTORY

Revision 0

Initial document.

02. OBJECTIVE

The objective of the present appendix is to present results and associated calculations for the determination of ductility demands of selected reinforced concrete section walls in the containment enclosure building subjected to moment and axial load demands. The selected section walls have been identified with the highest demand-to-capacity (D/C) ratios due to "Standard" and "Standard-Plus" load combinations and are subjected to moment redistribution.

03. RESULTS AND CONCLUSIONS

Wall section cuts showing the highest ductility demands are reported in Table O-1. These ductility demands are reported only for the "Standard-Plus" load combination due to the similarity of results with the "Standard" case. The highest ductility demand is 3.51 at section-cut 22. The corresponding strain in the steel is 0.00699 (0.7%) which is well below the strain limit of 0.070 (7%) for Grade 60 bars at fracture (Table 2 of ASTM Standard A615-78 [O-1]). Consequently, this wall section and all of the other wall sections with less ductility demands are adequate for moment redistribution.

04. ASSUMPTIONS

No assumptions are made in this calculation.

05. METHODOLOGY

The ductility demand in the reinforced concrete section wall is reported as the ratio between the maximum strain of the steel rebar to the yielding strain of the steel. The maximum strain of the rebar is calculated based on curvature in the section needed to store energy equivalent to the linear-elastic strain energy in the section due to the moment demand.



Energy that is stored on the section for a given curvature is calculated by integrating the nonlinear moment-curvature response curve of the section. The moment-curvature response of the section is calculated based on material models for the concrete and steel ([O-2] to [O-9]). The linear-elastic strain energy due to the moment demand is calculated based on the slope of the linear-elastic portion of the moment-curvature response curve of the section.

Ductility demand is calculated for wall sections of the containment enclosure building (Table O-1) which have been identified with the highest D/C ratios and subjected to moment redistribution.

O6. COMPUTATIONS

Ductility demand calculations for wall section cuts listed in Table O-1 for the "Standard-Plus" case are presented in the following pages. Section properties and moment and axial force demands used in the evaluation of the flexural-axial force capacity of the walls are used as inputs for the calculations. As noted in the main body of the calculation, rebar covers for the flexural-axial force capacity of the walls are computed with conservatism to account for possible variations in the rebar configuration. Because section-cut 22 shows the highest ductility demand (3.51), the moment-curvature response calculation of this section is performed based on design concrete covers.

07. TABLES

Load Combination	Section Cut	Demands		Steel Yielding Strain (ϵ_y)	Steel Strain (ϵ_s)	Ductility (ϵ_s/ϵ_y)
		Moment (kip*ft/ft)	Axial Load (kip/ft)			
STANDARD-PLUS	4 (Middle Segment)	911.5	11.4	1.989E-03	2.95E-03	1.48
	8	322.3	-140.8	1.989E-03	3.66E-03	1.84
	22	169.5	-30.9	1.989E-03	6.99E-03	3.51

Table O-1. Ductility Demands

1. REFERENCES

- [O-1] American Society for Testing and Materials (ASTM), 1979 Annual Book of ASTM Standards, Standard Specification for Deformed and Plain Billet-Steel Bars for Concrete Reinforcement A615-78, Pages 580-586.
- [O-2] Karthik and Mander, Stress-Block Parameters for Unconfined and Confined Concrete Based on a Unified Stress-Strain Model, ASCE Journal of Structural Engineering V137 N2 February 2011.
- [O-3] Eric Setzler, Modeling the Behavior of Lightly Reinforced Concrete Columns Subjected to Lateral Loads, MS Thesis, Ohio State University, 2005.
- [O-4] Pilkey, W. D. Formulas for Stress, Strain, and Structural Matrices, Second Edition, John Wiley & Sons 2005.
- [O-5] Mander, Priestley and Park, Theoretical Stress-Strain Model for Confined Concrete, ASCE Journal of Structural Engineering V114 N8 August 1988.
- [O-6] Cornelissen, H. A. W., Hordijk, D. A. and Reinhardt, H. W. Experimental determination of crack softening characteristic of normal weight and lightweight concrete. HERON 31(2), 45-56, 1986.
- [O-7] Roy, H. E. H. and Sozen M. A., Ductility of Concrete, ACI Special Publication: Flexural Mechanics of Reinforced Concrete, 1965
- [O-8] Halil Sezen, Eric Setzler, Reinforcement Slip in Reinforced Concrete Columns. ACI Structural Journal, May-June 2008.

Section Cut 22 "STANDARD-PLUS" Load Combination**INPUT DEFINITION**

Set starting index of all arrays to 1 (the default is 0)

ORIGIN \equiv 1

Input Reading

	1
1	"Seabrook1"
2	$4 \cdot 10^3$
3	$6 \cdot 10^4$
4	$6 \cdot 10^4$
5	$9 \cdot 10^4$
INPUTS = 6	3.95
7	1.495
8	12
9	27
10	324
11	9.01
12	...

INDEX = 1

colname := INPUTS_{1, INDEX}

colname = "Seabrook1"

Concrete strength

$f'_c := \text{INPUTS}_{2, \text{INDEX}} \cdot \text{psi}$

$f'_c = 4 \cdot \text{ksi}$

Steel yield strength

$f_y := \text{INPUTS}_{3, \text{INDEX}} \cdot \text{psi}$

$f_y = 60 \cdot \text{ksi}$

Ultimate strength of rebar

$f_{su} := \text{INPUTS}_{5, \text{INDEX}} \cdot \text{psi}$

$f_{su} = 90 \cdot \text{ksi}$

cover (to centroid of steel)	$\text{cover} := \text{INPUTS}_{6, \text{INDEX}} \cdot \text{in}$	$\text{cover} = 3.95 \cdot \text{in}$
Width of column	$b_{\text{col}} := \text{INPUTS}_{8, \text{INDEX}} \cdot \text{in}$	$b_{\text{col}} = 12 \cdot \text{in}$
Height of column	$h_{\text{col}} := \text{INPUTS}_{9, \text{INDEX}} \cdot \text{in}$	$h_{\text{col}} = 27 \cdot \text{in}$
Gross Area	$A_g := \text{INPUTS}_{10, \text{INDEX}} \cdot \text{in}^2$	$A_g = 324 \cdot \text{in}^2$
Area of longitudinal bar	$a_{\text{bar}} := \text{INPUTS}_{13, \text{INDEX}} \cdot \text{in}^2$	$a_{\text{bar}} = 1.27 \cdot \text{in}^2$
Diameter of bar	$d_{\text{bar}} := \text{INPUTS}_{14, \text{INDEX}} \cdot \text{in}$	$d_{\text{bar}} = 1.27 \cdot \text{in}$
Area of longitudinal steel	$A_{sL} := \text{INPUTS}_{18, \text{INDEX}} \cdot \text{in}^2$	$A_{sL} = 2.54 \cdot \text{in}^2$
Young's modulus of steel	$E_s := \text{INPUTS}_{20, \text{INDEX}} \cdot \text{psi}$	$E_s = 2.9 \times 10^4 \cdot \text{ksi}$
Ultimate strain of rebar	$\epsilon_{\text{su}} := \text{INPUTS}_{21, \text{INDEX}}$	$\epsilon_{\text{su}} = 0.07$
Modulus of strain hardening [O-2]	$E_{\text{sh}} := \text{INPUTS}_{22, \text{INDEX}} \cdot \text{psi}$	$E_{\text{sh}} = 1.16 \times 10^3 \cdot \text{ksi}$
Strain at strain hardening [O-3]	$\epsilon_{\text{sh}} := \text{INPUTS}_{23, \text{INDEX}}$	$\epsilon_{\text{sh}} = 8 \times 10^{-3}$
Young's modulus of concrete	$E_c := \text{INPUTS}_{24, \text{INDEX}} \cdot \text{psi}$	$E_c = 3.605 \times 10^3 \cdot \text{ksi}$
Poisson's ratio	$\nu := \text{INPUTS}_{25, \text{INDEX}}$	$\nu = 0.17$
Shear modulus of concrete	$G_c := \text{INPUTS}_{26, \text{INDEX}} \cdot \text{psi}$	$G_c = 1.541 \times 10^3 \cdot \text{ksi}$
Shear modification factor Table 2.4 of [O-4]	$\alpha := \text{INPUTS}_{27, \text{INDEX}}$	$\alpha = 1.185$
Torsional Constant Table 2.5 of [O-5]	$J := \text{INPUTS}_{28, \text{INDEX}} \cdot \text{in}^4$	$J = 1.121 \times 10^4 \cdot \text{in}^4$

Crack section index

crack := INPUTS_{140, INDEX}

crack = "yes"

Locate the longitudinal bars in the wall

bars := augment(submatrix(INPUTS, 40, 59, INDEX, INDEX), submatrix(INPUTS, 60, 79, INDEX, INDEX))·in

Area of bars

a_{bar} := submatrix(INPUTS, 80, 99, INDEX, INDEX)·in²

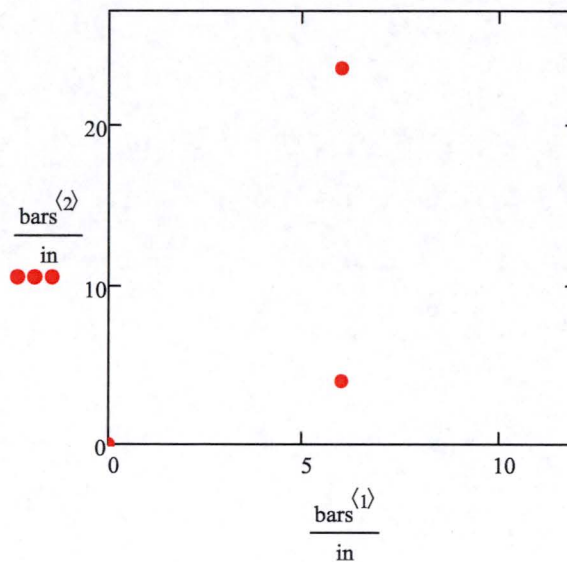
Diameter of bars

d_{bar} := submatrix(INPUTS, 100, 119, INDEX, INDEX)·in

index of bars

b := 1..20

Reinforcement Location



END OF INPUT

SECTION PROPERTIES

Elastic properties of uncracked cross section

$$I_{g1} := \frac{1}{12} \cdot b_{col} \cdot h_{col}^3$$

$$I_{g1} = 1.968 \times 10^4 \cdot \text{in}^4$$

$$I_{g2} := \frac{1}{12} \cdot h_{col} \cdot b_{col}^3$$

$$I_{g2} = 3.888 \times 10^3 \cdot \text{in}^4$$

$$A_v := b_{col} \cdot h_{col}$$

$$A_v = 2.25 \text{ ft}^2$$

Transverse Shear Stiffness

$$K_v := \frac{G_c \cdot A_v}{\alpha}$$

$$K_v = 4.211 \times 10^8 \cdot \text{lb} \cdot \text{f}$$

Flexural Stiffness

$$EI_2 := E_c \cdot I_{g2}$$

$$EI_2 = 1.402 \times 10^{10} \cdot \text{lb} \cdot \text{f} \cdot \text{in}^2$$

Axial Stiffness

$$EA := E_c \cdot A_g$$

$$EA = 1.168 \times 10^9 \cdot \text{lb} \cdot \text{f}$$

Torsional Stiffness

$$GJ := G_c \cdot J$$

$$GJ = 1.727 \times 10^{10} \cdot \text{lb} \cdot \text{f} \cdot \text{in}^2$$

CONCRETE MODEL

Peak strain of unconfined concrete
in compression assumed to be
0.002 [O-5]

$$\epsilon_{co} := 0.002$$

$$\epsilon_{co} = 2 \times 10^{-3}$$

From Table 1 of Karthik and Mander [O-2]

Ultimate strain of
unconfined concrete in
compression

$$\epsilon_{c1} := 0.0036$$

Failure strain of unconfined
concrete in compression

$$\epsilon_{sp} := 0.012 - 7 \cdot 10^{-7} \cdot \frac{f_c}{\text{psi}}$$

$$\epsilon_{sp} = 9.2 \times 10^{-3}$$

Peak strain of concrete in
tension

$$\epsilon_{to} := -0.1 \cdot \epsilon_{co}$$

$$\epsilon_{to} = -2 \times 10^{-4}$$

Concrete tensile strength

$$f_t := 7.5 \cdot \sqrt{\frac{f_c}{\text{psi}}}$$

$$f_t = 474.342 \text{ psi}$$

Use Cornelissen, Hordijk and Reinhardt (1986) to determine ultimate tension strain [O-6]

[O-6] Fig 6

$$\delta_o := 160 \mu\text{m}$$

[O-6] Eq 1

$$\sigma t(\delta) := \left[1 + \left(\frac{3 \cdot \delta}{\delta_o} \right)^3 \right] \cdot e^{-6.93 \cdot \frac{\delta}{\delta_o}}$$

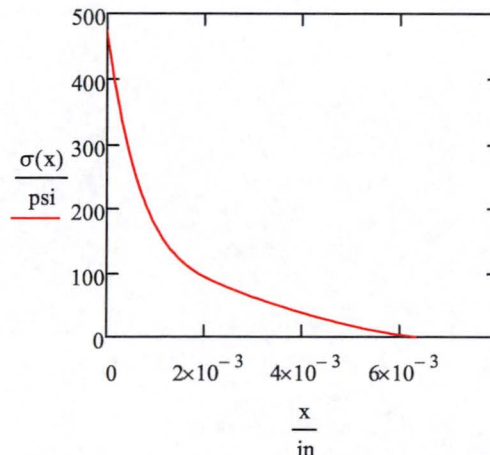
$$\sigma(\delta) := f_t \cdot \left[\sigma t(\delta) - \frac{\delta}{\delta_o} \cdot \sigma t(\delta_o) \right]$$

$$\epsilon_{cr} := \frac{f_t}{E_c}$$

$$\epsilon_{cr} = 1.316 \times 10^{-4}$$

$$x := 0 \mu\text{m}, 1 \mu\text{m}.. 160 \mu\text{m}$$

Tension Stress-Strain Curve



Fracture energy

$$g_f := \int_0^{\delta_o} \sigma(x) dx$$

$$g_f = 0.582 \cdot \frac{\text{lbf}}{\text{in}}$$

From Table 1 of Karthik and Mander [O-2]:

Failure strain of
concrete in tension

$$\epsilon_u := \frac{-18}{\text{in}} \cdot \frac{g_f}{5 \cdot f_t}$$

$$\epsilon_u = -4.415 \times 10^{-3}$$

Ultimate strain of
concrete in tension

$$\epsilon_{t1} := \frac{2 \cdot \epsilon_u}{9}$$

$$\epsilon_{t1} = -9.812 \times 10^{-4}$$

Ultimate stress of concrete in tension

$$f_{t1} := \frac{f_t}{3}$$

$$f_{t1} = 158.114 \cdot \text{psi}$$

Tension stress-strain curve, [O-2] Eq 1, 2 & 3

$$f_{ct}(\epsilon_c) := -1 \cdot \begin{cases} f_t \cdot \left[1 - \left(\left| 1 - \frac{\epsilon_c}{\epsilon_{to}} \right| \right)^{\frac{E_c \cdot \epsilon_{to}}{-f_t}} \right] & \text{if } \epsilon_{to} \leq \epsilon_c \leq 0 \\ f_t - \left(\frac{f_t - f_{t1}}{\frac{\epsilon_{t1}}{\epsilon_{to}} - 1} \right) \cdot \left(\frac{\epsilon_c}{\epsilon_{to}} - 1 \right) & \text{if } \epsilon_{t1} \leq \epsilon_c < \epsilon_{to} \\ f_{t1} \cdot \left(\frac{\epsilon_c - \epsilon_u}{\epsilon_{t1} - \epsilon_u} \right) & \text{if } \epsilon_u \leq \epsilon_c < \epsilon_{t1} \\ 0 & \text{if } \epsilon_c < \epsilon_u \end{cases}$$

[O-2] Table 1

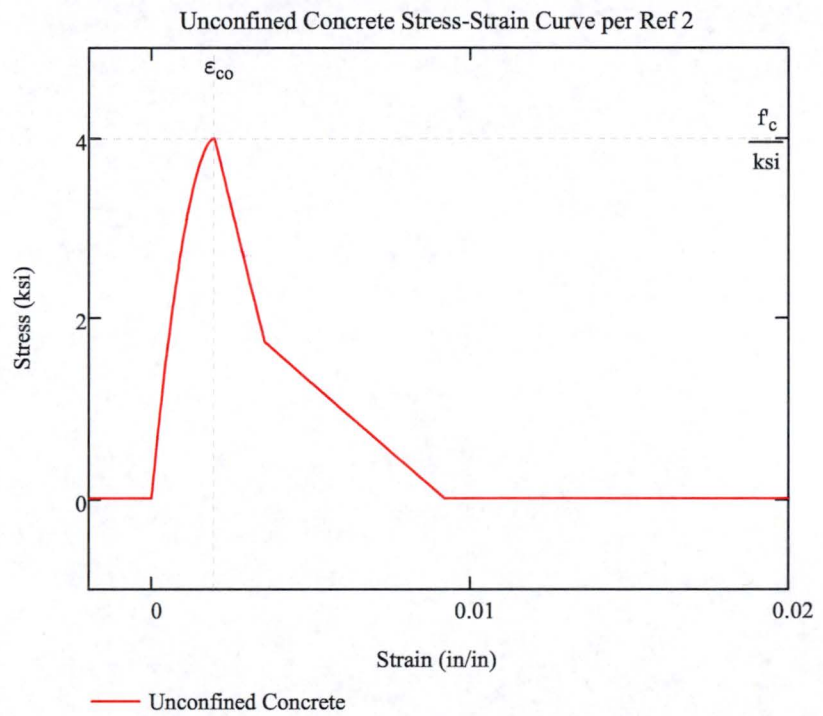
$$f_{c1} := 1.74 \text{ksi}$$

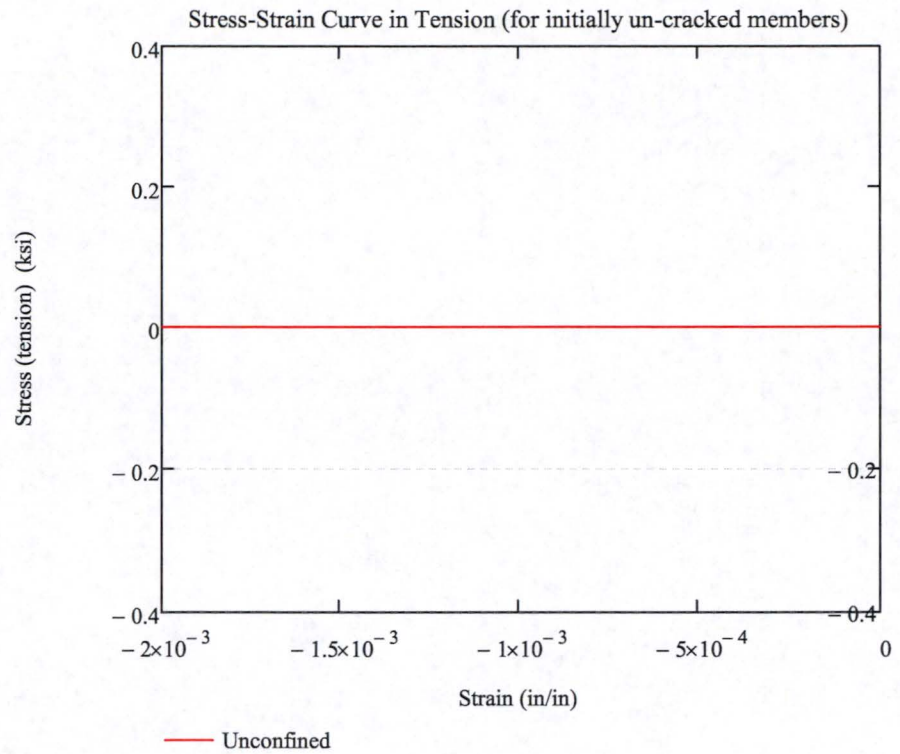
$$\text{mult_crack} := \begin{cases} 1 & \text{if crack} = \text{"no"} \\ 0 & \text{if crack} = \text{"yes"} \end{cases}$$

$$\text{mult_crack} = 0$$

Unconfined stress-strain curve [O-2] Eq 1, 2 & 3

$$f_c(\epsilon_c) := \begin{cases} f_{ct}(\epsilon_c) \cdot \text{mult_crack} & \text{if } \frac{\epsilon_c}{\epsilon_{co}} < 0 \\ f_c \cdot \left[1 - \left(\left| 1 - \frac{\epsilon_c}{\epsilon_{co}} \right| \right)^{\frac{E_c \cdot \epsilon_{co}}{f_c}} \right] & \text{if } 0 \leq \frac{\epsilon_c}{\epsilon_{co}} < 1 \\ f_c - \left(\frac{f_c - f_{cl}}{\frac{\epsilon_{cl}}{\epsilon_{co}} - 1} \right) \cdot \left(\frac{\epsilon_c}{\epsilon_{co}} - 1 \right) & \text{if } 1 \leq \frac{\epsilon_c}{\epsilon_{co}} < \frac{\epsilon_{cl}}{\epsilon_{co}} \\ f_{cl} \cdot \left(\frac{\frac{\epsilon_c}{\epsilon_{co}} - \frac{\epsilon_{sp}}{\epsilon_{co}}}{\frac{\epsilon_{cl}}{\epsilon_{co}} - \frac{\epsilon_{sp}}{\epsilon_{co}}} \right) & \text{if } \frac{\epsilon_{cl}}{\epsilon_{co}} \leq \frac{\epsilon_c}{\epsilon_{co}} < \frac{\epsilon_{sp}}{\epsilon_{co}} \\ 0 & \text{if } \frac{\epsilon_{sp}}{\epsilon_{co}} \leq \frac{\epsilon_c}{\epsilon_{co}} \end{cases}$$





Modified confinement per Roy and Sozen [O-7] Eq 5.3

$$\epsilon_{50u} := \frac{3\text{psi} + 0.002 \cdot f_c}{f_c - 1000\text{psi}} \quad \epsilon_{50u} = 3.667 \times 10^{-3}$$

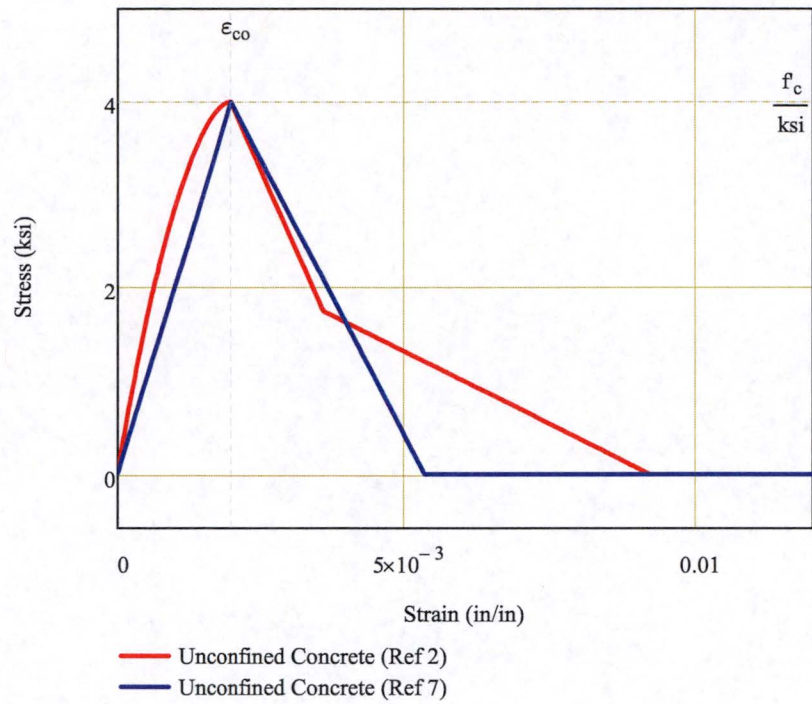
[O-7]

$$m_{\text{RoySozen}} := \frac{-0.5 \cdot f_c}{\epsilon_{50u} - 0.002} \quad m_{\text{RoySozen}} = -1.2 \times 10^3 \cdot \text{ksi}$$

$$b_{\text{RoySozen}} := 0.002 \cdot (-m_{\text{RoySozen}}) + (f_c) \quad b_{\text{RoySozen}} = 6.4 \cdot \text{ksi}$$

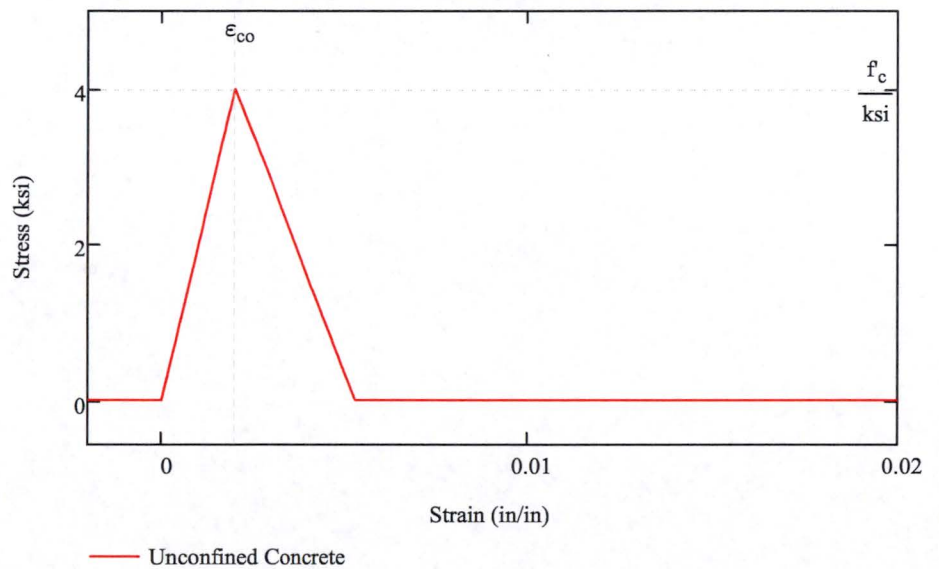
$$f_c_{\text{RoySozen}}(\epsilon_c) := \begin{cases} f_c(\epsilon_c) \cdot \text{mult_crack} & \text{if } \epsilon_c < 0 \\ \frac{f_c}{0.002} \cdot \epsilon_c & \text{if } 0 \leq \epsilon_c < 0.002 \\ \max(0, m_{\text{RoySozen}} \cdot \epsilon_c + b_{\text{RoySozen}}) & \text{if } 0.002 \leq \epsilon_c \end{cases}$$

Comparison of Mander (Ref 2) and Sezen (Ref 7) Concrete Models



$$f_c(\epsilon_c) := \begin{cases} f_{c_RoySozen}(\epsilon_c) & \text{if } INPUTS_{34, INDEX} = "RoySozen" \\ f_c(\epsilon_c) & \text{otherwise} \end{cases}$$

Concrete Model Used for Evaluation



REBAR MODEL

Stress - Strain curve of rebar

[O-2] Eq 5

$$P := \begin{cases} 1 & \text{if } f_{su} = f_y \\ \frac{E_{sh} \cdot (\epsilon_{su} - \epsilon_{sh})}{f_{su} - f_y} & \text{otherwise} \end{cases} \quad P = 2.397$$

[O-2] Eq 4.

$$f_{s_t}(\epsilon_s) := \left[\frac{E_s \cdot |\epsilon_s|}{\left[1 + \left(\left| \frac{E_s \cdot |\epsilon_s|}{f_y} \right| \right)^{20} \right]^{0.05}} + (f_{su} - f_y) \cdot \left[1 - \frac{(|\epsilon_{su} - |\epsilon_s||)^P}{\left[(|\epsilon_{su} - \epsilon_{sh}|)^{20 \cdot P} + (|\epsilon_{su} - |\epsilon_s||)^{20 \cdot P} \right]^{0.05}} \right] \right]$$

Based on the recommendation of Sezen and Setzler ([O-8], and [O-3]), the steel stress strain curve is modified slightly to make sure the plateau region as a slight positive slope

Slope of strain hardening

$$\alpha_s := 0.02$$

Adjust f_y such that area under the plateau stays the same

Steel yield strength

$$f_y = 60 \cdot \text{ksi}$$

Modified yield strength

$$f_{y'} := f_y - \frac{E_s \cdot \alpha_s \cdot \epsilon_{sh}}{2} \quad f_{y'} = 57.68 \cdot \text{ksi}$$

Yield strain

$$\epsilon_y := \frac{f_{y'}}{E_s} \quad \epsilon_y = 1.989 \times 10^{-3}$$

[O-3] strain at strain hardening

$$\epsilon_{sh} = 8 \times 10^{-3}$$

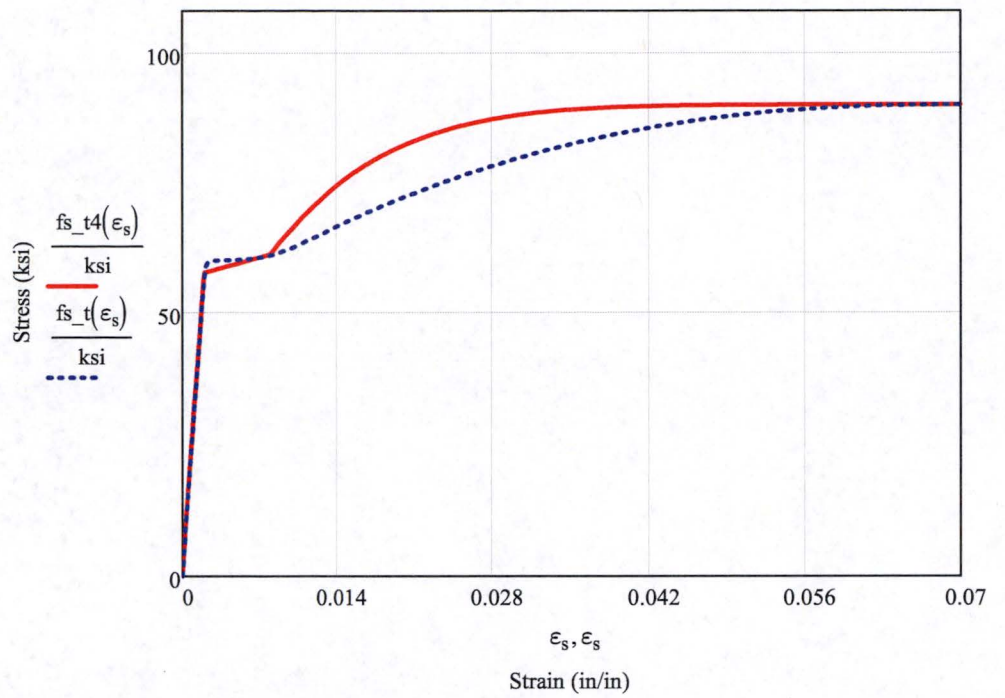
Steel material model [O-3] Eq 3.3

$$\epsilon_{cross} := \frac{f_y - f_{y'}}{\alpha_s \cdot E_s} + \epsilon_y = 5.989 \times 10^{-3}$$

$$f_{sh} := \begin{cases} f_{y'} + (\epsilon_{sh} - \epsilon_y) \cdot \alpha_s \cdot E_s & \text{if } P \neq 1 \\ \left[f_{y'} + (\epsilon_{cross} - \epsilon_y) \cdot \alpha_s \cdot E_s \right] & \text{otherwise} \end{cases} \quad f_{sh} = 61.166 \cdot \text{ksi}$$

Steel curve from Setzler thesis ([O-3]) (with correction per sezen for plateau region)

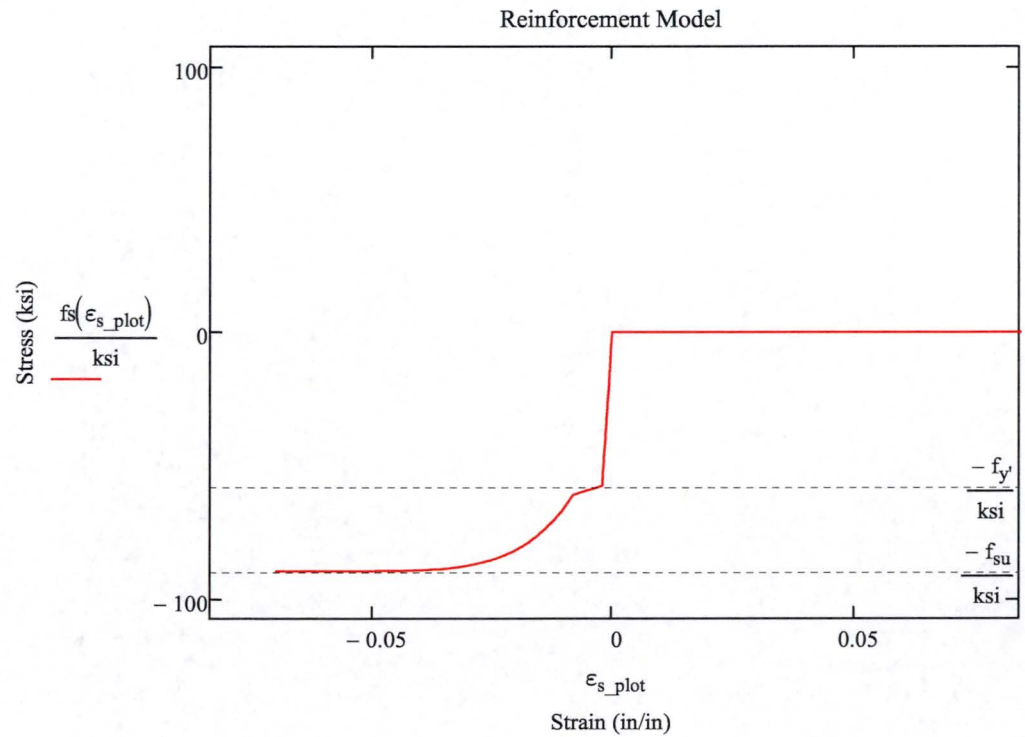
$$f_{s_t4}(\epsilon_s) := \begin{cases} \text{if } P \neq 1 \\ \begin{cases} E_s \cdot \epsilon_s & \text{if } \epsilon_s \leq \epsilon_y \\ f_{y'} + (\epsilon_s - \epsilon_y) \cdot \alpha_s \cdot E_s & \text{if } \epsilon_y < \epsilon_s \leq \epsilon_{sh} \\ f_{su} - (f_{su} - f_{sh}) \cdot \left(\frac{\epsilon_s - \epsilon_{sh}}{\epsilon_{su} - \epsilon_{sh}} \right)^6 & \text{if } \epsilon_{sh} < \epsilon_s \leq \epsilon_{su} \end{cases} \\ \text{otherwise} \\ \begin{cases} E_s \cdot \epsilon_s & \text{if } \epsilon_s \leq \epsilon_y \\ f_{y'} + (\epsilon_s - \epsilon_y) \cdot \alpha_s \cdot E_s & \text{if } \epsilon_y < \epsilon_s \leq \epsilon_{cross} \\ f_{su} - (f_{su} - f_{sh}) \cdot \left(\frac{\epsilon_s - \epsilon_{su}}{\epsilon_{su} - \epsilon_{sh}} \right)^6 & \text{if } \epsilon_{cross} < \epsilon_s \leq \epsilon_{su} \end{cases} \end{cases}$$



Combined tension and
compression behavior

$$f_s(\epsilon_s) := \begin{cases} -f_{s_t4}(|\epsilon_s|) & \text{if } \epsilon_s \leq 0 \\ 0 & \text{otherwise} \end{cases}$$

$$\epsilon_{s_plot} := -0.2, -0.1999 \dots 0.2$$



DUCTILITY CALCULATION

Section inertia of uncracked cross section

$$I_g := \frac{1}{12} \cdot b_{col} \cdot h_{col}^3 + \frac{E_s}{E_c} \cdot \sum_b \left[a_{bar_b} \cdot \left(bars_{b,2} - \frac{h_{col}}{2} \right)^2 \right] \quad I_g = 2.163 \times 10^4 \cdot \text{in}^4$$

Concrete stress at a location (x) given a curvature, and neutral axis

$$\sigma_{conc}(\phi, x, NA) := fc[\phi \cdot (x - NA)]$$

Steel stress in a bar (b) given a curvature and neutral axis

$$\sigma_{steel}(\phi, b, NA) := fs[\phi \cdot (bars_{b,2} - NA)]$$

Given

Integration across the section to combine concrete and steel stresses must equal the applied vertical load independent of the curvature. (integrate by parts to help convergence)

$$\int_0^{h_{col}} b_{col} \cdot \sigma_{conc}(\phi, x, na_{test}) dx \dots = F_v \\ + \sum_b \left(\sigma_{steel}(\phi, b, na_{test}) \cdot a_{bar_b} \right)$$

Function to execute the solve block and find the neutral axis location as a function of curvature.

$$na(\phi, F_v, na_{test}) := \text{Find}(na_{test})$$

$$F_{v_plot} := 0 \text{ kip}$$

$$\phi_{plot} := 3 \cdot 10^{-4} \cdot \frac{1}{\text{in}}$$

$$na(\phi_{plot}, F_{v_plot}, 0.8 \cdot h_{col}) = 22.409 \cdot \text{in}$$

$$h_{centroid} := \frac{h_{col}}{2}$$

$$h_{centroid} = 13.5 \cdot \text{in}$$

Function to solve for the moment about the centroid for a given curvature

$$\text{mom}(\phi, NA, F_v) := \int_0^{h_{col}} b_{col} \cdot \sigma_{conc}(\phi, x, NA) \cdot (x - h_{centroid}) dx \dots \\ + \sum_b \left[\sigma_{steel}(\phi, b, NA) \cdot a_{bar_b} \cdot (bars_{b,2} - h_{centroid}) \right]$$

$$\text{mom}(\phi_{plot}, na(\phi_{plot}, F_{v_plot}, 0.8h_{col}), F_{v_plot}) = 1.633 \times 10^3 \cdot \text{kip} \cdot \text{in}$$

$$\text{mom}(-\phi_{plot}, na(-\phi_{plot}, F_{v_plot}, 0.2h_{col}), F_{v_plot}) = -1.666 \times 10^3 \cdot \text{kip} \cdot \text{in}$$

Function to check the resulting axial force

$$\text{chk}(\phi, \text{NA}) := \int_0^{h_{\text{col}}} b_{\text{col}} \cdot \sigma_{\text{conc}}(\phi, x, \text{NA}) dx \dots$$

$$+ \sum_b \left(\sigma_{\text{steel}}(\phi, b, \text{NA}) \cdot a_{\text{bar}_b} \right)$$

$$F_{v_plot} = 0 \cdot \text{kip}$$

$$\text{chk}(\phi_{\text{plot}}, \text{na}(\phi_{\text{plot}}, F_{v_plot}, 0.8h_{\text{col}})) = -5.234 \times 10^{-14} \cdot \text{kip}$$

$$\text{max_bar} := \text{INPUTS}_{36, \text{INDEX}} \quad \text{max_bar} = 2$$

$$\text{min_bar} := \text{INPUTS}_{37, \text{INDEX}} \quad \text{min_bar} = 1$$

To this point, compression is positive and tension is negative, for computing steel strain and stress, use tension as positive values.

$$\text{steel_strain}(\phi, \text{NA}) := -1 \cdot \begin{cases} \phi \cdot (\text{bars}_{\text{min_bar}, 2} - \text{NA}) & \text{if } \phi \geq 0 \\ \phi \cdot (\text{bars}_{\text{max_bar}, 2} - \text{NA}) & \text{if } \phi < 0 \end{cases}$$

$$\text{steel_stress}(\phi, \text{NA}) := -1 \cdot \begin{cases} \sigma_{\text{steel}}(\phi, \text{min_bar}, \text{NA}) & \text{if } \phi \geq 0 \\ \sigma_{\text{steel}}(\phi, \text{max_bar}, \text{NA}) & \text{if } \phi < 0 \end{cases}$$

$$\text{depth_bar}(\phi) := \begin{cases} \text{bars}_{\text{min_bar}, 2} & \text{if } \phi \geq 0 \\ \text{bars}_{\text{max_bar}, 2} & \text{if } \phi < 0 \end{cases}$$

$$d_b(\phi) := \begin{cases} d_{\text{bar}_{\text{min_bar}}} & \text{if } \phi \geq 0 \\ d_{\text{bar}_{\text{max_bar}}} & \text{if } \phi < 0 \end{cases} \quad d_b(\phi_{\text{plot}}) = 1.27 \cdot \text{in}$$

$$\text{steel_strain}(\phi_{\text{plot}}, \text{na}(\phi_{\text{plot}}, F_{v_plot}, 0.8 \cdot h_{\text{col}})) = 5.538 \times 10^{-3}$$

$$\text{steel_stress}(\phi_{\text{plot}}, \text{na}(\phi_{\text{plot}}, F_{v_plot}, 0.8 \cdot h_{\text{col}})) = 59.738 \cdot \text{ksi}$$

$$\text{fname} := \text{INPUTS}_{124, \text{INDEX}} \quad \text{fname} = "001_Wall_uncracked_file1.txt"$$

Compute moment-curvature curves at various axial load, and curvatures. This requires the following programming loop, which writes results to a text file which is then read back in by this calculation.

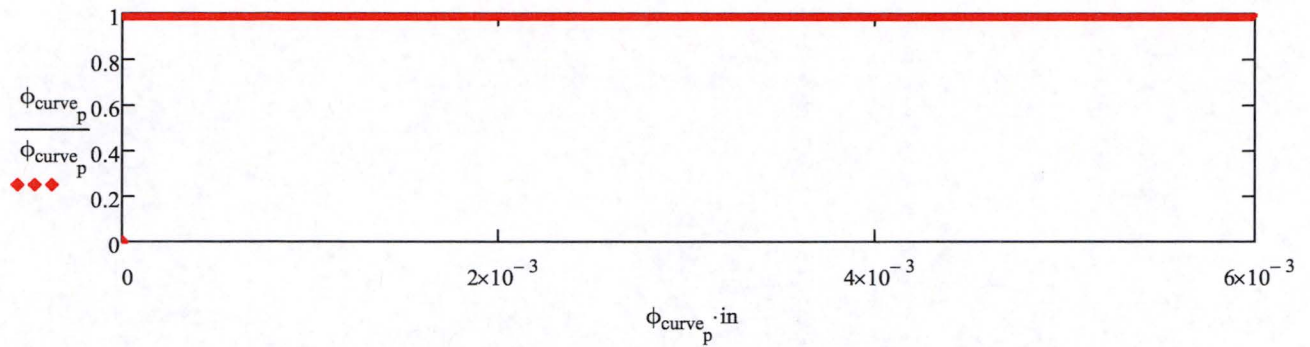
Index of curvatures

$$\text{numinc} := \text{INPUTS}_{139, \text{INDEX}}$$

$$p := 1 \dots \text{numinc}$$

$$\phi_{\text{int}} := \text{INPUTS}_{138, \text{INDEX}} \cdot \frac{1}{\text{in}} \quad \phi_{\text{int}} = 1 \times 10^{-5} \cdot \frac{1}{\text{in}}$$

$$\phi_{\text{curve}_p} := (p - 1) \cdot \phi_{\text{int}}$$



```
fv := submatrix(INPUTS,126,137,INDEX,INDEX)
```

```
fv := | new ← fv1
      | for j ∈ 2..rows(fv)
      |   new ← new if IsString(fvj)
      |   new ← stack(new, fvj) otherwise
      | return new.lbf
```

	1
1	907.2
2	793.8
3	680.4
4	567
5	453.6
fv = 6	340.2 ·kip
7	226.8
8	113.4
9	0
10	-43.2
11	-86.4
12	-129.6

```
f := 1..rows(fv)
```

Output _{1,1} := "Curvature (1/in)"	Output _{1,5} := "Concrete Strain"	Output _{1,9} := "Slip Rotation (rad)"
Output _{1,2} := "Moment (lbf*in)"	Output _{1,6} := "Concrete Strain"	Output _{1,10} := "Slip (in)"
Output _{1,3} := "Axial Load (lbf)"	Output _{1,7} := "Steel Strain"	Output _{1,11} := ""
Output _{1,4} := "neutral axis (in)"	Output _{1,8} := "Steel Strain"	Output _{1,12} := "LINE"

```
fname = "001_Wall_uncracked_file1.txt"
```

```
exist := "no" on error READPRN(fname)
```

zero(x,y) := 0

out := if exist = "no"

```

APPENDPRN[fname,(OutputT)<1>T]
for f ∈ 1..rows(fv)
  na_last ← ""
  continue ← "yes"
  errorcount ← 0
  for p ∈ 1..numinc
    if continue = "yes"
      M1 ← ϕcurvep·in
      m0 ← [0 on error (mom(ϕcurvep,na(ϕcurvep,fvf,na_last),fvf))]
      mout ← m0
      NA ← (0 on error na(ϕcurvep,fvf,na_last))
      if (m0 = 0 ∨ sign(m0) ≠ sign(ϕcurvep))
        m1 ← [0 on error (mom(ϕcurvep,na(ϕcurvep,fvf,0in),fvf))]
        m2 ← [0 on error (mom(ϕcurvep,na(ϕcurvep,fvf,sign(ϕcurvep)·0.5hcol),fvf))]
        m3 ← [0 on error (mom(ϕcurvep,na(ϕcurvep,fvf,sign(ϕcurvep)·0.9hcol),fvf))]
        if |m1| > max(|m2|,|m3|)
          NA ← (0 on error na(ϕcurvep,fvf,0in))
          mout ← m1
        if |m2| ≥ max(|m1|,|m3|)
          NA ← (0 on error na(ϕcurvep,fvf,sign(ϕcurvep)·0.5hcol))
          mout ← m2
        if |m3| ≥ max(|m1|,|m2|)
          NA ← (0 on error na(ϕcurvep,fvf,sign(ϕcurvep)·0.9hcol))
          mout ← m3
      M2 ←  $\frac{mout}{lbf \cdot in}$ 
      M3 ←  $\frac{fv_f}{lbf}$ 
      M4 ←  $\frac{NA}{in}$ 
      na_last ← NA
      M5 ← ϕcurvep·(0in - NA)
      M6 ← ϕcurvep·(hcol - NA)
      M7 ← ϕcurvep·(barsmin_bar,2 - NA)

```

```

M8 ←  $\phi_{\text{curve}_p} \cdot (\text{bars}_{\text{max\_bar}, 2} - \text{NA})$ 
M9 ← 0
M10 ← 0
M11 ← 0
M12 ← "LINE"
errorcount ← errorcount + 1 if (NA = 0) ∨ (sign(mout) ≠ sign( $\phi_{\text{curve}_p}$ )) ∨ (M6 > 0.010)
errorcount ← 0 otherwise
APPENDPRN(fname, MT)
M ← matrix(12, 1, zero)
continue ← "no" if errorcount > 3
"nothing" otherwise

```

```

data := READPRN(fname) if exist = "no"
        exist otherwise

```

	1	2	3
1	"Curvature (1/in)"	"Moment (lbf*in)"	"Axial Load (lbf)"
2	0	0	9.072·10 ⁵
3	1·10 ⁻⁵	3.937·10 ⁵	9.072·10 ⁵
4	2·10 ⁻⁵	7.873·10 ⁵	9.072·10 ⁵
5	3·10 ⁻⁵	1.181·10 ⁶	9.072·10 ⁵
6	4·10 ⁻⁵	1.575·10 ⁶	9.072·10 ⁵
7	5·10 ⁻⁵	1.937·10 ⁶	9.072·10 ⁵
8	6·10 ⁻⁵	2.141·10 ⁶	9.072·10 ⁵
9	7·10 ⁻⁵	2.2·10 ⁶	9.072·10 ⁵
10	8·10 ⁻⁵	2.13·10 ⁶	9.072·10 ⁵
11	9·10 ⁻⁵	1.927·10 ⁶	9.072·10 ⁵
12	1·10 ⁻⁴	1.567·10 ⁶	9.072·10 ⁵
13	1.1·10 ⁻⁴	9.671·10 ⁵	9.072·10 ⁵
14	1.2·10 ⁻⁴	0	9.072·10 ⁵
15	1.3·10 ⁻⁴	0	9.072·10 ⁵
16	1.4·10 ⁻⁴	0	...

```

data := d ← submatrix(data, 1, 1, 1, 12)
        for i ∈ 2..rows(data<1>)
            d ← d if (datai,2 ≤ 0 ∧ datai,1 ≠ 0)
            d ← stack(d, submatrix(data, i, i, 1, 12)) otherwise
        return d

```


cleandata := APPENDPRN(concat("clean_",fname),data)

cleandata =

	1	2	3
1	"Curvature (1/in)"	"Moment (lbf*in)"	"Axial Load (lbf)"
2	0	0	9.072·10 ⁵
3	1·10 ⁻⁵	3.937·10 ⁵	9.072·10 ⁵
4	2·10 ⁻⁵	7.873·10 ⁵	9.072·10 ⁵
5	3·10 ⁻⁵	1.181·10 ⁶	9.072·10 ⁵
6	4·10 ⁻⁵	1.575·10 ⁶	9.072·10 ⁵
7	5·10 ⁻⁵	1.937·10 ⁶	9.072·10 ⁵
8	6·10 ⁻⁵	2.141·10 ⁶	9.072·10 ⁵
9	7·10 ⁻⁵	2.2·10 ⁶	9.072·10 ⁵
10	8·10 ⁻⁵	2.13·10 ⁶	9.072·10 ⁵
11	9·10 ⁻⁵	1.927·10 ⁶	9.072·10 ⁵
12	1·10 ⁻⁴	1.567·10 ⁶	9.072·10 ⁵
13	1.1·10 ⁻⁴	9.671·10 ⁵	9.072·10 ⁵
14	0	0	7.938·10 ⁵
15	1·10 ⁻⁵	3.937·10 ⁵	7.938·10 ⁵
16	2·10 ⁻⁵	7.873·10 ⁵	7.938·10 ⁵
17	3·10 ⁻⁵	1.181·10 ⁶	7.938·10 ⁵
18	4·10 ⁻⁵	1.575·10 ⁶	7.938·10 ⁵
19	5·10 ⁻⁵	1.968·10 ⁶	7.938·10 ⁵
20	6·10 ⁻⁵	2.357·10 ⁶	7.938·10 ⁵
21	7·10 ⁻⁵	2.638·10 ⁶	7.938·10 ⁵
22	8·10 ⁻⁵	2.794·10 ⁶	7.938·10 ⁵
23	9·10 ⁻⁵	2.842·10 ⁶	7.938·10 ⁵
24	1·10 ⁻⁴	2.79·10 ⁶	7.938·10 ⁵
25	1.1·10 ⁻⁴	2.638·10 ⁶	7.938·10 ⁵
26	1.2·10 ⁻⁴	2.377·10 ⁶	7.938·10 ⁵
27	1.3·10 ⁻⁴	1.986·10 ⁶	7.938·10 ⁵
28	1.4·10 ⁻⁴	1.406·10 ⁶	7.938·10 ⁵
29	1.5·10 ⁻⁴	3.969·10 ⁵	7.938·10 ⁵
30	0	0	6.804·10 ⁵
31	1·10 ⁻⁵	3.937·10 ⁵	6.804·10 ⁵
32	2·10 ⁻⁵	7.873·10 ⁵	6.804·10 ⁵
33	3·10 ⁻⁵	1.181·10 ⁶	6.804·10 ⁵
34	4·10 ⁻⁵	1.575·10 ⁶	6.804·10 ⁵
35	5·10 ⁻⁵	1.968·10 ⁶	6.804·10 ⁵
36	6·10 ⁻⁵	2.362·10 ⁶	6.804·10 ⁵
37	7·10 ⁻⁵	2.756·10 ⁶	...

Strain limit

strain_lim := 0.005

lim = 5×10^{-3}

```

Column(d,i,strain_lim) :=
  account ← 1
  datas_account,1 ← 2
  for r ∈ 3..rows(d)
    if dr,3 ≠ dr-1,3
      datas_account,2 ← r - 1
      account ← account + 1
      datas_account,1 ← r
  datas_account,2 ← rows(d)
  sub ← submatrix(d,1,1,1,cols(d))
  out ← submatrix(d,datas_account,1,datas_account,2,1,cols(d))
  for j ∈ 1..rows(out)
    if [(outj,2 ≠ 0 ∧ sign(outj,2) = sign(outj,1)) ∨ outj,1 = 0]
      p2 ← submatrix(out,j,j,1,cols(d))
      sub ← stack(sub,p2)
    sub ← sub otherwise
  cutoff2 ← 0
  for i ∈ 2..rows(sub)
    cutoff2 ← i - 1 if (subi,6 > strain_lim) ∧ (cutoff2 = 0)
  cutoff2 ← rows(sub) if cutoff2 = 0
  cutoff1 ← 2
  cutoff1 ← 2 if sub2,1 = 0
  otherwise
    i ← 2
    while subi,5 > strain_lim
      cutoff1 ← i + 1
      i ← i + 1
  return stack(submatrix(sub,1,1,1,cols(sub)),submatrix(sub,cutoff1,cutoff2,1,cols(sub)))

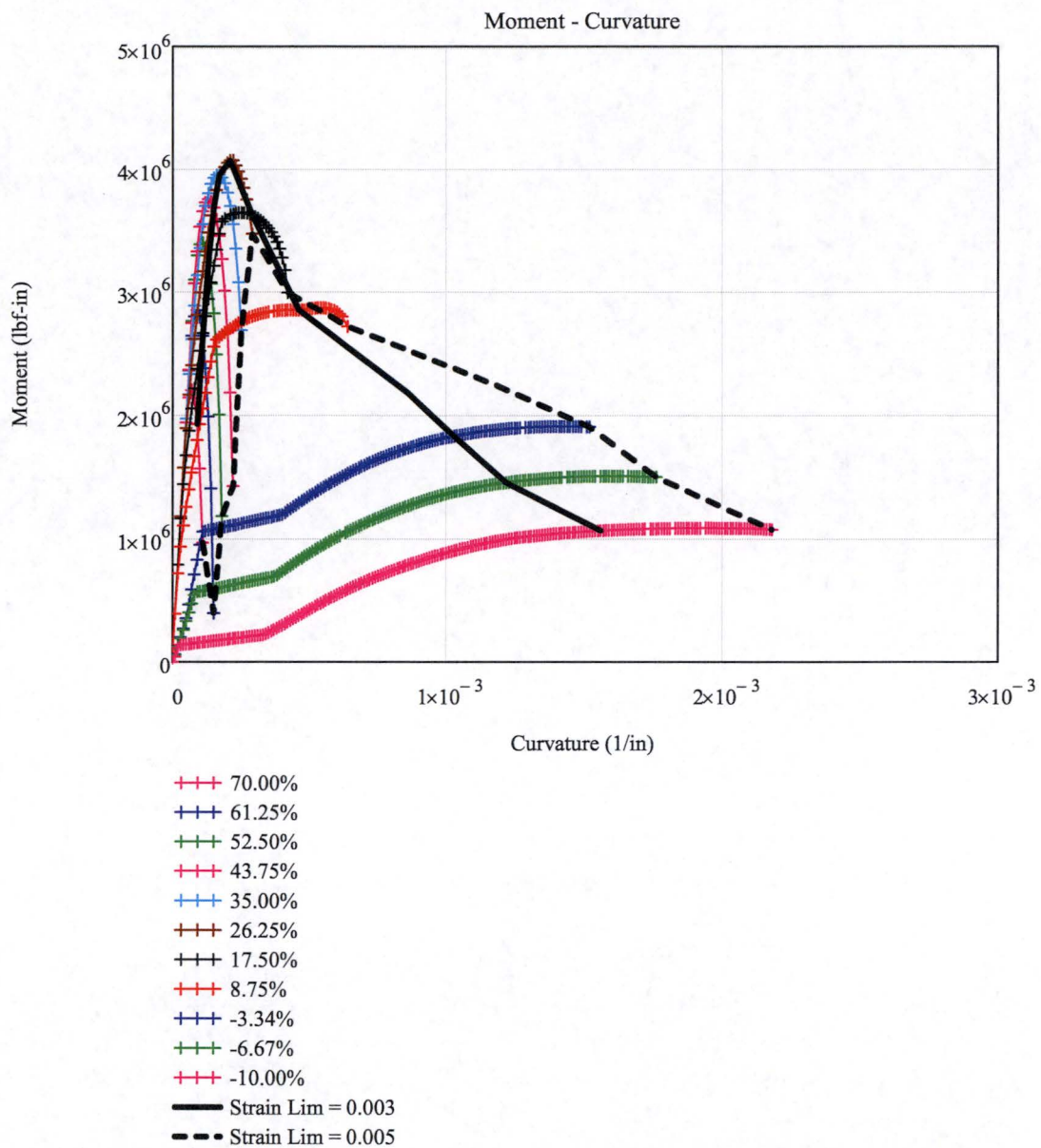
StrainLim(limit) :=
  StrainLim ← ("curvature" "moment" "Slip Rotation" "P/Ag*fc")
  for f ∈ 1..rows(fv)
    StrainLimf+1,1 ← Column(data,f,limit)rows(Column(data,f,limit)(1),1
    StrainLimf+1,2 ← Column(data,f,limit)rows(Column(data,f,limit)(1),2
    StrainLimf+1,3 ← Column(data,f,limit)rows(Column(data,f,limit)(1),9
    StrainLimf+1,4 ←  $\frac{fv_f}{A_g \cdot f_c}$ 
  return StrainLim

```

Moment - Curvature curves for different axial forces

```

plt := 1..12
plot_index_plt := | plt if plt ≤ rows(fv)
                  | 1 otherwise
    
```



Moment demand

$$\text{Moment_Sec} := 169.54 \frac{\text{kip} \cdot \text{ft}}{\text{ft}}$$

$$\text{Moment_Sec} = 169540 \cdot \frac{\text{lbf} \cdot \text{in}}{\text{in}}$$

$$\text{Moment} := \text{Moment_Sec} \cdot b_{\text{col}}$$

$$\text{Moment} = 2.034 \times 10^6 \cdot \text{lbf} \cdot \text{in}$$

Axial load demand

$$\text{Axial} := -30.93 \frac{\text{kip}}{\text{ft}}$$

$$\text{Axial} = -2.578 \times 10^3 \cdot \frac{\text{lbf}}{\text{in}}$$

Total axial load

$$\text{Axial_Sec} := \text{Axial} \cdot b_{\text{col}}$$

$$\text{Axial_Sec} = -30930 \text{ lbf}$$

Maximum axial load

$$\text{Max_axial} := A_g \cdot (f'_c)$$

$$\text{Max_axial} = 1296000 \text{ lbf}$$

Calculated percent tension or compression of $A_g \cdot f'_c$

$$\text{Percent} := \frac{\text{Axial_Sec}}{\text{Max_axial}}$$

$$\text{Percent} = -0.024$$

Percent compression or tension See below for options, tension is negative

$$\text{Axial_p} := -3.34$$

Stress level

$$\text{ap} := \begin{cases} 1 & \text{if } \text{Axial_p} = 70 \\ 2 & \text{if } \text{Axial_p} = 61.25 \\ 3 & \text{if } \text{Axial_p} = 52.50 \\ 4 & \text{if } \text{Axial_p} = 43.75 \\ 5 & \text{if } \text{Axial_p} = 35.00 \\ 6 & \text{if } \text{Axial_p} = 26.25 \\ 7 & \text{if } \text{Axial_p} = 17.50 \\ 8 & \text{if } \text{Axial_p} = 8.75 \\ 10 & \text{if } \text{Axial_p} = -3.34 \\ 11 & \text{if } \text{Axial_p} = -6.67 \\ 12 & \text{if } \text{Axial_p} = -10 \end{cases}$$

$$\text{ap} = 10$$

Slope of linear moment curvature plot

$$m_{ap} := \frac{\left[\left(\text{Column}(\text{data}, \text{plot_index}_{ap}, \text{lim})^{(2)} \right)_4 - \left(\text{Column}(\text{data}, \text{plot_index}_{ap}, \text{lim})^{(2)} \right)_2 \right]}{\left[\left(\text{Column}(\text{data}, \text{plot_index}_{ap}, \text{lim})^{(1)} \right)_4 - \left(\text{Column}(\text{data}, \text{plot_index}_{ap}, \text{lim})^{(1)} \right)_2 \right]}$$

$$m_{ap} \cdot (\text{lbf} \cdot \text{in}^2) = 6.565 \times 10^9 \cdot \text{lbf} \cdot \text{in}^2$$

Linear curvature parameters

Linear strain energy

$$L_Area_{ap} := \frac{\text{Moment}^2}{\left(2 \cdot m_{ap} \cdot \text{lbf} \cdot \text{in}^2 \right)}$$

$$L_Area_{ap} = 315 \text{ lbf}$$

Linear curvature at moment

$$L_Cur_{ap} := \frac{\text{Moment}}{m_{ap} \cdot \text{lbf} \cdot \text{in}^2}$$

$$L_Cur_{ap} = 3.099 \times 10^{-4} \cdot \frac{1}{\text{in}}$$

Curvature points

$$w := \begin{pmatrix} 0 \\ L_Cur_{ap} \cdot \text{in} \end{pmatrix}$$

$$w = \begin{pmatrix} 0 \\ 3.099 \times 10^{-4} \end{pmatrix}$$

Moment points

$$L_Mom_p(w) := m_{ap} \cdot w$$

$$L_Mom_p(w) = \begin{pmatrix} 0 \\ 2.034 \times 10^6 \end{pmatrix}$$

Max number of trapezoids to add when calculating moment under non-linear moment curvature curve

$$c_{max} := 37$$

Variables to calculate area under moment-curvature plot that represent width (b) and heights (h) of trapezoids

Height (Moment) $h1_{ap} := \text{Column}(\text{data}, \text{plot_index}_{ap}, \text{lim})^{(2)}$

$$h2_{ap} := \text{Column}(\text{data}, \text{plot_index}_{ap}, \text{lim})^{(2)}$$

Width (Curvature) $b1_{ap} := \text{Column}(\text{data}, \text{plot_index}_{ap}, \text{lim})^{(1)}$

$$b2_{ap} := \text{Column}(\text{data}, \text{plot_index}_{ap}, \text{lim})^{(1)}$$

Area under moment-curvature plot, based on summing trapezoidal areas

$$NL_Area_{ap} := \sum_{k=3}^{c_{max}} \left[\frac{1}{2} \cdot \left[(h1_{ap})_k \cdot \text{lbf} \cdot \text{in} + (h2_{ap})_{k-1} \cdot \text{lbf} \cdot \text{in} \right] \cdot \left[(b1_{ap})_k \cdot \frac{1}{\text{in}} - (b2_{ap})_{k-1} \cdot \frac{1}{\text{in}} \right] \right]$$

$$NL_Area_{ap} = 318 \text{ lbf}$$

Non-linear Curvature

$$NL_Cur_{ap} := \left(\text{Column}(\text{data}, \text{plot_index}_{ap}, \text{lim})^{(1)} \right)_{c_{max}} \cdot \frac{1}{\text{in}}$$

$$NL_Cur_{ap} = 3.500 \times 10^{-4} \cdot \frac{1}{\text{in}}$$

Vary c.max to make close to zero

$$NL_Area_{ap} - L_Area_{ap} = 3.075 \text{ lbf}$$

Parameters for plotting purposes

$$y := \begin{bmatrix} 0 \\ \left(\text{Column}(\text{data}, \text{plot_index}_{ap}, \text{lim})^{(2)} \right)_{c_{max}} \end{bmatrix} \quad z := \begin{bmatrix} 0 \\ \text{Moment} \cdot \frac{1}{\text{lbf} \cdot \text{in}} \end{bmatrix}$$

$$\text{Lim_NL}(y) := \begin{bmatrix} NL_Cur_{ap} \cdot \text{in} \\ NL_Cur_{ap} \cdot \text{in} \end{bmatrix} \quad \text{Lim_L}(z) := \begin{bmatrix} L_Cur_{ap} \cdot \text{in} \\ L_Cur_{ap} \cdot \text{in} \end{bmatrix}$$

Depth to neutral axis

$$d_{NA} := na(NL_Cur_{ap}, fv_{ap}, 0.8h_{col})$$

$$d_{NA} = 23.925 \cdot \text{in}$$

Distance for strain in steel calculation $d_{\text{strain}} := d_{NA} - \text{cover}$

$$d_{\text{strain}} = 19.975 \cdot \text{in}$$

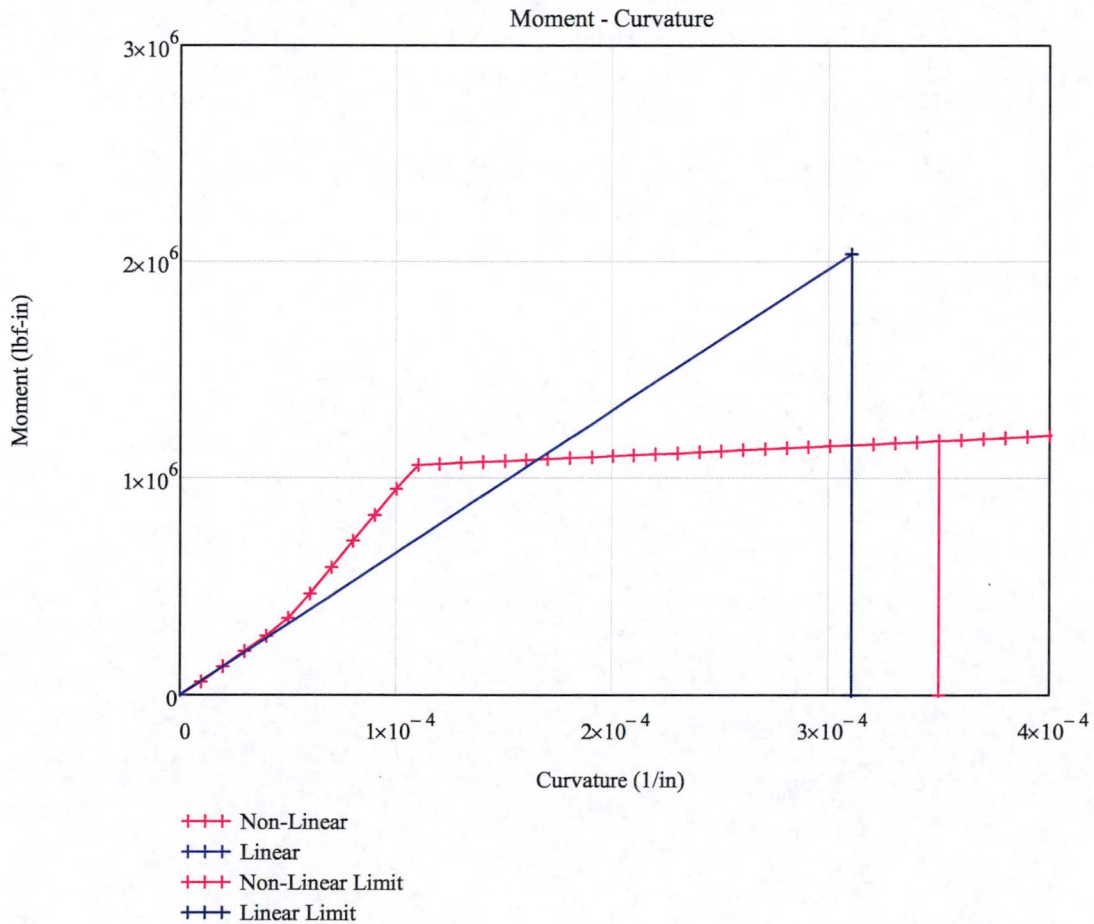
Strain in steel

$$\epsilon_{\text{steel}} := NL_Cur_{ap} \cdot d_{\text{strain}}$$

$$\epsilon_{\text{steel}} = 0.00699$$

Ductility Demand

$$\frac{\epsilon_{\text{steel}}}{\epsilon_y} = 3.51$$



Section Cut 8 "STANDARD - PLUS" Load Combination

INPUT DEFINITION

Set starting index of all arrays to 1 (the default is 0)

ORIGIN \equiv 1

Input Reading

	1
1	"Seabrook1"
2	$4 \cdot 10^3$
3	$6 \cdot 10^4$
4	$6 \cdot 10^4$
5	$9 \cdot 10^4$
INPUTS = 6	3.53
7	1.495
8	12
9	31
10	372
11	9.01
12	...

INDEX = 1

colname := INPUTS_{1, INDEX}

colname = "Seabrook1"

Concrete strength

$f'_c := \text{INPUTS}_{2, \text{INDEX}} \cdot \text{psi}$

$f'_c = 4 \cdot \text{ksi}$

Steel yield strength

$f_y := \text{INPUTS}_{3, \text{INDEX}} \cdot \text{psi}$

$f_y = 60 \cdot \text{ksi}$

Ultimate strength of rebar

$f_{su} := \text{INPUTS}_{5, \text{INDEX}} \cdot \text{psi}$

$f_{su} = 90 \cdot \text{ksi}$

cover (to centroid of steel)	$\text{cover} := \text{INPUTS}_{6, \text{INDEX}} \cdot \text{in}$	$\text{cover} = 3.53 \cdot \text{in}$
Width of column	$b_{\text{col}} := \text{INPUTS}_{8, \text{INDEX}} \cdot \text{in}$	$b_{\text{col}} = 12 \cdot \text{in}$
Height of column	$h_{\text{col}} := \text{INPUTS}_{9, \text{INDEX}} \cdot \text{in}$	$h_{\text{col}} = 31 \cdot \text{in}$
Gross Area	$A_g := \text{INPUTS}_{10, \text{INDEX}} \cdot \text{in}^2$	$A_g = 372 \cdot \text{in}^2$
Area of longitudinal bar	$a_{\text{bar}} := \text{INPUTS}_{13, \text{INDEX}} \cdot \text{in}^2$	$a_{\text{bar}} = 3.12 \cdot \text{in}^2$
Diameter of bar	$d_{\text{bar}} := \text{INPUTS}_{14, \text{INDEX}} \cdot \text{in}$	$d_{\text{bar}} = 0.5 \cdot \text{in}$
Area of longitudinal steel	$A_{sL} := \text{INPUTS}_{18, \text{INDEX}} \cdot \text{in}^2$	$A_{sL} = 9.36 \cdot \text{in}^2$
Young's modulus of steel	$E_s := \text{INPUTS}_{20, \text{INDEX}} \cdot \text{psi}$	$E_s = 2.9 \times 10^4 \cdot \text{ksi}$
Ultimate strain of rebar	$\epsilon_{\text{su}} := \text{INPUTS}_{21, \text{INDEX}}$	$\epsilon_{\text{su}} = 0.07$
Modulus of strain hardening [O-2]	$E_{\text{sh}} := \text{INPUTS}_{22, \text{INDEX}} \cdot \text{psi}$	$E_{\text{sh}} = 1.16 \times 10^3 \cdot \text{ksi}$
Strain at strain hardening [O-3]	$\epsilon_{\text{sh}} := \text{INPUTS}_{23, \text{INDEX}}$	$\epsilon_{\text{sh}} = 8 \times 10^{-3}$
Young's modulus of concrete	$E_c := \text{INPUTS}_{24, \text{INDEX}} \cdot \text{psi}$	$E_c = 3.605 \times 10^3 \cdot \text{ksi}$
Poisson's ratio	$\nu := \text{INPUTS}_{25, \text{INDEX}}$	$\nu = 0.17$
Shear modulus of concrete	$G_c := \text{INPUTS}_{26, \text{INDEX}} \cdot \text{psi}$	$G_c = 1.541 \times 10^3 \cdot \text{ksi}$
Shear modification factor Table 2.4 of [O-4]	$\alpha := \text{INPUTS}_{27, \text{INDEX}}$	$\alpha = 1.185$
Torsional Constant Table 2.5 of [O-5]	$J := \text{INPUTS}_{28, \text{INDEX}} \cdot \text{in}^4$	$J = 1.351 \times 10^4 \cdot \text{in}^4$

Crack section index

crack := INPUTS_{140, INDEX}

crack = "yes"

Locate the longitudinal bars in the wall

bars := augment(submatrix(INPUTS, 40, 59, INDEX, INDEX), submatrix(INPUTS, 60, 79, INDEX, INDEX))·in

Area of bars

$a_{\text{bar}} := \text{submatrix}(\text{INPUTS}, 80, 99, \text{INDEX}, \text{INDEX}) \cdot \text{in}^2$

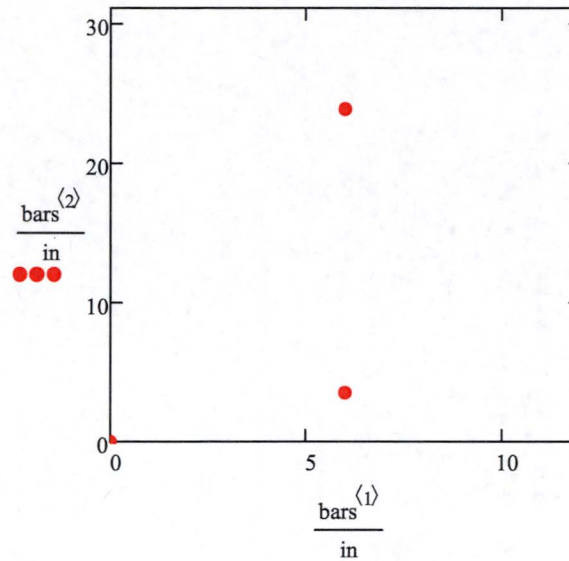
Diameter of bars

$d_{\text{bar}} := \text{submatrix}(\text{INPUTS}, 100, 119, \text{INDEX}, \text{INDEX}) \cdot \text{in}$

index of bars

b := 1..20

Reinforcement Location



END OF INPUT

SECTION PROPERTIES

Elastic properties of uncracked cross section

$$I_{g1} := \frac{1}{12} \cdot b_{col} \cdot h_{col}^3$$

$$I_{g1} = 2.979 \times 10^4 \cdot \text{in}^4$$

$$I_{g2} := \frac{1}{12} \cdot h_{col} \cdot b_{col}^3$$

$$I_{g2} = 4.464 \times 10^3 \cdot \text{in}^4$$

$$A_v := b_{col} \cdot h_{col}$$

$$A_v = 2.583 \text{ ft}^2$$

Transverse Shear Stiffness

$$K_v := \frac{G_c \cdot A_v}{\alpha}$$

$$K_v = 4.834 \times 10^8 \cdot \text{lb} \cdot \text{f}$$

Flexural Stiffness

$$EI_2 := E_c \cdot I_{g2}$$

$$EI_2 = 1.609 \times 10^{10} \cdot \text{lb} \cdot \text{f} \cdot \text{in}^2$$

Axial Stiffness

$$EA := E_c \cdot A_g$$

$$EA = 1.341 \times 10^9 \cdot \text{lb} \cdot \text{f}$$

Torsional Stiffness

$$GJ := G_c \cdot J$$

$$GJ = 2.081 \times 10^{10} \cdot \text{lb} \cdot \text{f} \cdot \text{in}^2$$

CONCRETE MODEL

Peak strain of unconfined concrete
in compression assumed to be
0.002 [O-5]

$$\epsilon_{co} := 0.002$$

$$\epsilon_{co} = 2 \times 10^{-3}$$

From Table 1 of Karthik and Mander [O-2]

Ultimate strain of
unconfined concrete in
compression

$$\epsilon_{c1} := 0.0036$$

Failure strain of unconfined
concrete in compression

$$\epsilon_{sp} := 0.012 - 7 \cdot 10^{-7} \cdot \frac{f_c}{\text{psi}}$$

$$\epsilon_{sp} = 9.2 \times 10^{-3}$$

Peak strain of concrete in
tension

$$\epsilon_{to} := -0.1 \cdot \epsilon_{co}$$

$$\epsilon_{to} = -2 \times 10^{-4}$$

Concrete tensile strength

$$f_t := 7.5 \cdot \sqrt{\frac{f_c}{\text{psi}}} \cdot \text{psi}$$

$$f_t = 474.342 \text{ psi}$$

Use Cornelissen, Hordijk and Reinhardt (1986) to determine ultimate tension strain [O-6]

[O-6] Fig 6

$$\delta_o := 160 \mu\text{m}$$

[O-6] Eq 1

$$\sigma_t(\delta) := \left[1 + \left(\frac{3 \cdot \delta}{\delta_o} \right)^3 \right]^{-6.93} \cdot \frac{\delta}{(\delta_o)}$$

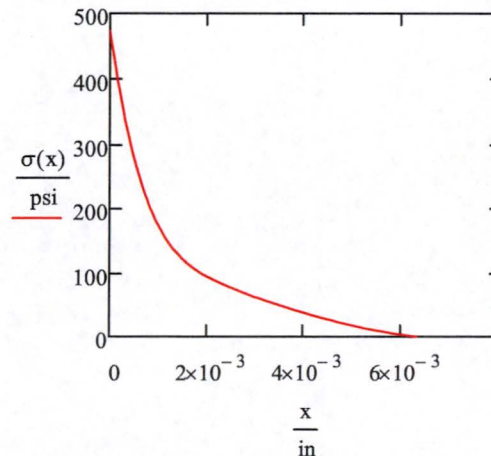
$$\sigma(\delta) := f_t \cdot \left[\sigma_t(\delta) - \frac{\delta}{(\delta_o)} \cdot \sigma_t(\delta_o) \right]$$

$$\epsilon_{cr} := \frac{f_t}{E_c}$$

$$\epsilon_{cr} = 1.316 \times 10^{-4}$$

$$x := 0 \mu\text{m}, 1 \mu\text{m}.. 160 \mu\text{m}$$

Tension Stress-Strain Curve



Fracture energy

$$g_f := \int_0^{\delta_o} \sigma(x) dx$$

$$g_f = 0.582 \cdot \frac{\text{lbf}}{\text{in}}$$

From Table 1 of Karthik and Mander [O-2]:

Failure strain of
concrete in tension

$$\epsilon_u := \frac{-18}{\text{in}} \cdot \frac{g_f}{5 \cdot f_t}$$

$$\epsilon_u = -4.415 \times 10^{-3}$$

Ultimate strain of
concrete in tension

$$\epsilon_{t1} := \frac{2 \cdot \epsilon_u}{9}$$

$$\epsilon_{t1} = -9.812 \times 10^{-4}$$

Ultimate stress of concrete in tension

$$f_{t1} := \frac{f_t}{3}$$

$$f_{t1} = 158.114 \cdot \text{psi}$$

Tension stress-strain curve, [O-2] Eq 1, 2 & 3

$$fct(\epsilon_c) := -1 \cdot \begin{cases} f_t \cdot \left[1 - \left(\left| 1 - \frac{\epsilon_c}{\epsilon_{to}} \right| \right)^{\frac{E_c \cdot \epsilon_{to}}{f_t}} \right] & \text{if } \epsilon_{to} \leq \epsilon_c \leq 0 \\ f_t - \left(\frac{f_t - f_{t1}}{\frac{\epsilon_{t1}}{\epsilon_{to}} - 1} \right) \cdot \left(\frac{\epsilon_c}{\epsilon_{to}} - 1 \right) & \text{if } \epsilon_{t1} \leq \epsilon_c < \epsilon_{to} \\ f_{t1} \cdot \left(\frac{\epsilon_c - \epsilon_u}{\epsilon_{t1} - \epsilon_u} \right) & \text{if } \epsilon_u \leq \epsilon_c < \epsilon_{t1} \\ 0 & \text{if } \epsilon_c < \epsilon_u \end{cases}$$

[O-2] Table 1

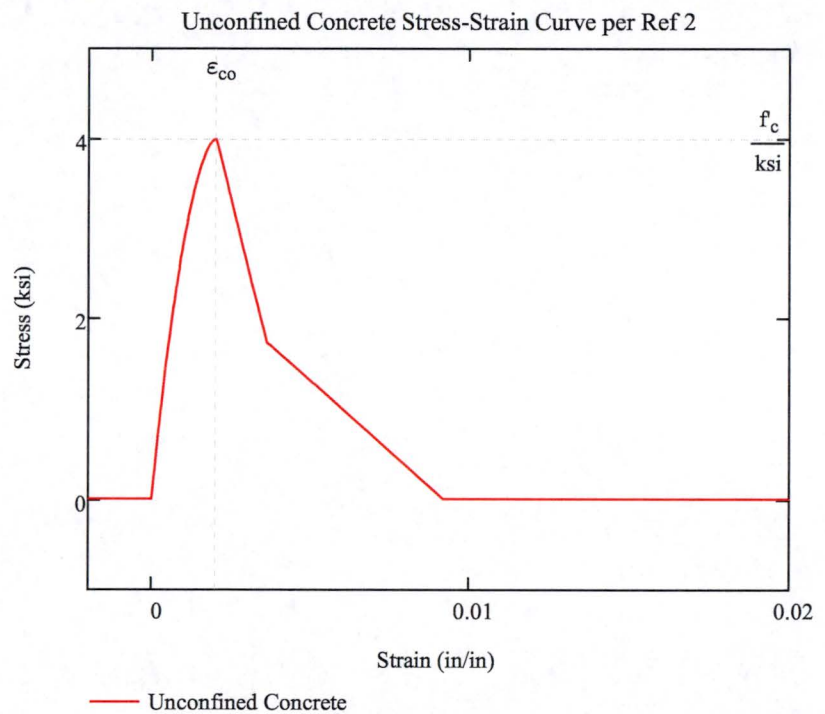
$$f_{c1} := 1.74 \text{ksi}$$

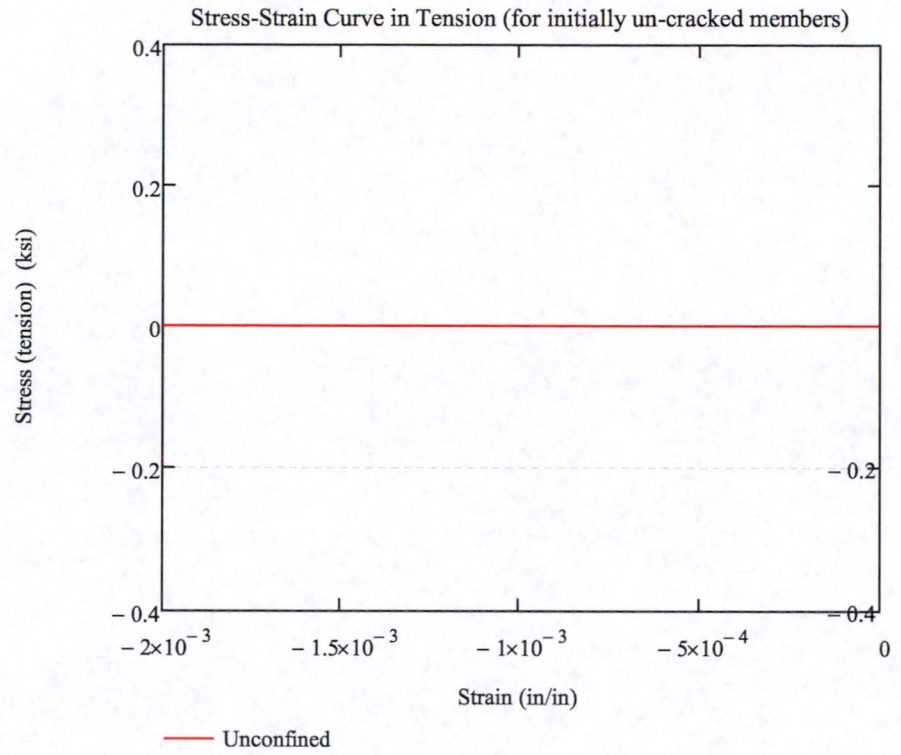
$$\text{mult_crack} := \begin{cases} 1 & \text{if crack} = \text{"no"} \\ 0 & \text{if crack} = \text{"yes"} \end{cases}$$

$$\text{mult_crack} = 0$$

Unconfined stress-strain curve [O-2] Eq 1, 2 & 3

$$f_c(\epsilon_c) := \begin{cases} f_{ct}(\epsilon_c) \cdot \text{mult_crack} & \text{if } \frac{\epsilon_c}{\epsilon_{co}} < 0 \\ f_c \cdot \left[1 - \left(\left| 1 - \frac{\epsilon_c}{\epsilon_{co}} \right| \right)^{\frac{E_c \cdot \epsilon_{co}}{f_c}} \right] & \text{if } 0 \leq \frac{\epsilon_c}{\epsilon_{co}} < 1 \\ f_c - \left(\frac{f_c - f_{cl}}{\frac{\epsilon_{cl}}{\epsilon_{co}} - 1} \right) \cdot \left(\frac{\epsilon_c}{\epsilon_{co}} - 1 \right) & \text{if } 1 \leq \frac{\epsilon_c}{\epsilon_{co}} < \frac{\epsilon_{cl}}{\epsilon_{co}} \\ f_{cl} \cdot \left(\frac{\frac{\epsilon_c}{\epsilon_{co}} - \frac{\epsilon_{sp}}{\epsilon_{co}}}{\frac{\epsilon_{cl}}{\epsilon_{co}} - \frac{\epsilon_{sp}}{\epsilon_{co}}} \right) & \text{if } \frac{\epsilon_{cl}}{\epsilon_{co}} \leq \frac{\epsilon_c}{\epsilon_{co}} < \frac{\epsilon_{sp}}{\epsilon_{co}} \\ 0 & \text{if } \frac{\epsilon_{sp}}{\epsilon_{co}} \leq \frac{\epsilon_c}{\epsilon_{co}} \end{cases}$$





Modified confinement per Roy and Sozen [O-7] Eq 5.3

$$\epsilon_{50u} := \frac{3\text{psi} + 0.002 \cdot f_c}{f_c - 1000\text{psi}} \quad \epsilon_{50u} = 3.667 \times 10^{-3}$$

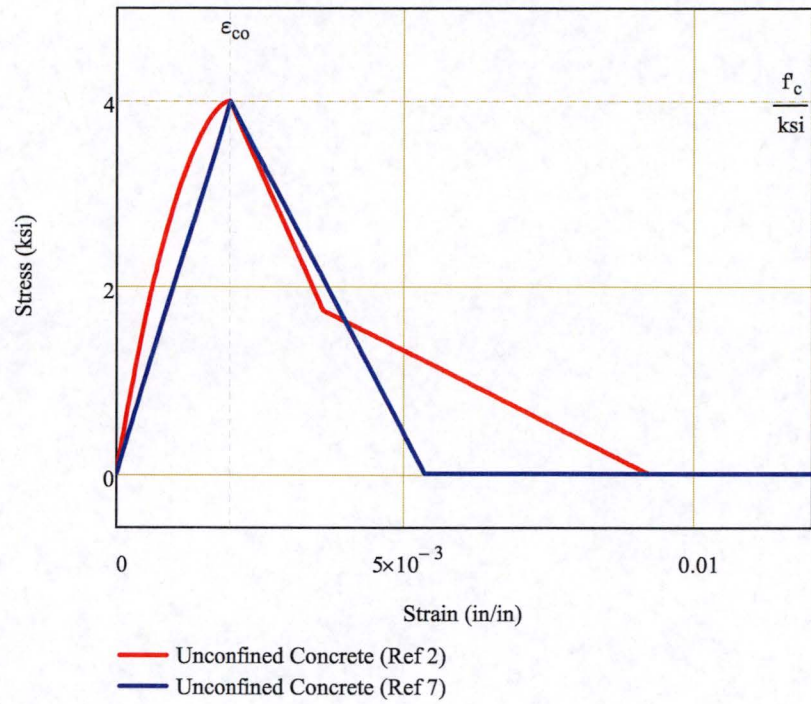
[O-7]

$$m_{\text{RoySozen}} := \frac{-0.5 \cdot f_c}{\epsilon_{50u} - 0.002} \quad m_{\text{RoySozen}} = -1.2 \times 10^3 \cdot \text{ksi}$$

$$b_{\text{RoySozen}} := 0.002 \cdot (-m_{\text{RoySozen}}) + (f_c) \quad b_{\text{RoySozen}} = 6.4 \cdot \text{ksi}$$

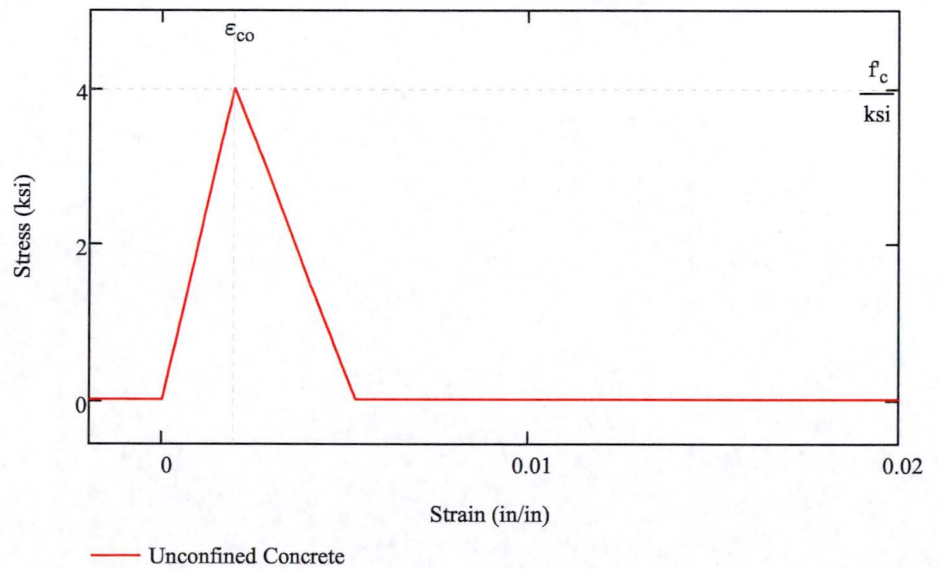
$$f_{c_RoySozen}(\epsilon_c) := \begin{cases} f_{ct}(\epsilon_c) \cdot \text{mult_crack} & \text{if } \epsilon_c < 0 \\ \frac{f_c}{0.002} \cdot \epsilon_c & \text{if } 0 \leq \epsilon_c < 0.002 \\ \max(0, m_{\text{RoySozen}} \cdot \epsilon_c + b_{\text{RoySozen}}) & \text{if } 0.002 \leq \epsilon_c \end{cases}$$

Comparison of Mander (Ref 2) and Sezen (Ref 7) Concrete Models



$$f_c(\epsilon_c) := \begin{cases} f_{c_RoySozen}(\epsilon_c) & \text{if } INPUTS_{34, INDEX} = "RoySozen" \\ f_c(\epsilon_c) & \text{otherwise} \end{cases}$$

Concrete Model Used for Evaluation



REBAR MODEL

Stress - Strain curve of rebar

[O-2] Eq 5

$$P := \begin{cases} 1 & \text{if } f_{su} = f_y \\ \frac{E_{sh} \cdot (\epsilon_{su} - \epsilon_{sh})}{f_{su} - f_y} & \text{otherwise} \end{cases} \quad P = 2.397$$

[O-2] Eq 4.

$$f_{s_t}(\epsilon_s) := \left[\frac{E_s \cdot |\epsilon_s|}{\left[1 + \left(\left| \frac{E_s \cdot |\epsilon_s|}{f_y} \right| \right)^{20} \right]^{0.05}} + (f_{su} - f_y) \cdot \left[1 - \frac{(|\epsilon_{su} - |\epsilon_s||)^P}{\left[(|\epsilon_{su} - \epsilon_{sh}|)^{20 \cdot P} + (|\epsilon_{su} - |\epsilon_s||)^{20 \cdot P} \right]^{0.05}} \right] \right]$$

Based on the recommendation of Sezen and Setzler ([O-8], and [O-3]), the steel stress strain curve is modified slightly to make sure the plateau region as a slight positive slope

Slope of strain hardening

$$\alpha_s := 0.02$$

Adjust f_y such that area under the plateau stays the same

Steel yield strength

$$f_y = 60 \cdot \text{ksi}$$

Modified yield strength

$$f_{y'} := f_y - \frac{E_s \cdot \alpha_s \cdot \epsilon_{sh}}{2} \quad f_{y'} = 57.68 \cdot \text{ksi}$$

Yield strain

$$\epsilon_y := \frac{f_{y'}}{E_s} \quad \epsilon_y = 1.989 \times 10^{-3}$$

[O-3] strain at strain hardening

$$\epsilon_{sh} = 8 \times 10^{-3}$$

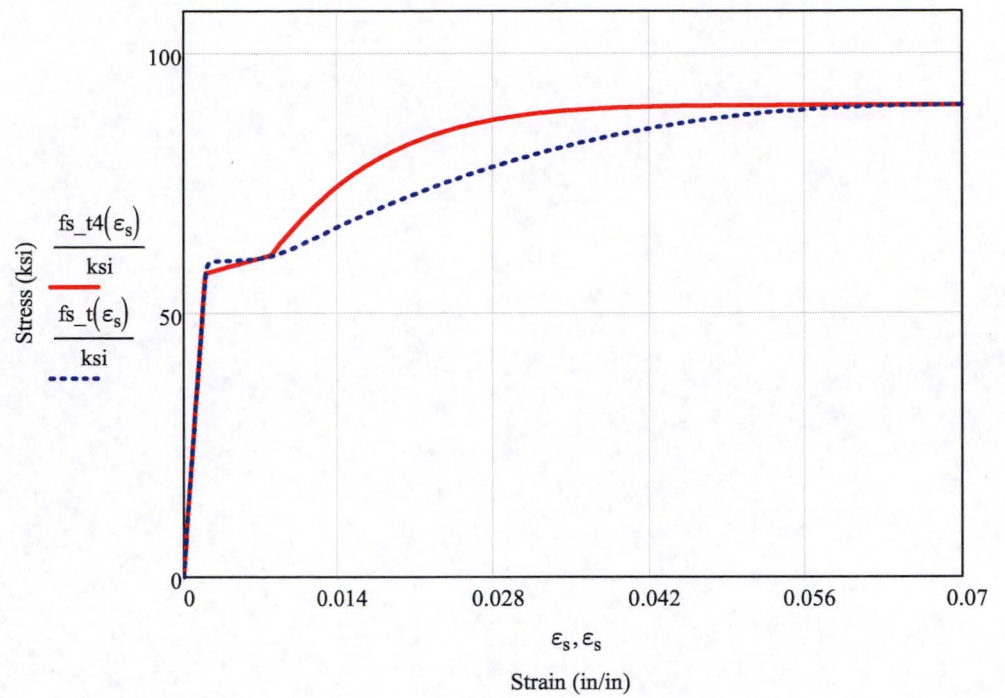
Steel material model [O-3] Eq 3.3

$$\epsilon_{cross} := \frac{f_y - f_{y'}}{\alpha_s \cdot E_s} + \epsilon_y = 5.989 \times 10^{-3}$$

$$f_{sh} := \begin{cases} f_{y'} + (\epsilon_{sh} - \epsilon_y) \cdot \alpha_s \cdot E_s & \text{if } P \neq 1 \\ \left[f_{y'} + (\epsilon_{cross} - \epsilon_y) \cdot \alpha_s \cdot E_s \right] & \text{otherwise} \end{cases} \quad f_{sh} = 61.166 \cdot \text{ksi}$$

Steel curve from Setzler thesis ([O-3]) (with correction per sezen for plateau region)

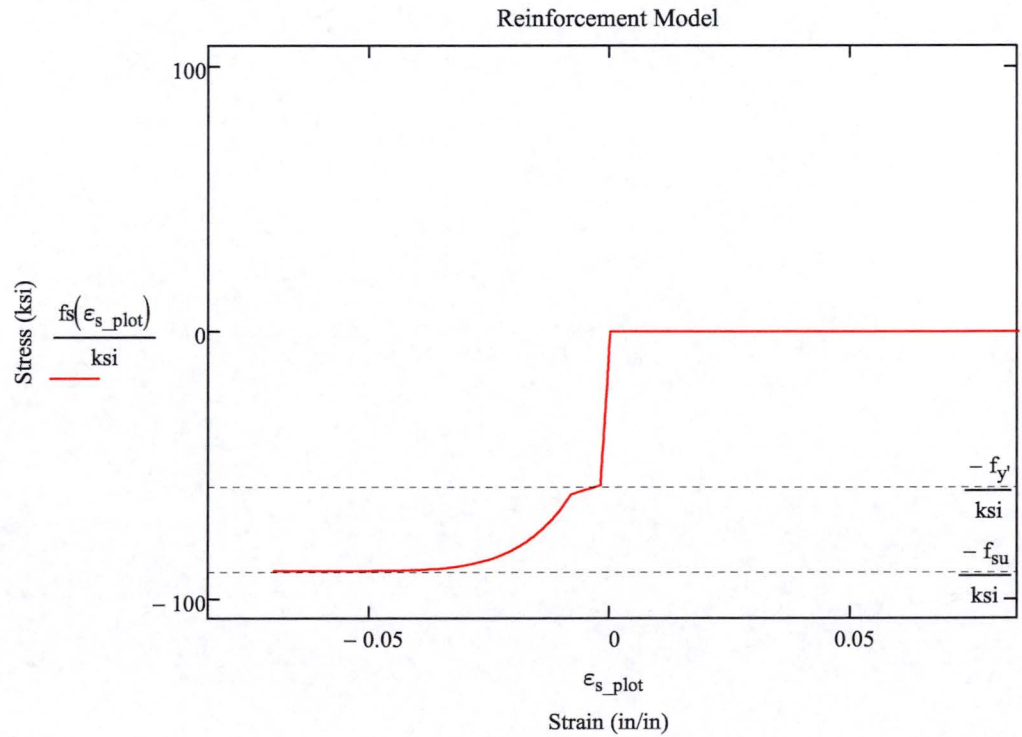
$$f_{s_t4}(\epsilon_s) := \begin{cases} \text{if } P \neq 1 \\ \begin{cases} E_s \cdot \epsilon_s & \text{if } \epsilon_s \leq \epsilon_y \\ f_{y'} + (\epsilon_s - \epsilon_y) \cdot \alpha_s \cdot E_s & \text{if } \epsilon_y < \epsilon_s \leq \epsilon_{sh} \\ f_{su} - (f_{su} - f_{sh}) \cdot \left(\frac{\epsilon_s - \epsilon_{su}}{\epsilon_{su} - \epsilon_{sh}} \right)^6 & \text{if } \epsilon_{sh} < \epsilon_s \leq \epsilon_{su} \end{cases} \\ \text{otherwise} \\ \begin{cases} E_s \cdot \epsilon_s & \text{if } \epsilon_s \leq \epsilon_y \\ f_{y'} + (\epsilon_s - \epsilon_y) \cdot \alpha_s \cdot E_s & \text{if } \epsilon_y < \epsilon_s \leq \epsilon_{cross} \\ f_{su} - (f_{su} - f_{sh}) \cdot \left(\frac{\epsilon_s - \epsilon_{su}}{\epsilon_{su} - \epsilon_{sh}} \right)^6 & \text{if } \epsilon_{cross} < \epsilon_s \leq \epsilon_{su} \end{cases} \end{cases}$$



Combined tension and
compression behavior

$$f_s(\epsilon_s) := \begin{cases} -f_{s_t4}(|\epsilon_s|) & \text{if } \epsilon_s \leq 0 \\ 0 & \text{otherwise} \end{cases}$$

$$\epsilon_{s_plot} := -0.2, -0.1999..0.2$$



DUCTILITY CALCULATION

Section inertia of uncracked cross section

$$I_g := \frac{1}{12} \cdot b_{col} \cdot h_{col}^3 + \frac{E_s}{E_c} \cdot \sum_b \left[a_{bar_b} \cdot \left(bars_{b,2} - \frac{h_{col}}{2} \right)^2 \right] \quad I_g = 3.684 \times 10^4 \cdot \text{in}^4$$

Concrete stress at a location (x) given a curvature, and neutral axis

$$\sigma_{conc}(\phi, x, NA) := fc[\phi \cdot (x - NA)]$$

Steel stress in a bar (b) given a curvature and neutral axis

$$\sigma_{steel}(\phi, b, NA) := fs[\phi \cdot (bars_{b,2} - NA)]$$

Given

Integration across the section to combine concrete and steel stresses must equal the applied vertical load independent of the curvature. (integrate by parts to help convergence)

$$\int_0^{h_{col}} b_{col} \cdot \sigma_{conc}(\phi, x, na_test) dx \dots = F_v \\ + \sum_b \left(\sigma_{steel}(\phi, b, na_test) \cdot a_{bar_b} \right)$$

Function to execute the solve block and find the neutral axis location as a function of curvature.

$$na(\phi, F_v, na_test) := \text{Find}(na_test)$$

$$F_{v_plot} := 0 \text{ kip}$$

$$\phi_{plot} := 3 \cdot 10^{-4} \cdot \frac{1}{\text{in}}$$

$$na(\phi_{plot}, F_{v_plot}, 0.8 \cdot h_{col}) = 23.749 \cdot \text{in}$$

$$h_{centroid} := \frac{h_{col}}{2} \quad h_{centroid} = 15.5 \cdot \text{in}$$

Function to solve for the moment about the centroid for a given curvature

$$mom(\phi, NA, F_v) := \int_0^{h_{col}} b_{col} \cdot \sigma_{conc}(\phi, x, NA) \cdot (x - h_{centroid}) dx \dots \\ + \sum_b \left[\sigma_{steel}(\phi, b, NA) \cdot a_{bar_b} \cdot (bars_{b,2} - h_{centroid}) \right]$$

$$mom(\phi_{plot}, na(\phi_{plot}, F_{v_plot}, 0.8 h_{col}), F_{v_plot}) = 4.689 \times 10^3 \cdot \text{kip} \cdot \text{in}$$

$$mom(-\phi_{plot}, na(-\phi_{plot}, F_{v_plot}, 0.2 h_{col}), F_{v_plot}) = -6.747 \times 10^3 \cdot \text{kip} \cdot \text{in}$$

Function to check the resulting axial force

$$\text{chk}(\phi, \text{NA}) := \int_0^{h_{\text{col}}} b_{\text{col}} \cdot \sigma_{\text{conc}}(\phi, x, \text{NA}) dx \dots$$

$$+ \sum_b \left(\sigma_{\text{steel}}(\phi, b, \text{NA}) \cdot a_{\text{bar}_b} \right)$$

$$F_{v_plot} = 0 \cdot \text{kip}$$

$$\text{chk}(\phi_{\text{plot}}, \text{na}(\phi_{\text{plot}}, F_{v_plot}, 0.8h_{\text{col}})) = 1.047 \times 10^{-13} \cdot \text{kip}$$

$$\text{max_bar} := \text{INPUTS}_{36, \text{INDEX}} \quad \text{max_bar} = 2$$

$$\text{min_bar} := \text{INPUTS}_{37, \text{INDEX}} \quad \text{min_bar} = 1$$

To this point, compression is positive and tension is negative, for computing steel strain and stress, use tension as positive values.

$$\text{steel_strain}(\phi, \text{NA}) := -1 \cdot \begin{cases} \phi \cdot (\text{bars}_{\text{min_bar}, 2} - \text{NA}) & \text{if } \phi \geq 0 \\ \phi \cdot (\text{bars}_{\text{max_bar}, 2} - \text{NA}) & \text{if } \phi < 0 \end{cases}$$

$$\text{steel_stress}(\phi, \text{NA}) := -1 \cdot \begin{cases} \sigma_{\text{steel}}(\phi, \text{min_bar}, \text{NA}) & \text{if } \phi \geq 0 \\ \sigma_{\text{steel}}(\phi, \text{max_bar}, \text{NA}) & \text{if } \phi < 0 \end{cases}$$

$$\text{depth_bar}(\phi) := \begin{cases} \text{bars}_{\text{min_bar}, 2} & \text{if } \phi \geq 0 \\ \text{bars}_{\text{max_bar}, 2} & \text{if } \phi < 0 \end{cases}$$

$$d_b(\phi) := \begin{cases} d_{\text{bar}_{\text{min_bar}}} & \text{if } \phi \geq 0 \\ d_{\text{bar}_{\text{max_bar}}} & \text{if } \phi < 0 \end{cases} \quad d_b(\phi_{\text{plot}}) = 0.5 \cdot \text{in}$$

$$\text{steel_strain}(\phi_{\text{plot}}, \text{na}(\phi_{\text{plot}}, F_{v_plot}, 0.8 \cdot h_{\text{col}})) = 6.066 \times 10^{-3}$$

$$\text{steel_stress}(\phi_{\text{plot}}, \text{na}(\phi_{\text{plot}}, F_{v_plot}, 0.8 \cdot h_{\text{col}})) = 60.044 \cdot \text{ksi}$$

$$\text{fname} := \text{INPUTS}_{124, \text{INDEX}} \quad \text{fname} = "001_Wall_uncracked_file1.txt"$$

Compute moment-curvature curves at various axial load, and curvatures. This requires the following programming loop, which writes results to a text file which is then read back in by this calculation.

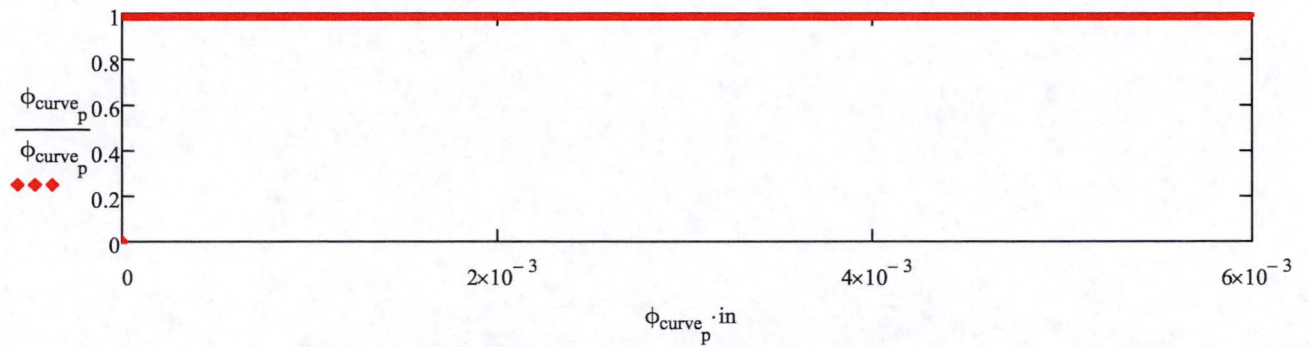
Index of curvatures

$$\text{numinc} := \text{INPUTS}_{139, \text{INDEX}}$$

$$p := 1 \dots \text{numinc}$$

$$\phi_{\text{int}} := \text{INPUTS}_{138, \text{INDEX}} \cdot \frac{1}{\text{in}} \quad \phi_{\text{int}} = 1 \times 10^{-5} \cdot \frac{1}{\text{in}}$$

$$\phi_{\text{curve}_p} := (p - 1) \cdot \phi_{\text{int}}$$



```
fv := submatrix(INPUTS,126,137,INDEX,INDEX)
```

```
fv := | new ← fv1
      | for j ∈ 2..rows(fv)
      |   new ← new if IsString(fvj)
      |   new ← stack(new,fvj) otherwise
      | return new.lbf
```

	1	
1	1.042·10 ³	
2	911.4	
3	781.2	
4	651	
5	520.8	
fv = 6	390.6	·kip
7	260.4	
8	130.2	
9	0	
10	-49.6	
11	-99.2	
12	-148.8	

```
f := 1..rows(fv)
```

Output _{1,1} := "Curvature (1/in)"	Output _{1,5} := "Concrete Strain"	Output _{1,9} := "Slip Rotation (rad)"
Output _{1,2} := "Moment (lbf*in)"	Output _{1,6} := "Concrete Strain"	Output _{1,10} := "Slip (in)"
Output _{1,3} := "Axial Load (lbf)"	Output _{1,7} := "Steel Strain"	Output _{1,11} := ""
Output _{1,4} := "neutral axis (in)"	Output _{1,8} := "Steel Strain"	Output _{1,12} := "LINE"

```
fname = "001_Wall_uncracked_file1.txt"
```

```
exist := "no" on error READPRN(fname)
```


zero(x,y) := 0

out := if exist = "no"

```

APPENDPRN[fname,(OutputT)<1>T]
for f ∈ 1..rows(fv)
  na_last ← ""
  continue ← "yes"
  errorcount ← 0
  for p ∈ 1..numinc
    if continue = "yes"
      M1 ← ϕcurvep·in
      m0 ← [0 on error (mom(ϕcurvep, na(ϕcurvep, fvf, na_last), fvf))]
      mout ← m0
      NA ← (0 on error na(ϕcurvep, fvf, na_last))
      if (m0 = 0 ∨ sign(m0) ≠ sign(ϕcurvep))
        m1 ← [0 on error (mom(ϕcurvep, na(ϕcurvep, fvf, 0in), fvf))]
        m2 ← [0 on error (mom(ϕcurvep, na(ϕcurvep, fvf, sign(ϕcurvep)·0.5hcol), fvf))]
        m3 ← [0 on error (mom(ϕcurvep, na(ϕcurvep, fvf, sign(ϕcurvep)·0.9hcol), fvf))]
        if |m1| > max(|m2|, |m3|)
          NA ← (0 on error na(ϕcurvep, fvf, 0in))
          mout ← m1
        if |m2| ≥ max(|m1|, |m3|)
          NA ← (0 on error na(ϕcurvep, fvf, sign(ϕcurvep)·0.5hcol))
          mout ← m2
        if |m3| ≥ max(|m1|, |m2|)
          NA ← (0 on error na(ϕcurvep, fvf, sign(ϕcurvep)·0.9hcol))
          mout ← m3
      M2 ←  $\frac{mout}{lbf \cdot in}$ 
      M3 ←  $\frac{fv_f}{lbf}$ 
      M4 ←  $\frac{NA}{in}$ 
      na_last ← NA
      M5 ← ϕcurvep·(0in - NA)
      M6 ← ϕcurvep·(hcol - NA)
      M7 ← ϕcurvep·(barsmin_bar,2 - NA)

```



```

M8 ←  $\phi_{curve_p} \cdot (\text{bars}_{\text{max\_bar},2} - \text{NA})$ 
M9 ← 0
M10 ← 0
M11 ← 0
M12 ← "LINE"
errorcount ← errorcount + 1 if (NA = 0) ∨ (sign(mout) ≠ sign( $\phi_{curve_p}$ )) ∨ (M6 > 0.010)
errorcount ← 0 otherwise
APPENDPRN(fname, MT)
M ← matrix(12, 1, zero)
continue ← "no" if errorcount > 3
"nothing" otherwise

```

```

data := READPRN(fname) if exist = "no"
        exist otherwise

```

	1	2	3
1	"Curvature (1/in)"	"Moment (lbf*in)"	"Axial Load (lbf)"
2	0	0	1.042·10 ⁶
3	1·10 ⁻⁵	5.958·10 ⁵	1.042·10 ⁶
4	2·10 ⁻⁵	1.192·10 ⁶	1.042·10 ⁶
5	3·10 ⁻⁵	1.787·10 ⁶	1.042·10 ⁶
6	4·10 ⁻⁵	2.38·10 ⁶	1.042·10 ⁶
7	5·10 ⁻⁵	2.773·10 ⁶	1.042·10 ⁶
8	6·10 ⁻⁵	2.901·10 ⁶	1.042·10 ⁶
9	7·10 ⁻⁵	2.801·10 ⁶	1.042·10 ⁶
10	8·10 ⁻⁵	2.469·10 ⁶	1.042·10 ⁶
11	9·10 ⁻⁵	1.848·10 ⁶	1.042·10 ⁶
12	1·10 ⁻⁴	6.486·10 ⁵	1.042·10 ⁶
13	1.1·10 ⁻⁴	0	1.042·10 ⁶
14	1.2·10 ⁻⁴	0	1.042·10 ⁶
15	1.3·10 ⁻⁴	0	1.042·10 ⁶
16	1.4·10 ⁻⁴	0	...

```

data := d ← submatrix(data, 1, 1, 1, 12)
        for i ∈ 2..rows(data)
            d ← d if (datai,2 ≤ 0 ∧ datai,1 ≠ 0)
            d ← stack(d, submatrix(data, i, i, 1, 12)) otherwise
        return d

```

cleandata := APPENDPRN(concat("clean_",fname),data)

cleandata =

	1	2	3
1	"Curvature (1/in)"	"Moment (lbf*in)"	"Axial Load (lbf)"
2	0	0	1.042·10 ⁶
3	1·10 ⁻⁵	5.958·10 ⁵	1.042·10 ⁶
4	2·10 ⁻⁵	1.192·10 ⁶	1.042·10 ⁶
5	3·10 ⁻⁵	1.787·10 ⁶	1.042·10 ⁶
6	4·10 ⁻⁵	2.38·10 ⁶	1.042·10 ⁶
7	5·10 ⁻⁵	2.773·10 ⁶	1.042·10 ⁶
8	6·10 ⁻⁵	2.901·10 ⁶	1.042·10 ⁶
9	7·10 ⁻⁵	2.801·10 ⁶	1.042·10 ⁶
10	8·10 ⁻⁵	2.469·10 ⁶	1.042·10 ⁶
11	9·10 ⁻⁵	1.848·10 ⁶	1.042·10 ⁶
12	1·10 ⁻⁴	6.486·10 ⁵	1.042·10 ⁶
13	0	0	9.114·10 ⁵
14	1·10 ⁻⁵	5.958·10 ⁵	9.114·10 ⁵
15	2·10 ⁻⁵	1.192·10 ⁶	9.114·10 ⁵
16	3·10 ⁻⁵	1.787·10 ⁶	9.114·10 ⁵
17	4·10 ⁻⁵	2.383·10 ⁶	9.114·10 ⁵
18	5·10 ⁻⁵	2.979·10 ⁶	9.114·10 ⁵
19	6·10 ⁻⁵	3.445·10 ⁶	9.114·10 ⁵
20	7·10 ⁻⁵	3.688·10 ⁶	9.114·10 ⁵
21	8·10 ⁻⁵	3.744·10 ⁶	9.114·10 ⁵
22	9·10 ⁻⁵	3.626·10 ⁶	9.114·10 ⁵
23	1·10 ⁻⁴	3.33·10 ⁶	9.114·10 ⁵
24	1.1·10 ⁻⁴	2.832·10 ⁶	9.114·10 ⁵
25	1.2·10 ⁻⁴	2.053·10 ⁶	9.114·10 ⁵
26	1.3·10 ⁻⁴	6.692·10 ⁵	9.114·10 ⁵
27	0	0	7.812·10 ⁵
28	1·10 ⁻⁵	5.958·10 ⁵	7.812·10 ⁵
29	2·10 ⁻⁵	1.192·10 ⁶	7.812·10 ⁵
30	3·10 ⁻⁵	1.787·10 ⁶	7.812·10 ⁵
31	4·10 ⁻⁵	2.383·10 ⁶	7.812·10 ⁵
32	5·10 ⁻⁵	2.979·10 ⁶	7.812·10 ⁵
33	6·10 ⁻⁵	3.575·10 ⁶	7.812·10 ⁵
34	7·10 ⁻⁵	4.085·10 ⁶	7.812·10 ⁵
35	8·10 ⁻⁵	4.365·10 ⁶	7.812·10 ⁵
36	9·10 ⁻⁵	4.468·10 ⁶	7.812·10 ⁵
37	1·10 ⁻⁴	4.467·10 ⁶	...

Strain limit

strain_lim := 0.005

lim = 5×10^{-3}

```

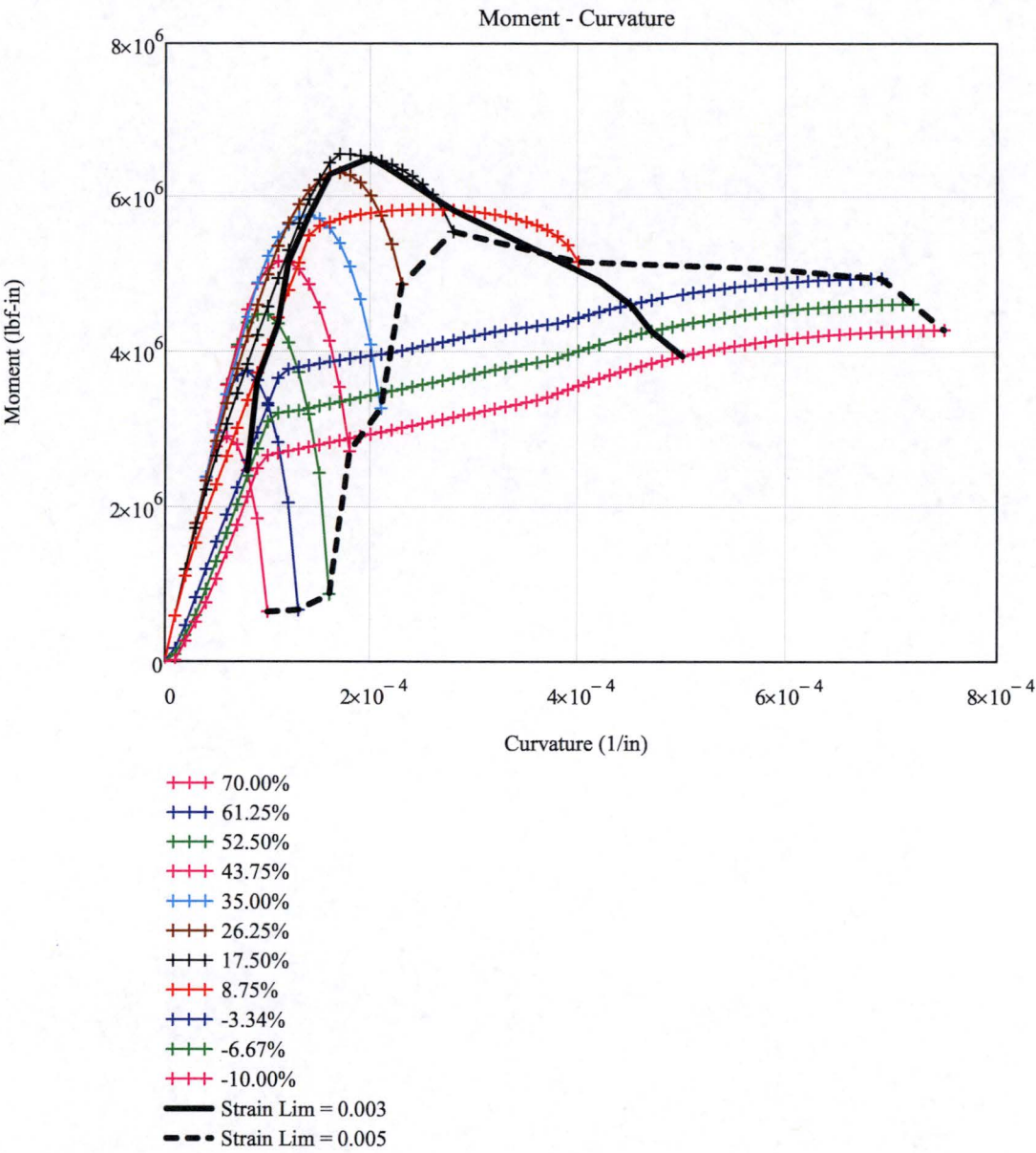
Column(d,i,strain_lim) :=
  account ← 1
  datas_account,1 ← 2
  for r ∈ 3..rows(d)
    if dr,3 ≠ dr-1,3
      datas_account,2 ← r - 1
      account ← account + 1
      datas_account,1 ← r
  datas_account,2 ← rows(d)
  sub ← submatrix(d,1,1,1,cols(d))
  out ← submatrix(d,datas_i,1,datas_i,2,1,cols(d))
  for j ∈ 1..rows(out)
    if [(outj,2 ≠ 0 ∧ sign(outj,2) = sign(outj,1)) ∨ outj,1 = 0]
      p2 ← submatrix(out,j,j,1,cols(d))
      sub ← stack(sub,p2)
    sub ← sub otherwise
  cutoff2 ← 0
  for i ∈ 2..rows(sub)
    cutoff2 ← i - 1 if (subi,6 > strain_lim) ∧ (cutoff2 = 0)
  cutoff2 ← rows(sub) if cutoff2 = 0
  cutoff1 ← 2
  cutoff1 ← 2 if sub2,1 = 0
  otherwise
    i ← 2
    while subi,5 > strain_lim
      cutoff1 ← i + 1
      i ← i + 1
  return stack(submatrix(sub,1,1,1,cols(sub)),submatrix(sub,cutoff1,cutoff2,1,cols(sub)))

StrainLim(limit) :=
  StrainLim ← ("curvature" "moment" "Slip Rotation" "P/Ag*fc")
  for f ∈ 1..rows(fv)
    StrainLimf+1,1 ← Column(data,f,limit) rows(Column(data,f,limit)(1)), 1
    StrainLimf+1,2 ← Column(data,f,limit) rows(Column(data,f,limit)(1)), 2
    StrainLimf+1,3 ← Column(data,f,limit) rows(Column(data,f,limit)(1)), 9
    StrainLimf+1,4 ←  $\frac{fv_f}{A_g \cdot f_c}$ 
  return StrainLim

```

Moment - Curvature curves for different axial forces

```
plt := 1..12      plot_index_plt := | plt if plt ≤ rows(fv)
                               | 1 otherwise
```



Moment demand

$$\text{Moment_Sec} := 322.26 \frac{\text{kip} \cdot \text{ft}}{\text{ft}}$$

$$\text{Moment_Sec} = 322260 \frac{\text{lbf} \cdot \text{in}}{\text{in}}$$

$$\text{Moment} := \text{Moment_Sec} \cdot b_{\text{col}}$$

$$\text{Moment} = 3.867 \times 10^6 \cdot \text{lbf} \cdot \text{in}$$

Axial load demand

$$\text{Axial} := -140.77 \frac{\text{kip}}{\text{ft}}$$

$$\text{Axial} = -1.173 \times 10^4 \frac{\text{lbf}}{\text{in}}$$

Total axial load

$$\text{Axial_Sec} := \text{Axial} \cdot b_{\text{col}}$$

$$\text{Axial_Sec} = -140770 \text{ lbf}$$

Maximum axial load

$$\text{Max_axial} := A_g \cdot (f_c)$$

$$\text{Max_axial} = 1488000 \text{ lbf}$$

Calculated percent tension or compression of $A_g \cdot f_{pc}$

$$\text{Percent} := \frac{\text{Axial_Sec}}{\text{Max_axial}}$$

$$\text{Percent} = -0.095$$

Percent compression or tension See below for options, tension is negative

$$\text{Axial_p} := -10$$

Stress level

$$\text{ap} := \begin{cases} 1 & \text{if } \text{Axial_p} = 70 \\ 2 & \text{if } \text{Axial_p} = 61.25 \\ 3 & \text{if } \text{Axial_p} = 52.50 \\ 4 & \text{if } \text{Axial_p} = 43.75 \\ 5 & \text{if } \text{Axial_p} = 35.00 \\ 6 & \text{if } \text{Axial_p} = 26.25 \\ 7 & \text{if } \text{Axial_p} = 17.50 \\ 8 & \text{if } \text{Axial_p} = 8.75 \\ 10 & \text{if } \text{Axial_p} = -3.34 \\ 11 & \text{if } \text{Axial_p} = -6.67 \\ 12 & \text{if } \text{Axial_p} = -10 \end{cases}$$

$$\text{ap} = 12$$

Slope of linear moment curvature plot

$$m_{ap} := \frac{\left[\left(\text{Column}(\text{data}, \text{plot_index}_{ap}, \text{lim})^{(2)} \right)_4 - \left(\text{Column}(\text{data}, \text{plot_index}_{ap}, \text{lim})^{(2)} \right)_3 \right]}{\left[\left(\text{Column}(\text{data}, \text{plot_index}_{ap}, \text{lim})^{(1)} \right)_4 - \left(\text{Column}(\text{data}, \text{plot_index}_{ap}, \text{lim})^{(1)} \right)_3 \right]}$$

$$m_{ap} \cdot (\text{lbf} \cdot \text{in}^2) = 2.477 \times 10^{10} \cdot \text{lbf} \cdot \text{in}^2$$

Linear curvature parameters

Linear strain energy

$$L_Area_{ap} := \frac{\text{Moment}^2}{\left(2 \cdot m_{ap} \cdot \text{lbf} \cdot \text{in}^2 \right)}$$

$$L_Area_{ap} = 302 \text{ lbf}$$

Linear curvature at moment

$$L_Cur_{ap} := \frac{\text{Moment}}{m_{ap} \cdot \text{lbf} \cdot \text{in}^2}$$

$$L_Cur_{ap} = 1.561 \times 10^{-4} \cdot \frac{1}{\text{in}}$$

Curvature points

$$w := \begin{pmatrix} 0 \\ L_Cur_{ap} \cdot \text{in} \end{pmatrix}$$

$$w = \begin{pmatrix} 0 \\ 1.561 \times 10^{-4} \end{pmatrix}$$

Moment points

$$L_Mom_p(w) := m_{ap} \cdot w$$

$$L_Mom_p(w) = \begin{pmatrix} 0 \\ 3.867 \times 10^6 \end{pmatrix}$$

Max number of trapezoids to add when calculating moment under non-linear moment curvature curve

$$c_{max} := 19$$

Variables to calculate area under moment-curvature plot that represent width (b) and heights (h) of trapezoids

Height (Moment)

$$h1_{ap} := \text{Column}(\text{data}, \text{plot_index}_{ap}, \text{lim})^{(2)}$$

$$h2_{ap} := \text{Column}(\text{data}, \text{plot_index}_{ap}, \text{lim})^{(2)}$$

Width (Curvature)

$$b1_{ap} := \text{Column}(\text{data}, \text{plot_index}_{ap}, \text{lim})^{(1)}$$

$$b2_{ap} := \text{Column}(\text{data}, \text{plot_index}_{ap}, \text{lim})^{(1)}$$

Area under moment-curvature plot, based on summing trapezoidal areas

$$NL_Area_{ap} := \sum_{k=3}^{c_{max}} \left[\frac{1}{2} \left[\left(h1_{ap} \right)_k \cdot \text{lbf} \cdot \text{in} + \left(h2_{ap} \right)_{k-1} \cdot \text{lbf} \cdot \text{in} \right] \left[\left(b1_{ap} \right)_k \cdot \frac{1}{\text{in}} - \left(b2_{ap} \right)_{k-1} \cdot \frac{1}{\text{in}} \right] \right]$$

$$NL_Area_{ap} = 310 \text{ lbf}$$

Non-linear Curvature

$$NL_Cur_{ap} := \left(\text{Column}(\text{data}, \text{plot_index}_{ap}, \text{lim})^{(1)} \right)_{c_{max}} \cdot \frac{1}{\text{in}}$$

$$NL_Cur_{ap} = 1.700 \times 10^{-4} \cdot \frac{1}{\text{in}}$$

Vary c.max to make close to zero

$$NL_Area_{ap} - L_Area_{ap} = 8.609 \text{ lbf}$$

Parameters for plotting purposes

$$y := \begin{bmatrix} 0 \\ \left(\text{Column}(\text{data}, \text{plot_index}_{ap}, \text{lim})^{(2)} \right)_{c_{max}} \end{bmatrix} \quad z := \begin{bmatrix} 0 \\ \text{Moment} \cdot \frac{1}{\text{lbf} \cdot \text{in}} \end{bmatrix}$$

$$\text{Lim_NL}(y) := \begin{pmatrix} NL_Cur_{ap} \cdot \text{in} \\ NL_Cur_{ap} \cdot \text{in} \end{pmatrix} \quad \text{Lim_L}(z) := \begin{pmatrix} L_Cur_{ap} \cdot \text{in} \\ L_Cur_{ap} \cdot \text{in} \end{pmatrix}$$

Depth to neutral axis

$$d_{NA} := na(NL_Cur_{ap}, fv_{ap}, 0.8h_{col})$$

$$d_{NA} = 25.04 \cdot \text{in}$$

Distance for strain in steel calculation $d_{strain} := d_{NA} - \text{cover}$

$$d_{strain} = 21.51 \cdot \text{in}$$

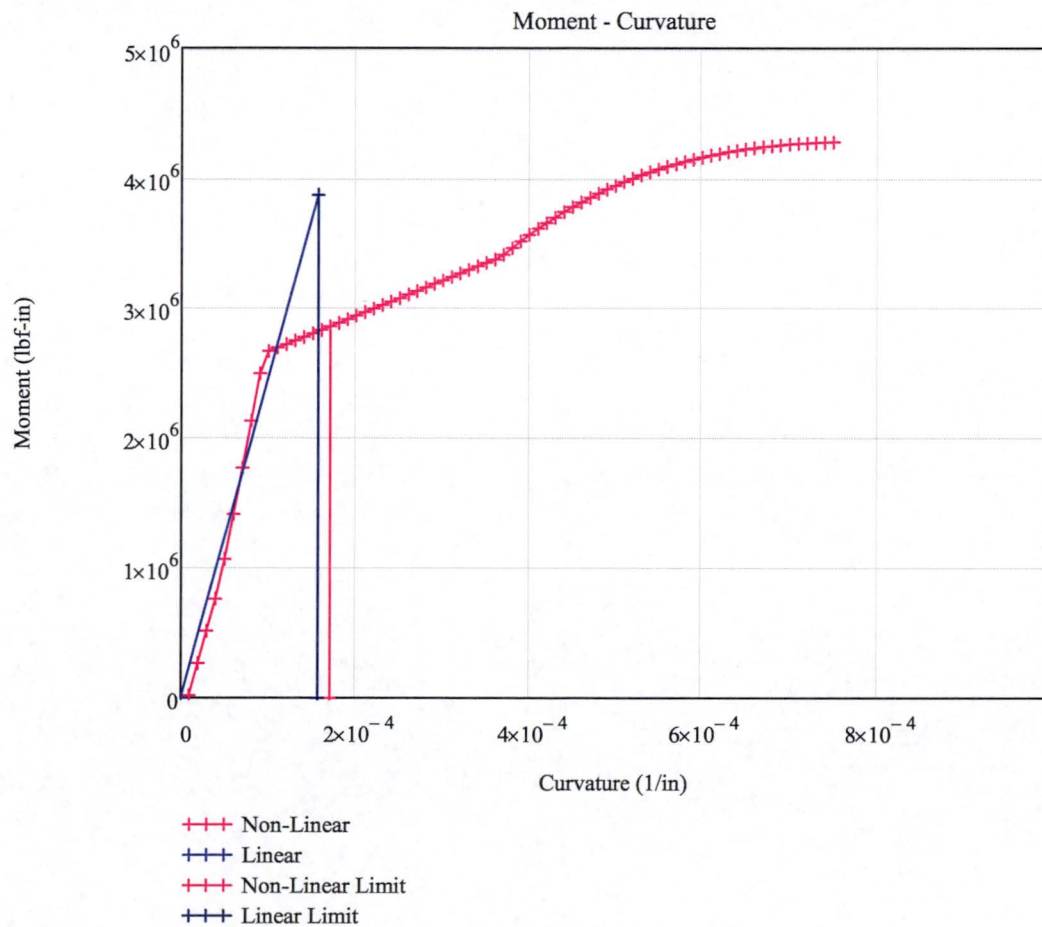
Strain in steel

$$\epsilon_{steel} := NL_Cur_{ap} \cdot d_{strain}$$

$$\epsilon_{steel} = 0.00366$$

Ductility Demand

$$\frac{\epsilon_{steel}}{\epsilon_y} = 1.84$$



Section Cut 4 (Middle Segment) "STANDARD - PLUS" Load Combination**INPUT DEFINITION**

Set starting index of all arrays to 1 (the default is 0)

ORIGIN \equiv 1

Input Reading

	1
1	"Seabrook1"
2	$4 \cdot 10^3$
3	$6 \cdot 10^4$
4	$6 \cdot 10^4$
5	$9 \cdot 10^4$
INPUTS = 6	3.705
7	1.495
8	12
9	36
10	432
11	9.01
12	...

INDEX = 1

colname := INPUTS_{1, INDEX}

colname = "Seabrook1"

Concrete strength

$f'_c := \text{INPUTS}_{2, \text{INDEX}} \cdot \text{psi}$

$f'_c = 4 \cdot \text{ksi}$

Steel yield strength

$f_y := \text{INPUTS}_{3, \text{INDEX}} \cdot \text{psi}$

$f_y = 60 \cdot \text{ksi}$

Ultimate strength of rebar

$f_{su} := \text{INPUTS}_{5, \text{INDEX}} \cdot \text{psi}$

$f_{su} = 90 \cdot \text{ksi}$

cover (to centroid of steel)	$\text{cover} := \text{INPUTS}_{6, \text{INDEX}} \cdot \text{in}$	$\text{cover} = 3.705 \cdot \text{in}$
Width of column	$b_{\text{col}} := \text{INPUTS}_{8, \text{INDEX}} \cdot \text{in}$	$b_{\text{col}} = 12 \cdot \text{in}$
Height of column	$h_{\text{col}} := \text{INPUTS}_{9, \text{INDEX}} \cdot \text{in}$	$h_{\text{col}} = 36 \cdot \text{in}$
Gross Area	$A_g := \text{INPUTS}_{10, \text{INDEX}} \cdot \text{in}^2$	$A_g = 432 \cdot \text{in}^2$
Area of longitudinal bar	$a_{\text{bar}} := \text{INPUTS}_{13, \text{INDEX}} \cdot \text{in}^2$	$a_{\text{bar}} = 1.56 \cdot \text{in}^2$
Diameter of bar	$d_{\text{bar}} := \text{INPUTS}_{14, \text{INDEX}} \cdot \text{in}$	$d_{\text{bar}} = 1.41 \cdot \text{in}$
Area of longitudinal steel	$A_{sL} := \text{INPUTS}_{18, \text{INDEX}} \cdot \text{in}^2$	$A_{sL} = 9.36 \cdot \text{in}^2$
Young's modulus of steel	$E_s := \text{INPUTS}_{20, \text{INDEX}} \cdot \text{psi}$	$E_s = 2.9 \times 10^4 \cdot \text{ksi}$
Ultimate strain of rebar	$\epsilon_{\text{su}} := \text{INPUTS}_{21, \text{INDEX}}$	$\epsilon_{\text{su}} = 0.07$
Modulus of strain hardening [O-2]	$E_{\text{sh}} := \text{INPUTS}_{22, \text{INDEX}} \cdot \text{psi}$	$E_{\text{sh}} = 1.16 \times 10^3 \cdot \text{ksi}$
Strain at strain hardening [O-3]	$\epsilon_{\text{sh}} := \text{INPUTS}_{23, \text{INDEX}}$	$\epsilon_{\text{sh}} = 8 \times 10^{-3}$
Young's modulus of concrete	$E_c := \text{INPUTS}_{24, \text{INDEX}} \cdot \text{psi}$	$E_c = 3.605 \times 10^3 \cdot \text{ksi}$
Poisson's ratio	$\nu := \text{INPUTS}_{25, \text{INDEX}}$	$\nu = 0.17$
Shear modulus of concrete	$G_c := \text{INPUTS}_{26, \text{INDEX}} \cdot \text{psi}$	$G_c = 1.541 \times 10^3 \cdot \text{ksi}$
Shear modification factor Table 2.4 of [O-4]	$\alpha := \text{INPUTS}_{27, \text{INDEX}}$	$\alpha = 1.185$
Torsional Constant Table 2.5 of [O-5]	$J := \text{INPUTS}_{28, \text{INDEX}} \cdot \text{in}^4$	$J = 1.639 \times 10^4 \cdot \text{in}^4$

Crack section index

crack := INPUTS_{140, INDEX}

crack = "yes"

Locate the longitudinal bars in the wall

bars := augment(submatrix(INPUTS, 40, 59, INDEX, INDEX), submatrix(INPUTS, 60, 79, INDEX, INDEX))·in

Area of bars

$a_{\text{bar}} := \text{submatrix}(\text{INPUTS}, 80, 99, \text{INDEX}, \text{INDEX}) \cdot \text{in}^2$

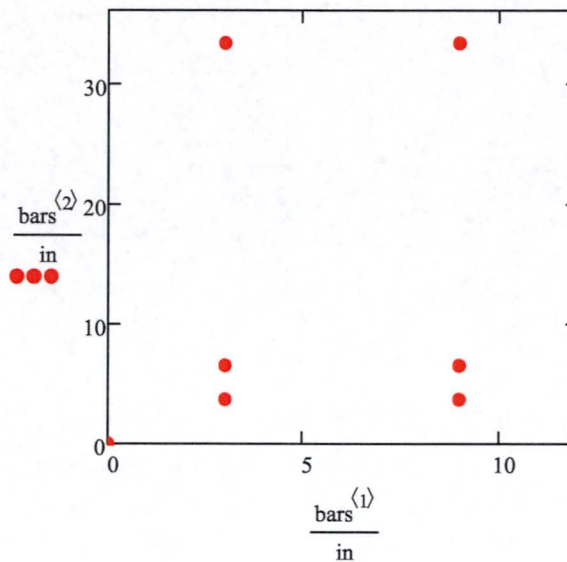
Diameter of bars

$d_{\text{bar}} := \text{submatrix}(\text{INPUTS}, 100, 119, \text{INDEX}, \text{INDEX}) \cdot \text{in}$

index of bars

b := 1..20

Reinforcement Location



END OF INPUT

SECTION PROPERTIES

Elastic properties of uncracked cross section

$$I_{g1} := \frac{1}{12} \cdot b_{col} \cdot h_{col}^3$$

$$I_{g1} = 4.666 \times 10^4 \cdot \text{in}^4$$

$$I_{g2} := \frac{1}{12} \cdot h_{col} \cdot b_{col}^3$$

$$I_{g2} = 5.184 \times 10^3 \cdot \text{in}^4$$

$$A_v := b_{col} \cdot h_{col}$$

$$A_v = 3 \text{ ft}^2$$

Transverse Shear Stiffness

$$K_v := \frac{G_c \cdot A_v}{\alpha}$$

$$K_v = 5.614 \times 10^8 \cdot \text{lb} \cdot \text{f}$$

Flexural Stiffness

$$EI_2 := E_c \cdot I_{g2}$$

$$EI_2 = 1.869 \times 10^{10} \cdot \text{lb} \cdot \text{f} \cdot \text{in}^2$$

Axial Stiffness

$$EA := E_c \cdot A_g$$

$$EA = 1.557 \times 10^9 \cdot \text{lb} \cdot \text{f}$$

Torsional Stiffness

$$GJ := G_c \cdot J$$

$$GJ = 2.524 \times 10^{10} \cdot \text{lb} \cdot \text{f} \cdot \text{in}^2$$

CONCRETE MODEL

Peak strain of unconfined concrete
in compression assumed to be

$$\epsilon_{co} := 0.002$$

$$\epsilon_{co} = 2 \times 10^{-3}$$

From Table 1 of Karthik and Mander [O-2]

Ultimate strain of
unconfined concrete in
compression

$$\epsilon_{c1} := 0.0036$$

Failure strain of unconfined
concrete in compression

$$\epsilon_{sp} := 0.012 - 7 \cdot 10^{-7} \cdot \frac{f_c}{\text{psi}}$$

$$\epsilon_{sp} = 9.2 \times 10^{-3}$$

Peak strain of concrete in
tension

$$\epsilon_{to} := -0.1 \cdot \epsilon_{co}$$

$$\epsilon_{to} = -2 \times 10^{-4}$$

Concrete tensile strength

$$f_t := 7.5 \cdot \sqrt{\frac{f_c}{\text{psi}}} \cdot \text{psi}$$

$$f_t = 474.342 \text{ psi}$$

Use Cornelissen, Hordijk and Reinhardt (1986) to determine ultimate tension strain [O-6]

[O-6] Fig 6

$$\delta_o := 160 \mu\text{m}$$

[O-6] Eq 1

$$\sigma t(\delta) := \left[1 + \left(\frac{3 \cdot \delta}{\delta_o} \right)^3 \right] \cdot e^{-6.93 \cdot \frac{\delta}{\delta_o}}$$

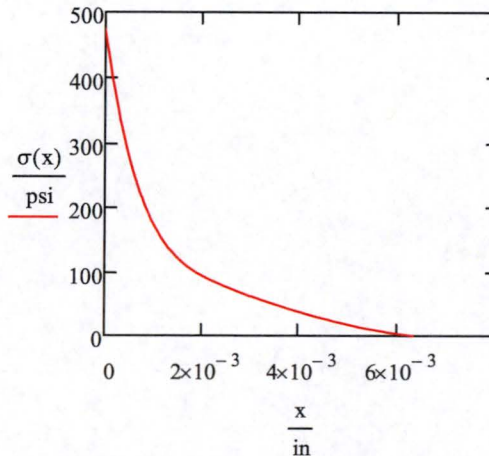
$$\sigma(\delta) := f_t \cdot \left[\sigma t(\delta) - \frac{\delta}{\delta_o} \cdot \sigma t(\delta_o) \right]$$

$$\epsilon_{cr} := \frac{f_t}{E_c}$$

$$\epsilon_{cr} = 1.316 \times 10^{-4}$$

$$x := 0 \mu\text{m}, 1 \mu\text{m}.. 160 \mu\text{m}$$

Tension Stress-Strain Curve



Fracture energy

$$g_f := \int_0^{\delta_o} \sigma(x) dx$$

$$g_f = 0.582 \cdot \frac{\text{lbf}}{\text{in}}$$

From Table 1 of Karthik and Mander [O-2]:

Failure strain of
concrete in tension

$$\epsilon_u := \frac{-18}{\text{in}} \cdot \frac{g_f}{5 \cdot f_t}$$

$$\epsilon_u = -4.415 \times 10^{-3}$$

Ultimate strain of
concrete in tension

$$\epsilon_{t1} := \frac{2 \cdot \epsilon_u}{9}$$

$$\epsilon_{t1} = -9.812 \times 10^{-4}$$

Ultimate stress of concrete in tension

$$f_{t1} := \frac{f_t}{3}$$

$$f_{t1} = 158.114 \cdot \text{psi}$$

Tension stress-strain curve, [O-2] Eq 1, 2 & 3

$$f_{ct}(\epsilon_c) := -1 \cdot \begin{cases} f_t \cdot \left[1 - \left(1 - \frac{\epsilon_c}{\epsilon_{to}} \right)^{\frac{E_c \cdot \epsilon_{to}}{-f_t}} \right] & \text{if } \epsilon_{to} \leq \epsilon_c \leq 0 \\ f_t - \left(\frac{f_t - f_{t1}}{\frac{\epsilon_{t1}}{\epsilon_{to}} - 1} \right) \cdot \left(\frac{\epsilon_c}{\epsilon_{to}} - 1 \right) & \text{if } \epsilon_{t1} \leq \epsilon_c < \epsilon_{to} \\ f_{t1} \cdot \left(\frac{\epsilon_c - \epsilon_u}{\epsilon_{t1} - \epsilon_u} \right) & \text{if } \epsilon_u \leq \epsilon_c < \epsilon_{t1} \\ 0 & \text{if } \epsilon_c < \epsilon_u \end{cases}$$

[O-2] Table 1

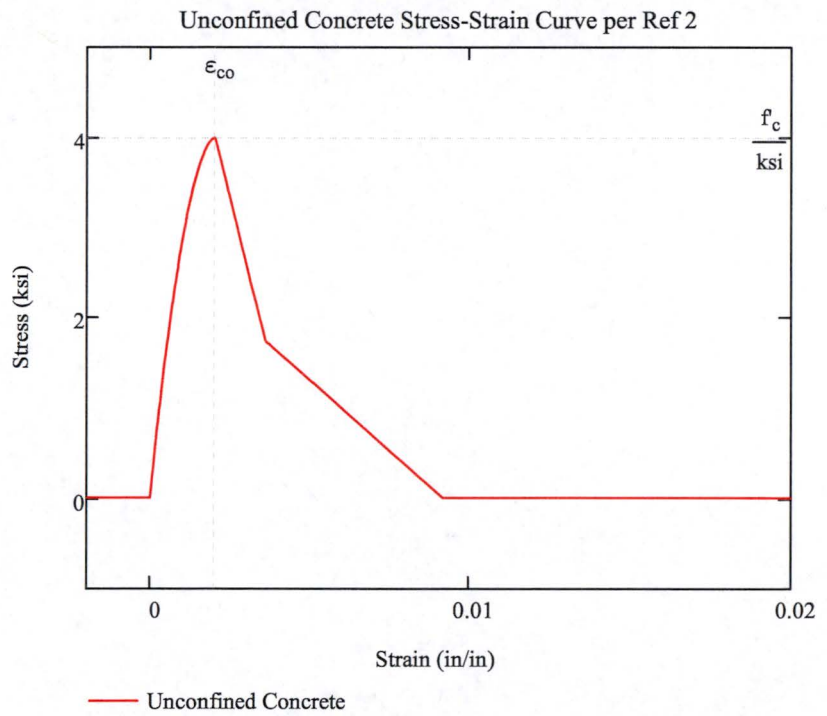
$$f_{c1} := 1.74 \text{ksi}$$

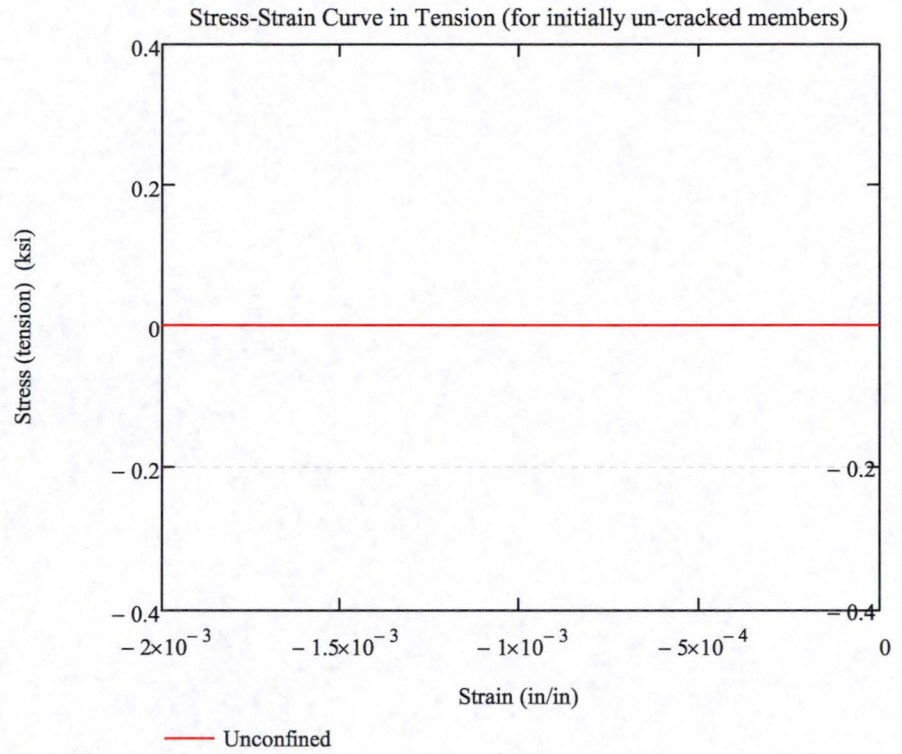
$$\text{mult_crack} := \begin{cases} 1 & \text{if crack} = \text{"no"} \\ 0 & \text{if crack} = \text{"yes"} \end{cases}$$

$$\text{mult_crack} = 0$$

Unconfined stress-strain curve [O-2] Eq 1, 2 & 3

$$f_c(\epsilon_c) := \begin{cases} f_{ct}(\epsilon_c) \cdot \text{mult_crack} & \text{if } \frac{\epsilon_c}{\epsilon_{co}} < 0 \\ f_c \cdot \left[1 - \left(\left| 1 - \frac{\epsilon_c}{\epsilon_{co}} \right| \right)^{\frac{E_c \cdot \epsilon_{co}}{f_c}} \right] & \text{if } 0 \leq \frac{\epsilon_c}{\epsilon_{co}} < 1 \\ f_c - \left(\frac{f_c - f_{cl}}{\frac{\epsilon_{cl}}{\epsilon_{co}} - 1} \right) \cdot \left(\frac{\epsilon_c}{\epsilon_{co}} - 1 \right) & \text{if } 1 \leq \frac{\epsilon_c}{\epsilon_{co}} < \frac{\epsilon_{cl}}{\epsilon_{co}} \\ f_{cl} \cdot \left(\frac{\frac{\epsilon_c}{\epsilon_{co}} - \frac{\epsilon_{sp}}{\epsilon_{co}}}{\frac{\epsilon_{cl}}{\epsilon_{co}} - \frac{\epsilon_{sp}}{\epsilon_{co}}} \right) & \text{if } \frac{\epsilon_{cl}}{\epsilon_{co}} \leq \frac{\epsilon_c}{\epsilon_{co}} < \frac{\epsilon_{sp}}{\epsilon_{co}} \\ 0 & \text{if } \frac{\epsilon_{sp}}{\epsilon_{co}} \leq \frac{\epsilon_c}{\epsilon_{co}} \end{cases}$$





Modified confinement per Roy and Sozen [O-7] Eq 5.3

$$\epsilon_{50u} := \frac{3\text{psi} + 0.002 \cdot f_c}{f_c - 1000\text{psi}} \quad \epsilon_{50u} = 3.667 \times 10^{-3}$$

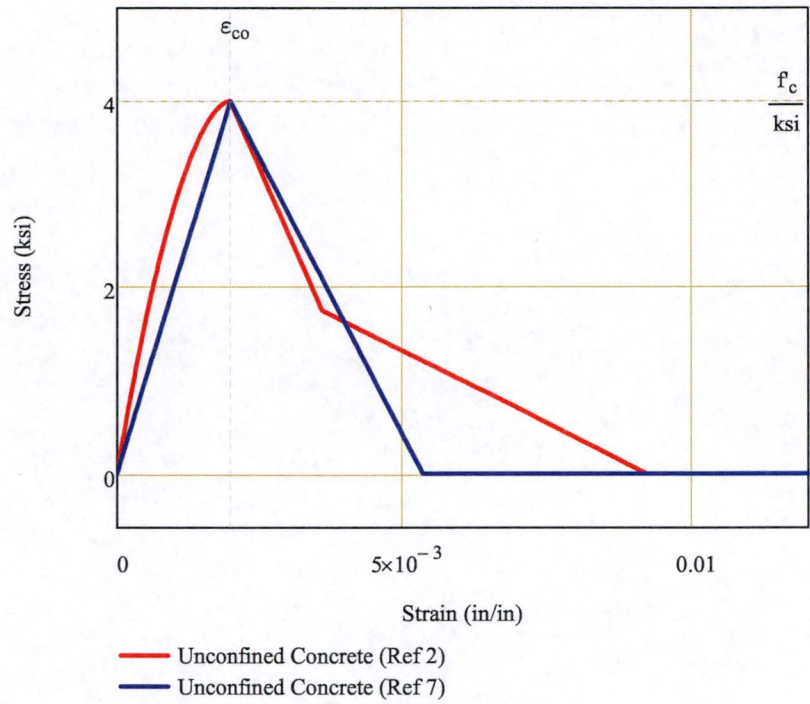
[O-7]

$$m_{\text{RoySozen}} := \frac{-0.5 \cdot f_c}{\epsilon_{50u} - 0.002} \quad m_{\text{RoySozen}} = -1.2 \times 10^3 \cdot \text{ksi}$$

$$b_{\text{RoySozen}} := 0.002 \cdot (-m_{\text{RoySozen}}) + (f_c) \quad b_{\text{RoySozen}} = 6.4 \cdot \text{ksi}$$

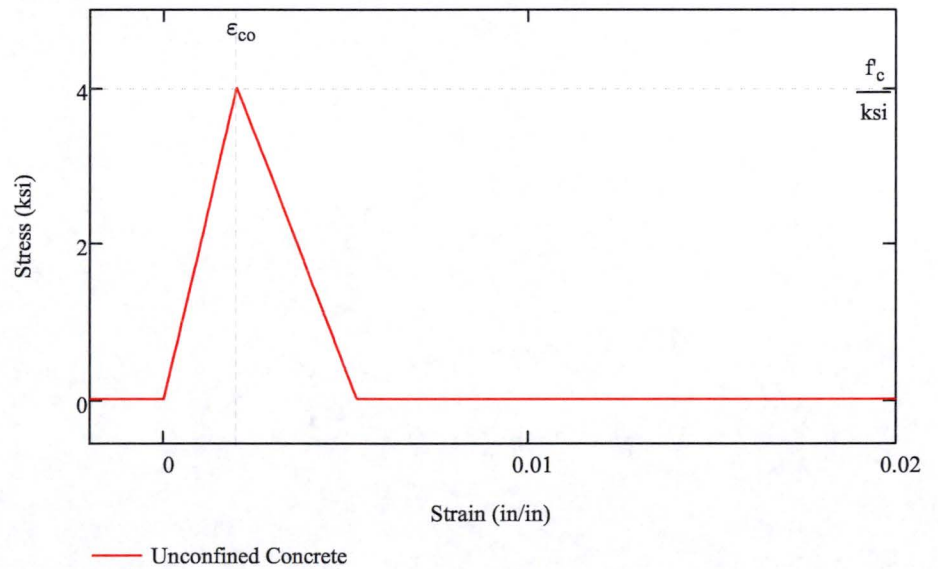
$$f_{c_RoySozen}(\epsilon_c) := \begin{cases} f_{ct}(\epsilon_c) \cdot \text{mult_crack} & \text{if } \epsilon_c < 0 \\ \frac{f_c}{0.002} \cdot \epsilon_c & \text{if } 0 \leq \epsilon_c < 0.002 \\ \max(0, m_{\text{RoySozen}} \cdot \epsilon_c + b_{\text{RoySozen}}) & \text{if } 0.002 \leq \epsilon_c \end{cases}$$

Comparison of Mander (Ref 2) and Sezen (Ref 7) Concrete Models



$$f_c(\epsilon_c) := \begin{cases} f_{c_RoySozen}(\epsilon_c) & \text{if } INPUTS_{34, INDEX} = "RoySozen" \\ f_c(\epsilon_c) & \text{otherwise} \end{cases}$$

Concrete Model Used for Evaluation



REBAR MODEL

Stress - Strain curve of rebar

[O-2] Eq 5

$$P := \begin{cases} 1 & \text{if } f_{su} = f_y \\ \frac{E_{sh} \cdot (\epsilon_{su} - \epsilon_{sh})}{f_{su} - f_y} & \text{otherwise} \end{cases} \quad P = 2.397$$

[O-2] Eq 4.

$$f_{s_t}(\epsilon_s) := \left[\frac{E_s \cdot |\epsilon_s|}{\left[1 + \left(\left| \frac{E_s \cdot |\epsilon_s|}{f_y} \right| \right)^{20} \right]^{0.05}} + (f_{su} - f_y) \cdot \left[1 - \frac{(|\epsilon_{su} - |\epsilon_s||)^P}{\left[(|\epsilon_{su} - \epsilon_{sh}|)^{20 \cdot P} + (|\epsilon_{su} - |\epsilon_s||)^{20 \cdot P} \right]^{0.05}} \right] \right]$$

Based on the recommendation of Sezen and Setzler ([O-8], and [O-3]), the steel stress strain curve is modified slightly to make sure the plateau region as a slight positive slope

Slope of strain hardening

$$\alpha_s := 0.02$$

Adjust f_y such that area under the plateau stays the same

Steel yield strength

$$f_y = 60 \cdot \text{ksi}$$

Modified yield strength

$$f_{y'} := f_y - \frac{E_s \cdot \alpha_s \cdot \epsilon_{sh}}{2} \quad f_{y'} = 57.68 \cdot \text{ksi}$$

Yield strain

$$\epsilon_y := \frac{f_{y'}}{E_s} \quad \epsilon_y = 1.989 \times 10^{-3}$$

[O-3] strain at strain hardening

$$\epsilon_{sh} = 8 \times 10^{-3}$$

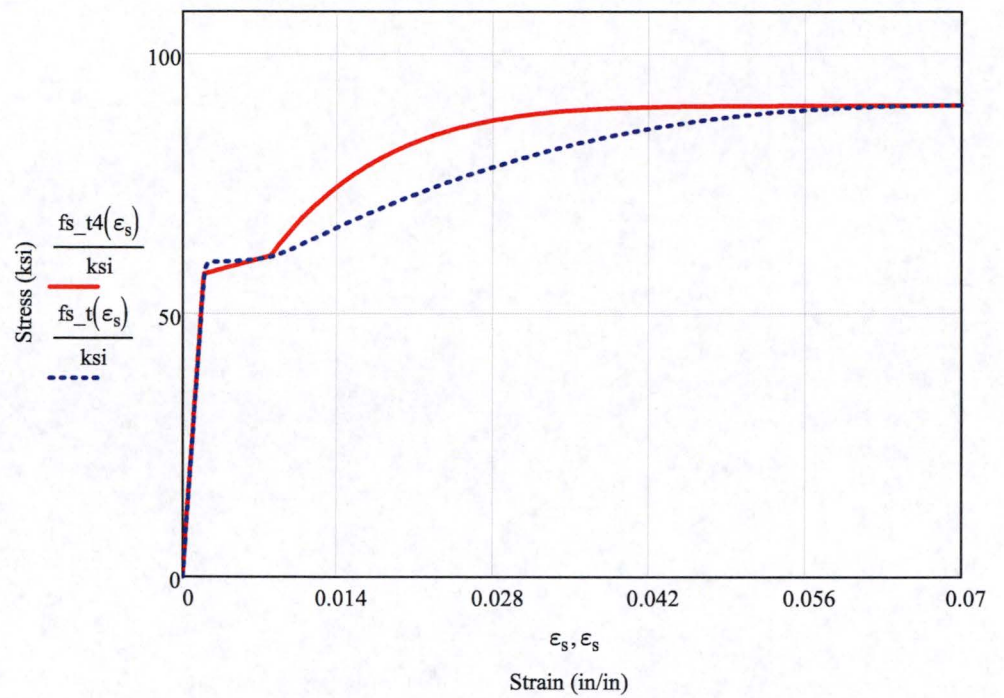
Steel material model [O-3] Eq 3.3

$$\epsilon_{cross} := \frac{f_y - f_{y'}}{\alpha_s \cdot E_s} + \epsilon_y = 5.989 \times 10^{-3}$$

$$f_{sh} := \begin{cases} f_{y'} + (\epsilon_{sh} - \epsilon_y) \cdot \alpha_s \cdot E_s & \text{if } P \neq 1 \\ \left[f_{y'} + (\epsilon_{cross} - \epsilon_y) \cdot \alpha_s \cdot E_s \right] & \text{otherwise} \end{cases} \quad f_{sh} = 61.166 \cdot \text{ksi}$$

Steel curve from Setzler thesis ([O-3]) (with correction per sezen for plateau region)

$$f_{s_t4}(\epsilon_s) := \begin{cases} \text{if } P \neq 1 \\ \begin{cases} E_s \cdot \epsilon_s & \text{if } \epsilon_s \leq \epsilon_y \\ f_{y'} + (\epsilon_s - \epsilon_y) \cdot \alpha_s \cdot E_s & \text{if } \epsilon_y < \epsilon_s \leq \epsilon_{sh} \\ f_{su} - (f_{su} - f_{sh}) \cdot \left(\frac{\epsilon_s - \epsilon_{su}}{\epsilon_{su} - \epsilon_{sh}} \right)^6 & \text{if } \epsilon_{sh} < \epsilon_s \leq \epsilon_{su} \end{cases} \\ \text{otherwise} \\ \begin{cases} E_s \cdot \epsilon_s & \text{if } \epsilon_s \leq \epsilon_y \\ f_{y'} + (\epsilon_s - \epsilon_y) \cdot \alpha_s \cdot E_s & \text{if } \epsilon_y < \epsilon_s \leq \epsilon_{cross} \\ f_{su} - (f_{su} - f_{sh}) \cdot \left(\frac{\epsilon_s - \epsilon_{su}}{\epsilon_{su} - \epsilon_{sh}} \right)^6 & \text{if } \epsilon_{cross} < \epsilon_s \leq \epsilon_{su} \end{cases} \end{cases}$$



Combined tension and
compression behavior

$$f_s(\epsilon_s) := \begin{cases} -f_{s_t4}(|\epsilon_s|) & \text{if } \epsilon_s \leq 0 \\ 0 & \text{otherwise} \end{cases}$$

$$\epsilon_{s_plot} := -0.2, -0.1999..0.2$$



DUCTILITY CALCULATION

Section inertia of uncracked cross section

$$I_g := \frac{1}{12} \cdot b_{col} \cdot h_{col}^3 + \frac{E_s}{E_c} \cdot \sum_b \left[a_{bar_b} \cdot \left(bars_{b,2} - \frac{h_{col}}{2} \right)^2 \right] \quad I_g = 6.096 \times 10^4 \cdot \text{in}^4$$

Concrete stress at a location (x) given a curvature, and neutral axis

$$\sigma_{conc}(\phi, x, NA) := fc[\phi \cdot (x - NA)]$$

Steel stress in a bar (b) given a curvature and neutral axis

$$\sigma_{steel}(\phi, b, NA) := fs[\phi \cdot (bars_{b,2} - NA)]$$

Given

Integration across the section to combine concrete and steel stresses must equal the applied vertical load independent of the curvature. (integrate by parts to help convergence)

$$\int_0^{h_{col}} b_{col} \cdot \sigma_{conc}(\phi, x, na_test) dx \dots = F_v \\ + \sum_b \left(\sigma_{steel}(\phi, b, na_test) \cdot a_{bar_b} \right)$$

Function to execute the solve block and find the neutral axis location as a function of curvature.

$$na(\phi, F_v, na_test) := \text{Find}(na_test)$$

$$F_{v_plot} := 0 \text{ kip}$$

$$\phi_{plot} := 3 \cdot 10^{-4} \cdot \frac{1}{\text{in}}$$

$$na(\phi_{plot}, F_{v_plot}, 0.8 \cdot h_{col}) = 23.235 \cdot \text{in}$$

$$h_{centroid} := \frac{h_{col}}{2}$$

$$h_{centroid} = 18 \cdot \text{in}$$

Function to solve for the moment about the centroid for a given curvature

$$\text{mom}(\phi, NA, F_v) := \int_0^{h_{col}} b_{col} \cdot \sigma_{conc}(\phi, x, NA) \cdot (x - h_{centroid}) dx \dots \\ + \sum_b \left[\sigma_{steel}(\phi, b, NA) \cdot a_{bar_b} \cdot (bars_{b,2} - h_{centroid}) \right]$$

$$\text{mom}(\phi_{plot}, na(\phi_{plot}, F_{v_plot}, 0.8 h_{col}), F_{v_plot}) = 9.443 \times 10^3 \cdot \text{kip} \cdot \text{in}$$

$$\text{mom}(-\phi_{plot}, na(-\phi_{plot}, F_{v_plot}, 0.2 h_{col}), F_{v_plot}) = -5.871 \times 10^3 \cdot \text{kip} \cdot \text{in}$$

Function to check the resulting axial force

$$\text{chk}(\phi, \text{NA}) := \int_0^{h_{\text{col}}} b_{\text{col}} \cdot \sigma_{\text{conc}}(\phi, x, \text{NA}) dx \dots$$

$$+ \sum_b \left(\sigma_{\text{steel}}(\phi, b, \text{NA}) \cdot a_{\text{bar}_b} \right)$$

$$F_{v_plot} = 0 \cdot \text{kip}$$

$$\text{chk}(\phi_{\text{plot}}, \text{na}(\phi_{\text{plot}}, F_{v_plot}, 0.8h_{\text{col}})) = 0 \cdot \text{kip}$$

$$\text{max_bar} := \text{INPUTS}_{36, \text{INDEX}} \quad \text{max_bar} = 5$$

$$\text{min_bar} := \text{INPUTS}_{37, \text{INDEX}} \quad \text{min_bar} = 1$$

To this point, compression is positive and tension is negative, for computing steel strain and stress, use tension as positive values.

$$\text{steel_strain}(\phi, \text{NA}) := -1 \cdot \begin{cases} \phi \cdot (\text{bars}_{\text{min_bar}, 2} - \text{NA}) & \text{if } \phi \geq 0 \\ \phi \cdot (\text{bars}_{\text{max_bar}, 2} - \text{NA}) & \text{if } \phi < 0 \end{cases}$$

$$\text{steel_stress}(\phi, \text{NA}) := -1 \cdot \begin{cases} \sigma_{\text{steel}}(\phi, \text{min_bar}, \text{NA}) & \text{if } \phi \geq 0 \\ \sigma_{\text{steel}}(\phi, \text{max_bar}, \text{NA}) & \text{if } \phi < 0 \end{cases}$$

$$\text{depth_bar}(\phi) := \begin{cases} \text{bars}_{\text{min_bar}, 2} & \text{if } \phi \geq 0 \\ \text{bars}_{\text{max_bar}, 2} & \text{if } \phi < 0 \end{cases}$$

$$d_b(\phi) := \begin{cases} d_{\text{bar}_{\text{min_bar}}} & \text{if } \phi \geq 0 \\ d_{\text{bar}_{\text{max_bar}}} & \text{if } \phi < 0 \end{cases} \quad d_b(\phi_{\text{plot}}) = 1.41 \cdot \text{in}$$

$$\text{steel_strain}(\phi_{\text{plot}}, \text{na}(\phi_{\text{plot}}, F_{v_plot}, 0.8 \cdot h_{\text{col}})) = 5.859 \times 10^{-3}$$

$$\text{steel_stress}(\phi_{\text{plot}}, \text{na}(\phi_{\text{plot}}, F_{v_plot}, 0.8 \cdot h_{\text{col}})) = 59.925 \cdot \text{ksi}$$

$$\text{fname} := \text{INPUTS}_{124, \text{INDEX}} \quad \text{fname} = "001_Wall_uncracked_file1.txt"$$

Compute moment-curvature curves at various axial load, and curvatures. This requires the following programming loop, which writes results to a text file which is then read back in by this calculation.

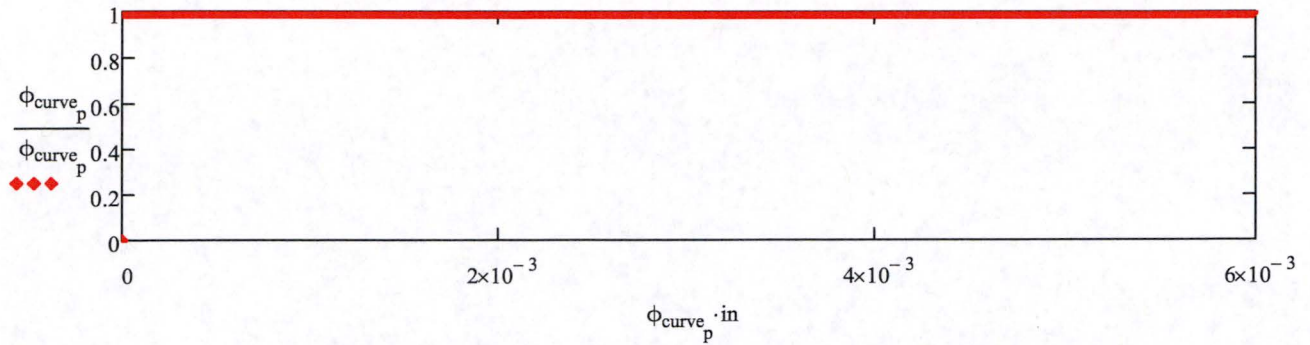
Index of curvatures

$$\text{numinc} := \text{INPUTS}_{139, \text{INDEX}}$$

$$p := 1 \dots \text{numinc}$$

$$\phi_{\text{int}} := \text{INPUTS}_{138, \text{INDEX}} \cdot \frac{1}{\text{in}} \quad \phi_{\text{int}} = 1 \times 10^{-5} \cdot \frac{1}{\text{in}}$$

$$\phi_{\text{curve}_p} := (p - 1) \cdot \phi_{\text{int}}$$



```
fv := submatrix(INPUTS,126,137,INDEX,INDEX)
```

```
fv := | new ← fv1
      | for j ∈ 2..rows(fv)
      |   new ← new if IsString(fvj)
      |   new ← stack(new,fvj) otherwise
      | return new.lbf
```

	1
1	1.21·10 ³
2	1.058·10 ³
3	907.2
4	756
5	604.8
fv = 6	453.6 ·kip
7	302.4
8	151.2
9	0
10	-57.6
11	-115.2
12	-172.8

```
f := 1..rows(fv)
```

Output _{1,1} := "Curvature (1/in)"	Output _{1,5} := "Concrete Strain"	Output _{1,9} := "Slip Rotation (rad)"
Output _{1,2} := "Moment (lbf*in)"	Output _{1,6} := "Concrete Strain"	Output _{1,10} := "Slip (in)"
Output _{1,3} := "Axial Load (lbf)"	Output _{1,7} := "Steel Strain"	Output _{1,11} := ""
Output _{1,4} := "neutral axis (in)"	Output _{1,8} := "Steel Strain"	Output _{1,12} := "LINE"

```
fname = "001_Wall_uncracked_file1.txt"
```

```
exist := "no" on error READPRN(fname)
```

zero(x,y) := 0

out := if exist = "no"

```

APPENDPRN[fname, (OutputT)<1>T]
for f ∈ 1..rows(fv)
  na_last ← ""
  continue ← "yes"
  errorcount ← 0
  for p ∈ 1..numinc
    if continue = "yes"
      M1 ← ϕcurvep · in
      m0 ← [0 on error (mom(ϕcurvep, na(ϕcurvep, fvf, na_last), fvf))]
      mout ← m0
      NA ← (0 on error na(ϕcurvep, fvf, na_last))
      if (m0 = 0 ∨ sign(m0) ≠ sign(ϕcurvep))
        m1 ← [0 on error (mom(ϕcurvep, na(ϕcurvep, fvf, 0in), fvf))]
        m2 ← [0 on error (mom(ϕcurvep, na(ϕcurvep, fvf, sign(ϕcurvep) · 0.5hcol), fvf))]
        m3 ← [0 on error (mom(ϕcurvep, na(ϕcurvep, fvf, sign(ϕcurvep) · 0.9hcol), fvf))]
        if |m1| > max(|m2|, |m3|)
          NA ← (0 on error na(ϕcurvep, fvf, 0in))
          mout ← m1
        if |m2| ≥ max(|m1|, |m3|)
          NA ← (0 on error na(ϕcurvep, fvf, sign(ϕcurvep) · 0.5hcol))
          mout ← m2
        if |m3| ≥ max(|m1|, |m2|)
          NA ← (0 on error na(ϕcurvep, fvf, sign(ϕcurvep) · 0.9hcol))
          mout ← m3
      M2 ←  $\frac{mout}{lbf \cdot in}$ 
      M3 ←  $\frac{fv_f}{lbf}$ 
      M4 ←  $\frac{NA}{in}$ 
      na_last ← NA
      M5 ← ϕcurvep · (0in - NA)
      M6 ← ϕcurvep · (hcol - NA)
      M7 ← ϕcurvep · (barsmin_bar, 2 - NA)

```

```

M8 ←  $\phi_{\text{curve}_p} \cdot (\text{bars}_{\text{max\_bar},2} - \text{NA})$ 
M9 ← 0
M10 ← 0
M11 ← 0
M12 ← "LINE"
errorcount ← errorcount + 1 if (NA = 0) ∨ (sign(mout) ≠ sign( $\phi_{\text{curve}_p}$ )) ∨ (M6 > 0.010)
errorcount ← 0 otherwise
APPENDPRN(fname, MT)
M ← matrix(12, 1, zero)
continue ← "no" if errorcount > 3
"nothing" otherwise

```

```

data := READPRN(fname) if exist = "no"
        exist otherwise

```

	1	2	3
1	"Curvature (1/in)"	"Moment (lbf*in)"	"Axial Load (lbf)"
2	0	0	1.21·10 ⁶
3	1·10 ⁻⁵	9.331·10 ⁵	1.21·10 ⁶
4	2·10 ⁻⁵	1.866·10 ⁶	1.21·10 ⁶
5	3·10 ⁻⁵	2.799·10 ⁶	1.21·10 ⁶
6	4·10 ⁻⁵	3.597·10 ⁶	1.21·10 ⁶
7	5·10 ⁻⁵	3.903·10 ⁶	1.21·10 ⁶
8	6·10 ⁻⁵	3.786·10 ⁶	1.21·10 ⁶
9	7·10 ⁻⁵	3.247·10 ⁶	1.21·10 ⁶
10	8·10 ⁻⁵	2.143·10 ⁶	1.21·10 ⁶
11	9·10 ⁻⁵	0	1.21·10 ⁶
12	1·10 ⁻⁴	0	1.21·10 ⁶
13	1.1·10 ⁻⁴	0	1.21·10 ⁶
14	1.2·10 ⁻⁴	0	1.21·10 ⁶
15	0	0	1.058·10 ⁶
16	1·10 ⁻⁵	9.331·10 ⁵	...

```

data := d ← submatrix(data, 1, 1, 1, 12)
        for i ∈ 2..rows(data<1>)
            d ← d if (datai,2 ≤ 0 ∧ datai,1 ≠ 0)
            d ← stack(d, submatrix(data, i, i, 1, 12)) otherwise
        return d

```


cleandata := APPENDPRN(concat("clean_",fname),data)

cleandata =

	1	2	3
1	"Curvature (1/in)"	"Moment (lbf*in)"	"Axial Load (lbf)"
2	0	0	$1.21 \cdot 10^6$
3	$1 \cdot 10^{-5}$	$9.331 \cdot 10^5$	$1.21 \cdot 10^6$
4	$2 \cdot 10^{-5}$	$1.866 \cdot 10^6$	$1.21 \cdot 10^6$
5	$3 \cdot 10^{-5}$	$2.799 \cdot 10^6$	$1.21 \cdot 10^6$
6	$4 \cdot 10^{-5}$	$3.597 \cdot 10^6$	$1.21 \cdot 10^6$
7	$5 \cdot 10^{-5}$	$3.903 \cdot 10^6$	$1.21 \cdot 10^6$
8	$6 \cdot 10^{-5}$	$3.786 \cdot 10^6$	$1.21 \cdot 10^6$
9	$7 \cdot 10^{-5}$	$3.247 \cdot 10^6$	$1.21 \cdot 10^6$
10	$8 \cdot 10^{-5}$	$2.143 \cdot 10^6$	$1.21 \cdot 10^6$
11	0	0	$1.058 \cdot 10^6$
12	$1 \cdot 10^{-5}$	$9.331 \cdot 10^5$	$1.058 \cdot 10^6$
13	$2 \cdot 10^{-5}$	$1.866 \cdot 10^6$	$1.058 \cdot 10^6$
14	$3 \cdot 10^{-5}$	$2.799 \cdot 10^6$	$1.058 \cdot 10^6$
15	$4 \cdot 10^{-5}$	$3.732 \cdot 10^6$	$1.058 \cdot 10^6$
16	$5 \cdot 10^{-5}$	$4.55 \cdot 10^6$	$1.058 \cdot 10^6$
17	$6 \cdot 10^{-5}$	$4.968 \cdot 10^6$	$1.058 \cdot 10^6$
18	$7 \cdot 10^{-5}$	$5.042 \cdot 10^6$	$1.058 \cdot 10^6$
19	$8 \cdot 10^{-5}$	$4.8 \cdot 10^6$	$1.058 \cdot 10^6$
20	$9 \cdot 10^{-5}$	$4.226 \cdot 10^6$	$1.058 \cdot 10^6$
21	$1 \cdot 10^{-4}$	$3.233 \cdot 10^6$	$1.058 \cdot 10^6$
22	$1.1 \cdot 10^{-4}$	$1.469 \cdot 10^6$	$1.058 \cdot 10^6$
23	0	0	$9.072 \cdot 10^5$
24	$1 \cdot 10^{-5}$	$9.331 \cdot 10^5$	$9.072 \cdot 10^5$
25	$2 \cdot 10^{-5}$	$1.866 \cdot 10^6$	$9.072 \cdot 10^5$
26	$3 \cdot 10^{-5}$	$2.799 \cdot 10^6$	$9.072 \cdot 10^5$
27	$4 \cdot 10^{-5}$	$3.732 \cdot 10^6$	$9.072 \cdot 10^5$
28	$5 \cdot 10^{-5}$	$4.666 \cdot 10^6$	$9.072 \cdot 10^5$
29	$6 \cdot 10^{-5}$	$5.494 \cdot 10^6$	$9.072 \cdot 10^5$
30	$7 \cdot 10^{-5}$	$5.916 \cdot 10^6$	$9.072 \cdot 10^5$
31	$8 \cdot 10^{-5}$	$6.051 \cdot 10^6$	$9.072 \cdot 10^5$
32	$9 \cdot 10^{-5}$	$5.993 \cdot 10^6$	$9.072 \cdot 10^5$
33	$1 \cdot 10^{-4}$	$5.701 \cdot 10^6$	$9.072 \cdot 10^5$
34	$1.1 \cdot 10^{-4}$	$5.167 \cdot 10^6$	$9.072 \cdot 10^5$
35	$1.3 \cdot 10^{-4}$	$3.115 \cdot 10^6$	$9.072 \cdot 10^5$
36	0	0	$7.56 \cdot 10^5$
37	$1 \cdot 10^{-5}$	$9.331 \cdot 10^5$...

Strain limit

strain_lim := 0.005

lim := strain_lim

lim = 5×10^{-3}

```

Column(d,i,strain_lim) :=
  account ← 1
  datas_account,1 ← 2
  for r ∈ 3..rows(d)
    if dr,3 ≠ dr-1,3
      datas_account,2 ← r - 1
      account ← account + 1
      datas_account,1 ← r
  datas_account,2 ← rows(d)
  sub ← submatrix(d,1,1,1,cols(d))
  out ← submatrix(d,datasi,1,datasi,2,1,cols(d))
  for j ∈ 1..rows(out)
    if [(outj,2 ≠ 0 ∧ sign(outj,2) = sign(outj,1)) ∨ outj,1 = 0]
      p2 ← submatrix(out,j,j,1,cols(d))
      sub ← stack(sub,p2)
    sub ← sub otherwise
  cutoff2 ← 0
  for i ∈ 2..rows(sub)
    cutoff2 ← i - 1 if (subi,6 > strain_lim) ∧ (cutoff2 = 0)
  cutoff2 ← rows(sub) if cutoff2 = 0
  cutoff1 ← 2
  cutoff1 ← 2 if sub2,1 = 0
  otherwise
    i ← 2
    while subi,5 > strain_lim
      cutoff1 ← i + 1
      i ← i + 1
  return stack(submatrix(sub,1,1,1,cols(sub)),submatrix(sub,cutoff1,cutoff2,1,cols(sub)))

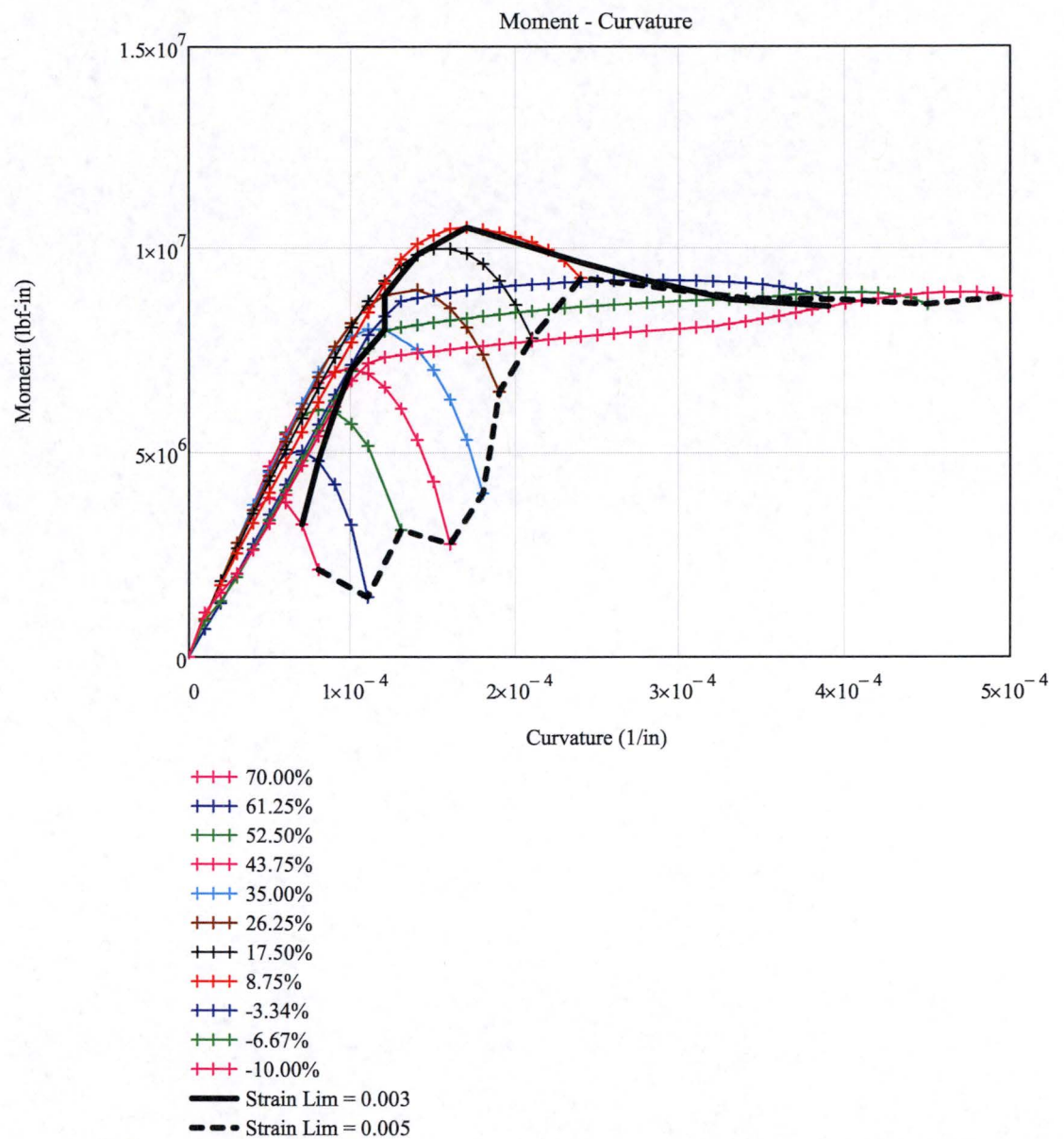
StrainLim(limit) :=
  StrainLim ← ("curvature" "moment" "Slip Rotation" "P/Ag*fc")
  for f ∈ 1..rows(fv)
    StrainLimf+1,1 ← Column(data,f,limit)rows(Column(data,f,limit)(1),1
    StrainLimf+1,2 ← Column(data,f,limit)rows(Column(data,f,limit)(1),2
    StrainLimf+1,3 ← Column(data,f,limit)rows(Column(data,f,limit)(1),9
    StrainLimf+1,4 ←  $\frac{fv_f}{A_g \cdot f_c}$ 
  return StrainLim

```

Moment - Curvature curves for different axial forces

```

plt := 1..12
plot_index_plt := | plt if plt ≤ rows(fv)
                  | 1 otherwise
    
```



Moment demand

$$\text{Moment_Sec} := 911.53 \frac{\text{kip} \cdot \text{ft}}{\text{ft}}$$

$$\text{Moment_Sec} = 911530 \cdot \frac{\text{lbf} \cdot \text{in}}{\text{in}}$$

$$\text{Moment} := \text{Moment_Sec} \cdot b_{\text{col}}$$

$$\text{Moment} = 1.094 \times 10^7 \cdot \text{lbf} \cdot \text{in}$$

Axial load demand

$$\text{Axial} := 11.41 \frac{\text{kip}}{\text{ft}}$$

$$\text{Axial} = 950.833 \cdot \frac{\text{lbf}}{\text{in}}$$

Total axial load

$$\text{Axial_Sec} := \text{Axial} \cdot b_{\text{col}}$$

$$\text{Axial_Sec} = 11410 \text{ lbf}$$

Maximum axial load

$$\text{Max_axial} := A_g \cdot (f_c)$$

$$\text{Max_axial} = 1728000 \text{ lbf}$$

Calculated percent tension or compression of $A_g \cdot f_{pc}$

$$\text{Percent} := \frac{\text{Axial_Sec}}{\text{Max_axial}}$$

$$\text{Percent} = 6.603 \times 10^{-3}$$

Percent compression or tension See below for options, tension is negative

$$\text{Axial_p} := -3.34$$

Stress level

$$\text{ap} := \begin{cases} 1 & \text{if } \text{Axial_p} = 70 \\ 2 & \text{if } \text{Axial_p} = 61.25 \\ 3 & \text{if } \text{Axial_p} = 52.50 \\ 4 & \text{if } \text{Axial_p} = 43.75 \\ 5 & \text{if } \text{Axial_p} = 35.00 \\ 6 & \text{if } \text{Axial_p} = 26.25 \\ 7 & \text{if } \text{Axial_p} = 17.50 \\ 8 & \text{if } \text{Axial_p} = 8.75 \\ 10 & \text{if } \text{Axial_p} = -3.34 \\ 11 & \text{if } \text{Axial_p} = -6.67 \\ 12 & \text{if } \text{Axial_p} = -10 \end{cases}$$

$$\text{ap} = 10$$

$$\text{ap} := 9$$

Slope of linear moment curvature plot

$$m_{ap} := \frac{\left[\left(\text{Column}(\text{data}, \text{plot_index}_{ap}, \text{lim})^{(2)} \right)_4 - \left(\text{Column}(\text{data}, \text{plot_index}_{ap}, \text{lim})^{(2)} \right)_2 \right]}{\left[\left(\text{Column}(\text{data}, \text{plot_index}_{ap}, \text{lim})^{(1)} \right)_4 - \left(\text{Column}(\text{data}, \text{plot_index}_{ap}, \text{lim})^{(1)} \right)_2 \right]}$$

$$m_{ap} \cdot (\text{lbf} \cdot \text{in}^2) = 7.295 \times 10^{10} \cdot \text{lbf} \cdot \text{in}^2$$

Linear curvature parameters

Linear strain energy

$$L_Area_{ap} := \frac{\text{Moment}^2}{\left(2 \cdot m_{ap} \cdot \text{lbf} \cdot \text{in}^2 \right)}$$

$$L_Area_{ap} = 820 \text{ lbf}$$

Linear curvature at moment

$$L_Cur_{ap} := \frac{\text{Moment}}{m_{ap} \cdot \text{lbf} \cdot \text{in}^2}$$

$$L_Cur_{ap} = 1.499 \times 10^{-4} \cdot \frac{1}{\text{in}}$$

Curvature points

$$w := \begin{pmatrix} 0 \\ L_Cur_{ap} \cdot \text{in} \end{pmatrix}$$

$$w = \begin{pmatrix} 0 \\ 1.499 \times 10^{-4} \end{pmatrix}$$

Moment points

$$L_Mom_p(w) := m_{ap} \cdot w$$

$$L_Mom_p(w) = \begin{pmatrix} 0 \\ 1.094 \times 10^7 \end{pmatrix}$$

Max number of trapezoids to add when calculating moment under non-linear moment curvature curve

$$c_{max} := 18$$

Variables to calculate area under moment-curvature plot that represent width (b) and heights (h) of trapezoids

Height (Moment) $h1_{ap} := \text{Column}(\text{data}, \text{plot_index}_{ap}, \text{lim})^{(2)}$

$$h2_{ap} := \text{Column}(\text{data}, \text{plot_index}_{ap}, \text{lim})^{(2)}$$

Width (Curvature) $b1_{ap} := \text{Column}(\text{data}, \text{plot_index}_{ap}, \text{lim})^{(1)}$

$$b2_{ap} := \text{Column}(\text{data}, \text{plot_index}_{ap}, \text{lim})^{(1)}$$

Area under moment-curvature plot, based on summing trapezoidal areas

$$NL_Area_{ap} := \sum_{k=3}^{c_{max}} \left[\frac{1}{2} \left[\left(h1_{ap} \right)_k \cdot \text{lbf} \cdot \text{in} + \left(h2_{ap} \right)_{k-1} \cdot \text{lbf} \cdot \text{in} \right] \left[\left(b1_{ap} \right)_k \cdot \frac{1}{\text{in}} - \left(b2_{ap} \right)_{k-1} \cdot \frac{1}{\text{in}} \right] \right]$$

$$NL_Area_{ap} = 895 \text{ lbf}$$

Non-linear Curvature

$$NL_Cur_{ap} := \left(\text{Column}(\text{data}, \text{plot_index}_{ap}, \text{lim})^{(1)} \right)_{c_{max}} \cdot \frac{1}{\text{in}}$$

$$NL_Cur_{ap} = 1.600 \times 10^{-4} \cdot \frac{1}{\text{in}}$$

Vary c.max to make close to zero

$$NL_Area_{ap} - L_Area_{ap} = 74.975 \text{ lbf}$$

Parameters for plotting purposes

$$y := \begin{bmatrix} 0 \\ \left(\text{Column}(\text{data}, \text{plot_index}_{ap}, \text{lim})^{(2)} \right)_{c_{max}} \end{bmatrix} \quad z := \begin{bmatrix} 0 \\ \text{Moment} \cdot \frac{1}{\text{lbf} \cdot \text{in}} \end{bmatrix}$$

$$\text{Lim_NL}(y) := \begin{pmatrix} NL_Cur_{ap} \cdot \text{in} \\ NL_Cur_{ap} \cdot \text{in} \end{pmatrix} \quad \text{Lim_L}(z) := \begin{pmatrix} L_Cur_{ap} \cdot \text{in} \\ L_Cur_{ap} \cdot \text{in} \end{pmatrix}$$

Depth to neutral axis

$$d_{NA} := na(NL_Cur_{ap}, fv_{ap}, 0.8h_{col})$$

$$d_{NA} = 22.154 \cdot \text{in}$$

Distance for strain in steel calculation $d_{strain} := d_{NA} - \text{cover}$

$$d_{strain} = 18.449 \cdot \text{in}$$

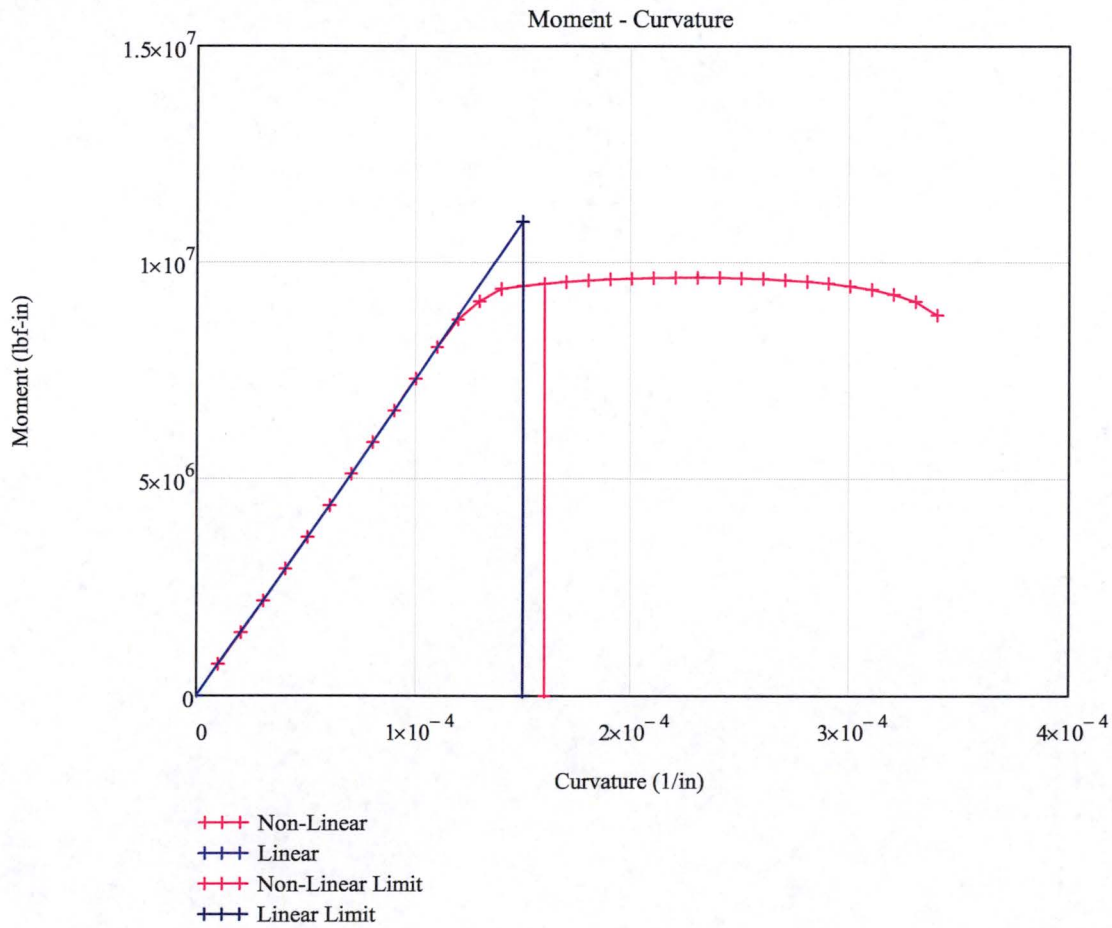
Strain in steel

$$\epsilon_{steel} := NL_Cur_{ap} \cdot d_{strain}$$

$$\epsilon_{steel} = 0.00295$$

Ductility Demand

$$\frac{\epsilon_{steel}}{\epsilon_y} = 1.48$$



PROJECT NO: 150252DATE: July 2016CLIENT: NextEra Energy SeabrookBY: R.M. MonesSUBJECT: Evaluation and Design Confirmation of As-Deformed CEBVERIFIER: A.T. Sarawit**APPENDIX Y****Source Code of Project-Specific Computer Routines****NOTE:**

For brevity, the first 5 pages and last 5 pages of this appendix (not including this title page) are included in this calculation. The full version of this appendix is 179 pages long (including this page) and the last page number is Y-179. The page numbers for the shortened version of this appendix are renumbered to Y-1 through Y-11. All source code in this appendix is also provided in the attached 150252-CA-02-CD-01.



File: SR_MISC_ACCPROF_r0.apdl

Notes: None

Line	Source Code
1	! RMMones
2	! SR_MISC_ACCPROF_r0.apdl
3	! JUNE 2016
4	! ANSYS 15
5	!
6	! Define seismic acceleration profiles
7	! Ref: UE SBSAG-4CE Sheets 22 through 26
8	!
9	! Elev. E-W N-S Vertical
10	! -0360.00 0.130000 0.130000 0.130000
11	! -0152.00 0.130000 0.130000 0.130000
12	! 0000.00 0.130000 0.130000 0.130000
13	! 0240.00 0.130000 0.130000 0.130000
14	! 0444.00 0.130000 0.130000 0.144000
15	! 0612.00 0.162000 0.150000 0.171000
16	! 0816.00 0.215000 0.204000 0.208000
17	! 1020.00 0.265000 0.256000 0.243000
18	! 1224.00 0.310000 0.303000 0.274000
19	! 1428.00 0.354000 0.348000 0.303000
20	! 1620.50 0.397000 0.391000 0.327000
21	! 1813.50 0.442000 0.435000 0.347000
22	! 2006.00 0.487000 0.481000 0.362000
23	! 2198.50 0.531000 0.526000 0.371000
24	! 2391.00 0.570000 0.567000 0.375000
25	AccPro_Size = 15
26	*DIM,AccPro_Elevation,ARRAY,15
27	AccPro_Elevation(1) = -360.00
28	AccPro_Elevation(2) = -152.00
29	AccPro_Elevation(3) = 0.00
30	AccPro_Elevation(4) = 240.00
31	AccPro_Elevation(5) = 444.00
32	AccPro_Elevation(6) = 612.00
33	AccPro_Elevation(7) = 816.00
34	AccPro_Elevation(8) = 1020.00
35	AccPro_Elevation(9) = 1224.00
36	AccPro_Elevation(10) = 1428.00
37	AccPro_Elevation(11) = 1620.50
38	AccPro_Elevation(12) = 1813.50
39	AccPro_Elevation(13) = 2006.00
40	AccPro_Elevation(14) = 2198.50
41	AccPro_Elevation(15) = 2391.00
42	*DIM,AccPro_OBE_EW,ARRAY,15
43	AccPro_OBE_EW(1) = 0.13
44	AccPro_OBE_EW(2) = 0.13
45	AccPro_OBE_EW(3) = 0.13
46	AccPro_OBE_EW(4) = 0.13
47	AccPro_OBE_EW(5) = 0.13
48	AccPro_OBE_EW(6) = 0.16
49	AccPro_OBE_EW(7) = 0.22
50	AccPro_OBE_EW(8) = 0.27
51	AccPro_OBE_EW(9) = 0.31

CONTINUED ON NEXT PAGE



CLIENT NextEra Energy Seabrook

SUBJECT Evaluation and Design-Confirmation of As-Deformed CEB

PROJECT NO. 150252

DATE July 2016

BY R.M. Mones

CHECKED BY A.T. Sarawit

File: SR_MISC_ACCPROF_r0.apdl (Continued)

Notes: None

Line	Source Code
52	AccPro_OBE_EW(10) = 0.35
53	AccPro_OBE_EW(11) = 0.40
54	AccPro_OBE_EW(12) = 0.44
55	AccPro_OBE_EW(13) = 0.49
56	AccPro_OBE_EW(14) = 0.53
57	AccPro_OBE_EW(15) = 0.57
58	*DIM,AccPro_OBE_NS,ARRAY,15
59	AccPro_OBE_NS(1) = 0.13
60	AccPro_OBE_NS(2) = 0.13
61	AccPro_OBE_NS(3) = 0.13
62	AccPro_OBE_NS(4) = 0.13
63	AccPro_OBE_NS(5) = 0.13
64	AccPro_OBE_NS(6) = 0.15
65	AccPro_OBE_NS(7) = 0.20
66	AccPro_OBE_NS(8) = 0.26
67	AccPro_OBE_NS(9) = 0.30
68	AccPro_OBE_NS(10) = 0.35
69	AccPro_OBE_NS(11) = 0.39
70	AccPro_OBE_NS(12) = 0.44
71	AccPro_OBE_NS(13) = 0.48
72	AccPro_OBE_NS(14) = 0.53
73	AccPro_OBE_NS(15) = 0.57
74	*DIM,AccPro_OBE_V,ARRAY,15
75	AccPro_OBE_V(1) = 0.13
76	AccPro_OBE_V(2) = 0.13
77	AccPro_OBE_V(3) = 0.13
78	AccPro_OBE_V(4) = 0.13
79	AccPro_OBE_V(5) = 0.14
80	AccPro_OBE_V(6) = 0.17
81	AccPro_OBE_V(7) = 0.21
82	AccPro_OBE_V(8) = 0.24
83	AccPro_OBE_V(9) = 0.27
84	AccPro_OBE_V(10) = 0.30
85	AccPro_OBE_V(11) = 0.33
86	AccPro_OBE_V(12) = 0.35
87	AccPro_OBE_V(13) = 0.36
88	AccPro_OBE_V(14) = 0.37
89	AccPro_OBE_V(15) = 0.38
90	! Elev. E-W N-S Vertical
91	! -0360.00 0.250000 0.250000 0.250000
92	! -0152.00 0.250000 0.250000 0.250000
93	! 0000.00 0.250000 0.250000 0.250000
94	! 0240.00 0.250000 0.250000 0.250000
95	! 0444.00 0.250000 0.250000 0.250000
96	! 0612.00 0.268000 0.250000 0.294000
97	! 0816.00 0.350000 0.334000 0.353000
98	! 1020.00 0.424000 0.411000 0.407000
99	! 1224.00 0.491000 0.481000 0.457000
100	! 1428.00 0.555000 0.547000 0.504000
101	! 1620.50 0.620000 0.610000 0.544000
102	! 1813.50 0.687000 0.677000 0.579000

CONTINUED ON NEXT PAGE



File: SR_MISC_ACCPROF_r0.apdl (Continued)

Notes: None

Line	Source Code
103	! 2006.00 0.758000 0.747000 0.606000
104	! 2198.50 0.829000 0.822000 0.622000
105	! 2391.00 0.893000 0.889000 0.628000
106	*DIM,AccPro_SSE_EW,ARRAY,15
107	AccPro_SSE_EW(1) = 0.25
108	AccPro_SSE_EW(2) = 0.25
109	AccPro_SSE_EW(3) = 0.25
110	AccPro_SSE_EW(4) = 0.25
111	AccPro_SSE_EW(5) = 0.25
112	AccPro_SSE_EW(6) = 0.27
113	AccPro_SSE_EW(7) = 0.35
114	AccPro_SSE_EW(8) = 0.42
115	AccPro_SSE_EW(9) = 0.49
116	AccPro_SSE_EW(10) = 0.56
117	AccPro_SSE_EW(11) = 0.62
118	AccPro_SSE_EW(12) = 0.69
119	AccPro_SSE_EW(13) = 0.76
120	AccPro_SSE_EW(14) = 0.83
121	AccPro_SSE_EW(15) = 0.89
122	*DIM,AccPro_SSE_NS,ARRAY,15
123	AccPro_SSE_NS(1) = 0.25
124	AccPro_SSE_NS(2) = 0.25
125	AccPro_SSE_NS(3) = 0.25
126	AccPro_SSE_NS(4) = 0.25
127	AccPro_SSE_NS(5) = 0.25
128	AccPro_SSE_NS(6) = 0.25
129	AccPro_SSE_NS(7) = 0.33
130	AccPro_SSE_NS(8) = 0.41
131	AccPro_SSE_NS(9) = 0.48
132	AccPro_SSE_NS(10) = 0.55
133	AccPro_SSE_NS(11) = 0.61
134	AccPro_SSE_NS(12) = 0.68
135	AccPro_SSE_NS(13) = 0.75
136	AccPro_SSE_NS(14) = 0.82
137	AccPro_SSE_NS(15) = 0.89
138	*DIM,AccPro_SSE_V,ARRAY,15
139	AccPro_SSE_V(1) = 0.25
140	AccPro_SSE_V(2) = 0.25
141	AccPro_SSE_V(3) = 0.25
142	AccPro_SSE_V(4) = 0.25
143	AccPro_SSE_V(5) = 0.25
144	AccPro_SSE_V(6) = 0.29
145	AccPro_SSE_V(7) = 0.35
146	AccPro_SSE_V(8) = 0.41
147	AccPro_SSE_V(9) = 0.46
148	AccPro_SSE_V(10) = 0.50
149	AccPro_SSE_V(11) = 0.54
150	AccPro_SSE_V(12) = 0.58
151	AccPro_SSE_V(13) = 0.61
152	AccPro_SSE_V(14) = 0.62
153	AccPro_SSE_V(15) = 0.63

END OF FILE



File: SR_ILC_01_I_r0.apdl

Notes: None

Line	Source Code
1	! RMMones
2	! SR_ILC_01_I_r0.apdl
3	! JUNE 2016
4	! ANSYS 15
5	!
6	! DUMMY MODEL, NO LOADS
7	
8	!Generate the model...
9	/PREP7
10	/INPUT, SR_MODEL1_PROPERTIES_A_r0, apdl
11	/INPUT, SR_MODEL1_NODES_r0, apdl
12	/INPUT, SR_MODEL1_ELEMENTS_CONCRETE_r0, apdl
13	/INPUT, SR_MODEL1_ELEMENTS_STEEL_r0, apdl
14	/INPUT, SR_MODEL1_CONN_BASE_r0, apdl
15	/INPUT, SR_MODEL1_CONN_RADIAL_r0, apdl
16	/INPUT, SR_MODEL1_CONN_TANGENT_r0, apdl
17	/INPUT, SR_MODEL1_BOUNDARY_A_r0, apdl
18	
19	SAVE
20	
21	!(No loads)
22	
23	!SOLVE
24	ALLSEL, ALL, ALL
25	/SOLU
26	ANTYPE,STATIC
27	OUTPR, ALL, NONE
28	OUTRES, ALL
29	ALLSEL, ALL, ALL
30	SOLVE
31	SAVE
32	FINISH

END OF FILE



CLIENT NextEra Energy Seabrook

SUBJECT Evaluation and Design-Confirmation of As-Deformed CEB

PROJECT NO. 150252

DATE July 2016

BY R.M. Mones

CHECKED BY A.T. Sarawit

File: SR_ILC_02_I_r0.apdl

Notes: None

Line	Source Code
1	! RMMones
2	! SR_ILC_02_I_r0.apdl
3	! JUNE 2016
4	! ANSYS 15
5	!
6	! EXTRACT MASS TRIBUTARY TO EACH NODE
7	
8	!Generate the model...
9	/PREP7
10	/INPUT, SR_MODEL1_PROPERTIES_A_r0, apdl
11	/INPUT, SR_MODEL1_NODES_r0, apdl
12	/INPUT, SR_MODEL1_ELEMENTS_CONCRETE_r0, apdl
13	/INPUT, SR_MODEL1_ELEMENTS_STEEL_r0, apdl
14	/INPUT, SR_MODEL1_CONN_BASE_r0, apdl
15	/INPUT, SR_MODEL1_CONN_RADIAL_r0, apdl
16	/INPUT, SR_MODEL1_CONN_TANGENT_r0, apdl
17	!/INPUT, SR_MODEL1_BOUNDARY_A_r0, apdl
18	
19	! Modify dome material cards so density term includes 25%
20	! of the snow load and self weight
21	MP, DENS,10, 0.000241+0.0000222*0.2
22	MP, DENS,12, 0.000241+0.0000222*0.4
23	MP, DENS,14, 0.000241+0.0000222*0.6
24	MP, DENS,16, 0.000241+0.0000222*0.8
25	MP, DENS,18, 0.000241+0.0000222*1.0
26	
27	ALLSEL, ALL
28	D,ALL,ALL
29	ACEL,0,0,1
30	
31	!SOLVE
32	/SOLU
33	ANTYPE,STATIC
34	OUTPR, ALL, NONE
35	OUTRES, ALL
36	ALLSEL, ALL, ALL
37	SOLVE
38	SAVE
39	FINISH
40	
41	!POST
42	/POST1
43	NSEL,S,NODE,,2000000,2999999
44	*GET, nodeNum, NODE, 0, COUNT
45	*GET, nodeMin, NODE, 0, NUM, MIN
46	*GET, nodeMax, NODE, 0, NUM, MAX
47	nodeOperate = nodeMin
48	/OUTPUT,SR_MISC_NODEMASS_r0,apdl
49	/NOPR
50	*DO,i,1,nodeNum

SIMPSON GUMPERTZ & HEGEREngineering of Structures
and Building Enclosures

CLIENT NextEra Energy Seabrook

SUBJECT Evaluation and Design-Confirmation of As-Deformed CEB

PROJECT NO. 150252

DATE July 2016

BY R.M. Mones

CHECKED BY A.T. Sarawit

51 ESEL,A,ELEM,, 2303726

CONTINUED ON NEXT PAGE

File: SR_ILC_48_1_r0.apdl (Continued)

Notes: None

Line

Source Code

```
52 ESEL,A,ELEM,, 2303728
53 ESEL,A,ELEM,, 2303734
54 ESEL,A,ELEM,, 2303735
55 ESEL,A,ELEM,, 2303736
56 ESEL,A,ELEM,, 2303737
57 ESEL,A,ELEM,, 2303869
58 ESEL,A,ELEM,, 2303871
59 ESEL,A,ELEM,, 2303875
60 ESEL,A,ELEM,, 2303876
61 ESEL,A,ELEM,, 2303877
62 ESEL,A,ELEM,, 2303878
63 ESEL,A,ELEM,, 2303879
64
65 inistate,set,CSYS,-2
66 inistate,set,DTYP,EPEL
67 inistate,defi,,,1,1,-0.0000001
68 inistate,defi,,,1,3,0.0000001
69
70 !SOLVE
71 ALLSEL, ALL, ALL
72 /SOLU
73 ANTYPE,STATIC
74 OUTPR, ALL, NONE
75 OUTRES, ALL
76 ALLSEL, ALL, ALL
77 SOLVE
78 SAVE
79 FINISH
80
81 /POST1
82 ESEL,S,ELEM,, 2303576
83 ESEL,A,ELEM,, 2303577
84 ESEL,A,ELEM,, 2303583
85 ESEL,A,ELEM,, 2303585
86 ESEL,A,ELEM,, 2303586
87 ESEL,A,ELEM,, 2303587
88 ESEL,A,ELEM,, 2303594
89 /PAGE,,,1
90 PRESOL,SMIS,4
91 PRESOL,SMIS,5
92 FINISH
```

END OF FILE



File: SR_ILC_49_I_r0.apdl

Notes: None

Line	Source Code
1	! RMMones
2	! SR_ILC_49_I_r0.apdl
3	! JULY 2016
4	! ANSYS 15
5	!
6	!MOMENT REDISTRIBUTION 13
7	!PLACEHOLDER
8	
9	!Generate the model...
10	/PREP7
11	/INPUT, SR_MODEL1_PROPERTIES_C_r0, apdl
12	/INPUT, SR_MODEL1_NODES_DEFORMED_r0, apdl
13	/INPUT, SR_MODEL1_ELEMENTS_CONCRETE_r0, apdl
14	/INPUT, SR_MODEL1_ELEMENTS_STEEL_r0, apdl
15	/INPUT, SR_MODEL1_CONN_BASE_HINGE_r0, apdl
16	/INPUT, SR_MODEL1_CONN_RADIAL_r0, apdl
17	/INPUT, SR_MODEL1_CONN_TANGENT_r0, apdl
18	/INPUT, SR_MODEL1_BOUNDARY_A_r0, apdl
19	
20	SAVE
21	
22	!(No loads)
23	
24	!SOLVE
25	ALLSEL, ALL, ALL
26	/SOLU
27	ANTYPE,STATIC
28	OUTPR, ALL, NONE
29	OUTRES, ALL
30	ALLSEL, ALL, ALL
31	SOLVE
32	SAVE
33	FINISH

END OF FILE



CLIENT NextEra Energy Seabrook

SUBJECT Evaluation and Design-Confirmation of As-Deformed CEB

PROJECT NO. 150252

DATE July 2016

BY R.M. Mones

CHECKED BY A.T. Sarawit

File: SR_ILC_50_I_r0.apdl

Notes: None

Line	Source Code
1	! RMMones
2	! SR_ILC_50_I_r0.apdl
3	! JULY 2016
4	! ANSYS 15
5	!
6	!MOMENT REDISTRIBUTION 14
7	!PLACEHOLDER
8	
9	!Generate the model...
10	/PREP7
11	/INPUT, SR_MODEL1_PROPERTIES_C_r0, apdl
12	/INPUT, SR_MODEL1_NODES_DEFORMED_r0, apdl
13	/INPUT, SR_MODEL1_ELEMENTS_CONCRETE_r0, apdl
14	/INPUT, SR_MODEL1_ELEMENTS_STEEL_r0, apdl
15	/INPUT, SR_MODEL1_CONN_BASE_HINGE_r0, apdl
16	/INPUT, SR_MODEL1_CONN_RADIAL_r0, apdl
17	/INPUT, SR_MODEL1_CONN_TANGENT_r0, apdl
18	/INPUT, SR_MODEL1_BOUNDARY_A_r0, apdl
19	
20	SAVE
21	
22	!(No loads)
23	
24	!SOLVE
25	ALLSEL, ALL, ALL
26	/SOLU
27	ANTYPE,STATIC
28	OUTPR, ALL, NONE
29	OUTRES, ALL
30	ALLSEL, ALL, ALL
31	SOLVE
32	SAVE
33	FINISH

END OF FILE



File: SR_ILC_51_I_r0.apdl

Notes: None

```

Line   Source Code
1       ! RMMones
2       ! SR_ILC_51_I_r0.apdl
3       ! JULY 2016
4       ! ANSYS 15
5       !
6       ! SIMULATE MERIDIONAL STIFFNESS REDUCTION ABOVE EL. 45 ft AT AZ~240
7
8       !Generate the model...
9       /PREP7
10      /INPUT, SR_MODEL1_PROPERTIES_C_r0, apdl
11      /INPUT, SR_MODEL1_NODES_DEFORMED_r0, apdl
12      /INPUT, SR_MODEL1_ELEMENTS_CONCRETE_r0, apdl
13      /INPUT, SR_MODEL1_ELEMENTS_STEEL_r0, apdl
14      /INPUT, SR_MODEL1_CONN_BASE_HINGE_r0, apdl
15      /INPUT, SR_MODEL1_CONN_RADIAL_r0, apdl
16      /INPUT, SR_MODEL1_CONN_TANGENT_r0, apdl
17      /INPUT, SR_MODEL1_BOUNDARY_A_r0, apdl
18
19      SAVE
20
21      ALLSEL,ALL
22
23      !Top nodes:
24      D,2200841,UZ,0.0001
25      D,2200968,UZ,0.0001
26      D,2201114,UZ,0.0001
27      D,2201263,UZ,0.0001
28      D,2201377,UZ,0.0001
29      D,2201504,UZ,0.0001
30      D,2201650,UZ,0.0001
31      D,2201807,UZ,0.0001
32      D,2201940,UZ,0.0001
33      D,2202103,UZ,0.0001
34      !Bottom Nodes:
35      D,2200840,UZ,-0.0001
36      D,2200967,UZ,-0.0001
37      D,2201113,UZ,-0.0001
38      D,2201262,UZ,-0.0001
39      D,2201376,UZ,-0.0001
40      D,2201503,UZ,-0.0001
41      D,2201649,UZ,-0.0001
42      D,2201806,UZ,-0.0001
43      D,2201939,UZ,-0.0001
44      D,2202102,UZ,-0.0001
45
46      !SOLVE
47      ALLSEL, ALL, ALL
48      /SOLU
49      ANTYPE,STATIC
50      OUTPR, ALL, NONE
    
```



CLIENT NextEra Energy Seabrook

SUBJECT Evaluation and Design-Confirmation of As-Deformed CEB

PROJECT NO. 150252

DATE July 2016

BY R.M. Mones

CHECKED BY A.T. Sarawit

51 OUTRES, ALL

CONTINUED ON NEXT PAGE

File: SR_ILC_51_I_r0.apdl (Continued)

Notes: None

Line	Source Code
52	ALLSEL, ALL, ALL
53	SOLVE
54	SAVE
55	FINISH
56	
57	/POST1
58	esel,S,elem,, 2300487
59	esel,a,elem,, 2300567
60	esel,a,elem,, 2300651
61	esel,a,elem,, 2300737
62	esel,a,elem,, 2300851
63	esel,a,elem,, 2300945
64	esel,a,elem,, 2301031
65	esel,a,elem,, 2301131
66	esel,a,elem,, 2301241
67	esel,a,elem,, 2301345
68	esel,a,elem,, 2301460
69	esel,a,elem,, 2301576
70	/PAGE,,,1
71	PRESOL,SMIS,1
72	PRESOL,SMIS,2
73	PRESOL,SMIS,3
74	PRESOL,SMIS,4
75	PRESOL,SMIS,5
76	PRESOL,SMIS,6
77	FINISH

END OF FILE

PROJECT NO: 150252DATE: July 2016CLIENT: NextEra Energy SeabrookBY: R.M. MonesSUBJECT: Evaluation and Design Confirmation of As-Deformed CEBVERIFIER: A.T. Sarawit

APPENDIX Z

FEA Model Definition

NOTE:

For brevity, the first 5 pages and last 5 pages of this appendix (not including this title page) are included in this calculation. The full version of this appendix is 1420 pages long (including this page) and the last page number is Z-1420. The page numbers for the shortened version of this appendix are renumbered to Z-1 through Z-11. All source code in this appendix is also provided in the attached 150252-CA-02-CD-01.



CLIENT NextEra Energy Seabrook

SUBJECT Evaluation and Design-Confirmation of As-Deformed CEB

PROJECT NO. 150252

DATE July 2016

BY R.M. Mones

CHECKED BY A.T. Sarawit

File: SR_MODEL1_BOUNDARY_A_r0.apdl

Notes: None

Line	Source Code
1	! RMMones
2	! SR_MODEL01_BOUNDARY.apdl
3	! JUNE 2016
4	! ANSYS 15
5	!
6	! DEFINE BOUNDARY CONDITIONS
7	
8	CSYS,1
9	
10	!Vertical support at base of fdn:
11	NSEL,S,NODE,,1000000,1999999
12	NSEL,R,LOC,Z,-485,-475
13	D,ALL,UZ
14	
15	!Tangential support (concrete mat):
16	NSEL,S,NODE,,5000000,5999999
17	D,ALL,ALL
18	
19	!Radial support (concrete fill):
20	NSEL,S,NODE,,4000000,4999999
21	D,ALL,ALL

END OF FILE



CLIENT NextEra Energy Seabrook

SUBJECT Evaluation and Design-Confirmation of As-Deformed CEB

PROJECT NO. 150252

DATE July 2016

BY R.M. Mones

CHECKED BY A.T. Sarawit

File: SR_MODEL1_CONN_BASE_HINGE_r0.apdl

Notes: Only used in Moment Redistribution Cases

Line	Source Code
1	! RMMones
2	! SR_MODEL1_CONN_BASE_HINGE_r0.apdl
3	! JUNE 2016
4	! ANSYS 15
5	!
6	
7	! Model the connection between wall and foundation as hinge
8	
9	! Make coincident nodes at the base to insert hinge release moment about the hoop axis
10	*DO,ii,1,124,1
11	N,3100000+ii,NX(2100000+ii),NY(2100000+ii),NZ(2100000+ii)
12	*ENDDO
13	
14	! Rotate the new nodes to cylindrical coordinate system
15	CSYS, 1
16	NSEL,S,,,3100001,3100124
17	NROTAT, ALL
18	ALLSEL,ALL
19	
20	! Constraint all DOF except rotation about the hoop axis
21	*DO,ii,1,124,1
22	CE,NEXT,0.,3100000+ii,UX,1.0,2100000+ii,UX,-1.0
23	CE,NEXT,0.,3100000+ii,UY,1.0,2100000+ii,UY,-1.0
24	CE,NEXT,0.,3100000+ii,UZ,1.0,2100000+ii,UZ,-1.0
25	CE,NEXT,0.,3100000+ii,ROTX,1.0,2100000+ii,ROTX,-1.0
26	CE,NEXT,0.,3100000+ii,ROTZ,1.0,2100000+ii,ROTZ,-1.0
27	*ENDDO
28	
29	! Spiders connect wall (hinge connection) to foundation
30	TYPE, 1841
31	EN, 3400001, 3100001, 1001989
32	EN, 3400002, 1002000, 3100001
33	EN, 3400003, 3100002, 1002022
34	EN, 3400004, 1002035, 3100002
35	EN, 3400005, 3100003, 1001960
36	EN, 3400006, 1001947, 3100003
37	EN, 3400007, 3100004, 1002063
38	EN, 3400008, 1002076, 3100004
39	EN, 3400009, 3100005, 1001904
40	EN, 3400010, 1001917, 3100005
41	EN, 3400011, 3100006, 1002104
42	EN, 3400012, 1002116, 3100006
43	EN, 3400013, 3100007, 1001864
44	EN, 3400014, 1001875, 3100007
45	EN, 3400015, 3100008, 1002146
46	EN, 3400016, 1002157, 3100008
47	EN, 3400017, 3100009, 1001821
48	EN, 3400018, 1001838, 3100009
49	EN, 3400019, 3100010, 1002183
50	EN, 3400020, 1002198, 3100010
51	EN, 3400021, 3100011, 1001784

CONTINUED ON NEXT PAGE

SIMPSON GUMPERTZ & HEGEREngineering of Structures
and Building Enclosures

CLIENT NextEra Energy Seabrook

SUBJECT Evaluation and Design-Confirmation of As-Deformed CEB

PROJECT NO. 150252

DATE July 2016

BY R.M. Mones

CHECKED BY A.T. Sarawit

File: SR_MODEL1_CONN_BASE_HINGE_r0.apdl (Continued)

Notes: Only used in Moment Redistribution Cases

Line	Source Code
52	EN, 3400022, 1001797, 3100011
53	EN, 3400023, 3100012, 1002228
54	EN, 3400024, 1002241, 3100012
55	EN, 3400025, 3100013, 1001743
56	EN, 3400026, 1001756, 3100013
57	EN, 3400027, 3100014, 1002268
58	EN, 3400028, 1002282, 3100014
59	EN, 3400029, 3100015, 1001699
60	EN, 3400030, 1001714, 3100015
61	EN, 3400031, 3100016, 1002310
62	EN, 3400032, 1002322, 3100016
63	EN, 3400033, 3100017, 1001661
64	EN, 3400034, 1001673, 3100017
65	EN, 3400035, 3100018, 1002358
66	EN, 3400036, 1002383, 3100018
67	EN, 3400037, 3100019, 1001590
68	EN, 3400038, 1001611, 3100019
69	EN, 3400039, 3100020, 1002431
70	EN, 3400040, 1002465, 3100020
71	EN, 3400041, 3100021, 1001506
72	EN, 3400042, 1001529, 3100021
73	EN, 3400043, 3100022, 1002506
74	EN, 3400044, 1002547, 3100022
75	EN, 3400045, 3100023, 1001420
76	EN, 3400046, 1001460, 3100023
77	EN, 3400047, 3100024, 1002588
78	EN, 3400048, 1002629, 3100024
79	EN, 3400049, 3100025, 1001339
80	EN, 3400050, 1001378, 3100025
81	EN, 3400051, 3100026, 1002678
82	EN, 3400052, 1002731, 3100026
83	EN, 3400053, 3100027, 1001248
84	EN, 3400054, 1001303, 3100027
85	EN, 3400055, 3100028, 1002756
86	EN, 3400056, 1002814, 3100028
87	EN, 3400057, 3100029, 1001169
88	EN, 3400058, 1001221, 3100029
89	EN, 3400059, 3100030, 1002824
90	EN, 3400060, 1002895, 3100030
91	EN, 3400061, 3100031, 1001148
92	EN, 3400062, 1001085, 3100031
93	EN, 3400063, 3100032, 1002911
94	EN, 3400064, 1002975, 3100032
95	EN, 3400065, 3100033, 1001009
96	EN, 3400066, 1001065, 3100033
97	EN, 3400067, 3100034, 1002991
98	EN, 3400068, 1003054, 3100034
99	EN, 3400069, 3100035, 1000924
100	EN, 3400070, 1000988, 3100035
101	EN, 3400071, 3100036, 1003075
102	EN, 3400072, 1003128, 3100036

CONTINUED ON NEXT PAGE



CLIENT NextEra Energy Seabrook

SUBJECT Evaluation and Design-Confirmation of As-Deformed CEB

PROJECT NO. 150252

DATE July 2016

BY R.M. Mones

CHECKED BY A.T. Sarawit

File: SR_MODEL1_CONN_BASE_HINGE_r0.apdl (Continued)

Notes: Only used in Moment Redistribution Cases

Line	Source Code
103	EN, 3400073, 3100037, 1000842
104	EN, 3400074, 1000907, 3100037
105	EN, 3400075, 3100038, 1003217
106	EN, 3400076, 1003156, 3100038
107	EN, 3400077, 3100039, 1000759
108	EN, 3400078, 1000827, 3100039
109	EN, 3400079, 3100040, 1003307
110	EN, 3400080, 1003229, 3100040
111	EN, 3400081, 3100041, 1000675
112	EN, 3400082, 1000748, 3100041
113	EN, 3400083, 3100042, 1003312
114	EN, 3400084, 1003393, 3100042
115	EN, 3400085, 3100043, 1000581
116	EN, 3400086, 1000669, 3100043
117	EN, 3400087, 3100044, 1003386
118	EN, 3400088, 1003482, 3100044
119	EN, 3400089, 3100045, 1000497
120	EN, 3400090, 1000593, 3100045
121	EN, 3400091, 3100046, 1003567
122	EN, 3400092, 1003475, 3100046
123	EN, 3400093, 3100047, 1000414
124	EN, 3400094, 1000504, 3100047
125	EN, 3400095, 3100048, 1003552
126	EN, 3400096, 1003646, 3100048
127	EN, 3400097, 3100049, 1000332
128	EN, 3400098, 1000431, 3100049
129	EN, 3400099, 3100050, 1003698
130	EN, 3400100, 1003589, 3100050
131	EN, 3400101, 3100051, 1000241
132	EN, 3400102, 1000362, 3100051
133	EN, 3400103, 3100052, 1003782
134	EN, 3400104, 1003680, 3100052
135	EN, 3400105, 3100053, 1000177
136	EN, 3400106, 1000291, 3100053
137	EN, 3400107, 3100054, 1003872
138	EN, 3400108, 1003762, 3100054
139	EN, 3400109, 3100055, 1000106
140	EN, 3400110, 1000211, 3100055
141	EN, 3400111, 3100056, 1003956
142	EN, 3400112, 1003843, 3100056
143	EN, 3400113, 3100057, 1000071
144	EN, 3400114, 1000172, 3100057
145	EN, 3400115, 3100058, 1003926
146	EN, 3400116, 1004058, 3100058
147	EN, 3400117, 3100059, 1004156
148	EN, 3400118, 1003974, 3100059
149	EN, 3400119, 3100060, 1004253
150	EN, 3400120, 1004049, 3100060
151	EN, 3400121, 3100061, 1004129
152	EN, 3400122, 1004347, 3100061
153	EN, 3400123, 3100062, 1004199

CONTINUED ON NEXT PAGE



CLIENT NextEra Energy Seabrook

SUBJECT Evaluation and Design-Confirmation of As-Deformed CEB

PROJECT NO. 150252

DATE July 2016

BY R.M. Mones

CHECKED BY A.T. Sarawit

File: SR_MODEL1_CONN_BASE_HINGE_r0.apdl (Continued)

Notes: Only used in Moment Redistribution Cases

Line	Source Code
154	EN, 3400124, 1004467, 3100062
155	EN, 3400125, 3100063, 1004285
156	EN, 3400126, 1004538, 3100063
157	EN, 3400127, 3100064, 1004636
158	EN, 3400128, 1004362, 3100064
159	EN, 3400129, 3100065, 1004437
160	EN, 3400130, 1004690, 3100065
161	EN, 3400131, 3100066, 1004763
162	EN, 3400132, 1004478, 3100066
163	EN, 3400133, 3100067, 1004519
164	EN, 3400134, 1004790, 3100067
165	EN, 3400135, 3100068, 1004572
166	EN, 3400136, 1004814, 3100068
167	EN, 3400137, 3100069, 1004589
168	EN, 3400138, 1004841, 3100069
169	EN, 3400139, 3100070, 1004602
170	EN, 3400140, 1004855, 3100070
171	EN, 3400141, 3100071, 1004631
172	EN, 3400142, 1004874, 3100071
173	EN, 3400143, 3100072, 1004607
174	EN, 3400144, 1004862, 3100072
175	EN, 3400145, 3100073, 1004593
176	EN, 3400146, 1004848, 3100073
177	EN, 3400147, 3100074, 1004579
178	EN, 3400148, 1004820, 3100074
179	EN, 3400149, 3100075, 1004525
180	EN, 3400150, 1004792, 3100075
181	EN, 3400151, 3100076, 1004769
182	EN, 3400152, 1004485, 3100076
183	EN, 3400153, 3100077, 1004448
184	EN, 3400154, 1004699, 3100077
185	EN, 3400155, 3100078, 1004373
186	EN, 3400156, 1004645, 3100078
187	EN, 3400157, 3100079, 1004291
188	EN, 3400158, 1004544, 3100079
189	EN, 3400159, 3100080, 1004204
190	EN, 3400160, 1004471, 3100080
191	EN, 3400161, 3100081, 1004354
192	EN, 3400162, 1004136, 3100081
193	EN, 3400163, 3100082, 1004061
194	EN, 3400164, 1004258, 3100082
195	EN, 3400165, 3100083, 1003984
196	EN, 3400166, 1004162, 3100083
197	EN, 3400167, 3100084, 1003930
198	EN, 3400168, 1004068, 3100084
199	EN, 3400169, 3100085, 1003848
200	EN, 3400170, 1003958, 3100085
201	EN, 3400171, 3100086, 1000078
202	EN, 3400172, 1000171, 3100086
203	EN, 3400173, 3100087, 1000214
204	EN, 3400174, 1000112, 3100087

CONTINUED ON NEXT PAGE



CLIENT NextEra Energy Seabrook

SUBJECT Evaluation and Design-Confirmation of As-Deformed CEB

PROJECT NO. 150252

DATE July 2016

BY R.M. Mones

CHECKED BY A.T. Sarawit

File: SR_MODEL1_PROPERTIES_D_r0.apdl (Continued)

Notes: Only used in Moment Redistribution Cases

Line	Source Code
154	
155	!!STEEL, 1#10@12EF + 1#8@12IF
156	SECTYPE, 612, SHELL, ,612
157	SECDATA, A10*2/12+A08*1/12
158	SECOFFSET, MID
159	
160	!!STEEL, 1#10@12EF + 1#6@6EF + 1#8@12IF
161	SECTYPE, 613, SHELL, ,613
162	SECDATA, A10*2/12+A06*2/6+A08*1/12
163	SECOFFSET, MID
164	
165	!!STEEL, H #11@12 EF
166	SECTYPE, 614, SHELL, ,614
167	SECDATA, A11*2/12
168	SECOFFSET, MID
169	
170	!!STEEL, H #10@12 EF
171	SECTYPE, 615, SHELL, ,615
172	SECDATA, A10*2/12
173	SECOFFSET, MID
174	
175	!!STEEL, H #11@6 EF
176	SECTYPE, 616, SHELL, ,616
177	SECDATA, A11*2/6
178	SECOFFSET, MID
179	
180	!!STEEL, H #10@6 EF
181	SECTYPE, 617, SHELL, ,617
182	SECDATA, A10*2/6
183	SECOFFSET, MID
184	
185	!!STEEL, H #11@6 EF & #6@6 EF
186	SECTYPE, 618, SHELL, ,618
187	SECDATA, A11*2/6+A06*2/6
188	SECOFFSET, MID
189	
190	!!STEEL, H #10@6 EF & #6@6 EF
191	SECTYPE, 619, SHELL, ,619
192	SECDATA, A10*2/6+A06*2/6
193	SECOFFSET, MID
194	
195	!!STEEL, H #10@12 EF & #6@6 EF
196	SECTYPE, 620, SHELL, ,620
197	SECDATA, A10*2/12+A06*2/6
198	SECOFFSET, MID
199	
200	!!STEEL, H #11@12 EF & #6@6 EF
201	SECTYPE, 621, SHELL, ,621
202	SECDATA, A11*2/12+A06*2/6
203	SECOFFSET, MID
204	

CONTINUED ON NEXT PAGE



CLIENT NextEra Energy Seabrook

SUBJECT Evaluation and Design-Confirmation of As-Deformed CEB

PROJECT NO. 150252

DATE July 2016

BY R.M. Mones

CHECKED BY A.T. Sarawit

File: SR_MODEL1_PROPERTIES_D_r0.apdl (Continued)
Notes: Only used in Moment Redistribution Cases

Line	Source Code
205	!!STEEL, H 1#10@12EF & 1#6@6IF
206	SECTYPE, 622, SHELL, ,622
207	SECDATA, A10*2/12+A06*1/6
208	SECOFFSET, MID
209	
210	!!STEEL, H UNASSIGNED
211	SECTYPE, 699, SHELL, ,H_NULL
212	SECDATA, 0.001
213	SECOFFSET, MID
214	
215	!!STEEL, 2#11@6OF + 1#14@12IF + 1#11@12IF
216	SECTYPE, 701, SHELL, ,701
217	SECDATA, A11*2/6 + A14*1/12 + A11*1/12
218	SECOFFSET, MID
219	
220	!!STEEL, 1#9@12EF
221	SECTYPE, 702, SHELL, ,702
222	SECDATA, A09*2/12
223	SECOFFSET, MID
224	
225	!!STEEL, V #11@6 EF
226	SECTYPE, 703, SHELL, ,703
227	SECDATA, A11*2/6
228	SECOFFSET, MID
229	
230	!!STEEL, 1#8@12EF
231	SECTYPE, 704, SHELL, ,704
232	SECDATA, A08*2/12
233	SECOFFSET, MID
234	
235	!!STEEL, 1#9@6EF
236	SECTYPE, 705, SHELL, ,705
237	SECDATA, A09*2/6
238	SECOFFSET, MID
239	
240	!!STEEL, 1#8@6EF
241	SECTYPE, 706, SHELL, ,706
242	SECDATA, A08*2/6
243	SECOFFSET, MID
244	
245	!!STEEL, V 2#14@6OF & 1#11@6IF
246	SECTYPE, 707, SHELL, ,707
247	SECDATA, A14*2/6+A11*1/6
248	SECOFFSET, MID
249	
250	!!STEEL, V 1#6@12EF
251	SECTYPE, 708, SHELL, ,708
252	SECDATA, A06*2/12
253	SECOFFSET, MID
254	
255	!!STEEL, V 2#11@6 OF & 1#11@6 IF

CONTINUED ON NEXT PAGE

SIMPSON GUMPERTZ & HEGER


Engineering of Structures
and Building Enclosures

CLIENT NextEra Energy Seabrook

SUBJECT Evaluation and Design-Confirmation of As-Deformed CEB

PROJECT NO. 150252

DATE July 2016

BY R.M. Mones

CHECKED BY A.T. Sarawit

File: SR_MODEL1_PROPERTIES_D_r0.apdl (Continued)

Notes: Only used in Moment Redistribution Cases

Line	Source Code
256	SECTYPE, 709, SHELL, ,709
257	SECDATA, A11*3/6
258	SECOFFSET, USER, -3.5
259	
260	!!STEEL, V Steel Pilaster Low Elevations
261	SECTYPE, 710, SHELL, ,710
262	SECDATA, A11*3/6+A11*6/60
263	SECOFFSET, USER, -4.5
264	
265	!!STEEL, V Steel Pilaster Upper Elevations
266	SECTYPE, 711, SHELL, ,711
267	SECDATA, A11*2/6+A11*6/60
268	SECOFFSET, MID
269	
270	!!STEEL, V 2#14@6OF & 1#14@12IF & 1#11@12IF
271	SECTYPE, 712, SHELL, ,712
272	SECDATA, A14*2/6+A11*1/12+A14*1/12
273	SECOFFSET, USER, -3.5
274	
275	!!STEEL, V 1#6@6EF
276	SECTYPE, 713, SHELL, ,713
277	SECDATA, A06*2/6
278	SECOFFSET, MID
279	
280	!STEEL, V UNASSIGNED
281	SECTYPE, 799, SHELL, ,V_NULL
282	SECDATA, 0.001
283	SECOFFSET, MID
284	
285	!STRUCTURAL CONCRETE, CEB
286	MP, EX,1, 3605000
287	MP, NUXY,1, 0.15
288	MP, DENS,1, 0.000225
289	MP, REFT, 1, 0.00
290	
291	!STRUCTURAL CONCRETE, FDN
292	MP, EX,2, 3120000
293	MP, NUXY,2, 0.15
294	MP, DENS,2, 0.000225
295	MP, REFT, 2, 0.00
296	
297	!HORIZONTAL STEEL FOR APPLICATION OF ASR EXPANSION
298	MP, EX,6, 1000
299	MP, EY,6, 1000
300	MP, EZ,6, 1000
301	MP, GXY,6, 1000
302	MP, GYZ,6, 1000
303	MP, GXZ,6, 1000
304	MP, NUXY,6, 0.000001
305	MP, NUYZ,6, 0.000001
306	MP, NUXZ,6, 0.000001

CONTINUED ON NEXT PAGE

SIMPSON GUMPERTZ & HEGEREngineering of Structures
and Building Enclosures

CLIENT NextEra Energy Seabrook

SUBJECT Evaluation and Design-Confirmation of As-Deformed CEB

PROJECT NO. 150252

DATE July 2016

BY R.M. Mones

CHECKED BY A.T. Sarawit

File: SR_MODEL1_PROPERTIES_D_r0.apdl (Continued)

Notes: Only used in Moment Redistribution Cases

Line	Source Code
307	MP, DENS,6, 0.000001
308	MP, REFT, 6, 0.00
309	
310	!!VERTICAL STEEL FOR APPLICATION OF ASR EXPANSION
311	MP, EX,7, 1000
312	MP, EY,7, 1000
313	MP, EZ,7, 1000
314	MP, GXY,7, 1000
315	MP, GYZ,7, 1000
316	MP, GXZ,7, 1000
317	MP, NUXY,7, 0.000001
318	MP, NUYZ,7, 0.000001
319	MP, NUXZ,7, 0.000001
320	MP, DENS,7, 0.000001
321	MP, REFT, 7, 0.00
322	
323	!STRUCTURAL CONCRETE, FOR DOME ELEMENTS WITH
324	!PROJECTED AREA/TOTAL AREA = 0 to 0.2
325	!INCLUDES ADDED WT OF PERMANENT FORMWORK
326	MP, EX,10, 3605000
327	MP, NUXY,10, 0.15
328	MP, DENS,10, 0.000241
329	MP, REFT, 10, 0.00
330	
331	!STRUCTURAL CONCRETE, FOR DOME ELEMENTS WITH
332	!PROJECTED AREA/TOTAL AREA = 0.2 to 0.4
333	!INCLUDES ADDED WT OF PERMANENT FORMWORK
334	MP, EX,12, 3605000
335	MP, NUXY,12, 0.15
336	MP, DENS,12, 0.000241
337	MP, REFT, 12, 0.00
338	
339	!STRUCTURAL CONCRETE, FOR DOME ELEMENTS WITH
340	!PROJECTED AREA/TOTAL AREA = 0.4 to 0.6
341	!INCLUDES ADDED WT OF PERMANENT FORMWORK
342	MP, EX,14, 3605000
343	MP, NUXY,14, 0.15
344	MP, DENS,14, 0.000241
345	MP, REFT, 14, 0.00
346	
347	!STRUCTURAL CONCRETE, FOR DOME ELEMENTS WITH
348	!PROJECTED AREA/TOTAL AREA = 0.6 to 0.8
349	!INCLUDES ADDED WT OF PERMANENT FORMWORK
350	MP, EX,16, 3605000
351	MP, NUXY,16, 0.15
352	MP, DENS,16, 0.000241
353	MP, REFT, 16, 0.00
354	
355	!STRUCTURAL CONCRETE, FOR DOME ELEMENTS WITH
356	!PROJECTED AREA/TOTAL AREA = 0.8 to 1.0
357	!INCLUDES ADDED WT OF PERMANENT FORMWORK

CONTINUED ON NEXT PAGE



File: SR_MODEL1_PROPERTIES_D_r0.apdl (Continued)

Notes: Only used in Moment Redistribution Cases

Line	Source Code
358	MP, EX, 18, 3605000
359	MP, NUXY, 18, 0.15
360	MP, DENS, 18, 0.000241
361	MP, REFT, 18, 0.00
362	
363	!<<ALL INPUTS BELOW ARE FOR CRACKED SECTION PROPERTIES>>
364	
365	kcr=0.50
366	
367	!STRUCTURAL CONCRETE, CEB, <<FOR CRACKED SECTIONS>>
368	MP, EX, 3, 3605000/(kcr**0.5)
369	MP, NUXY, 3, 0.15
370	MP, DENS, 3, 0.000318/(kcr**0.5)
371	MP, REFT, 3, 0.00
372	
373	!CONCRETE, THICKNESS = 36 in. (CEB WALL) <<FOR CRACKED SECTIONS>>
374	SECTYPE, 236, SHELL, , Crck36in
375	SECDATA, 36*(kcr)**0.5
376	
377	!CONCRETE, THICKNESS = 27 in. (CEB WALL) <<FOR CRACKED SECTIONS>>
378	SECTYPE, 227, SHELL, , Crck27in
379	SECDATA, 27*(kcr)**0.5
380	
381	!CONCRETE, THICKNESS = 15 in. (CEB WALL) <<FOR CRACKED SECTIONS>>
382	SECTYPE, 215, SHELL, , Crck15in
383	SECDATA, 15*(kcr)**0.5
384	
385	!CONCRETE, THICKNESS = 48 in. (PILASTERS) <<FOR CRACKED SECTIONS>>
386	SECTYPE, 248, SHELL, , Crck48in
387	SECDATA, 48*(kcr)**0.5
388	
389	!CONCRETE, THICKNESS = 39 in. (PILASTERS) <<FOR CRACKED SECTIONS>>
390	SECTYPE, 239, SHELL, , Crck39in
391	SECDATA, 39*(kcr)**0.5

END OF FILE